Queen Mary
University of London

Barts & The London

Wingate Institute of Neurogastroenterology,
Blizard Institute

Characterisation of the Sensory Phenotype of the Oesophageal Mucosa in Adults with Gastroesophageal Reflux Disease

A thesis submitted in partial fulfilment of the requirements of the Degree Doctor of Philosophy

Ahsen Ustaoglu

Abstract

As the first line of defence against noxious luminal contents, the oesophageal mucosa plays an important role in the pathogenesis of gastroesophageal reflux disease (GORD). We hypothesised that the heterogeneity of symptom perception between heartburn patients may be dependent on the interactions between neuronal and inflammatory cells in the oesophageal mucosa.

Studies were conducted with endoscopic oesophageal biopsies from GORD patients (N=83) to characterise the phenotype of afferent mucosal nerve endings by assessing expression of ion channels TRPV1, ASIC3, and TRPM8 involved in pain transduction. Neuro-immune interactions in the oesophageal mucosa of heartburn patients and healthy individuals (N=14) was studied by assessing the expression of inflammatory cytokine receptors CXCR2, TNFR1, IL1R, IL6R, and RAMP1. Infiltration of immune cell populations was characterised among GORD groups. Mast cell co-expression of NGF was also studied. Cytokine release profiles were measured in supernatant from mucosal biopsies from ERD patients and healthy controls exposed to acid using a multiplex assay. RNA extracted from mucosal GORD biopsies and healthy controls were bulk-sequenced to assess the differences in the molecular gene signature between patients with heartburn and asymptomatic subjects, and among GORD phenotypes.

TRPV1 was expressed only on mucosal superficial sensory afferent nerve endings of NERD patients, while ASIC3 was most frequently expressed on oesophageal epithelial cells in NERD and ERD patients. CXCR2 was localised on epithelial cells surrounding the papillae in all GORD phenotypes and healthy controls, but was also detected on deep sensory afferent nerves innervating papillae in FH patients. NGF expression was significantly higher in mast cells in patients with GORD compared to healthy controls, and these mast cells were detected in close proximity to sensory deep afferent nerves in patients with ERD. IL8 secretion was increased with acid exposure in both healthy control oesophageal mucosa and ERD, while NGF was released at higher levels with acid exposure from ERD oesophageal mucosa. RNA sequencing detected important differences in expression of genes with structural and regenerative roles between NERD, ERD and BO oesophageal mucosa and asymptomatic subjects.

We demonstrated distinct sensory phenotypes in the oesophageal mucosa of patients with ERD, NERD, BO, FH, and healthy controls. These phenotypes include differences in mucosal afferent innervation, immune cell profiles, cytokine release when challenged with acid, and gene expression signatures. Collectively, these findings may contribute to heartburn

pathogenesis in the oesophageal epithelium of GORD patients. Improved understanding of mucosal targets identified in this study, including TRPV1, ASIC3, and NGF, in functional studies will enable development of targeted topical treatments to alleviate heartburn symptoms.

Statement of Originality

I, Ahsen Ustaoglu, confirm that the research included within this thesis is my own work or that where it has been carried out in collaboration with, or supported by others, that this is duly acknowledged below and my contribution is indicated. Previously published material is also acknowledged below.

All the studies were performed and analysed by myself except when stated. Mr Manfredi D'Afflitto obtained immunohistochemistry images for T and B lymphocyte staining, and contributed to IHC staining for dendritic cells under my supervision. Dr Fatema Arif Daudali obtained immunohistochemistry images for GAP-43/PGP9.5 and NGF/mast cell tryptase staining panels under my supervision. Dr Jan Soetaert assisted in acquisition of confocal Z-stack images.

I attest that I have exercised reasonable care to ensure that the work is original, and does not to the best of my knowledge break any UK law, infringe any third party's copyright or other Intellectual Property Right, or contain any confidential material.

I accept that the College has the right to use plagiarism detection software to check the electronic version of the thesis.

I confirm that this thesis has not been previously submitted for the award of a degree by this or any other university.

The copyright of this thesis rests with the author and no quotation from it or information derived from it may be published without the prior written consent of the author.

Signature: AHSEN USTAOGLU

Date: 13/03/2022

Publications:

Ustaoglu A, Sawada A, Lee C, Lei WY, Chen CL, Hackett R, Sifrim D, Peiris M, Woodland P. (2021). **Heartburn sensation in nonerosive reflux disease: Pattern of superficial sensory nerves expressing TRPV1 and epithelial cells expressing ASIC3 receptors.** *American Journal of Physiology - Gastrointestinal and Liver Physiology* vol. 320, (5) G804 - G815.

Ustaoglu A, Woodland P (2021). **Esophageal afferent innervation and its role in gastro-esophageal reflux disease symptoms.** *Current opinion in gastroenterology* vol. 37, (4)372-377.

Ustaoglu A, Nguyen A, Spechler S, Sifrim D, Souza R, Woodland P (2020). **Mucosal pathogenesis in gastro-esophageal reflux disease.** *Neurogastroenterology and Motility* vol. 32, (12)

Acknowledgements

I would like to thank my supervisors, Professor Daniel Sifrim, Dr Madusha Peiris, and Dr Philip Woodland for giving me the opportunity to undertake a PhD at Barts and the London School of Medicine and Dentistry. I am incredibly thankful to Professor Daniel Sifrim for his endless enthusiasm, advice, and support throughout my doctorate studies. I am grateful to Dr Madusha Peiris for continuously supporting me with my experiments and writing, and teaching me how to be a true scientist. I am also grateful to Dr Philip Woodland for his invaluable advice and insight, and always encouraging me in my many moments of self-doubt.

I am thankful to many of the Wingate and Blizard Institute staff for their assistance during my PhD. Chung Lee became a great friend and mentor. I am fortunate to have had his endless attention, help, and constructive feedback which has undoubtedly made me a better scientist. Professor Qasim Aziz was always on hand to offer support and the benefit of his advice. Stephen Murtough provided excellent assistance in RNA sequencing analysis- without him I could not have gotten through coding on R to visualise my sequencing data. Dr Diana Blaydon gave insightful feedback on my RNA sequencing chapter, and patiently listened to and answered my many questions. I am indebted to Professor David Kelsell for his invaluable advice, guidance, and insight which fuelled the progression of this PhD project. I am also grateful to Dr Estefania Moreno, Adrian Ramdass, and all of the staff at the Royal London Hospital Endoscopy Unit for their very generous help in obtaining biopsy samples, particularly during a pandemic.

I am eternally grateful to my dear brother, mum and dad for their unconditional love, support, and belief in my potential. Thank you for always nurturing my growth and being my best role models. I am also thankful to my wonderful friends for listening, motivating, and supporting me during the most challenging endeavour of my life so far. Finally, words cannot express my gratitude for my husband, Burhan, who I met and married during this journey. Thank you for being my unwavering pillar of strength, biggest source of motivation, and for your endless love.

I dedicate this thesis to my beautiful grandmother, whose battle against disease was my first motivation for studying the medical sciences.

London, 2022.

Table of Contents

Table of Figures

1 Introduction

Gastroesophageal reflux disease (GORD) is a condition that develops following reflux of gastric contents into the oesophagus leading to troublesome symptoms and/or complications [1]. In most GORD patients, it presents as troublesome heartburn and regurgitation which worsen after eating or lying down [2]. It has global impact on health and quality of life, affecting 20% of Western populations [3]. Most patients respond well to the standard therapy of proton pump inhibitors (PPIs) which are prodrugs that suppress gastric acid secretion by inhibiting H^+/K^+-ATPase on parietal cells [4]. However, attention is now being directed to the 30-40% of GORD patients who do not respond adequately to acid suppressant therapy [5]. Heartburn is the most common and important symptom of GORD, but remains a challenge to treat due to our incomplete knowledge of oesophageal pain sensing mechanisms [1]. Moreover, prevalence of the disease appears to be increasing, not only in the conventionally affected Western populations, but also in Eastern parts of the world including Asia [6]. The economic burden of GORD is significant, with annual healthcare expenditure for oesophageal diseases totalling $18 billion, and GORD being among the top three outpatient diagnostics in the Unites States [7]. Thus, GORD presents a significant burden to healthcare economy, has a negative effect on health-related quality of life, and a sub-set of patients with chronic GORD develop Barrett's oesophagus and oesophageal adenocarcinoma [8]. Thus, GORD is a growing global problem that leads to significant impairment of quality of life, making it essential to understand the cellular mechanisms underlying symptom generation.

1.1 Pathophysiology of GORD

1.1.1 The Anti-Reflux Barrier

The high prevalence of GORD can be explained by the proximity of the acid and pepsin secreting mucosa of the stomach to the squamous mucosa of the oesophagus at and above the gastroesophageal junction (GOJ). While the columnar mucosa of the stomach is designed to withstand low pH and the high proteolytic activity of gastric acid and pepsin, the stratified squamous mucosa of the oesophagus is readily digested and damaged when exposed to this chemical environment [9]. Under normal physiology, excessive reflux exposure is prevented by the anti-reflux barrier which is a complex anatomical structure made up of several components at the GOJ including the lower oesophageal sphincter (LOS), extrinsic crural diaphragm, and the gastro-intestinal flap valve (Figure 1).

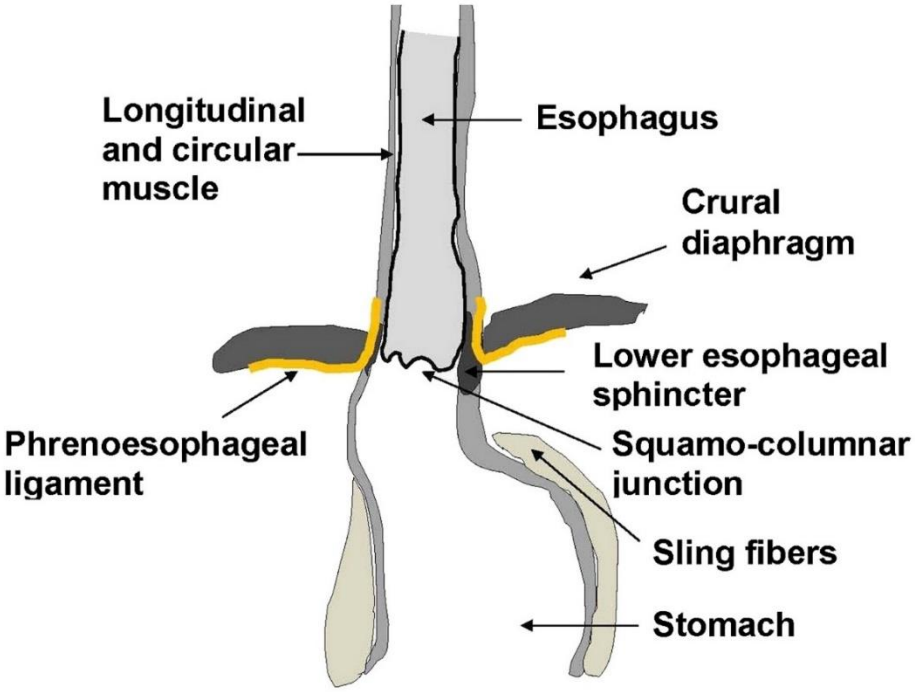

Figure 1 Anatomy of the gastroesophageal junction (GOJ) [10]

Diagram demonstrating the structure of the GOJ, where the lower oesophageal sphincter prevents retrograde flow of bolus from the stomach into the oesophagus.

The GOJ is designed to facilitate the flow of acid secreted from the proximal gastric mucosa into the stomach, and not up to the distal oesophageal mucosa [10]. This function is served in large by the LOS which acts as a one-way valve during swallowing to allow the passage of bolus from the oesophagus to the stomach, while simultaneously exerting pressure to prevent retrograde flow towards the oesophagus [11]. The resting tone of the LOS varies between 10-30 mmHg among healthy individuals, relative to intragastric pressure, providing a barrier to offset the pressure gradient across the GOJ. This pressure is modified by myogenic and

neurogenic factors which are affected by many factors including food, medication, peptides, hormones, intra-abdominal pressure, and gastric distention. Thus, the LOS prevents ingested material refluxing into the oesophagus during fluctuations of the GOJ pressure gradient [12]. When these protective mechanisms are compromised, the deleterious effects are additive.

The physiology of the anti-reflux barrier occurring at the GOJ is complex, and can be involved in inducing reflux when associated with factors such as increased intra-abdominal pressure [11]. Studies suggest that transient lower oesophageal sphincter relaxations (TLOSRs) are the most common mechanism by which reflux occurs during periods of normal LOS pressure (>10 mmHg) [2], [13]. During a TLOSR both the intrinsic and extrinsic oesophageal sphincter relaxes and longitudinal smooth muscle contracts, causing the GOJ to move proximally into the thorax by 2-8cm [14]. This stimulates the intraganglionic lamellar endings (IGLEs) of vagal afferents which project to the nucleus tractus solitarii in the brainstem, and subsequently the vagal dorsal motor nuclei [15]. Neurons of the dorsal motor nucleus then project to inhibitory neurons in the myenteric plexus of the distal oesophagus which induces a motor response to cause tension-mediated relaxation of the LOS and crural diaphragmatic inhibition, and costal diaphragmatic contraction [2], [13].

While most patients with a normal GOJ experience reflux almost exclusively via TLOSRs, patients who present with hiatus hernia can experience swallow-induced reflux, as well as during periods of LOS hypotension [15]. Many patients with severe reflux disease show evidence of having a hiatus hernia which is where the GOJ is displaced proximally, moving the intrinsic LOS proximally to the hiatus formed by the crural diaphragm [16]. Thus, a portion of the proximal stomach lies in the chest above the diaphragm, forming a sac (Figure 2) [17]. Hiatus herniation has been shown to induce reflux through various mechanisms including trapping of acid within the hernia sac. Ambulatory pH studies which recorded pH in different regions of the gastrointestinal tract using pH sensors 1 cm apart found that the pH in the region just below the GOJ remains highly acidic post prandially, and does not undergo buffering like the rest of the stomach [19], [20]. This post-prandial gastric juice layer of unbuffered acid is known as the acid pocket. Importantly, in patients with hiatus hernia the acid pocket provides a large reservoir of unbuffered acid which becomes available to reflux when the LOS fails [21]. However, acid pockets are not the only mechanism through which hiatus hernia promotes acid reflux. Other mechanisms include impaired oesophageal clearance, re-refluxing following a peristaltic wave, and decreased sphincter pressure [22], [23].

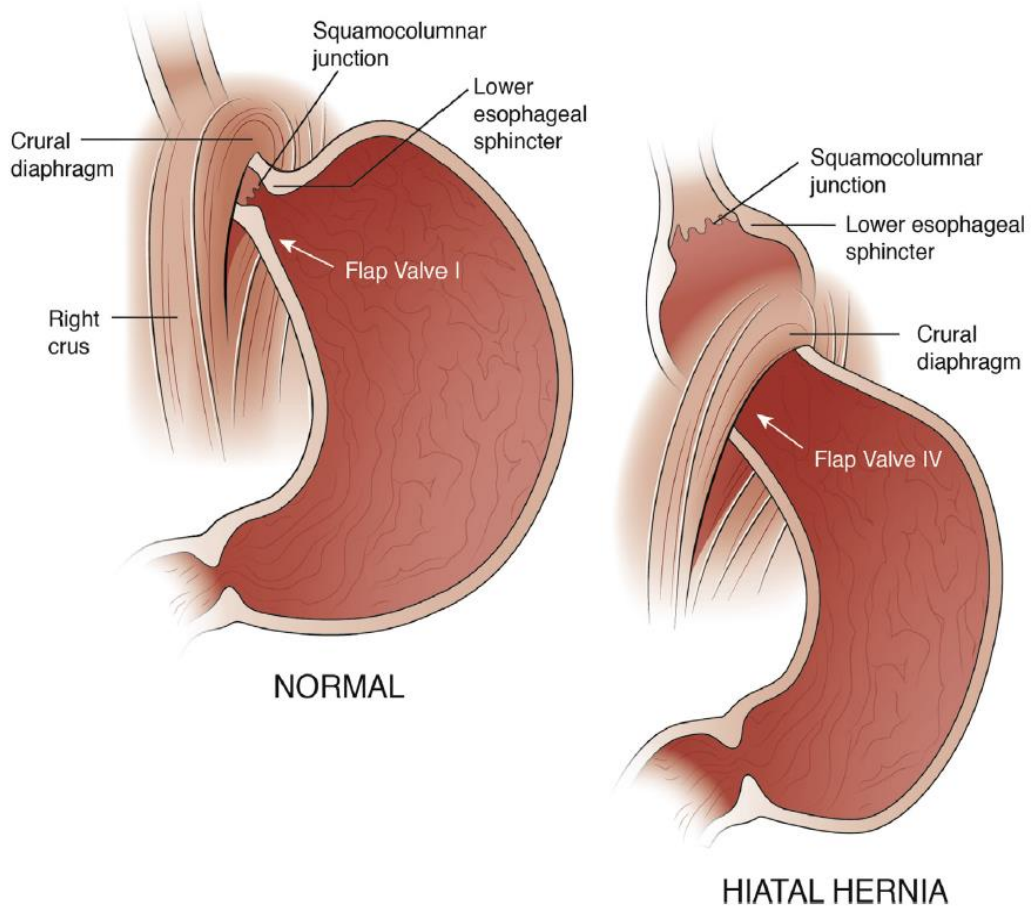

Figure 2: The gastroesophageal junction, without and with hiatus hernia (right)

In patients with hiatus hernia, the GOJ is displaced proximally. This moves the intrinsic LOS several cm proximally to the hiatus formed. The proximal stomach lies above the diaphragm, which compromises the function of the crural diaphragm due to its axial displacement [16]

1.1.2 The Gastric Refluxate and gastro-oesophageal mucosa

The mucosal glands of the gastric body contain parietal cells which secrete gastric acid for the breakdown of proteins in the stomach, solubilisation of food components, and promotion of nutrient absorption [24]. Parietal cells contain the hydrogen (H^+)/potassium (K^+)-ATPase (more commonly known as proton pump), which transports H^+ out of the cell and K^+ from the gastric lumen into the cell. The chloride (Cl^-) component of hydrochloric acid (HCl) is secreted separately by Cl channels in the stomach [25]. Gastric juice is a noxious blend of HCl, bile, and digestive enzymes that collectively create an acidic environment in the stomach that induces the conversion of proenzyme pepsinogen to pepsin [26]. Pepsin is an endopeptidase which breaks down proteins into smaller peptides that can later be processed and absorbed

in the small intestine [27]. The physiological functions of gastric acid also extend to protection of the gastrointestinal tract (GIT) by reducing bacterial colonisation of the stomach and duodenum as many pathogens are inactivated or killed at an intragastric pH of 1-2 [28].

Not only is the gastric mucosa lined by columnar epithelium, but also contains mucous neck cells which secrete mucus that line the gastric and duodenal epithelium [29]. The mucus layer serves as both a lubricant and a protectant against mechanical and chemical injury from gastric acid [30]. Mucus is composed of glycoproteins which have high molecular weight giving it viscoelastic properties, which prevent the penetration of pepsin into the underlying epithelium [31]. Despite the squamous oesophageal epithelium being considered to be non-mucus secreting, the expression of mucin (*MUC*) genes was detected in the submucosal glands and squamous epithelium of the normal oesophagus with *in situ* hybridization and northern blot [32]. *MUC* gene expression also correlated with oesophageal cell differentiation, with *MUC5AC*, the most enzymatically protective mucin in the intestine, and *MUC6* expression being associated with gastric differentiation as a protective mechanism against acid in the form of Barrett's oesophagus [32]. Thus, MUC genes could be considered a phenotypic marker of oesophageal cell differentiation, even in the absence of a mucus layer in the oesophagus [32], [33].

The presence of surface bicarbonate ions (HCO_3^-) in the stomach and duodenum acts as another pre-epithelial defence mechanism [33]. While mucus blocks pepsin diffusion into the epithelium, it is not an effective barrier to H^+. However, HCO_3^- residing in the water layer of the lumen neutralizes H^+ as it penetrates the mucous layer before reaching the epithelium [34]. The capacity of HCO_3^- to act as an alkaline sink has been demonstrated in animals and humans [35], [36]. These studies passed pH-sensitive electrodes from the lumen to the epithelium and showed a luminal pH of 2, while the pH at the epithelial surface ranged from 5-7. In contrast, the pH measured 2 both at the oesophageal lumen and the oesophageal epithelial surface [36]. The lack of HCO_3^- at the oesophagus is due to the inability of the unspecialised cells of the stratified squamous epithelium to secrete HCO_3^- [37]. Moreover, the absence of a mucus layer in the human oesophagus leaves it vulnerable to the injurious threat posed by gastric acid, loading a major burden on the epithelial layer to mount a defence mechanism against gastric refluxate [37].

The stratified squamous epithelial lining of the oesophagus, as seen in Figure 3, provides a tight protective barrier separating luminal contents (including food and gastric reflux) from having close contact with neurons and other cells (e.g. secretory glands). Oesophageal epithelial apical cell membranes have junctional complexes which are composed of tight junctions, adherens junctions, and desmosomes which act as a barrier to the movement of

ions [38]. However, unlike the acid and pepsin-secreting columnar mucosa of the stomach which are designed to withstand very low pH and high proteolytic activity, unspecialised cells of the oesophageal mucosa can be damaged when exposed to chemical stimuli [8]. The threat imposed by a high luminal acid concentration is normally met by mucosal defence mechanisms such as local homeostatic repair initiated by acid-sensing cells including epithelial cells and acid-sensitive neurons. Acid-related diseases including GORD may ensue when these defence systems are defective or suboptimal [39]. Importantly, normal concentrations of gastric juice components are sufficient to cause mucosal injury when oesophageal exposure is increased [17].

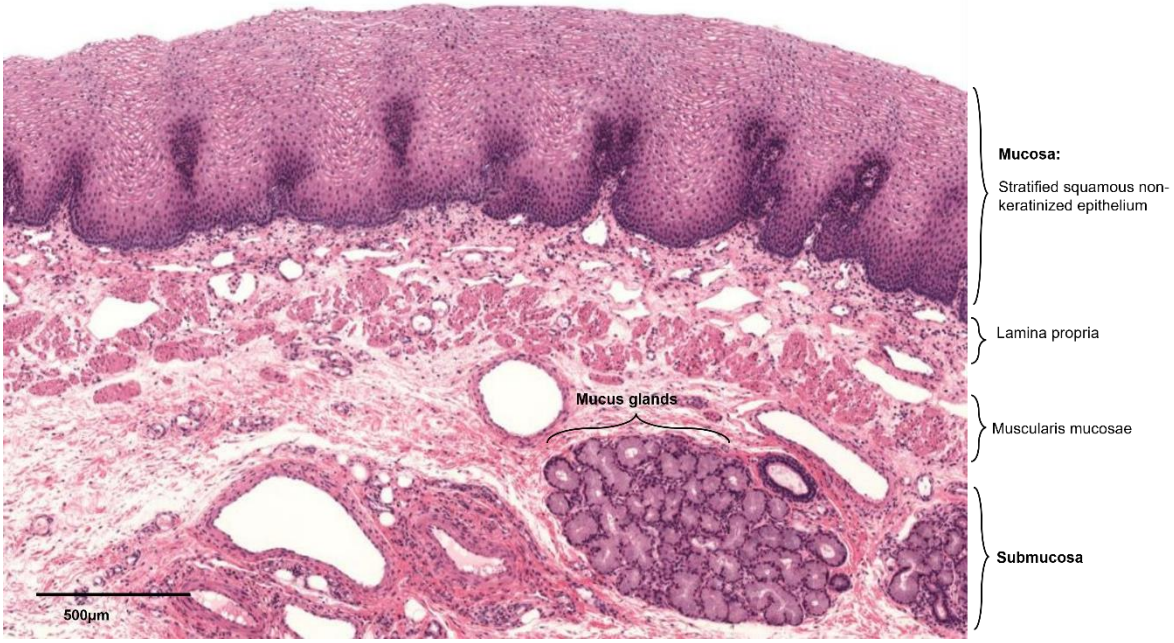

Figure 3 Histology of the oesophageal mucosa and submucosa

Figure taken from the Histology Guide, highlighting the mucosa and submucosa of the normal oesophagus [40] Scale bar represents 500µm.

The cells in the most luminal part of the oesophageal epithelium are the oldest in the epithelial layer and are at varying stages of degeneration. This layer may thus provide some mechanical protection, but gives little protection against H^+ [33]. Besides acid, other noxious components of gastric juice, such as pepsin, can also damage the oesophagus and induce symptoms [40]. Bile acids can disrupt cell function by damaging membrane structure, which in turn alters the integrity of the mucosal barrier [42]. However, while pepsin and bile are important noxious factors which cause mucosal damage, it is difficult to target these components, and treatment remains limited predominantly to acid suppression therapy in the form of PPIs [17].

Several studies have highlighted the loss of mucosal barrier function in patients with GORD as a potential peripheral mechanism underlying oesophageal hypersensitivity to reflux (see section 1.4 Peripheral pathways of pain sensation in the oesophagus). Impairment of oesophageal mucosal integrity can even be seen in macroscopically normal tissue, apparent in the histologic finding of so-called dilated intercellular spaces (DIS): a widely accepted morphologic model of GORD pathophysiology. This model describes the increased space between neighbouring epithelial cells in the oesophageal mucosa which has been suggested to result in a more 'leaky' epithelium facilitating the easy passage of noxious refluxate [42]. The constituents of the refluxate including H^+ are therefore proposed to be able to reach nerve endings in the deeper oesophageal mucosa and submucosa and stimulate acid-sensitive receptors more easily, as demonstrated in Figure 4 [17].

DIS has been suggested to be initially caused by an increase in permeability to Cl^- which is closely followed by water which osmotically flows through the epithelium, filling intercellular spaces and causing dilation [43]. This ultrastructural change is sometimes also accompanied by functional changes in the epithelium. *In vitro* Ussing chamber studies in our group have previously shown a decrease in transepithelial electrical resistance (TER) in human oesophageal biopsies upon exposure to acid solutions, suggesting that patients with heartburn in the absence of mucosal damage have mucosal vulnerability to acid [45]. Continuous measurement of TER as a functional marker of mucosal integrity gives a dynamic measurement of changes in integrity in response to acid exposure over time, unlike DIS which is a static, all-or-nothing measurement [44]. Although PPI treatment has been reported to

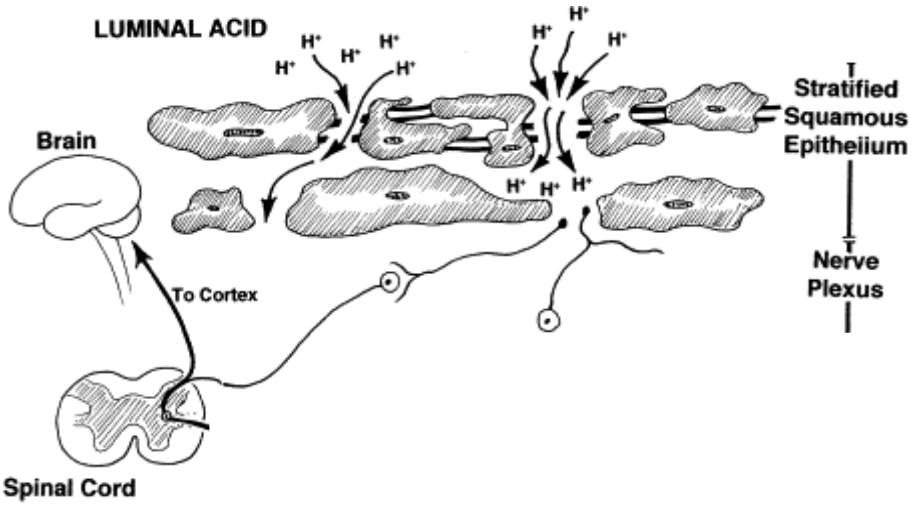

Figure 4: Impaired oesophageal mucosal integrity in GORD [39]

This schematic representation of the oesophageal mucosa shows defects in the intercellular junctional complex between epithelial cells at the lumen of the stratified squamous epithelium. This allows passage of gastric acid into the intercellular space, causing dilation and subsequent DIS. Within this space, acid encounters nerve fibres which become activated and transmit signals to the brain via the spinal cord, inducing heartburn.

improve DIS, its occurrence in both health, and non-reflux disorders like eosinophilic oesophagitis alludes to the possibility of DIS being a non-specific response to epithelial injury, rather than a mechanism of reflux symptom generation [45], [46].

In line with the association between increased epithelial permeability and GORD pathophysiology, animal studies have described the dysregulation of claudin-dominated tight junction and e-cadherin-dominated adherens junctions [47], [48]. A study investigating the molecular mechanisms for the acid-induced increase in paracellular permeability found an association between increased fluorescein flux and reduced TER with the cleavage of the adherens junction protein e-cadherin [49]. Western blot analysis revealed the presence of the C-terminal fragment of e-cadherin, and immunostaining highlighted A disintegrin And Metalloproteinase (ADAM-10) as the metalloproteinase responsible for the cleavage [49]. Moreover, a rat model of erosive reflux disease identified interleukin-6 as the mediator for defective desmosomes and hence cell-cell contacts [48]. Thus, the molecular mechanisms underlying defects in barrier function involve changes in the structure and function of adhesion molecules at the oesophageal epithelial surface.

The integrity of the oesophageal epithelial barrier has paramount importance in protection against gastric reflux-induced symptoms. When gastric juice enters the oesophagus, several protective factors help to clear the refluxate to protect the mucosa. It is the breakdown of these factors that promotes the onset of reflux disease. However, heartburn symptoms can also occur in individuals with a normal reflux burden, possibly when there is poor epithelial resistance and increased visceral sensitivity [17]. Recent studies suggest that oesophageal hypersensitivity contributes to symptom perception in patients with physiological levels of acid. Taken together, the pathogenesis of reflux disease is undoubtedly very complex, and determined by interactions among multiple aggressive and defensive factors. A deeper characterisation of the sensory mechanisms which determine the relationship between reflux exposure and symptom generation is fundamental to an improved understanding of GORD pathophysiology.

1.2 Diagnostic evaluation of GORD

While the relationship between reflux episodes and symptom generation is incompletely understood and varies, there are clinical tests in place to aid the diagnostic evaluation of patients presenting with heartburn. GORD can be divided into several phenotypes based upon the severity of oesophageal mucosal damage, the severity of oesophageal acid exposure, and the association of reflux events with symptom manifestation (Figure 5) [51]. Accurate phenotyping can be done by endoscopy, and by ambulatory reflux monitoring. Endoscopy distinguishes erosive reflux disease (ERD) and Barrett's oesophagus (BO), while 96-hour pH impedance monitoring enables objective assessment of gastro-oesophageal reflux (usually only required in patients with normal endoscopic appearances). The severity of reflux assessed with a 96-hour pH measurement often correlates with the severity of mucosal damage, as patients with oesophagitis usually have higher total oesophageal acid exposure than patients without macroscopic lesions [52]. However, there is important variability within this, as patients with similar levels of acid exposure can sometimes exhibit very different macroscopic appearances.

In patients with macroscopic damage and inflammation (ERD), the cause of symptoms is relatively easy to understand. However, in 70% of GORD patients, the macroscopic appearance of the oesophagus is normal, with no obvious erosion (non-erosive reflux disease, NERD) [53]. Importantly, NERD can only be diagnosed when there are no abnormalities at endoscopy, and when the 96-hour pH monitoring provides objective evidence for pathological acid exposure being responsible for patients' symptoms [51]. Studies have also identified patients with oesophageal acid exposure within physiological limits, but with a clear association between reflux events and heartburn perception [54], [55]. These patients are also considered to have GORD, and are categorised as having a hypersensitive oesophagus according to Rome IV criteria [53]. Moreover, some patients experience a lot of heartburn that does not appear to be associated with gastro-oesophageal reflux and are classified as functional heartburn (FH). Conversely, patients with Barrett's oesophagus often do not present with heartburn despite having had years of high acid reflux levels, suggesting oesophageal hyposensitivity (Figure 5).

1.2.1 Oesophageal Sensitivity of GORD

Differences in oesophageal sensitivity significantly affect symptom presentation during reflux episodes [54]. Increased sensitivity to gastrointestinal reflux has been implied in NERD patients who are refractory to acid suppression therapy. Bernstein acid perfusion studies demonstrated a heightened sensitivity to oesophageal acid perfusion in patients with NERD

and ERD compared to healthy controls [56], [57]. NERD patients are suggested to be more sensitive than their erosive counterparts, showing hypersensitivity to saline infusion in some cases [58], [59].

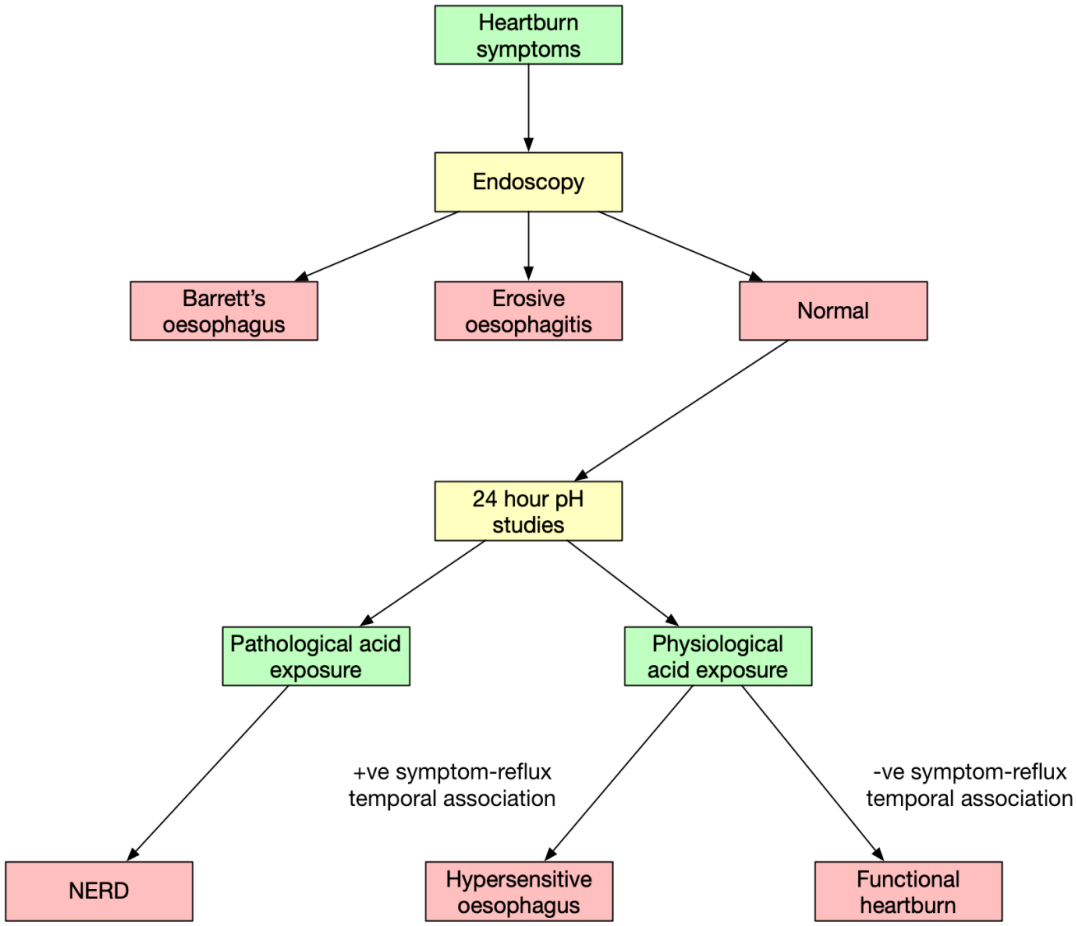

Figure 5: Subgroups of GORD based on the severity of the oesophageal mucosal damage, the severity of the oesophageal acid exposure, and the relation between reflux events and symptoms

Patients with macroscopic damage and inflammation at endoscopy are diagnosed as erosive oesophagitis or erosive reflux disease (ERD). In 70% GORD patients, the endoscopy is negative, with no obvious erosion but pathological acid exposure; these patients are classified as non-erosive reflux disease (NERD). A proportion of patients experience painful perception to a normal level of reflux (hypersensitive oesophagus). Some patients have high levels of heartburn but no association with acid reflux (functional heartburn, FH). Patients with Barrett's oesophagus (BO) sometimes do not present with heartburn despite having the highest acid exposure.

In contrast to this hypersensitive NERD group, patients with Barrett's have been suggested to be much less sensitive to oesophageal acid perfusion, reporting relatively mild reflux symptoms or being fully asymptomatic [51]. Acid perfusion tests in BO patients showed patients to be less sensitive to the perfused acid solution compared to other GORD phenotypes [60]. However, these findings are not universal. BO patients were reported to be

hyposensitive to mechanical, thermal, and electrical pain stimuli in a study which recorded the stimulation intensity and evoked brain potentials from both the normal and metaplastic part of the BO [61]. Another study by the same group detected hyposensitivity in BO patients to mechanical, thermal and electrical stimulation, but hypersensitivity to acid stimuli in these same patients [62]. This finding of acid hypersensitivity correlates with the finding of decreased mucosal baseline impedance in BO compared to healthy controls, but also sheds light to the apparent existence of symptomatic and asymptomatic subgroups within BO [62]. The analysis of the association between noxious gastric acid with GORD lesions suggest that the presence and severity of ERD is dependent predominantly on acid reflux, while there is a suggestion that both bile and acid exposure influence development of BO [63], [64]. Moreover, the mechanism underlying hyposensitivity to acid exposure in BO remains unclear. The multi-layered epithelium, comprised of both squamous and columnar cells and thus thickened mucosa, may partially explain the reduced symptom severity seen in BO patients [65]. Figure 6 summarises the current general understanding of oesophageal sensitivity among GORD phenotypes [51]. These observations support the role of oesophageal sensitivity in determining GORD symptoms and suggest that the mechanism of reflux among phenotypes may represent different ends of a spectrum rather than distinct pathophysiological mechanisms [10], [55].

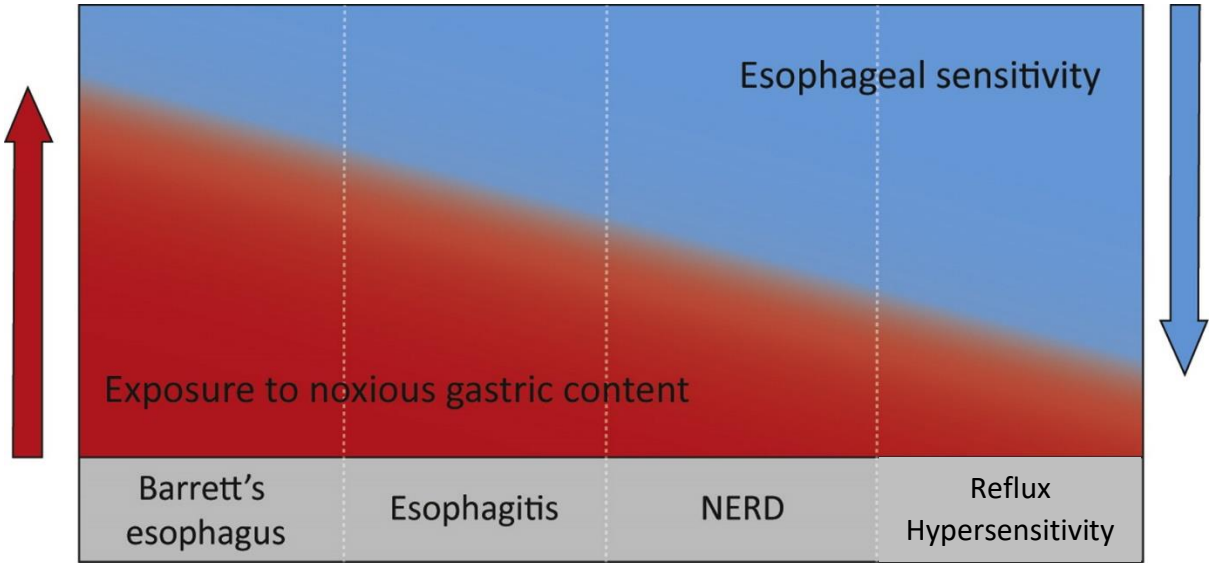

Figure 6: A representation of the association of oesophageal sensitivity with different GORD phenotypes.

A spectrum of oesophageal sensitivity among GORD phenotypes, with reflux hypersensitivity patients on one end of the spectrum having heightened sensitivity to normal levels of acid exposure, and hyposensitivity in BO with much higher exposure to noxious gastric content at the other end. *(Figure adapted from [22])*

1.3 Central pathways of pain sensation in the oesophagus

Oesophageal sensation is regulated by the strength of sensory receptor activation in the GIT, and the processing in the central nervous system (CNS) which often leads to the amplification or suppression of the afferent signal that gets transmitted to the cortical regions causing perception [66]. Peripheral and central mechanisms both play a role in the pathogenesis of oesophageal hypersensitivity by increasing signal transmission following stimuli [66]. Central mechanisms are signals that alter the sensitivity of dorsal horn neurons in the spinal cord and high centres which process incoming (afferent) signals from the oesophagus [17]. These central processes can involve the amplification of the incoming signal, as well as a lack of inhibition by descending pathways. Factors such as stress and anxiety affect these central mechanisms and control the downstream regulation of the signal [54]. Most GORD patients report that increased stress aggravates their symptoms [67]. A study which assessed emotional and perceptual responses to intraoesophageal acid during auditory stress stimuli in ERD and NERD patients demonstrated how acute auditory stress can augment heartburn symptoms in GORD patients [68]. The study found a significant reduction in the lag time to initial symptom perception, increased intensity, and increased sensitivity during the stress period in both patient groups compared to healthy controls, which was associated with higher emotional responses to the stress stimulus [68]. More recent studies have suggested that oesophageal hypervigilance, a psychological process that results in the increased awareness and amplification of oesophageal symptoms and sensations, is positively associated with increased symptom severity, irrespective of acid burden [69], [70]. A retrospective study on a cohort of patients with reflux symptoms who underwent 96-hour pH monitoring and were stratified into groups based on positive acid exposure time demonstrated that hypervigilance significantly predicted symptom severity [69]. This suggests that hypervigilance results in a systemic stress response via activation of the sympathetic nervous system, and thus represents an independent factor contributing to the onset and maintenance of oesophageal symptom perception [71].

Psychosocial comorbidities have also been found to determine the severity of symptoms. Sleep deprivation was shown to be hyperalgesic in a study which measured sensitivity to acid perfusion after sleep deprivation compared with a good night's sleep. Healthy control subjects showed no differences in stimulus response between good sleep and sleep deprivation, whereas GORD patients showed a significant rise in the intensity rating and acid perfusion sensitivity score in the symptom report [72]. In a prospective study which assessed anxiety and depression levels in patients with FH and hypersensitivity, increased levels of anxiety were associated with more severe heartburn and reduced quality of life [73]. The impact of

sleep deprivation, anxiety, and depression on increasing sensitization in the oesophagus can be said to reflect the decreased activity of anti-nociceptive pathways which normally prevent afferent painful stimuli from reaching the GIT [66], [74].

While the GIT possesses intrinsic neural plexuses that allow a degree of autonomy over gastrointestinal (GI) functions including digestion and nutrient absorption, the CNS provides extrinsic neural outputs which control and modify these functions [76]. The sympathetic nervous system primarily exerts an inhibitory effect on gastrointestinal muscle and regulates blood flow via splanchnic efferents [66]. In contrast, the parasympathetic nervous system exerts both excitatory and inhibitory control over GI motility, implying a more complex influence over GI functions [76]. The vagus nerve is a major component of the parasympathetic nervous system and facilitates brain and GIT communication [77]. In humans, a high percentage of the LOS tone is due to cholinergic vagal efferent innervation [78]. In a study which retrogradely labelled sensory cell bodies by fast blue injection into striated and smooth muscle of the cat oesophagus and LOS, more vagal afferent fibres were labelled than spinal afferents [79]. Moreover, proximal stomach distension during LOS relaxation is known to stimulate IGLEs which project to the dorsal motor nuclei of the vagus, suggesting that the swallow induced relaxation of the LOS is modulated by the dorsal motor nucleus of the vagus nerve [80]. Sensory information from the oesophagus is conveyed from the GIT to the CNS via two important and distinct afferent pathways [81]. Action potentials generated by noxious stimuli in the oesophageal mucosa are transmitted to the CNS via either vagal or spinal afferent nerves (Figure 7) [82]. Cell bodies of the vagal afferent neurons reside in jugular or nodose ganglia and vagal afferent fibres innervate all layers of the oesophageal wall except the distal oesophagus [83]. Vagal nerve density is highest in the upper cervical region of the oesophagus and decreases in distal regions in rats [84]. Vagal afferents connect to central pathways through their axons which project to the solitary tract nucleus in the brainstem [82]. In contrast, cell bodies of spinal afferents are in the cervical and thoracic dorsal root ganglia, with central endings in the spinal dorsal horn [83]. Spinal afferent innervation extends from the cervical to the spinal cord's upper lumbar segment through thoracic spinal nerves and splanchnic nerves [85]. Their nerve endings reach the lamina propria and the epithelial layer of the oesophagus. Calcitonin gene-related protein (CGRP) stains for both spinal afferent and vagal afferent nerves in the oesophagus, revealing a fine network of nerve fibres in the mucosa [86], [87].

Acid has been shown to be a potent stimulator of primary afferent neurons [88]. There are two types of proton-gated inward currents in DRG neurons. The first is a fast, rapidly inactivating current carried by Na^+ which is highly sensitive to protons seen in most DRG neurons where the threshold activation can occur at pH7 [89]The second is a slow, non-desensitising current

carried by Na^+, Ca^{2+}, and K^+ which is less sensitive to H^+ and activated only at pH levels below 6.2 [90], [91]. While the fast and highly proton-sensitive current resembles that carried by acid-sensing ion channels (ASICs), the second and slower current resembles the acid-evoked current carried by the transient receptor potential channel of vanilloid type 1 (TRPV1), and is only seen in neurons activated by capsaicin [92], [93]. Acid-induced activation of sensory neurons in the GIT evokes two systemic responses: the local release of neuropeptides such as CGRP from the peripheral axons in the tissue, and pain sensation [94].

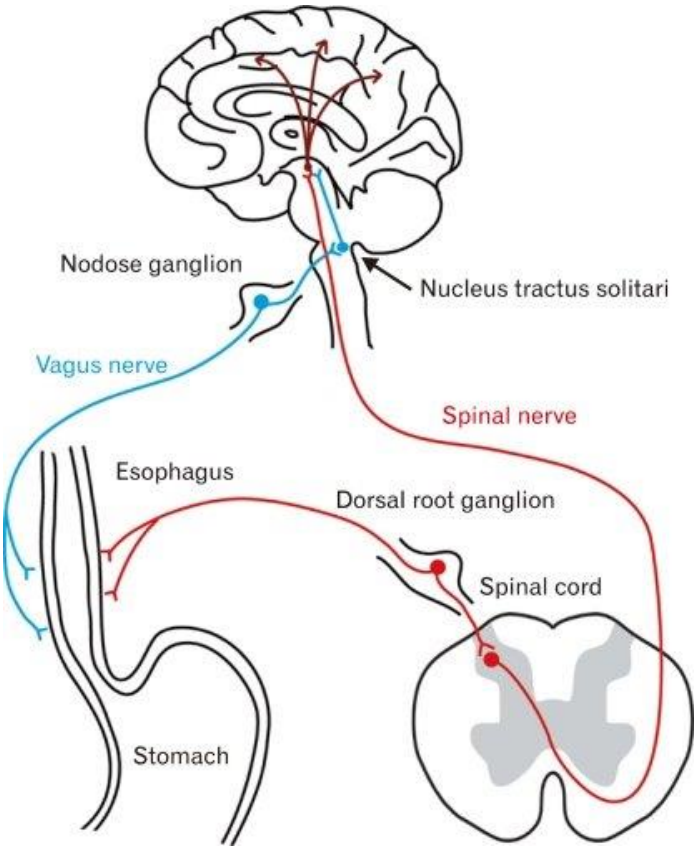

Figure 7: **The two major afferent sensory pathways (vagal and spinal) from the oesophagus to the brain.**

In the vagal pathway, noxious information gets transmitted to the nucleus tractus solitarius through the nodose ganglia. In the spinal nerve pathway, the AP is transmitted to the dorsal horn of the spinal cord via the DRG, and then gets transmitted to the thalamus of the brain [81].

The process whereby primary afferent nerve fibres of the somatosensory system detect noxious stimuli is called ‘nociception’ [95]. Noxious stimuli including chemical (acid-induced heartburn), mechanical (balloon distention), and thermal (cold and hot fluid-induced chest pain) stimulation of the oesophageal mucosa activate nociceptive (pain-sensing) receptors on peripheral nerve endings to generate action potentials (AP) [96]. Sensitisation of these oesophageal afferent fibres is thought to occur following acid-induced inflammation as

nocifensive mechanisms to prevent tissue damage leads to visceral hypersensitivity [97], [98]. However, symptom severity does not always correlate with the degree of macroscopic inflammation, so the management of reflux pain with acid suppression is not always sufficient [81].

Repetitive generation of APs within the oesophageal mucosa also activates intracellular signalling mechanisms in neurons of the spinal dorsal horn as seen in Figure 8, leading to central sensitisation. This results in an amplified response to noxious stimuli, and subsequent hyperalgesia [99]. The presynaptic release of neurotransmitters such as substance-P (SP), glutamate and brain-derived neurotrophic factor (BDNF) triggers intracellular calcium signalling upon binding their respective receptors [100]. There is an increased level of intracellular calcium and subsequent calcium-dependent activation of protein kinases A and C. Activated protein kinases then phosphorylate *N*-methyl-D-aspartate (NMDA) receptors which induces a change in receptor kinetics, decreasing the voltage-dependence of the magnesium block. As a result, the responsiveness to glutamate is increased [101].

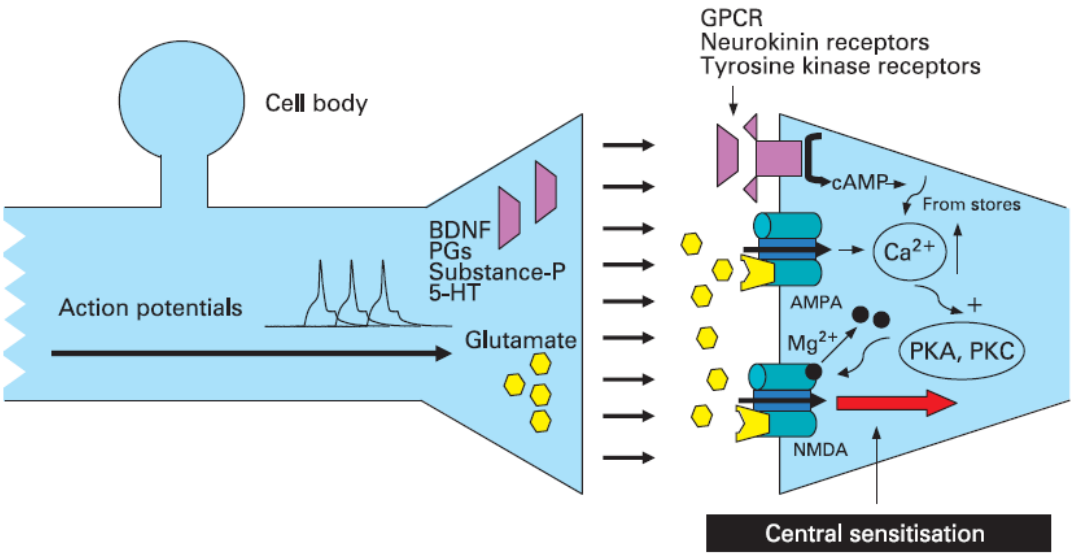

Figure 8: Molecular mechanisms of central sensitisation [63]

Incoming APs induce the release of neurotransmitters (BDNF, SP, 5-HT, PG) and neuromodulators which act via G-protein-coupled receptors and ligand-gated ion channels. Subsequent intracellular increase of calcium and activation of protein kinases A and C causes phosphorylation of NMDA receptors which reduces the voltage-dependence of the magnesium block. This induces a response to glutamate and eventual central sensitisation in the neuron and those adjacent to it (secondary hyperalgesia).

In addition to the intracellular effects, central sensitisation also activates adjacent spinal neurons through previously silent nociceptors, leading to hypersensitivity in somatic and

visceral areas [65]. This mechanism is known as secondary hyperalgesia. Studies investigating the association between responses of vagal afferents innervating the oesophagus and brainstem neurons after acute infusion of acid and pepsin in cat oesophagus have shown central sensitisation following noxious stimulation [102], [103]. Infusion of acid and pepsin into the cat oesophagus significantly increased AP firing rate indicating that brainstem neurons, recorded extracellularly by making an incision into the cisterna magna to expose the caudal brainstem, undergo central sensitisation [103]. Furthermore, the role of NMDA receptors in central sensitisation was confirmed in another cat model which showed the upregulation of the NR1 subunit of the NMDA receptor in the thoracic DRG and nodose ganglia as a result of long-term acid infusion into the oesophagus [104]. Patients with heartburn symptoms report longer periods of visceral pain hypersensitivity compared to healthy volunteers upon acid infusion into the oesophagus suggesting the contribution of central sensitisation to enhance sensory transfer in visceral pain disorders [105]. For example, the prostaglandin E2 receptor-1 (PGE_2) antagonist ZD6416 attenuates secondary hyperalgesia in a randomized, placebo-controlled crossover study suggesting that prostaglandin E2 contributes to visceral hypersensitivity [106]. PGE_2 levels increase following inflammation in both the inflamed tissue and the spinal cord, where it facilitates neurotransmitter release from the central terminals of nociceptors [107]. Moreover, PGE_2 can increase neuronal excitability by inducing depolarisation of the membrane of dorsal horn neurons through the activation of a nonselective cation channel, as seen in Figure 8 [108]. Another randomized, placebo-controlled study investigated the role of NMDA in the modulation of visceral hypersensitivity. The NMDA receptor, located within dorsal horn neurons in the spinal cord, prevented and reversed the induction of oesophageal hypersensitivity by acid when blocked by its antagonist ketamine [109]. These findings collectively reinforce the role of central sensitisation as a mechanism of visceral pain hypersensitivity following noxious stimulation in the oesophageal mucosa [65].

1.4 Peripheral pathways of pain sensation in the oesophagus

Several hypotheses have been proposed to explain the mechanism of visceral hypersensitivity in the oesophagus [99]. Peripheral sensitisation of afferent nerves in the GIT also plays a key role in the pathogenesis of pain sensation [66]. To understand the underlying molecular peripheral sensitisation pathways, it is important to first describe the functional anatomy of the afferent peripheral innervation.

The GIT is unique compared to other peripheral organs in having its own intrinsic nervous system named the enteric nervous system (ENS) [110]. The GIT is innervated by both intrinsic enteric neurons located within the GIT wall, and extrinsic afferent and efferent neurons. Although the ENS can control GI functions such as motility, local blood flow and transmucosal movement of fluids separately from the CNS, it is not completely autonomous as there is bidirectional flow between the two nervous systems [111]. The ENS is composed of aggregations of nerve cells, two major layers of ganglia named the myenteric and submucosal plexuses, and neural connections between these ganglia [112]. The myenteric plexus resides between the circular and longitudinal muscle layers of the GIT, where it regulates the contraction and relaxation of these muscle layers [109]. In the oesophageal body, motility is controlled and modulated by both the ENS and CNS together. However, damaged vagal nerve endings in the proximal oesophagus prevented food propulsion, suggesting that the CNS provides the primary control of proximal oesophageal motility [114].

The extrinsic afferent innervation of the oesophagus is predominantly via vagal afferent nerve endings known as IGLEs. A study in the guinea-pig oesophagus investigated whether IGLEs are chemically activated by neurotransmitters or via mechano-gated ion channels. In this study, extracellular recordings were performed from mechanically sensitive vagal afferent branches, and demonstrated that chemical transmission is not involved [115]. Thus, IGLEs directly respond to mechanical stimuli via low intensity stretch-activated ion channels, and are distributed homogenously along the length of the oesophagus in animal models [14]. Other types of vagal afferent endings include intramuscular arrays (IMAs) which are specialised terminal structures with parent axon branches innervating circular and longitudinal muscle layers [116]. In smooth muscle layers, IMA endings create a distinct pattern of parallel elements known as the interstitial cells of Cajal (ICCs) which mediate the communication between the autonomic nervous system and smooth muscle [117].

Vagal afferent nerves innervate the whole GIT except the distal colon [66]. Sensory information from the distal colon is transmitted to the spinal cord through the lumbar splanchnic nerves (LSN) and sacral pelvic nerves (SPN) as demonstrated in retrogradely labelled colonic

sensory rat neurons which functionally express 5-HT_3 receptors on their peripheral ends [119]. The response of these mechanosensitive afferent nerves from the LSN and SPN to mechanical stimuli in the form of probing, circular stretch, and mucosal stretching was electrically recorded using an *in vitro* preparation from a mouse colon. This identified five classes of afferent nerves, each of which responded to different mechanical stimuli. The five categories of sensory afferent fibres were defined by the location of their mechanoreceptive field: mucosal, muscular (tension receptor), muscular-mucosal, serosal, and mesenteric afferents [120]. Thus, the mechanosensory properties of afferent neurons are diverse, and comparable to those which innervate the skin [121]. In the oesophagus, afferent fibres which terminate in the muscle layers respond to intraluminal distention and are thus known as tension-sensitive afferent fibres. They are mostly unmyelinated C-fibres or thinly myelinated Aδ-fibres carried in both the vagus and the spinal nerves [122].

Spinal afferent fibres are equally important in pain perception because spinal nociceptors have a wide dynamic range which makes them capable of transmitting high intensity pain [111]. Two subtypes of afferent fibres have been described in cat oesophagus: 1. isolated bundles of fibres in myenteric connectives, and 2. fibres within the myenteric ganglia [123]. A study that selectively labelled spinal primary afferent fibres in the cat GOJ found labelled fibres in the squamous oesophageal epithelium, suggesting a local mechanosensory and nociceptive role via release of neurotransmitters such as SP and CGRP that act on myenteric neurons [124]. These tension-sensitive fibres have also shown sensitivity to chemical stimuli; 15-30% of muscle afferents in animal models displayed excitation to intraluminal acid perfusion [103], [125], [126]. While pepsin infusion alone did not change the resting firing of afferent fibres, there was increased firing in response to acute acid and pepsin exposure in the cat oesophagus [127]. An electrophysiological study in human visceral afferents demonstrated sensitivity of serosal afferents to key algesic mediators including bradykinin and Adenosine Triphosphate (ATP), while muscular afferents were largely insensitive to chemical stimuli [128]. In contrast, muscle afferents in mice were not excited by HCl, but responded to chemical mediators such as 5-HT and agents like capsaicin when applied to the mucosal surface [129]. Thus, spinal afferents are distributed evenly throughout the oesophagus, and consist mainly of Aδ fibres and unmyelinated C-fibres which are normally silent but may become activated by chemical and noxious stimuli [130].

Studies investigating the peripheral nervous system have highlighted the molecular events underlying peripheral sensitisation of these afferent neurons (Figure 9) [66]. Excessive noxious stimulation and eventual tissue damage leads to the release of inflammatory mediators such as histamine, bradykinin, ATP, and prostaglandins which reduce the transduction threshold of nociceptors (Aδ fibres and unmyelinated C-fibres) and increase the

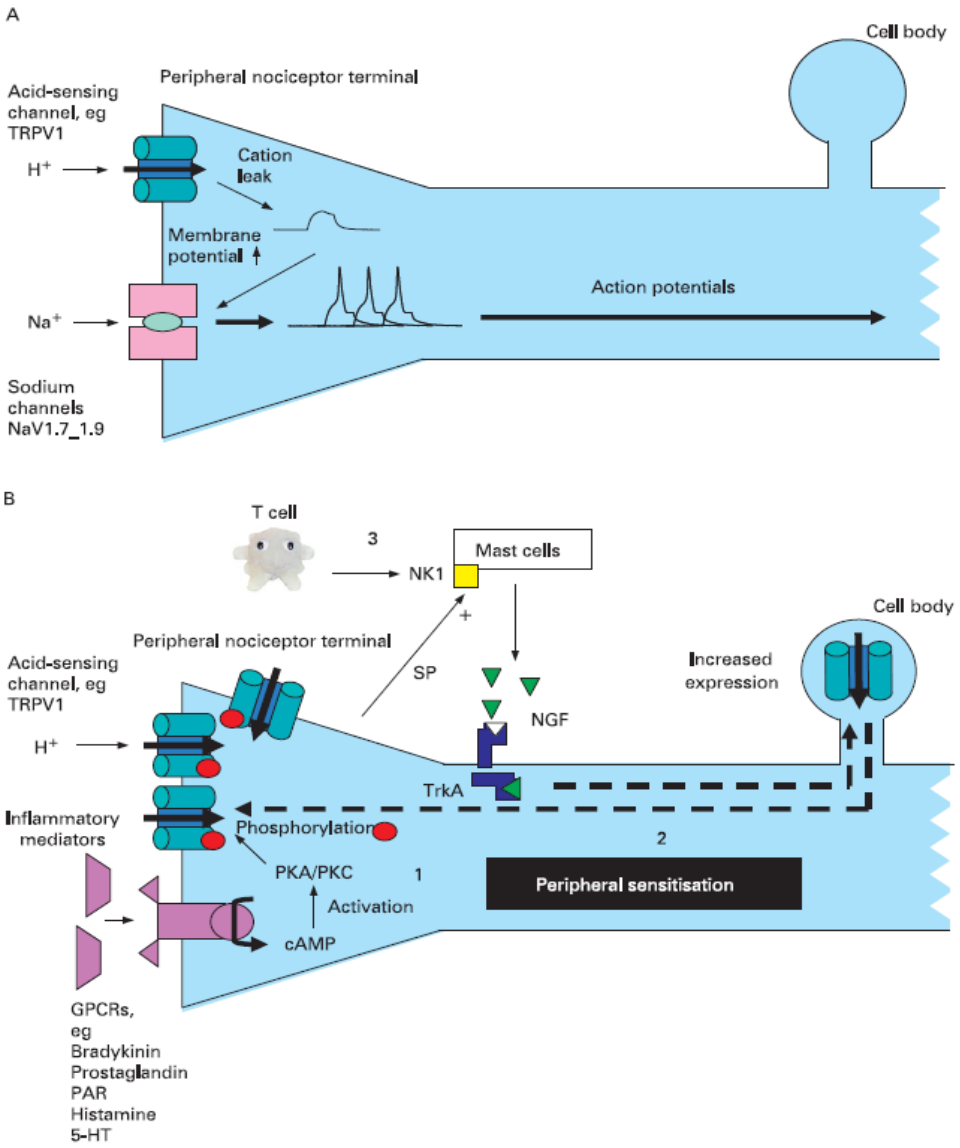

Figure 9: Molecular mechanisms of peripheral sensitisation [66]

A) A common pathway to an AP generation in nociceptors when exposed to acid. Cations leak from ion channels, leading to a less negative membrane potential which activates sodium channels and subsequent axonal firing. B) 3 mechanisms of peripheral sensitisation upon exposure to noxious stimuli such as inflammatory mediators. 1: G-protein-coupled receptor releases cAMP upon activation by inflammatory mediator, subsequent phosphorylation of ion channels which reduces its transduction threshold. 2: Upregulation of ion channel expression in response to NGF, subsequent transport to the cell body and finally to the nerve terminals. 3: Neuroimmune interactions; SP release by nociceptor activates mast cells to release NGF, leading to a bidirectional cycle.

magnitude of response (Figure 9b) [131]. *In vitro* single-fibre recordings of propagated APs from cutaneous sensory nerve endings in the mouse skin revealed two classes of nociceptor activated by noxious stimuli [132]. Nociceptors can be subcategorised based on their receptor expression and cell content [133]. Analysis of sensory neurons in gene-targeted mice showed that 70-80% DRG neurons contain neuropeptides such as SP and/or CGRP and are hence named ‘peptidergic’. These peptide nerves are further defined by the expression of the nerve

growth factor receptor trkA [134]. The second subpopulation of nerves express the phospholipid label isolectin-B4 (IB4), and are further defined by the expression of RET, the receptor for glial cell line-derived neurotrophic factor (GDNF) [134].

Importantly, a more recently established route to hyperalgesia includes the activation of sodium channels NaV1.7-1.9 on nociceptors. This is when inflammatory mediators such as H^+ induce a leakage of cations, causing the resting potential at the peripheral nerve terminal to become less negative [135]. In Nav1.8-null mice, there was normal nociception in response to acute noxious stimulation by intracolonic saline stimulation, but blunted pain and no hyperalgesia in response to intracolonic capsaicin and mustard oil [136]. Taken together, these findings highlight an important role for sodium channels in inducing spontaneous activity in sensitised nociceptors (Figure 9a). The increased expression of receptors which play a role in the sensation of reflux could be another important peripheral mechanism underlying oesophageal hypersensitivity [17].

1.5 Ion channels in pain sensation

Increasing evidence from molecular biology studies demonstrate the ability of primary afferent neurons expressing various membrane-bound receptors/channels capable of responding to thermal, mechanical, and chemical stimuli [137]. Voltage-gated ion channels are one of the most studied class of cell surface proteins expressed on sensory neurons and have a key role in determining neuronal excitability and sensory transduction [138]. Studies which have investigated ion channels in nociception and hypersensitivity over the last 20 years have shown that changes in expression, biophysical properties, and distribution of ion channels underlies aberrant afferent activity in preclinical neuropathic models of pain [133], [139].

Ion channels are multimeric proteins which reside in the plasma membrane of excitable cells such as neurons and form a passageway from one side of the membrane to the other [140], [141]. As shown in Figure 9, some ion channels can directly induce transduction (TRP channels), while others (like NaV1.8) act indirectly. These ion channels are expressed throughout the GIT, and human biopsies from patients with functional GIT disorders such as irritable bowel syndrome (IBS) revealed altered expression of various types of ion channels including: 5-HT_3 receptor, P2X receptors, transient receptor potential (TRP) channels, and acid-sensing ion channels (ASICs) [142].

Briefly, 5-HT is a vital paracrine signalling molecule in the brain-gut axis, with the GIT storing over 80% of the total body 5-HT and its receptor. While most serotonin receptors belong to the family of G protein-coupled receptors (GPCRs), the 5-HT_3 receptor is the only ligand-gated ion channel. When serotonin binds the 5-HT_3 receptor, its ion-conducting pore opens and enables cations to flow into the neuron leading to an excitatory response [143]. The 5-HT_3 receptor antagonist Alosetron significantly reduced pain perception induced by colonic distension in IBS patients, suggesting a pathogenic role of 5-HT_3 in IBS [144]. P2X ($P2X_1$-$P2X_7$) purinoreceptors are another type of ligand-gated cation channel that open when their ligand, extracellular ATP is bound [145]. In a rat model, chronic oesophageal acid exposure was found to increase P2X3 protein expression in the DRG [146], while in the inflamed human bowel, peripheral P2X receptor expression was increased in the subepithelial layer [147].

In contrast, TRP channels are activated by the generation of a transient depolarisation in response to an influx of cations into the cell and are expressed by both vagal and spinal afferents throughout the GIT of animal models and humans [148]. In a chronic rat reflux model, TRPV1 expression was increased in response to acid exposure, and ulceration was reduced with TRVP1 antagonists [149]. Of further relevance to acid-related disorders are acid-sensing ion channels (ASIC1-3) which belong to the voltage-insensitive, amiloride-sensitive epithelial

Na^+ channel family of cation channels [66]. The changes in transgenic animal responses to mucosal acid exposure [150], and the upregulation of ASICs with inflammation in the GIT suggest a nociceptive role of ASIC channels in the GIT [151]. As the most commonly studied ion channels in oesophageal hypersensitivity, TRP and ASIC channels will be the focus for the remainder of this section.

1.5.1 Transient receptor potential (TRP) channels

TRP channels are one of the most promising receptor superfamily of ion channel targets for visceral hypersensitivity. These nonselective cation channels are diverse, with varied physiological functions ranging from thermo-sensation to magnesium and iron transport [152]. In mammals, TRP channels are subclassified into 6 groups: TRP channel subfamily V (vanilloid; TRPV), TRP channel subfamily A (ankyrin; TRPA), TRP channel subfamily C (canonical; TRPC), TRP channel subfamily M (melastatin; TRPM), TRP channel polycystin subfamily (TRPP), and TRP channel mucolipin subfamily (TRPML) [153]. The latter two TRP channels were named after the diseases they are associated with; TRPP for polycystic kidney disease, and TRPML for mucolipidosis. The TRPM1, the first member of the TRPM subfamily to be found, was identified through comparative gene analyses of benign and malignant melanoma [154]. TRPA1, the only member of the TRPA channel subgroup was so named because of its high number of ankyrin repeats at the amino terminus of the protein. The TRPV group was identified as a result of expression cloning of TRPV1- the receptor for the vanilloid irritant capsaicin [155].

There is little structural similarity among TRP channel subfamilies, as seen in Figure 10 [148]. Most TRP channels comprise of 6 putative transmembrane domains, and large intracellular amino and carboxyl termini at either end [156], [157]. It is these terminal domains which contain very different motifs (Figure 10). Like other 6 transmembrane (TM) pore-forming channel proteins, functional TRP channels assemble to form cation-permeable pores [158]. Unsurprisingly, these channels have functional, as well as structural versatility. While most TRP family members are non-selective calcium channels, there are exceptions like TRPV5 and TRPV6 which are Ca^{2+}-selective, and TRPM4 and TRPM5 which are Na^+ selective [153]. Most TRP channels are suggested to function downstream of GPCRs as shown in Figure 9b. Agonist binding to its membrane receptor that is distinct from the TRP channel activates phospholipase C, inducing downstream secondary messengers such as diacylglycerol which lead to TRP channel activation and eventual Ca^{2+} influx [159]. The most important candidate

TRP channel receptors involved in sensing reflux in the oesophagus are TRPV1, TRPM8, and TRPA1 and will thus be discussed in further detail in this section.

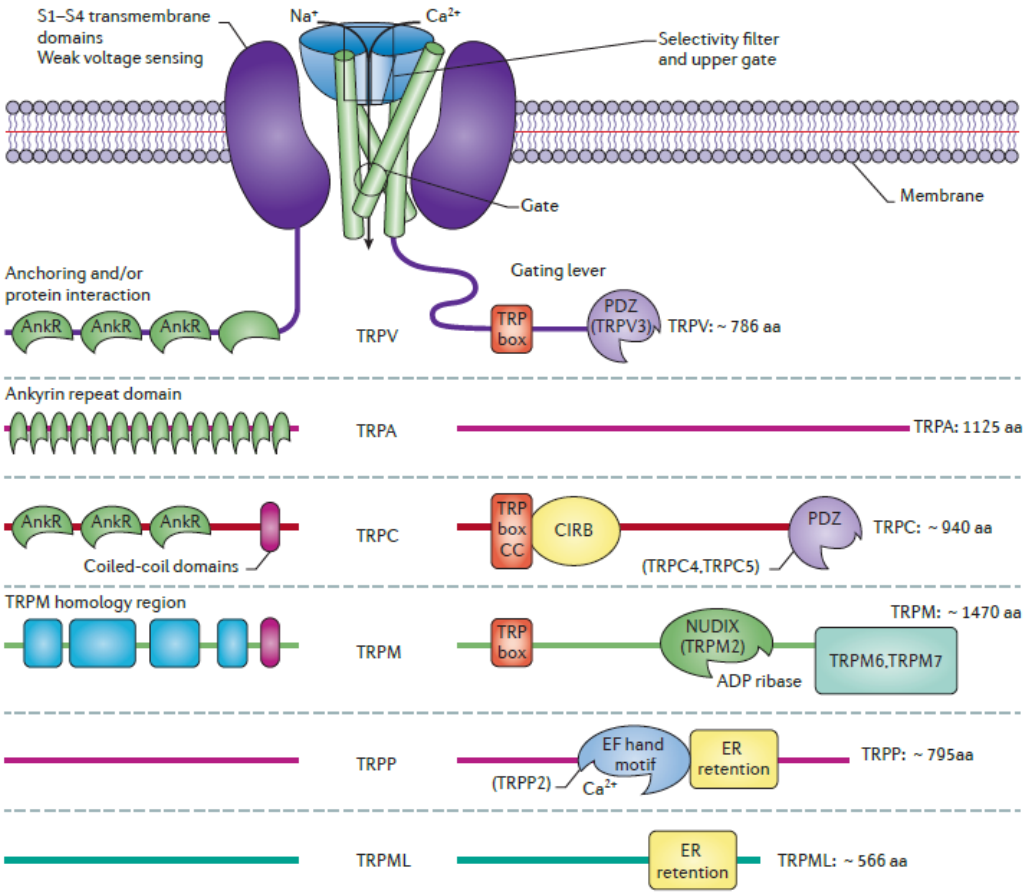

Figure 10: Structural diversity among TRP channel subfamilies [156]

Figure emphasising the diversity of TRP cytoplasmic domains of the 6 TRP channel subfamilies. The selectivity filter is formed by amino acids that dip into the pore loops of the plasma membrane bilayer. The gating comprises the S5-S6 domains. TRPV, TRPA, and TRPC families contain an ankyrin repeat (AnkR) domain in their amino terminal which are absent in other TRP families. The TRP box found in the TRPV, TRPM, and TRPC channels has been suggested to play a role in gating. TRPP and TRPML subfamilies have an endoplasmic reticulum (ER) retention domain that could be due to their functional localisation in intracellular organelles. CC indicates a coiled-coil domain; Numbers on the right indicate range in amino acid length; CIRB, calmodulin/inositol-1,4,5-tris-phosphate (Ins (1,4,5) P_3 receptor binding domain; NUDIX, nucleoside diphosphate-linked moiety X; PDZ, acronym for postsynaptic density protein 95

1.5.2 TRPV1

The TRPV subfamily, notably the vanilloid subfamily member 1 (TRPV1) activated by the vanilloid chilli extract capsaicin, is the most well-known TRP channel for pain [160]. TRPV1 is a non-selective Ca^{2+}-permeant channel which is also activated by noxious heat (>43°C), and endogenous H^+ released during inflammation [155]. The thermal sensitivity of TRPV1 is enhanced by endogenous factors including bradykinin and nerve growth factor which hydrolyse inhibitors via phospholipase C (PLC) and release the inhibition of the channel [161]. TRPV1 activity can be modulated by several intracellular molecules including calmodulin (CaM) which interacts with the C and N terminals of the ion channel and induces desensitisation by cross-linking the termini [162]. Intracellular ATP can suppress the desensitising effect of CaM by competing to bind the overlapping ankyrin repeat domain of TRPV1, thereby augmenting TRPV1 currents [162]. Intracellular phosphatidylinositol-4,5-bisphosphate (PIP_2) is another molecule which can modulate TRPV1 activation. While the consensus for the mechanism of action of PIP_2 on TRPV1 modulation remains paradoxical, there is growing evidence to suggest that PIP_2 sensitises TRPV1 [163]. PIP_2 has been shown to compete with CaM and bind the C terminus of the channel to enhance the TRPV1 current [163]. The dynamic balance of Ca^{2+}-dependent phosphorylation and dephosphorylation is another important modulator of TRPV1 [164]. In mammalian cells, GPCRs catalyse the G protein nucleotide exchange which forms active Gα and Gβγ subunits which then activate phospholipase C (PLCβ), or in the case of tyrosine kinase receptors, they activate PLCγ [165]. PLC hydrolyses the membrane component PIP_2 into soluble messengers including diacylglycerol (DAG) and inositol 1,4,5-triphosphate ($InsP_3$) [166]. The $InsP_3$ then binds its receptor on the endoplasmic reticulum of the cell, releasing intracellular Ca^{2+}. Importantly at resting state, the cytosolic concentration of Ca^{2+} is considerably lower than outside the cell [157]. Thus, the influx of Ca^{2+} into the intracellular compartment of nociceptive neurons reduces the membrane potential to cause depolarisation, generating action potential firing and eventually resulting in pain [167]. While the activation of protein kinase A and C increase TRPV1 channel activity [168], the channel becomes desensitised through the activation of protein phosphatase calcineurin which causes dephosphorylation of the channel [169].

TRPV1 was discovered through a mammalian cell expression cloning method on the basis of capsaicin triggering Ca^{2+} influx into sensory neurons *in vitro* [170]. VR1 is located on chromosome 17p13.3 and encodes a protein receptor of a length of 828 amino acids, 6 TM segments (S1-S6) with a short hydrophobic region between S5 and S6 which forms the pore [165]. There are 3 ankyrin repeats in the N terminal, and a TRP domain in the C terminus as shown in Figure 10. An *in vivo* study in mice disrupted the VR1 gene by deleting an exon

encoding S5 and S6 of the TM domain of the channel. The ability of vanilloid compounds to increase cytosolic Ca^{2+} was assessed in cultured DRG neurons from wild-type (WT) and $VR1^{-/-}$ mice, where capsaicin induced rapid Ca^{2+} increase in the WT neurons, but was completely inactive in the $VR1^{-/-}$ neurons. Similarly, measurements of the membrane current of these neurons after exposure to an acidified solution of pH 5 showed inward currents in 75% of WT neurons, compared with only 7% in $VR1^{-/-}$ neurons. The $VR1^{-/-}$ neurons also exhibited clear deficits in heat-evoked responses, thus demonstrating that sensory neurons in $VR1^{-/-}$ mice were significantly deficient in their response to vanilloid compounds, protons, and noxious heat and supporting a tissue injury-induced role of TRPV1 in acute thermal nociception and hyperalgesia [171].

TRPV1 is expressed on various cell types in both excitable and non-excitable tissues including sensory neurons [172]. Whilst being highly expressed by myelinated (Aδ) and unmyelinated (C) nociceptive fibres of the DRG and trigeminal ganglia, spinal and peripheral nerve terminals and cutaneous sensory nerve fibres, TRPV1 is also expressed by multiple non-neural cell-types like epidermal keratinocytes, and various immune cells including mast cells [173]. TRPV1 is localised on the plasma membrane [172]. TRPV1 expression has been well described in different animal species. The role of TRPV1 expression in primary sensory neurons was investigated in a study which induced pancreatitis in mice by injecting caerulein over a period of 12 hours, with one group of mice receiving the TRPV1-antagonist capsazepine at 4-hour intervals [174]. The study demonstrated endogenous SP release in mice which received repeated caerulein administration, whereas the pharmacological antagonism of TRPV1 significantly suppressed SP release and reduced the severity of pancreatitis, and suggested an important role of TRPV1 expression on sensory neurons in the inflammatory response to tissue injury in pancreatitis [174]. Similarly, TRPV1 expression in primary afferent neurons in the bladder was also found to be critical in cystitis-induced visceral pain in a study which compared the effect of cystitis on bladder function between$TRPV1^{-/-}$ mice and WT mice [175]. Cystitis was only induced in the bladder of WT mice, but not in the knockout mice which also lacked an increase in the mRNA expression of inflammatory mediators nerve growth factor, nitric oxide synthase, and bradykinin [176]. Moreover, TRPV1-positive spinal nerve fibres have been described in each layer of the GIT in mouse, rat, and guinea pig, and these immunoreactive fibres often co-expressed CGRP [177].

Evidence from visceral pain studies in the lower GIT highlight a nociceptive role for TRPV1. In the stomach, an *in vivo* rat study found that noxious mechanical stimulation with gastric distention caused an increase in ERK1/2 phosphorylation (p-ERK1/2) in small-diameter neurons [178]. In a previous study, p-ERK1/2 was reported to increase in response to peripheral noxious stimulation [179]. Importantly, the present study also showed TRPV1 co-

expression in the p-ERK1/2-immunoreactive neurons after noxious gastric distention, thus suggesting a role of TRPV1 in mediating nociception in the stomach [178]. In the intestine, electrophysiological readings in mesenteric afferent nerve preparations from WT and TRPV1 knockout mice found that the afferent response was significantly lower for both mechanical distention and intraluminal HCl in the TRPV1$^{-/-}$ mice [180]. Another study investigated the roles of TRPV1 and CGRP in the context of lipopolysaccharide (LPS)-induced sepsis in the mice ileus [181]. LPS injection has been previously shown to induce a cellular inflammatory response by activating resident intestinal macrophages in the muscle layer which causes dysmotility in the intestine [182]. While inflammatory mediators such as NO can directly hinder activity in the smooth muscle, they can also activate afferent nerves which trigger inhibitory neuronal pathways that in turn disturb motility throughout the whole GIT [183]. In the present study, the administration of CGRP and TRPV1 antagonists (CGRP8-37 and BCTC, respectively) were found to reverse the LPS-induced delay in gastric emptying, suggesting involvement of afferent neurons in endotoxin-induced dysmotility through CGRP and TRPV1 signalling [181].

In the colon, inflammation-induced TRPV1 sensitisation has been extensively studied [81]. An *ex vivo* preparation of the mouse colon recorded sensory neurons during colonic distension, and in the presence and absence of noxious stimulants. From the two populations of colonic afferents identified, only TRPV1-positive neurons with a low-firing frequency were sensitised by capsaicin and H^+. While neurons with a high-firing frequency were sensitised by distension at a lower threshold, they were unresponsive to capsaicin and H^+ [184]. In a study which investigated the role of TRPV1 in a trinitrobenenesulfonic acid (TNBS)-induced colitis model in the rat colon, TRPV1 immunoreactivity was assessed in the thoraco-lumbar and lumbo-sacral DRG neurons. In the group of rats which received TRPV1 antagonist JYL1421 administration, microscopic colitis was found to be significantly decreased, thus suggesting an active role of TRPV1 during the development of inflammation [185]. Moreover, a study in humans compared TRPV1 expression between inflammatory bowel disease (IBD) patients with abdominal pain to asymptomatic IBD patients and controls using rectosigmoid biopsies. They found a significantly higher number of TRPV1-immunoreactive fibres in biopsies from patients with IBD experiencing abdominal pain symptoms compared with controls and asymptomatic patients [186]. Taken together, these findings reinforce the notion that TRPV1 may contribute to the pathophysiology of visceral pain throughout the lower GIT.

Functional studies of TRPV1 in the human oesophagus are relatively limited. However, TRPV1 expression in sensory neurons and afferent nerve endings has been well described in the oesophagus of different animals [65]. A study which investigated the role of TRPV1 in surgically induced oesophagitis in WT and TRPV1 knockout mice found that TRPV1$^{-/-}$ mice

exhibited significantly less histological damage, SP receptor endocytosis, and myeloperoxidase activity following acid exposure compared to WT mice. Moreover, inflammatory parameters were considerably reduced following acid suppression and administration of the TRPV1 antagonist capsazepine in WT mice, suggesting that acid-induced oesophagitis may act through TRPV1 [187]. Similarly in a rat oesophagitis model, TRPV1 expression was shown to be significantly increased with acid-induced oesophagitis in both SP and isolectin B4-immunoreactive sensory neurons innervating the oesophagus [149]. The acid-induced excitation of vagal sensory afferents in rats with oesophagitis was blocked by the TRPV1 antagonist AMG9810, suggesting that TRPV1 may play a role in sensitizing acid-sensitive nerve fibres and thus reflux hypersensitivity [188]. A more recent study investigating the role of TRPV1 in a murine model of NERD found that pharmacological blockade of TRPV1 reduced acid-induced damage to the mucosal integrity of the epithelium [189]. While the murine oesophageal mucosa demonstrated an acid-induced decrease in TER, this was suppressed upon administration of the TRPV1 antagonist SB366791 and long-term TRPV1 desensitisation by resiniferatoxin. In addition, the basal permeability to fluorescein was also significantly reduced with the blockade and deletion of TRPV1, suggesting a potential role for TRPV1 in mucosal barrier impairment in NERD [189].

Furthermore, a recent study looking at acid-induced inflammation in the cat oesophagus demonstrated TRPV1 expression in oesophageal epithelial cells, where it was found to release substance P and CGRP through intrinsic neurons when exposed to HCl [190]. Moreover, in the mucosal supernatant, a HCl-induced increase in platelet activating factor (PAF) was found [190]. PAF is a chemoattractant for immune cells and has an important role in mediating inflammation [191]. PAF also selectively induces eosinophil transmigration through the basement membrane, as well as their adherence to vascular endothelial cells and eosinophilic release of reactive oxygen species [192]. Importantly, PAF has also been shown to play a role in oesophageal mucosal damage [193]. The epithelial cell lining was directly exposed to acid reflux, suggesting a possible catalyst role of PAF release by epithelial cells for the triggering of the inflammatory cascade. Using the oesophageal epithelial cell line HET-1A, another study also demonstrated epithelial cell expression of TRPV1 and highlighted its potentially pivotal role in initiating the inflammatory process, disproving the previous consensus that TRPV1 was only expressed by neurons in the submucosa [191]. A study by Wu *et al* showed how the activation of protease-activated receptor-2 (PAR2) in cultured human oesophageal epithelial cells plays a role in pain sensation and inflammation by modulating the sensitivity of TRPV1 [194]. This study demonstrated epithelial cell release of ATP upon acid exposure which was significantly attenuated after treatment with the TRPV1 antagonist 5-iodoresiniferatoxin. Treatment of the oesophageal epithelial cells with the PAR2 agonist trypsin or mast cell

tryptase also increased acid-induced ATP release, and this effect was also blocked by 5-iodoresiniferatoxin. Taken together, these results suggest that PAR2 activation sensitises oesophageal epithelial cells to acid through TRPV1 phosphorylation [194]. Thus, the expression pattern of TRPV1 and the inflammatory response to acid activation may differ between GORD phenotypes, and may shape future therapeutic targets.

In the human oesophagus, RNA studies have shown a higher expression of TRPV1 in the inflamed oesophageal mucosa and in the mucosa of NERD patients compared to normal [195]. The distribution of TRPV1-expressing nerve fibres was studied in oesophageal biopsies from patients with ERD and control subjects. This study demonstrated the presence of TRPV1-immunoreactive nerve fibres in the papilla of both healthy controls and ERD patients, but a marked increase in the percentage of papilla positive for TRPV1 in the ERD biopsies [196]. TRPV1 activation has since been shown to evoke pain sensations including heartburn by releasing neurotransmitters such as substance P and CGRP which activate postsynaptic receptors in the spinothalamic tract neurons and induce neurogenic inflammation [197]. Taken together, these findings highlight TRPV1 as a target with therapeutic potential for the treatment of visceral pain. Whilst systemic therapy with TRPV1 antagonist failed, possibly due to the difficult balance between efficacy of the drug and systemic side effects, topical therapy would avoid this [198]. Further studies in the oesophagus of patients with different phenotypes of GORD are therefore needed for an improved understanding of its mechanism of action and potential pathophysiological role in causing heartburn.

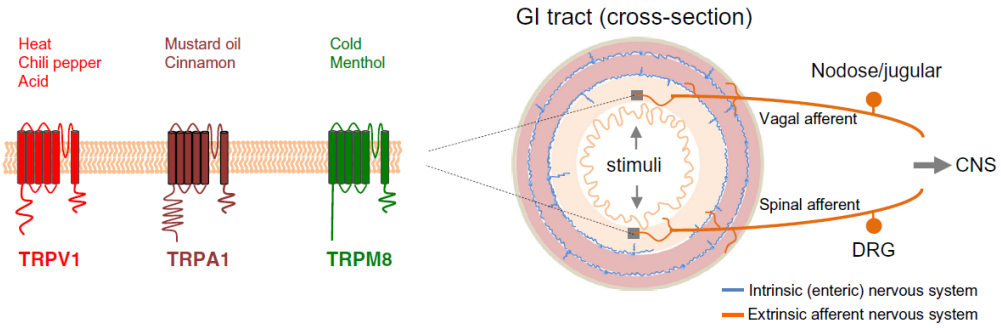

Figure 11: TRP channels in vagal and spinal afferent nerves in the GIT [81]

Figure showing the stimulants and localisation of TRPV1, TRPA1, and TRPM8 in the plasma membrane. The cross-section on the right shows neuronal innervation of the GIT by both vagal and spinal afferent neurons which express these TRP channels. Once the ion channels are activated by a noxious stimulus in the GIT, the nerve fibre becomes excited and transmits the signal (pain) to the CNS in the form of an AP via the nodose or dorsal root ganglion, respectively.

1.5.3 TRPA1

Transient receptor potential ankyrin-1 (TRPA1) is a permeable cation channel which is activated by both endogenous and exogenous stimuli including noxious cold temperatures (below 17ºC) and allyl isothiocyanate (constituent of mustard oil), regulating numerous cellular processes including pain [199],[200]. TRPA1 is the sole member of the TRPA gene subfamily in mammals. Structurally, the TRPA1 (ANKTM1) channel is characterised by approximately 14 ankyrin repeats on the N terminus, as seen in Figure 10 and Figure 11 [201]. The mechanism of action of mustard oil was discovered through a study which used calcium imaging to investigate whether allyl isothiocyanate (at 20 µM) activates disassociated sensory neurons from the rat trigeminal ganglia. Mustard oil was found to induce Ca^{2+} influx into 35% of sensory neurons, while all neurons activated by mustard oil were also sensitive to capsaicin. This led to the hypothesis that mustard oil activates a Ca^{2+}-permeable ion channel in neurons which express TRPV1 [202]. A different study which combined bioinformatic and expression analysis searched for cDNA sequences containing both multiple ankyrin domains and 6TM domains found TRPA1 in a small sub-population of DRG neurons [203]. Importantly, 97% of the TRPA1-expressing neurons also expressed CGRP and TRPV1, but only 30% of TRPV1-positive neurons expressed TRPA1. Conversely, the other cold receptor TRPM8 was not co-expressed with CGRP and TRPV1 in DRG neurons [204]. In situ hybridization reinforced this finding by demonstrating no expression overlap between TRPA1 and TRPM8, leading to the indication that TRPA1 is expressed in a subgroup of nociceptive neurons that express TRPV1, but not the cold-activated TRPM8 [203]. Moreover, a study in $TRPA1^{-/-}$ mice demonstrated a lack of acute pain-related behaviour following topical mustard oil application. Cultured sensory neurons from TRPA1-deficient mice also remained insensitive to mustard oil, showing failed activation and lack of Ca^{2+} influx. Taken together, these studies demonstrate that TRPA1 channel activation by mustard oil induces Ca^{2+} influx into sensory neurons and subsequent release of neuropeptides such as CGRP and SP from nerve endings which activate neurogenic inflammation in a way that closely resembles TRPV1 [205].

At a molecular level, electrophysiological data demonstrates TRPA1 to be coupled to bradykinin signalling through PLC downstream, suggesting a nociceptive role for TRPA1 [206]. Bradykinin is an inflammatory mediator released during tissue injury and inflammation, and has been shown to induce acute excitation in sensory neurons by acting through its GPCR [207]. Specifically, bradykinin activates the PLC signalling pathway as described in section 1.5.1 [208]. PLC activation regulates the downstream activity of many TRP channels including TRPA1 by breaking down PIP2 into DAG and IP3, which then releases Ca^{2+} from the ER and causes Ca^{2+} influx into sensory neurons. The present study found that the DAG analog 1-

oleoyl-2-acetyl-sn-glycerol (OAG) activated TRPA1-expressing DRG cell cultures, suggesting a potential mechanism by which bradykinin signalling and TRPA1 activity are connected [206].

The GIT has been extensively studied with regards to the nociceptive and inflammatory role of TRPA1 [209]. In a chemically induced mouse model of colitis, TRPA1 agonists were found to amplify visceral hypersensitivity in afferent nerves, reinforcing a sensitising role of TRPA1 during inflammatory conditions [210]. GPCR-induced activation of protease-activated receptor-2 (PAR-2) has also been shown to induce colitis. Importantly, in rat DRG neurons, PAR-2 and TRPA1 have been observed to be colocalised, and TRPA1 was shown to be activated downstream of PAR-2 signalling, suggesting TRPA1 regulation by PAR-2 [211]. In line with the observation described with bradykinin, PAR-2 also sensitises TRPA1 via the PLC signalling pathway, which is suggested to be activated in various GI disorders [209]. In a visceral pain study in mice, intracolonic PAR-2 activating peptide was found to induce hyperalgesia in $TRPA1^{+/+}$ mice, but not in $TRPA1^{-/-}$ mice. The same study demonstrated that the inflammatory agent trinitrobenzene sulfonic acid-induced colitis caused an increase in visceromotor responses to colorectal distention, and activated c-fos in spinal neurons in $TRPA1^{+/+}$ mice only [212]. Thus, TRPA1 has an important role in visceral nociception in the colon and could be a potential therapeutic target for visceral pain. Paradoxically, a recent study reported an unexpected anti-inflammatory role of TRPA1 in CD4+ T lymphocytes. Double immunofluorescence staining between TRPA1 and TRPV1 showed co-localisation between the two channels in wild-type (WT) CD4+ T cells suggesting their direct interaction, whereas TRPV1 channel activity was increased in *Trpa1*$^{-/-}$ CD4+ T cells [213]. Moreover, the adoptive transfer of *Trpa1*$^{-/-}$ and *Trpa1*$^{-/-}$*Trpv1*$^{-/-}$ CD4+ T cells to *Rag*$^{-/-}$ recipient mice showed more severe colitis in the *Trpa1*$^{-/-}$ T cells [213]. These findings highlight that TRPA1 expressed on CD4+ T cells decreases the severity of colitis, suggesting an unexpected anti-inflammatory role by restraining TRPV1 channel activity [213].

In the oesophagus, PAR-2 has been shown to sensitise sensory nerves and induce hyperalgesia via mast cell activation. A study in the guinea pig oesophagus showed co-expression between TRPA1 and PAR-2 on 80% of TRPA1-positive sensory neurons [214]. Moreover, the mechanical response of C-fibres to oesophageal distention was found to be significantly increased by both mast cell activation and by the PAR-2 activating peptide [214]. TRPA1 inhibition significantly decreased mechanical hypersensitivity by either mast cell activation or PAR-2 activating peptide, suggesting that TRPA1 is sensitised through PAR2 activation and has a regulatory role in hypersensitivity caused by mast cell activity in vagal nodose C-fibres [214]. Another study in the guinea pig oesophagus performed extracellular recordings of APs from vagal nodose and jugular neurons following oesophageal distension and allyl isothiocyanate perfusion. Neuronal activation by bradykinin was found to significantly

increase following oesophageal distension, and was prohibited by the bradykinin receptor antagonist WINK64338 [215]. In addition, the TRPA1 inhibitor HC-030031 reduced bradykinin-induced hypersensitivity in the oesophagus, further suggesting TRPA1 may have a role in mediating inflammatory nociception [215]. Taken together, the studies discussed in this section highlight the contribution of TRPA1 ion channels in sensory neurons in the GIT to acute and inflammatory pain, and reveal its potential as a neuronal target underlying oesophageal hypersensitivity.

1.5.4 TRPM8

Transient receptor potential melastatin 8 (TRPM8) is a Ca^{2+}-permeable, nonselective cation channel which is activated by cold (temperatures between 8-23ºC) and cooling compounds such as menthol and icilin [216]. The *trp-p8* gene was originally discovered in a cDNA screening of prostate-specific genes, where a 5694-base pair cDNA encoding 1104 amino acids was found to compose a putative protein with 7TM domains [217]. The sensory role of this protein was uncovered by a study which isolated and cloned the menthol receptor from trigeminal sensory neurons and demonstrated its activation by thermal stimuli in the cool range [218]. A high throughput mutagenesis screening study highlighted the S1-S2 TM segments as the determinants of sensitivity to TRPM8 agonists [219]. This corresponds to the binding site on the TRPV1 receptor, suggesting that the gating mechanisms for sensitisation are conserved amongst TRP channels [220].

TRPM8 is widely expressed, but its most renowned function is as a cold and menthol-induced sensory transducer in a subgroup of $TrkA^+$ primary sensory neurons [218]. Multiple studies in mice have independently demonstrated the lack of response to cold stimuli in TRPM8 null mice [221], [222]. Fluorometric calcium imaging demonstrated a significant decrease in the response of sensory neurons derived from $TRPM8^{-/-}$ mice to cold (18ºC) and menthol (100 µM) stimuli [222]. Thus, TRPM8 is a potent detector of cool temperatures *in vivo*, suggesting a possible role in nociception and development of analgesia [153].

While TRPV1, TRPA1, and TRPM8 channels all interact with inflammatory GPCRs, inflammatory mediators including bradykinin inhibit TRPM8 in sensory neurons. Upon TRPM8 binding to a Gq-coupled receptor, a novel signalling pathway is activated which directly inhibits TRPM8 [223]. Another signalling mechanism for TRPM8 involves the menthol induced Ca^{2+} influx which activates downstream PLC signalling. Activation of PLC results in the breakdown of the membrane phospholipid phosphatidylinositol 4,5-bisphosphate ($PtdIns(4,5)P_2$), which shifts the voltage dependence of the TRPM8 channel and causes desensitisation to its ligands [224], [225]. Moreover, PLC also activates PKC downstream which initiates the

dephosphorylation of TRPM8 and results in the channel's inactivation [226]. The activation of PKA downstream of PLC is yet another mechanism by which the TRPM8 channel becomes desensitised [227]. Moreover, the TRPM8 agonist icilin was found to prevent desensitisation caused by the TRPV1 agonist capsaicin and the TRPA1 agonist allyl isothiocyanate, demonstrating that TRPM8 couples to TRPV1 and TRPA1 and suppresses their chemosensory and mechanosensory actions [228]. Taken together, the molecular mechanisms of TRPM8 activation and desensitisation explain the cooling sensation that menthol infusion has been reported to cause and highlight a possible nociceptive role in alleviating pain symptoms.

Anatomical and molecular data have shown TRPM8 expression in colonic sensory neurons, where it induces initial activation followed by mechanical desensitisation. TRPM8 immunoreactivity was observed in colonic nerve endings throughout the layers of the colon (mucosa, submucosa, muscle, and serosa) where it usually co-expressed CGRP [228]. The role of TRPM8 in nociception has been described in a DSS-induced mice colitis model where the administration of TRPM8 agonist WS-12 increased visceral pain-like symptoms [229]. Conversely, another study showed that distention-induced colonic CGRP release in TRPM8-deficient mice decreased at higher distension pressure levels compared to TRPA1-deficient mice. This demonstrates that the TRPM8 channel has a different activation threshold compared to TRPA1, which may reflect TRPM8 expression in high threshold mechanosensitive fibres [230]. Studies have also highlighted a role of TRPM8 in colonic inflammation. CGRP levels were elevated in a $TRPM8^{-/-}$ DSS mice colitis model, while TRPM8 activation by icilin (pre-treatment) blocked TRPV1-induced CGRP release and attenuated the severity of colitis, reinforcing the possible regulatory role of TRPM8 in neurogenic inflammation [231]. Moreover, $Trpm8^{-/-}$ mice were found to be hypersusceptible to colitis. TRPM8 and CGRP immunoreactivity in mucosal fibres were both significantly increased in DSS-treated mice compared with WT controls, suggesting that colitis activates TRPM8 signalling in a subset of mucosal sensory neurons and induces CGRP release [232]. CGRP is then suggested to attenuate the production of pro-inflammatory cytokines by $CD11c^{+}$ dendritic cells, suggesting an indispensable role of TRPM8 signalling in innate immune responses via CGRP regulation [232]. The use of menthol for relief of abdominal pain and colonic inflammation further reinforces an immunoregulatory role for TRPM8 [233].

However, there are currently no studies of TRPM8 in the human oesophageal mucosa. A study in neurons from nodose and jugular ganglia from the guinea pig oesophagus highlighted a distinctive role of TRPM8 in oesophageal sensory transduction [234]. Acid perfusion evoked APs and suppressed the response to oesophageal distension in jugular C fibres, but not nodose C fibres, showing distinctive responses to acid in subtypes of vagal afferent nerves

[235]. Observations in humans have demonstrated that cold water induces oesophageal pain, while infusion of menthol into the oesophagus of GORD patients induces heartburn, suggesting a visceral nociceptive role of TRPM8 in the oesophagus [236]. Understanding TRPM8 function in afferent nerves in the oesophageal mucosa will not only elucidate the effect of menthol-induced relief on heartburn but may also be a potential therapeutic target in the oesophageal mucosa of GORD patients.

1.5.5 Acid sensing ion channels

Acid sensing ion channels (ASICs) belong to an epithelial Na^+ channel/degenerin (ENaC/DEG) family of voltage-insensitive, amiloride sensitive cation channels [237]. ASICs are sensors of extracellular pH and have an activation threshold of pH 7.2, exhibiting diverse response dynamics ranging from fast and rapidly deactivating, to slow and sustained responses [238]. In mammals, proton-sensitive ASIC members are encoded by 3 different genes: *ACCN1, ACCN2* and *ACCN3*. These genes are alternatively spliced to produce 5 subunits: ASIC1a, ASIC1b, ASIC2a, ASIC2b, and ASIC3. All these subunits are directly proton-gated as homomultimers except ASIC2b which only responds to increased acid exposure when expressed as a heteromultimer with ASIC3 [39]. Structurally, ASICs share the characteristics of other ENaC/DEG family members, with two hydrophobic TM domains, an extracellular cysteine-rich loop, and short intracellular N- and C- domains [239]. The channel's proton sensor is proposed to be situated in multiple sites of the extracellular loop, but particularly His-72 and Gly-430 [239], [240]. When activated by extracellular protons, the only known activator of ASICs, the channel becomes permeable to Na^+ [92], [241]. Inflammatory mediators such as NGF have been shown to directly modulate ASIC3 gene expression in sensory neurons, suggesting an immunomodulatory role in determining the sensitivity of primary afferent nociceptors [242].

Kress and Waldmann have described two principal mechanisms of sensitisation in sensory neurons: the first type involves a fast, rapidly inactivating Na^+ current which is highly H^+-sensitive (activated at pH 7), while the second type is a slow current carried by Na^+, K^+ , and Ca^{2+} which is much less sensitive to H^+ (activated at pH 6.2) [88]. The latter mechanism is only seen in DRG neurons activated by capsaicin, whereas the first mechanism which is fast and rapidly inactivating closely resembles the gating mechanism of ASICs [93]. Activation of ASIC channels leads to an influx of Na^+, desensitising the neuron and initiating an AP which is fed into nociceptive pathways of the CNS. The evidence showing expression of ASICs on peripheral sensory neurons and spinal nociceptive pathways highlight ASICs as major sensors of acid-induced pain [243] ASIC3 was localised in sensory nerve endings of the skin in a study

in mice, which demonstrated decreased sensitivity to noxious pinch and acid infusion in ASIC3- deficient mice [244].

ASICs are predominantly expressed on the peripheral fibres of extrinsic primary afferent neurons originating from the DRGs and nodose ganglia [245]. However, a recent *in vivo* study by Akiba *et al* found ASIC1-3 expression in other cells including oesophageal epithelial cells, and ASIC3 expression in the muscularis mucosa [246]. In this study, the distal oesophageal mucosa of the rat was perfused with acid solutions via a mucosal perfusion chamber. Following continuous super-fusion of a Krebs buffer solution of pH7 to stabilise blood flow, the perfusate was changed to pH6.4 saline, a solution with high CO_2 concentration, or an acid solution of pH 1, with or without the addition of various antagonists and inhibitors. While CO_2 challenge was found to induce hyperaemia, the generic ASIC inhibitor amiloride inhibited the CO_2 response [246]. Moreover, immunofluorescence analysis revealed expression of ASIC1-3 isoforms in the prickle cell layer of the oesophageal mucosa, as well as in nerve fibres in the muscularis mucosa [246]. Taken together, these results suggest that luminal CO_2 diffuses and interacts with epithelial membrane-bound ASICs and activates these acid sensors, leading to signals being conducted to afferent nerves, resulting in hyperaemia [246].

ASIC3 plays a major role in visceral hypersensitivity in the GIT following neurogenic inflammation. In a study which examined whether the knockout of *ASIC2* or *ASIC3* modified afferent signalling of a gastric acid insult in the inflamed stomach, acid-evoked expression of c-Fos in the brainstem during gastritis was found to be attenuated following the disruption of the *ASIC3* gene. In contrast, *ASIC2* gene knockout did not induce change in the afferent signalling causing inflammatory hypersensitivity, but was found to enhance c-Fos expression in response to acidification of the normal stomach [247]. This finding is consistent with the inference that the expression of ASIC3, but not ASIC3 and ASIC2 is increased in the colonic mucosa of patients with Chron's disease [151].

In the oesophagus, acid sensing mechanisms in epithelial cells and acid-sensitive afferent neurons have been demonstrated to initiate a rapid series of protective mechanisms including increase in thickness of mucous, HCO_3^- secretion and mucosal blood flow following oesophageal exposure to excess acid [94]. The detection of CO_2 in epithelial cells sensed by carbonic anhydrases and ion transporters induces the hydration of CO_2 into H^+ and HCO_3^- [248]. Consequently, there is intracellular acidification, interstitial pH decreases, and acid-sensing afferent nerves release CGRP to induce vasodilation [249]. Importantly, the nociceptive responses of vagal afferent neurons to acidification at the oesophageal mucosa is likely to depend on the sensitisation and downstream activity of more than one acid-sensing ion channel [250], as the attenuation of acid-induced oesophageal vagal afferent nerve fibre

excitation was only seen when both *ASIC3* and *TRPV1* underwent knockout [251]. While there have been no functional studies of ASICs in humans in health or following acid exposure to date, Wu *et al* demonstrated a potential role for ASIC3 in the mechanism for heartburn sensation using cultured human oesophageal epithelial cells. This study demonstrated ATP release by these primary oesophageal epithelial cells upon exposure to weak acid (pH 5), and showed this effect to be significantly reduced when pre-treated with the ASIC3 antagonist amiloride [194]. Moreover, ATP release was enhanced when the primary cells were treated with PAR2 agonists trypsin and tryptase, and this effect was also blocked with amiloride or a PAR2 antagonist. PAR2 is a GPCR whose involvement has been reported in neuroinflammatory epithelial responses in the gut [252]. The results of this study suggest that PAR2 activation sensitises human oesophageal epithelial cells to weak acid, partially through the phosphorylation of ASIC3 [194]. The functional role of ASICs in peripheral nociception, as well as their involvement in the development of central sensitisation and pain hypersensitivity have highlighted ASICs as important transmitters in chronic pain sensation. Hence, ASICs are emerging potential therapeutic targets for visceral pain, and their role needs to be investigated in the oesophageal mucosa of GORD patients.

1.6 Mucosal neuroanatomy of the oesophagus

There is limited data describing mucosal innervation of the human oesophagus. While the proximal oesophagus has been suggested to be more sensitive to chemical, electrical, and mechanical stimuli than its distal counterpart, oesophageal sensation is likely to have a multifactorial mechanism of action [253]. Our group previously examined biopsies from the distal and proximal healthy human oesophagus for the presence of mucosal sensory afferent nerves. The location of these afferent fibres were found to be significantly closer to the oesophageal lumen in the proximal oesophagus compared to the distal, as demonstrated by immunoreactivity for both CGRP and PGP 9.5 [254]. Increasing evidence from animal studies suggests that CGRP-positive mucosal fibres in the proximal oesophagus are vagal, and play a role in nociception which might be relevant to pain perception in GORD patients [84], [255]. The superficial nature of afferent nerves in the proximal oesophagus might mean that they are amenable to topical protectant therapies which could reduce their sensitivity and provide an effective alternative strategy to treating PPI-refractory GORD [254].

Furthermore, our group subsequently demonstrated that NERD patients have a greater density of superficial nerves in the proximal and distal oesophagus compared to healthy controls and patients with BO and ERD [256]. In keeping with the previous study, the proximity of nerves to the lumen was measured in terms of the number of intercellular junction layers, as this has been suggested to be a more accurate representation of the physiological barrier to diffusion compared to measuring the distance in micrometres [256]. In this way, the measurement avoided bias from basal cell hyperplasia which is a common feature of NERD, as well as the varying epithelial thickness that is often seen in oesophageal biopsies from GORD patients [257]. Mucosal afferent nerves in both the proximal and distal oesophagus were found to lie in closest proximity to the luminal surface in NERD patients, whereas the fibre location in ERD and BO was similar to that seen in healthy volunteers (Figure 12). While the precise function of these afferent nerves is yet to be fully understood in humans, their CGRP and substance P immunoreactivity suggests a possible nociceptive role. A previous study on oesophageal mucosal fibres in patients with NERD demonstrated TRPV1 expression on these fibres, and there is a plethora of evidence indicating that TRPV1-immunoreactive nerve fibres belong to a nociceptive spinal afferent pathway [258], [259]. Thus, acid hypersensitivity in patients with NERD might be partially explained by the increased proximity of their afferent nerves to the oesophageal lumen, and therefore greater exposure to noxious substances in the refluxate [256]. However, further studies are needed to investigate the nociceptive pathways related to these mucosal afferent nerves in the human oesophagus in greater detail.

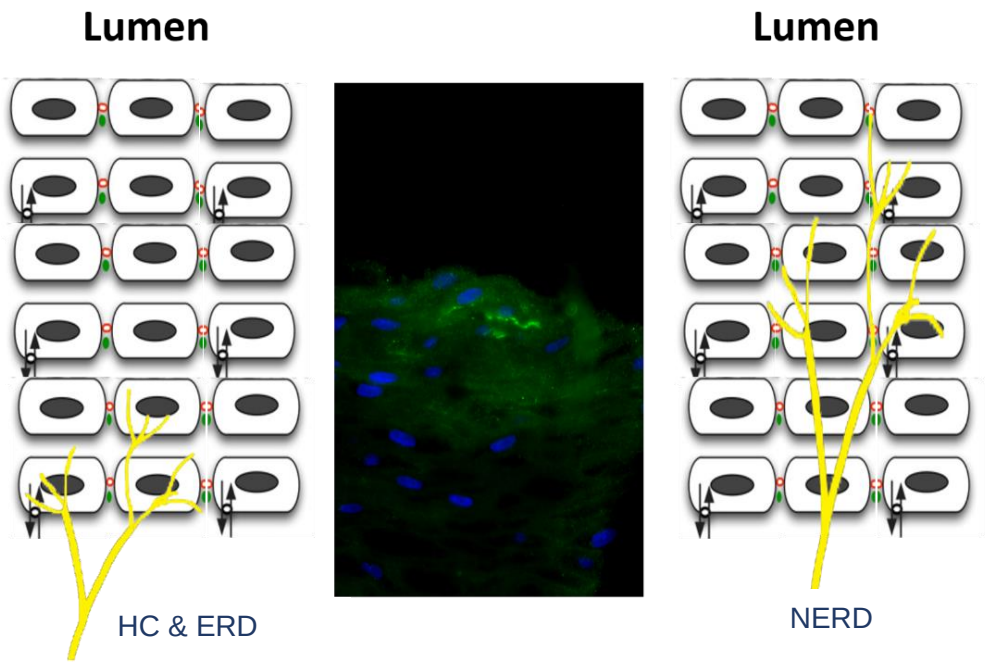

Figure 12: Mucosal afferent nerve location in patients with NERD, ERD, and healthy controls.

Mucosal afferent fibres are closer to the oesophageal lumen in NERD, whereas in ERD, the fibre location is similar to that seen in HC. Yellow structures represent nerve fibres, red structures represent tight junction protein occludins and green structures represent adherens junction protein e-cadherin[256].

1.7 Neuroimmune crosstalk in the oesophagus

There is accumulating evidence highlighting an active role of non-neuronal cells such as immune cells in the pathogenesis and resolution of pain [260]. Acute/nociceptive pain is a cardinal feature of acute inflammation, with most inflammatory mediators inducing pain by binding their receptors located on sensory nerves that innervate the injured tissue [98]. On the other hand, chronic pain has been shown to be maintained by neuronal plasticity, with peripheral sensitisation of nociceptors regulating chronic pain [261]. Moreover, the relationship between pain and inflammation is bidirectional; nociceptive neurons are not only activated by signals from immune cells but can also directly regulate inflammation by producing inflammatory mediators such as SP and CGRP when activated by noxious stimuli [262]. Sensory neurons signal to tissue resident innate immune cells such as mast cells and dendritic cells during the early phases of inflammation. Anatomical studies have demonstrated a direct connection between these nerve terminals and mast cells and dendritic cells (DCs), where neuropeptides released from nociceptors induced the production of inflammatory cytokines in these immune cells [263], [264]. Functional assays on epidermal dendritic cells (Langerhans cells) showed that CGRP exposure enhanced antigen presentation on Langerhans cells to a Th2 clone, demonstrating enhanced DC function for Th2 responses in response to CGRP [267]. On the other hand, monocytes and macrophages induce pain by releasing inflammatory mediators such as interleukin-1β (IL-1β) which transduce pain by modulating ion channels like TRPA1 and TRPV1 [262]. Toll-like receptors (TLRs) have also been shown to be instrumental in their interactions between neurons and non-neuronal cells [261]. Although mainly expressed by immune cells, sensory neurons in the DRG also express various TLRs, and each TLR modulates a different sensory function. For example, tissue injury caused by bacterial infections releases pathogen-activated molecular patterns such as LPS [266]. TLR4 has been shown to be functionally coupled to TRPV1 in the sensory neuron terminal, so LPS binding its receptor TLR4 leads to a Ca^{2+} influx in the neuron and subsequent pain [266], [267].

In the intestine, inflammatory mediators released by the mucosa of patients with IBS regulate the function of sensory nerves [268]. Several studies have suggested an overlap between GORD and functional disorders such as IBS through questionnaire-based diagnoses which showed a positive association between heartburn symptoms and IBS [269]. Dothel *et al*. analysed mucosal biopsies from IBS patients and healthy controls by measuring the levels of mucosal mediators using immunohistochemistry and enzyme-linked immunosorbent assays. This study demonstrated that mucosal nerve fibres had increased fibre sprouting and density in patients with IBS, as indicated by a higher expression of nerve growth factor (NGF) and tyrosine kinase receptor A (NTRK1) [268]. Increased neuronal sprouting was demonstrated

by the higher expression of GAP43, a neuronal membrane phosphoprotein involved in neuronal sprouting through polymerising actin monomers [270]. The results of this study also showed that NGF was predominantly expressed by tryptase-immunoreactive mast cells, demonstrating mast cells as an important source of this growth factor. NGF acts on its receptor NTRK1, which was found to be expressed on nerve fibres, as well as mast cells. NTRK1 is suggested to subsequently drive neuronal differentiation by increasing GAP43 transcription [271]. Moreover, a previous study highlighted a relationship between the frequency and severity of abdominal pain, and the close vicinity of mast cells to colonic mucosal nerves [271]. Taken together, these studies suggest that NGF produced by mast cells acts on receptors expressed by nerve fibres, leading to nerve sprouting and pathological pain transmission. An increase in NGF levels has also been shown to upregulate ASIC3 expression and ASIC3 current amplitudes in sensory neurons during inflammation by directly interacting with the promoter region of the ASIC3 gene [242]. The important role of NGF in determining the sensitivity of afferent nociceptors leads to the concept that neuroimmune crosstalk may have a critical role in the pathophysiology of visceral hypersensitivity and pain persistence through the induction of neuroplastic changes [272].

The role of inflammation on oesophageal conditions such as GORD is poorly understood. Despite recent evidence demonstrating the production of neurogenic mediators in the pathogenesis of GORD, the relationship between inflammation and oesophageal hypersensitivity remains unclear [273]. However, recent studies are beginning to describe mechanisms by which acid may induce an inflammatory state. For example, excessive acid stimulates oesophageal epithelial cells to secrete chemokines such as IL-8 which is transcribed via NF-κB signalling, and is closely associated with inflammation induced by neutrophils [274]. A study which evaluated histologic features of oesophageal inflammation in acute ERD by stopping PPI treatment for 2 weeks highlighted significant increases in intraepithelial lymphocyte infiltration characterised by T cells [275]. Moreover, inflammation characterised by neutrophil and eosinophil infiltration has been more commonly observed in ERD than NERD phenotypes [276]. Therefore, inflammatory mediators may mediate mucosal immune responses specific to different GORD phenotypes [277].

As described in section 1.5.2 TRPV1, acid-induced activation of TRPV1 receptors in the oesophageal mucosa increase the synthesis of PAF by oesophageal epithelial cells [278]. PAF acts as a chemoattractant for peripheral blood leukocytes which produce inflammatory mediators such as H_20_2 which could be a potential mechanism for the initiation of acid-induced inflammation in GORD [196]. The activation of TRPV1 in primary afferent nerves also leads to the release of other neurogenic mediators, namely SP and CGRP, which can cause a burning pain sensation by inducing neurogenic inflammation [278]. Moreover, a histological study

found CGRP expression in Langerhans cells in the oesophageal mucosa, particularly during inflammation, highlighting an immunomodulatory role for CGRP in antigen presentation *in vitro* [279]. Thus, while there are gaps in our understanding of the neuro-immune interaction in the oesophageal mucosa, there is accumulating evidence suggesting a close link between nociceptors and non-neuronal cells in pain studies in different regions of the body. The neuro-immune interaction in the oesophageal mucosa could be an important mechanism underlying heartburn symptoms in GORD, and must be investigated to better understand the mucosal pathogenesis of heartburn.

1.7.1 Cytokine Receptors in Neuroimmune crosstalk

It has become apparent that soluble mediators, including cytokines, contribute critically to the integration of the nervous and immune systems both in the healthy state and in pathological conditions [280]. Immune cytokines, including tumour necrosis factor (TNF), interleukin-1β (IL-1β), IL6, and IL8 are important mediators of cell recruitment and activation, potentially driving pain transmission during local tissue damage, as evident in conditions such as inflamed arthritis [281]. Several mechanisms could be responsible for the link between these inflammatory cytokines and nociception. As reviewed in sections 1.3 Central pathways of pain sensation in the oesophagus and 1.4 Peripheral pathways of pain sensation in the oesophagus, many chemical stimuli, including those released during inflammation and tissue damage, can sensitise nociceptors. Thus, the 'inflammatory soup' that is detected by nerve endings is made up of many sensitising agents, including growth factors, cytokines, chemokines, protons, and ATP [97], [282]. Until recently, cytokines were assumed only to activate nociceptive terminals through inducing release of neurostimulators including kinins and amines from non-neuronal cells. However, recent data has shown the ability of cytokines to directly sensitise and mediate pain during inflammation [281], [283].

With the increasing recognition of cytokines as important mediators of nociceptive pain, there are now two established mechanisms through which cytokines are known to induce nociceptor sensitisation. First, inflammatory cytokines can indirectly sensitise nerve endings though release of mediators which prime neurons and result in their increased responsiveness to otherwise innocuous stimuli. Second, such cytokines may directly activate neurons via their specific receptors expressed on the nerves themselves [280]. Recent RNA-sequencing data for cytokine receptor expression in purified murine DRG neurons has highlighted the importance of inflammatory cytokines acting on the CNS to process noxious stimuli in neuropathic pain [284]. The most important candidate inflammatory cytokine receptors involved in pain sensation will thus be discussed in further detail in this section.

1.7.2 Type I TNF Receptor (TNFR1)

TNF is a pleiotropic cytokine which functions as an important regulator of many cellular responses ranging from apoptosis in tumour cells, to induction of inflammatory gene expression programmes, and stimulation of immune cell proliferation [285], [286]. The most well-known member of the TNF superfamily, TNFα, is the prototypic ligand of TNF which is expressed both as a single spanning transmembrane protein, and as a soluble variant which gets released from the transmembrane form [287]. Both of these forms interact with the two TNF receptors, type I TNF receptor (TNFR1) and type II TNF receptor (TNFR2), which are single-spanning type I transmembrane proteins with several characteristic cysteine-rich regions in their extracellular domain [288]. This N-terminal cysteine-rich domain regulates self-association in the inactive state of the receptor prior to ligand binding, and has been named the pre-ligand binding assembly domain (PLAD) (Figure 13) [289]. Interestingly, alternate splicing has been described to result in soluble forms of TNFR1 and TNFR2, but these have been suggested to act as TNF inhibitors by competing with the TNF cytokine for binding the transmembrane form of the receptor [288], [290], [291]. Moreover, TNFR1 has been described as a 'death receptor' due to the death domain (DD) in its cytoplasmic region which associates the receptor with cytotoxic signalling pathways that trigger apoptosis or necroptosis [292]. However, studies have also highlighted the engagement of TNFR1 in pathways activating transcription factors such as NFκB and MAP kinases, suggesting a role for TNFR1 in proinflammatory gene-activating signalling [286], [293]. Although the transmembrane form of TNFα can bind and activate TNFR1 and 2 with high efficacy, soluble TNFα has been shown to result in TNFR1 activation only (Figure 13).

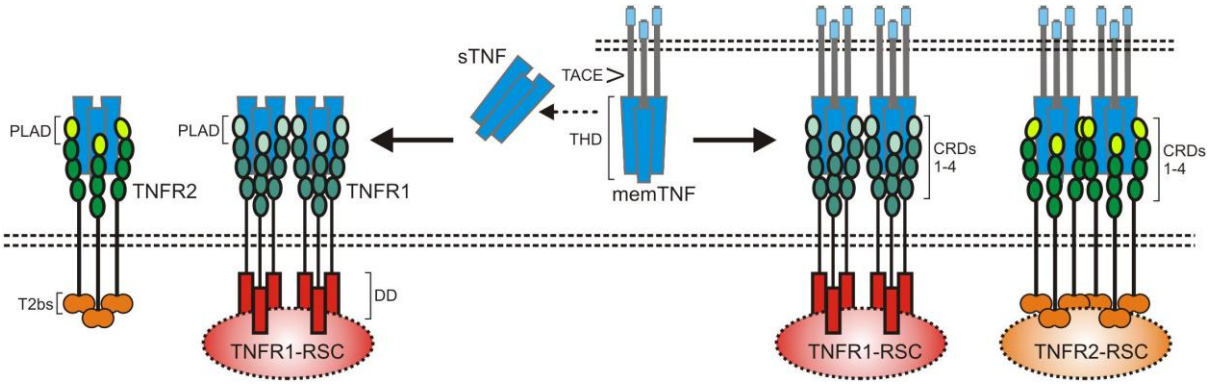

Figure 13: The TNF-TNFR System

TNFR1 and 2 both exhibit cysteine-rich domains (CRD) in their N terminals, known as pre-ligand assembly domain (PLAD). TNFR1 also has a death domain (DD) in its intracellular domain, while TNFR2 has a TRAF2 binding site (T2bs). TNFα can bind in two forms: a membrane-bound ligand (memTNF), and a soluble cytokine (sTNF). TACE can convert memTNF to sTNF. Although the transmembrane form of TNF can bind and activate both TNFRs, binding of the soluble form of TNF can only activate TNFR1 [289].

Following the binding of TNFα, TNFR1 activation occurs through the formation of a core signalling complex on the C-terminal of the receptor [294]. Initially, TNFR1 gets trimerized when bound by TNFα, enabling the DD to recruit TNFR1-associated death domain (TRADD) which acts as a scaffold [295]. Next, TNF receptor-associated factor (TRAF) 2 or 5, and receptor-interacting serine/threonine-protein kinase 1 (RIPK1) are recruited to the complex, allowing downstream signalling to occur [296], [297]. TRAF2 then recruits cellular inhibitor of apoptosis protein (cIAP) $_1$ and cIAP$_2$, forming the core signalling complex of activated TNFR1. The signalling outcome is then determined by the ubiquitination of RIPK1: the complete ubiquitination of RIPK1 forms Complex I which ultimately activates NFκB, JNK, and p38 pathways activate inflammatory cytokine signalling, and incomplete ubiquitination of RIPK1 results in Complex IIa or IIb, leading to apoptosis pathways [298]–[300]. Cell culture studies and knockout studies in mice have shown that both proinflammatory and apoptotic pathways activated by TNFα and linked to tissue injury are mediated predominantly through TNFR1 [301].

Whilst TNFR2 expression is restricted primarily to cells of haematopoietic lineage including immune cell subsets, fibroblasts, and endothelial cell types, TNFR1 is constitutively expressed by most cell types [302], [303]. In resting cells, TNFR1 resides in the Golgi apparatus, where it is suggested to act as a reservoir which gets mobilised to the cell surface to become activated [304]. Importantly, TNFRs are highly regulated by inflammatory tissue injury *in vivo*. In the kidney, where expression of TNFR1 is largely confined to microvascular and glomerular endothelial cells under normal conditions, TNFR1 expression is significantly reduced in endothelial cells in kidney allografts subjected to ischaemic injury [301]. Mediators such as nitric oxide have been shown to activate matrix metalloproteinases involved in the shedding of TNR1 [308]. Thus, TNFR1 shedding from the endothelial cell surface could be a result of inflammatory mediators in the injured tissue [306], [307]. The expression of both TNFR1 and 2 have also been reported in 40-60% of DRG neurons of an antigen-induced arthritis model in rats. In this model, systemic neutralisation of TNF was found to rapidly attenuate mechanical and thermal hypersensitivities in the inflamed knee. Electrophysiological recordings highlighted that the response reduction of nociceptive sensory Aδ and C fibres to mechanical stimuli 30 minutes after injection of the TNFR fusion protein etanercept was found to be more rapid than the reduction of inflammation, suggesting TNF to induce arthritic pain by directly activating its neuronal receptor target [308]. TNFR expression in neurons has been further highlighted using immunohistochemistry and immunofluorescence approaches, whereby basal levels of both TNFR1 and TNFR2 in naïve rodent DRG neurons was shown to increase during nerve injury [309], [310]. Conversely, in situ mRNA hybridization data detected no basal

TNFR1 expression in naïve murine DRG neurons, but was only found after nerve injury [311], [312].

The involvement of TNF in pain processing pathways has become increasingly clear, but how much neurons express TNFR1, and whether TNF acts directly on neurons alone or requires downstream mediators to induce pain, remains incompletely understood [280]. A study in isolated rat skin showed that administration of TNF augments the heat-evoked CGRP release from nociceptors [313]. Moreover, long-term TNFα exposure of cultured mouse and rat DRG neurons was found to enhance BDNF, tyrosine kinase B, and TRPV1 immunoreactivity [311], [314]. This effect was abrogated in cultured neurons obtained from *tnfr1/2*$^{-/-}$ and *tnfr1*$^{-/-}$ mice, but not *tnfr2*$^{-/-}$ mice. In this study investigating the somata of primary afferent fibres, TNFα-induced increase of TRPV1 expression was found to involve the activation of ERK [314]. In an *IL10*$^{-/-}$ Chron's colitis mouse which was bred with *tnfr1*$^{-/-}$ mice to create a double-knockout animal model, TNFR1 deletion induced colonic epithelial dysfunction, neutrophil infiltration and B cell depletion in the colonic mucosa, suggesting increased susceptibility to colitis [315]. This could partially explain the ineffective results seen with anti-TNF antibody treatments in patients with IBD [316], [317]. In another *tnfr1*$^{-/-}$ murine model of chronic ulcerative colitis, TNF was found to activate a p53-dependent pathway of apoptosis of intestinal epithelial cells. The inhibition of this apoptotic pathway could be one way to enable mucosal healing in ulcerative colitis patients treated with anti-TNF therapy [318]. Moreover, a histopathology study investigating the colons of *tnfr1*$^{-/-}$ and *tnfr2*$^{-/-}$ mice revealed that although both KOs had a similar histopathological damage score, *tnfr1*$^{-/-}$ mice had more severe colitis and reduced infiltration of macrophages compared to *tnfr2*$^{-/-}$ and WT mice [319]. The role of TNFα/TNFR1 signalling has also been associated with an increased risk of gastric cancer, whereby a *tnfr1*$^{-/-}$*Gan* mouse model of gastric tumorigenesis demonstrated a significant suppression of tumour progression, highlighting the TNFα/TNFR1 pathway as a potential therapeutic target for gastric cancer [320].

In the oesophagus, the role of TNFR has been highlighted in relation to BO and oesophageal adenocarcinoma. Importantly, analysis of oesophageal adenocarcinomas has suggested a correlation between reduced expression of the epithelial cell adhesion marker and tumour suppressant e-cadherin, and increased TNFα stimulation [321]. Moreover, immunohistochemistry and western blot analysis of oesophageal tissue showed an increased epithelial expression of TNFα with metaplastic progression of BO, suggesting an oncogenic role of TNFα in transcription of the c-myc pathway [322]. However, there is no literature on the potential role of TNFα/TNFR1 signalling in the oesophagus of patients with GORD, and its potential role in the processing of oesophageal pain needs to be investigated.

1.7.3 IL1R

IL-1β is a prototypic pro-inflammatory cytokine that has been frequently implicated as a driver of many inflammatory and autoimmune disorders and pain [323]. Whilst having homeostatic functions including sleep and temperature regulation under physiological conditions, its overproduction has been highlighted in the progression of many inflammatory diseases such as rheumatoid arthritis, IBD, neuropathic pain, and Alzheimer's disease [324], [325]. Recent studies have shed light on the complexity of the IL-1β secretory process during inflammation and pain via the inflammasome- an intracellular multi-protein complex that acts as a scaffold for proteolytic enzymes that cleave and secrete cytokines known as caspases [326]. IL-1β secretion, predominantly by circulating monocytes, is divided into two steps [327]: first, activation of TLR4 or 2 induces transcription of pro- IL-1β precursor protein, and second, conversion of pro- IL-1β into mature IL-1β via the inflammasome. The inflammasome complex forms upon the activation and oligomerisation of nod-like receptors by pathogen-associated molecular patterns or by nonmicrobial danger signals released by damaged cells [328]. The inflammasome then subsequently activates caspase-1, which cleaves and activates pro- IL-1β into its bioactive IL-1β form [329]. Although literature suggests the existence of two IL-1 receptors, IL-1R type 1 (IL-1R1) and IL-1 type 2 receptor (IL-1R2), IL-1β signals through binding IL-1RI, and IL-1RII is a decoy receptor which does not activate cell signalling when bound [330]. The binding of IL-1β to IL-1RI recruits an accessory protein (IL-1RAcP) to the cell membrane, forming a high affinity binding receptor complex [323]. This is followed by the rapid recruitment of adaptor protein myeloid differentiation factor 88 (MyD88) to the IL-1RI complex which also recruits interleukin-1 receptor-associated kinase 1 and 4 (IRAK1/4) to the receptor complex by interacting with the death domain of MyD88 (as shown in Figure 14) [331]. This subsequently activates the intracellular IL-1β signalling pathway, resulting in translocation of NF-κB to the nucleus, followed by transcription of proinflammatory genes, thus further perpetuating the inflammatory cascade [332], [333]. In this way, IL-1R can be considered an alarm receptor of the innate immune system which gets turned on by its endogenous alarmin (IL-1β) by indicating the breach of a barrier [334]. This is closely followed by the infiltration of leukocytes to the area of damage with the aim to repair this breach, resulting in acute inflammation at the site of injury via the canonical inflammasome signalling pathway [335], [336].

Expression of IL1R1 has been widely described for many different cell types including immune cells such as macrophages, T cells, dendritic cells, and B cells, but also non-immune cells including most epithelial cells [331]. Moreover, studies conducting qRT-PCR and *in situ* hybridization in rat dorsal root ganglia also detected IL1R1 expression in sensory neurons,

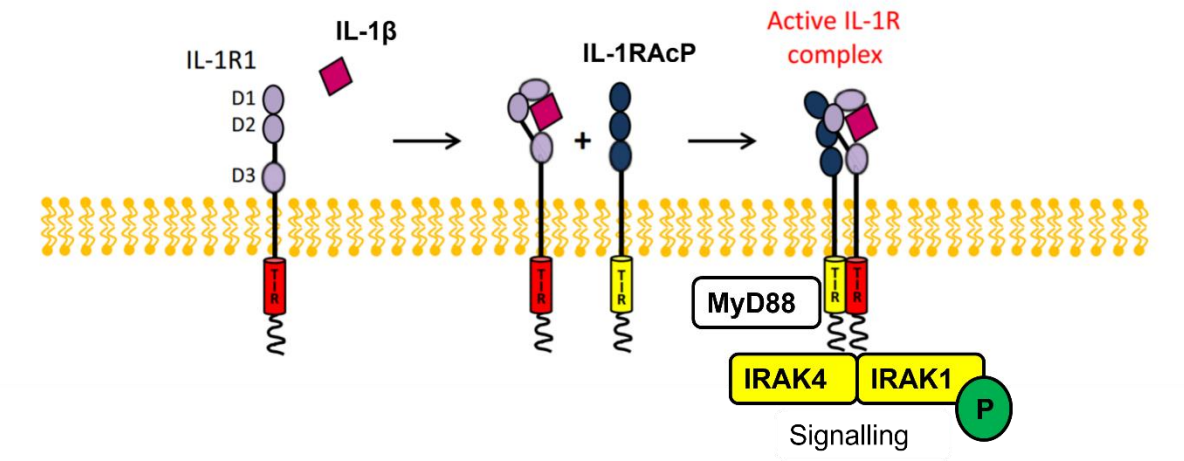

Figure 14 IL1R Signalling Complex Activation

Agonist cytokine IL-1β binds its receptor IL-1R via the receptor domains D1/D2 and D3, which induces a conformational change and recruits the accessory protein IL-1RAcP. Signalling is activated when the TIR domains dimerise, MyD88 is recruited and binds IRAK1 and 4 via its death domain. Figure adapted from Boraschi *et al*.

where IL-1β was found to sensitise sensory neurons to noxious heat in an IL-1R-signalling complex-dependent mechanism [337], [338]. Another *in vivo* rat study also demonstrated IL-1R1 colocalisation with NR1 subunit of the NMDA receptor in neurons of the spinal trigeminal complex using immunostaining experiments, suggesting the coupling of NMDA receptor phosphorylation through IL-1R signalling [339]. Moreover, recent literature has suggested the expression of IL-1R1 on almost all cells of the body, and its requirement of relatively little regulation.

IL-1R signalling has been indicated in immune responses to inhaled particulate matter such as asbestos, whereby inhalation of such particles induced IL-1β secretion in the lung. Moreover, experiments using IL-1R$^{-/-}$ mice collectively suggested attenuated pulmonary inflammatory response to toxic airborne particles in the absence of IL-1β signalling [340], [341]. The involvement of IL-1β signalling has also been implicated in neuropathic pain generation in several studies in animal models of neuropathic pain, where IL-1β expression was found to increase upon injury to the sciatic nerve, DRG, and spinal cord [342], [343]. A mutant murine model with delayed immune response to nerve injury at the site of lesion also exhibited decreased expression of IL-1β in macrophages and Schwann cells [344]. There is also evidence highlighting the ability of IL-1β to directly induce neuronal excitability by regulating nociceptors including TRPV1, GABA receptors, and NMDA receptors [345]. One such evidence is presented by a study which administered IL-1β to an *in vitro* hind-paw skin preparation by a plantar injection and recorded action potentials of the rat DRG in response to mechanical and thermal stimulation [346]. This study demonstrated that IL-1β reduced the threshold pressure for neuronal firing by 58%, suggesting an important role for IL-1β in

cutaneous hyperalgesia [346]. Additionally, an *in vitro* study on a rat skin model demonstrated heat-induced release of CGRP from cutaneous nociceptors when administered with 2.7ng/ml IL-1β, further demonstrating an important role of IL1R signalling in hyperalgesia in the skin [313]. Importantly, the intrathecal administration of IL-1β neutralising antibody was found to significantly reduce allodynia in a mouse model of neuropathic pain, highlighting the possibility that IL-1β regulates neuropathic pain at several different sites in the organism [342]. These findings have been further supported by studies in genetically engineered mice models ($IL1R1^{-/-}$ and mice overexpressing the naturally occurring IL1R antagonist in astrocytes) where both the knockout of IL1R1, and its antagonism were found to decrease thermal hyperalgesia and mechanical allodynia [347]. These collectively implicate the IL1R signalling pathway in painful and inflammatory settings both peripherally and centrally.

In the intestine, the release of IL-1β from the inflammasome and subsequent activation of IL1R signalling has been shown to recruit neutrophils to prevent bacterial colonisation [348]–[350]. More recent studies assessed epithelial tight junction barrier permeability response in mice by administering intraperitoneal injections of IL-1β and measuring the marker inulin in intestinal tissue collected from mice with colitis and analysed immunohistochemically and with RT-PCR [351]. This study reported increased levels of *IL-1β* mRNA and decreased expression of occludin mRNA by enterocytes and subsequently increased barrier permeability and thereby increased penetration of luminal antigens into the intestinal mucosa [351]. Moreover, inhibiting this IL-1β-induced disruption to the intestinal epithelial tight junction barrier with an antagonist to MIR200C-3p, miRNA that binds to the occludin 3'UTR to decrease occludin mRNA, was found to protect against development of colitis [351]. This gives rise to the possibility that the barrier breach induced by IL-1β signalling contributes to intestinal inflammation [352].

Similarly, in the oesophageal mucosa, expression of IL-1β highly correlated with histopathological grades of inflammation. In a study which performed PCR and immunohistochemical analysis of biopsy samples from patients with NERD, ERD, and BO, mRNA expression of IL-1β was upregulated 3-10-fold more than in NERD and BO samples [277]. Moreover, another study assessing the IL-1β expression in patients with long segment BO using an ELISA following organ culture of BO patient biopsies detected increased IL-1β expression following exposure of the BO oesophageal mucosal culture to acid and bile acid, which positively correlated with the histopathological inflammation score [277]. Despite the functional studies on IL-1β expression in the oesophageal mucosa of patients with BO and ERD, data on the localisation and function of IL1R in the oesophagus remains limited. Given IL1R's role as an 'alarm' receptor of the innate immune response and the pivotal role it plays in sensing irregularities that requires the swift attention of the cells of the immune system in

other systems, and the therapeutic potential of IL-1β inhibition, IL1R is an important cytokine receptor whose function should be further investigated in the context of GORD.

1.7.4 IL6ST

IL6ST, also known as gp130, is a signal transducing receptor that forms part of a receptor complex with the non-signalling IL6 receptor (IL6R) for several cytokines including IL6 to mediate signal transduction [353]. Molecular cloning studies of gp130 cDNA revealed its single transmembrane domain, and increased affinity IL6-binding sites following IL6ST/gp130 association with the non-signalling IL6R as shown in Figure 15 [354]–[356]. The binding of IL6 to IL6R triggers the formation of a heterodimeric receptor complex with an IL6ST homodimer and two IL6R domains [357]. Janus kinases JAK1 and JAK2 are constitutively bound to IL6ST cytosolic domain, but receptor engagement of IL6 with IL6ST and IL6R induces their phosphorylation and subsequent activation [358]. JAK1/2 then phosphorylates STAT in turn, initiating its translocation to the nucleus and activation of gene transcription. However, as shown in Figure 15, the activation of IL6ST signalling can trigger the downstream activation of three different signalling cascades, with JAK-STAT pathway being the most common, and less being known about the IL6-mediated MAPK or PI3K/AKT pathways [353].

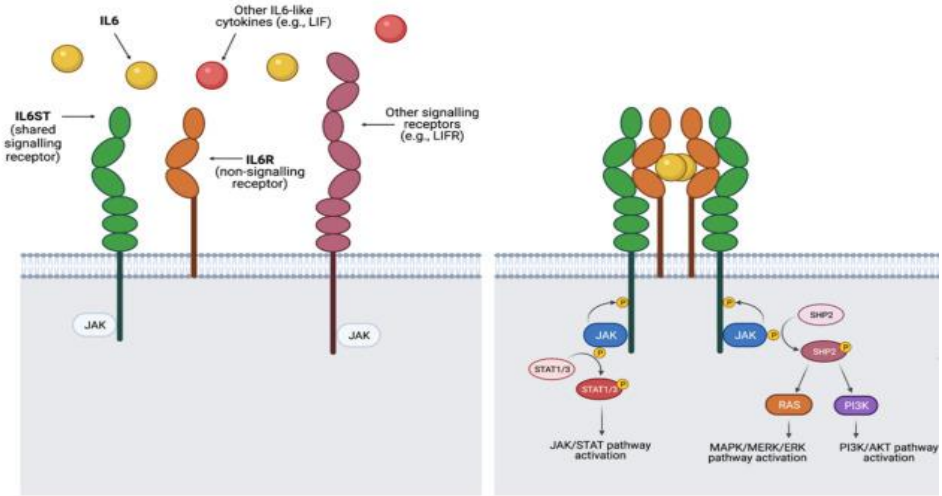

Figure 15 IL6ST Signalling When Bound by IL6

Diagram summarises IL6 signalling via IL6ST/IL6R complex. IL6-family of cytokines bind transmembrane IL6R complex, of which at least 1 strand is always IL6ST. Following the dimerization of the receptor, cytoplasmic tyrosine kinases (JAK) get activated which can trigger 3 signalling pathways: JAK/STAT, MAPK/ERK, and PI3K/AKT signalling depending on the cytokine that binds the receptor complex. In the case of IL6, the cytokine binds IL6R which lacks cytoplasmic tyrosine kinase domains, leading to the formation of a heterodimeric signalling complex with the IL6ST homodimer. Figure from Martinez-Perez *et al*.

Although initially described in mice as a membranous glycoprotein on activated T cells, but not on resting lymphocytes, its expression has since been recognised on both haematopoietic and nonhematopoietic cells ubiquitously [353]. A study which assessed surface expression of IL6ST on peripheral T cells found them to be expressed in a regulated manner, with T cells being physiologically $IL6ST^{+}IL6R^{+}$, but downregulated upon T cell receptor engagement both *in vitro* and *in vivo* [359]. More recently, IL6ST expression has also been reported in gastric epithelial cells in a study which examined the effect of *Helicobacter pylori* infection of gastric epithelial cell lines AGS and MKN-28 by RT-qPCR [360]. Moreover, a luciferase reporter gene assay detected higher mRNA and protein expression levels of IL6ST in asthmatic airway epithelial cells compared to normal human bronchial epithelial cells. In this study, IL6ST was found to be a downstream target of miR-200c-3p, whereby miR-200c-3p inhibition downregulated IL6ST expression at both mRNA and protein level, thus suggesting a role for IL6ST signalling in asthmatic inflammation [361].

IL6ST has been shown to be critically involved in a range of biological processes by studies which demonstrated development of myocardial and haematopoietic defects in $IL6ST^{-/-}$ mice embryos [362]. In the colon of mice with DSS-induced colitis, IL6ST mRNA was found to be upregulated in microRNA 31 (MIR31)-knockout mice with colitis compared to control mice, suggesting that the inflammatory response in murine colonic epithelium is activated when MIR31 loses its direct ability to suppress IL6ST and thus fails in suppressing the immune response [363]. Moreover, IHC of sections from a preclinical $IL6ST^{F/F}$ gastric cancer model in mice demonstrated expression of phosphorylated STAT3+ cells in tertiary lymphoid structures formed in the gastric submucosa, suggesting the dependence of tumorigenesis on IL6ST signalling [364] Importantly, the role of IL6ST signalling has also recently been implicated in pain pathogenesis. An *in vivo* $IL6ST^{-/-}$ mouse model with selective deletion of IL6ST from peripheral sensory nerves alleviated heat hyperalgesia in these $IL6ST^{-/-}$ mice injected with CFA compared to $IL6ST^{fl/fl}$ mice which remained hypersensitive [365]. Moreover, application of hyper-IL6 (HIL6) into the foot pad of a hindpaw in $TRPV1^{-/-}$ mice demonstrated a reduced paw withdrawal latency to heat stimulation in TRPV1 KO mice compared to WT, suggesting an important role for neuronal IL6ST expression in regulation of TRPV1 activation in inflammatory pain disorders [365]. These findings were further supported by a recent transgenic mouse model with conditional IL6ST depletion in $Nav1.8^{+}$ neurons, which reported significantly less mechanical hypersensitivity in the von Frey test *in vivo* following nerve injury in the $IL6ST^{-/-}$ mice compared to WT [366]. In this study, the reduced mechanical hypersensitivity in afferent nerves was associated with a downregulation of TRPA1 mRNA, highlighting another nociceptive receptor regulated by IL6ST signalling in sensory nerves in neuropathic pain disorders. Furthermore, antigen-induced arthritis in a $IL6ST^{-/-}$ mouse model

recently highlighted significantly lower serum concentrations of CGRP and IL6, and presented with a lack of upregulation of CGRP in sensory neurons compared to IL6ST$^{fl/fl}$ mice, suggesting a role of IL6ST signalling in neurogenic and joint swelling in arthritis. Thus, IL6ST signalling in sensory neurons is not only a regulator of pain pathogenesis but is also involved in modulating the inflammatory response.

In the oesophageal mucosa, increased levels of IL6 secretion have been detected in BO segment compared to the squamous epithelium from adjacent sites in the same patients at both mRNA and protein level, and suggested to contribute towards the development of oesophageal adenocarcinoma [367]. In oesophageal squamous cell carcinoma, IL6 secreted by cancer associated fibroblasts was found to modulate chemoresistance by upregulating CXCR7 expression via the activation of the NF-KB pathway [368]. However, data on the role of IL6 signalling in the oesophageal mucosa of patients with BO, ERD, NERD, and FH in the context of heartburn pathogenesis is lacking. Given the bidirectional coordination of pain and inflammation via IL6ST signalling in the process of arthritis and models of neuropathic pain, the inflammatory and sensory role of this cytokine receptor should also be investigated in the oesophageal mucosa of patients with GORD.

1.7.5 CXCR2

C-X-C chemokine receptor 2 (CXCR2) is an important multifunctional receptor which has been increasingly highlighted as a mediator of inflammation, wound healing, tumorigenesis, and the development and maintenance of chronic pain through its activation by CXCL8 (IL8), the endogenous ligand for CXCR2 [369], [370]. Like all other chemokine receptors, CXCR2 is a GPCR with a DNA sequence containing a single long open reading frame encoding an amino acid sequence matching that of the rhodopsin superfamily of GPCRs, as identified by a study which isolated DNA encoding CXCR2 from human neutrophils [371]. A recent study which assessed the crystal structure of CXCR2 using cryo-electron microscopy demonstrated that IL8, can bind and activate CXCR2 in both a monomer and dimer form, with its ELR motif binding TM5 and TM6 regions of the receptor by forming hydrogen bonds and electrostatic interactions [315]. Original studies demonstrated CXCR2 coupling to cytoplasmic Gαi subunits by administering neutralising-Gαi peptides into human neutrophil suspensions which was found to completely block calcium release upon stimulation with IL8 [372]. Thus, CXCR2 activation initiates intracellular signalling cascades by inducing the disassociation of Gαi from Gβγ subunits of its G protein as shown in Figure 16. A study investigating expression of different G protein subunits in COS-7 cells detected IL8-induced activation of endogenous

inositide-specific phospholipase C (PLC) when transfected with Gα subunits, suggesting Gα release from its βγ subunits to activate the PLC β2 isoform [373]. This was further reinforced by a recent study which detected a CXCR2/PLC-β2 macromolecular complex in neutrophils by co-immunoprecipitation and found this to be critical in calcium mobilisation and subsequent chemotaxis of neutrophils [374]. Thus, Gαi disassociation from Gβγ subunits of the G protein activates several downstream signalling cascades including rapid release of Ca^{2+} from the endoplasmic reticulum via the activation of phospholipase C-β2 (PLC-β2) (as shown in Figure 16). Moreover, CXCR2 activation and Gαi/Gβγ disassociation has also been shown to induce rapid phosphorylation of growth kinases such as ERK1/2 in human neutrophils, as shown in Figure 16. This was demonstrated by a study which showed suppressed IL8-induced chemotaxis of polymorphonuclear leukocytes when treated with the MEK inhibitor PD98059 *in vitro* [375]. Importantly, a structural cryo-electron microscopy study also used a highly selective allosteric CXCR2 antagonist (00767013) to assess the structure of inactive CXCR2, demonstrating a more compact extracellular region in the ligand activated form of CXCR2 compared to the inhibited form, and suggested the possibility of pharmacological application of small molecule antagonism of CXCR2 to inhibit its pathological effects [315].

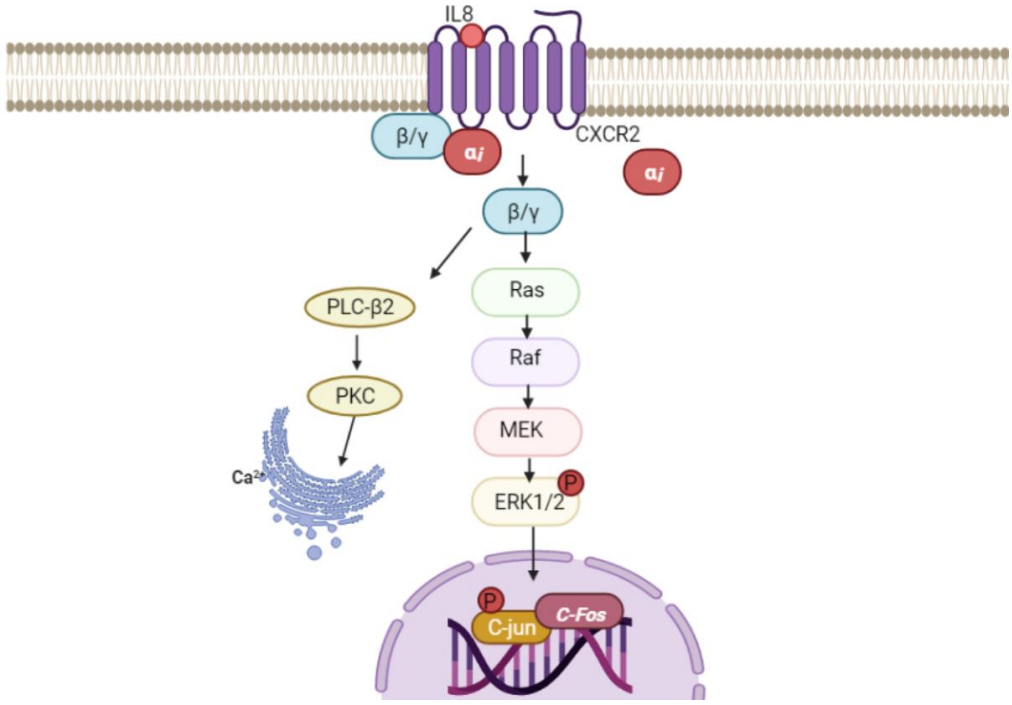

Figure 16 IL8/CXCR2 Signalling Cascade

IL8 binding CXCR2 can activate multiple G-protein mediated signalling mechanisms. Upon CXCR2 activation, Gαi subunit disassociates from the G protein βγ subunits, enabling subsequent phosphorylation of ERK1/2 to enable translocation of ERK1/2 to the nucleus and gene transcription to enable cell survival, proliferation, and chemotaxis. Moreover, Gβγ can also activate PLC-β2, inducing rapid release of Ca2+ from the endoplasmic reticulum. Figure created using BioRender.com

CXCR2 expression has been reported on a range of immune cells including granulocytes, monocytes, mast cells, and natural killer cells [370]. Double colour flow cytometry studies on human peripheral blood leukocytes reported variation in the level of CXCR2 expression among leukocyte subsets, with all neutrophils and monocytes, 7-42% CD8+ T cells, and 39-76% CD56+ NK cells being found to express CXCR2, while CD20+ B cells and CD4+ T cells exhibited no CXCR2 expression [376]. Moreover, another flow cytometry study on a B16F10 tumour-bearing mouse model detected CXCR2 expression on $CD45^{+}Ly6G^{-}$ bone marrow cells which increased in number in correlation with tumour growth. The same study also found compromised growth of macrophage progenitor cells which would otherwise regulate myeloid cell differentiation in the tumour microenvironment of CXCR2-deficient mice, suggesting a regulatory role for CXCR2 in tumour progression [377]. However, CXCR2 expression has also been demonstrated in the squamous epithelium of skin, oesophagus, and ectocervix in a membranous staining pattern, while epithelial cells in the stomach, small intestine, colon, lung, and kidney did not express any CXCR2 in archival neuroendocrine tissues [378]. Moreover, in a study which performed double staining IF and *in situ* hybridisation, CXCR2 expression was also detected on cultured spinal cord neurons which was upregulated at both mRNA and protein level with intraplantar CFA injection 3 days after injection [379], [380]. CXCR2 thus shows a highly variable expression pattern throughout inflammatory, pain and cancer settings and plays important regulatory roles in the tissue in which it is detected.

In the maintenance of inflammatory pain, many studies have investigated the role of CXCR2. One such study knocked down CXCR2 in mouse DRGs by injecting CXCR2 specific small interfering RNAs (siRNA) into the perisciatic nerve, and demonstrated attenuation of CFA-induced neuropathic pain symptoms including mechanical allodynia and heat hyperalgesia [381]. These findings have been further corroborated by studies in other neuropathic pain models including spinal nerve ligation and sciatic chronic constriction injury which reported an upregulation of CXCR2 in both peptidergic and nonpeptidergic neurons with IF, suggesting a regulatory role for CXCR2 signalling in peripheral mechanisms of neuropathic pain [382]. However, CXCR2 has also been widely suggested to regulate neutrophil chemotaxis from peripheral blood to inflamed tissue in the innate immune response [383]. In a murine model of autoantibody-induced arthritis, synovial fluid leukocytes isolated from the ankle joints were analysed for CXCR2 expression and demonstrated increased CXCR2 mRNA expression on neutrophils recruited into the joint, suggesting the preferential recruitment of CXCR2+ polymorphonuclear cells into the inflamed joint [384]. This study also revealed delayed initiation of arthritis in mice deficient for CXCR2 compared to WT mice, reinforcing the notion that CXCR2 is required for neutrophil chemotaxis into a site of inflammation [384]. Moreover, increased numbers of neutrophils within intestinal epithelial crypts in IBD patient mucosal

biopsies has been found to directly correlate with the severity of epithelial damage and clinical disease progression [385]. Thus, CXCR2-induced neutrophil migration could serve as an important marker of mucosal inflammatory disease activity and neuropathic pain pathogenesis.

Unsurprisingly, oesophageal literature on the role of CXCR2 signalling in pain and inflammation exists predominantly in relation to the development of oesophageal squamous cell carcinoma. In a study which examined the relationship between IL8/CXCR2 expression by IHC analysis and oesophageal squamous cell carcinoma progression, increased IL8/CXCR2 was found to be directly associated with a shorter overall survival, thus highlighting CXCR2 as a prognostic marker in oesophageal cancer [386]. In another IHC study of CXCR2 expression in archival specimens from oesophageal squamous cell carcinoma patients who underwent oesophagectomy, recurrence-free survival rates were significantly lower in patients who expressed CXCR2 compared to the CXCR2-negative group [387]. Moreover, in another study which transfected oesophageal cancer cell lines with siRNA against CXCR2, rates of cell growth and invasion were significantly reduced in oesophageal cancer cells with silenced CXCR2 compared to controls, highlighting CXCR2 as a therapeutic target for oesophageal cancer [388]. Although data on the role of CXCR2 in the oesophageal mucosa of patients with GORD is limited, recent studies have investigated mechanisms involved in IL8 production by human oesophageal epithelial cells (HEEC). In HEECs stimulated with bile acids and inflammatory cytokines and assessed with ELISA and qPCR, there was significantly higher IL8 secretion by epithelial cells stimulated with bile acids compared to neutral-pH media. Moreover, the same group also assessed biopsies from patients with heartburn, and detected a positive correlation between IL8 expression at mRNA level and the severity of oesophagitis and inflammatory cell infiltration [389]. Despite lower IL8 expression in NERD patients compared to ERD, NERD patients had higher IL8 expression than healthy controls, suggesting that IL8 expression in the oesophageal mucosa could be an important regulator of oesophageal inflammation, even in patients with NERD [390]. IL8/CXCR2 is thus an important marker involved in many complex pain and inflammatory mechanisms, and its role in GORD pathogenesis needs further investigation.

1.7.6 RAMP1

Receptor activity-modifying protein 1 (RAMP1) has been implicated as a contributor to the development of CGRP-induced chronic pain [391]. RAMP1 is a single membrane-spanning protein which forms part of the CGRP heterodimer receptor complex with seven

transmembrane spanning GPCR calcitonin receptor-like protein (CLR), and receptor component protein (RCP) as shown in Figure 17 **CGRP Receptor Complex** [392]. In the discovery of the CGRP receptor, CLR was long suspected to be the sole receptor for CGRP. However, expression-cloning of CLR in model cell line SK-N-MC from human neuroblastoma found that CLR did not traffic to the cell surface, making CGRP unable to bind and elicit cellular response [393]. Subsequent studies in Xenopus oocytes injected with complementary RNA from the model cell line recorded inward currents in response to CGRP application that were larger than the endogenous response in Xenopus oocytes without the SK-N-MC cRNA [393]. Repeatedly isolating the pool of clones according to their CGRP response identified a 148-amino acid protein which is now known as RAMP1, and whose response was inhibited by a CGRP antagonist [393], suggesting that co-expression of RAMP1 with CLR was necessary to induce a substantial cellular response to CGRP. Moreover, the role of RCP in CGRP-induced signalling was later examined by using RCP antisense RNA to silence RCP expression in model cell lines which contained endogenous RCP. Whilst the level of CGRP receptor expression at the cell surface remained unaffected, CGRP-induced cAMP production was significantly attenuated, highlighting an important role for RCP in downstream CGRP receptor signalling [394]. Kinetic and biophysical evidence of increased neuronal production of cAMP in cultured trigeminal ganglion neurons when transfected with adenoviral RAMP1 vector further highlights that CLR needs RAMP1 for both its trafficking to the cell surface and its binding to CGRP, and RCP for its coupling to Gαs [395]. Upon CGRP binding the N-terminal pocket formed by CLR and RAMP1 in the extracellular domain (as shown in Figure 17), the CGRP receptor most frequently activates the cAMP signalling pathway to regulate gene expression and ion channel activity [396]. Moreover, as with most GPCRs, the CGRP receptor complex also undergoes a conformational change that results in serine and threonine

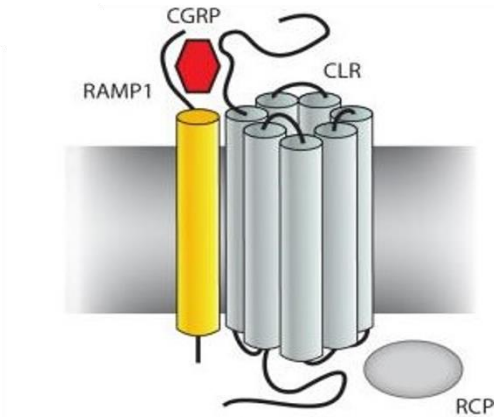

Figure 17 CGRP Receptor Complex

RAMP1-CLR-RCP heterodimer complex with CGRP bound to the extracellular N-terminal pocket formed by CLR and RAMP1 together. RCP interacts with CLR via its second intracellular cytoplasmic loop. Figure by Russo *et al*.

residues' phosphorylation by G protein kinases [397]. This phosphorylation event increases the affinity of the CGRP receptor for β-arrestins which translocate to the plasma membrane, where they act as a molecular scaffold for clathrin and adapter proteins such as AP-1 to induce the internalisation and endocytosis of the GPCR [398].

Most literature around CGRP signalling is in the context of primary headaches and migraines, in which CGRP has been shown to play a pivotal role [399]. RAMP1 expression has been recently described on neurons of the rat trigeminal ganglion with IHC [400]. Moreover, RAMP1 immunoreactivity has also been found within arterial blood vessels, mononuclear cells, and Schwann cells within the cranial dura mater [401]. However, RAMP1 expression has also been widely reported on numerous immune cells, thereby enabling CGRP modulation of the immune response [392]. RAMP1 immunoreactivity was also recently reported on CD11b-immunoreactive macrophages and S100A4-immunoreactive fibroblast, but not blood vessel endothelial cells, nor lymphatic endothelial cells [402]. Moreover, in a mouse model of DSS-induced colitis, RAMP1 expression was shown on macrophages, mast cells, and T cells [408]. RAMP1 expression has also been reported on Kupffer cells in the liver, where it was found to play an important role in immune-mediated hepatitis [404]. Thus, RAMP1 is widely expressed on immune cells where it acts as a key regulator of the immune response in multiple disease settings.

The immunosuppressive actions of CGRP signalling via RAMP1 has been well described in the colon [405]. An *in vivo* study in a mouse colitis model which assessed colonic mucosal changes found increased accumulation of inflammatory cells including macrophages, mast cells, and T cells in RAMP1$^{-/-}$ mice, which also exhibited increased levels of TNFα, IL1β, IFNγ, and IL17 compared to WT, suggesting a mucosal protective role for RAMP1 via the attenuation of inflammatory cell recruitment to the site of inflammation [405]. Moreover, RAMP1 signalling has also been shown to play an important role in immune cells during inflammation-related lymphangiogenesis, where RAMP1$^{-/-}$ mice injected with LPS had suppressed lymphangiogenesis compared to WT mice, which was coupled with reduced expression of vascular endothelial growth factors (VEGF), and infiltration of fewer CD4+ T cells [406]. These findings were further supported by a study investigating skin wound healing in RAMP1$^{-/-}$ mice which demonstrated suppressed wound healing and wound-induced angiogenesis in mice with silenced RAMP1, coupled with decreased expression of VEGF-C [407]. Indeed, RAMP1 signalling has also been highlighted in the growth of endometrial tissue and angiogenesis and lymphangiogenesis in the pathogenesis of endometriosis, whereby transplant of endometrial tissue from donor WT mice into the peritoneal wall of RAMP1$^{-/-}$ mice resulted in reduced implant growth and angiogenesis compared to transplant into WT mice where the endometrial implant grew with increased density of blood and lymphatic vessels [402]. This study also

demonstrated limited endometrial growth and angio/lymphangiogenesis when endometrial implants were administered with CGRP receptor antagonist CGRP8-37 [402]. A recent study which silenced RAMP1 expression by conditional gene-targeting reported high blood pressure by vascular contraction in mice which was caused by deficient CGRP signal transduction [408]. Moreover, LPS administration into $RAMP1^{-/-}$ mice induced a significant increase in serum levels of CGRP compared to $RAMP1^{+/+}$ mice. In this study, LPS administration was also found to supress TNFα secretion and induce IL-10 release by bone marrow-derived dendritic cells in $RAMP1^{+/+}$ but not $RAMP1^{-/-}$ mice, suggesting CGRP-induced immunosuppression via RAMP1 activation on dendritic cells [408]. However, CGRP signalling also contributes critically to peripheral sensitisation of nociceptive nerves in migraine pathogenesis. For example, intravenous infusion of the known migraine trigger nitric oxide in a rat migraine model was found to induce increased RAMP1 expression on trigeminal ganglion neurons, suggesting enhanced RAMP1 signalling underlying the pathological mechanism of migraine attacks [409]. Recent IHC findings of RAMP1 expression on human and rat trigeminal ganglion neurons and glial cells further suggests a site and mechanism of action for migraine therapy [410]. However, co-expression with CGRP was very rare, suggesting CGRP and RAMP1 expression on separate neurons [401]. The development and FDA approval of CGRP receptor monoclonal antibody erenumab as a therapeutic for migraine further highlights the potential of manipulating RAMP1 signalling to alleviate chronic or episodic pain [391], [411].

Despite the importance of RAMP1 signalling in the regulation of peripheral sensitisation, neuropathic pain, and the immune response, little is known about the distribution and function of RAMP1 in the oesophagus, where 90% spinal afferent neurons are known to contain the RAMP1 ligand CGRP [412]. In the mouse oesophagus, RAMP1 was detected immunohistochemically on IGLEs in contact with CGRP-immunoreactive spinal afferent nerve endings, and in the myenteric plexus. This suggests a possible modulatory role of RAMP1 signalling in regulating hypersensitivity or motility reflexes [412]. However, neither the anatomical nor the functional basis for RAMP1 in the human oesophagus has been investigated. Thus, the role of RAMP1 signalling remains a promising therapeutic avenue to explore in the context of heartburn in patients with GORD.

1.8 Inflammation in GORD

The traditional consensus for the pathophysiology of ERD is assumed to develop as a caustic chemical injury, whereby refluxed gastric acid and pepsin damage the squamous epithelial cells [413]. However, studies in a rat model of reflux oesophagitis demonstrated that disease onset follows infiltration of T lymphocytes and leads to basal cell hyperplasia [414]. Subsequently, a new concept for ERD pathogenesis included the possibility in which refluxed acid does not damage squamous epithelial cells lining the oesophagus, but rather induces them to secrete cytokines to activate proliferation and attract T cells which in turn cause damage to the mucosa [414]. In a clinical study where patients with healed ERD through PPI usage got induced acute oesophagitis by interrupting their PPI therapy, disease onset was found to begin with a T lymphocyte-predominant inflammation of the oesophagus, followed by the development of hyperplasia [275].

Hypoxia-inducible factors (HIFs) are a family of transcription factors that respond to hypoxic stress and promote inflammation, and have been recently highlighted as critical mediators of oesophageal inflammation [415], [416]. Patients with acute oesophagitis after stopping PPI treatment showed an associated increase in HIF-2α in the oesophageal epithelium [414]. Moreover, human oesophageal squamous epithelial cell lines exposed to bile acid *in vitro* demonstrated decreased prolyl hydroxylase activity by generating intracellular reactive oxygen species and causing a sustained increase in HIF-2α [417]. In the normal state, HIF-α subunits are degraded and inactivated by proteasomes such as prolyl hydroxylase which catalyse HIFs [415]. Thus, exposure to bile acid induced HIF-2α accumulation by preventing its degradation (as seen in a state of hypoxia) [418]. This increase in HIF-2α was shown to be coupled to increased epithelial activity of NF-KB, increased immunostaining for p65, and an upregulation of mRNA levels of proinflammatory cytokines (COX-2, IL8, IL1β, TNFα, and ICAM-1) (Figure 18) [417]. When stabilised, HIFs have been reported to translocate to the nucleus and stimulate the transcription of target genes, explaining why the stabilisation of HIF-2α activated the NF-KB-dependent inflammatory pathway in epithelial cells in the present study [419]. Thus, epithelial cells in the oesophageal mucosa secrete T cell chemokines as a result of HIF2α signalling. The findings of this study support the novel hypothesis that ERD development is initiated by T lymphocyte-led inflammation, causing damage to the oesophagus as a result of increased HIF-2α activity [420].

Furthermore, the oesophageal mucosa of GORD patients produces higher levels of various inflammatory cytokines compared with healthy controls [390]. Interleukin-8 (IL-8), a known neutrophil chemoattractant, was overexpressed in mucosa of GORD patients compared to

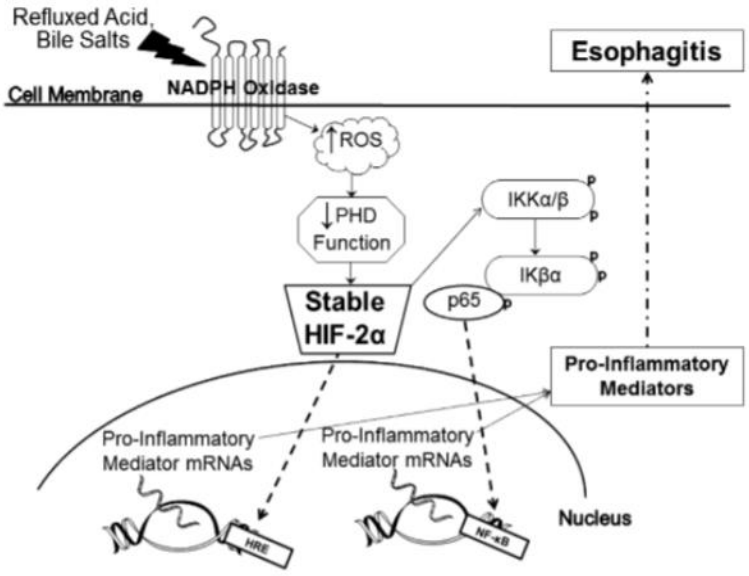

Figure 18: Signalling mechanism of stabilised HIF-2α

Diagram demonstrating the mechanism of bile acid-induced HIF-2α stabilisation and subsequent stimulation of proinflammatory cytokines which contribute to the development of ERD. Bile acid salts reduce PHD function by activating the NADPH oxidase system to generate ROS which causes a stable increase in HIF-2α. HIF-2α in turn activates the NF-κB/p-65 signalling pathway which increases the transcription of pro-inflammatory cytokines. PHD, prolyl hydroxylase; ROS, reactive oxygen species [416]

controls, and was correlated with histological disease severity [421]. Huo *et al* demonstrated that oesophageal epithelial cells secrete IL-8 when exposed to acidic bile salts which activate the IL-8 promoter by binding NF-KB and AP-1 DNA binding sites. They also showed that IL-8 secretion is suppressed when omeprazole is administered by blocking the nuclear translocation of the NF-KB subunit p65, thereby preventing the binding of p65 with AP-1 subunits c-jun and c-fos [422]. Importantly, acid-induced production of IL-8 by oesophageal epithelial cells acts as a chemoattractant for lymphocytes, and there is a direct relationship between IL-8 levels and severity of ERD [423].

The chronic inflammatory state induced by obesity in GORD has also been recently highlighted. A study that assessed the relationship between obesity and OGJ pressure segment morphology using high- resolution manometry demonstrated positive correlation between body mass index, waist circumference, and intragastric pressure [424]. This suggests that obese patients have increased likelihood of developing OGJ disruption, resulting in development of hiatal hernia, and an increased gastroesophageal pressure gradient leading to more reflux episodes. However, more recent data suggests that visceral obesity may induce systemic inflammation via the production of proinflammatory cytokines, which may have direct effects on oesophageal barrier function through downregulation of tight junction proteins

including claudin and occludin [425]. A recent study that assessed the influence of obesity on baseline impedance by using ambulatory pH impedance monitoring found that oesophageal impedance was significantly lower in obese patients without reflux, and non-obese patients with reflux compared to healthy controls [426]. These data suggest that obesity is associated with abnormal oesophageal impedance, which is a functional measurement of oesophageal barrier integrity. As such, it is important to consider the inflammatory effect that obesity may induce in the oesophageal mucosa when studying inflammatory mechanisms underlying heartburn pathogenesis.

1.8.1 Microinflammation

Unlike ERD where the mucosal injury apparent at endoscopy is clearly responsible for the troublesome heartburn symptoms induced by acid reflux, the absence of macroscopic mucosal injury suggests symptoms of NERD and FH occur via different mechanisms [427]. While IL-8 is known to mediate lymphocyte trafficking via its receptors in ERD, IL-8 mRNA levels have also been reported to be significantly higher in the oesophageal mucosa of patients with endoscopy-negative GORD compared to healthy controls. Moreover, there was an association between high levels of IL-8 mRNA and the presence of basal hyperplasia and intraepithelial neutrophils [428], suggesting that microscopic damage may underlie the pathogenesis of NERD [429]. Microscopic inflammation is a common type of oesophageal epithelial injury seen in patients with GORD [430]; the table below summarises the prevalence of individual lesions in ERD patients, as well as endoscopy-negative heartburn patients [431]. The prevalence of basal cell hyperplasia was significantly higher in ERD (95%), NERD (73%), and hypersensitive oesophagus (65%) compared to patients with FH (27%) and healthy controls (35%) [431]. Moreover, the concentration of eosinophils and neutrophil-led erosions in ERD (65%) and NERD (32%) were relatively higher than patients with FH (13%) and healthy volunteers (10%), suggesting that microscopic inflammation plays a role in endoscopy-negative GORD patients including NERD and those with hypersensitive oesophagus, but not in FH [432]. While these histological changes are not specific to GORD, occurring in other inflammatory conditions such as eosinophilic oesophagitis, it is important to consider these histological abnormalities when characterising the sensory phenotype of different GORD phenotypes.

Table 1 summarising the prevalence of individual lesions in GORD phenotypes [431]

Histological abnormalities *n* (%)	EE ($n = 20$)	NERD pH-POS ($n = 22$)	HE ($n = 20$)	FH ($n = 15$)	HVs ($n = 20$)	*p* value
Basal cell hyperplasia	19 (95 %)	16 (73 %)	13 (65 %)	4 (27 %)	7 (35 %)	0.0023
Papillae elongation	17 (85 %)	15 (68 %)	7 (35 %)	3 (20 %)	3 (15 %)	0.0002
Dilated intercellular spaces	19 (95 %)	21 (95 %)	14 (70 %)	5 (33 %)	5 (25 %)	0.0001
Eosinophils/neutrophils/erosion/necrosis	13 (65 %)	7 (32 %)	5 (25 %)	2 (13 %)	2 (10 %)	0.0073

EE erosive esophagitis, *NERD* non-erosive reflux disease, *HE* hypersensitive esophagus, *FH* functional heartburn, *HVs* healthy volunteers

It is thus possible to suggest that pain in the absence of overt inflammation, and persistent heartburn in the 30% of PPI-refractory GORD patients, could be explained by the concept of microinflammation in the oesophageal mucosa. A recent study measured low-grade inflammation with electrical conductivity of the oesophageal mucosa of heartburn patients without visible macroscopic breaks administered with rabeprazole for 2 weeks [433]. *In vivo* bioelectrical admittance measurements from these patients after short-term PPI treatment demonstrated higher admittance in patients with good responses to PPI, and assessment of histological alterations highlighted significant association between severity of microinflammation and oesophageal permeability [433]. These results suggest that in the absence of overt inflammation, more subtle inflammation in the oesophageal mucosa, possibly with small numbers of leukocytes releasing inflammatory mediators to sensitize sensory afferent nerves, could be an important underlying mechanism for pain in the absence of macroscopic injury [434].

1.9 Hypothesis

Neuronal acid-sensing and neuro-immune interactions generate oesophageal symptoms and vary between different reflux phenotypes.

1.9.1 Aims

- Investigate the expression of candidate acid-sensing receptors on epithelial nerves in NERD, FH ERD, and Barrett's oesophagus patients, and healthy volunteers
- RNA analysis of the genes expression level of ion channels: *TRPM8, TRPV1, TRPA1, ASIC1-3*), nerve growth factors (*NGF* and *GAP43*), and inflammatory mediators (*IL8, TNF-α, IL-1β, IL6*) in endoscopic mucosal biopsies from NERD, FH ERD, and Barrett's oesophagus patients and healthy volunteers
- Investigate the relation between the characterisation of mucosal afferent nerves and inflammatory mechanisms in endoscopic mucosal biopsies from NERD, FH, ERD and BO patients.
- Assess the global transcriptome in GORD and healthy control oesophageal mucosa to enable further understanding of the functions and regulatory mechanisms of genes involved in heartburn pathogenesis and insight into novel genes that may be useful to investigate as potential biomarkers for further research.

2 Characterisation of mucosal afferent nerves in the oesophageal mucosa of patients with GORD

2.1 Introduction

The overwhelming majority (70%) of GORD patients belong to the sub-group NERD as defined by increased oesophageal acid exposure but macroscopically 'normal' oesophageal mucosa. As described in section 1.2 Diagnostic evaluation of GORD, these non-erosive patients are a unique group who exhibit heightened sensitivity to intra-oesophageal perfusion of acidic and nonacidic solutions compared to healthy controls, and equal or higher sensitivity compared to patients with endoscopically visible inflammation (ERD) [59]. Woodland *et al*. has shown superficial localisation of sensory afferent nerves in patients with NERD, but deeper lying nerves in the oesophageal mucosa of patients with ERD, BO, and controls [256]. This could be a partial explanation for acid hypersensitivity in patients with NERD due to the increased proximity of sensory nerve endings to the noxious refluxate and, therefore, greater exposure of their afferent nerves to acid reflux. However, the neurochemical profiles of these afferent nerve endings have not been further characterised.

This is in contrast to the lower GIT where primary afferent neurons innervating the gut have been extensively characterised morphologically (cell size, location, microscopic structure of nerve endings), according to neurochemical profile (their neurochemistry, the ion channels and receptors that they express), and functional neuronal properties (basal firing rate, thresholds), as detailed in section 1.4 Peripheral pathways of pain sensation in the oesophagus [435]. Importantly, colon-projecting sensory neurons in mice were further refined by a novel single-cell RNA sequencing study into seven neuronal subtypes that selectively express marker genes [436]. Human intestinal studies have also highlighted how mucosal inflammatory mediators released by IBS patients regulate hypersensitivity through increased expression of receptors for neurotrophins (such as NTRK1), as detailed in section 1.7 Neuroimmune crosstalk in the oesophagus [270]. Therefore, the rationale behind our study was to investigate how similar alterations in the neurochemical profiles of sensory mucosal afferents innervating the human oesophageal mucosa of GORD patients may be involved in sensing noxious stimuli.

The chemosensitive function of sensory neurons is attributed to their expression of a range of ion channels and receptors, as described in section 1.5 Ion channels in pain sensation. Increased TRPV1 expression in sensory afferent nerves is associated with hypersensitivity,

with pro-inflammatory mediators including nerve growth factors indirectly sensitising the channel by lowering its activation threshold [437]. Moreover, submucosal capsaicin injection into the oesophagus of healthy subjects induces chest pain that resembles the description of symptoms by patients with reflux disease and oesophageal motility disorders [438], [439]. TRPA1 has also emerged as an important sensory transductor in the context of visceral hypersensitivity and inflammation in the GIT, inducing colitis in experimental models which demonstrate the upregulation of sensory mediators SP and CGRP release from nerve fibre endings [440]. Expression studies in guinea pig have shown TRPM8 to be highly expressed in oesophageal vagal jugular neurons and C-fibres [234], while clinical studies have shown menthol infusion into the oesophagus of GORD patients induces heartburn symptoms, suggesting a potential mechanism involving sensory neurons driving hypersensitivity [236]. ASIC3 protein expression has also been detected in the oesophageal epithelium of human oesophageal mucosal biopsies, where patients with more severe GORD symptoms demonstrated higher ASIC3 expression [441], and ASIC3 receptor expression in peripheral sensory nerves was shown to be upregulated via NGF during mucosal inflammation [242].

Alterations in the neurochemical profiles of sensory mucosal nerves innervating the oesophageal mucosa in GORD patients may be involved in heartburn sensation mechanisms. We hypothesise that nerve endings in the oesophageal mucosa have an acid-sensing role, and that their neurochemical profiles may differ in different reflux phenotypes. This chapter investigates the neuroanatomy and neurochemical profiles of sensory afferent nerve endings innervating the oesophageal mucosa of patients with GORD. It presents IHC data assessing the expression of ion channels (TRPM8, TRPV1, ASIC3) on neuronal subtypes in endoscopic mucosal biopsies from NERD, FH, ERD, and Barrett's oesophagus patients. In addition, RNA analysis data on the gene expression levels of these sensory ion channels (*TRPM8, TRPV1, TRPA1, ASIC3*) in endoscopic mucosal biopsies from NERD, FH, ERD, and BO patients will be presented. Taken together, these results fulfil our aim of characterising the differences in the sensory innervation of the oesophageal mucosa among subgroups of GORD patients, and give guidance for potential future topical therapies to alleviate heartburn symptoms.

2.2 Materials and Methods

2.2.1 Patient Biopsies

All patients were prospectively recruited following informed consent and were required to have a clinical history of problematic heartburn requiring investigation. A total of 57 patients were recruited from the Royal London Hospital (Barts and the London School of Medicine and Dentistry, Queen Mary University of London, UK) for immunohistochemistry analysis and gene expression analysis. An additional 12 patients were recruited from Hualien Tzu Chi Hospital (Buddhist Tzu Chi Medical Foundation and Tzu Chi University, Hualien, Taiwan) and included in gene expression analysis based on our inclusion and exclusion criteria. This study was peer reviewed and approved by the Joint Research Management Office, Queen Mary University of London, and was also reviewed and granted ethical approval by the NRES Committee London- Queensquare (Study reference: 19/LO/1506) and the Research Ethics Committee - Hualien Tzu Chi Hospital (Study reference: IRB107-180-A). All patients provided written informed consent , and completed a Reflux Disease Questinnaire (RDQ) to assess symptom severity.Patients were included if they: 1) were aged between 18 to 70 years old, 2) had symptoms of at least moderate heartburn more than 3 times per week, and 3) had a clinical referral for endoscopic examination for investigation of symptoms. Patients were excluded if they: 1) had previous upper gastrointestinal surgery, 2) if they had severe upper gastrointestinal motility disorders, 3) if they took coagulopathy or concurrent anticoagulant medication, 4) if they were pregnant, 5) if they were allergic or hypersensitive to local anaesthetic, or 6) if they had any other medical condition that would make it unsafe for the subject to participate, determined by the treating physician. Patient demographic is presented in **Table 10**, appendix.

Patients underwent endoscopy +/- wireless ambulatory reflux monitoring. All patients (except those with known Barrett's esophagus) had stopped PPI treatment for > 7 days before endoscopy and reflux testing. Post-procedure, patients were divided according to phenotypes into; 1. erosive reflux disease (ERD), 2. non-erosive reflux disease (NERD), 3. Barrett's oesophagus (BO) and 4. functional heartburn (FH) according to the definitions under the subheadings below.

<u>Enrolment criteria for erosive reflux disease patients</u>

Symptomatic patients with at least LA Grade B oesophagitis [53] at endoscopy were included in this group. Five distal esophageal mucosal biopsies were taken per patient from non-eroded epithelium 3 cm above the squamo-columnar junction.

Enrolment criteria for nonerosive reflux disease and functional heartburn patients

Where symptomatic patients had normal endoscopic appearances, 5 distal esophageal mucosal biopsies per patient were obtained (3 cm above the squamo-columnar junction). At the same session a wireless intra-esophageal pH sensor capsule was placed (systems used: OMOM, Jinshan Science & Technology (Group) Co Ltd, Chongqing, China; or Bravo, Medtronic, Shoreview MN). 96-hours pH recording was performed. PPI was not allowed for 7 days before or during the reflux study. pH impedance monitoring was used to diagnose FH patients obtained from the second research site. Both methods are validated methods of reflux phenotyping.

Patients with confirmed pathological acid exposure (>4.2% over the study period, as per standard practice at the time in which this study was started) [442] on analysis of their reflux studies were diagnosed with NERD. Patients whose reflux testing scores did not meet pathological acid exposure and had negative reflux/symptom association were diagnosed with FH and included in the study. Of note, the acid exposure time (AET) was >6% for all NERD patients included in the study (Table 10, appendix).

Enrolment criteria for Barrett's oesophagus patients

Adults from BO endoscopic surveillance lists or those undergoing screening for suspected BO following previous ERD diagnosis were recruited from the Royal London Hospital. PPI therapy was not stopped before endoscopy, in keeping with treatment guidelines. Patients were diagnosed with BO upon the clear visualisation of columnar epithelium ≥1 cm above the gastro-esophageal junction on endoscopy and histopathologic recognition of columnar metaplasia. In addition to the clinical surveillance biopsies, five distal esophageal mucosal biopsies were taken from squamous mucosa within 1 cm above the squamo-columnar junction (away from the BO segment) for the purposes of this study.

2.2.2 Tissue Processing and Sectioning for Immunohistochemistry

Of the 5 distal oesophageal biopsies taken at endoscopy, 3 were fixed in 4% paraformaldehyde (PFA) (Sigma-Aldrich, Cat. Number 158127) in phosphate-buffered saline (PBS) (Sigma, Cat. Number P4417) for 2h, followed by cryoprotection in 30% sucrose in PBS for 24h at +4ºC, and 2 oesophageal biopsies were placed in RNA later solution and stored at -80ºC until further use. PFA-fixed tissue was embedded in optimum cutting temperature (Sakura Tissue-Tek, Cat. Number 4583) compound, frozen at -25ºC and (4 serial) 10µm sections were cut perpendicular to the mucosal surface on a cryostat (Leica 180UV) and mounted on positive-charged glass slides (Thermo Scientific, Cat. Number J1800AMNZ).

Table 2 Demographic data of patients

Phenotype	Number of patients studied for TRPV1 IHC analysis	Mean age (years)	Age range (years)	Women: Men
NERD	10	52	30-71	5:5
ERD	10	45	22-61	2:8
FH	7	46	22-70	4:3
BO	8	58	32-73	4:4
Phenotype	**Additional patients studied for ASIC3 IHC analysis**			
FH	11	46	33-69	7:5
BO	11	63	50-78	4:7
Phenotype	**Additional RNA samples studied for gene expression analysis**			
ERD	5	44	31-54	3:2
FH	7	49	41-54	4:3

35 biopsies were analysed for IHC assessment of TRPV1, while 57 biopsies were studied for ASIC3 expression analysis including additional samples from previous studies (recruited using identical inclusion/exclusion criteria). Residual tissue from previous studies was adequate for analysis of epithelial cell expression, but not neuronal analysis which required serial optimal sections throughout the biopsy to be studied. An additional 12 mucosal biopsies were obtained from the second site for qPCR analysis only.

2.2.3 Immunofluorescence-Immunohistochemistry

Sections were air-dried for 1 hour, washed with PBS to rehydrate sections for 5 minutes and serum blocked to reduce non-specific binding for 2 hours (Protein Block Serum-Free Ready-to-use, Dako, Cat. Number X0909). Sections were then incubated with a combination of primary antibodies made up in protein block for 16-18h at +4ºC. All primary antibodies used are listed in

Table 3. Sections were then washed 3 times for 10 minutes with PBS with gentle agitation on an orbital shaker (Titramax 100, Heidolph) the following day, and secondary antibodies subsequently applied and incubated for 1h at room temperature (donkey anti-mouse 488nm, donkey anti-rat 488nm, and donkey anti-rabbit 568nm, Invitrogen, Thermo Fisher Scientific, 1:400 concentration). Sections were then washed 3 times for 10min in PBS before being mounted in Vectashield HardSet antifade mounting medium with DAPI fluorescent stain (4',6-diamidino-2-phenylindole; Vector Laboratories, H-1500) and a 0.16-0.19mm cover slip (Thermo Fisher Scientific, 22X30-1.5).

Slides were examined for fluorescence using a Leica DM4000 Epi-Fluorescence Microscope (upright) using MetaMorph microscopy software for image capture. Images were viewed with a 20x, 40x, or 63x oil lens and processed using FIJI (win64).

Table 3 Source, clones, and dilution of all primary antibodies used.

Antigen	Clone	Species	Company	Product Code	Dilution Used
CGRP	Monoclonal	Mouse	Thermo Fisher Scientific	025-05-02	1:400
TRPM8	Polyclonal	Rabbit	Alomone	ACC-049	1:200
TRPV1	Polyclonal	Rabbit	Alomone	ACC-030	1:400
TRPV1	Polyclonal	Rabbit	Abcam	Ab31895	1:1000
TRPA1	Polyclonal	Rabbit	Alomone	ACC-037	1:200
ASIC3	Polyclonal	Rabbit	Thermo Fisher Scientific	PA5-61898	1:200
CD45	Monoclonal	Mouse	Dako	M0701	1:100
Mast Cell Tryptase	Monoclonal	Mouse	Dako	M7052	1:400
E-cadherin	Monoclonal	Rat	Sigma-Aldrich	MABT26	1:100

2.2.4 Image analysis

We first confirmed the distance of sensory CGRP-positive nerve endings from the luminal surface by counting the number of cell layers from the luminal surface to the identified neuronal ending. The results from all sections for each whole biopsy were compiled, and the mean representative value was used in downstream analysis for that sample. Nerve fibres between 1-10 cell layers away from the esophageal lumen were classed as ‘superficial’, while those more than 10 cell layers away from the lumen were classified as ‘deep’ nerves, in keeping with the group’s previous projects [254], [256].

2.2.4.1 Manders coefficient

Images were processed using FIJI (win64) and co-localisation was quantitatively analysed using a JaCOP plugin, where the overlap of one pixel labelled in the red channel and the other pixel labelled in the green channel was measured to give a final value, giving the total percentage overlap. Acquired images were converted to black and white. A threshold was set to highlight positive signals in black and background in white, creating a binary image in each channel. Then, the positive area was highlighted using the freehand tool to give a region of interest (ROI). The ROI was applied to the corresponding image in the other channel, and pixel number measured. Thus, two values were obtained for each image: the number of positive pixels in the green channel, and the number of positive pixels in the red channel, within the same ROI.

The overlap of positive pixels between the two images were quantified by using the Manders coefficient which measures the percentage positive pixel overlap in one channel and the other where 1.0= complete overlap and 0= no overlap.

2.2.4.2 Automated cell counting

Automated cell counting was done using FIJI. Images were converted to greyscale before processing. A threshold was set to highlight all the cells positive for DAPI, and then a separate threshold was set to highlight all the cells positive for the marker of interest. This generated binary images for counting. All positive particles were then automatically counted by using the 'Analyse particles' tool. The percentage of cells positive for marker of interest were calculated from the total DAPI-positive cell count. 5 images were quantified per sample, and a mean cell count per sample was calculated. Submucosal cells were excluded from the count to ensure that only the epithelial expression of protein of interest was analysed.

2.2.5 Qualitative Real Time Polymerase Chain Reaction (qRT-PCR)

2.2.5.1 RNA Extraction

Endoscopic biopsies from the distal oesophagus were placed in RNA later solution (Sigma, Cat. Number R0901-100ml) and kept at -80ºC until RNA extraction. RNA was extracted using the RNeasy Mini Kit (Qiagen, Cat. Number 74016). Briefly, biopsies were placed in 600 µl of buffer RLT with 1% β-mercaptoethanol and disrupted with a TissueRuptor (Qiagen). The lysate was centrifuged for 3 min at full speed. The supernatant was removed and transferred to a new microcentrifuge. Subsequently, 600 µl of 70% ethanol was added to the lysate and mixed immediately by pipetting. A 700 µl volume of the sample was added to the spin column in a 2 mL collection tube and centrifuged at >10000 rpm for 15 sec. Flow through was discarded and 700 µl buffer RW1 was added to the RNeasy spin column and centrifuged at >10000 rpm. Flow-through was discarded, and the membrane was washed with 500 µl buffer RPE centrifuged for 15 sec at >10000 rpm. Flow-through was discarded and the membrane washed with 500 µl buffer RPE and centrifuged for 2 min. The old collection tube was discarded, column was placed in a new collection tube and centrifuged for 1 min at full speed to dry the membrane. A 30 µl volume of RNAse free water was added directly to the centre of the spin column membrane and centrifuged for 1 min at >10000 rpm to elute RNA. Eluted RNA was quantified using Nanodrop (Thermo Scientific). Only samples with >100 ng/µl RNA and a 260/280 ratio >2.0 were used for qPCR experiments.

2.2.5.2 Reverse transcription for cDNA Synthesis

0.5 µg total RNA was reverse transcribed into cDNA using the QuantiTect reverse transcription kit (Qiagen, Cat. Number 205310). A maximum of 2 µg RNA was incubated with the reverse transcription MasterMix (reverse transcriptase, RT buffer, RT primer mix) in a PCR max Alpha cycler using the following settings: incubate for 15 min at 42ºC, incubate for 3 min at 95 ºC to inactivate quantiscript reverse transcriptase, then hold at 4 ºC.

2.2.5.3 qRT-PCR

qRT-PCR was performed on the AB7300 Real-Time PCR system (Applied Biosystems) using the QuantiFast SYBR Green PCR kit (Cat. Number 204056). QuantiTect Primer Assays were used for 18S, TRPM8, TRPV1, TRPA1, and ASIC3 genes (See Table *4*).

Gene product	Product no.	Cat. No.
18S	249900	QT00199367
GAPDH	249900	QT00273322
TRPM8	249900	QT00038906
TRPV1	249900	QT01010219
TRPA1	249900	QT00025054
ASIC3	249900	QT01012557

Table 4: QuantiTect Primer Assays (Qiagen), and their sources

2.2.6 Statistical Analysis

Relative gene expression by qPCR was calculated using the $2^{-\Delta CT}$ method, where gene expression change was relative to the housekeeping gene. GORD phenotypes were compared to each other by one-way ANOVA followed by Bonferroni's post-hoc test for multiple comparison. Values are presented as mean ± SD.

2.3 Results

2.3.1 Localisation of sensory afferent nerves in GORD phenotypes

First, previous findings on sensory afferent neuronal innervation of CGRP immunoreactive fibres in the oesophageal mucosa of GORD patients was confirmed using immunohistochemical analysis. We previously established the co-expression of PGP9.5 on CGRP-positive nerve fibres innervating the esophageal squamous epithelium [256], therefore, only CGRP containing sensory nerves were identified in this study.

In NERD patients, CGRP immunoreactive (IR) afferent nerve endings were located superficially in the distal oesophageal mucosa, where they were found to innervate the uppermost layer of epithelial cells (Figure 19A). Conversely, in patients with ERD, FH, and BO, CGRP-IR afferent nerves were found deeper in the distal squamous epithelium (mean 22 cell layers away from the lumen surface) (Figure 19B). These deep nerves were most often intrapapillary, regardless of disease phenotype (Figure 19A). CGRP-IR nerves were identified in 3/8 BO patients, 5/10 ERD patients, 4/7 FH patients and 7/10 NERD patients. In patients where sensory nerves were identified, superficial expression of CGRP-IR afferent nerves was significantly higher in NERD patients compared to FH, ERD and BO ($p = <0.01$) (Figure 19B).

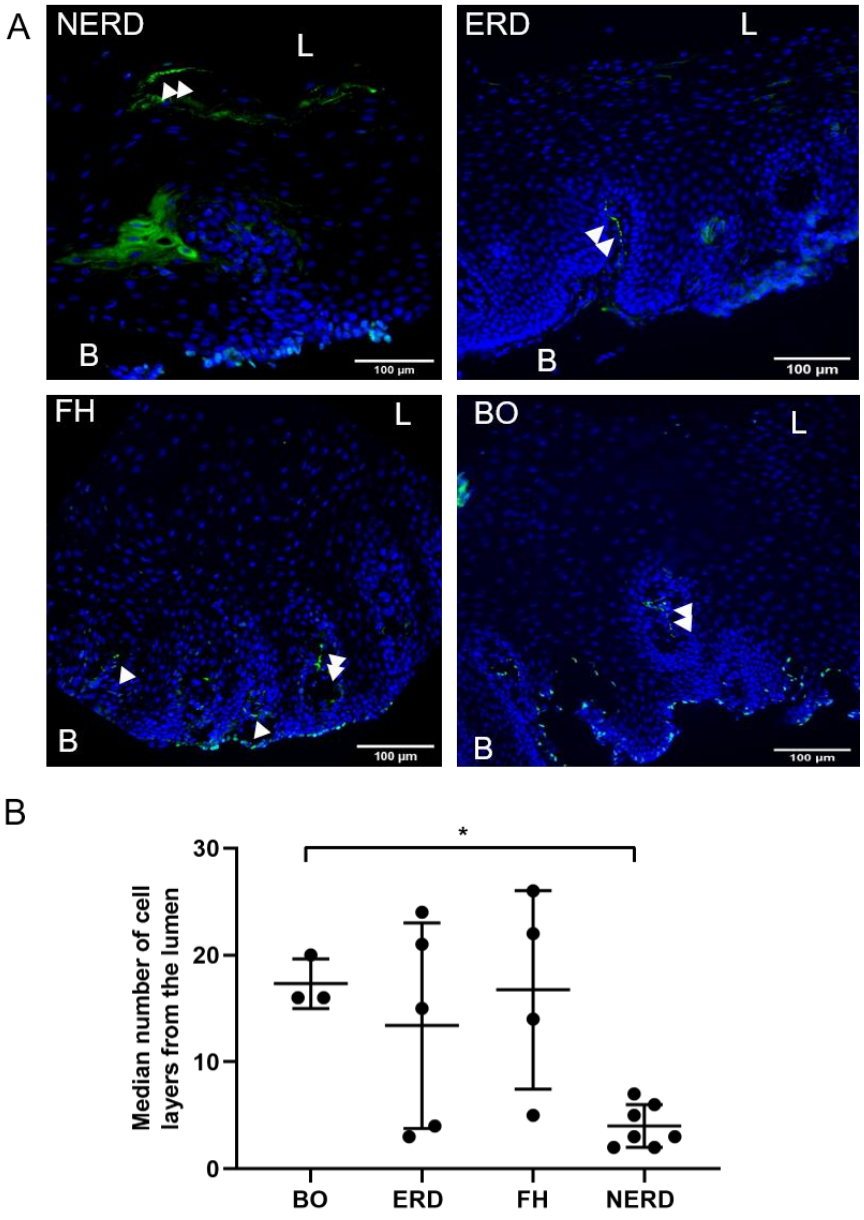

Figure 19 Localisation of CGRP-IR nerves in GORD phenotypes

A) Top left panel demonstrates a superficial afferent nerve in a NERD patient with arrows pointing to a CGRP-IR sensory nerve ending. The ERD, FH, and BO panels demonstrate deep nerve fibres typically found in these patients as demonstrated by arrows pointing to the CGRP-IR nerves in the papillae. B) CGRP-positive nerves are significantly closer to the lumen in NERD ($p=<0.01$). L= lumen, B= basal layer. Error bars represent SD. Scale bar: 100µm. Images are representative of the mean taken from 3 experimental repeats per patient, over 5 fields of view.

2.3.2 TRPV1 expression in the oesophageal mucosa of adults with GORD

TRPV1 has been extensively reported as an ion channel involved in hypersensitivity, but its expression on oesophageal mucosal afferent nerves in patients with heartburn has not been characterised. TRPV1 expression in the oesophageal mucosa of GORD patients was assessed using IF-IHC. Specific binding of the TRPV1 antibody was confirmed using control IBD colon tissue kindly donated by Dr Rubina Aktar for the purpose of antibody validation (Figure 20) and abdominoplasty skin tissue (post-fixed with 4% PFA for 15 minutes prior to IF-IHC) kindly donated by Dr Lisa McGinty as a positive control (Figure 21A). Literature demonstrates that mucosal macrophages, submucosal plasma cells, and leukocytes near the epithelial layer express TRPV1 in the inflamed mouse and human colon [443]. Moreover, TRPV1 is highly expressed on nociceptive sensory nerve endings in the skin, where it was shown to have sensory afferent functions [444]. In the colonic mucosa, cellular TRPV1 expression was observed between crypts, and there was some co-localisation with CGRP (Figure 20A). In the epidermis of the abdominoplasty skin, TRPV1 was expressed on CGRP-immunoreactive nerve fibres (Figure 21A). Negative controls with no primary antibody showed no labelling in the colon (Figure 20B), nor skin (Figure 21B). Additionally, control antigen was also run alongside the antibody according to the manufacturer's instructions to confirm the specificity of the antibody. Slides were incubated in parallel with and without the antigen in a ratio of 1:2 (Appendix 1).

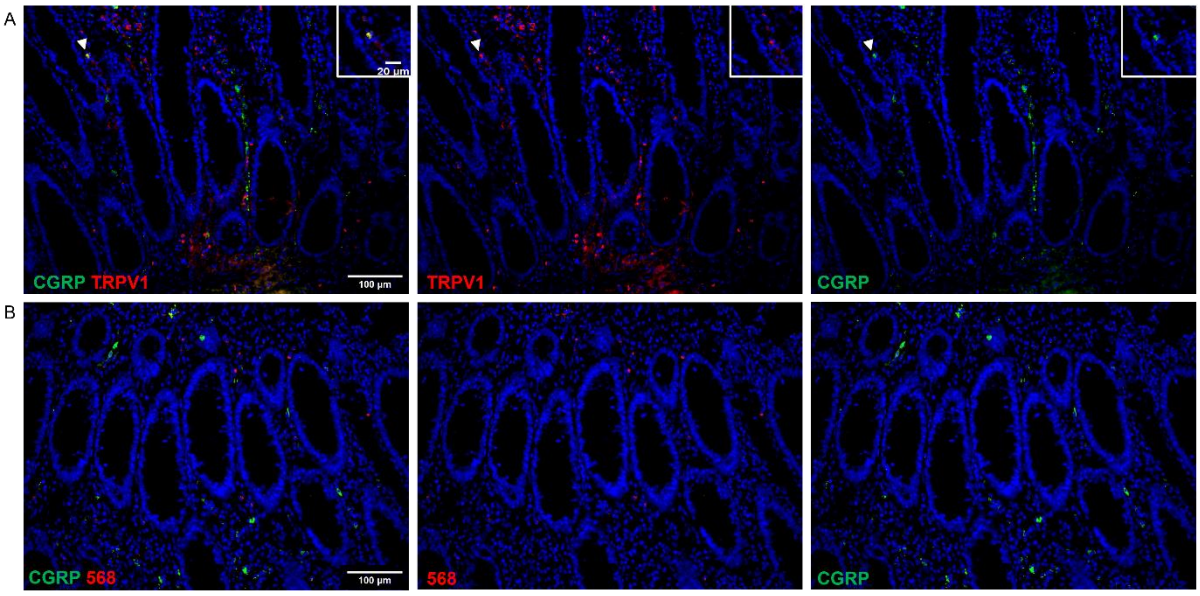

Figure 20: TRPV1 is expressed in colon tissue isolated from IBD patient biopsies

A) TRPV1 optimisation in the IBD colon co-stained with CGRP, showing TRPV1-immunoreactive cells between colonic crypts. Arrowhead highlights a TRPV1+CGRP+ cell B) Negative control showing no TRPV1 immunoreactivity in the same IBD colon sample. A total of 2 IBD colon samples and 2 normal colon samples were used for optimisation. Scale bar: 100µm, insert scale bar: 20µm.

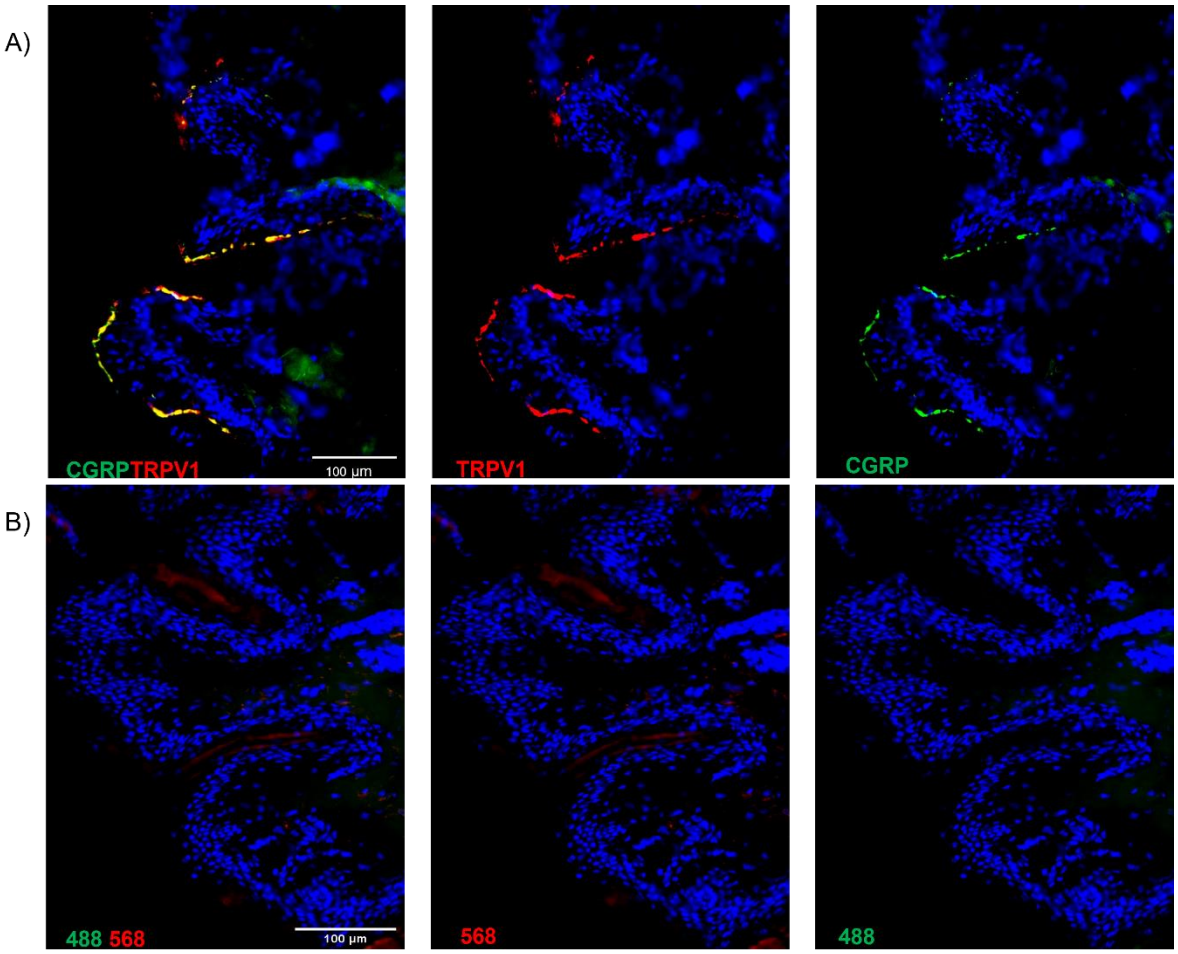

Figure 21 CGRP-immunoreactive nerves in the obese skin are TRPV1-positive

A) TRPV1 optimisation in abdominoplasty skin tissue, co-stained with CGRP to highlight sensory nerve endings. TRPV1 was expressed by CGRP-immunoreactive afferent nerves in the epidermis layer. B) Negative control for TRPV1 and CGRP, showing no immunoreactivity in the same abdominoplasty skin sample. Scale bar: 100 µm

After successful antibody optimisation, immunohistochemical expression of TRPV1 was assessed in mucosal biopsies from 35 patients presenting with heartburn phenotyped endoscopically and with objective reflux studies into ERD (N=10), NERD (N=10), FH (N=7), and BO (N=8). A total of 160 µm per sample (4 slides per patient, with each slide containing 4 serial sections at 10 µm each) was evaluated to locate nerve fibres. TRPV1 was frequently expressed on superficial CGRP-immunoreactive nerves in NERD patient samples (Figure 22A). Quantitative analysis to assess the degree of co-expression found significantly increased co-expression of TRPV1 on CGRP-immunoreactive superficial nerves in NERD, compared to ERD (p = 0.028) or BO (p = 0.017) patients (Figure 22E).

Papillary CGRP-immunoreactive nerves in patients with ERD, FH, and BO did not express TRPV1 (Figure 22B-D). TRPV1 expression was only occasionally observed in oesophageal epithelial cells (5/35 GERD patients studied, including 3 FH patients, 1 ERD patient, and 1 BO patient) (Figure 23). This was reflected in RNA quantitation studies which confirmed expression of *TRPV1* at mRNA level, but showed high variability between patient phenotypes and no significant differences in *TRPV1* gene expression (Figure 22F). While the study requires healthy control data, there appears to be no relationship between *TRPV1* expression at mRNA level and phenotype.

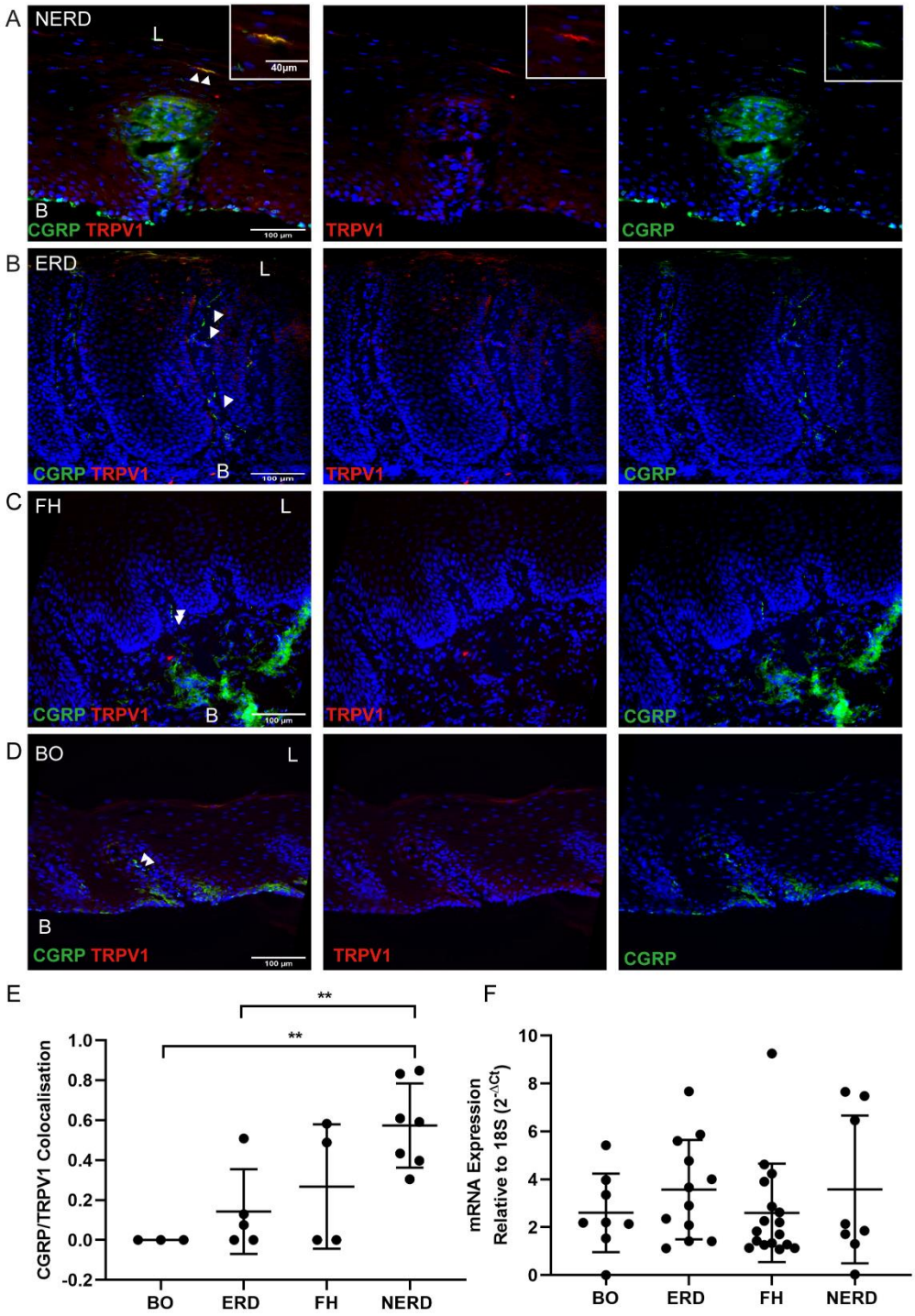

Figure 22 TRPV1 expression and co-localisation with CGRP in GORD phenotypes

A) Superficial mucosal nerve identified with CGRP (arrows) which co-localised with TRPV1 in a NERD patient. B) Intrapapillary mucosal nerve identified with CGRP (arrows) did not express TRPV1 in an ERD patient. C) Deep intrapapillary mucosal nerve identified with CGRP (arrows) did not express TRPV1 in a patient with FH. D) Deep interpapillary mucosal nerve identified with CGRP (arrows) did not express TRPV1 in a patient with BO. Images are representative of the mean taken from 3 experimental repeats per patient, from 5 fields of view. E) Co-localisation of CGRP-IR sensory endings with TRPV1 is significantly increased in NERD compared to ERD, and BO as assessed by one-way ANOVA and Bonferroni's test. F) TRPV1 mRNA expression in oesophageal mucosal biopsies from GORD patients. BO: N=8, ERD: N=12, FH: N=17, NERD: N=8. Error bars represent S.D. qPCR included duplicate samples/patient, and plotted data is the mean of 3 independent experimental repeats. L= lumen, B= basal layer. Scale bar: 100µm.

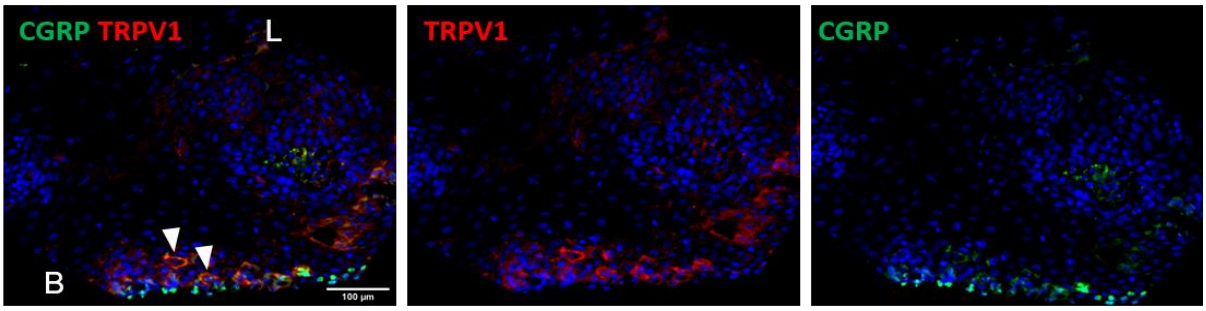

Figure 23: Cellular TRPV1 expression

Epithelial TRPV1 expression in a representative ERD sample. Arrows highlight epithelial cells showing membranous TRPV1 expression. L= luminal, B= basal layer. Scale bar: 100µm

2.3.3 ASIC3 expression in the oesophageal mucosa of adults with GORD

ASIC3 expression in the oesophageal mucosa of patients with GORD was assessed using IF-IHC. Efficacy of the ASIC3 antibody was confirmed using full thickness inflamed colon tissue as positive control as previously described, where ASIC3 was found to be expressed in the myenteric plexus (Figure 24A). Negative control slides were prepared as previously described and showed no ASIC3 immunoreactivity in the myenteric plexus (Figure 24B).

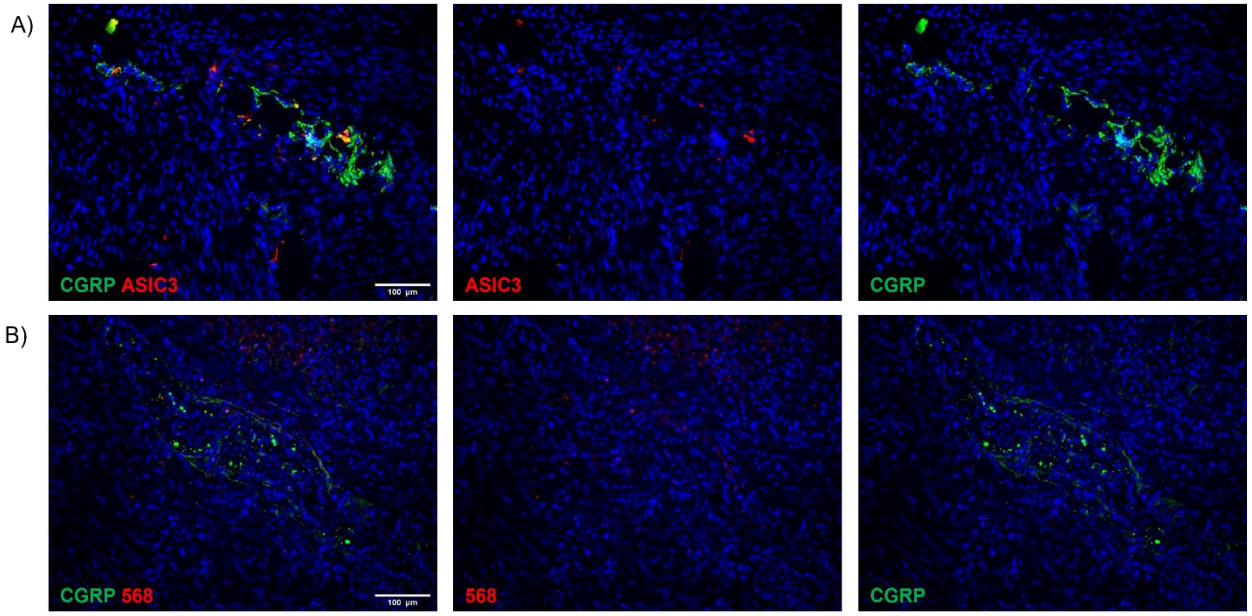

Figure 24: ASIC3 is expressed in the myenteric plexus of the IBD colon

A) ASIC3 optimisation in inflamed colon tissue, co-stained with CGRP to highlight sensory nerve fibres of the myenteric plexus. ASIC3 was expressed by CGRP-immunoreactive nerves in the myenteric plexus (yellow) B) Negative control for ASIC3 and CGRP, showing no immunoreactivity in the same colon sample. Scale bar represents 100 µm.

Immunohistochemical expression of ASIC3 was assessed in mucosal biopsies from 56 GORD samples phenotyped endoscopically and with objective reflux studies into ERD (N=9), NERD (N=10), FH (N=18), BO (N=19), and healthy controls (N=7). This included a total of 80 µm per sample (2 slides per patient, with each slide containing 4 serial sections at 10 µm each). ASIC3 expression was not detected on either superficial or deep CGRP-IR nerves but was observed on epithelial cells in ERD, FH, NERD, and BO, where ASIC3-positive cells co-stained for e-cadherin (Figure 25A-D).

DAPI-positive cells and ASIC3-positive cells were counted and calculated as a percentage of the total number of DAPI-positive cells expressing ASIC3 (as described in section 2.2.4 Image analysis). Epithelial expression of ASIC3 was significantly increased in ERD and NERD compared to healthy controls (p = <0.0002 for both comparisons), FH (p = <0.01 for both comparisons) and BO patients (p = <0.0001) (Figure 25E). Healthy controls and BO had the lowest level of ASIC3 expression while the NERD and ERD subgroups appeared to have two clusters: a group of patients with a high level of ASIC3 positivity, and a group of patients with considerably lower ASIC3 expression (Figure 25E). However, there was also no correlation between symptom severity as assessed by RDQ score, nor between acid exposure time (AET), and ASIC3 expression (Appendix *2*, Appendix *4*).

RNA quantitation studies were conducted to study the relative level of *ASIC3* gene expression (in relation to the reference gene *18S)*. There was no significant difference in the level of *ASIC3* gene expression between the different GORD phenotypes (Figure 25F). While the study requires healthy control data, there appears to be no correlation between *ASIC3* expression at mRNA level and disease phenotype.

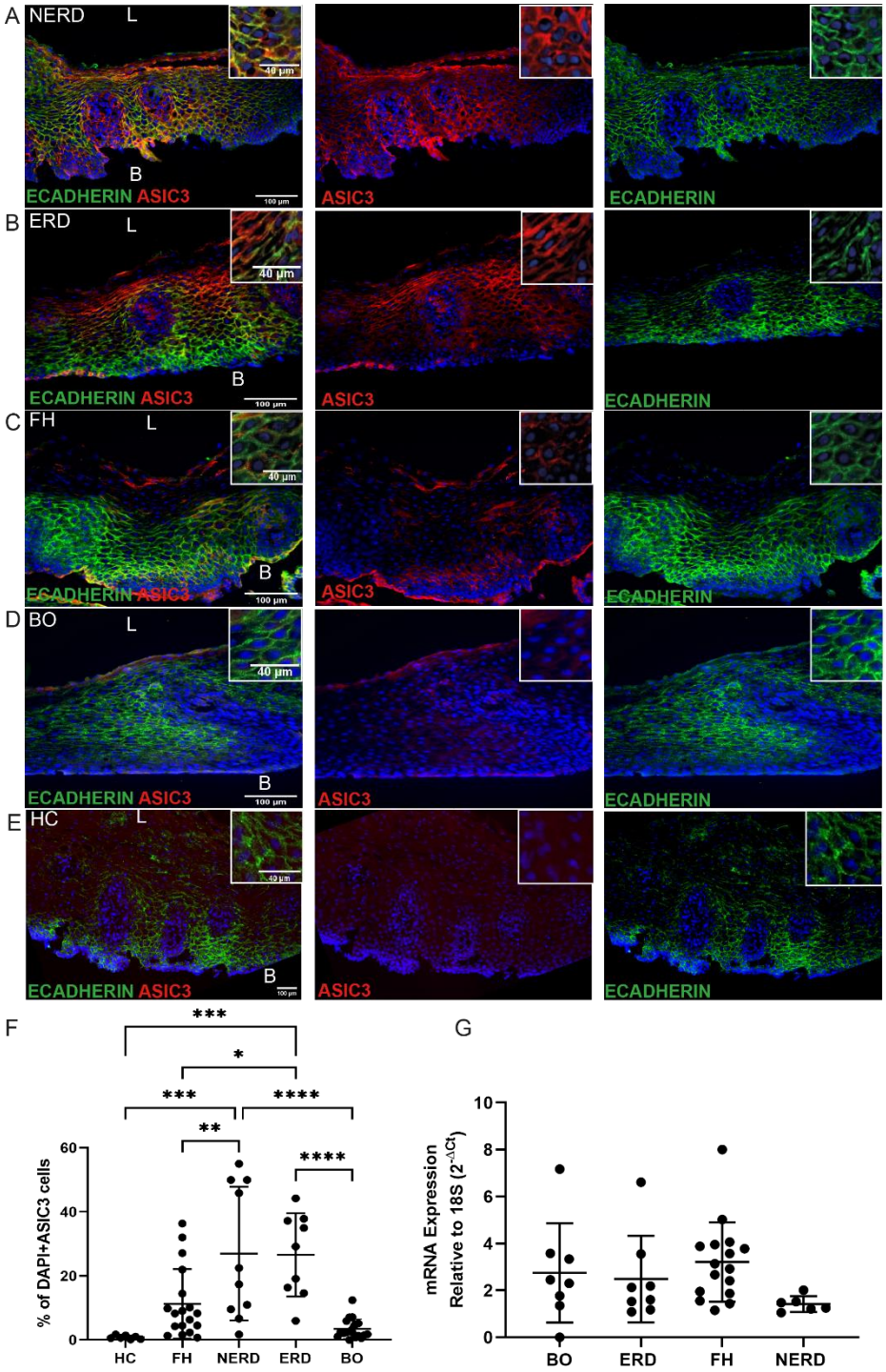

Figure 25: ASIC3 expression by oesophageal epithelial cells in GORD phenotypes

A) ASIC3 is expressed on e-cadherin immunoreactive oesophageal epithelial cells in a patient with NERD, B) e-cadherin immunoreactive oesophageal epithelial cells express ASIC3 in an ERD patient C) e-cadherin immunoreactive oesophageal epithelial cells co-express ASIC3 in a patient with FH, D) e-cadherin immunoreactive oesophageal epithelial cells have low ASIC3 expression in a patient with BO. E) e-cadherin immunoreactive oesophageal epithelial cells do not express ASIC3 in healthy controls (HCs). F) The percentage of ASIC3 cells was significantly higher in ERD and NERD patients as assessed by one-way ANOVA and Bonferroni's test. G) qPCR analysis of ASIC3 in esophageal mucosal biopsies in GERD patients. Error bars represent S.D. NERD: N=8, BO: N=8, ERD: N=8, FH: N=16. qPCR analyses included duplicate samples/patient, and plotted data is the mean of 3 independent experimental repeats. L=lumen, B= basal layer. Scale bars: 100µm, inset scale bars: 40µm.

2.3.3.1 Assessment of ASIC3 on intra-epithelial leukocytes in the oesophageal mucosa

As co-localisation between ASIC3 and e-cadherin was not exclusive, ASIC3-immunoreactive cells were further characterised by double-staining with the pan-leukocyte marker CD45. However, there was no co-localisation between CD45 and ASIC3 in any of the disease groups. While all GORD phenotypes presented with immune cell infiltration in the mucosa, CD45+ lymphocytes were ASIC3-negative (Figure 26A). The highest density of immune cell was observed in the submucosa of NERD patient biopsies. In the epithelium, CD45+ lymphocytes were mostly intrapapillary, whilst FH samples showed sparse immune cell infiltration in the epithelium (Figure 26A). CD45+ lymphocyte infiltration was not significantly different between the GORD groups ($p = 0.52$) (Figure 26B).

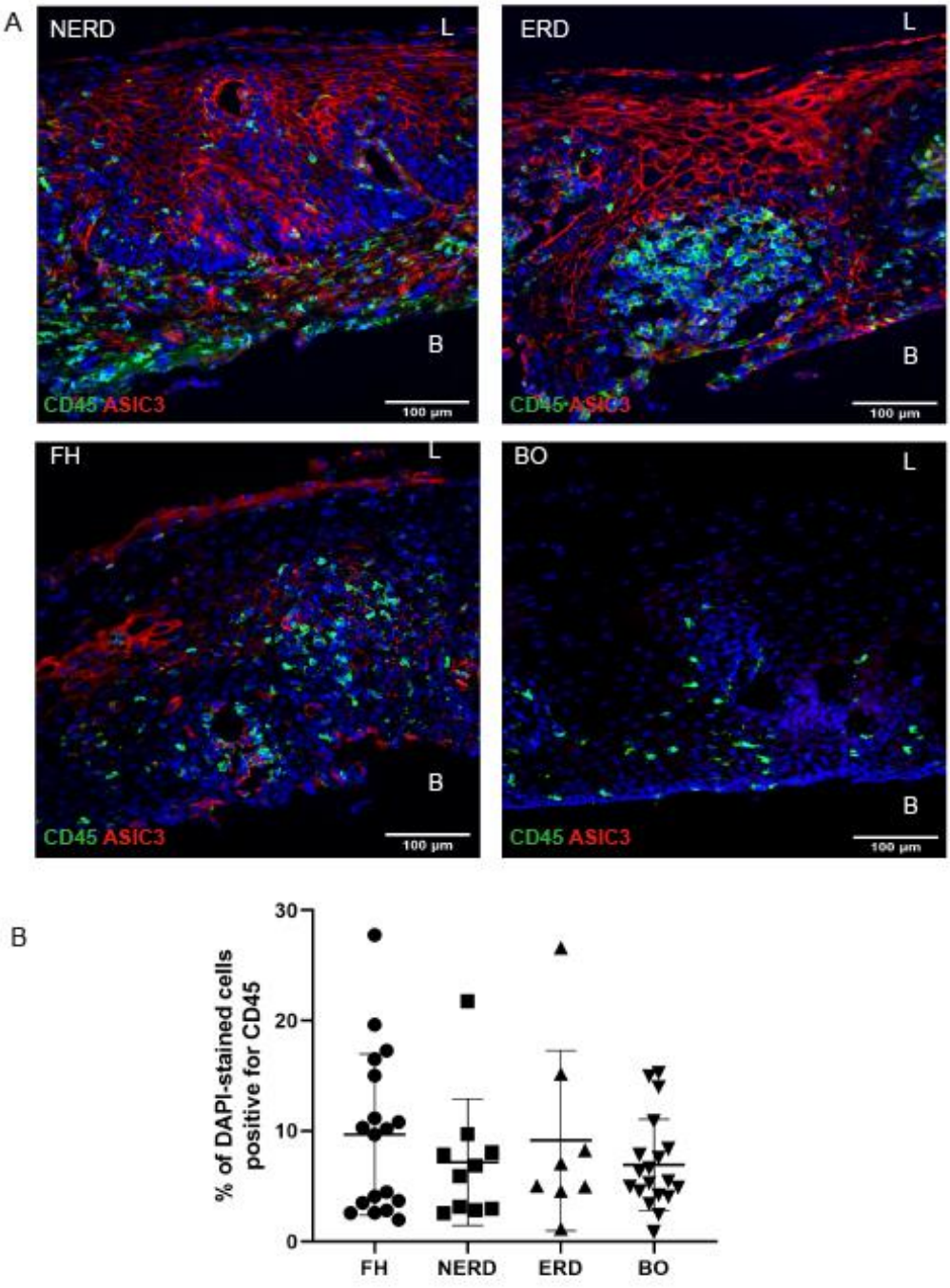

Figure 26: Immune cells in the oesophageal mucosa of GORD patients do not express ASIC3

A) ASIC3 is not expressed by CD45-immunoreactive lymphocytes in NERD, ERD, FH, and BO. B) The percentage of CD45-IR cells was not significantly different between GORD phenotypes as assessed by one-way ANOVA. B, basal layer; L, lumen. Scale bar: 100 µm

2.3.4 TRPM8 expression in the oesophageal mucosa of adults with GORD

We hypothesised that TRPM8 might be expressed on afferent nerves in the oesophageal mucosa, and that it might have a sensory role in inducing heartburn symptoms. TRPM8 expression was investigated using IF-IHC. Positive staining using the TRPM8 antibody was determined with IBD colon tissue as a positive control (Figure 27). This was justified as literature demonstrated increased TRPM8 immunoreactivity in the inflamed colon [229]. Negative controls were prepared as previously described and showed no labelling. In the mucosa of a patient with IBD, cellular TRPM8 expression was observed between the crypts (Figure 27A and C). These co-localised with CD45, a pan-leukocyte marker (Figure 27A), and CGRP, a marker for sensory neurons (Figure 27C). TRPM8 expression was also observed in the submucosa, but did not co-localise with protein gene product 9.5 (PGP), pan-neuronal marker (Figure 27B). Furthermore, an antigen control test was performed according to the manufacturer's instructions to confirm antibody specificity. Slides were incubated with the antibody in parallel with and without the control antigen in a ratio of 1:2.

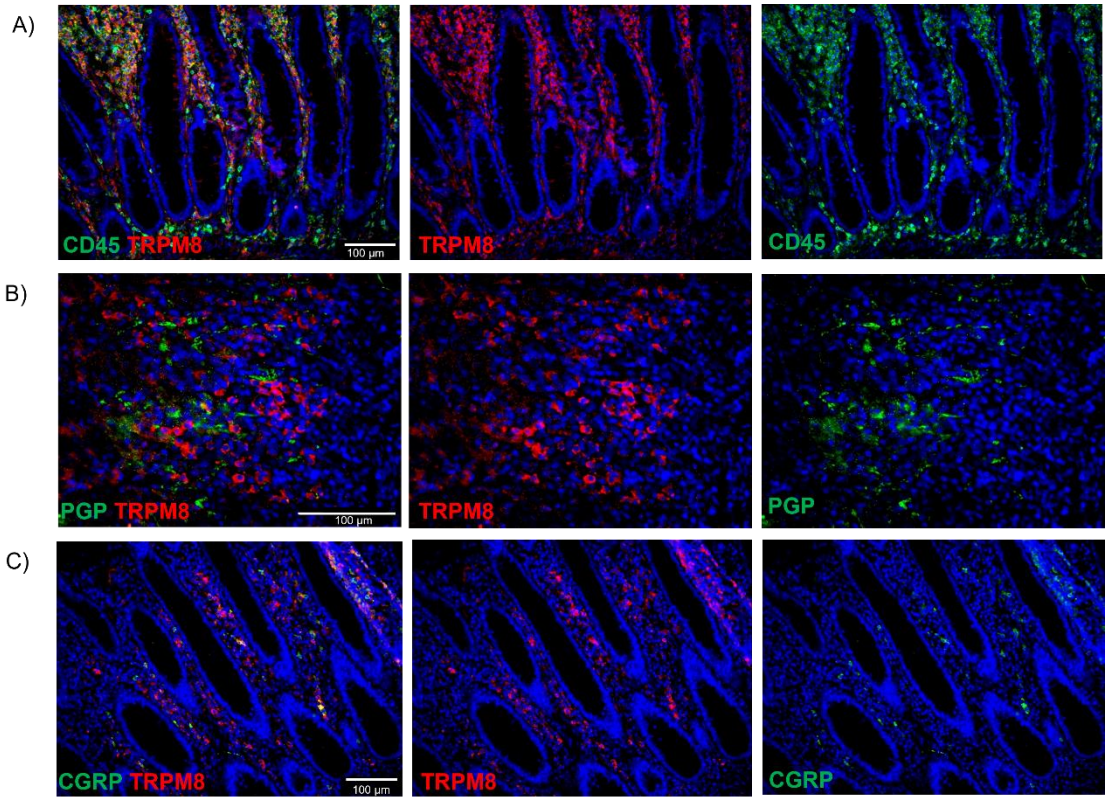

Figure 27: TRPM8 expression in the IBD colon

TRPM8 antibody optimisation on positive control tissue, IBD colon. CD45 was used to highlight lymphocytes (A) and PGP was used as a neuronal marker (B). TRPM8 was expressed on immune cells in the epithelial layer of the colon. There was colocalisation between TRPM8 and CGRP in the epithelium of the IBD colon (C). Scale bar: 100µm

Oesophageal mucosal biopsies from 20 GORD patients (ERD N=10, FH N=4, NERD N=4, BO N=2) were immunohistochemically assessed for expression of TRPM8. A total of 160 µm of oesophageal epithelium was studied per patient sample (4 slides per patient, with each slide containing 4 serial sections at 10 µm each). Neither epithelial cells nor sensory afferent nerves in the oesophageal mucosa of heartburn patients expressed TRPM8 (Figure 28A-B). In ERD samples where submucosa was present, TRPM8 expression was observed on a subset of CD45-positive lymphocyte infiltrates (Figure 28C).

To assess TRPM8 expression at mRNA level, RT-qPCR was performed. TRPM8 expression was absent in 2/20 patients whilst remaining samples had detectable but low levels of *TRPM8* expression (Figure 28D). A concentration of 100ng RNA was initially used, and subsequently increased to 500ng to test whether detection could be improved. TRPM8 levels remained relatively low at mRNA level despite the increase of RNA concentration. The mRNA data agrees with the IF-IHC findings of limited *TRPM8* expression in the epithelium. Most oesophageal biopsies do not contain the submucosa region where the protein was found to be expressed, hence it is unsurprising that the gene was not detected in the samples analysed.

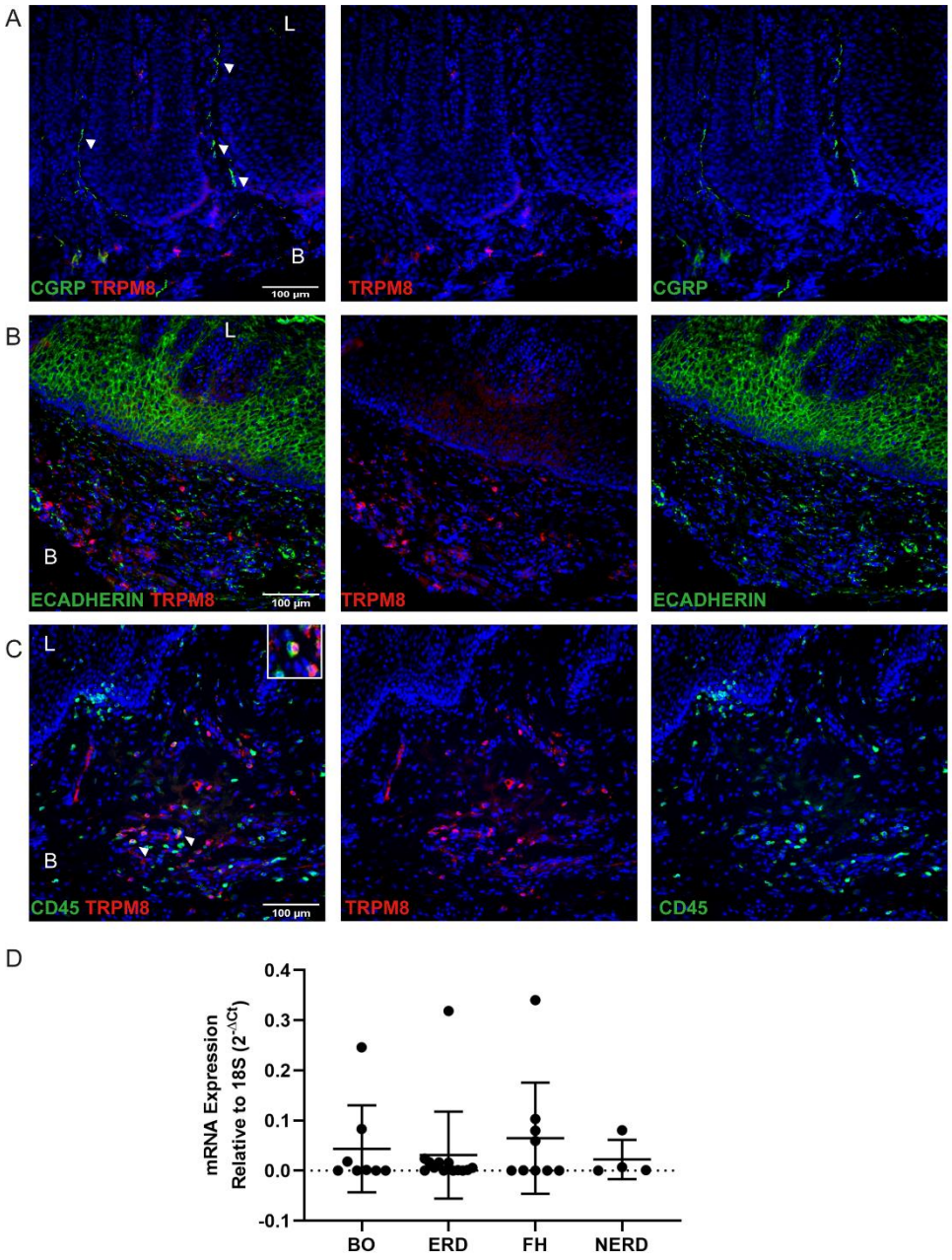

Figure 28: TRPM8 is expressed on CD45+ leukocytes in the oesophageal mucosa of ERD patients

A) CGRP-immunoreactive mucosal afferents negative for TRPM8 in a patient with ERD. B) Esophageal epithelial cells identified with e-cadherin did not express TRPM8 in patients with ERD. C) TRPM8 is expressed on CD45+ leukocytes in the esophageal submucosa of ERD patients. Images are representative of the mean taken from 3 experimental repeats per patient, from 5 fields of view D) TRPM8 gene expression in esophageal mucosal biopsies in GERD patients. Error bars represent S.D. NERD: N=4, BO: N=8, ERD:N=9, FH:N=9. qPCR analyses included duplicate samples/patient, and plotted data is the mean of 3 independent experimental repeats. L=lumen, B=basal layer. Scale bar represents 100µm.

2.3.5 TRPA1 expression in the oesophageal mucosa of adults with GORD

TRPA1 has been implicated as another ion channel which may play a sensitising role in sensory neurons innervating the oesophageal mucosa. The relative level of *TRPA1* gene expression in the oesophageal mucosa of patients with GORD was assessed via RNA quantification studies. There was no significant difference in the level of *TRPA1* gene expression among GORD phenotypes (Figure 29). The study requires healthy control data, as well as TRPA1 protein localisation studies with IF-IHC in the oesophageal mucosa.

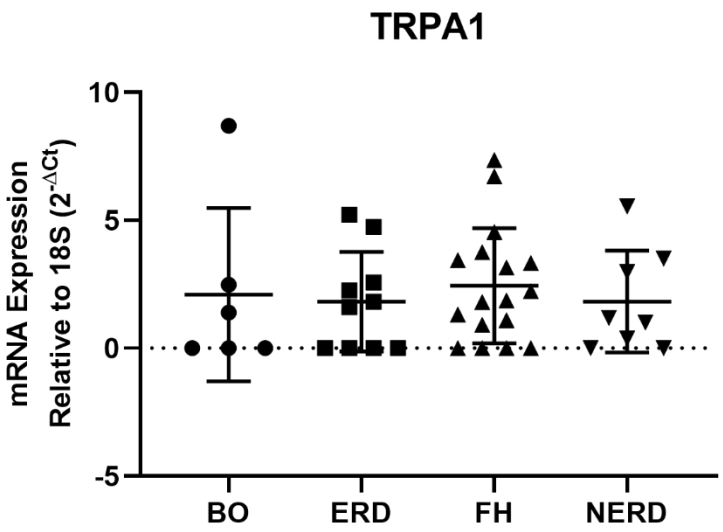

Figure 29: qPCR analysis of TRPA1 in the oesophageal mucosa of GORD patients

The relative expression of the gene of interest is in relation to the reference gene 18S. Error bars represents SD. Results were statistically insignificant. NERD N= 6; Barrett's N= 6; ERD N=9; FH N= 19

2.4 Discussion

This section aimed to characterise sensory afferent nerves innervating the oesophageal mucosa for an improved understanding of the mucosal mechanisms underlying oesophageal hypersensitivity in patients with GORD. TRPM8, TRPV1, ASIC3, and TRPA1 expression was investigated using IF-IHC and qPCR studies in endoscopic mucosal biopsies from patients with BO, ERD, FH, and NERD. At the time in which the studies for this section of the study were undertaken, healthy volunteers had just been recruited following ethical approval issued by the Health Research Authority in January 2020. However, the collection of healthy control biopsies was disrupted due to the SARS-CoV-2 outbreak soon after. Thus, analysis of results in this section compares the subgroups of GORD to one another.

Findings from this study confirm our group's previous findings describing superficial nerves (close to the lumen) found in NERD, but not other reflux phenotypes [256]. They are seen much closer to the luminal surface in NERD than in other GORD phenotypes, where nerve fibres are located deeper in the epithelium and are most often papillary. The uniquely superficial nerves of NERD are ideally located to sense and be activated by acidic luminal stimuli without need for significant breach of the oesophageal mucosal barrier integrity and is likely to explain why patients with NERD can experience similar severity of heartburn as patients with erosive disease.

Unlike deep mucosal nerves, superficial mucosal nerves (found most frequently in NERD) express TRPV1. The superficial expression of TRPV1 may have a role in pathogenesis of heartburn [256]. The acid-induced activation of TRPV1 on superficial afferent fibres innervating the oesophageal mucosa could be a possible mechanism of oesophageal perception of reflux events or hypersensitivity, as previously suggested by animal studies which demonstrate that pharmacological blockade of TRPV1 reduces acid-induced damage to the mucosal integrity in NERD [149], [189]. The mechanism of TRPV1-mediated hypersensitivity could also involve neuro-immune interactions. There is evidence in the literature to suggest that activation of TRPV1 in primary afferent nerves induces the release of CGRP and SP when exposed to HCl, causing an increase in platelet-activating factor (PAF) which can induce inflammation and mucosal damage [190], [193]. The finding of co-localisation of TRPV1 and CGRP on superficial afferent nerves in the current study thus suggests a nociceptive function of TRPV1 on these fibres, where excessive H^+ in the refluxate lowers the transduction threshold of the ion channel, subsequent influx of H^+ causes membrane depolarisation and leads to the active firing of the neuron, thus increasing sensitisation to the noxious stimulus [66]. Moreover, the observation that in hyposensitive

Barrett's patients only deep intra-papillary sensory nerves were identified, while superficial afferent sensory nerves co-expressed TRPV1 most frequently in hypersensitive NERD patients suggests that heartburn symptoms in patients without mucosal injury could be explained by the superficial location of TRPV1-immunoreactive nerves. Physiologically, TRPV1 can be activated by H^+ released during inflammation [155]. Our findings suggest that TRPV1 could be activated by luminal H^+ present in the refluxate, even in the absence of inflammation. Thus, pathological levels of acid reflux could lead to the increased sensitisation of TRPV1 even in the absence of apparent mucosal lesions and cause increased action potential firing, ultimately resulting in troublesome heartburn symptoms [445]. This highlights TRPV1 as a topical mucosal target which could be pharmacologically blocked to attenuate its activation by H^+ in the refluxate to block the peripheral mechanisms responsible for increased sensitivity, and thus alleviate heartburn in patients with NERD.

Furthermore, electrophysiological recordings have demonstrated that capsaicin injection into the marrow cavity increases the afferent neuronal activity in C fibres and Aδ fibres, while also sensitising both to mechanical stimuli [446]. These findings provide further evidence supporting the role of TRPV1 in pain pathogenesis. There have also been suggestions of nociceptive neuroplasticity associated with the pathogenesis of GORD. A gene expression study which investigated the correlation between TRPV1 upregulation with neurotrophic factors such as NGF and glial cell-derived neurotrophic factor (GDNF) demonstrated an association between NGF and GDNF in the upregulation of TRPV1 gene expression in patients with ERD, highlighting the neuroplastic alterations which may drive the change in the location of afferent nerve endings, their expression of TRPV1, and hence explain the increased sensitivity and heartburn symptoms in GORD [447]. However, whilst the TRPV1 receptor was detected on afferent nerve endings in the oesophageal mucosa of NERD and occasionally FH patients with IF-IHC, there was no significant difference in the expression of TRPV1 among the subgroups of GORD at mRNA level. This can be partially explained by the lack of RNA in nerve endings innervating the oesophageal mucosa and hence the lack of detection of differences in mRNA levels of TRPV1 between the NERD group and other phenotypes of GORD. In addition, there may be technical reasons for why we did not see a difference in TRPV1 gene expression when other studies have reported *TRPV1* upregulation in the oesophageal mucosa of NERD and ERD patients [448]. Studies which report a significant increase in *TRPV1* gene expression in oesophageal endoscopic biopsies from GORD patients reverse transcribe 1 mg (1000µg) [447], or 1 µg [448] of total RNA isolated with the Trizol reagent. In this study, RNA was extracted using solid-phase RNA extraction with silica-membrane spin columns, and the concentration of total RNA used for cDNA synthesis was increased from the manufacturer instructions of 0.1 µg to 0.5 µg, half the

concentration of that used in the real-time polymerase chain reaction study by Guarino *et al*. Moreover, both studies report a significant increase of *TRPV1* gene expression in GORD groups in relation to healthy subjects, not in relation to different GORD subgroups. In our study, the analysis compares *TRPV1* expression between NERD, ERD, FH, and BO, relative to the housekeeping gene. Hence, the significance of *TRPV1* gene expression could still be relatively higher in the GORD subgroups when compared to healthy control samples.

Pain sensation in the oesophagus of patients with heartburn symptoms could be further explained by our finding that epithelial cells within the mucosa in NERD and ERD patients express ASIC3 significantly more than in FH and BO. The observation that NERD and ERD patients (who have increased acid exposure) have more epithelial expression of ASIC3 than FH (who do not have increased acid exposure) and BO (who also have low exposure due to patients being on PPI treatment at the time of endoscopy) is interesting, and could mean that there is a direct link between ASIC3 expression and acid exposure. The difference could also be due to a fundamental difference in the sensory phenotype of Barrett's patients. The lack of co-expression between CD45 and ASIC3 suggests that ASIC3 primarily regulates epithelial cells, and that the mechanism of ASIC3 upregulation is likely to be unrelated to immune cell infiltration. The presence of specific epithelial ASIC3 in the oesophageal mucosa was shown to be associated with an increased symptom severity in GORD patients previously and was highlighted as a potential objective biomarker of symptom severity [441], thus supporting our findings. Another recent study which assessed gene and protein expression of ASIC3 using qPCR, western blot, and IF analysis confirmed our findings, demonstrating increased ASIC3 protein expression in oesophageal mucosa and DRG neurons in rodent models of ERD and NERD compared to sham operated controls [449].

ASIC3 is reported to be a peripheral sensory receptor with nociceptive functions which is activated by changes in pH in both the physiological and pathophysiological range [450]. While it has been reported to be found predominantly on sensory nerves, a role for ASIC3 in heartburn has been described in a recent study using primary human oesophageal epithelial cells [194]. In this study, the phosphorylation of ASIC3 and TRPV1 by acid-induced release of ATP was shown to be a mechanism sensitising oesophageal epithelial cells to acid. Moreover, the activation of the GPCR receptor PAR2 via mast cell tryptase was found to enhance ATP release following acid exposure [194]. Thus, although we did not observe co-localisation between CD45-immunoreactive leukocytes and ASIC3 in our GORD samples, immune cells such as mast cells may be sensitising ASIC3-expressing epithelial cells to acid indirectly. Our observation of differential ASIC3 expression in the oesophageal epithelium among GORD subgroups could explain the mechanisms of acid-induced heartburn, and particularly the role that epithelial cells play in the pathogenesis of heartburn. Importantly, ASIC3 and TRPV1

could heighten sensitivity to acid together, and topical therapy with ASIC3 antagonists could be another possible new sensory pharmacological treatment strategy for GORD patients experiencing pathological acid exposure.

Although previous studies suggested a possible sensory role of TRPM8 in the oesophageal mucosa, we demonstrate expression of this ion channel on CD45-positive lymphocytes in the submucosa of ERD patients. Unlike the colon where TRPM8 is on sensory nerve fibres [228], in the oesophagus it did not co-label with CGRP immunoreactive nerve fibres in the mucosal layer. This finding is in contrary to a previous study in humans which suggested that menthol infusion was able to induce heartburn in GORD patients [228]. While our results suggest that TRPM8 is unlikely to be a candidate target for future topical therapy, we highlight a potential immune role of TRPM8 as a small subpopulation of TRPM8-expressing cells were immunoreactive for CD45, a pan-leukocyte marker. TRPM8 could have a possible functional role as a modulator of macrophage function in the context of inflammation. While the underlying mechanisms through which TRPM8 controls macrophage function remains incompletely understood, TRPM8 activation in macrophages *in vitro* was shown to attenuate pro-inflammatory TNF-α secretion and increase immunomodulatory IL-10 secretion [451]. Whether such an anti-inflammatory role exists in the human oesophagus may be relevant to the submucosal immune expression of TRPM8 that we detected, and requires further investigation.

TRPA1 remains a promising target to our improved understanding and characterisation of the oesophageal mucosa in GORD patients. Our qPCR data shows *TRPA1* expression in all GORD phenotypes, with a trend towards higher expression in patients with FH. While lacking control data makes interpretation difficult, there is functional evidence for the activation of TRPA1-expressing sensory neurons through the activity of PAR2 in the guinea pig oesophagus during hyperalgesia [214]. IF-IHC studies to evaluate the localisation of TRPA1 in the epithelium of our GORD samples will extend our characterisation of the sensory phenotype of the oesophageal mucosa in these patients.

2.5 Limitations of Methodology

This study was limited by the absence of patients with acid hypersensitive oesophagus. However, these patients represent only a small proportion of the patients we investigated during the study period, which may be explained by our use of the wireless pH recording technique which detects only strongly acidic reflux events (<pH 4) and therefore cannot assess the association between symptoms and weakly acidic reflux. Whilst the lack of reflux hypersensitive patients in our cohort is a limitation, for the purpose of our study investigating the targets of acid hypersensitivity, pH data obtained through objective acid reflux monitoring

is most important. However, we acknowledge the limitation that AET data could not be obtained for 5/19 patients with normal endoscopy included in the study who were phenotyped into FH or NERD groups based on PPI response, meaning that they might not be 'true' NERD or FH. Additionally, BO patients included in the study were "on" PPI at the time of endoscopy, unlike ERD, NERD, and FH patients who discontinued PPI use two weeks prior to biopsy collection. This was in keeping with standard clinical practice which issues long-term PPI therapy for BO patients to decrease risk of esophageal adenocarcinoma [452]. Treatment with PPI could have modified mucosal structure and function, for example by resolving DIS [5], [453]. Moreover, biopsies represent only a small percentage of esophageal surface area, giving only a snapshot for anatomical localisation studies, and the method of biopsy needs to be improved with a more precise protocol. Finally, the lack of normal controls in this study is also a limitation. Expanding our study to investigate normal expression levels of TRPV1 and TRPM8 in our recruited healthy volunteers will be a critical follow-up to the current study.

2.6 Future Work

While the sensory phenotype of the oesophageal mucosa of adults with GORD has been substantially characterised, the phenotype of the normal oesophagus remains largely unknown. Ethical approval for collection of healthy volunteer biopsies was granted in January 2020, and recruitment began shortly after. 1 set of healthy volunteer biopsy were collected before endoscopies were cancelled due to the COVID-19 outbreak. Thus, future work for completion of this aspect of the study includes:

1) Evaluating the expression of TRPM8 and TRPV1 on healthy control samples with IF-IHC
2) Evaluating the gene expression of *TRPM8, TRPV1, ASIC3* and *TRPA1* by qPCR on healthy control biopsies

3 RNA sequencing the oesophageal mucosa of patients with GORD

3.1 Introduction

The molecular signature of the oesophageal mucosa of patients with GORD is yet to be clearly established. We recently identified expression of TRPV1 on superficial sensory nerves in patients with NERD, alongside increased epithelial cell expression of ASIC3 in erosive oesophagitis and NERD, collectively highlighting mucosal mechanisms for heartburn sensation in different reflux phenotypes [445]. However, acid reflux-induced alterations to epithelial barrier integrity, mucosal inflammation and sensitivity are likely to have an overlapping role in heartburn pathogenesis in GORD. We sought to better understand why some patients with heartburn symptoms develop oesophagitis and BO while others develop NERD or FH, using a bulk RNA sequencing approach.

While IF-IHC analysis provides important anatomical data, particularly in relation to sensory afferent nerves, it fails to capture the fine details of the disease, including cellular subpopulations, cell-type specific expression, cell-cell interactions, and pathways associated with different disease states and disease restitution. RNA sequencing is a technique that comprehensively maps cell types and states within a tissue of interest that allows detailed understanding of molecular signatures relevant to specific diseases. High-throughput technologies have become increasingly used to profile differential gene and protein expression in human disease states as compared with normal tissues [454]. While important progress has been made in unravelling the expression profiles of diseases such as cancers and the oesophageal adenocarcinoma precursor lesion BO, there is relatively limited insight into the biology of the oesophageal mucosa of ERD, FH, and NERD patients at the molecular level.

A comprehensive framework for the molecular basis of visceral hypersensitivity in the colorectum was recently described by single-cell RNA sequencing, whereby thoracolumbar and lumbosacral DRG were collected from healthy mice and individual colonic sensory neurons isolated and sequenced [436]. This expanded upon the previously described five subsets of sensory neurons (described in section 1.4 Peripheral pathways of pain sensation in the oesophagus) identifying seven distinct colonic sensory neuron subtypes by highlighting novel molecular markers associated with each mouse colonic neuron. Importantly, the study revealed differential expression of specific receptors to be responsible for response to currently used therapies. Compared with other neuronal subgroups, *TRPA1*, *TRPV1*, and

TRPV4 were most highly expressed in mPeptidergic-b neurons, while *ASIC3* showed greatest expression in mNeuroFilament-b and mPeptidergic-a neuronal subgroups [436]. What is clear from this data is that multiple sensory channels are expressed within the same colonic neuronal subtype [436]. Such molecular fingerprinting of colonic sensory neurons could facilitate drug development in conditions such as IBS, and with a similar approach applied to GORD.

Such comprehensive bioinformatic analysis has not previously been done in the human oesophagus of patients with reflux disease. A recent bulk-RNA sequencing study of oesophageal biopsies from achalasia patients and control subjects revealed 111 differentially expressed genes likely to be involved in neuronal and ICC changes that underlie primary achalasia [455]. Moreover, there have been 14 published studies on gene expression profiling of human BO, 6 of which have their raw data publicly available [456]–[461]. Analysis by Wang *et al*. applying serial analysis of gene expression (SAGE) and significance analysis of microarrays (SAM) identified 68 differentially expressed genes between BO and normal oesophagus (55 BO-associated genes and 13 normal oesophageal genes), which were then confirmed using IHC [454]. The data retrieved from both SAM and SAGE highlighted an important role of *CDX2* and *CDX1* in the development of BO, and the list of genes confirmed with IHC are likely to shape future studies on the pathophysiology of BO [454]. Moreover, a recent study used a single-cell sequencing approach to molecularly define distinct cell types in the human oesophagus, stomach, and duodenum, and described a quiescent COL17A1^{high}KRT15^{high} stem cell population in the basal layer of healthy oesophageal epithelium [462]. However, the use of high-throughput technologies to investigate the discrepancies between symptom presentation and level of acid exposure between the oesophageal mucosa of GORD phenotypes remains an unexplored territory.

The oesophageal mucosal gene expression signature in GORD phenotypes may highlight molecular markers important in targeting heartburn pathogenesis. We hypothesise that the gene expression profile of GORD patients will differ from healthy control samples, and possibly also from each other. In an attempt to advance our understanding of the signalling pathways which differentiate symptom profiles of GORD patients, as well as to identify genes/pathways for evaluation as therapeutic targets, this chapter will present a global assessment of the oesophageal mucosa at the molecular level via a bulk RNA sequencing approach. We identified marker genes selectively expressed in the oesophageal mucosa of each of the GORD phenotypes, providing insight for the first time into the potential molecular mechanisms contributing to the apparent discrepancies between endoscopic findings and heartburn perception in patients with GORD.

3.2 Materials and Methods

3.2.1 Patient Biopsies and Healthy Control Biopsies

Patient samples were collected and phenotyped as described in section 2.2.1 Patient Biopsies. Data from patients with ERD, NERD, FH, and BO were compared with data from a group of healthy and asymptomatic volunteers. Fourteen asymptomatic volunteers (aged 18-80) were recruited (detailed in Appendix Table 11). None of these volunteers had a history of gastrointestinal symptoms, or a history of anti-reflux medication use. All healthy controls (HCs) had a Reflux Disease Questionnaire score of 0. Healthy controls were excluded if they: 1) had previous upper GI surgery, 2) had severe upper GI motility disorders, 3) were pregnant, 4) were taking coagulopathy or concurrent anticoagulant medication, or 5) if they had any severe midface trauma or recent nasal surgery.

All subjects had normal oesophageal appearance on endoscopy. Five distal oesophageal biopsies were obtained per volunteer (3 cm above the gastroesophageal junction) at the Royal London Hospital. Distal oesophageal biopsies of these HCs were prepared and analysed in an identical fashion to the patient biopsies used in this study. Demographic data for patients and healthy control samples analysed can be found in Table 5 below, and in **Table 10**-11, appendix.

Table 5 Demographic data for patient and healthy control samples

Phenotype	Number of participants studied for RNA Sequencing Analysis	Mean Age (years)	Age Range (years)	Female: Male
NERD	9	44	28-53	3:6
ERD	10	46	21-74	2:8
FH	9	41	20-71	3:6
BO	9	54	31-75	4:5
HC	8	27	20-35	6:2

3.2.2 RNA Sequencing

3.2.2.1 RNA extraction

Endoscopic biopsies from the distal oesophagus were placed in RNA later solution (Sigma, Cat. Number R0901-100ml) and kept at -80ºC until RNA extraction. A total of 9-10 biopsy samples were selected for sequencing from each GORD phenotype. RNA isolation was performed using the RNeasy Mini Kit (Qiagen, Cat. Number 74016) as described in section 2.5.1, with the addition of DNase treatment (Qiagen, Cat. Number 79254). Briefly, after the first wash in buffer RW1 centrifuged for 15 sec, 80 µl of buffer RDD with 14% DNAse I (Qiagen)

was added to the column membrane and left to stand at room temperature for 15 min. The spin column was then washed again with 350 µl buffer RW1 and centrifuged for 15 sec at 10000 rpm, and the isolation was resumed as earlier described with wash steps in buffer RPE.

A maximum of 30 mg of tissue was used for each RNA extraction to ensure sufficient RNA yield for sequencing.

3.2.2.2 Library preparation and sequencing

Nanodrop and bioanalyzer were used to perform quality control (QC) checks of RNA supplied to the Genome Centre. RNA samples with RNA integrity less than 7 were excluded from library preparation. Representative bioanalyser reads can be found in Appendix 5.

cDNA libraries were generated using the NEBNext Ultra II Directional RNA Library Preparation Kit with the mRNA isolation module using the manufacturer's instructions (Illumina). Briefly, RNA samples were first diluted to 20ng/µl using RNAse-free water. First strand synthesis reaction buffer was prepared and left on ice until reaction. NEBNext oligo d(T) beads were washed with RNA binding buffer, placed on a plate and subsequently resuspended in RNA binding buffer on a magnetic rack. The plate was then sealed and placed on a thermal cycler with the lid heated to 75°C, at 65°C for 5min to denature RNA and facilitate binding of the poly-A mRNA to the beads. Following centrifugation, resuspension, and washing of the beads, the plate was placed on the magnetic rack again and supernatant was discarded. Next, 50µl of Tris buffer was added per well, plate sealed and incubated at 80°C for 2min with the lid heated to 90°C. The plate was removed when the temperature reached 25°C, centrifuged, and 50µl RNA binding buffer added per well to allow mRNA to re-bind beads. The supernatant was removed using the magnetic rack, and mRNA eluted from the beads by adding 11.5µl of the first strand synthesis buffer and placing in the thermal cycler with the lid heated to 105°C for 10min at 94°C. Following completion of incubation, the plate was removed from the thermal cycler, centrifuged, and purified mRNA collected by transferring 10µl of supernatant to a clean nuclease-free PCR plate. The plate was then placed on ice and first strand cDNA synthesis was immediately started.

The first strand enzyme mastermix (composed of NEBNext strand specificity reagent and NEBNext first strand synthesis enzyme mix) was added to the fragmented and primed mRNA, gently mixed, and the plate sealed and placed in the thermal cycler with the heated lid set to 80°C using the following conditions: 25°C for 10min, 42°C for 50min, 70°C for 15min, hold at 4°C. Plate was then removed, briefly centrifuged, and second strand cDNA synthesis reaction began immediately. Next, 60µl second strand mastermix (composed of nuclease free water, NEBNext second strand synthesis buffer, and NEBNext second strand synthesis enzyme mix) was added to the first strand synthesis reaction. The plate was sealed and placed in thermal

cycler for 60min at 16°C. AMPure XP beads were resuspended and added to the second strand synthesis reaction to purify the double-stranded cDNA. The supernatant was subsequently discarded and washed in 80% ethanol, airdried, and the DNA target was eluted from the beads by adding 53µl 0.1x TE buffer to the beads. The end prep mastermix was prepared by combining NEBNext Ultra II end prep reaction buffer and NEBNext Ultra II end prep enzyme mix, and added to the purified cDNA. The sealed plate was then placed in a thermal cycler at 20°C for 30min, and 65°C for 30min, and removed when the incubation reached 4°C.

Following adaptor ligation and purification using AMPure XP beads, the PCR library was enriched by adding 25µl of NEBNext Q5 Hot start HiFi PCR master mix and 10µl of pre-assigned index primer to each well and incubation. The thermal cycler lid was heated to 105°C, and samples went through: 1 cycle of 98°C for 30sec, 98°C for 10sec, 13 cycles of 65°C for 75sec, 1 cycle of 65°C for 5min, and held at 4°C. The PCR reaction was then purified using Agencourt AMPure XP beads. All resulting libraries were quantified using the Qubit HS dsDNA kit and qualified on the appropriate 1000bp ScreenTape according to concentration.

Paired end mRNA sequencing was performed using the NextSeq 500 High Output Kit (Blizard Genome Centre) with 20M reads and a read length of 75bp per sample.

3.2.2.3 Sequencing data analysis

3.2.2.3.1 Quality Control

Sequencing analysis was conducted using Partek Flow software, as shown in Figure 31. FASTQ files were demultiplexed and underwent pre-alignment QC to ensure that the collected data did not have any obvious systematic errors before alignment (Table 12, Figure 30). Next, Spliced Transcripts Alignment to a Reference (STAR) was used to align sequenced reads to the hg38 human genome [463]. Adapter sequence overrepresentation was insignificant, so trimming was not necessary. Post-alignment QC was performed to check the quality of alignment. All samples had more than 97% alignment to the genome as shown in **Figure *32***A. The total number of reads was more variable, but most samples had more than 17M reads (**Figure *32***B, Appendix Table 13). There was no parameter for removing outliers based on QC metrics, as advised by a bioinformatician.

Principal component analysis (PCA) was then performed including the first two principal components. The PCA shows the similarity between healthy controls (Figure 33A), where they spatially arranged close to one another. Samples NE8 (FH), SH061119 (BO), and RC110320 (BO) appeared to be outliers as they were spatially dissimilar to the other GORD samples. These samples were further evaluated using a selection of Barrett's segment (*SOX9,*

MUC5AC) and stromal collagen genes (*COL3-6A*) to check the significant expression of these genes among any of the samples. As seen in Figure 33D, the three outliers identified by PCA had significantly higher expression of stromal collagen genes (NE8), and Barrett's segment genes (SH061119 and RC110320), and were excluded from downstream analysis, as agreed by bioinformatician. Figure 33C shows PCA once outliers have been removed.

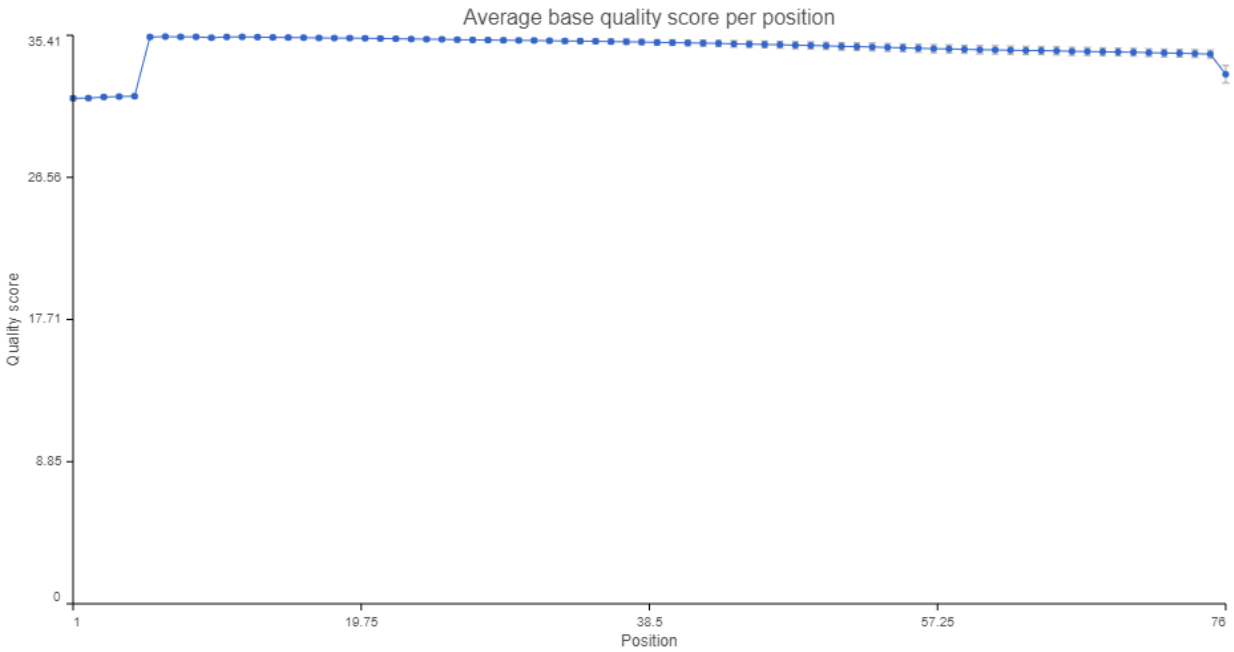

Figure 30 Pre-alignment QC

Average read quality was above 33 for all samples. Pre-alignment QC was performed on Partek flow.

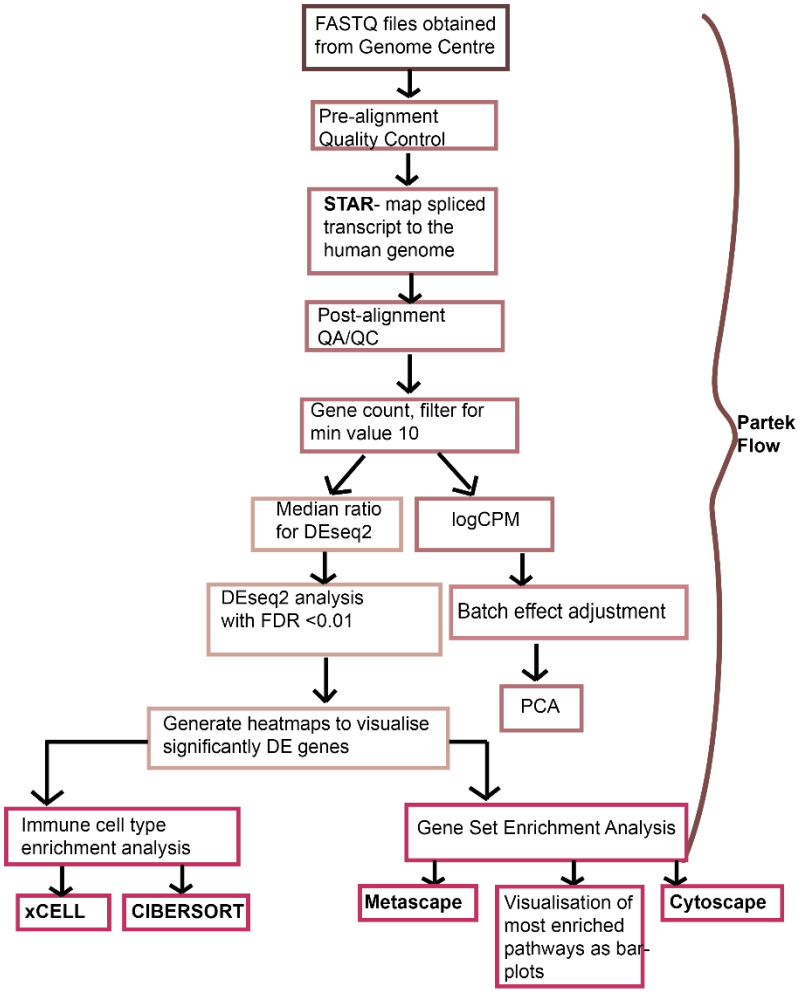

Figure 31: RNA Sequencing Analysis Workflow

A flow diagram demonstrating the methods and software used to analyse RNA Sequencing data.

3.2.2.3.2 Differential Expression Analysis

Aligned genes were normalised using median ratio for DEseq2 on Partek Flow, as seen in Figure 31. Differentially expressed genes between phenotypes were calculated using the Wald test in DESeq2 R package [464] with an FDR-adjusted *p* value of less than 0.01. The most biologically significantly differentially expressed genes were visualised as hierarchical clustering heatmaps on Partek Flow.

3.2.2.3.3 Gene Set Enrichment Analysis

Gene set enrichment analysis of FDR filtered differentially expressed genes was performed on Partek flow with a 0.01 *p* value cut off. R was used to visualise the most significantly biologically enriched gene functions. Metascape and Cytoscape were used to visualise functionally enriched gene ontologies, and compare GSEA results[465].

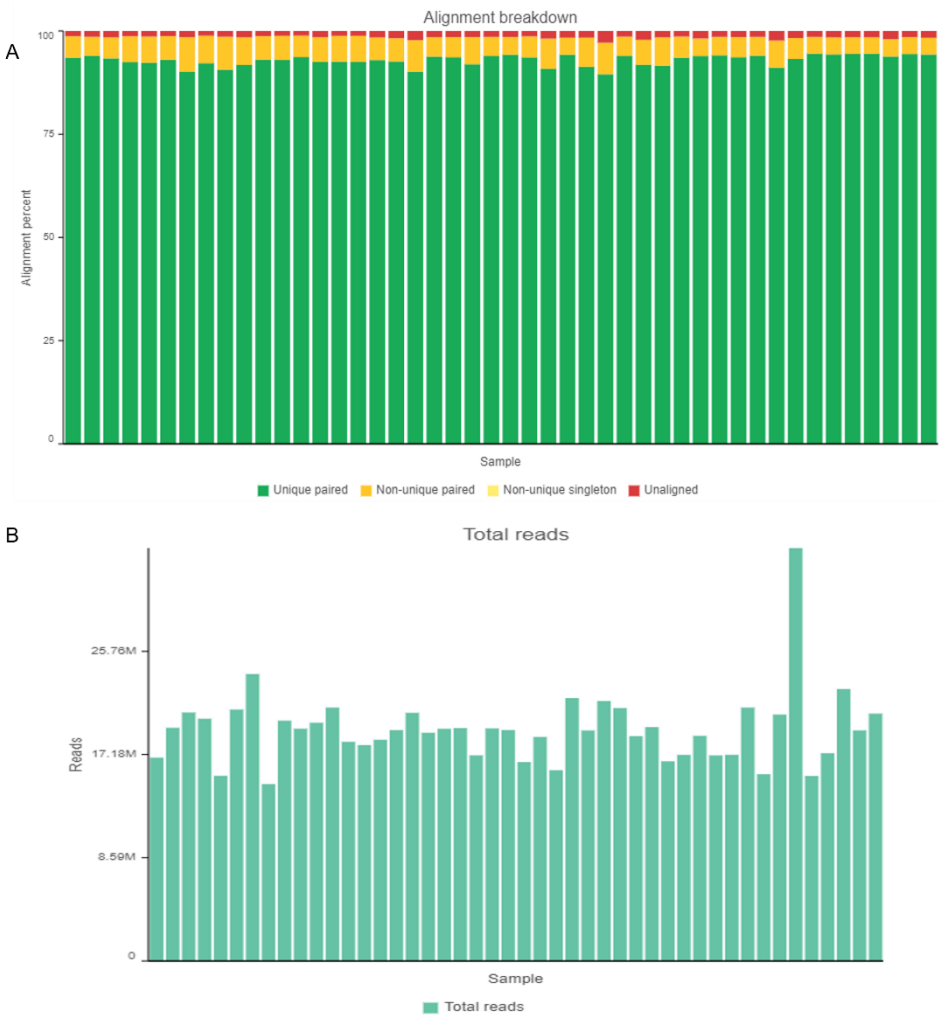

Figure 32 Post-alignment QC

General quality information about the whole data set subsequent to alignment using STAR. A) More than 97% of the reads were aligned to the genome. B) The total number of reads is more variable, but most samples had more than 17M reads. A more detailed report can be found in Appendix, table 13.

3.2.2.4 Cellular deconvolution

Deconvolution analysis for quantification of relative levels of distinct cell types in each tissue samples was carried out on normalised counts using xCell and CIBERSORT. xCell performed immune cell type enrichment analysis to infer 64 immune and stromal cell composition profile of oesophageal mucosal tissue from 1822 pure human cell type transcriptomes [466]. This was validated using CIBERSORT, another machine learning method which inferred an estimation of the immune cell composition of our mixed cell population.

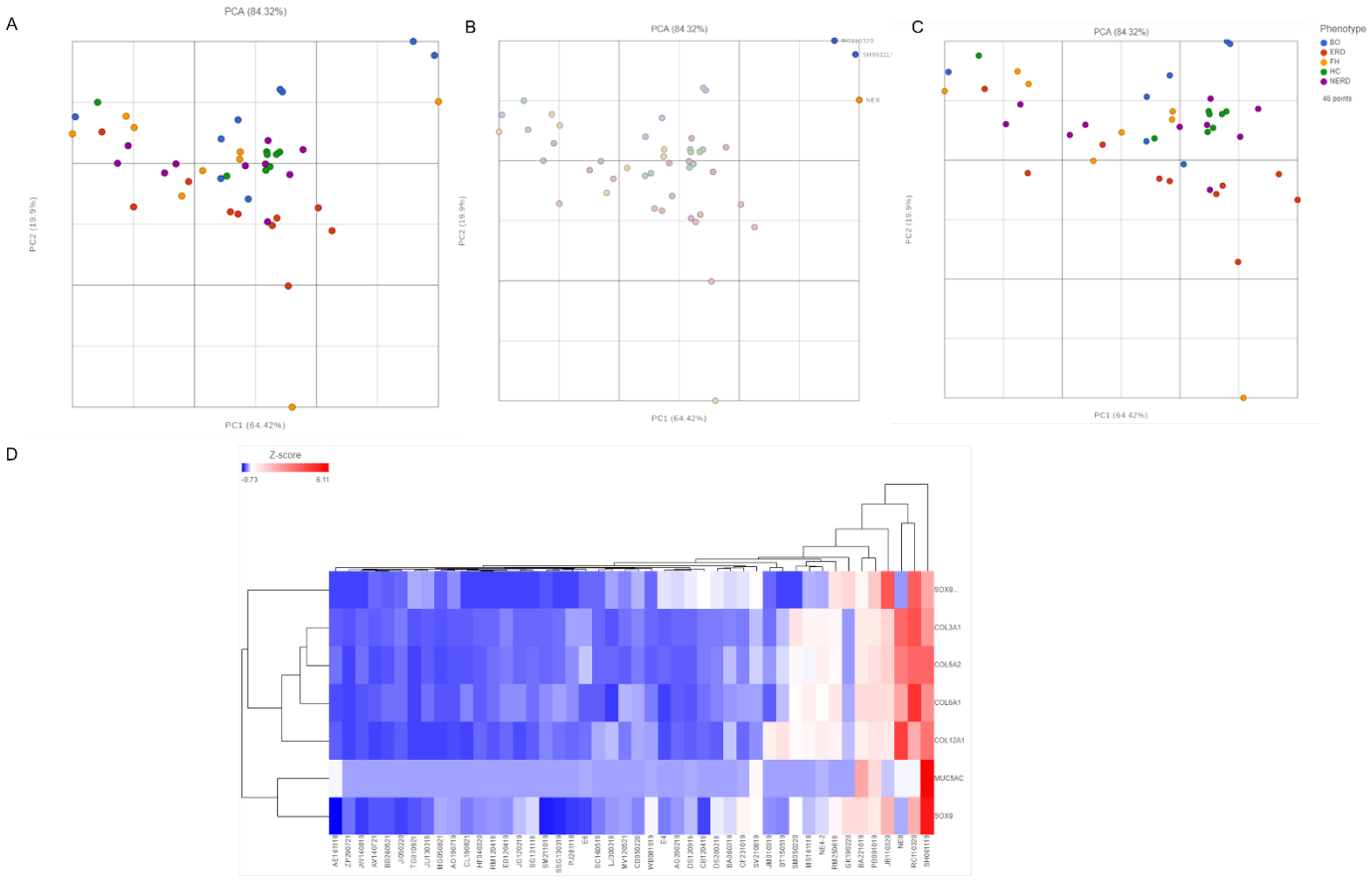

Figure 33 PCA plot of expression similarity between samples

A) PCA plot showing a scatter plot of samples along the first two principal components, where the spatial arrangement of the points reflects data similarity between samples. B) Three outliers highlighted from the PCA: NE8 (FH), SH061119 (BO), and RC110320 (BO). C) Refined PCA with outliers removed based on biological characteristics, i.e. high expression of stromal collagen and Barrett's segment genes. D) Samples filtered for expression of stromal collagen genes and Barrett's segment genes. NE8 (FH) had significantly higher expression of stromal collagens COL5A, while samples SH061119 (BO), and RC110320 (BO) had significantly higher expression of stromal collagen genes and Barrett's segment genes SOX9 and MUC5AC.

3.2.2.5 Tissue Structure

Corresponding PFA-fixed frozen biopsies from patients and healthy controls included in the RNA sequencing study were stained with haematoxylin and eosin (H&E) to determine sample size variability. Figure 34 shows that all samples had an intact basal layer of the epithelium, and contained papillary structures, indicating adequate tissue thickness across the phenotypes studied. Submucosa was occasionally seen in some samples, such as in the representative ERD sample in Figure 34.

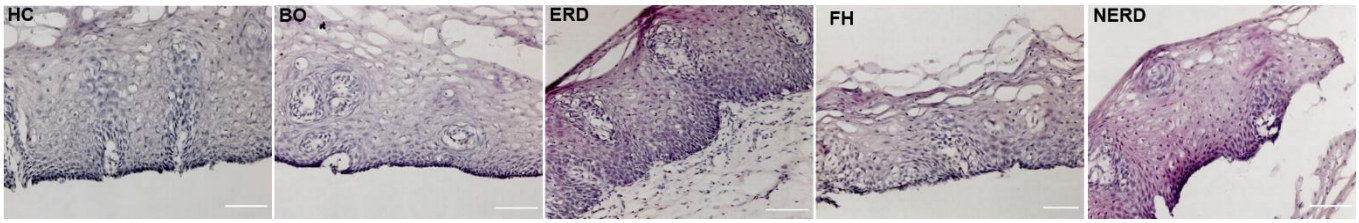

Figure 34 H&E staining of corresponding biopsies of RNA-sequenced samples

H&E staining of fixed corresponding biopsies of samples included in the RNA sequencing (and immunofluorescence) studies highlights that all samples had an intact basal layer, and papillary structures indicating an acceptable tissue thickness. Submucosa was occasionally seen in some samples, such as the representative ERD sample here. Images were taken using TissueFax. Scale bar represents 100µm.

3.2.3 Validation of RNA Sequencing Data with IF

A representative number of corresponding PFA-fixed frozen biopsies from patients and healthy controls included in the RNA sequencing study were evaluated with IF to validate the finding of differential gene expression data, following the methodology described in section 2.2.3 Immunofluorescence-Immunohistochemistry. Primary antibodies used included CD1a (monoclonal Mouse, Dako, M3578, 1:200), mast cell tryptase (monoclonal mouse, Dako, M7052, 1:400), keratin 14 (monoclonal mouse, Cell Signalling, LL02, 1:200), keratin 16 (polyclonal rabbit, Abcam ab181055, 1:100), and keratin 17 (polyclonal rabbit, Abcam ab51056, 1:300). Positive signals were quantified as described in section 2.2.4 Image analysis.

3.3 Results

3.3.1 Differential Gene Expression in Normal and GORD Oesophageal mucosa

In order to assess quantitative changes in gene expression levels between oesophageal mucosa of healthy controls and GORD patients, differential expression (DEseq2) analysis [464] was performed between healthy controls (N=8) and GORD patients (N=37) phenotyped endoscopically and with objective reflux studies and pooled into one group. An FDR filter of <0.01 was applied, and detected 979 differentially expressed (DE) genes between the normal oesophageal mucosa and that of GORD patients, as shown in Figure 35A, and Appendix table 14. There were more genes upregulated in GORD than genes downregulated compared to asymptomatic individuals. The most differentially expressed genes are highlighted in Figure 35B.

Using R, an adjusted *p* value of less than 0.01 and filter for DE genes with TPM over 100 were applied to visualise the most biologically significant DE genes among the two groups, highlighting genes with important structural functions. These DE genes included members of the keratin gene family and included: *KRT8, KRT14, KRT16, KRT17*, and *KRT78* (Appendix 5). Keratins are major structural proteins with critical functions in forming the cytoskeletal scaffold of epithelial cells that gives them the ability to withstand both mechanical and non-mechanical stress [467]. While *KRT78* and *MUC21* were highly expressed in the normal oesophageal mucosa, they were significantly downregulated in oesophageal mucosa of GORD patients (Appendix 5). In contrast, *KRT8* was upregulated predominantly in BO oesophageal mucosal patients, and *KRT14, 16,* and *17* were upregulated in ERD patients (Appendix 5). Collectively, these DE patterns were associated with increased organisation of the extracellular matrix, actin-filament processes, and regulation of cell adhesion.

Next, in order to infer important biological processes and molecular functions associated with DE genes between healthy and GORD oesophageal mucosa, gene set enrichment analysis (GSEA) was performed on Partek. A total of 979 significantly DE genes were taken as input for this enrichment analysis, and were highlighted in 896 molecular pathways including regulation of immune system process, extracellular matrix (ECM) organisation, and humoral immune response as statistically significative (*p*=<0.01). The most significantly enriched 20 pathways were visualised as a bar graph against log scaled *p* values (Figure 35C).

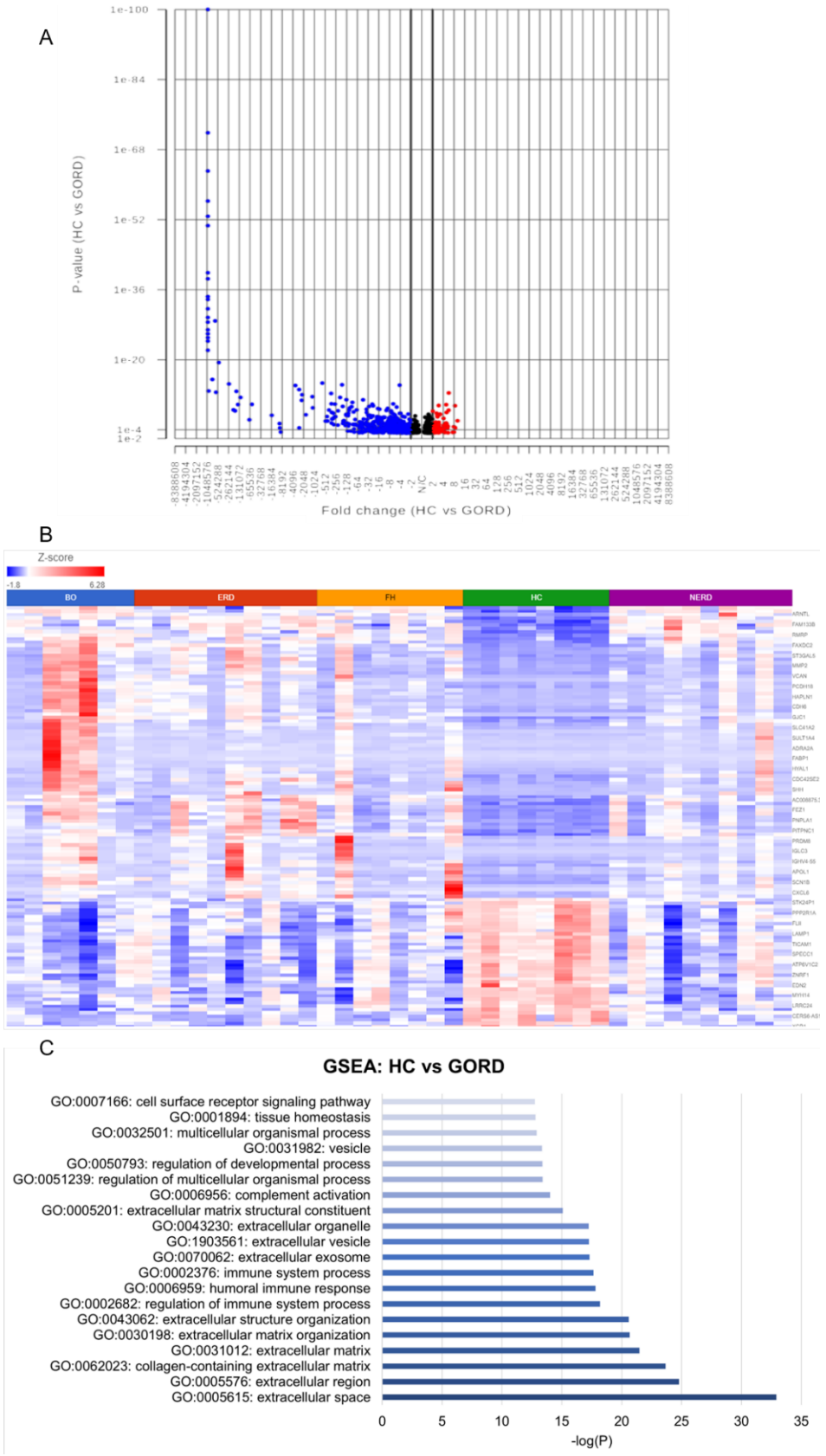

Figure 35 Differential gene expression between healthy control and GORD oesophageal mucosa

A) Volcano plot showing 979 genes upregulated in HCs as log2 scaled fold change in red dots on the right of the graph, and genes downregulated in HCs compared to GORD on the left. 94 genes were upregulated and 589 genes were downregulated in HCs compared to GORD. B) heatmap displaying the most significantly DE genes between healthy controls and GORD with FDR p=0.01. C) Bar graph displaying the most biologically enriched pathways from GSEA as log scaled p values (p<0.01). Graphs made using Partek. HC: N=8, BO: N=7, ERD: N=10, FH: N=8, NERD: N=9

3.3.2 Differential Gene Expression in Normal and FH Oesophageal Mucosa

To identify molecular markers associated with mucosal differences between FH patients and healthy controls, DESeq2 analysis was performed on RNA sequenced FH (N=8) and HC (N=8) samples. A FH sample (NE8) was excluded from DESeq2 analysis due to the detection of high stromal collagen expression in this sample, suggesting a large submucosal region as opposed to a purely squamous epithelial cell origin, as shown in Figure 33. Compared to the oesophageal mucosa of healthy asymptomatic subjects, FH patients had 711 significantly differentially expressed genes, as seen in Figure 36A. An FDR filter of <0.01 was then applied to visualise the most significantly DE genes. Interestingly, circadian rhythm-related genes *PER1* and *CIART,* normally highly expressed in the oesophagus [468], [469] were found to be downregulated in FH (Figure 36B). While *CIART* is involved in the circadian regulation of gene expression, *PER1* is known as a 'clock gene' which acts as the primary circadian pacemaker in the mammalian brain [477], [478].

GSEA of these most significantly DE genes between HC and FH highlighted circadian regulation of gene expression, immune system processes, and defence response, as statistically significative (p=0.01) (Figure 36C).

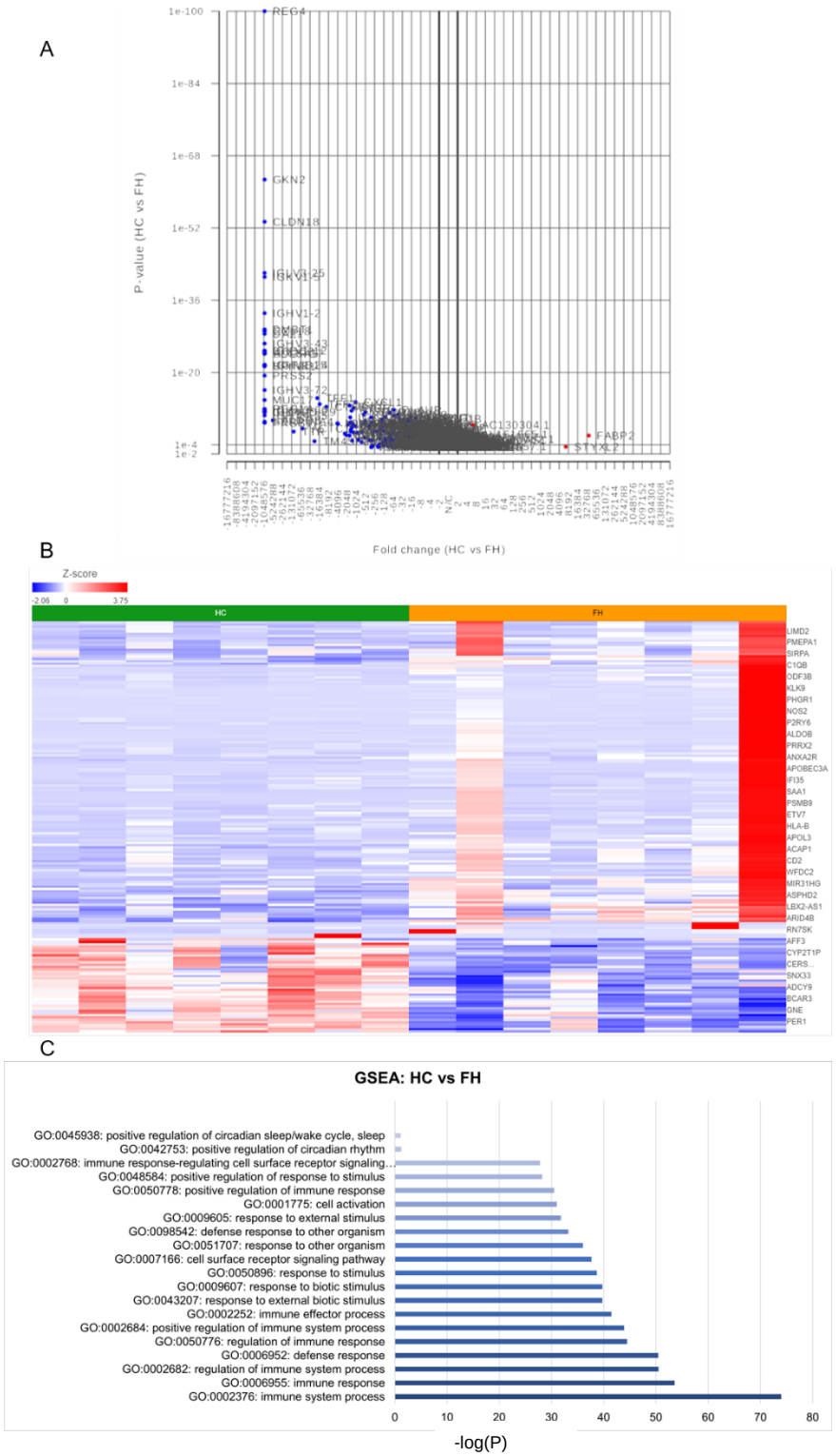

Figure 36 Differentially Expressed Genes Between Normal and FH Oesophageal Mucosa

A) Volcano plot showing 711 DE genes between HCs and FH: 24 genes upregulated and 647 genes downregulated in HCs compared to FH. Most significantly DE genes are highlighted. B) Heatmap displaying FDR filtered DE genes Z score= Log2 fold change in gene expression. C) Bar graph of most statistically significative functional categories highlighted (p<0.01). HC: N=8, FH: N=8

3.3.3 Differential Gene Expression in Normal and NERD Oesophageal Mucosa

To identify molecular markers associated with mucosal differences between NERD patients and healthy controls, DESeq2 analysis was performed on RNA sequenced NERD (N=9) and HC (N=8) samples. Compared to the oesophageal mucosa of healthy asymptomatic subjects, NERD patients had 137 significantly differentially expressed genes, as seen in Figure 37A. Upregulated genes included *HOXA7, ADAM9, DES, IGHV3*, and *MMP9* in NERD, and downregulation of genes such as *ACTN4* which encodes for the actin-binding protein α-actinin-4 and participates in reorganisation of the cytoskeleton [470], [471] (Figure 37B). Manually filtering for DE genes with TPM over 25 and *p* value <0.01 detected two clusters of NERD patients (Appendix 6). While 8/9 NERD patients had no log2 fold change of expression of *KRT14*, *IGKC, LYZ, AGR2, REG4, TFF1*, and *TFF2*, a single NERD patient showed 3log2 fold change of expression of these genes (Appendix 6). Similarly, while 6/9 NERD patients showed 2log2 fold change of *AKR1C3* and *WFDC21P*, 3/9 NERD samples showed a slight downregulation of these genes. These DE genes were highlighted in several molecular pathways including maintenance of gastrointestinal epithelium, regulation of innate immune response, and epithelial structure maintenance, as shown in Figure 37C.

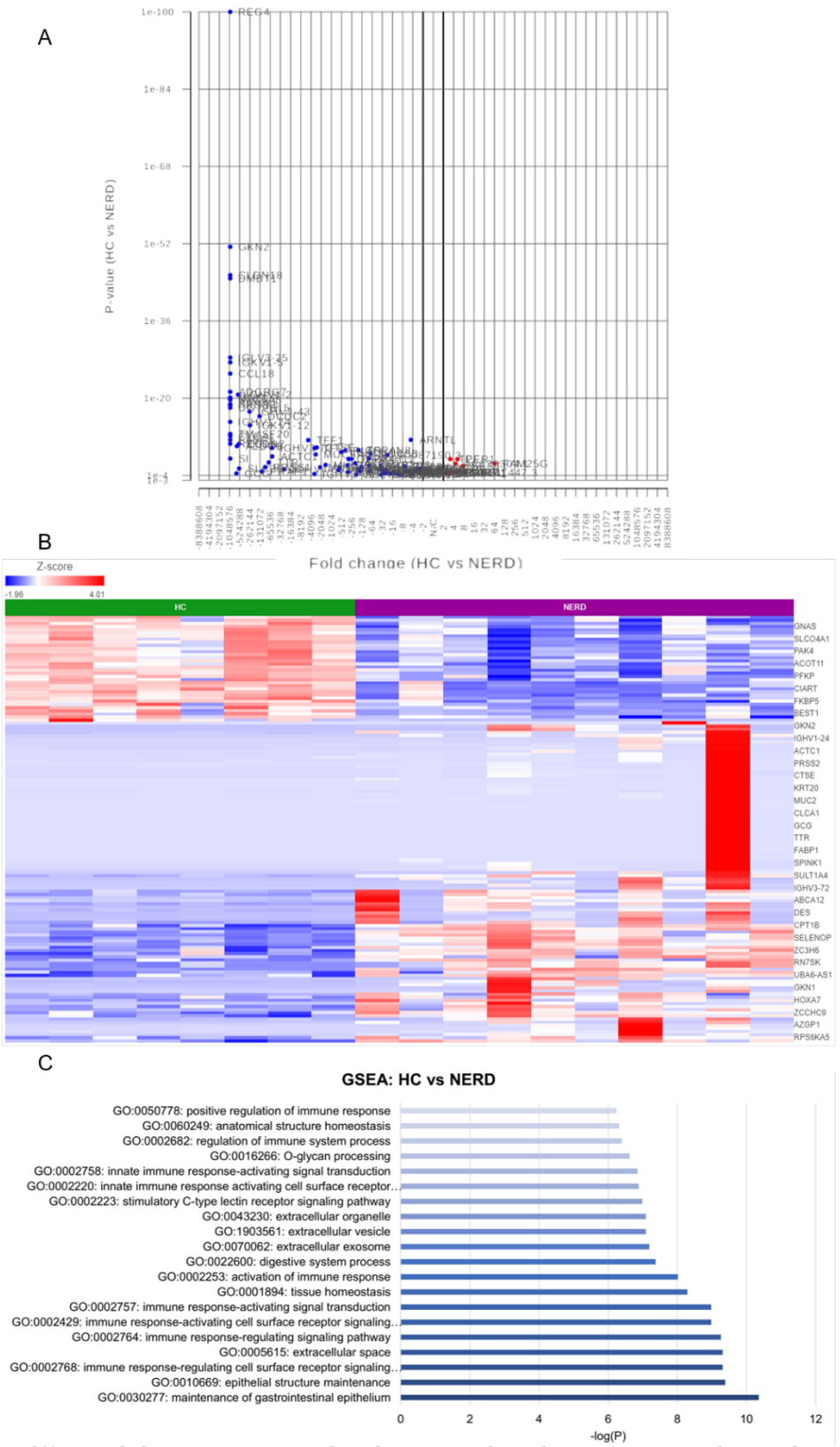

Figure 37 Differential Gene Expression in Normal and NERD Oesophageal Mucosa

A) Volcano plot showing 137 DE genes: 12 genes upregulated and 88 genes downregulated in HCs compared to NERD. B) Heatmap displaying the top significantly DE genes between HC and NERD. C) Bar graph of statistically significantly enriched biological pathways against log transformed *p* values ($p<0.01$). HC: N=8, NERD: N=9.

3.3.4 Differential Gene Expression in Normal and ERD Oesophageal Mucosa

To identify molecular markers associated with mucosal differences between ERD patients and healthy controls, DESeq2 analysis was performed on RNA sequenced ERD (N=10) and HC (N=8) samples. Compared to the oesophageal mucosa of healthy asymptomatic subjects, ERD patients had 356 significantly DE genes, as seen in Figure 38A. Significantly upregulated genes included *CXCL1, KRT10*, *KRT16*, *TNC,* and *CCL21* (Figure 38B). DE genes downregulated in ERD compared to HC included *CLDN10,* a gene important in tight junction formation and function [472]. Applying a filter for DE genes with TPM over 150 and *p* value <0.01 using R to determine the most significantly DE genes, we detected two clusters of ERD patients (Appendix 9). Interestingly, this highlighted downregulation of genes including *KRT78, KRT4, IL18*, and *LYPD2* in ERD compared to healthy controls, while *S100A6-7, KRT17, KRT14, KRT16*, *KRT6A-C*, and *S100A2* were highly upregulated in 5/10 ERD patients (Appendix 7). The remaining 5 ERD samples showed 0log2 fold change of these highly upregulated genes. These DE genes were highlighted in several molecular pathways including positive regulation of cell proliferation, humoral immune response, and complement activation as statistically significative (*p*=<0.01) (Figure 38C).

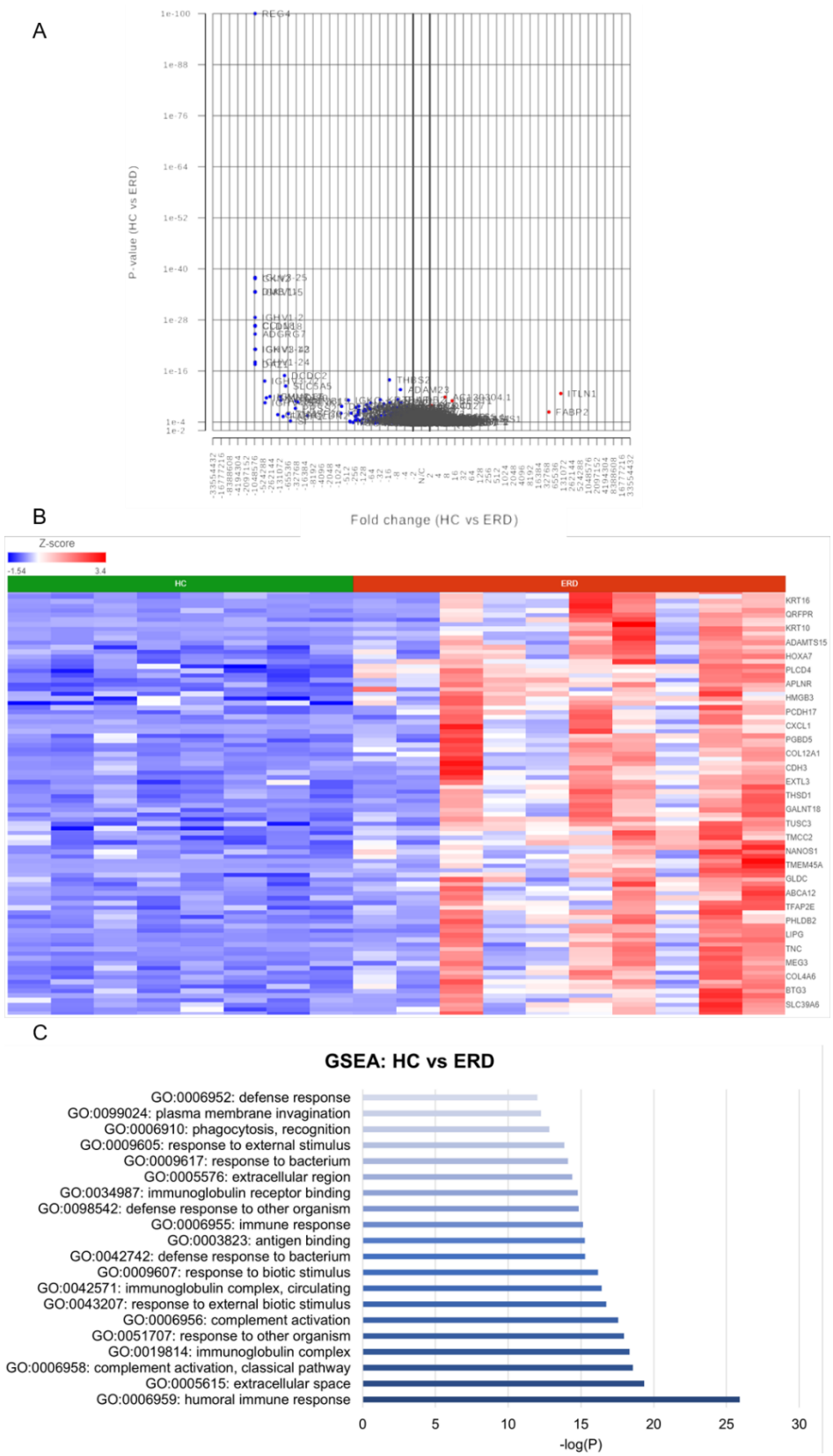

Figure 38 Differential Gene Expression Between ERD and Normal Oesophageal Mucosa

A) Volcano plot showing 356 DE genes between HCs and ERD patients as log2 scaled fold change: 55 genes upregulated and 245 genes downregulated in HCs compared to ERD patients. B) Heatmap displaying the top significantly DE genes between HC and ERD. C) Bar graph of the most statistically significantly enriched biological pathways against log transformed *p* values ($p<0.01$). HC: N=8, ERD: N=10.

3.3.4.1 Validation of Differential Keratin Expression in Oesophageal Mucosa of GORD Patients

To validate the finding of increased keratin 14 in NERD and ERD, and increased expression of keratin 16-17 in ERD oesophageal mucosa, IF was performed on a representative number of GORD patient tissue phenotyped into ERD (N=4), NERD (N=4), FH (N=6), BO (N=3), and healthy controls (N=4).

Keratin 14 protein expression was not frequently observed on oesophageal epithelial cells in healthy controls, patients with FH or BO, but was seen in the basal layer in patients with ERD and NERD (Figure 39A). There was no significant difference in the level of keratin 14 protein expression among HCs, FH, BO, and patients with ERD and NERD (Figure 39B). Keratin 16 and 17 were most frequently observed on oesophageal epithelial cells in the basal layer, as seen in Figure 40A and Figure 41A. There was no significant difference in the expression of keratin 16 or 17 proteins among HCs or GORD patients (Figure 40B, Figure 41B).

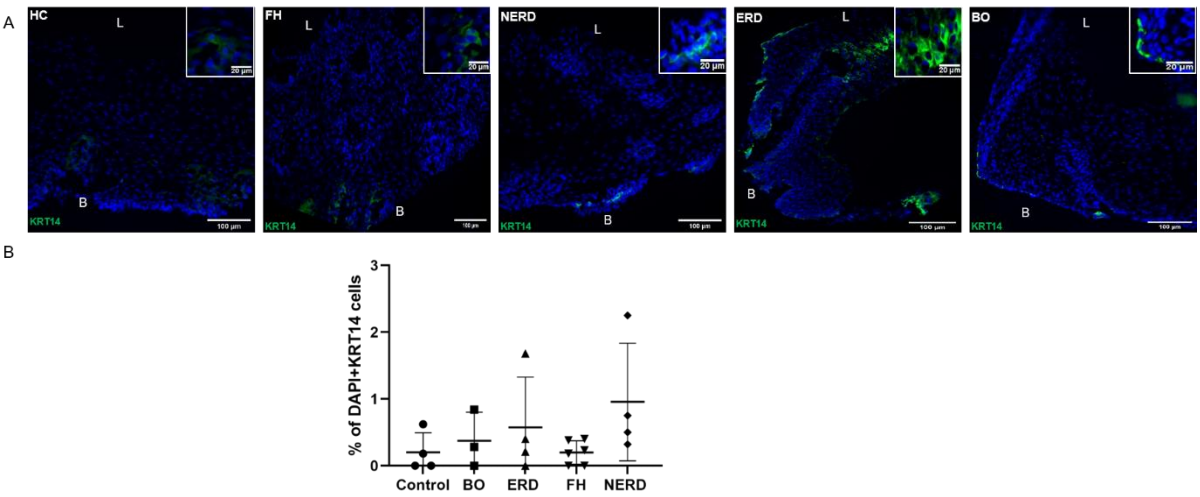

Figure 39 Validation of Keratin 14 Protein Expression in the Oesophageal Mucosa of Patients with ERD and NERD

A) KRT14 is not frequently expressed by oesophageal epithelial cells in healthy controls, patients with FH, or BO. In ERD and NERD patients, KRT14 is expressed by epithelial cells in the basal layer. B) There is no significant difference in KRT14 protein expression among HCs nor GORD patients, but a slight increase in NERD and ERD patients. Scale bar: 100μm. Inset scale bar: 20μm. L=lumen, B= basal layer.

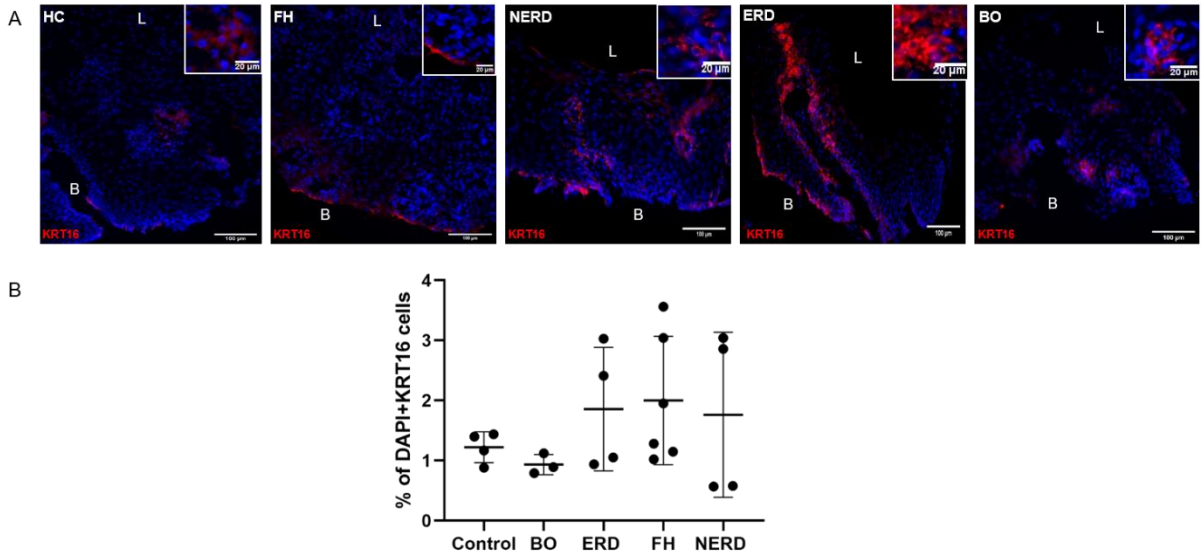

Figure 40 Validation of Keratin 16 Protein Expression in the Oesophageal Mucosa of Patients with ERD

A) KRT16 is most frequently expressed by oesophageal epithelial cells in the basal layer. B) There is no significant difference in KRT16 protein expression among HCs nor GORD patients. Scale bar: 100µm. Inset scale bar: 20µm. L=lumen, B= basal layer.

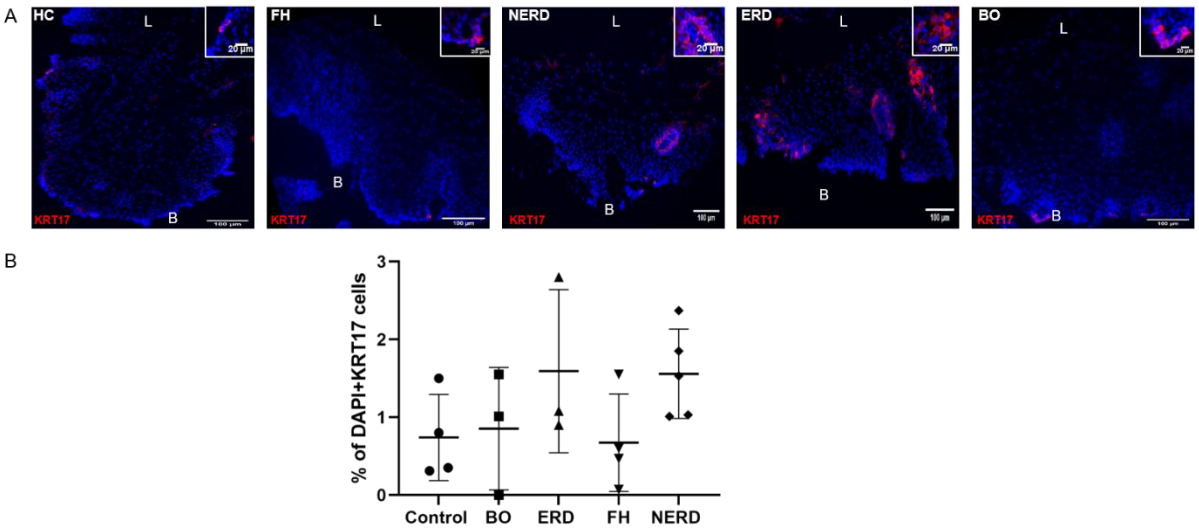

Figure 41 Validation of Keratin 17 Protein Expression in the Oesophageal Mucosa of Patients with ERD

A) KRT17 is most frequently expressed by oesophageal epithelial cells in the basal layer. B) There is no significant difference in KRT17 protein expression among HCs nor GORD patients, but a slight increase in ERD patients. Scale bar: 100μm. Inset scale bar: 20μm. L=lumen, B= basal layer.

3.3.5 Differential Gene Expression in Normal and BO Oesophageal Mucosa

To identify molecular markers associated with mucosal differences between BO patients and healthy controls, DESeq2 analysis was performed on RNA sequenced BO (N=7) and HC (N=8) samples. Two BO samples (SH061119 and RC110320) were excluded from DESeq2 analysis due to the detection of high stromal collagen expression and Barrett's segment genes in these samples, suggesting columnar as opposed to purely squamous epithelial cell origin, as shown in Figure 33. Compared to the oesophageal mucosa of healthy asymptomatic subjects, BO patients had 3010 significantly DE genes, as seen in Figure 42A. Genes involved in the formation of the immunoglobulin complex such as *IGKV1-12* and *NRCAM* were among the most significantly upregulated genes in BO compared to healthy controls (Figure 42B). *MUC21*, *TGM1* and *TGM3* were among the most significantly downregulated genes in BO compared to HC. *MUC21* is a transmembrane-like mucin that acts as an epithelial defence molecule [473], while *TGM1* (and *TGM3*) encodes transglutaminase-1 (or transglutaminase-3)- catalytic membrane-bound enzymes that regulates cornified cell envelope formation in the epidermis [474]. These DE genes were highlighted in several biological pathways including igA immunoglobulin complex, extracellular matrix organisation, and regulation of cell migration, as shown in Figure 42C.

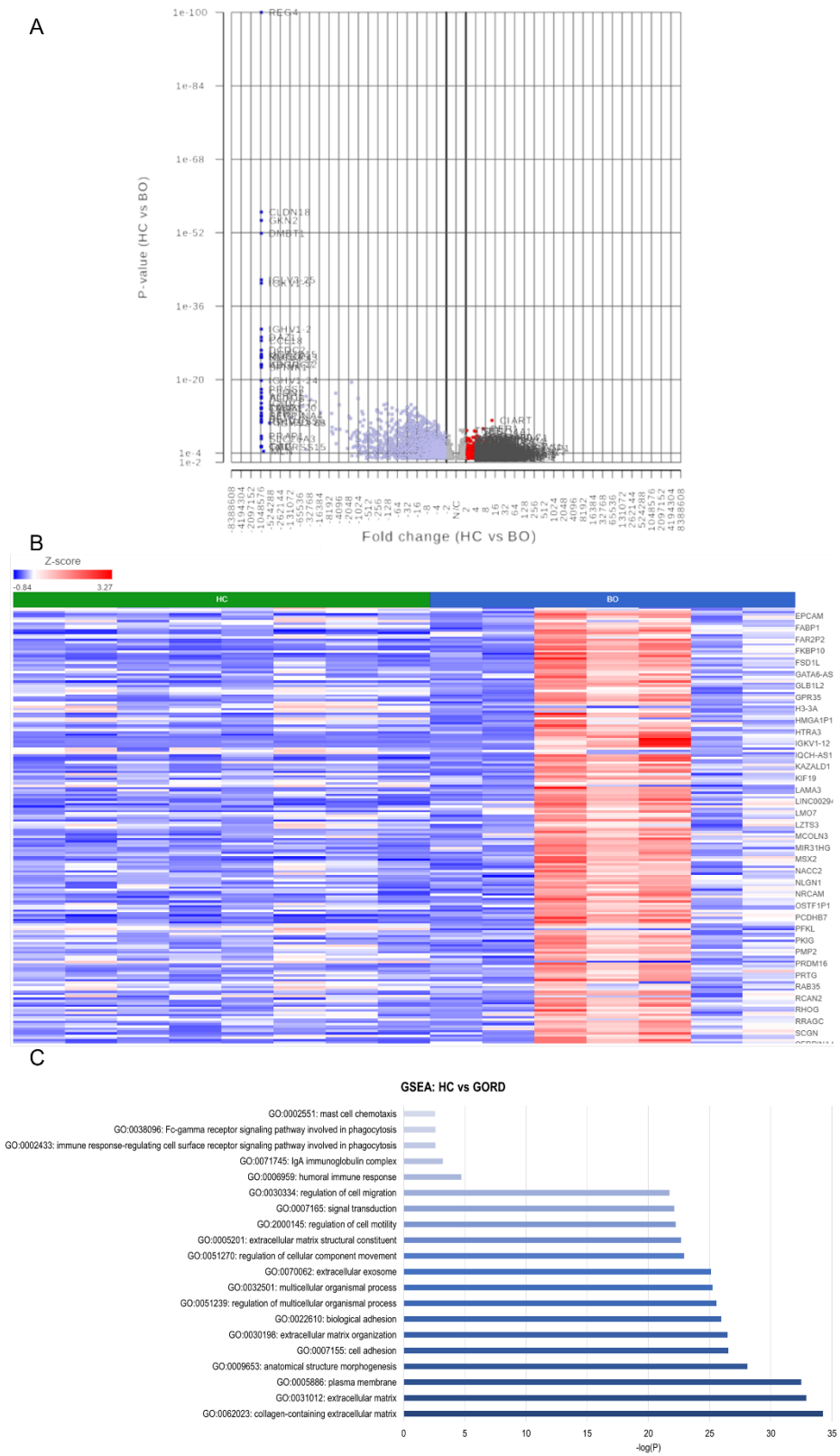

Figure 42 Differential Gene Expression Between Normal and BO Oesophageal Mucosa

A) Volcano plot showing 3010 DE genes between HCs and BO patients as log2 scaled fold change: 251 genes upregulated and 1978 genes downregulated in HCs compared to BO patients. B) Heatmap displaying the top significantly DE genes between HC and BO. C) Bar graph of the most statistically significantly enriched biological pathways against log transformed *p* values ($p<0.01$). HC: N=8, BO: N=7.

3.3.6 Differential Gene Expression Among GORD Phenotypes

3.3.6.1 DESeq2 in FH:NERD Oesophageal Mucosa

To identify molecular markers associated with mucosal differences between FH and NERD patients, DESeq2 analysis was performed on RNA sequenced FH (N=6) and NERD (N=10) samples. FH samples (NE8 and NE4-2) were excluded from the analysis, as explained in section 3.2.2.3.1 Quality Control. Compared to the oesophageal mucosa of FH patients, there were 137 DE genes in NERD patients (Figure 43A). The most significantly upregulated genes in NERD compared to FH included *CLCA1*, a gene encoding a member of the calcium sensitive chloride channel family that is associated with neuropathic pain- signalling in dorsal root horn neurons (Figure 43A-B) [475]. GSEA highlighted cytokine-mediated signalling, leukocyte activation, and regulation of immune response, as significantly enriched pathways, as shown in Figure 43C.

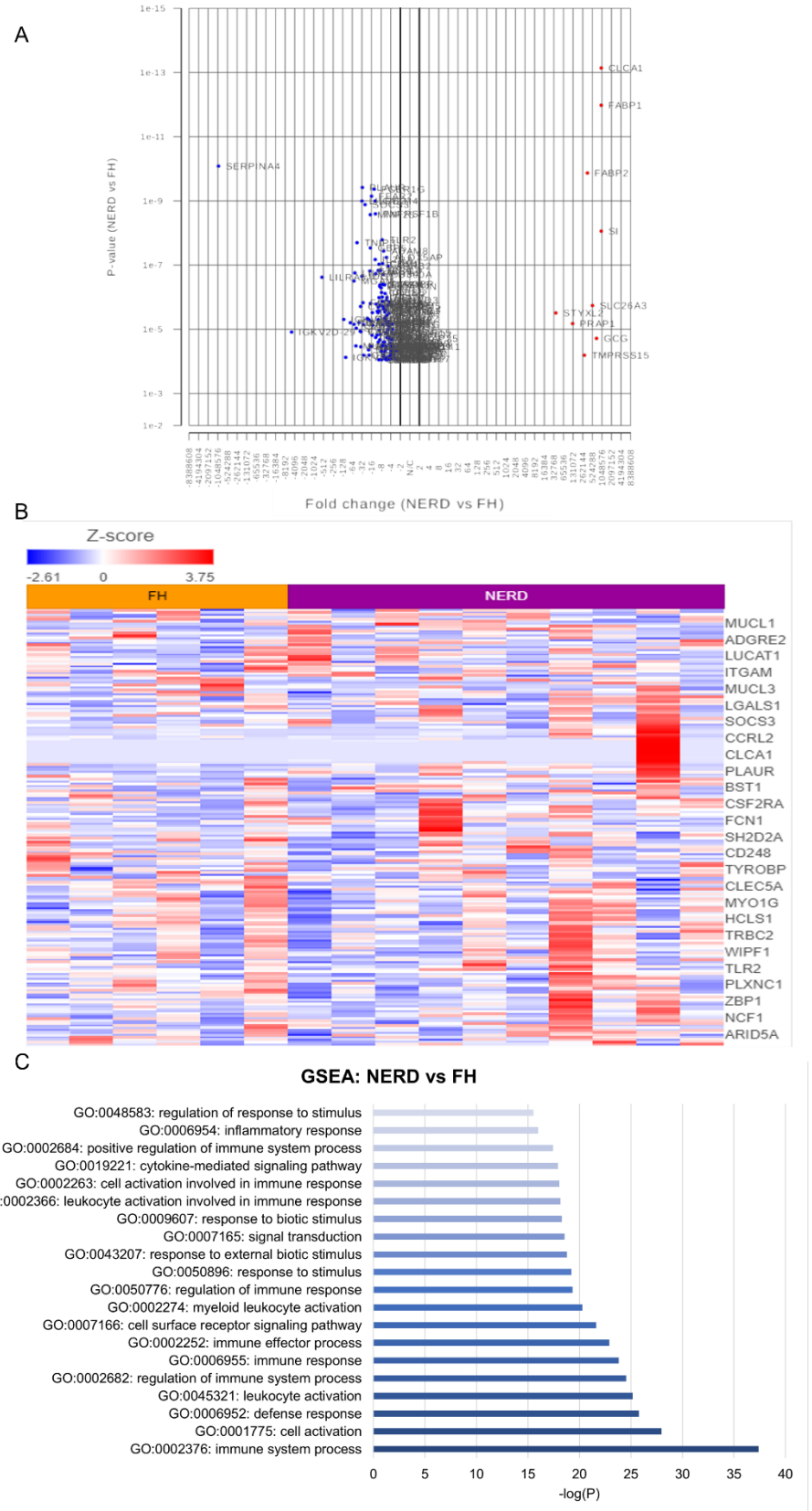

Figure 43 Differential Gene Expression Between NERD and FH Oesophageal Mucosa

A) Volcano plot showing 186 DE genes between NERD and FH patients as log2 scaled fold change: 9 genes upregulated and 177 genes downregulated in NERD compared to FH patients. B) Heatmap displaying the top significantly DE genes between NERD and FH. C) Bar graph of the most statistically significantly enriched biological pathways against log transformed *p* values ($p<0.01$). NERD: N=10, FH: N=6.

3.3.6.2 DESeq2 in ERD:NERD Oesophageal Mucosa

We next sought to identify possible molecular mechanisms that result in some heartburn patients developing oesophagitis while others develop NERD. DESeq2 analysis was performed on RNA sequenced ERD (N=10) and NERD (N=9) samples. Interestingly, this revealed only 13 significantly DE genes between the two disease groups (Figure 44A). These 13 DE genes included *PLTP, TNC*, and *SNCA*, which are implicated in increased extracellular matrix organisation in ERD compared to NERD as statistically significative (p=<0.01) (Figure 44B-C). None of the 10 DE genes identified appeared to be involved directly in barrier function. In contrast, genes upregulated in NERD compared to ERD included *ITLN1* gene involved in the innate immune response, *FABP2* and *ALDOB* genes enriched in fatty acid binding and enzyme transfer activity (Figure 44B-C).

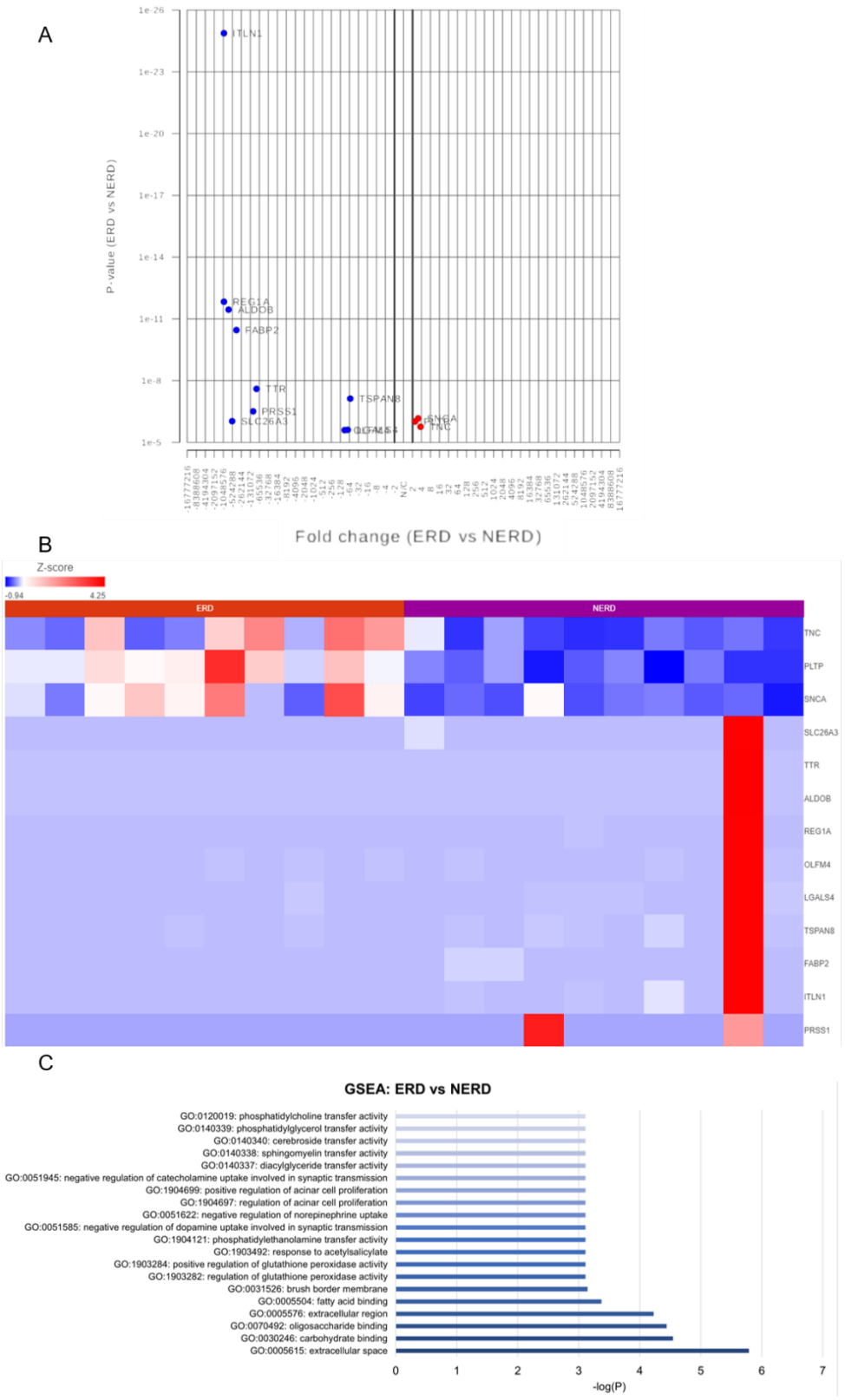

Figure 44 Differential Gene Expression in ERD and NERD Oesophageal Mucosa

A) Volcano plot showing 3 genes upregulated in ERD as log2 scaled fold change in red dots on the right of the graph, and 10 genes downregulated in ERD compared to NERD on the left. B) Heatmap displaying the most significantly DE genes between ERD NERD samples. C) Bar graph of statistically significantly enriched biological pathways from DE genes between ERD and NERD (p<0.01). Graphs made using Partek Flow. ERD: N=10, NERD: N=10.

3.3.6.3 DESeq2 in ERD:FH Oesophageal Mucosa

To identify molecular markers associated with mucosal differences between ERD and FH patients, DESeq2 analysis was performed on RNA sequenced ERD (N=10) and FH (N=7) samples. FH samples (NE8 and NE4-2) were excluded from the analysis, as explained in section 3.2.2.3.1 Quality Control. DESeq2 analysis revealed 120 DE genes between ERD and FH patients (Figure 45A). These included *CLCA1, KRT10, FSCN1*, and *ADAM23*, as seen in Figure 45A-B. Genes downregulated in ERD compared to FH included *MUCL3,* which encodes mucin-like 3 that forms an integral part of the plasma membrane [476], TFF1 and *CLDN18,* both involved in intestinal barrier function [477], [478]. These DE genes were enriched in biological pathways including cell surface receptor signalling, neutrophil degranulation, and leukocyte activation as statistically significative (p=<0.01) (Figure 45C).

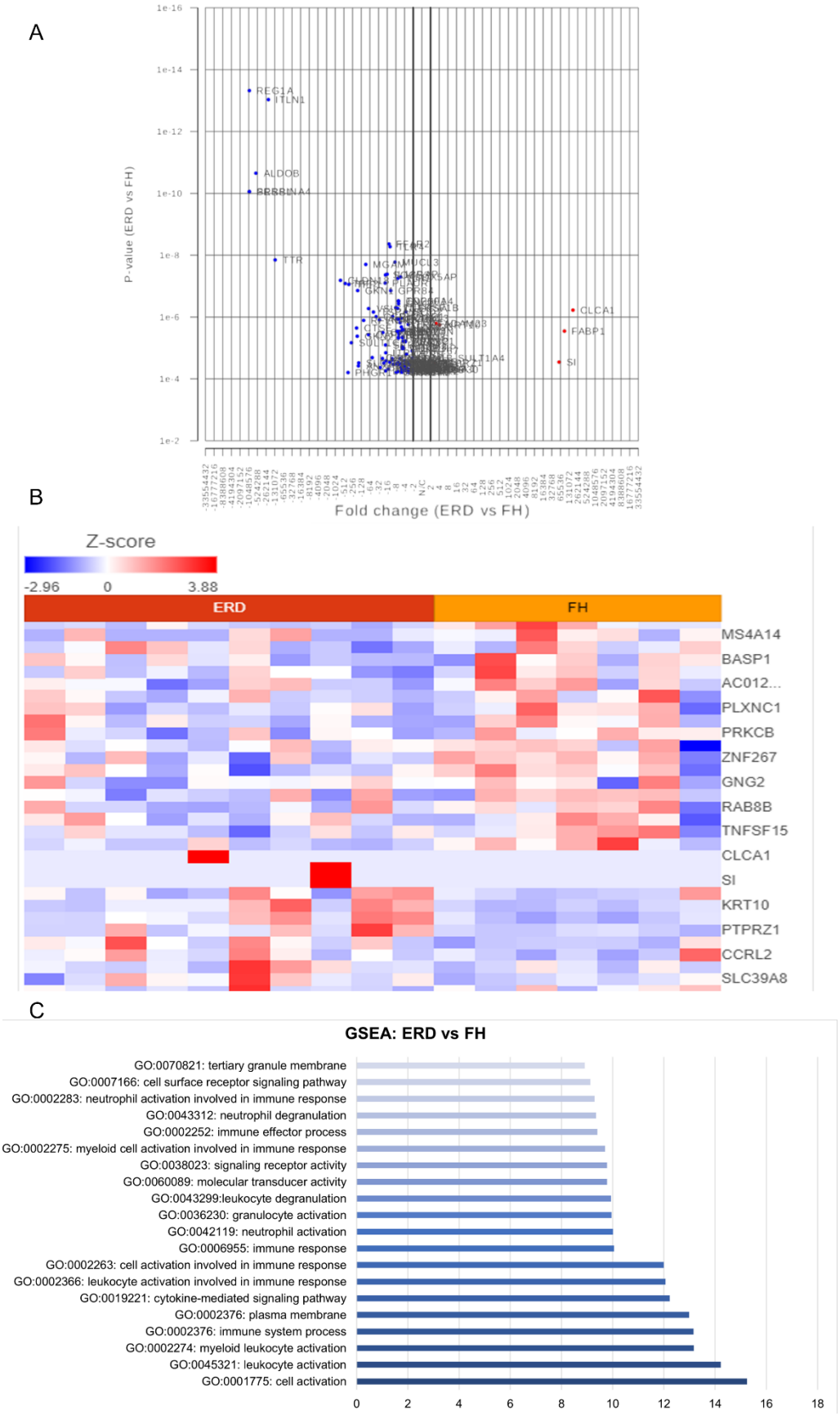

Figure 45 Differential Gene Expression Between ERD and FH Oesophageal Mucosa

A) Volcano plot showing 120 DE genes between ERD and FH patients: 6 genes upregulated and 113 genes downregulated in ERD compared to FH B) Heatmap displaying the most significantly DE genes between FH and ERD. C) Bar graph of the most enriched biological pathways from GSEA between ERD and FH DE genes. ERD: N=10, FH: N=7.

3.3.6.4 DESeq2 in BO:ERD Oesophageal Mucosa

We subsequently assessed molecular markers associated with mucosal differences between ERD and BO patients. Two BO samples (SH061119 and RC110320) were excluded from DESeq2 analysis as explained in section 3.3.4.1. DESeq2 analysis was performed on RNA sequenced BO (N=7) and ERD (N=10) samples revealing 1936 DE genes between ERD and BO patients (Figure 46A). There were more genes upregulated in BO compared to ERD oesophageal mucosa, including *COLEC12*, *TIMP3,* and *SMOC2*, as shown in Figure 46B. *ADAM23* was downregulated in BO compared to ERD (Figure 46B). To determine the most significantly DE genes between BO and ERD, R was used to manually filter for DE genes with normalised counts over 200 and *p* value <0.01. This detected upregulation *of KRT6A-C, KRT14, KRT16, KRT17*, and *KRT5* in ERD compared to their -1Log2 fold change in BO patient samples (Appendix 10). These DE genes were highlighted in calcium ion binding, cell-matrix adhesion, and extracellular matrix constituent BO oesophageal mucosa compared to ERD as statistically significative (Figure 46C).

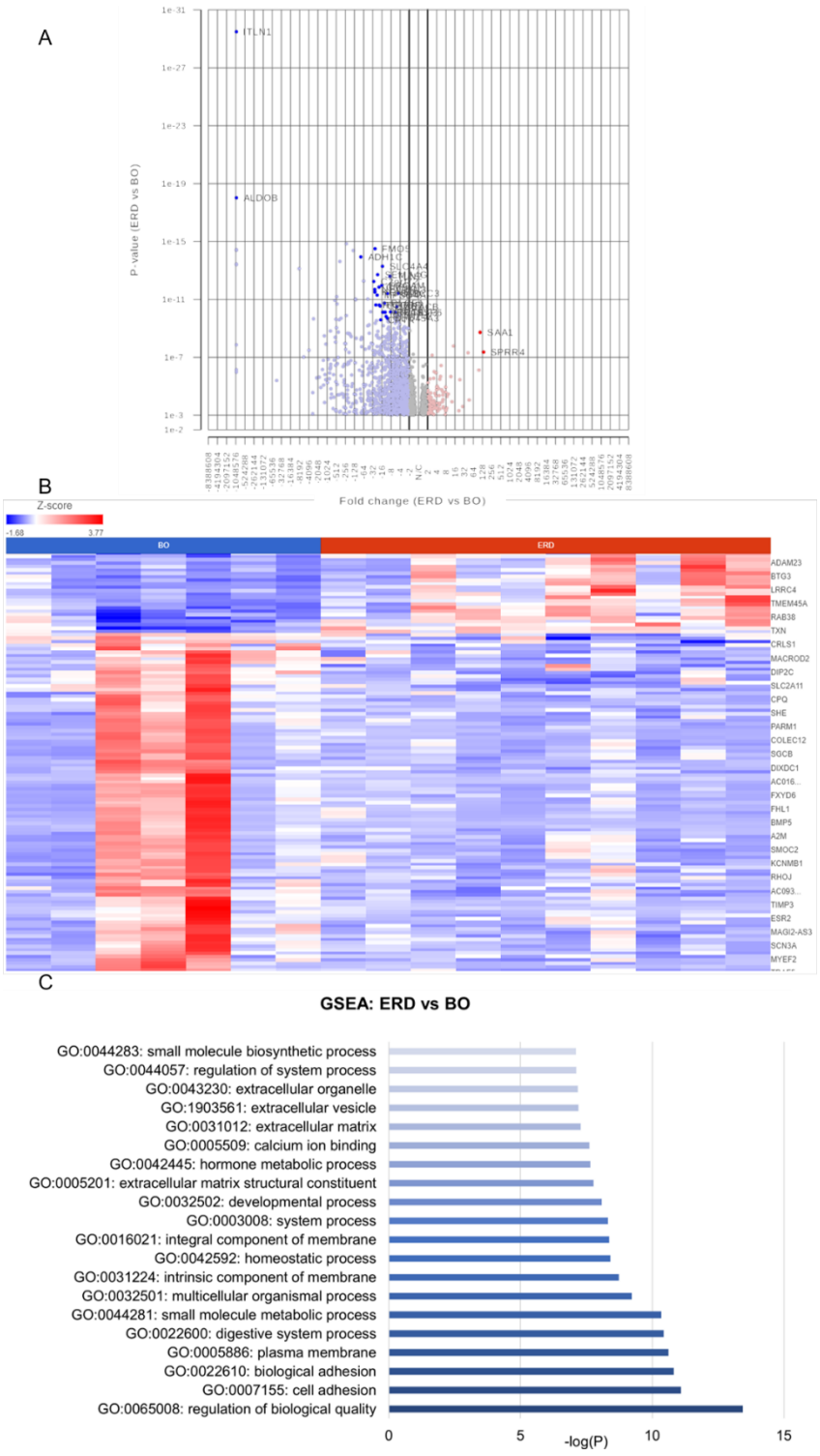

Figure 46 Differential Gene Expression Between BO and ERD Oesophageal Mucosa

A) Volcano plot showing 1936 DE genes between ERD and BO patients: 110 genes were upregulated and 1238 genes downregulated in ERD compared to BO B) Heatmap displaying the most significantly DE genes between BO and ERD. C) Bar graph of most significantly enriched biological pathways from DE genes between ERD and BO. ERD: N=10, BO: N=7.

3.3.6.5 DESeq2 in BO:FH Oesophageal Mucosa

To identify molecular markers associated with mucosal differences between BO and FH patients, DESeq2 analysis was performed on RNA sequenced BO (N=7) and FH (N=8) samples. FH sample NE8, and BO samples SH061119 and RC110320 were excluded from analysis as explained in section 3.2.2.3.1 Quality Control. This revealed 884 significantly DE genes between BO and FH oesophageal mucosa, where the majority of DE genes were upregulated in BO compared to FH (Figure 47A). Genes upregulated in BO compared to FH oesophageal mucosa included *NECTIN3, COL4A6, TFF3, and CLDN11* while *CLEC7A* was upregulated in FH compared to BO oesophageal mucosa (Figure 47B).

To determine the most significantly DE genes, R was used to manually filter for DE genes with normalised expression values over 50 and *p* value <0.01. This detected heterogeneity in the BO groups, with 5/9 patients showing significant upregulation of genes including *COL3A1, EPCAM, KRT20* and *ACTA2*, while 4/9 BO patients did not show a detectable expression fold change (Appendix 11). In contrast, FH oesophageal mucosal expression of these most significantly DE genes were more homogenous, with all FH samples displaying 0log2 fold change across these genes, as seen in Appendix 11.

These DE genes were collectively implicated in myeloid leukocyte activation, positive regulation of TNF signalling, and regulation of cell migration in BO compared to FH as statistically significative (*p*=<0.01) (Figure 47C).

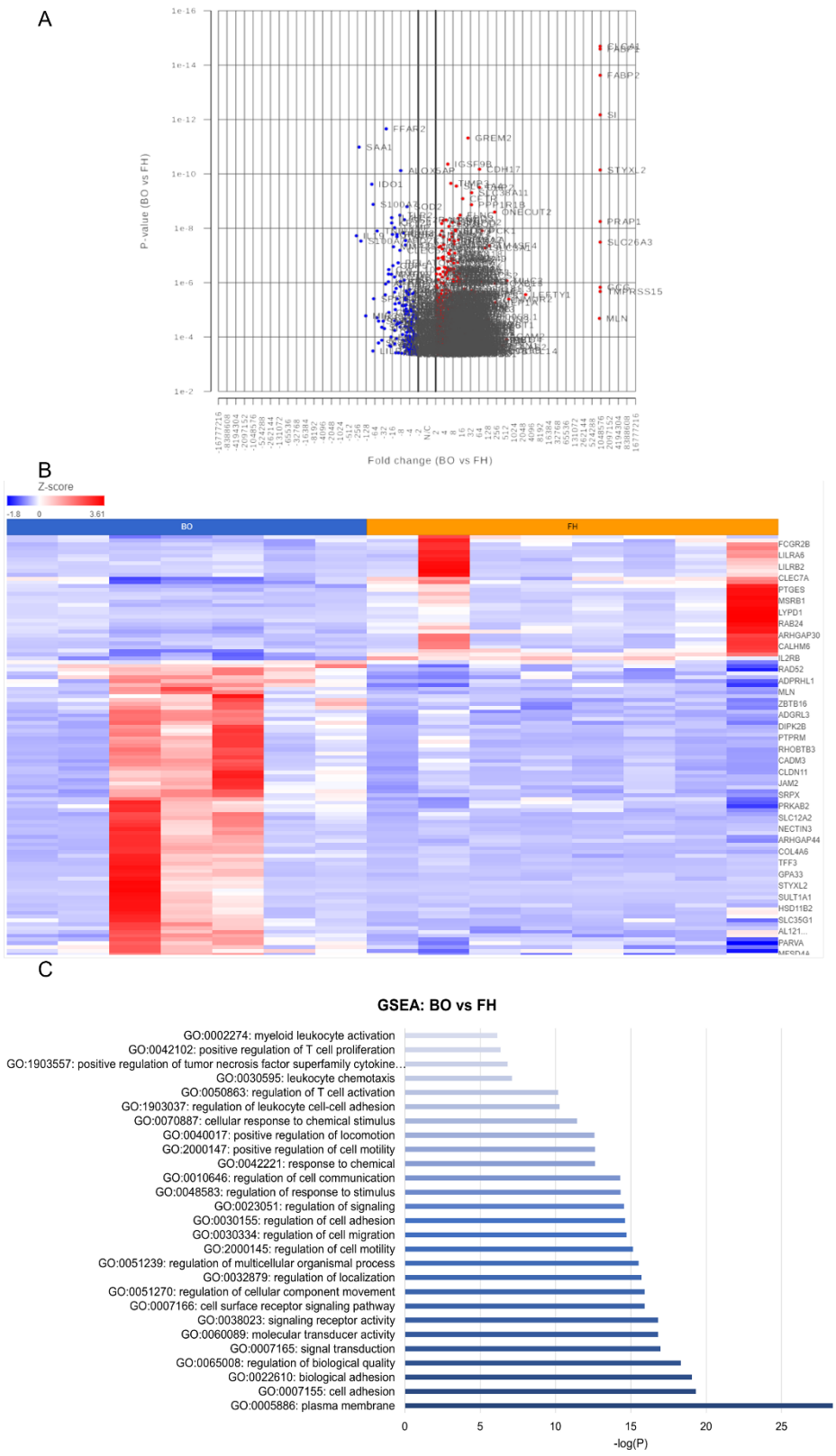

Figure 47 Differential Gene Expression Among BO and FH Oesophageal Mucosa

A) Volcano plot showing 884 DE genes between BO and FH patients: 535 genes were upregulated and 217 genes downregulated in BO compared to FH. B) Heatmap displaying the most significantly DE genes between BO and FH. C) Bar graph of most significantly enriched biological pathways from DE genes between BO and FH. BO: N=7, FH: N=8.

3.3.6.6 DESeq2 in BO:NERD Oesophageal Mucosa

To identify molecular markers associated with mucosal differences between NERD and BO patients, DESeq2 analysis was performed on RNA sequenced NERD (N=10) and BO (N=7) samples. BO samples SH061119 and RC110320 were excluded from analysis as explained in section 3.2.2.3.1 Quality Control. This highlighted 1302 DE genes between NERD and BO patients (Figure 48A). There were more genes upregulated in BO compared to NERD, as seen in Figure 48A-B. Genes upregulated in BO oesophageal mucosa compared to NERD included *JCHAIN, COL5A1,* and *LAMA4*, while genes including *RAB12* and *PDCD10* were upregulated in NERD compared to BO oesophageal mucosa (Figure 48B).

These DE genes were highlighted in molecular pathways including increased positive regulation of B cell activation, cell adhesion, and collagen-containing extracellular matrix in BO compared to NERD as statistically significative (p=<0.01) (Figure 48C).

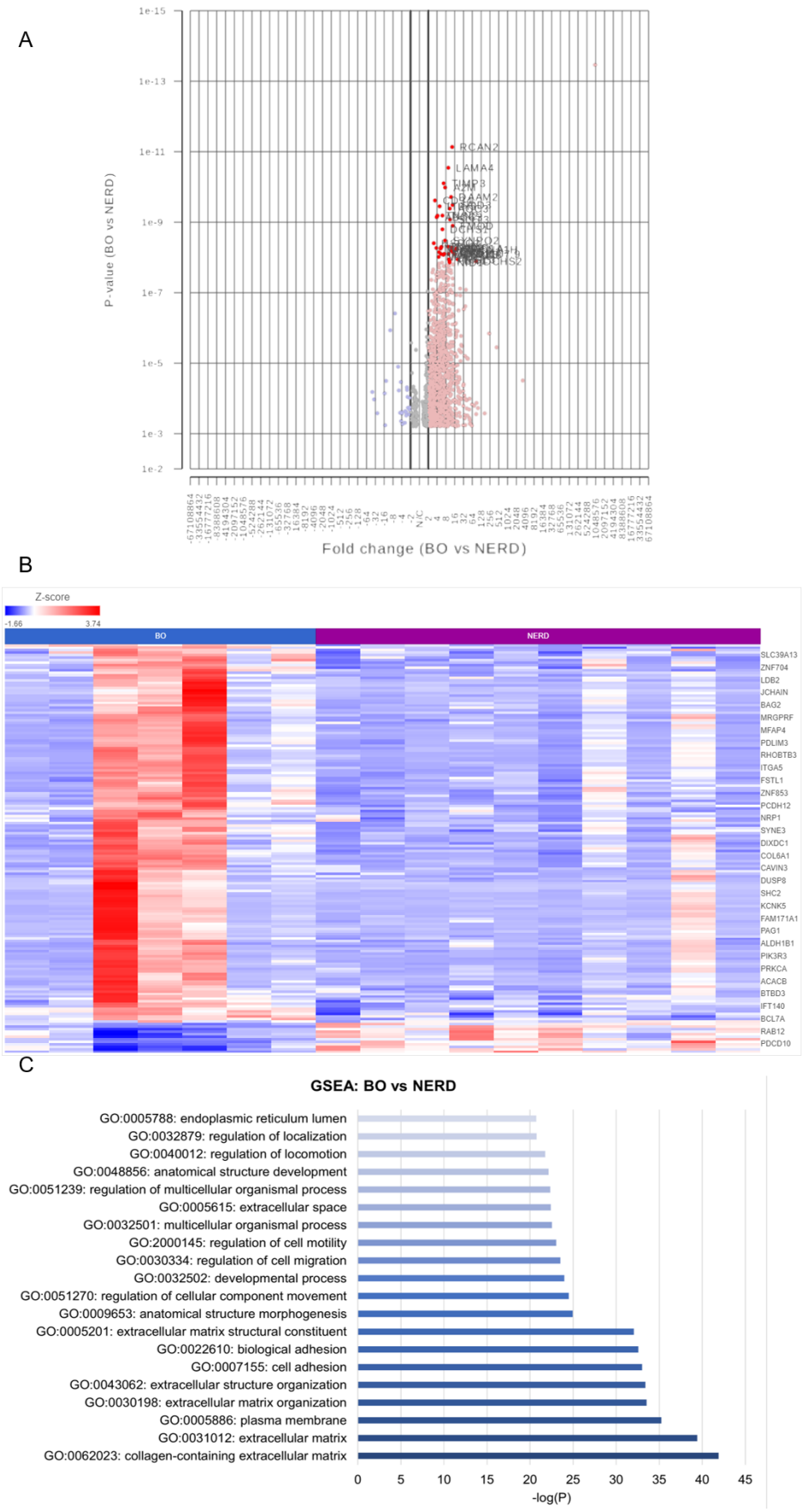

Figure 48 Differential Gene Expression Between NERD and BO Oesophageal Mucosa

A) Volcano plot showing 1302 DE genes between BO and NERD patients: 1089 genes were upregulated and 28 genes downregulated in BO compared to NERD. B) Heatmap displaying the most significantly DE genes between BO and NERD. C) Bar graph of most significantly enriched biological pathways from DE genes between BO and NERD. BO: N=7, NERD: N=10.

3.3.6.7 DESeq2 Summary

Comparison	Number of DE genes	Classes of most highly DE genes	Associated GO pathways
HC: GORD	979	Keratin gene family, immunoglobulins, trefoil factors 1-2	Immunoglobulin production, adaptive immune response, ECM organisation, cell-cell adhesion
HC: FH	711	'Clock' gene family, endothelin 2, circadian associated repressor of transcription	Circadian regulation of gene expression, regulation of circadian rhythm
HC: NERD	137	Metalloproteases, trefoil factors 1-2, Reg multigene family, lysozyme	Actin cytoskeleton organisation, leukocyte migration, proteolysis
HC: ERD	356	Inflammatory chemokine genes, keratin genes, calcium-binding proteins	Leukocyte migration, positive regulation of cell proliferation, immune response
HC: BO	3010	Immunoglobulins, mucins, pepsinogens	Complement activation, B cell activation, immune response
FH: NERD	186	Calcium sensitive chloride channel family	Neuropathic pain regulation
ERD: NERD	13	Fascin family of actin-binding proteins, tenascin C, collagen	ECM organisation, cell proliferation, lipid binding
ERD: FH	120	Keratins, fascin family of actin-binding proteins	Keratinisation, positive regulation of GPCR signalling
BO: ERD	1936	Epithelial cell adhesion molecules	Cell adhesion, cell-matrix adhesion
BO: FH	884	Endothelial cell chemokine genes, collagen, mucins	Complement activation, angiogenesis
BO: NERD	1302	Immunoglobins, calcium binding proteins	B cell activation, wound healing, collagen-containing ECM

Table 6 DESeq2 analysis summary table

Table detailing the number of significantly DE genes between specified subgroups, classes of the top DE genes, and most significantly associated GO pathways with these genes.

3.3.7 Cellular Deconvolution

3.3.7.1 Cellular Deconvolution with CIBERSORT

In order to estimate the proportions of different immune cell types present in our oesophageal mucosal tissue sequenced in bulk, two different computational deconvolution methods were used. First, the relative levels of distinct immune cells within oesophageal mucosal RNA isolated from bulk sequenced FH (N=8), NERD (N=9), ERD (N=10), BO (N=9) and HC (N=8) samples were determined using CIBERSORT and filtered for $p<0.05$ [479]. This inferred a slightly higher CD8+ T cell component in FH oesophageal mucosa compared to BO, HC, and NERD patients, as seen in Figure 49A. The dendritic cell component of the oesophageal mucosa was also higher in FH patients and healthy controls compared to BO and ERD patients (Figure 49B). Interestingly, M2 macrophages and mast cells both showed higher expression across the GORD phenotypes, with BO, ERD, and NERD patients having the highest M2 macrophage and mast cell component compared to HC (Figure 49C-D). However, memory B cells and plasma cells were only detected in the BO oesophageal mucosa, with ERD, FH and NERD patients showing a similar level of detection for these differentiated B cells as the healthy controls (Figure 49E-F).

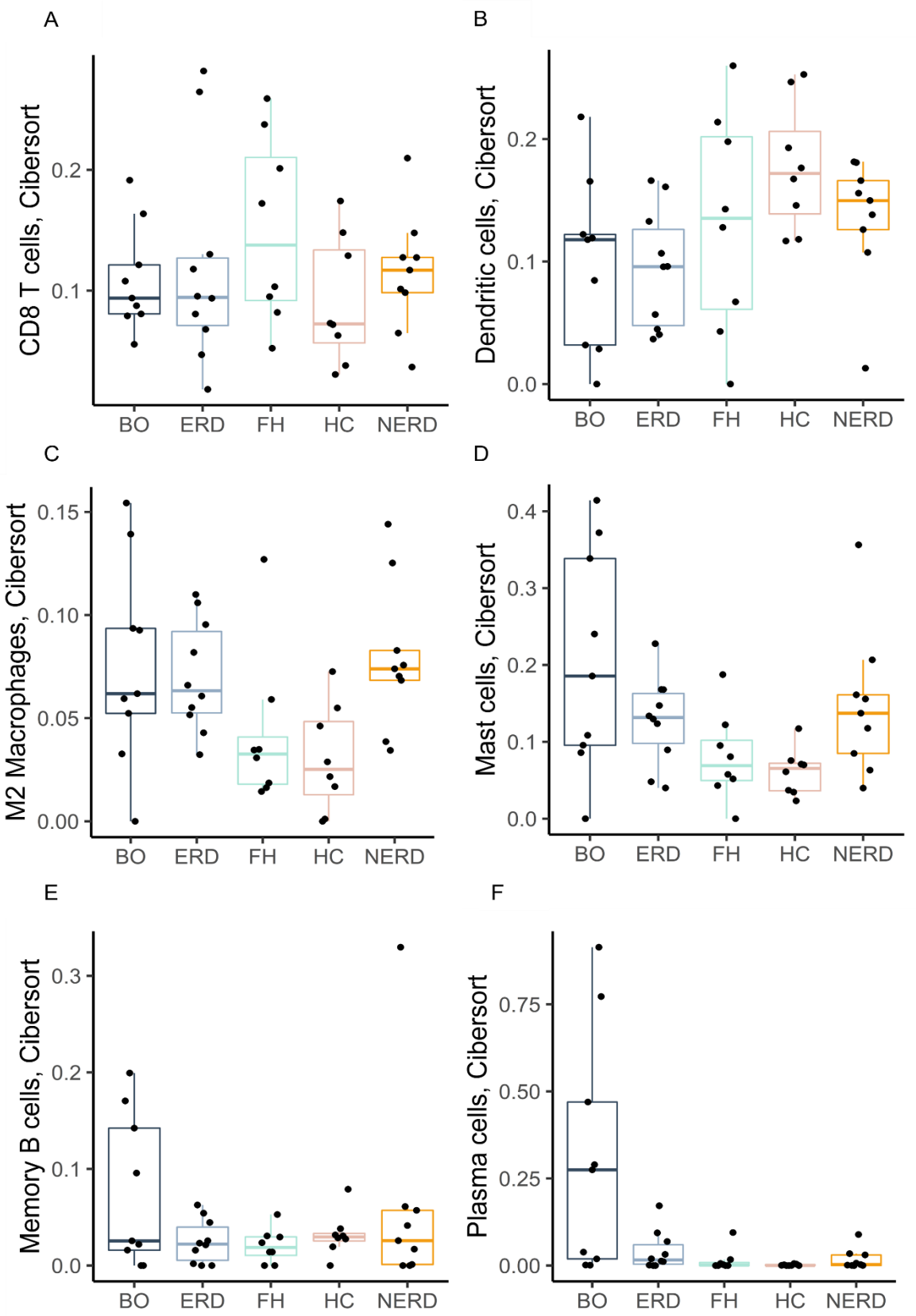

Figure 49 Immune Cell Composition of Normal and GORD Oesophageal Mucosa Determined with CIBERSORT

Boxplots displaying immune cell proportions in the oesophageal mucosa of patients with GORD and healthy controls. Displayed immune cell types are from among the 14 immune cell types with median absolute scores above 1 and *p*= <0.05. Graphs coded manually using R using data output from CIBERSORT. BO: N=9, ERD: N=10, FH: N=8, HC: N=8, NERD: N=9.

3.3.7.2 Cellular Deconvolution with xCell

Next, to confirm the cellular deconvolution data produced by CIBERSORT, we used xCell. The latter tool has been shown to outperform other similar methods due to its conductance of cell type enrichment analysis from a gene signature-based method learned from 1822 pure human cell type transcriptomes from various independent sources [466]. The relative levels of distinct immune populations within oesophageal mucosal RNA isolated from bulk sequenced FH (N=8), NERD (N=9), ERD (N=10), BO (N=9) and HC (N=8) samples were determined using xCell. This detected the highest Th2 cell abundance in ERD oesophageal mucosa compared to BO, FH, NERD, and healthy controls as seen in Figure 50A. Interestingly, CD8+ T cell compositions were significantly higher in ERD and FH patients compared to HCs (Figure 50B). Dendritic cell fractions were most abundant in healthy controls compared to patients with GORD, but FH patients were also observed to have an increased dendritic cell composition compared to patients with BO, ERD, and NERD (Figure 50C). Mast cell abundance was increased in patients with BO, ERD, and NERD compared to FH and healthy controls (Figure 50D). Moreover, M2 macrophages were most abundant in patients with BO, but ERD patients also showed an increased composition of M2 macrophages compared to patients with FH and NERD, and healthy controls (Figure 50E). In contrast, plasma cells were only detected in 1 BO, 1 ERD, and 1 FH patient (Figure 50F).

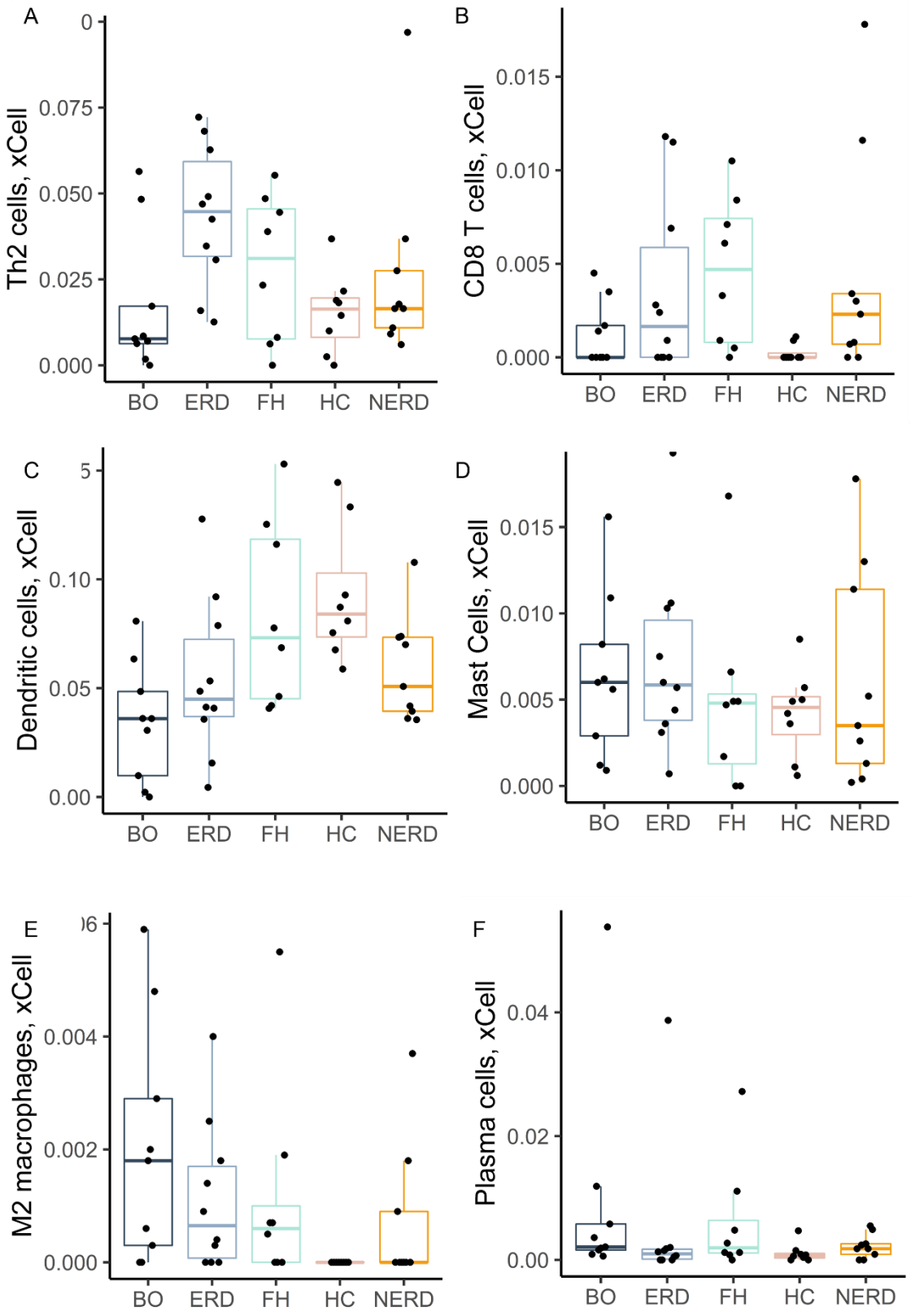

Figure 50 Immune Cell Composition of Normal and GORD Oesophageal Mucosa Determined with xCell

Boxplots displaying immune cell proportions in the oesophageal mucosa of patients with GORD and healthy controls. Displayed immune cell types are from among the 23 immune cell types with median absolute scores above 1. Graphs coded manually using R using data output from xCell. BO: N=9, ERD: N=10, FH: N=8, HC: N=8, NERD: N=9.

3.3.8 Validation of Immune Cell Enrichment in Oesophageal Mucosal Tissue from GORD Patients

3.3.8.1 Dendritic Cell Infiltration in the Oesophageal Mucosa of GORD Patients

Recent studies have highlighted the ability of neurotransmitters such as norepinephrine to modulate numerous dendritic cell functions including migration, antigen presentation, and cytokine production in the skin and intestinal mucosa [480]–[482]. IF-IHC studies were undertaken to assess the presence and possible function of arguably the most important myeloid cell type in the oesophageal mucosa, and its possible interactions with oesophageal epithelial neuronal innervation. CD1a (previously optimised by the group, antibody detailed in section 3.2.3 Validation of RNA Sequencing Data with IF), a well-described dendritic cell subset marker [483], was used to identify dendritic cells present in the oesophageal mucosa of biopsies from healthy controls and GORD patients.

GORD samples phenotyped into ERD (N=22), NERD (N= 10), FH (N= 17), and BO (N= 18), and healthy controls (N=10) were evaluated for $CD1a^+$ dendritic cells in the oesophageal mucosa. $CD1a^+$ dendritic cells were most frequently interpapillary in nature, being detected on the outside of and in between papillary structures, as seen in Figure 51A. The abundance of $CD1a^+$ dendritic cells was significantly higher in healthy controls compared to BO (p=0.0005), ERD (p=0.0004), and FH patients (p=0.0096) (Figure 51B). CD1a was also found to be expressed at a higher level in HCs compared to GORD patients at RNA level, as seen in Figure 52.

The localisation of dendritic cells was also assessed in relation to deep afferent nerve endings previously detected in a representative number of ERD samples and healthy controls with PGP9.5. There appeared to be no anatomical relationship between afferent nerves and dendritic cells in the oesophageal mucosa. $PGP9.5^+$ afferent nerves were detected in the submucosa and were not in close proximity to interpapillary dendritic cells detected in the oesophageal mucosa in ERD patients nor healthy controls (Appendix 13).

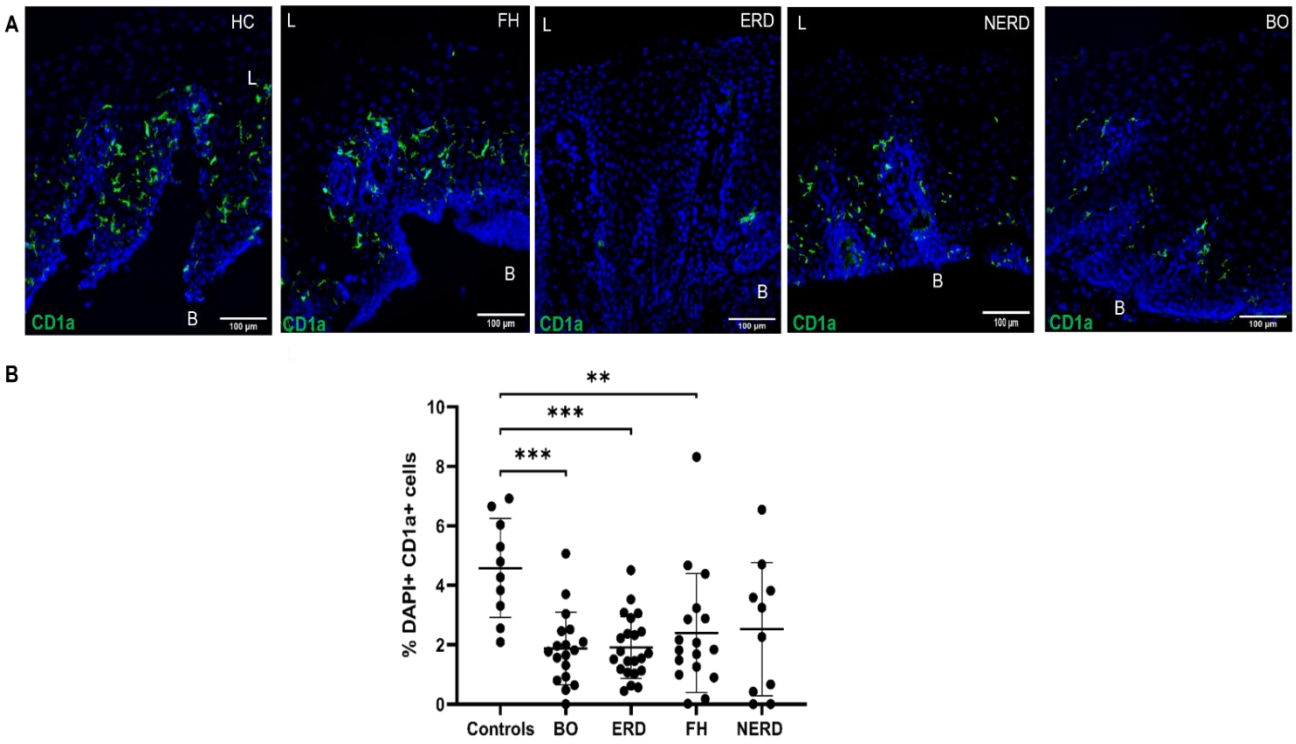

Figure 51 CD1a+ Dendritic Cells are More Abundant in the Healthy Oesophageal Mucosa than in Patients with GORD

A) Interpapillary CD1a^{+} dendritic cells residing in the oesophageal mucosa in healthy controls and patients with GORD. Scale bar: 100µm. B) Quantification of dendritic cells in healthy controls: N=10, BO patients: N=18, ERD: N=22, FH: N=17, NERD: N=10. One-way ANOVA and subsequent Bonferroni's test revealed significantly higher dendritic cell residence in healthy controls compared to patients with BO (p=0.0005), ERD (p=0.0004), and FH (p=0.0096). Error bars represent SD.

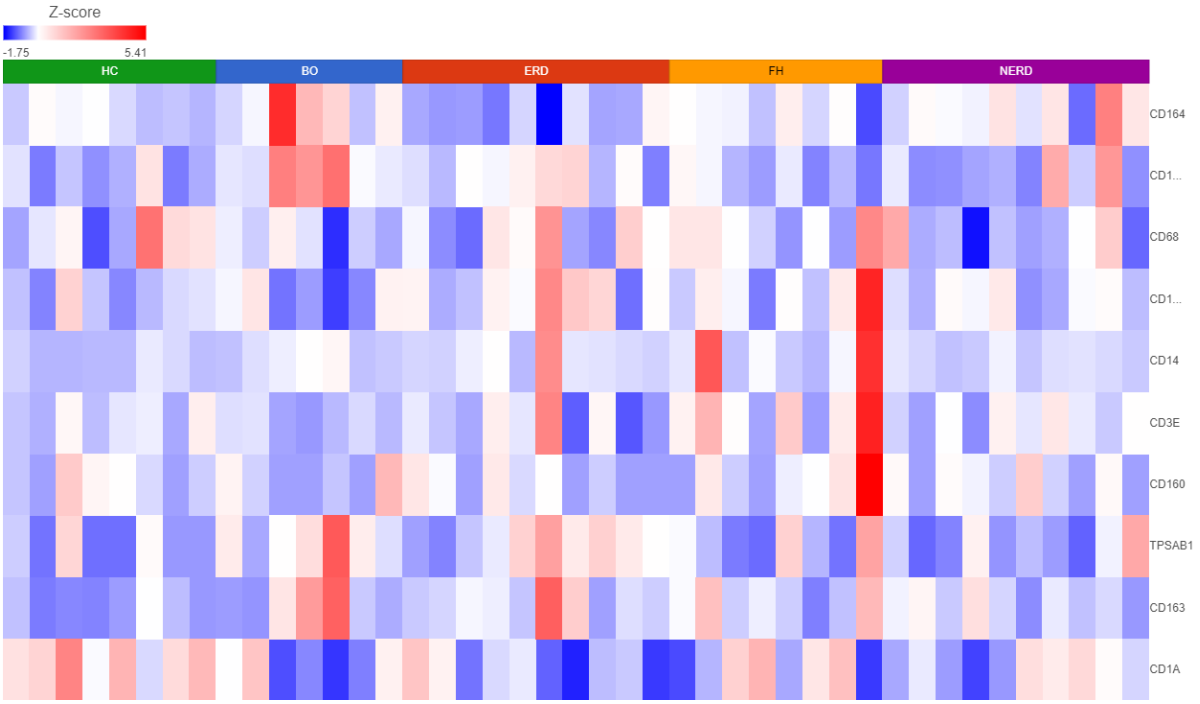

Figure 52 RNA Expression of Immune Cell Marker Genes

DESeq2 expression matrix for the comparison between HCs and GORD patients was manually filtered for immune cell markers on Partek. HCs: (N=8), BO: (N=7), ERD: (N=10), FH: (N=8), NERD: (N=10), p = 0.05.

3.3.8.2 Mast Cell Infiltration in the Oesophageal Mucosa of GORD Patients

Immune enrichment analysis of the RNA sequencing dataset highlighted a higher abundance of mast cells in oesophageal mucosal biopsies from patients with NERD, ERD, and BO compared to patients with FH and healthy controls (as seen in Section 3.3.8 Cellular Deconvolution with xCell). Mast cell tryptase (previously optimised by the group, antibody detailed in section 3.2.3 Validation of RNA Sequencing Data with IF) was the cell marker of choice, given the requirement for exocytosis of their cytoplasmic secretory effector granules to take place in order for mast cells to actively contribute to the inflammatory process. The protease tryptase is the most abundant protein among the array of bioactive effector molecules released during mast cell activation and was therefore used to assess the localisation of mast cells in this part of the study [484].

Mast cells were most often seen surrounding the papillae near the basal layer of the squamous epithelium (as seen in Figure 77), but tryptase granules were occasionally also detected around the more superficial layers of the mucosa. Mast cells that were detected appeared to predominantly conform to three types of morphologies: 1) oval-shaped mast cells with intracellular tryptase granules, in 'resting' form, 2) those with a highly granulated morphology, in anaphylactic degranulation, and 3) a combination of oval-shaped cells which appeared to be releasing tryptase granules or 'piecemeal degranulation', as shown in a representative ERD sample in Figure 53A. These morphologies were seen across all GORD phenotypes and healthy controls, with no notable morphologic differences between healthy controls and GORD phenotypes.

Although there was no significant difference in the infiltration of mast cells among GORD patients or healthy controls (p=0.0751), there was an increased mast cell abundance in patients with ERD (Figure ***53***B). Moreover, the mean cell count in the upper quartile of all GORD groups shows increased mast cell infiltration in GORD compared to healthy controls (Figure ***53***B). Moreover, there was no significant correlation between mast cell infiltration and severity of inflammation in ERD patients (Appendix 14).

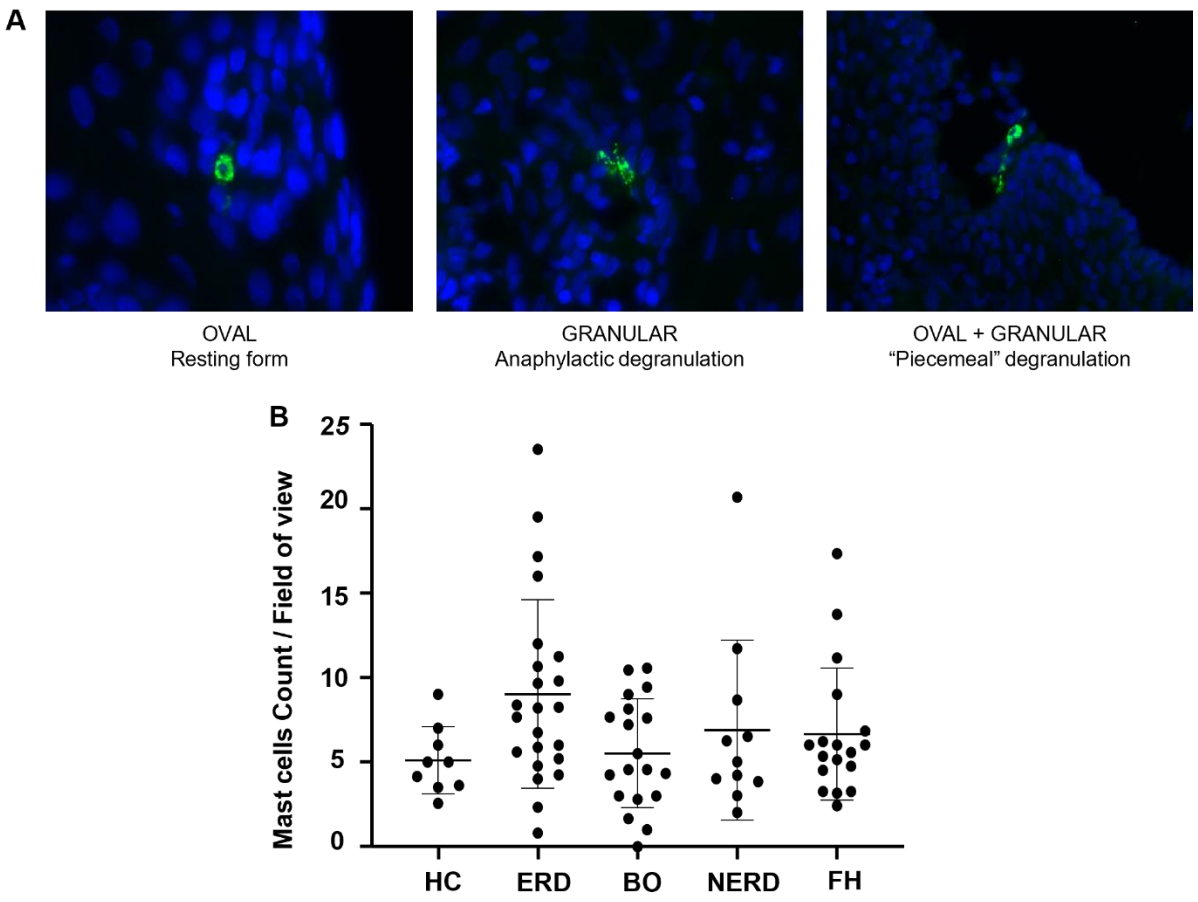

Figure 53 Mast Cells Detected in Three Morphologies in the Oesophageal Mucosa

A) Morphology and activity status of mast cells in the oesophageal epithelium of patients with GORD. A mix of mast cell morphologies were often seen in the same representative ERD sample. B) Quantification of mast cells in the oesophageal mucosa of patients with GORD and healthy controls. Mast cell infiltration among the disease groups was not statistically different (p=0.0751). Error bars represent SD.

3.3.9 Ion Channel Gene Expression Profiles

DESeq2 expression matrix for the comparison between HCs and GORD patients was manually filtered for ion channels explored in section 2 Characterisation of mucosal afferent nerves in the oesophageal mucosa of patients with GORD. *ASIC3* and *TRPV1* were found to be increased in NERD patient samples, while *TRPA1* expression was increased in BO patients compared to ERD, NERD and FH (Figure 54).

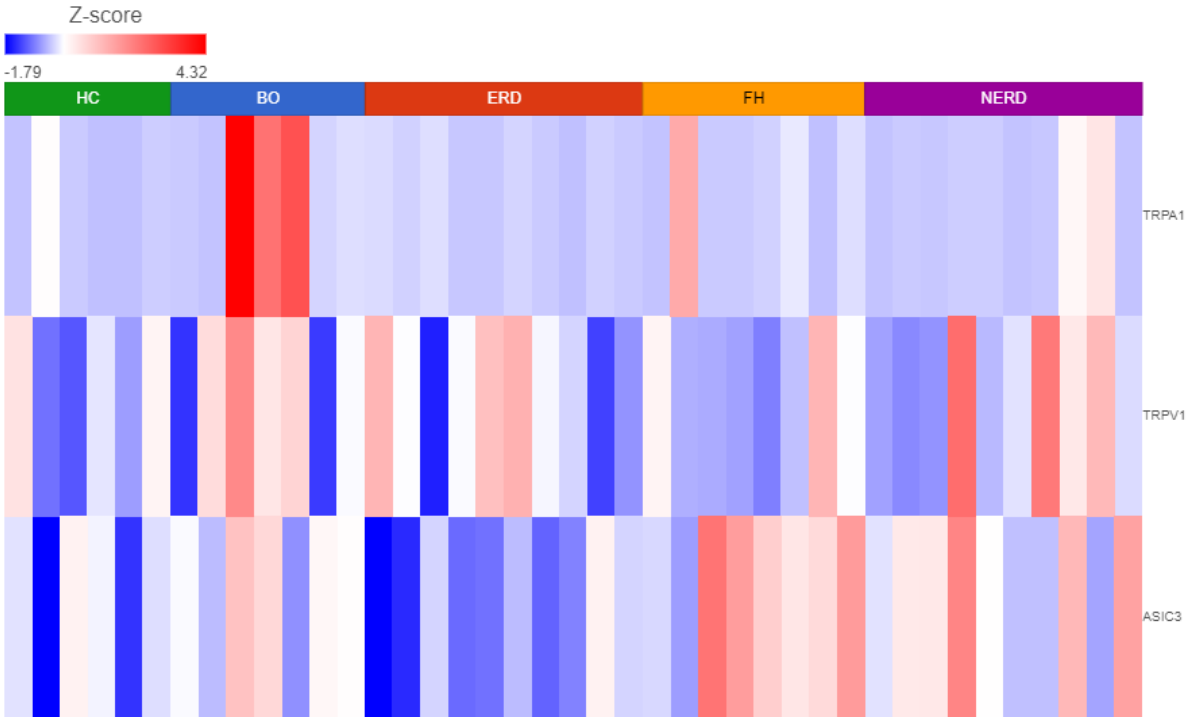

Figure 54 RNA Expression of Ion Channel Genes

DESeq2 expression matrix for the comparison between HCs and GORD patients was manually filtered for ion channel genes on Partek. HCs: (N=8), BO: (N=7), ERD: (N=10), FH: (N=8), NERD: (N=10), $p = 0.05$.

3.4 Discussion

This section aimed to characterise the gene expression signature of the oesophageal mucosa for an improved understanding of the molecular mechanisms underlying heartburn pathogenesis in patients with GORD. Differential expression analysis was performed between healthy controls and phenotyped GORD patient samples that underwent bulk RNA sequencing. Biological interpretation of gene expression data was conducted using GSEA. Moreover, computational cellular deconvolution analysis was performed to characterise the immune cell composition of each GORD phenotype using CIBERSORT and xCell, and the finding of decreased dendritic cell population in GORD oesophageal mucosa compared to healthy controls was validated immunohistochemically. This section of the study provides novel transcriptomic data on candidate molecular markers which may play important roles in oesophageal hypersensitivity, inflammation, and barrier functions in the oesophageal mucosa of heartburn patients.

There are important differences in expression of genes encoding several structural proteins between normal and GORD oesophageal mucosa. The downregulation of *ACTN4*, a cytoskeletal protein involved in binding actin to the cell membrane in adherens-type junctions, and *CLDN10*, a claudin which is an integral component of tight junctions that collectively form a physical barrier to prevent solutes and water passing freely into the cell, could highlight a novel structural change in oesophageal epithelial cells in GORD patients resulting in reduced barrier integrity enabling passage of refluxate through the mucosa (Appendix table 14) [485], [486]. The loss of *ACTN4* and *CLDN10* expression in GORD, including in patients with NERD, is a likely consequence of high acid exposure which may result in the loss of integrity of adherens and tight junction strands. Moreover, another lost protective mechanism highlighted by differential expression analysis is decreased *MUC17* expression in GORD compared to healthy controls. *MUC17* encodes a glycoprotein which is a membrane-bound protein that forms a protective mucous barrier on epithelial surfaces and also has a role in intracellular signalling [487]. This finding is supported by an earlier study which examined *MUC17* expression in peptic ulcers, and found MUC17 to be significantly decreased in idiopathic ulcers compared to ulcers induced by Helicobacter pylori and NSAIDs, suggesting altered protective efficiency in idiopathic ulcers against acid and pepsin [488]. These findings were coupled with a significantly decreased *ADAM23* expression in GORD, in particular, ERD oesophageal mucosa, suggesting a potential mechanism of breakdown of structural proteins *CLDN10* and *ACTN4* by a metalloprotease [489]. Collectively, these results highlight a possible protective structural mechanism that is lost in GORD oesophageal mucosa, including in patients without

apparent macroscopic injury (NERD), which might expose the oesophageal epithelium to damage induced by acid and bile content of the refluxate.

Keratins are major structural proteins critical in forming the cytoskeleton scaffold in epithelial cells which gives them the ability to withstand mechanical and non-mechanical stress [476]. *KRT6, KRT10, KRT14, KRT16*, and *KRTDAP* were upregulated in ERD patients compared to healthy controls. The DE of these keratins in ERD was significantly associated with increased epithelial cell differentiation, tissue development, and cytoskeleton organisation, suggesting that there is active regeneration in the ERD oesophageal mucosa. The selective expression of these keratins in epithelial cells of ERD patients likely plays a regulatory role in metabolic processes and signalling pathways that control the differentiation of the oesophageal epithelium. A recent study described *KRT16* to play a role in the process of keratinocyte activation following skin injury. In the newborn skin of keratin-16 transgenic mice, there was significantly altered response of skin keratinocytes to signalling cues including increased tyrosine phosphorylation of the epithelial growth factor receptor [491]. Keratin-14 expression has been demonstrated in mitotically active basal layer cells, together with its partner keratin-5, with their expression being downregulated with epithelial cell differentiation [492]. A study which inhibited KRT14 in stratified epithelial cell lines using RNA inference reported reduced cell proliferation and delayed cell cycle progression, coupled with reduced phosphorylated Akt levels. Equally, keratin-6 has also been described in mouse embryos where it was found to be rapidly induced in epithelial cells activated at the edge of a wound, and wound closure was significantly delayed in mice null for keratin-6 and 17 [493]. These results are significant in increased epithelial cell proliferation and differentiation, as determined by functional enrichment analysis of DE genes. Thus, our differential expression data suggests that much like the skin epithelium, the ERD oesophagus also triggers a response to restore its vital barrier function in response to acid-induced damage, which likely includes a rapid switch in gene expression whereby type II keratin 6 and type I keratin 16 are upregulated in epithelial cells at the wound edge.

Another important finding is the differentially expressed genes related to the immune response in individual GORD phenotypes compared to the normal oesophageal mucosa. The upregulation of genes such as *CXCL1* and *CXCL6* in the ERD oesophageal mucosa compared to normal controls highlights the functional involvement of these genes in the cellular response to chemokines resulting in leukocyte migration. In contrast, DE genes in BO oesophageal mucosa detected an upregulation of *IGHA1-2* and *JCHAIN*, which were highlighted in B cell receptor signalling and complement activation, suggesting a humoral immune response profile in BO compared to the other GORD phenotypes which overexpressed genes involved in innate and cellular adaptive immune responses. *JCHAIN* encodes the joining chain of

multimeric IgA and IgM [494]. In the intestine, immune protection of the intestinal mucosa was demonstrated to depend on IgA secretion by plasma cells in the gut lumen which provides protection for the mucosal barrier, suggesting the presence of a similar protective mechanism in the BO oesophageal mucosa [495]. However, these results need to be interpreted with caution because BO patients were biopsied while being on PPI treatment (due to the ethical restrictions of stopping PPI in patients with known Barrett's) – the only 'on PPI' group included in the study. Surprisingly, genes DE in FH oesophageal mucosa compared to healthy controls were also found to be functionally enriched in immune response processes. However, *IGKC* and *IGHA2*, genes involved in the IgA immunoglobulin complex, were only found to be upregulated in a single FH sample, suggesting that the diagnosis may have been wrong for this FH patient. As such, the immune response profile in FH appears to be similar to that seen in the normal oesophagus, while NERD and ERD oesophageal mucosa highly expresses genes involved in both the innate and adaptive immune response, and BO oesophageal mucosa has an enriched humoral immune response.

It was also interesting to compare gene expression profiles between GORD phenotypes in the current study. Although the oesophageal mucosal gene expression signature was heterogeneous between healthy controls and heartburn patients, with BO oesophageal mucosa having the highest number of DE genes (3010) compared to the normal oesophageal mucosa, in erosive and non-erosive reflux disease it is strikingly similar at a molecular level, with only 13 genes DE between the two groups. These 13 DE genes between ERD and NERD were implicated in fatty acid binding and enzyme transfer activity, but interestingly, none of the 13 DE genes identified were critically involved in barrier function. This finding was unexpected and suggests that the chemical composition of refluxate/amount of reflux is important in the mucosal differentiation between erosive oesophagitis and NERD patients. In contrast, FH, NERD and ERD patients were all strikingly different from BO at a molecular level, with each differentially expressing 884, 1302, and 1936 genes, respectively. According to these data, it is possible that BO represents a distinct entity that has a vastly different genetic signature, and it is unlikely for patients with NERD or ERD to progress over time to BO once metaplastic transformation begins, a concept previously debated by experts [496]. However, the genetic similarity detected between FH, NERD, and ERD patients and their distinct genetic difference compared to the normal oesophageal mucosa in the present study broadly supports the ongoing debate that these phenotypes represent a continuum of a single disorder [497]–[499]. Comparison of these findings with those of other studies confirms the significant overlap in oesophageal acid exposure of 47.4% between NERD and ERD, suggesting that the content of the refluxate could induce the progression of NERD into ERD [498]. The assessment of mucosal immune cell populations in the oesophagus of healthy controls and GORD patients

via cellular deconvolution of the bulk RNA dataset has expanded the characterisation of immune factors regulating homeostasis under normal conditions, and how these change with the pathogenesis of GORD. Both xCell and CIBERSORT reported a higher concentration of dendritic cells in the normal and FH oesophageal mucosa compared to patients with NERD, ERD, and BO. The interesting finding of significantly increased mucosal dendritic cell population in the oesophagus of healthy controls compared to patients with GORD was validated immunohistochemically. This suggests that the loss of oral tolerance to food antigens may underlie the onset of mucosal inflammation in GORD. The mucosal immune system is known to regulate the active suppression of cellular and humoral responses to orally ingested antigens through a process known as oral tolerance, which is maintained by dendritic cells which screen mucosal surfaces and capture these ingested antigens [502]. This subsequently induces naïve CD4+ T cells to differentiate into regulatory T cells which release anti-inflammatory cytokines such as TGF-β and IL-10 to supress immune responses against harmless oral antigens [503]. These findings are similar to those reported by literature on conventional dendritic cells in the skin [504]. In the steady state, immature dendritic cells residing in the skin have been shown to probe their homeostatic environment for invading pathogens. The rhythmic extension and retraction of their dendrites through the intracellular spaces between keratinocytes was demonstrated in a study which visualised Langerhans cells in l-Abeta-enhanced green fluorescent protein knock-in mice by confocal microscopy [504], [505]. It is probable that immature dendritic cells in the oesophageal mucosa, a squamous epithelium exposed to antigens from the lumen, could also be surveying the normal oesophageal epithelium for foreign invaders. Dendritic cells were often interpapillary, residing between the papillary structures, suggesting that they reside in the epithelial layer rather than infiltrate from the submucosa, as often seen with other immune cells. This mechanism appears to be significantly compromised in patients with FH, ERD, and BO, and appears to be decreased in patients with NERD. However, the insignificant difference between healthy controls and NERD patients was possibly due to the lower sample number in this group of patients compared to the other GORD phenotypes. A recent study demonstrated breakdown of oral tolerance by infecting BALB mice with *Citrobacter rodentium* while exposing them to OVA. Following the clearance of infection, continuous OVA administration induced IBS symptoms such as diarrhoea in the previously infected, but not the uninfected mice. Moreover, in the mice which developed IBS, subsequent oral ingestion of antigens was found to induce a mast cell-dependent mechanism of visceral hypersensitivity, whereby mast cells became activated by exposure to the antigen and degranulated to release histamine which in turn sensitised visceral afferent nerves [506]. Thus, our findings of reduced dendritic cells in the GORD patient population, coupled with an increased population of mast cells, highlights a

potential peripheral mechanism for food-induced heartburn symptoms in patients with GORD, and in particular, FH patients whose symptom generation is not associated with acid reflux.

The reduced dendritic cell population in NERD, ERD, and BO oesophageal mucosa was coupled with an increased mast cell population in these patients compared to healthy controls and FH patients according to both CIBERSORT and xCell estimations. Although CIBERSORT detected a slightly increased mast cell composition in FH patients compared to healthy controls, the difference between FH and normal oesophageal mucosa was negligible according to xCell findings. Although IF studies failed to detect a significant difference in mast cell infiltration between GORD samples and healthy controls, the median number of mast cells detected by mast cell tryptase staining was notably higher in ERD compared to HCs. The increased mast cell composition in GORD oesophageal mucosa compared to asymptomatic subjects could be attributed to increased hypersensitivity in these patients. Indeed, mast cells have been widely recognised for their role in initiating a reciprocal communication with nociceptors on sensory nerve fibres in a range of inflammatory conditions [268], [507]–[509]. Being one of the first responders of the immune system present near externally exposed surfaces such as the epithelial lining of the skin and mucosa of the GIT enables their orchestration of other immune cells involved in the immune defence [510]. Moreover, the proximity of peripheral mast cells to primary afferent nerve endings expressing nociceptors has been reported to be critical in pain transmission in IBS [508], [509]. The present study raises the possibility that increased mast cell composition of the oesophageal mucosa of patients with NERD, ERD, and BO underlies the mechanism of oesophageal hypersensitivity by releasing substances that interact with and activate sensory afferent nerve endings previously identified as innervating the deeper layers of oesophageal epithelium in these patients.

3.4.1 Limitations of Methodology

Although this study produced novel characterisation data on the oesophageal mucosal gene expression signature of healthy subjects and patients with heartburn, there were also several sources for error. First, due to the global pandemic which introduced a three-month break from experimental work, healthy control samples could only be collected at a later date. This meant that GORD samples were sequenced in a separate batch from healthy controls, which may have introduced an experimental error into the dataset. However, this was minimised as much as possible, by using the same RNA extraction kit by the principal researcher, and using the same genome centre and equipment for sequencing. Moreover, xCell provides an enrichment score of cellular composition in heterogeneous tissue, so cannot be interpreted as proportions of cells. xCell also does not provide statistical significance by calculating an empirical p value

as done by Newman *et al*. in CIBERSORT. This arguably makes xCell the inferior technique of cellular deconvolution. However, due to xCell being a gene signature-based method learned from gene expression data for 64 immune and stroma cell types, it provided useful estimations of immune cell populations enriched in our bulk RNA samples, some of which were not present in the CIBERSORT signature. To increase confidence in our computational analyses, we performed computational tissue dissection analysis with two widely accepted and published webtools, but validating the findings with a wet-lab method will increase the impact of our findings in this section of the study. Moreover, the method of biopsy taking is not precise, and a more defined protocol would improve the comparability between patient samples included in molecular studies in the future. The possibility of some FH patients being misdiagnosed should also not be overlooked.

4.4.2 Future Work

Further research should be undertaken to validate the immune cell type enrichment data generated by xCell and CIBERSORT using visualisation techniques such as IF-IHC, and quantitative methods such as qPCR by measuring mRNA levels of specific markers for each immune cell type of interest. Similarly, for differentially expressed genes of clinical relevance, qPCR should be performed to validate the difference in levels of expression between healthy control RNA samples and GORD samples, respectively. Moreover, the gene expression data can be further expanded by using more novel technology such as spatial transcriptomics (Visium) to identify anatomical regions of the oesophageal mucosa displaying changes in gene expression. However, this was beyond the scope of the current study, given the limitations in time and funding. Sequencing a number of fresh frozen biopsies from patients with ERD, NERD, FH, and BO, and healthy controls with spatial transcriptomics will produce more useful transcriptomic data on the localisation of differentially expressed genes of interest, which may help identify potential biomarkers to improve treatment of heartburn in GORD patients.

4: Neuro-immune Crosstalk in the Pathogenesis of Heartburn Symptoms in GORD

4.1 Introduction

Neuron-to-neuron signalling via pain neurotransmitters such as CGRP, substance P, and glutamate was, until recently, considered to be the key neuronal pathway mediating chronic pain [515]. However, recent evidence has emerged to indicate that the acidic microenvironment created by cytokine-induced inflammation could also activate acid-sensing receptors on oesophageal mucosal afferent nerves and epithelial cells, as detailed in section 1.8 Inflammation in GORD. Nociceptive neurons can both be activated by cytokines released from immune cells, and directly regulate inflammation by releasing neuropeptides upon activation by noxious stimuli [262]. Release of inflammatory mediators such as IL8, IL1β, and TNFα are likely to activate or heighten the sensitisation of peripheral afferent nerves. This has been shown in animal studies of the colon, where silent visceral afferent nerves were activated by chemical and inflammatory mediators which led to continuous neuronal firing [516]. Studies of the colon have also highlighted that the neuronal budding and localisation of neuronal endings may also be regulated by inflammatory factors, as described in section 1.7 Neuroimmune crosstalk in the oesophagus. However, such neuro-immune interactions have not been investigated in the oesophagus of patients with GORD.

Sensory neuronal expression of receptors of inflammatory mediators is becoming an increasingly accepted concept. A comprehensive transcriptome analysis of 622 single murine neurons found that 9% expressed TNFR1, one of two cell-surface receptors for the pro-inflammatory cytokine TNFα, and 2.4% expressed TNFR2 mRNA [517]. Interestingly, a single-cell real-time PCR analysis demonstrated TNFR1 expression solely in neurons, and TNFR2 expression only in non-neuronal cells [518]. IL1R has also been reported to be expressed by 9.1% murine DRG neurons [337], [517], with increased expression in inflammatory conditions including articular arthritis induced by complete Freund adjuvant (CFA) [519]. Similarly, the gene expression database generated by Usoskin *et al*. showed expression of gp130, a subunit of IL6R, in 38% of mouse DRG neurons [517]. CXCR2, the receptor of the most frequently cited inflammatory chemokine in GORD literature: IL8, has also been suggested to be expressed in the majority of rat DRG neurons, where the release of IL8 could activate CXCR2 on peripheral nociceptors via an autocrine or paracrine mechanism [520]. Moreover, CXCR2 was found to be upregulated both at mRNA and protein level following the peripheral injection of CFA, and co-expressed CGRP. In contrast, the knockout of CXCR2 via perisciatic nerve injection of CXCR2 siRNA attenuated CFA-induced allodynia and thus suggested its likely role

in maintaining inflammatory pain [381]. The concept that sensory neurons express receptors for inflammatory mediators, including cytokine receptors such as IL-1R, TNFR, and IL6R, supports the notion of direct immune modulation of neuronal action as a mechanistic driver of peripheral sensitisation [521].

As discussed in Chapter 3, RNA sequencing is a relatively unbiased omics technique with the capacity to provide novel insights into biological systems and disease models. Immune cell deconvolution analysis of bulk RNA sequencing on our 38 GORD samples revealed an enrichment of mast cells, M2 macrophages, B cells, and Th2 cells in heartburn patients compared to the healthy control tissue. Literature on immune contributions to pathological pain suggests that macrophages and neutrophils are the first immune cell populations to be recruited to the site of inflammation, where they secrete cytokines such as TNFα, IL-1β, IL-6, NGF, and chemokines such as IL-8/CXCL8 which recruit T lymphocytes and simultaneously sensitise nociceptors [522]. Moreover, recent studies have detected differences in the expression profile of inflammatory cytokines including TNFα, IL-1β, IL-8, and IL-10 across GORD phenotypes [277], [523]. However, the data on differences between GORD groups is conflicting, with Fitzgerald *et al*. demonstrating a 3-10-fold upregulation of IL-1β, IL-8, and IFN-γ in ERD compared to NERD and BO patients [277], while Solares *et al.* suggest a predominance of IL-8 in BO and increased expression of IL-1β and IL-6 in ERD and NERD [523].

Acid-induced inflammation in the oesophageal mucosa is likely to play an overlapping role in the pathogenesis of oesophageal pain and sensitivity. We hypothesise that there are differences in the expression and localisation of inflammatory cytokine receptors on oesophageal mucosal afferents or epithelial cells between healthy asymptomatic individuals and patients with GORD. This chapter seeks to validate some of the cellular deconvolution analysis of our sequencing data from chapter 3 RNA sequencing the oesophageal mucosa of patients with GORD, and to assess the expression and interaction of inflammatory mediators with sensory afferent nerves using IF-IHC, qPCR, and cytokine release assays. An improved understanding of immune contributions to peripheral sensitisation and eventually pathological pain in the oesophagus of patients with different clinical GORD phenotypes, with a particular focus on the role of inflammatory cytokines and their receptors, will likely reveal novel neuro-immune targets that may improve therapeutic options for heartburn patients in future.

4.2 Materials and Methods

4.2.1 Patient and Healthy Control Biopsies

Patient samples were collected and phenotyped as described in section 2.2.1 Patient Biopsies. Healthy volunteers were recruited and biopsies collected as detailed in section 3.2.1 Patient Biopsies and Healthy Control Biopsies. Demographic data for patients and healthy control samples analysed in this section of the study can be seen in Table 7 below, and in Table 10-11, appendix.

4.2.2 IF-IHC

IF-IHC experiments were performed as described in section 2.2.3 Immunofluorescence-Immunohistochemistry, with the use of the antibodies detailed in Table 8.

4.2.3 Image Analysis

Nerve positions were calculated as previously described in section 2.2.4 Image analysis. Cell counting was performed as detailed in section 2.2.4.2 Automated cell counting. Co-expression analysis was performed as described in section 2.2.4.1 Manders coefficient.

2.2.3.4 Pixel analysis

Acquired images were converted to black and white. A threshold was set to highlight positive signals in black and background in white, creating a binary image in each channel. Then, the positive area was highlighted using the freehand tool to give a region of interest (ROI), and positive pixels in the ROI were measured. Pixels per field of view were calculated on Excel using the following formula:$\%\ area\ x\ total\ \frac{area}{100}$. Standard deviation was calculated per sample based on a minimum of 5 fields of view, and the mean value was plotted on Graphpad Prism 8.4.

Table 7 Demographic data of patients and healthy controls

Phenotype	**Number of patients studied for IHC Analysis**	**Mean Age (years)**	**Age Range (years)**	**Female: Male**
NERD	11	52	30-71	5:6
ERD	23	45	22-61	7:16
FH	18	46	22-70	10:8
BO	19	60	32-78	8:11
HC	10	31	20-70	6:4

Table 8 Source, clones, and dilution of all primary antibodies used

Antigen	Clone	Species	Company	Product Code	Dilution Used
CGRP	Monoclonal	Mouse	Thermo Fisher Scientific	025-05-02	1:400
PGP9.5	Monoclonal	Mouse	AbD serotec	7863-1004	1:200
CD45	Monoclonal	Mouse	Dako	M0701	1:100
Mast Cell Tryptase	Monoclonal	Mouse	Dako	M7052	1:400
E-cadherin	Monoclonal	Rat	Sigma-Aldrich	MABT26	1:100
HIF-2α	Polyclonal	Rabbit	Abcam	Ab20654	1:250
TNFR1	Polyclonal	Rabbit	Abcam	Ab19139	1:200
IL6ST	Polyclonal	Rabbit	Thermo Fisher Scientific	BS-1459R	1:200
IL1R1	Polyclonal	Rabbit	Thermo Fisher Scientific	PA5-28834	1:200
CXCR2	Polyclonal	Rabbit	Thermo Fisher Scientific	PA5-83213	1:200
RAMP1	Polyclonal	Rabbit	Abcam	Ab203282	1:400
NGF	Monoclonal	Rabbit	Abcam	Ab52918	1:200
GAP-43	Polyclonal	Rabbit	Thermo Fisher Scientific	PA5-34943	1:500
CD1a	Monoclonal	Mouse	Dako	M3571	1:200
CD20	Monoclonal	Mouse	Dako	M0755	1:200
CD3	Polyclonal	Rabbit	Dako	IR503	Readymade

4.2.4 Qualitative Real Time Polymerase Chain Reaction (qRT-PCR)

4.2.4.1 RNA Extraction

RNA extraction was performed as previously detailed in section 2.2.5.1 RNA Extraction.

4.2.4.2 Reverse transcription for cDNA Synthesis

RNA was reverse transcribed into cDNA as detailed in section 2.2.5.2 Reverse transcription for cDNA Synthesis

4.2.4.3 qRT-PCR

qRT-PCR was performed on the AB7300 Real-Time PCR system (Applied Biosystems) using the QuantiFast SYBR Green PCR kit (Cat. Number 204056). QuantiTect Primer Assays were used for 18S, NGF, GAP-43, and CXCL8 genes (See Table 9).

Table 9: QuantiTect Primer Assays (Qiagen), and their sources

Gene product	**Product no.**	**Cat. No.**
18S	249900	QT00199367
GAPDH	249900	QT00273322
NGF	249900	QT00001589
GAP-43	249900	QT00023639
CXCL8	249900	QT00000322

4.2.4.4 Statistical Analysis

Relative gene expression by qPCR was calculated using the $2^{-\Delta\Delta CT}$ method as described previously [524]. Fold changes in gene expression were calculated relative to the average control group in gene expression studies in this section. GORD phenotypes were compared to the healthy control group and each other by two-way ANOVA using GraphPad Prism 9.0, respectively. Values are presented as mean ± SD.

4.2.5 *Ex Vivo* Assay of Oesophageal Mucosal Biopsies

Three oesophageal mucosal biopsies from a total of 3 ERD patients and 5 healthy volunteers were taken at endoscopy and immediately transported on ice in Dulbecco's Modified Eagle Medium (DMEM) liquid (High Glucose) with GlutaMAX I (Life technologies, cat. No. 31966021) supplemented with 0.4% Penicillin/Streptomycin (50U/ml) (Sigma, cat. No. P4333-20ML) and processed within 15 min. Biopsies were individually weighed (weight of biopsy= weight of 1.5ml Eppendorf containing biopsy in 1ml DMEM - weight of 1.5ml Eppendorf containing 1ml DMEM media but no biopsy). In a sterilised hood, biopsies were carefully placed in 200µl warm DMEM media in 96-well plates, ensuring minimal disruption to biopsies. Biopsies were incubated at 37ºC with 95% O_2 and 5% CO_2 to allow normalisation for 30 min. The plate was then taken out, supernatant carefully removed and aliquots stored at -80ºC until used for cytokine quantification as the 'baseline' concentration. Wells with biopsies were replaced with fresh 200µl DMEM and placed on ice. Mucosal biopsies were sequentially and carefully orientated using a stereomicroscope to have an apical to basolateral polarity, thereby anchoring the submucosal aspect of the biopsy onto a 0.4µm membrane in a Transwell insert (from 6-well Transwell plate), as shown in Figure 55. Luminal aspect of each biopsy was sequentially challenged with pH7 (control), pH5, and pH2 for 5 min, washed with PBS, and placed back in their respective wells with 200 µl DMEM media in 96-well plate, and subsequently maintained at 37ºC with 95% O_2 and 5% CO_2 overnight (18h). The supernatant was then removed and aliquots stored at -80ºC.

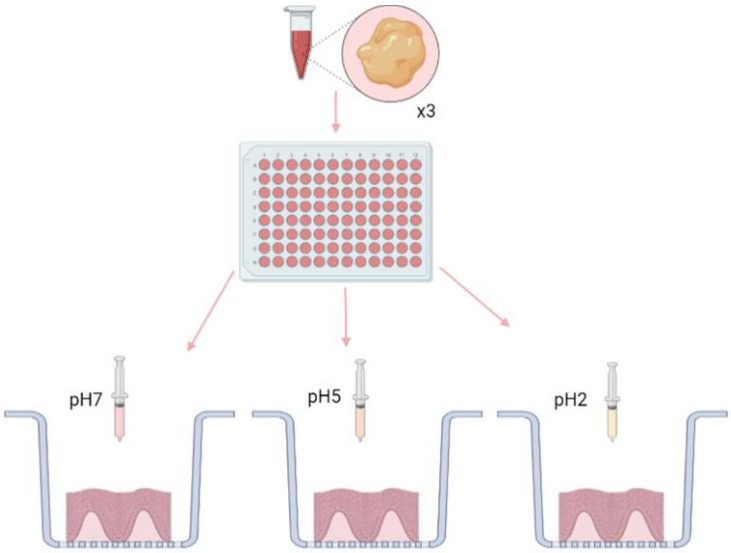

Figure 55 Ex Vivo Assay Setup

Diagram demonstrating apical to basolateral orientation of biopsy specimen and ex vivo challenge to acid. Figure created using biorender.com

4.2.6 Cytokine Quantification

Quantification of cytokines IL-1β, IL-6, TNF-α, IL-8, β-NGF, and MCP-1 was performed using a 6-plex Bio-Plex Pro Human Cytokine Assay (171304090M, Bio-Rad) as per Bio-Rad instructions. Briefly, standards were reconstituted by adding 250µl DMEM media, and vortexed at medium speed for 5 sec. A fourfold standard dilution series and blank was prepared, and each standard vortexed. Magnetic coupled beads were protected from light and vortexed at medium speed for 30 sec and diluted to 1x in DMEM media. A 50 µl volume of diluted (1x) beads were added to each well of the assay plate. The plate was then washed twice with 100 µl Bio-plex wash buffer using a handheld magnetic wash station (A14179, Life technologies). Samples, standards, and blank were vortexed, and 50µl of each were added to each well of the assay plate. Samples were run in duplicates. Plate was covered with sealing tape and incubated on a shaker at 900 rpm at RT for 30 min. Detection antibodies were prepared in the last 10 min of the incubation, whereby they were first vortexed for 5 sec and diluted to 1x. The assay plate was then washed 3 times with 100µl wash buffer, and 25µl detection antibodies added to each well. Assay plate was covered with fresh sealing tape and incubated at 900rpm for 30 min at RT. During the detection antibody incubation, XPONENT software on a MAGPIX detection system was prepared with standard S1 values and units provided in the assay kit. In the last 10 min of the incubation, 100x streptavidin-PE (SA-PE) was vortexed for 5 sec, diluted to 1x, and protected from light. Assay plate was then washed 3 times with 100µl wash buffer, the diluted SA-PE vortexed, and 50µl added to each well. New sealing tape was used to cover the assay plate again and incubated for 10 min at RT at 900 rpm. The plate was washed 3 times with 100µl wash buffer, and beads finally resuspended in 125µl assay buffer. The covered plate was shaken at 900 rpm for 30 sec before removing the sealing tape and reading plate using MAGPIX instrument settings.

4.2.7 Statistical Analysis

Following completion of the plate reading on XPONENT software, the raw results file was extracted and analysed in Bio-plex Manager. Standard curves for each analyte and error margins between sample reads were checked, and final report table saved. The observed concentration that fell within the range of the standard concentrations were extracted from the report table, and the Concentration in Range for baseline supernatant was subtracted from Sample Post- pH challenge to give the concentration of cytokine release (pg/ml). Cytokine release between ERD and healthy controls, and cytokine release with different pH conditions was compared by two-way ANOVA using GraphPad Prism 9.0. Values are presented as mean ± SD.

4.3 Results

4.3.1 Characterisation of TNFR1 Localisation in the Oesophageal Mucosa of GORD Patients

4.3.1.1 TNFR1 Antibody Optimisation

TNFR1 has been extensively reported as a therapeutic target in IBD treatment [525], but its role in other inflammatory diseases of the GIT, particularly the oesophageal mucosa, has not been characterised. TNFR1 expression in the oesophageal mucosa of GORD patients was assessed using IF-IHC. Specific binding of the TNFR1 antibody was confirmed using IBD colon tissue as a positive control. Literature demonstrates that TNFR1 signalling in intestinal epithelial cells is crucial for the pathogenesis of Crohn's colitis, and TNFR1 expression in

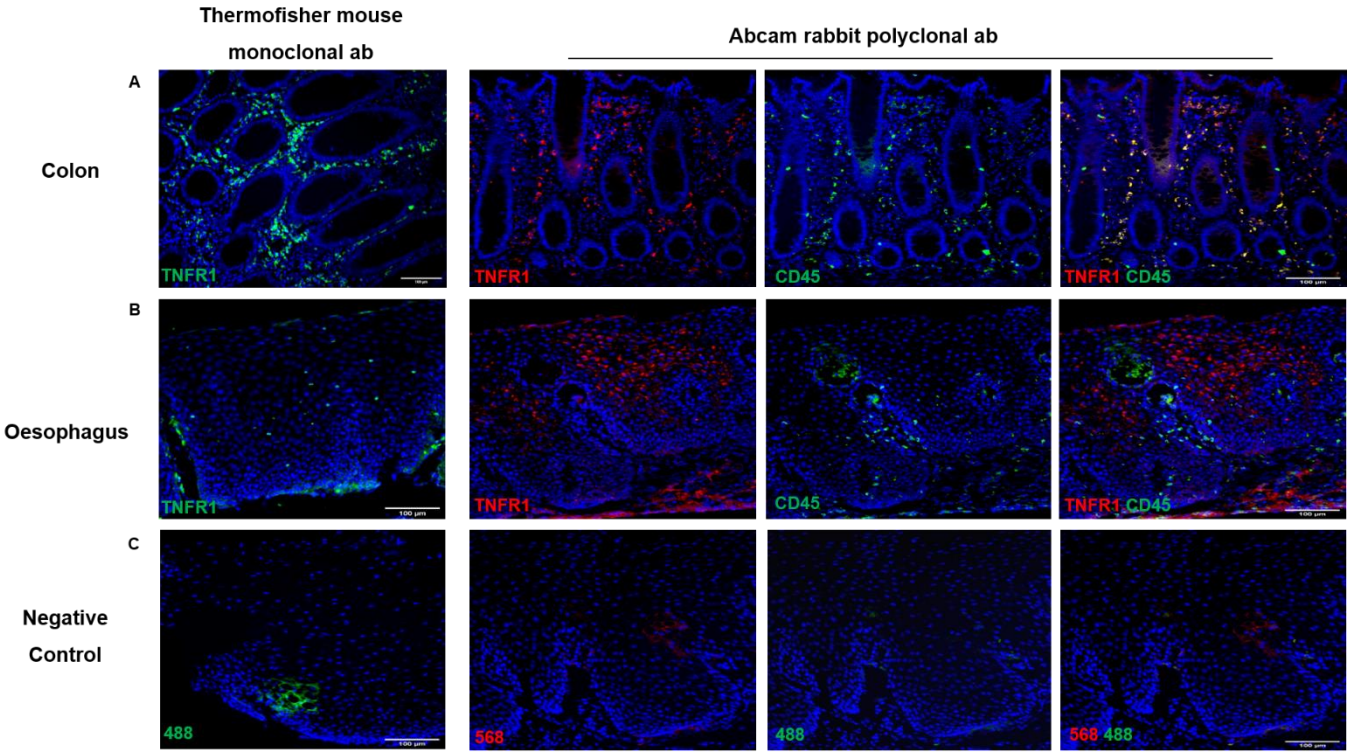

Figure 56 Expression pattern of TNFR1 in the IBD colonic mucosa and GORD oesophageal mucosa are different

A) A mouse monoclonal TNFR1 antibody from Thermofisher, and a rabbit polyclonal antibody from Abcam were tested in positive control tissue, inflamed intestinal mucosa. Both antibodies show TNFR1-immunoreactivity on lymphocyte infiltrates, as confirmed by CD45 colocalisation between colonic crypts. B) In the oesophagus, TNFR1 staining with Thermofisher monoclonal mouse antibody was less specific, and showed a nuclear pattern of staining which looked less specific than in the colon. The polyclonal rabbit antibody from Abcam was specifically expressed in the cytoplasm of epithelial cells, and did not co-express CD45. C) Negative controls showing no TNFR1 immunoreactivity for either antibody. Scale bar: 100 µm.

colonic lamina propria cells have been suggested to regulate epithelial regeneration following intestinal injury [526], [527].

In the inflamed colonic mucosa, cellular TNFR1 expression was observed between crypts, where TNFR1-immunoreactive cells detected with the polyclonal rabbit antibody were identified as CD45-positive lymphocytes (Figure 56A). A similar pattern of staining was observed in the colon with the monoclonal mouse TNFR1 antibody, which also identified TNFR1-immunoreactive cells between the colonic crypts (Figure 56A). In contrast, in human oesophagus, the monoclonal mouse antibody scarcely detected nuclear TNFR1-immunoreacvtivity in the epithelium, whilst the polyclonal rabbit antibody detected cytosolic expression of TNFR1 which had a much higher signal: background ratio (Figure 56B). Neither antibody detected TNFR1 expression on lymphocytes, as there was no colocalisation between TNFR1 and CD45 in the oesophagus (Figure 56B). Negative controls with no primary antibody were also prepared and showed no labelling. The rabbit polyclonal TNFR1 antibody was selected and used for the rest of the characterisation study.

4.3.1.2 TNFR1 Expression in the Oesophageal Mucosa of patients with GORD

A total of 70 GORD samples phenotyped endoscopically and with objective reflux studies into ERD (N=22), NERD (N=10), FH (N=18), and BO (N=20), and healthy controls (N=10) were evaluated for TNFR1 expression. This included a total of 80 µm of biopsy per sample (2 slides per patient, with each slide containing 4 serial sections at 10 µm each). TNFR1 expression was not detected on either superficial or deep CGRP-IR nerves (Figure 57). Cytosolic expression was, however, seen in oesophageal epithelial cells in ERD, FH, NERD, and BO, and in a limited number of HC samples (Figure 58). TNFR1 was not labelled on the cell membrane where epithelial cells express e-cadherin, but was found in the cell cytoplasm (Figure 58).

DAPI-positive cells and TNFR1-positive cells were counted in an automated manner and calculated as a percentage of the total number of DAPI-positive cells expressing TNFR1 (as described in section 2.2.4 Image analysis). The relative expression of TNFR1 in oesophageal epithelial cells was not significantly different among GORD phenotypes (*p=0.1566*) (Figure 58B).

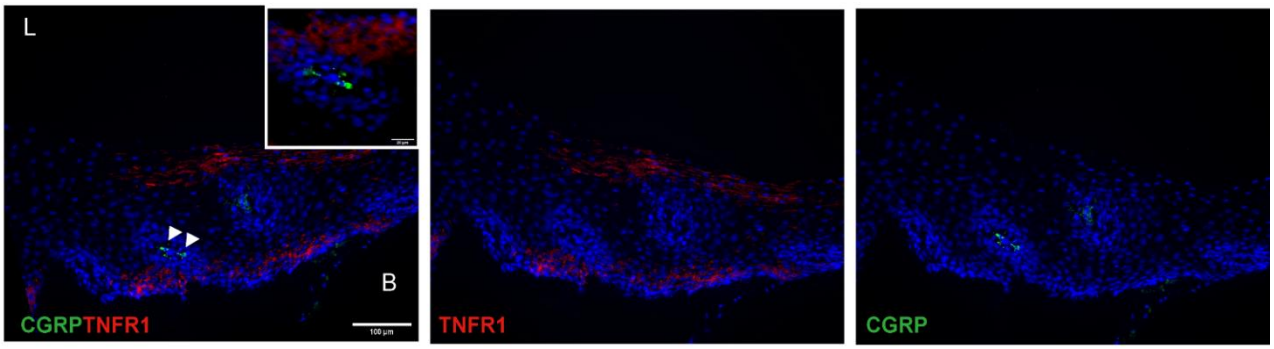

Figure 57 TNFR1 is not expressed in CGRP-positive nerves in the oesophageal mucosa

A representative GORD sample demonstrating a deep, intrapapillary sensory nerve which is negative for TNFR1. Sensory nerves did not express TNFR1 in patients with heartburn, regardless of phenotype. Scale bar:100µm. Insert scale bar: 40µm.

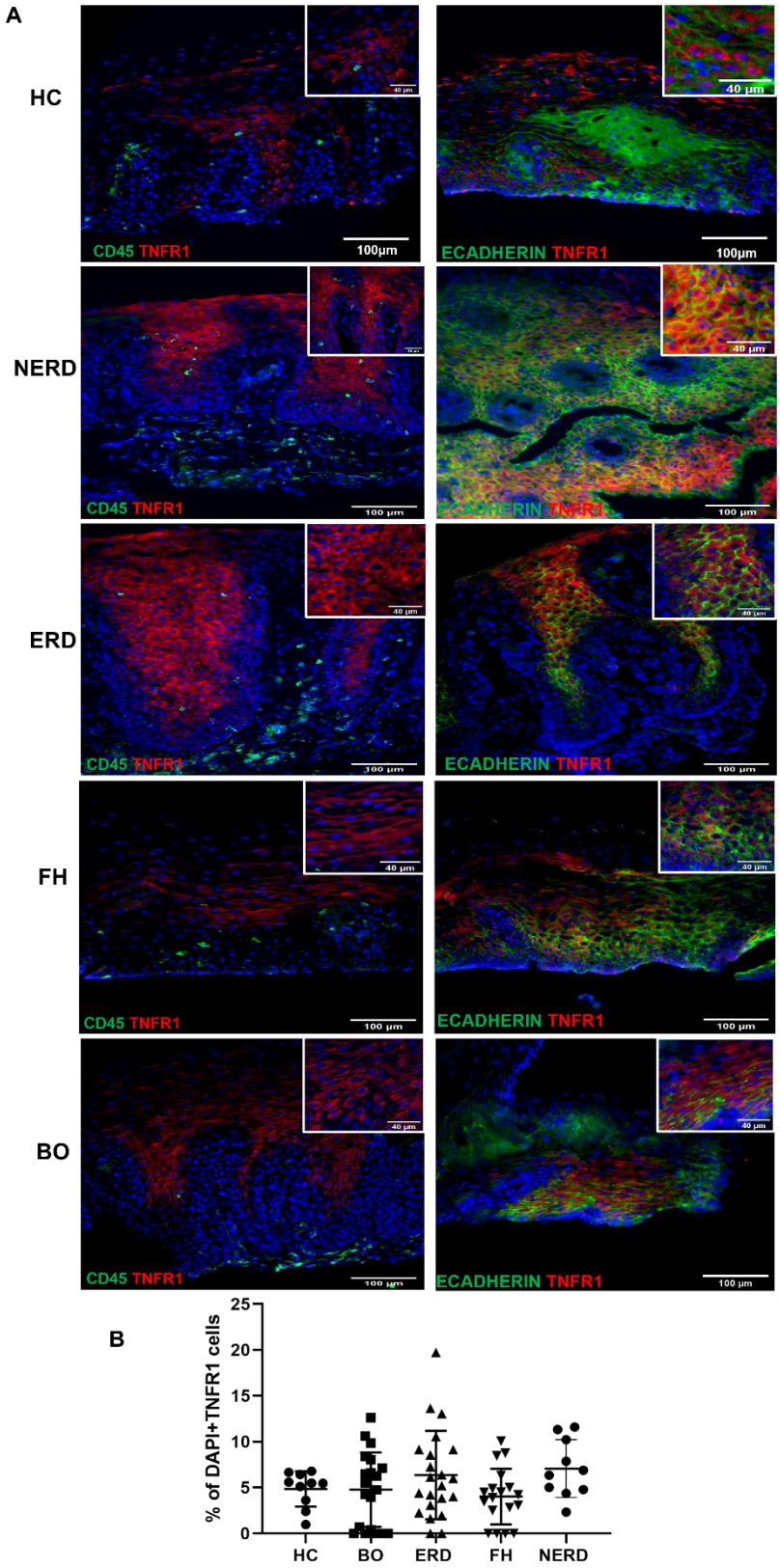

Figure 58 TNFR1 is Expressed by Oesophageal Epithelial Cells

A) TNFR1 was expressed in the cytoplasm of oesophageal epithelial cells in all GORD phenotypes and healthy controls, but was not expressed by immune cells identified with CD45. B) TNFR1 expression was not significantly different in epithelial cells among GORD phenotypes, nor between GORD patients and healthy controls. Error bars represent SD. HC: N=10, NERD: N=10, BO: N=20, ERD: N=22, FH: N=18. Scale bar: 100µm. Inset scale bar: 40µm.

4.3.2 Characterisation of CXCR2 Localisation in the Oesophageal Mucosa of GORD Patients

4.3.2.1 CXCR2 Antibody Optimisation

CXCR2 has been widely suggested to regulate the immune response of neutrophils in the pathogenesis of inflammatory disease models such as Ulcerative Colitis (UC) [528]. However, its role in other inflammatory diseases of the GIT, particularly the oesophageal mucosa, has not been characterised. To establish where CXCR2 resides in the oesophageal epithelium of patients with heartburn, IF-IHC was performed. Specific binding of the CXCR2 antibody was confirmed using IBD colon tissue as a positive control. Literature demonstrates increased CXCR2 expression on neutrophils infiltrating colonic mucosa of patients with active ulcerative colitis, and decreased secretion of inflammatory cytokines upon pre-treatment of peripheral blood neutrophils with CXCR2 inhibitor SB225002 [529].

In the inflamed colonic mucosa, cellular CXCR2 expression was observed between crypts, where they frequently colocalised with the pan-leukocyte marker CD45 (Figure 59A), supporting similar reports of CXCR2 expression on neutrophils in the colon in recent literature [528], [529]. Negative controls with no primary antibody were also prepared and showed no labelling (Figure 59B).

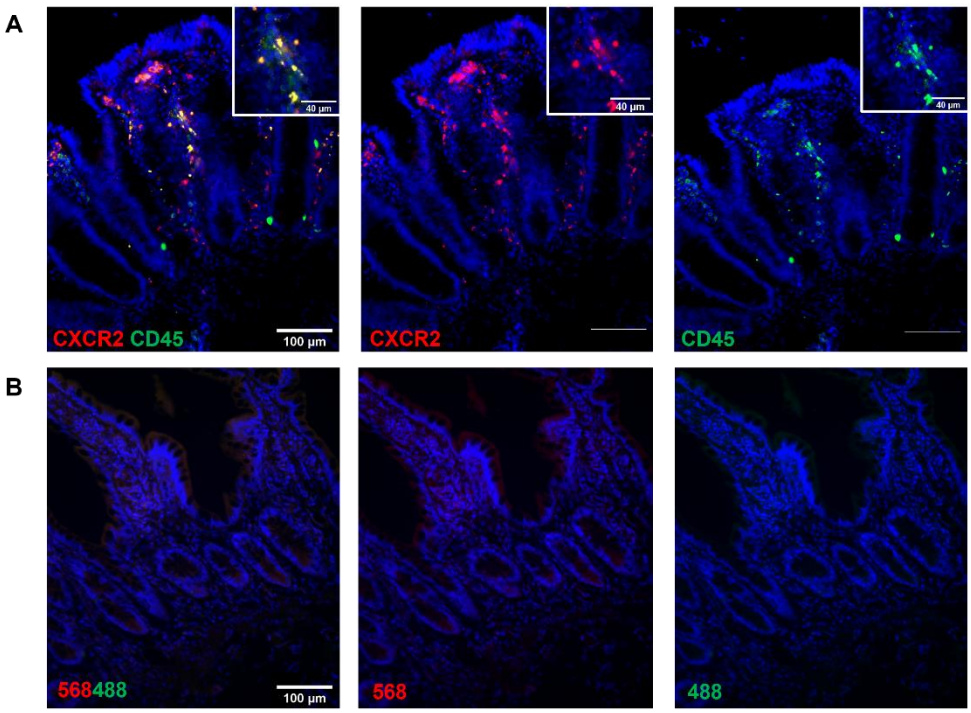

Figure 59 CXCR2 is Expressed on Immune Cells in Inflamed Colonic Mucosa

A) CXCR2 antibody optimisation on positive control tissue, IBD colon. CD45 was used to highlight lymphocytes. CXCR2 was expressed on immune cells in the colonic mucosa. There was colocalisation between CXCR2 and CD45 in the epithelium of the IBD colon B). Negative controls showing no immunoreactivity for CXCR2 in the IBD colon. Scale bar: 100µm. Inset scale bar: 40µm.

4.3.2.2 CXCR2 Expression in the Oesophageal Mucosa of Patients with GORD

A representative number of GORD samples phenotyped into ERD (N= 9), NERD (N= 13), FH (N= 10), and BO (N= 8), and healthy controls (N=10) were evaluated for CXCR2 expression in the oesophageal mucosa. CXCR2 expression was detected on oesophageal epithelial cell membranes in healthy controls, ERD, FH, NERD, and BO, and was frequently localised around the papillae (Figure 60). However, CXCR2 pixel quantification (as described in section 2.2.3.4 Pixel analysis) ascertained that relative expression of CXCR2 on oesophageal epithelial cells was not significantly different among GORD phenotypes, nor between GORD patients and healthy controls (Figure 60, p= 0.428).

To establish the spatial relationship between CXCR2-immunoreactive epithelial cells and sensory afferent nerves, IF data was further evaluated. CXCR2 co-expression was detected on deep CGRP-immunoreactive nerves innervating oesophageal mucosal papillae of FH patients (Figure 61). Interestingly, maximum intensity projection of a confocal z-stack also revealed the close apposition of a deep CXCR2/CGRP-immunoreactive sensory nerve innervating oesophageal papillae in a FH patient and the epithelial cells expressing membranous CXCR2 surrounding the papillae (Figure 61), (Appendix 12). While a representative number of GORD patients were assessed, sensory nerves were only identified in 2/10 FH patients. CGRP-immunoreactive nerve endings were not identified in the other GORD phenotypes in this panel of staining, despite experimental repeats. This is due to the scarcity of sensory afferent nerve endings in a relatively small biopsy specimen.

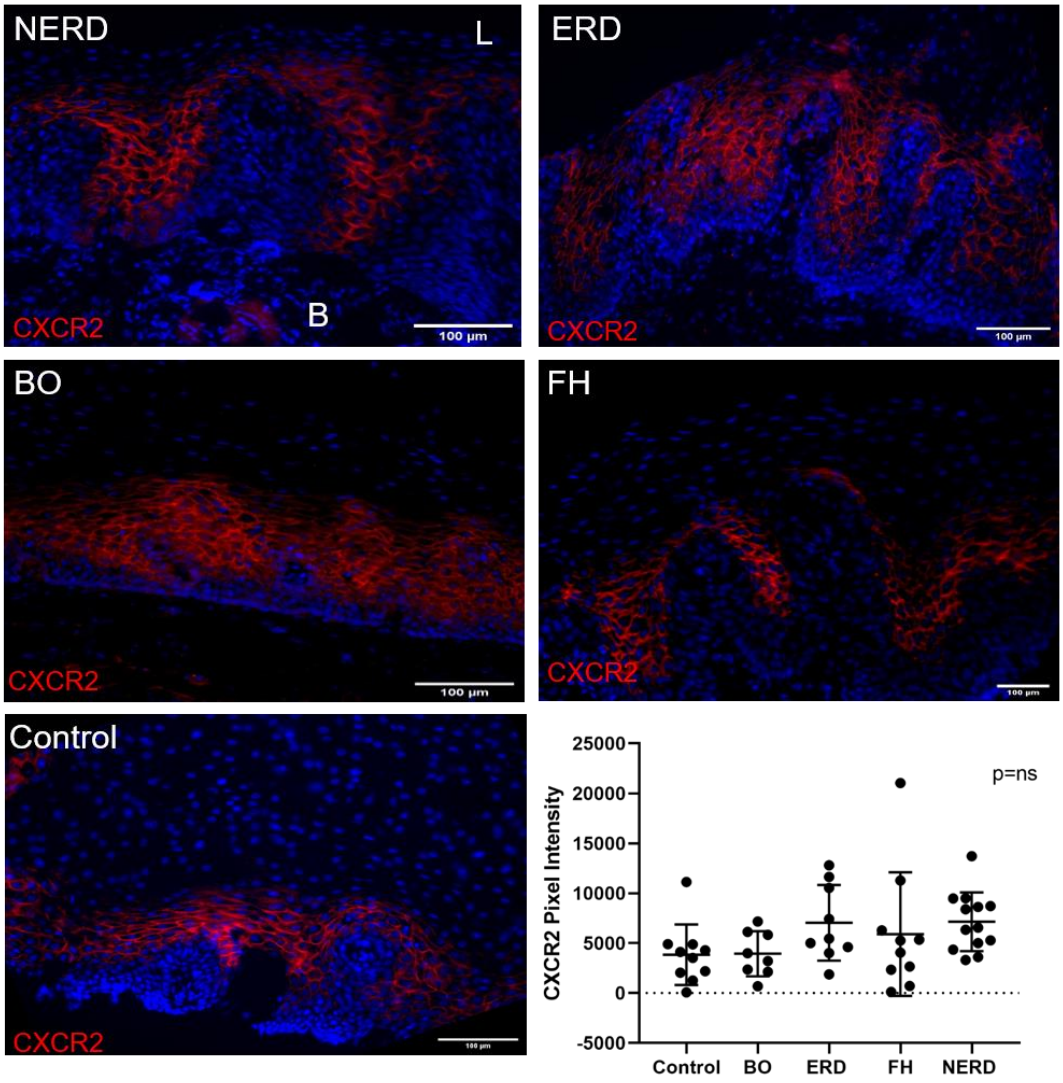

Figure 60 CXCR2 is expressed on epithelial cell membrane in GORD

CXCR2 is expression is localised on epithelial cells around the papillae of all GORD phenotypes and healthy controls. Pixel analysis found no significant difference in the level of CXCR2 expression among GORD groups, nor between GORD patients and healthy controls. L=lumen, B=basal layer. Scale bar: 100µm. Images are representative of the mean taken from 3 experimental repeats per patient, from 5 fields of view. Error bars represent S.D. Healthy control: N=10, ERD: N= 9, NERD: N= 13, FH: N= 10, and BO: N= 8.

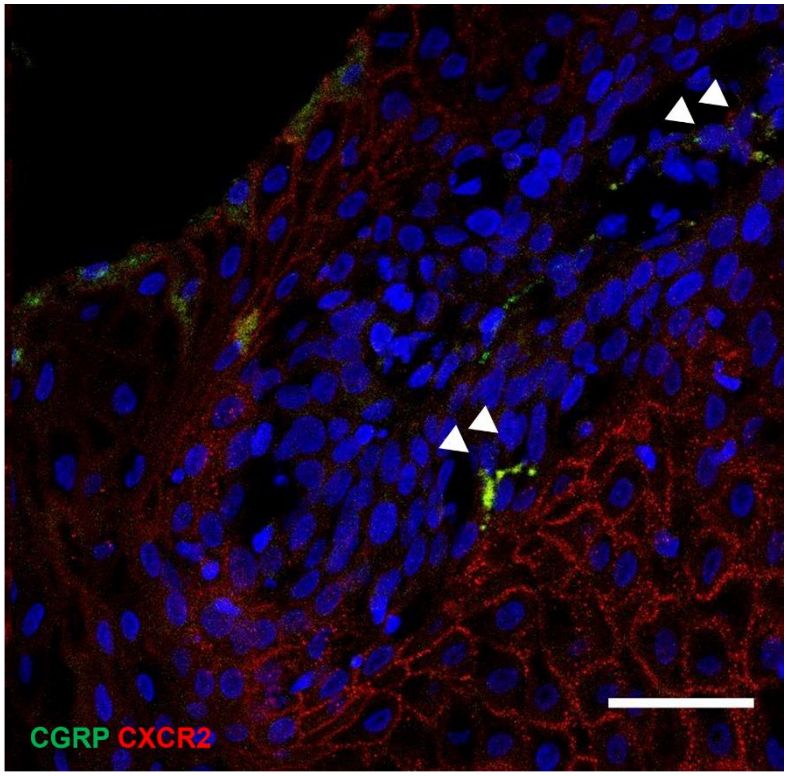

Figure 61 CXCR2 Expression on a deep sensory nerve in a patient with functional heartburn

Confocal Z-stack maximum intensity projection of a representative functional heartburn patient co-expressing CXCR2 on a deep sensory afferent nerve in the papillae in close association with CXCR2-immunoreactive epithelial cells surrounding the papillae. L=lumen, B= basal layer. Scale bar: 10µm

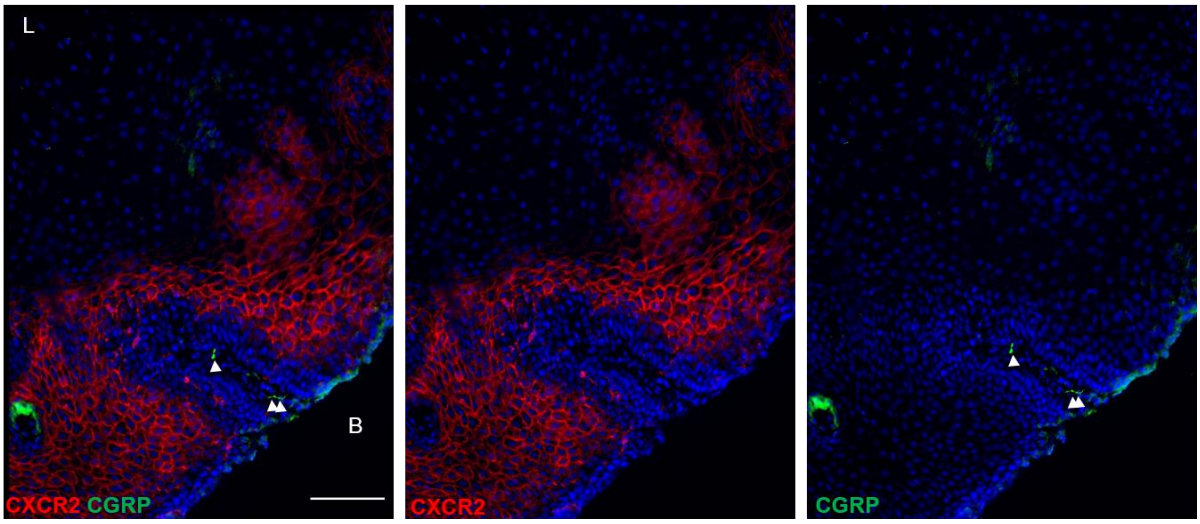

Figure 62 CGRP+ intrapapillary sensory afferent nerves in healthy controls do not express CXCR2

A representative healthy control oesophageal mucosa with CXCR2+ epithelial cells localised around the papillae, and CGRP+ sensory afferent nerve where CXCR2 expression was not detected. L=lumen, B= basal layer. Scale bar: 100µm

Whilst this spatial relationship between CXCR2+ epithelial cells and sensory afferent nerves was also assessed in healthy oesophageal mucosa, the intrapapillary sensory afferent nerves did not co-express CXCR2, nor were in as close proximity to the CXCR2+ epithelial cells as that seen in FH patients (Figure 62).

5.3.3 IL8 Gene Expression in the Oesophageal Mucosa of GORD Patients

The relative level of *IL8* gene expression in the oesophageal mucosa of patients with GORD was assessed via qPCR studies. *IL8* gene expression was significantly higher in GORD oesophageal mucosa compared to healthy oesophageal mucosa (p=0.0172) (Figure 63). ERD and NERD patients had the highest level of *IL8* gene expression among the GORD phenotypes, although the difference between ERD/NERD samples and healthy controls did not reach statistical significance (p=0.09, and p=0.12 respectively), as seen in Figure 63. In contrast, FH patients expressed *IL8* at levels similar to that seen in healthy controls (p= >0.99) (Figure 63). *IL8* expression fold change was also slightly higher in BO patients compared to FH (p= >0.99) (Figure 63).

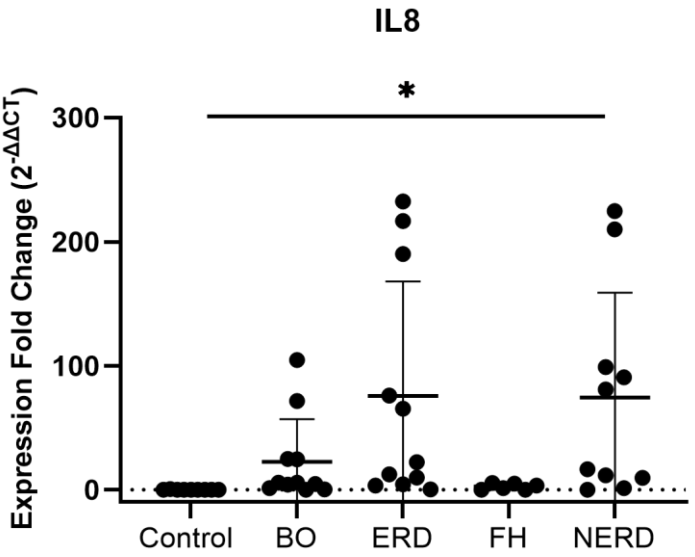

Figure 63 IL8 Expression Fold Change in GORD Oesophageal Mucosa

The normalised expression fold change of *IL8* in relation to the reference gene 18S, normalised against healthy control samples. Error bars represents SD. One-way ANOVA detected significant difference among control and GORD samples (p=0.0172). Bonferroni's NERD: N= 10, BO: N= 11, ERD: N=11, FH: N= 6, Control N=9

4.3.3 Characterisation of IL1R Localisation in the Oesophageal Mucosa of GORD Patients

4.3.3.1 IL1R Antibody Optimisation

The role of IL1R has been implicated in the inflammasome signalling pathway in intestinal inflammation, where it was shown to regulate neutrophil recruitment [350]. Upon bacterial infection, IL1R expression was increased in the ileum 7 days after inoculation with *Toxoplasma gondii*, and intestinal inflammation was attenuated in IL1R$^{-/-}$ mice [530]. In this part of the study, IL1R localisation in the oesophageal mucosa of patients with GORD was assessed using IF-IHC to elucidate the potential role IL1R signalling might have in heartburn pathogenesis. First, a suitable IL1R antibody was optimised using UC colon tissue. Figure 64A demonstrates extensive IL1R expression in CD45^{-} cells throughout the colonic epithelium. Negative controls with no primary antibody were also prepared simultaneously and showed no labelling (Figure 64B).

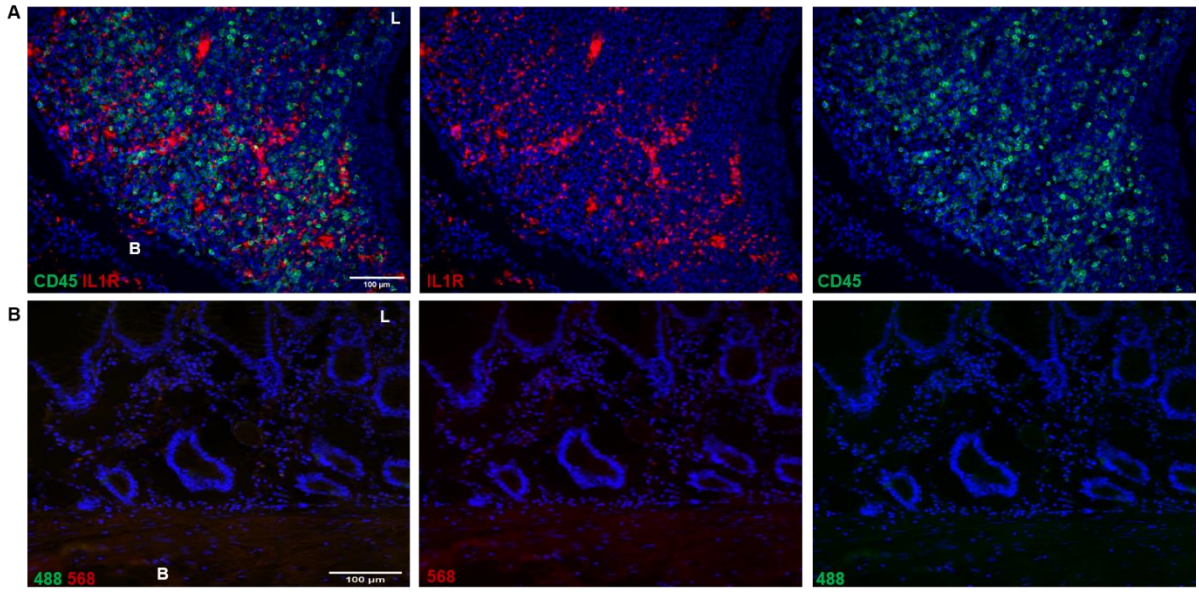

Figure 64 IL1R is Widely Expressed Throughout the IBD Colonic Mucosa

A) IL1R^{+}CD45^{-} cells are extensively present throughout the colonic mucosa of a representative IBD patient. IL1R-immunoreactive cells do not co-express CD45. B) Negative control of a colon sample of an IBD patient stained side by side with positive control tissue but with primary antibody omitted. Scale bar: 100µm. Inset scale bar: 40µm. L=lumen, B= basal layer.

4.3.3.2 IL1R Expression in the Oesophageal Mucosa of Patients with GORD

A representative number of GORD samples phenotyped into ERD (N= 9), NERD (N= 13), FH (N= 10), and BO (N= 8) were evaluated for IL1R expression in the oesophageal mucosa. IL1R showed two distinct patterns of expression in a small subset of oesophageal epithelial cells; 1) cytosolic expression as seen exclusively in a representative ERD patient sample in Figure 65A, and 2) membranous expression as seen in a representative NERD patient sample in Figure 65B where there is co-expression with e-cadherin, a membranous epithelial cell marker. However, IL1R expression was limited compared to the extensive mucosal expression observed with TNFR1 and CXCR2 receptors in sections 4.3.1.2 TNFR1 Expression in the Oesophageal Mucosa of patients with GORD and 4.3.2.2 CXCR2 Expression in the Oesophageal Mucosa of Patients with GORD.

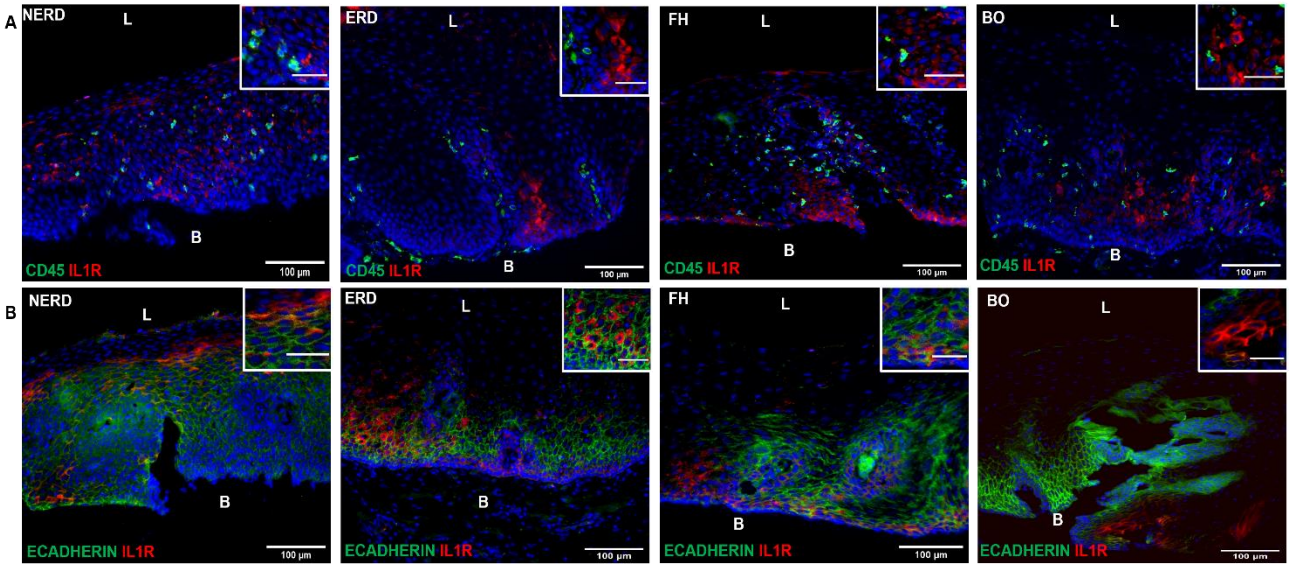

Figure 65 IL1R is Expressed in a Relatively Small Subset of Oesophageal Epithelial Cells in GORD Patients

A) IL1R is not expressed by lymphocytes infiltrating the oesophageal mucosa of patients with GORD. B) There is some cytosolic and some membranous expression of IL1R in a small subset of epithelial cells in the oesophageal mucosa of patients with GORD. Scale bar: 100µm. Inset scale bar: 40µm. L=lumen, B= basal layer.

4.3.4 Characterisation of IL6ST Localisation in the Oesophageal Mucosa of GORD Patients

4.3.4.1 IL6ST Antibody Optimisation

The importance of IL6ST in modulating the colonic mucosal inflammatory response in colitis has been well established, but its role in regulating mucosal mechanisms in the context of GORD is yet to be understood. Silencing MIR-31, which has a direct ability to suppress IL6ST activity, was found to induce an epithelial inflammatory response in a DSS-induced mouse model of colitis, highlighting the proinflammatory role of IL6ST in the colon [361]. In this part of the study, the localisation of IL6ST was assessed in the oesophageal mucosa of patients with heartburn to understand its potential role in oesophageal hypersensitivity. Inflamed colonic tissue from patients with UC was used as a positive control. IL6ST was extensively detected on intraepithelial lymphocytes between colonic crypts in the inflamed colonic mucosa, as seen in Figure 66. However, in the oesophageal mucosa of a patient with heartburn (phenotype undetermined), IL6ST showed a membranous pattern of staining on epithelial cells (Figure 66). Negative controls with no primary antibody were also prepared simultaneously and showed no labelling (Figure 66).

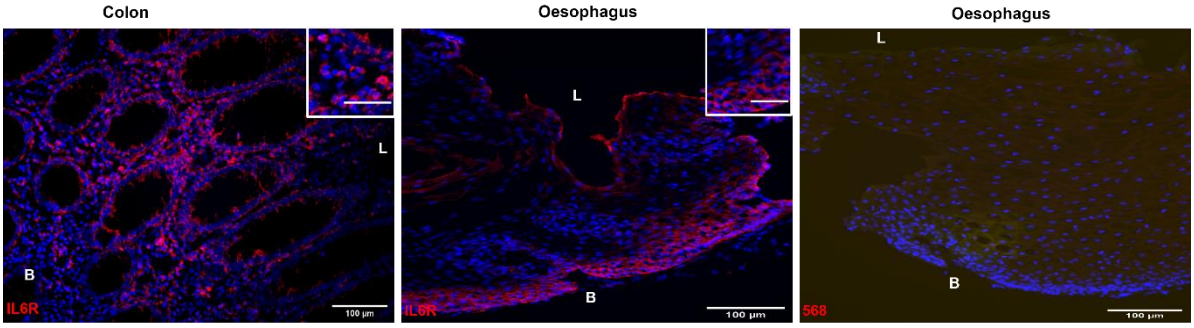

Figure 66 IL6ST is Densely Expressed on Intraepithelial Lymphocytes in the Colonic Mucosa and on Epithelial Cells in the Oesophagus

IL6ST was widely expressed on intraepithelial lymphocytes between colonic crypts in the inflamed colonic mucosa, while the expression pattern in the oesophagus of a heartburn patient appeared to be epithelial. The negative control of a oesophageal sample stained side by side with positive control tissue but with primary antibody omitted showed no positive signal. Scale bar: 100µm. Inset scale bar: 40µm. L=lumen, B= basal layer.

4.3.4.2 IL6ST Expression in the Oesophageal Mucosa of Patients with GORD

A representative number of GORD samples phenotyped into ERD (N= 9), NERD (N= 13), FH (N= 10), and BO (N= 8) were evaluated for IL6ST expression in the oesophageal mucosa. IL6ST expression was only detected in the cytoplasm of epithelial cells in the oesophageal epithelium of all GORD phenotypes, as shown in Figure 67. There was no colocalisation of e-cadherin and IL6ST in the GORD samples studied. Moreover, IL6ST expression was much more limited compared to the extensive mucosal expression observed with TNFR1 and CXCR2 receptors in sections 4.3.1.2 TNFR1 Expression in the Oesophageal Mucosa of patients with GORD and 4.3.2.2 CXCR2 Expression in the Oesophageal Mucosa of Patients with GORD.

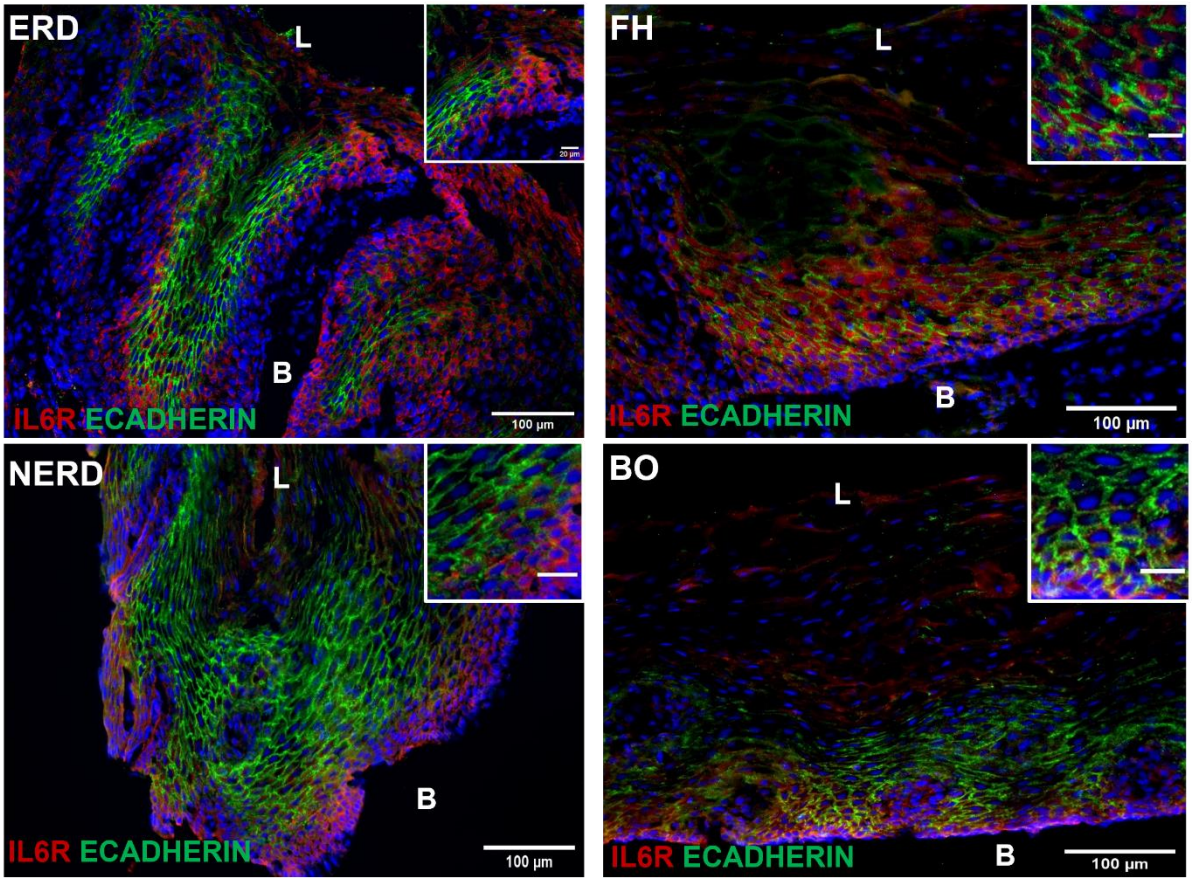

Figure 67 IL6ST is Expressed in the Cytoplasm of a Subset of Epithelial Cells in GORD Patients

IL6ST expression was detected in the cytoplasm of a subset of epithelial cells in all phenotypes of GORD. There was no expression of IL6ST on the epithelial cell membrane, as IL6ST and e-cadherin did not colocalise in any of the patient biopsies assessed. Scale bar: 100µm; Inset scale bar: 20µm. L=lumen, B= basal layer.

4.3.5 Characterisation of RAMP1 Localisation in the Oesophageal Mucosa of GORD Patients

4.3.5.1 RAMP1 Antibody Optimisation

RAMP1, an important protein component of the CGRP receptor complex, is an established target in treating chronic pain conditions such as migraine [391]. However, its role in the mechanism of pain sensation by CGRP-immunoreactive afferent nerves in the oesophageal mucosa of patients with GORD remains undetermined. In this part of the study, RAMP1 localisation and potential role regulating heartburn pathogenesis in the oesophageal mucosa was assessed using immunofluorescence. In a mouse model of DSS-induced colitis, RAMP1 immunoreactivity was reported on macrophages, mast cells, and T cells [402], [405]. As such, colon tissue from patients with UC was used to optimise the RAMP1 antibody. Interestingly, RAMP1 expression was detected on a small subset of myenteric neurons, as shown in Figure 68A. RAMP1 expression was also detected on a small subset of lymphocytes in the colonic mucosa, in between crypts (Figure 68B). Negative controls with no primary antibody were also prepared simultaneously and showed no labelling (Figure 68C).

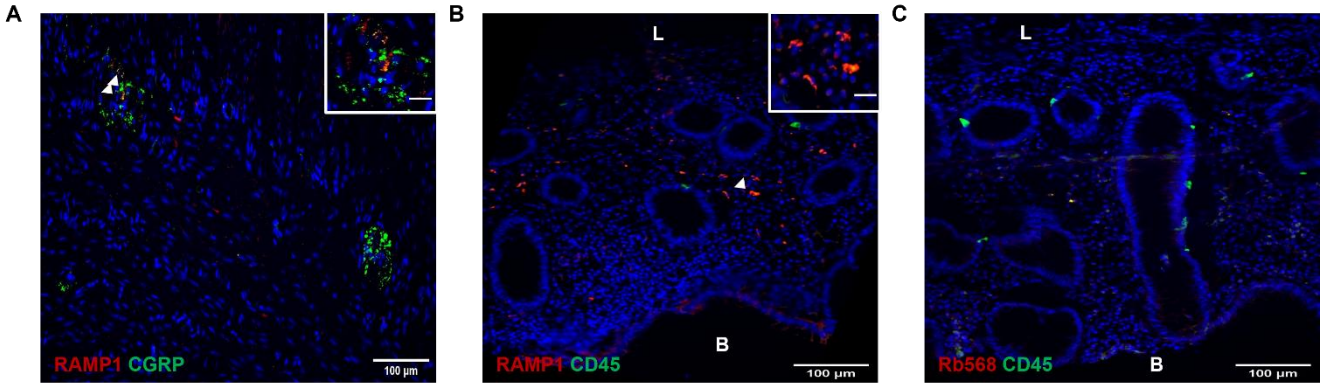

Figure 68 RAMP1 is Expressed on a Subset of Myenteric Neurons and on Lymphocytes in the Colonic Mucosa

A) RAMP1 is expressed on a very small number of CGRP+ myenteric neurons in the colon of an IBD patient. B) RAMP1 is expressed on a subset of intraepithelial lymphocytes between colonic crypts in the colonic mucosa of an IBD patient. C) The negative control of a oesophageal sample stained side by side with positive control tissue but with primary antibody omitted showed no positive signal. Scale bar: 100µm; inset scale bar: 20µm. L=lumen, B= basal layer.

4.3.5.2 RAMP1 Expression in the Oesophageal Mucosa of Patients with GORD

A representative number of GORD samples phenotyped into ERD (N= 9), NERD (N= 10), FH (N= 9), and BO (N= 9), and healthy controls (N=9) were evaluated for RAMP1 expression in the oesophageal mucosa. RAMP1 was most frequently detected on epithelial cell subsets in the oesophageal mucosa of patients with NERD and ERD, as shown in Figure 69A. However, RAMP1 was also occasionally detected on intrapapillary lymphocytes in patients with ERD (Figure 69B). Moreover, oesophageal epithelial expression of RAMP1 was not significantly different between patients with GORD, nor between healthy controls and phenotypes of GORD (p=0.639) (Figure 69C). The level of RAMP1 expression on epithelial cells was also lower than expression of other cytokine receptors such as TNFR1 (Figure 58B), which was expressed in the range of 5-15% DAPI+ cells in samples where it was detected, compared to a range of 1-3% DAPI+ cells expressing RAMP1.

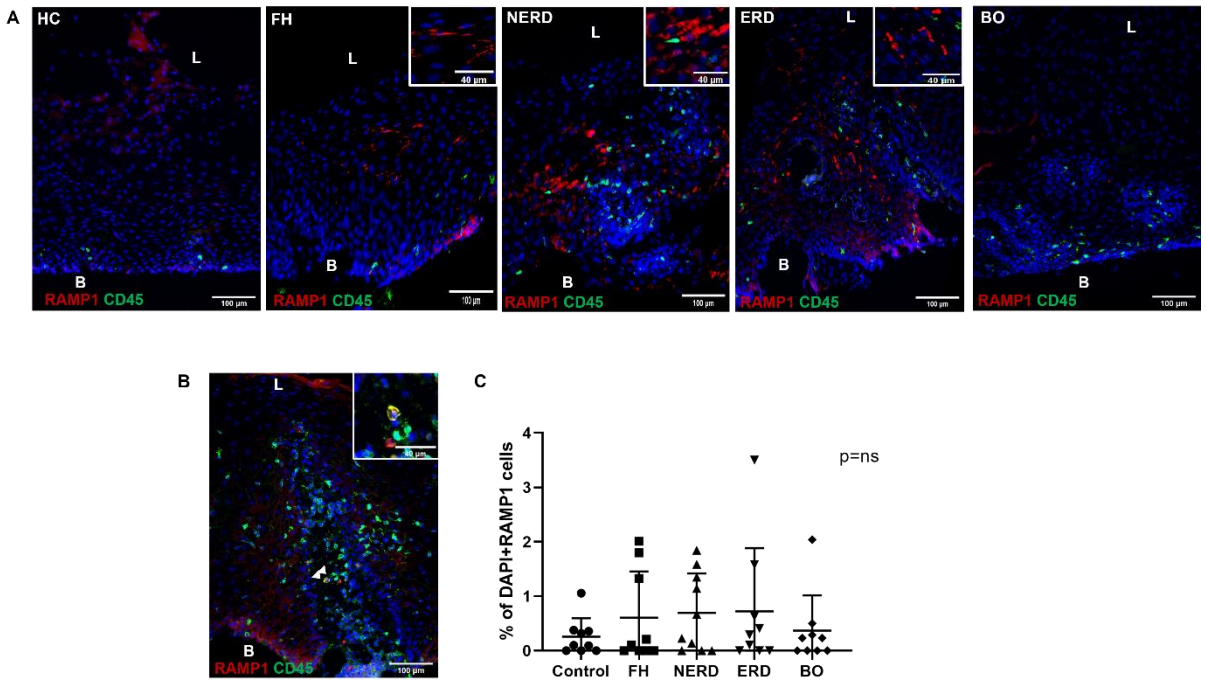

Figure 69 RAMP1 is Expressed by a Subset of Oesophageal Epithelial Cells in Patients with GORD, and Occasionally on Intrapapillary Lymphocytes

A) RAMP1 expression was frequently detected on small subsets of oesophageal epithelial cells in NERD and ERD patients, but never in healthy controls. B) RAMP1 expression on a CD45-immunoreactive lymphocyte in the papillae of a representative ERD patient. C) RAMP1 expression was not significantly different in epithelial cells among GORD phenotypes, nor between GORD patients and healthy controls. Error bars represent SD. HC: N=9, NERD: N=10, BO: N=9, ERD: N=9, FH: N=9. Scale bar: 100µm; inset scale bar: 40µm.

4.3.6 Differential Expression of Inflammatory Cytokine Receptor Genes in Oesophageal Mucosa of GORD Patients

DESeq2 expression matrix for the comparison between HCs and GORD patients was manually filtered for inflammatory cytokine receptors studied above. *TNFR* variants and *NTRK*1 were found to be increased in BO patients, while *NGF* and histamine receptor gene *HRH1* increased in ERD patients, as seen in Figure 70. Interestingly, healthy controls had increased expression of *RAMP1* and *IL1R* genes (Figure 70). *CXCR2* expression did not change across healthy controls or GORD patients (Figure 70).

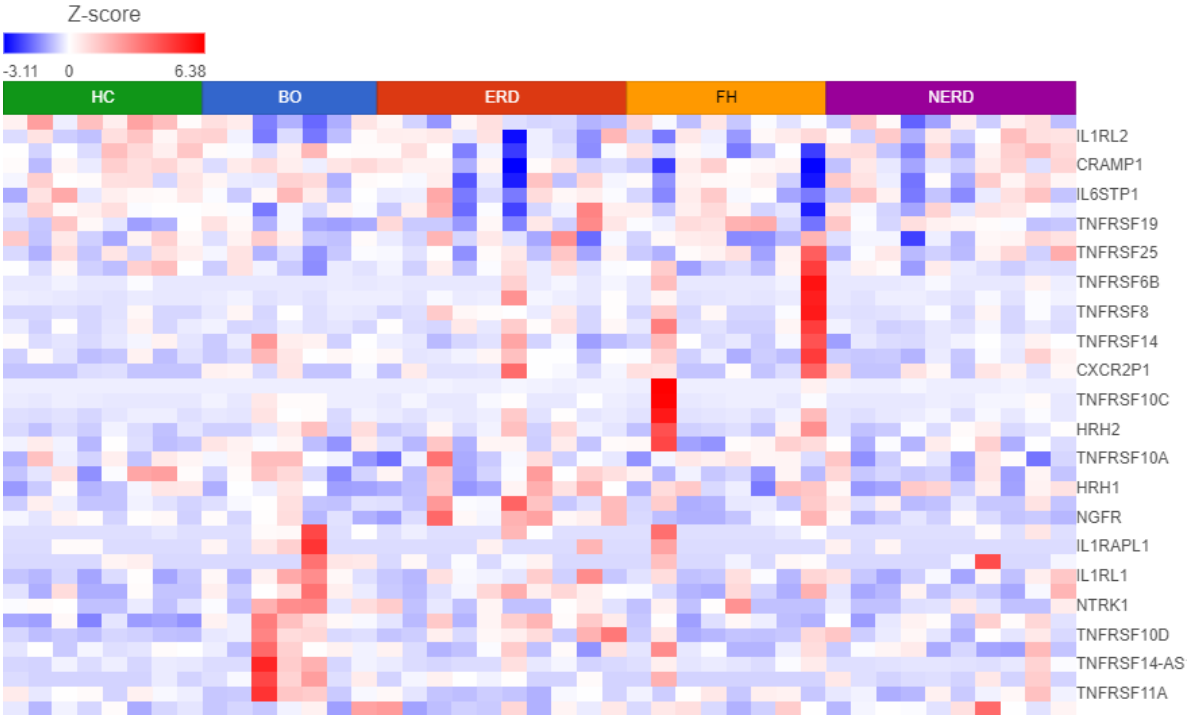

Figure 70 RNA Expression of Inflammatory Cytokine Receptors in GORD Oesophageal Mucosa

DESeq2 expression matrix for the comparison between HCs and GORD patients was manually filtered for ion channel genes on Partek. HCs: (N=8), BO: (N=7), ERD: (N=10), FH: (N=8), NERD: (N=10), $p = 0.05$.

4.3.7 Characterisation of Immune Cell Populations in the Oesophageal Mucosa of Patients with GORD

4.3.7.1 T-cell Infiltration in the Oesophageal Mucosa of GORD Patients

The stimulatory roles of T cells in pain sensation through amplification of neuroinflammation have been increasingly discussed [531]. Th1 and Th17 cells were recently shown to facilitate macrophage infiltration into areas of chimeric mice with damaged nerve endings [532]. As explained in section 1.8 Inflammation in GORD, a rat model of ERD also demonstrated infiltration of $CD3^{+}CD20^{-}$ lymphocytes in the inflamed oesophageal mucosa [418]. However, the potential role of T cells has not been extensively assessed in other heartburn phenotypes, including NERD. Thus, CD3+ T cell localisation was assessed using IF-IHC across well-defined phenotypes of GORD patients and healthy controls. A CD3 antibody previously optimised by the group was used to assess the presence of T cells in the oesophageal mucosa (antibody detailed in Table *8*).

GORD samples phenotyped into ERD (N=18), NERD (N= 10), FH (N= 16), and BO (N= 16), and healthy controls (N=7) were evaluated for $CD3^{+}$ T cells in the oesophageal mucosa. CD3+ T cells were most often detected near the papillae in the oesophageal mucosa of patients with GORD, as seen in Figure 71A. Although T cells were found more frequently in the oesophageal mucosa of patients with GORD compared to healthy controls, there was no significant difference in the number of T cells infiltrating the oesophageal mucosa between heartburn patients and healthy controls, nor among the GORD phenotypes (Figure 71B).

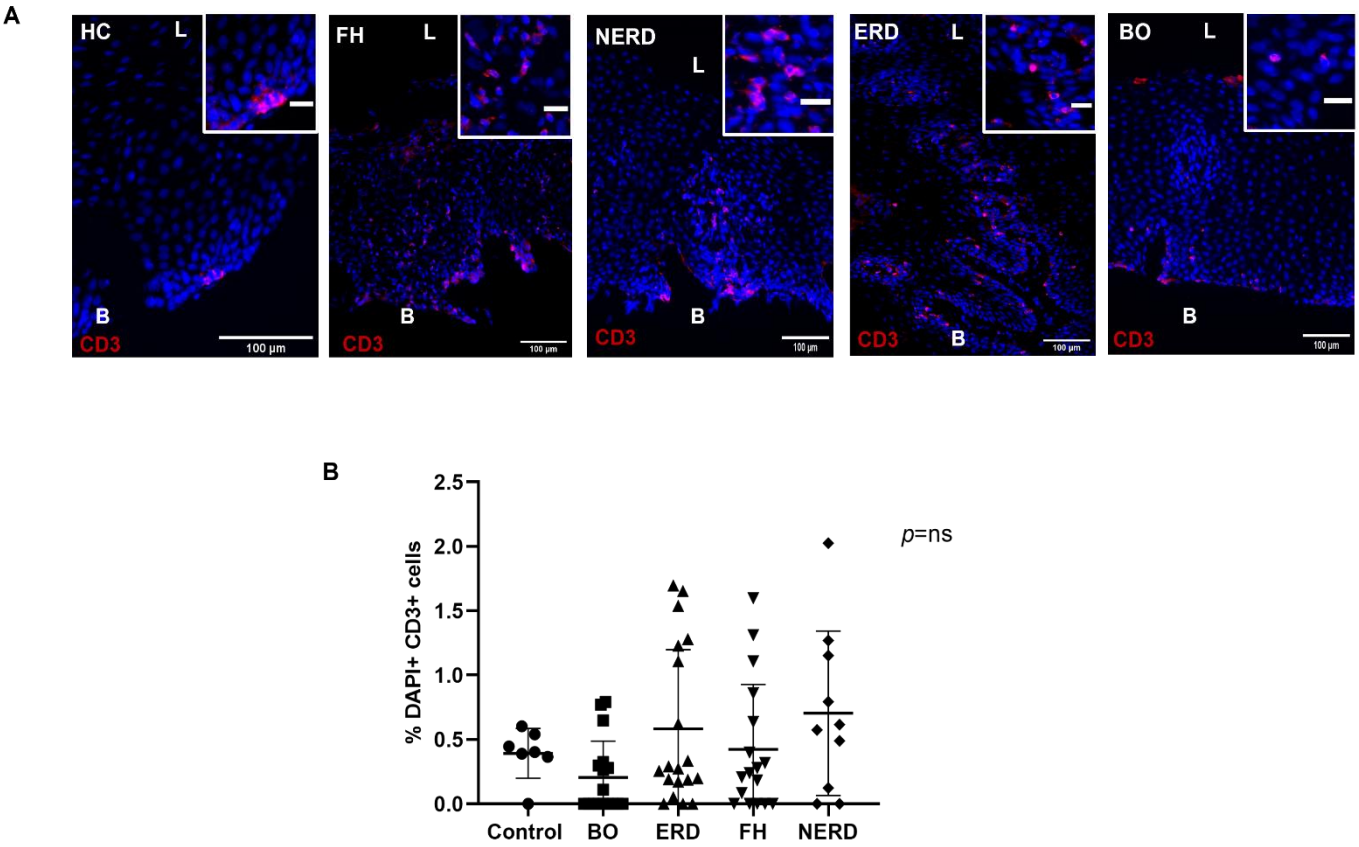

Figure 71 CD3+ T Cells are Localised around the Papillae in the Oesophageal Mucosa of Patients with GORD

A) CD3+ T cells were most frequently detected in close proximity to the papillae in patients with GORD. B) There was no significant difference in the levels of T cell infiltration across GORD patients, nor between GORD patients and healthy controls. Scale bar represents 100µm Error bars represent SD. Healthy controls: N=7, BO patients: N=16, ERD: N=18, FH: N=16, NERD: N=10

4.3.7.2 B-cell Infiltration in the Oesophageal Mucosa of GORD Patients

The humoral arm of the adaptive immune response has not been previously studied in the oesophageal mucosa of patients with GORD [522]. To validate functional enrichment analysis findings from the RNA sequencing data of this study, and to understand whether B lymphocytes have a modulatory role in heartburn pathogenesis, the localisation of CD20+ B cells was assessed with IF-IHC. A CD20 antibody previously optimised by the group was used to assess the presence of T cells in the oesophageal mucosa (antibody detailed in Table *8*).

GORD samples phenotyped into ERD (N=18), NERD (N= 10), FH (N= 16), and BO (N= 16), and healthy controls (N=7) were evaluated for $CD20^{+}$ B cells in the oesophageal mucosa. Although sparse in their numbers, CD20+ B cells were most often detected in papillary structures in patients with heartburn, as seen in Figure 72A. There was no significant difference in B cell infiltration among the GORD phenotypes, nor between GORD patients and healthy controls (Figure 72B), but a small increase in B cell abundance in ERD patients was observed.

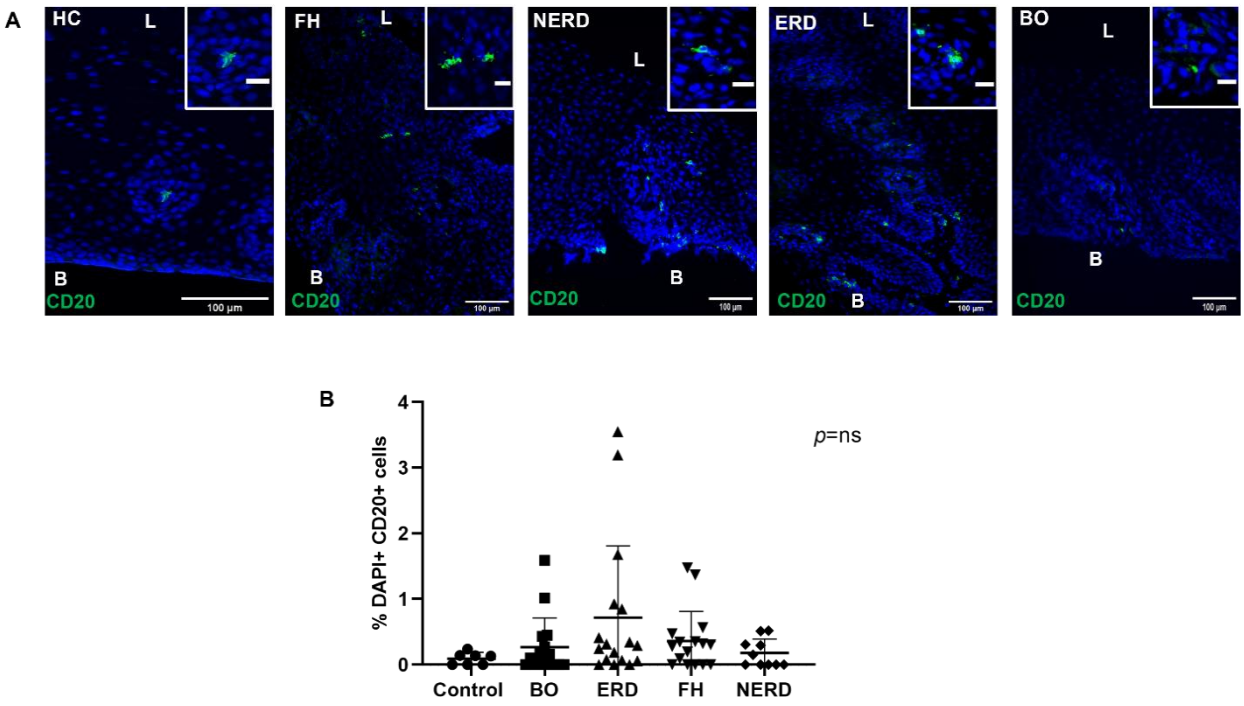

Figure 72 CD20+ B cells are Scarcely Expressed in the Papillae in Patients with GORD

A) CD20+ B cells were most frequently detected near the papillae in patients with GORD. B) There was no significant difference in the levels of T cell infiltration across GORD patients, nor between GORD patients and healthy controls. Scale bar represents 100µm Error bars represent SD. Healthy controls: N=7, BO patients: N=16, ERD: N=18, FH: N=16, NERD: N=10

4.3.8 Expression of Neurotrophic Mediators in the Oesophageal Mucosa of Patients with GORD

4.3.8.1 Optimisation of GAP43 Antibody

Growth-associated protein-43 (GAP43) has been traditionally reported to regulate peptidergic nerve growth and sprouting [533]. Recently, its involvement has also been implicated in hypersensitivity in IBS patients with increased colonic innervation of TRPV1+ nerves positively associated with abdominal pain, where increased neuronal sprouting as a result of GAP43 expression could play a propagative role [268], [534]. Its localisation in patients with oesophageal hypersensitivity has not, however, been previously investigated. To understand the neuroplastic changes involved in development of pain in patients with heartburn, IF-IHC experiments were performed on oesophageal biopsies from patients with GORD and healthy controls.

In the inflamed colonic tissue used as positive control, GAP43 co-expression was detected on both PGP9.5+ and CGRP+ afferent nerves in the lamina propria around colonic crypts (as shown in Figure 73A and B), supporting the observation of GAP43 expression in the colonic mucosa in recent literature [268]. Negative controls with no primary antibody were also prepared and showed no labelling (Figure 73C).

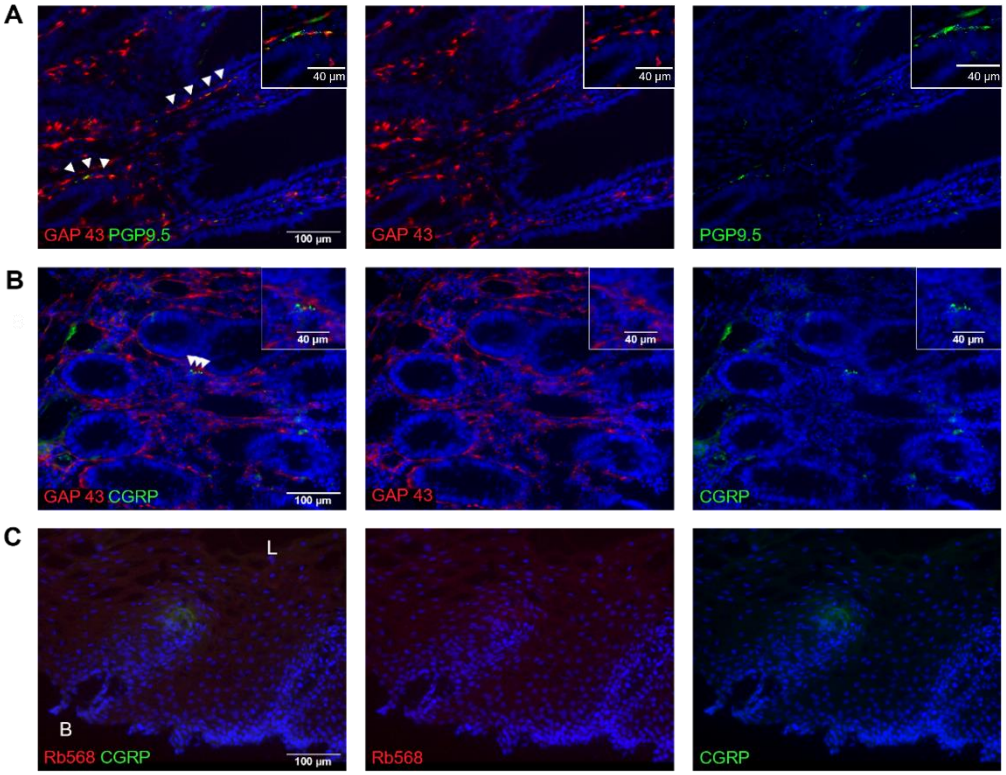

Figure 73 GAP43 is Expressed on Afferent Mucosal Nerves Innervating the Inflamed Colonic Mucosa

GAP43 antibody optimisation on positive control tissue, IBD colon. A) PGP9.5 was used to highlight total nerve fibres GAP43 is expressed by PGP9.5+ nerves innervating the lamina propria. B) CGRP was used as marker for sensory nerve fibres. GAP43 is co-expressed by CGRP+ afferent nerves innervating the lamina propria. C) Negative controls showing no immunoreactivity for GAP43 in the GORD oesophagus. Scale bar: 100µm; insert scale bar: 40µm.

4.3.8.2 GAP43 Expression in the Oesophageal Mucosa of GORD Patients

GORD samples phenotyped into ERD (N= 23), NERD (N= 11), FH (N= 18), and BO (N= 19), and healthy controls (N=10) were evaluated for GAP43 expression on oesophageal mucosal afferent nerves. This included a total of 80 µm per sample (2 slides per patient, with each slide containing 4 serial sections at 10 µm each). In this part of the study, PGP9.5 was the neuronal marker of choice, as GAP43 co-expression was detected on both CGRP and PGP9.5+ nerves in the inflamed colonic mucosa (Figure 73). Moreover, as a pan-neuronal marker, PGP9.5 maximised the chance of finding nerve endings in mucosal oesophageal biopsies as opposed to the use of CGRP, which only stains a subset of sensory nerves.

PGP9.5-immunoreactive nerves were found to innervate the deeper layers of the oesophageal mucosa, were mostly intrapapillary in healthy controls and all GORD groups, and frequently co-expressed GAP-43 (Figure 74). However, superficial PGP9.5+ nerves were also detected in 4/11 NERD patients but did not co-express GAP-43 (Figure 74C). Quantitative analysis to assess the degree of GAP43 co-expression on afferent nerves among the GORD patients and healthy controls found no statistical significance (p=0.0508). However, there was increased co-expression of GAP43 on PGP9.5+ nerve endings in patients with ERD compared to the other GORD groups and healthy controls (Figure 74F).

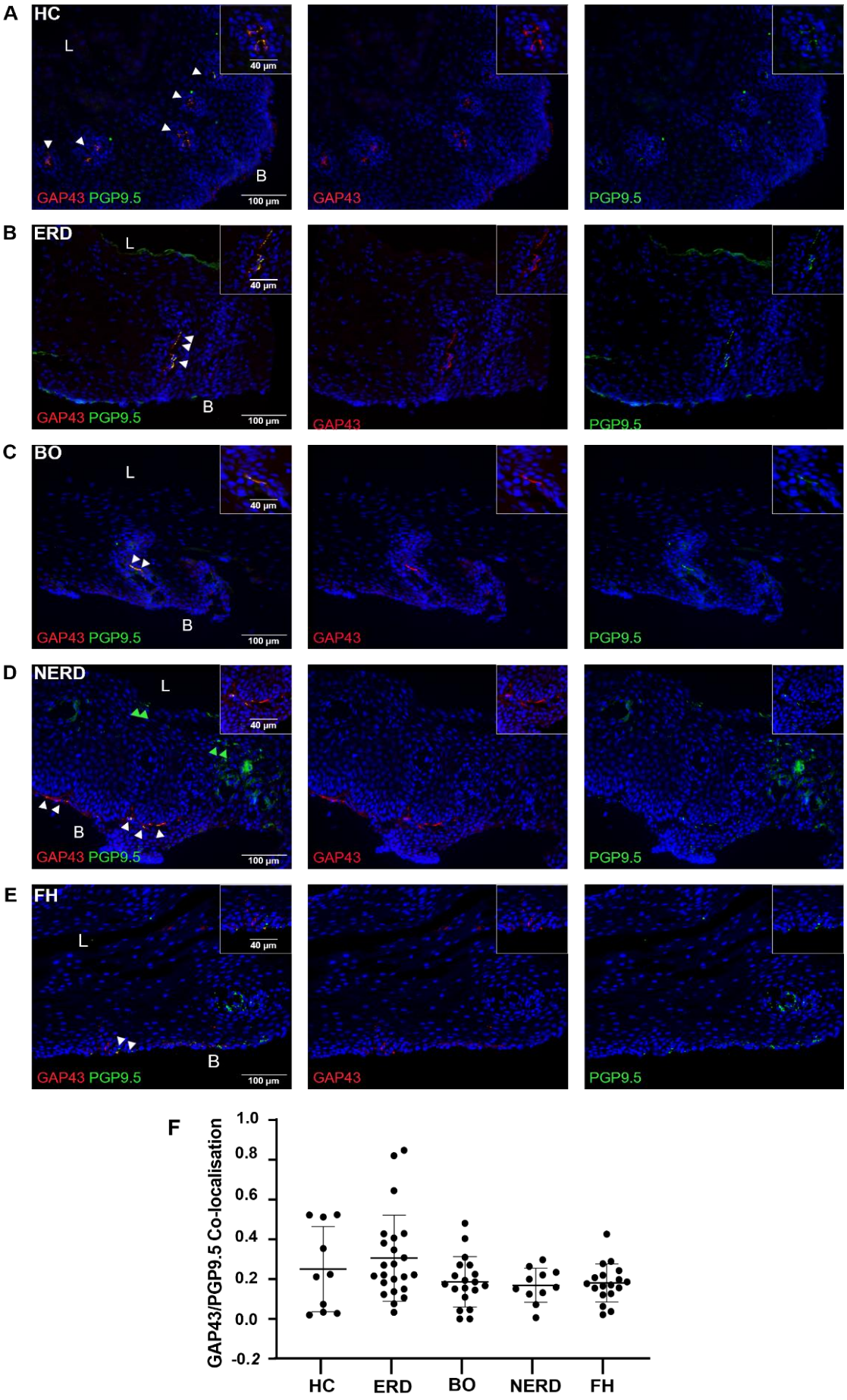

Figure 74 GAP43 is frequently co-expressed by deep afferent nerves innervating the oesophageal mucosa

(*Caption continued on next page…)*

A) Intrapapillary afferent nerves (white arrows) identified with PGP9.5 co-express GAP43 in a representative healthy control. B) PGP9.5+ nerve innervating the hyperplastic papillae (white arrow) expresses GAP43 in a patient with ERD. C) Intrapapillary afferent nerve (white arrows) inside hyperplastic papillae protruding into the epithelium in a patient with BO co-expressing GAP43. D) PGP9.5+ superficial nerves are observed in a NERD patient (green arrows); PGP9.5+ afferent deep intrapapillary nerves in NERD co-express GAP43 (white arrows). E) PGP9.5+ deep intrapapillary nerves in FH co-express GAP43. Scale bar: 100μm; insert scale bar: 40μm. F) Quantification of GAP43/PGP9.5 colocalisation using Manders coefficient (M1) on FIJI found no significant difference between controls and GORD patients.

4.3.8.3 GAP43 Gene Expression in the Oesophageal Mucosa of GORD Patients

The relative level of *GAP43* gene expression in the oesophageal mucosa of patients with GORD was assessed via qPCR studies. There was no significant difference in the level of *GAP43* gene expression among GORD phenotypes, nor between GORD patients and healthy oesophageal mucosa (p=0.2093) (Figure 75). However, there was slight increase in *GAP43* expression in ERD and BO oesophageal mucosa compared to controls, FH, and NERD patients, as seen in Figure 75.

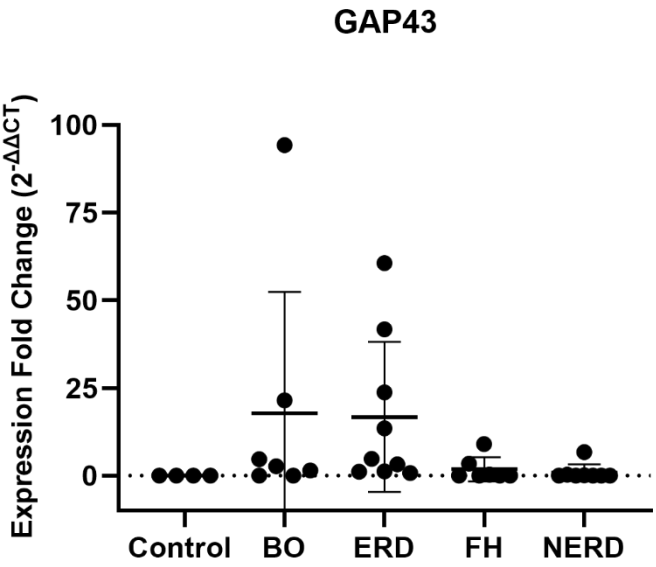

Figure 75 Expression Fold Change of *GAP43* in GORD Oesophageal Mucosa

The normalised expression fold change of *GAP43* in relation to the reference gene 18S, normalised against healthy control samples. Error bars represents SD. Results were statistically insignificant. NERD: N= 8, BO: N= 7, ERD: N=9, FH: N= 7, Control N=4.

4.3.8.4 Optimisation of NGF Antibody

NGF, a neuropeptide known to be secreted by mast cells during inflammation, has been highlighted not only as a key regulator of neuronal activity of peripheral neurons, but also as a direct driver of innate and adaptive immune responses [535]. Thus, NGF could be a mediator in the cross-talk between neuronal outgrowth and immune cell activity in the oesophageal mucosa. Based on literature suggesting that mast cells are proficient synthesisers of NGF [509], and to assess whether mast cell infiltration into the oesophageal mucosa of patients with GORD causes neuroplastic changes through NGF release, we performed NGF and tryptase double-labelling IF-IHC experiments in oesophageal mucosa of patients with GORD and healthy controls. Inflamed colonic tissue was used as a positive control, as increased colonic infiltration of mast cells in patients with IBS was found to induce NGF release [268]. Although the mentioned study by Dothel *et al*. detected NGF expression in different structures within the lamina propria, the majority of NGF expression was detected on tryptase-immunoreactive mast cells through double-labelling IF-IHC.

Similarly, positive control staining found NGF co-expression on a subset of mast cells surrounding colonic crypts identified with mast cell tryptase, as seen in Figure 76A. Negative control slides were also prepared as previously described and showed no labelling around the colonic crypts (Figure 76B).

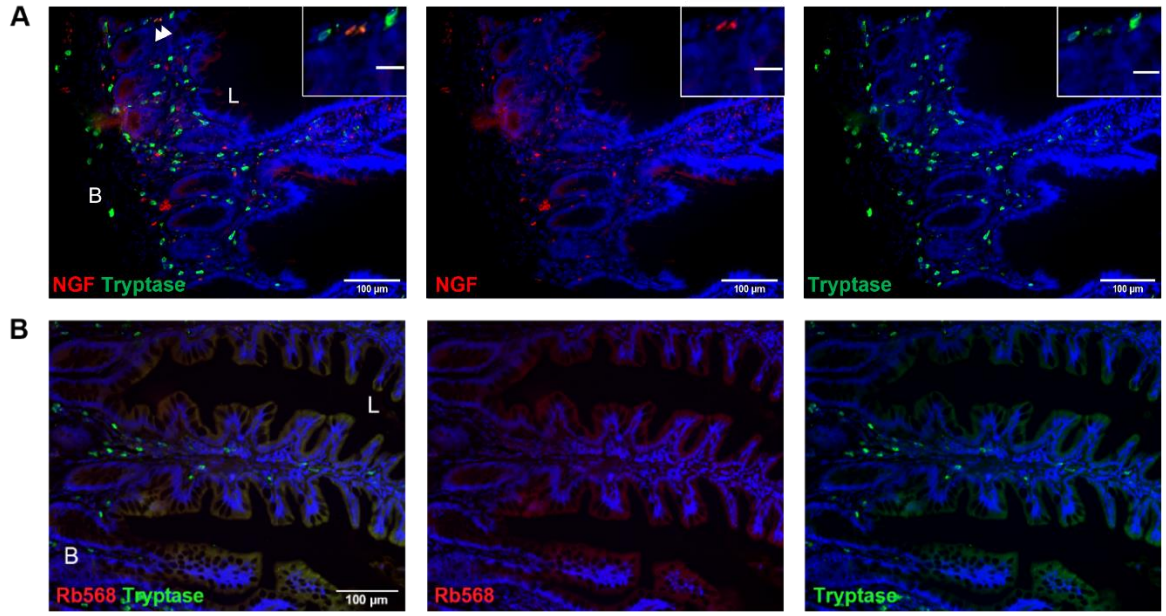

Figure 76 NGF is Expressed on a Subset of Mast Cells Surrounding Colonic Crypts in the IBD Colon

NGF antibody optimisation on IBD control tissue. A) NGF is co-expressed on a subset of mast cells identified with mast cell tryptase. B) Negative control slide shows mast cells in the colonic crypt, but no labelling for NGF in any of the mast cells identified. Scale bar: 100µm, insert scale bar: 40µm.

4.3.8.5 NGF Expression in the Oesophageal Mucosa of GORD Patients

GORD samples phenotyped into ERD (N=23), BO (N=19), NERD (N=11), and FH (N=18), and healthy controls (N=9) were assessed for NGF expression on mast cells infiltrating the oesophageal mucosa using IF-IHC. A total of 80 µm per sample (2 slides per patient, with each slide containing 4 serial sections at 10 µm each) was assessed. Tryptase+ mast cells detected in the oesophageal mucosa were found to frequently co-express NGF in all GORD groups (Figure 77B, C, D, E). $NGF^{+}Tryptase^{+}$ mast cells were intrapapillary, as seen in Figure 77B, C, D, and E. There was also some detection of NGF released into the epithelium which did not co-localise with mast cell tryptase, as seen in the healthy control and FH sample in Figure 77A and E.

Quantitative analysis (as described in 2.2.4.1 Manders coefficient) highlighted NGF co-expression on mast cells in GORD patients to be significantly higher than in healthy controls (Figure 77F) (p=0.0087). Further analysis with Bonferroni's test detected significantly higher NGF/tryptase colocalisation in patients with BO (p=0.0094) and patients with FH (p=0.0458) compared with healthy controls (Figure 77F). However, all GORD groups were heterogeneous, with the BO and ERD patients both exhibiting two clusters: half of the ERD patients had higher NGF/tryptase colocalisation whilst the other half had relatively low NGF co-expression (Figure 77F).

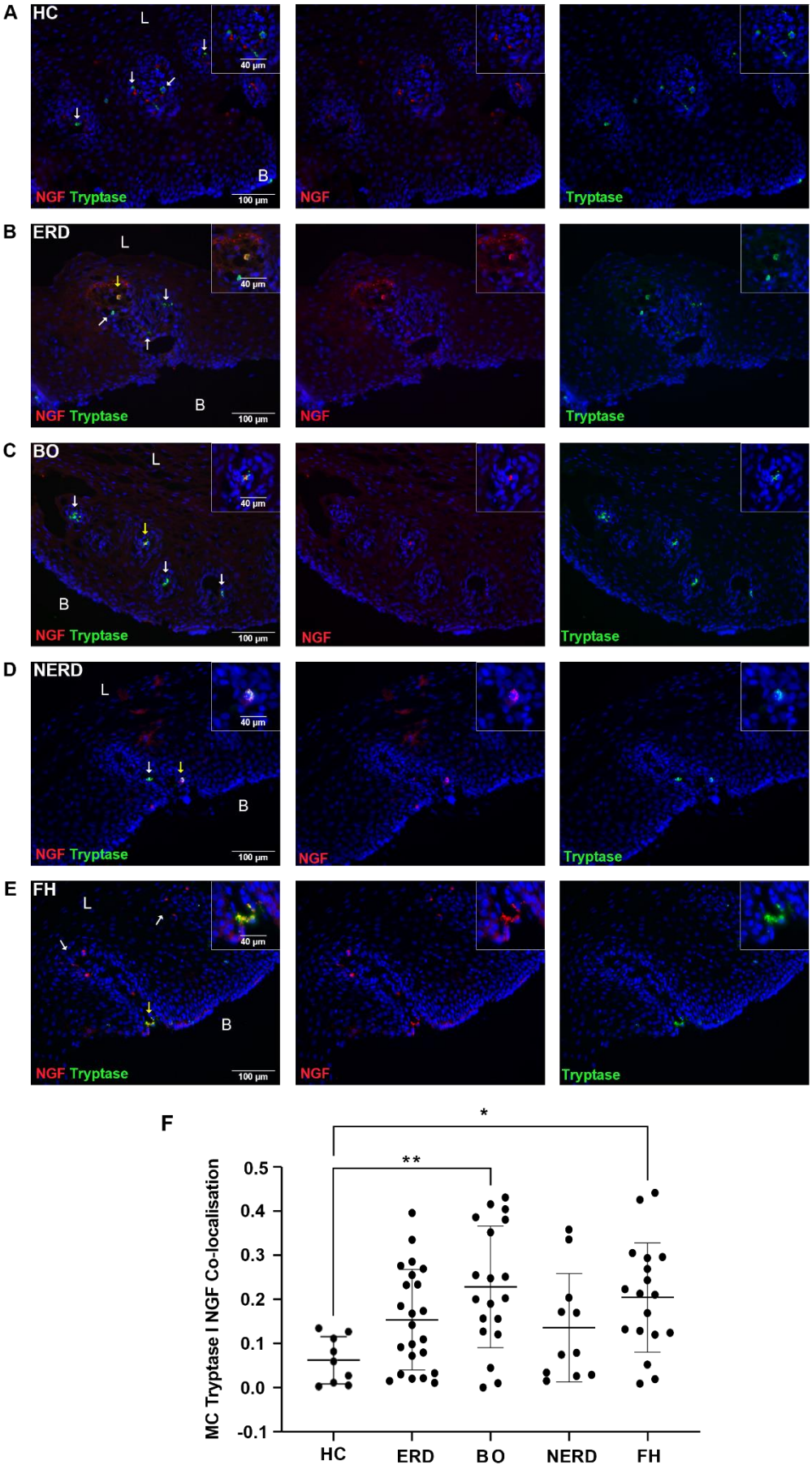

Figure 77 NGF Co-expression on Mast Cells Infiltrating the Oesophageal Mucosa is Significantly Higher in GORD than in Healthy Controls

(*Caption continued on next page…*)

A) Oval-shaped mast cells identified with mast cell tryptase (shown by white arrows) adjacent to the papillae do not express NGF. Released NGF/ NGF expressed by other immunocyte near mast cells. B) Intrapapillary mast cell co-express NGF (yellow arrow) in patient with ERD. C) Intrapapillary mast cells co-express NGF (yellow arrow) and mast cell without NGF expression in nearby papillae (white arrow) in a representative BO patient. D) Deep intrapapillary mast cell co-expressing NGF (yellow arrow) while another mast cell in close proximity (white arrow) did not express NGF in a patient with NERD. E) NGF and tryptase colocalisation in a degranulating intrapapillary mast cell (yellow arrow) and released NGF detected in the same papillae in a patient with FH. Scale bar represents 100μm, insert scale bar represents 40μm. F) Quantification of colocalisation between mast cell tryptase and NGF using Manders Coefficient (M1) detected significantly higher NGF co-expression in BO (p=0.0094) and FH (p=0.0458) compared to HCs. Error bars represent SD.

4.3.8.6 Spatial Relationship Between Mast Cells and Afferent Nerves in the Oesophageal Mucosa of GORD Patients

To assess whether tissue infiltration of mast cells induces neuroplastic and inflammatory changes in the oesophageal mucosa of patients with GORD, as reported in the colonic mucosa of patients with IBS, IF data was further evaluated to qualitatively assess the spatial relationship between mast cells residing in the oesophageal mucosa and afferent nerve endings. This revealed the innervation of a deep PGP9.5-immunoreactive afferent nerve in the same oesophageal mucosal papillary structures of ERD patients where mast cell infiltration was observed, as seen in Figure 78. While a representative number of GORD patients were assessed, deep afferent nerve endings were only identified in 2/10 ERD patients. PGP9.5-immunoreactive nerve endings were not identified in the other GORD phenotypes in this panel of staining, as previously explained (4.3.2.2 CXCR2 Expression in the Oesophageal Mucosa of Patients with GORD).

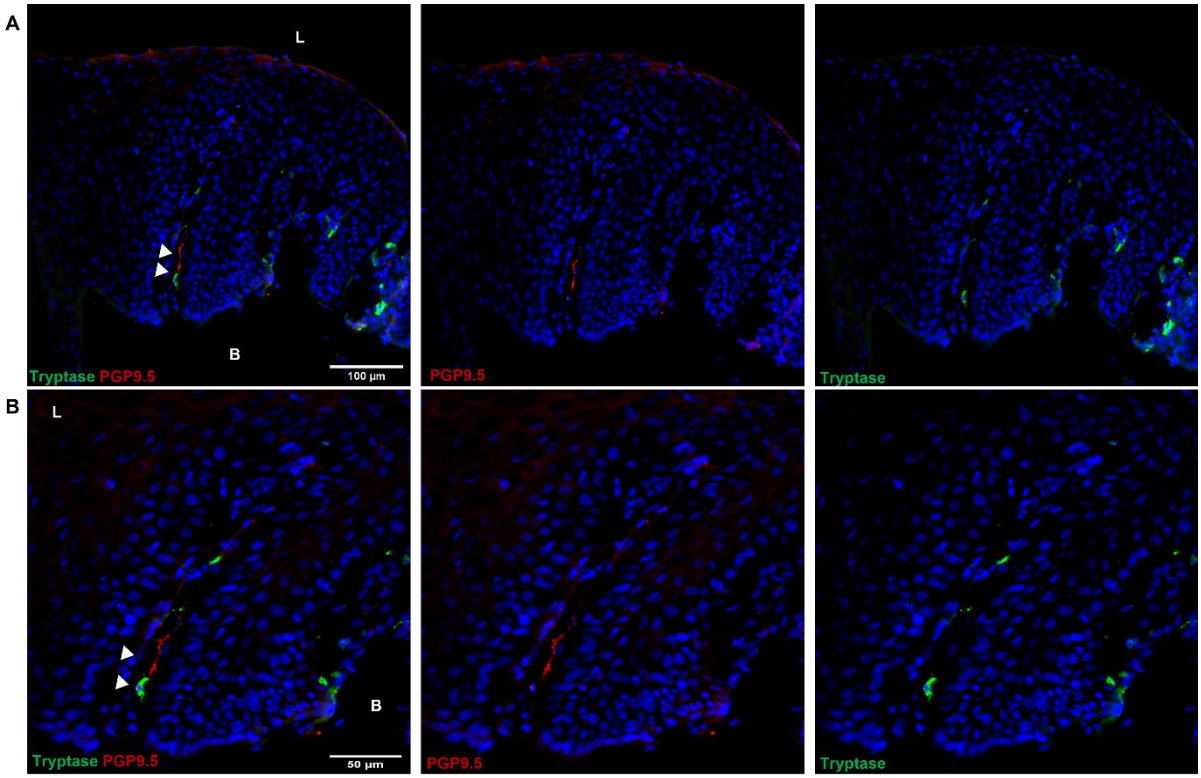

Figure 78 Deep Afferent Nerves and Mast Cells Innervate and Reside in the Same Papillae in ERD Patients

A) A representative ERD sample with deep afferent nerve marked by PGP9.5 in the same mucosal papillae as a mast cell. Scale bar: 100µm B) The same papillae at higher magnification with an afferent nerve ending and mast cell in close proximity. Scale bar: 50µm.

4.3.8.7 NGF Gene Expression in the Oesophageal Mucosa of GORD Patients

The relative level of *NGF* gene expression in the oesophageal mucosa of patients with GORD was assessed via qPCR studies. *NGF* gene expression was significantly higher in GORD oesophageal mucosa compared to healthy oesophageal mucosa (p=0.03) (Figure 79). ERD and NERD patients had the highest level of *NGF* gene expression among the GORD phenotypes, although the difference between ERD/NERD samples and healthy controls did not reach statistical significance (p= 0.09, and p= 0.66, respectively) as seen in Figure 79. BO patients also showed slightly increased *NGF* expression compared to healthy controls (p= >0.99). In contrast, FH patients expressed *NGF* at levels similar to that seen in healthy controls (p= >0.99) (Figure 79). There was no correlation between *NGF* expression and reflux disease symptom severity (Appendix 15).

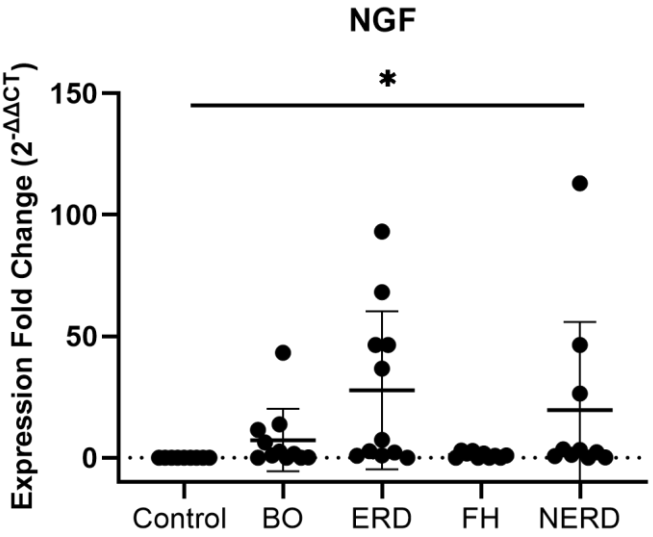

Figure 79 Expression Fold Change of NGF in GORD Oesophageal Mucosa

The normalised expression fold change of *NGF* in relation to the reference gene 18S, normalised against healthy control samples. Error bars represents SD. One-way ANOVA detected significant difference among control and GORD samples (p=0.03). NERD: N= 10, BO: N= 11, ERD: N=11, FH: N= 10, Control N=9.

4.3.9 Functional Cytokine Release from Ex Vivo Assay of Oesophageal Mucosal Biopsies Upon Acid Challenge

To assess the response of the healthy and inflamed oesophageal mucosa to acid challenge at different concentrations, an *ex vivo* biopsy culture model was used as described in section 4.2.5, and six inflammatory cytokines released measured using a Bio-plex multiplex system. This method has been previously validated to test the efficacy of drugs and responses of individual patient samples with a robust read-out that is truly representative of the response in human tissue, unlike *in vivo* animal models, or *in vitro* cell culture models where an inflammatory response must be artificially induced [536]. Healthy control mucosal biopsies (N=3) and ERD patient mucosal biopsies (N=3) collected at endoscopy were orientated using stereomicroscopy and sequentially challenged to pH7, pH5, and pH2 acid buffer on their luminal aspect on a Transwell insert. Levels of cytokines IL8, NGF, IL-1β, IL6, TNFα, and MCP-1 in the cell culture medium used to incubate mucosal biopsies were consistently detectable within the range of the assay standard curve (Appendix 16).

Although there were no significant differences in cytokine release between normal and inflamed oesophageal mucosa when analysed with two-way ANOVA, there were some patterns in this preliminary dataset. IL6 and NGF were released at higher levels in the ERD mucosa at baseline, pH5, and pH2 (Figure 80). Also, MCP-1 release from the oesophageal mucosa was significantly highest in ERD when challenged with pH5 buffer (Figure 80). However, IL8 was released at the highest level in ERD in terms of concentration of cytokine in pg/ml compared to the other cytokines, despite the normal and inflamed mucosa both responding to acid challenge at similar levels (Figure 80). IL8 levels in culture media from both normal and ERD oesophageal mucosal biopsies were significantly higher at pH5 challenge than the other cytokines assessed (Figure 80). IL-1β was released at relatively low levels compared to the levels of other cytokines and was undetected in several samples (Figure 80). TNFα release did not appear to change with changing acid concentration from normal nor ERD oesophageal mucosa (Figure 80).

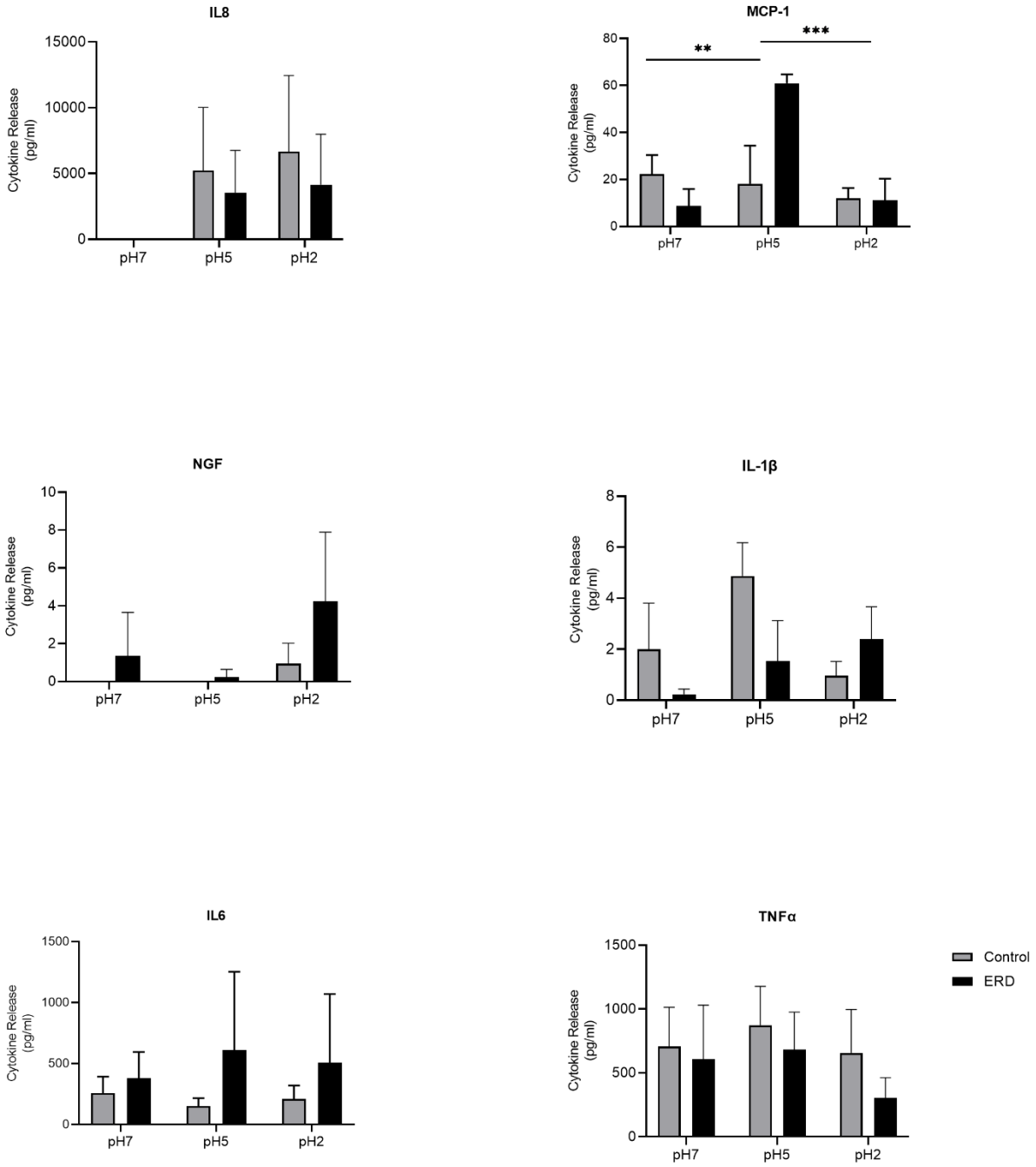

Figure 80 Inflammatory Cytokine Release from the Oesophageal Mucosa After *Ex Vivo* Acid Challenge

Cytokine release into tissue culture media from 3 biopsies from the same patients, sequentially challenged with pH7, pH5, and pH2 buffer *ex vivo*. No significant differences in IL8, NGF, IL-1β, IL6, or TNFα were observed (P>0.05, two-way ANOVA), but MCP-1 release was significantly highest when challenged with Ph5 (pH7 vs pH5: P=0.0017, pH5 vs pH2: P=0.0005), regardless of the phenotype of the oesophageal sample. 3 biopsies taken from each Control: N=3, ERD: N=3. Cytokine levels (pg/ml) are expressed as mean ± SD.

4.4 Discussion

This section of the study provides anatomical and preliminary quantitative data on candidate sensory and inflammatory markers potentially underlying heartburn pathogenesis in patients with GORD. We demonstrate increased NGF content in mast cells infiltrating the oesophageal mucosa of GORD patients compared to healthy controls, and the close vicinity of these NGF^+ mast cells to deep afferent nerves in ERD. This highlights the reflux-sensing role of mucosal nerves in heartburn perception, and highlights neuro-immune markers as potential targets for topical pharmacological therapy in ERD. The finding of GAP-43 expression on afferent nerve endings throughout healthy controls and GORD patients highlights the physiological sprouting mechanism of nerves in the oesophageal epithelium. We also report a decreased $CD1a^+$ dendritic cell population in GORD oesophageal mucosa compared to healthy controls. In this study, differences in the levels of T or B lymphocyte infiltration across GORD phenotypes and healthy controls was not detected. We also characterise the localisation of inflammatory cytokine receptors: TNFR1, CXCR2, IL1R, IL6R, and RAMP1 in the oesophageal mucosa of healthy controls and GORD patients. Findings from this study also confirmed literature describing increased IL8 release in patients with ERD when exposed to acid [390]. Finally, we report insignificant levels of IL6, TNFα, IL1β, MCP-1, and NGF release with *ex vivo* exposure of normal and inflamed oesophageal biopsies to acid.

There is increased co-expression of NGF in mast cells infiltrating the oesophageal mucosa of patients with GORD compared to healthy controls, which may be one of the key mechanisms behind heartburn sensation (Figure 77). Elevated mast cell numbers and NGF content characterise a number of inflammatory conditions including the derma of patients with early systemic sclerosis, the synovium of rats with rheumatoid synovitis, and the colonic mucosa in IBD patients [537]–[539]. The increase in NGF content in mast cells infiltrating the oesophageal mucosa of GORD patients could be a possible mechanism of nerve fibre sprouting leading to sensitivity. This has been previously suggested by studies in the human contact eczema skin which demonstrate a significant increase in NGF content as measured by enzyme-linked immunofluorescence assay, and a simultaneous increase in length of epidermal PGP9.5+ nerve fibres in lesional skin biopsies compared with normal skin as assessed by IHC [540]. Moreover, intestinal inflammation in a rat model infected with nematode was also immunocytochemically found to be accompanied by the remodelling of mucosal nerve fibres in conjunction with increased mast cell density [541]. A more recent study importantly highlighted increased nerve fibre density and sprouting, and increased expression of NGF on tryptase+ mast cells in mucosal colon tissues from IBS patients

compared to controls, highlighting a role for NGF in increasing nerve sprouting by signalling via NTRK1 receptors expressed on nerve fibres [268].

The observation of intrapapillary mast cells in very close apposition to deep afferent nerve endings in the papillae of patients with ERD suggests another critical mechanism for increased pain transmission in this group of patients who do not present with superficial afferent nerves (Figure 78). Literature on colonic mast cells in close vicinity to mucosal innervation has previously found to correlate with the intensity of abdominal pain [508]. This could be due to the histamine and protease released from mast cells which may induce activation of sensory fibres, as seen in sensory rat neurons *in vitro* when challenged with mast cell mediators released from the colonic mucosa of IBS patients [508]. The finding of mast cells in resting, granulated, and combination morphologies across all GORD groups enabled another way to postulate the activity status of the mast cells that were detected. The morphology of intrapapillary mast cells detected near mucosal afferent nerves in ERD patients being 'anaphylactic' suggests that they could be releasing NGF, histamine, or proteases which lower the activation threshold of the nerve endings and perpetuate oesophageal sensitivity. Transgenic animal skin overexpressing NGF has been shown to display hyperalgesic responses to noxious mechanical stimulation, and NGF widely reported to evoke neuronal excitability by inducing increased TRPV1 expression involved in transmission of pain stimuli [539], [542]. Thus, increased NGF expression on mast cells in patients with GORD (Figure 77), coupled with the infiltration of papillary mast cells in the same mucosal papillae as deep afferent nerve endings in patients with ERD (Figure 78) and the borderline significant increase in mast cell infiltration in patients with ERD compared to other GORD phenotypes (Figure ***53***) highlights NGF-releasing mast cells as a key modulator of neuronal plasticity and heartburn pathogenesis in patients with GORD. This is supported by findings from the *ex vivo* biopsy experiments in this section of the study, which detected increased NGF release from ERD oesophageal mucosal biopsies at baseline, pH5, and pH2 compared to healthy control oesophageal mucosa (Figure 80), further suggesting an important role of NGF in pain sensation in patients with ERD. Although these experiments were only done comparing healthy control oesophageal mucosa to ERD patients, the increase of NGF concentration in the biopsy culture media at pH2 compared to baseline and pH5 in patients with ERD suggests that there may be a correlation between mucosal exposure to acid and NGF release. Our finding of significant *NGF* expression fold increase in ERD and NERD patient samples compared to healthy controls with qPCR studies (Figure 79) further supports the *ex vivo* cytokine release data, implicating increased NGF expression and release by mast cells in the oesophageal mucosa as a sensory mechanism behind increased heartburn sensation in these patients.

Although the nerve sprouting mechanisms induced by NGF have been suggested to involve the upregulation of the neurotrophin GAP-43, in this study we did not detect significant differences in the gene expression of *GAP-43* by qPCR studies (Figure 75), nor GAP-43 protein expression levels among GORD groups or between GORD patients and healthy control oesophageal mucosa (Figure 74). There was a notable increase in GAP-43 co-expression by deep afferent PGP9.5+ nerve endings in papillary structures in ERD patients, suggesting that ERD patients might be sensing pain through a more extensive network of nerve endings which have increased likelihood of being activated by proinflammatory factors in the papillae (Figure 74F). However, GAP-43 co-expression on deep afferent nerves detected in the healthy control oesophageal mucosa was not significantly lower than the level of GAP43 co-expression in deep afferent nerves in ERD (Figure 74F). These results suggest that deep afferent nerve endings might be undergoing sprouting under physiological as well as reflux conditions, perhaps as a response to mucosal inflammation which has recently been shown to induce peripheral nerve lesions and thus trigger neuroregeneration and neuroplasticity to recover damaged neural networks [543]. Moreover, GAP43 expression was assessed on nerves identified with the pan-neuronal marker PGP9.5, which is not pain specific. Therefore, sprouting nerves may not necessarily be pain-sensing. Nevertheless, our data indicates GAP43-induced polymerisation of actin monomers as an unlikely mechanism for increased oesophageal sensitivity in patients with heartburn.

Heartburn symptoms in patients with FH may be partially explained by the expression of CXCR2 on deep sensory afferent nerves in the papillae (Figure 61). A note of caution is due here since CGRP-expressing sensory nerves could only be identified in 2/10 FH patients investigated, and as such the findings reported in relation to CXCR2 expression on nerve endings are merely descriptive. However, the detection of both membranous epithelial cell expression of CXCR2 closely surrounding papillae innervated by deep sensory nerves in FH, and the observation of CXCR2 co-expression on CGRP-immunoreactive nerves in these patients is an interesting avenue that warrants further investigation (Figure 61). The observation that deep sensory afferent nerves residing inside papillae in healthy control oesophageal mucosa did not express CXCR2 (Figure 62) suggests a potential mucosal difference between asymptomatic healthy individuals and patients with negative symptom association with physiological levels of reflux exposure. A recent study demonstrated increased CXCR2 expression on CGRP-immunoreactive DRG neurons upon peripheral injection of CFA, suggesting an important role for CXCR2 expressed on sensory nerves in the development and maintenance of pathological pain during inflammation [544]. However, CGRP-immunoreactive nerves could not be identified in the remaining GORD groups in this part of the study due to limited sample material. Therefore, while we demonstrate the lack of

CXCR2 expression on deep intrapapillary sensory afferent nerves in healthy controls, it remains unclear whether CXCR2 is expressed on deep sensory afferent nerves across all GORD phenotypes, or only in FH. These findings need to be confirmed on higher numbers of subjects. Interestingly, expression of CXCR2 on the cell membrane of epithelial cells was not significantly different among GORD patients, nor between healthy controls and GORD. This suggests that CXCR2 may only be expressed on the oesophageal epithelial cell membrane under physiological conditions, and perhaps only initiates signalling when bound by its high affinity ligand CXCL8 (or IL8). Being a GPCR, binding of IL8 to CXCR2 has been shown to induce a conformational change in the receptor that activates downstream G protein signalling which results in the activation of several inflammatory, proliferative, and metabolic genes (as discussed further in Section 1.7.5 CXCR2) [370]. Studies measuring IL8 mRNA expression in endoscopic biopsies from patients with ERD, NERD and asymptomatic subjects detected significantly increased IL8 gene expression in patients with Grade A-C ERD and NERD compared to asymptomatic subjects, where IL8 mRNA expression correlated with the endoscopic grade of oesophagitis [390]. These findings were also confirmed recently in a HEEC line model which showed upregulation of IL8 mRNA when exposed to acidic bile salts [422]. IL8 production has also been demonstrated to increase in an air-liquid interface model of HEECs upon apical trypsin stimulation, and later when challenged with unconjugated bile acids under weakly acidic conditions [545], [546]. These findings are in line with the preliminary data generated from the present study via the *ex vivo* biopsy culture exposed to weakly and highly acidic buffers. IL8 cytokine release when challenged with pH2 and pH5 acid buffer was significantly higher than all other inflammatory cytokines measured in the assay (Figure 80). Importantly, IL8 secretion was detected from both the normal and inflamed oesophageal mucosa when challenged with pH5 and pH2 acid (Figure 80). Our preliminary *ex vivo* experiments in biopsy cultures from healthy volunteers and ERD patients thus confirm the detection of increased IL8 with ELISA and qPCR in normal squamous epithelial cells from oesophageal cell culture models. Importantly, *IL8* gene expression studies in RNA extracted from healthy controls and GORD oesophageal mucosal biopsies detected a significant expression fold change in *IL8* mRNA levels in GORD patients compared to healthy controls, which is in keeping with the findings from earlier PCR studies (Figure 63) [390]. However, unlike patients with BO, ERD, and NERD, where there is a significant upregulation of *IL8* compared to control oesophageal mucosa, FH patients expressed *IL8* at levels similar to that of asymptomatic subjects, which suggests that CXCR2 expression in these patients is unlikely to induce hypersensitivity via IL8/CXCR2 signalling (Figure 63).

This section of the study has also expanded the anatomical characterisation of the oesophageal mucosa in patients with GORD and in healthy, asymptomatic subjects.

Importantly, unlike CXCR2, the other inflammatory cytokine receptors of interest showed a largely cytosolic pattern of expression in oesophageal epithelial cells. Of these receptors, TNFR1 was the most widely expressed across all GORD phenotypes, with 5-15% DAPI-stained cells showing cytosolic expression of TNFR1, compared to 5-6% DAPI-stained cells in healthy controls (Figure 58). Although there was a slightly increased TNFR1 presence in oesophageal epithelial cells in heartburn patients compared to healthy subjects, this difference did not reach statistical significance. However, there was considerably less variance in the level of TNFR1 expression in the healthy controls compared to the heterogeneity seen in the GORD group. This suggests that given a larger sample size, the differences observed between GORD and healthy oesophageal mucosa may have been more significant. The role of TNFR1 in propagating pain transmission has been recently demonstrated in a rat model of arthritis using electrophysiological recordings which highlighted that TNF neutralisation reduced the sensory response of TNFR1-immunoreactive Aδ and C fibres to mechanical stimuli [311]. However, in this study, TNFR1 expression was not detected on deep afferent CGRP-immunoreactive sensory nerves (Figure 57). Moreover, the cytosolic pattern of expression of TNFR1 makes it an unlikely candidate target mediating neuro-immune mechanisms underlying hypersensitivity, as TNFR1 is known to reside in the Golgi apparatus in resting cells where it acts as a reservoir, and only get mobilised to the cell surface to become activated [307]. Thus, in the oesophageal mucosa of patients with heartburn, TNFR1 was only detected in its inactive form, as seen in the healthy oesophageal epithelium.

Similarly, IL1R, IL6ST, and RAMP1 also showed a cytosolic expression pattern throughout the oesophageal epithelium of patients with GORD. However, the level of detection of these inflammatory cytokine receptors was considerably lower when compared with TNFR1 expression, with RAMP1 expression in GORD patients ranging from 0-4% DAPI-stained cells expressing RAMP1, and 0-1% DAPI-stained cells expressing RAMP1 in healthy oesophageal mucosa, and these differences did not reach statistical significance (Figure 69). Interestingly, RAMP1 was occasionally also detected on CD45-immunoreactive lymphocytes in the papillae of patients with ERD, suggesting that CGRP released from sensory afferent nerves can bind and activate signalling in both oesophageal epithelial cells, and immune cells infiltrating from the submucosa (Figure 69B). Given that deep afferent sensory nerves in ERD, BO and FH are often found in the papillae, this could highlight an important mechanism of communication between immune cells and nerve endings residing in papillary structures. However, the focus of this project is on mucosal sensory mechanisms, and it can be argued that the papillae is technically a submucosal structure which protrudes into the epithelium, separated by a layer of basal cells. As such, epithelial cells are a more likely candidate for CGRP-induced pain transmission in the oesophageal mucosa. However, the cytosolic pattern of RAMP1

expression in oesophageal epithelial cells also suggests the receptor to be in its inactive form, demonstrating that epithelial cell transmission of pain is not achieved via RAMP1. This can also be argued for IL1R and IL6ST, which showed an even more limited cytosolic expression pattern in oesophageal epithelial cells in patients with GORD (Figure 65 and Figure 67). The unlikeliness of IL1R and IL6ST to play roles in oesophageal hypersensitivity is enhanced by RNA sequencing data which showed a relatively low expression of both IL6ST and IL1R variants (Figure 70). These findings are further corroborated by the cytokine release data from *ex vivo* biopsy cultures, where IL1β was released at very low concentrations of 2-6 pg/ml, and IL6 released at 200 pg/ml, compared to IL8 which was released at 5000 pg/ml respectively (Figure 80). Moreover, although there was a slight increase in IL1β release from oesophageal mucosal biopsies challenged with pH5 compared to baseline, and pH2 compared to pH5 and baseline readings, these changes were negligible, and far from significant (Figure 80). Similarly, there was also a slight increase in IL6 release from the oesophageal mucosa when luminally challenged with pH5 and pH2 acid, but these differences were not significant. A recent study which assessed differences in inflammatory cytokine expression profiles between GORD phenotypes by qPCR demonstrated increased expression of *IL-1β* and *IL-6* in ERD and NERD compared to healthy controls, which does not align with our data [523]. However, our assessment of IL-1β and IL-6 levels was via a multiplex immunoassay, while the said study assessed gene expression levels with qPCR. Hence, the gene expression levels and cytokines released upon acid challenge into culture may account for these different findings in expression levels between patients with ERD and healthy controls. Collectively, the preliminary multiplex immunoassay and IF-IHC data from the present study suggest IL6/IL6ST and IL1β/IL1R to be unlikely candidates for heartburn pathogenesis in the oesophageal mucosa of GORD patients.

In contrast, IF-IHC assessment of CD3+ T cell infiltration in the oesophageal mucosa of patients with GORD did not appear to be significantly different from healthy controls (Figure 71). There was a slightly increased T cell abundance in patients with ERD, NERD, and FH compared to healthy controls and BO patients, but this difference was not significant. A recent study which characterised the immune cell subsets which composed the lymphocytic inflammation in GORD patients described a CD8+ T cell-predominant immunophenotype [547]. Whilst our study used the pan-T cell marker CD3 to identify T cells, using a more specific marker to differentiate T helper cells from cytotoxic T cells may have resulted in a more significant difference in T cell numbers in GORD patients compared to asymptomatic subjects. As CD3 covers regulatory T cells, as well as cytotoxic T cells, the CD3+ T cells identified in healthy controls could be part of the oral tolerance mechanism induced together with dendritic cells. However, the characterisation of T cell infiltration in the present study is also in contrast

to the data demonstrating increased CD3+ T cells in a recent study which investigated histologic events of oesophagitis in a rat model of ERD, where the inflammation measured 1 week-post oesophagoduodenostomy comprised of CD3+ lymphocytes [418]. The same findings were also observed in biopsies from ERD patients who stopped PPIs for 2 weeks, where at 1 and 2 weeks off PPIs, there was a significant increase in CD3+ T cell infiltration in the oesophageal mucosa compared to baseline [278]. However, there are major differences between the experimental design in this study and ours. First, while we compared levels of CD3+ T cells between healthy control biopsies and GORD patients who stopped PPIs for 7 days before endoscopy at a single time point, the mentioned study investigated differences in T cell infiltration in the same 12 patients at baseline (while they were taking PPIs as part of their routine treatment), 1 week off PPI, and 2 weeks off PPI. Second, the mentioned study used a different Dako CD3 antibody optimised for use in paraffin embedded tissue sections, while our Dako CD3 antibody was optimised for use on frozen tissue. Third, whilst we investigated CD3 expression on fixed frozen biopsies using IF-IHC, the mentioned study used IHC on formalin-fixed, paraffin-embedded tissue. This may have resulted in small differences in the numbers of T cells detected, as demonstrated by a comparative study which found optimum staining at highest primary antibody dilutions in frozen tissue, but better tissue morphology in paraffin sections [549]. Given the time limit on the project, it was not possible to collect follow-up biopsies from patients at different time points, and investigating the effect of PPIs on changes in T cell infiltration was not the primary objective of the present study. It might be interesting to assess differences in presence of more specific T cell markers, such as CD4 and CD8 to distinguish between levels of regulatory T cells and cytotoxic T cells infiltrating the oesophageal mucosa across GORD phenotypes and healthy controls for a more accurate characterisation of the immune landscape in GORD.

Similarly, although the population of CD20+ B cells were slightly increased in ERD patients compared to other GORD phenotypes and healthy controls, this difference did not reach statistical significance (Figure 72). Moreover, the abundance of B cells (and T cells) were lower compared to the other immune cells assessed, with B and T cells being detected at levels of 0.2-3% DAPI-stained cells, while dendritic cells were detected in 1-8% DAPI-stained cells, and mast cells were detected in 1-20% DAPI-stained cells, suggesting that B and T lymphocytes might play a less critical role in heartburn pathogenesis in the GORD oesophageal mucosa. However, B lymphocytes were most frequently detected surrounding the papillae, as with T lymphocytes, dendritic cells, and mast cells, suggesting that signals in the oesophageal mucosa recruit these immune cells ‘bottom-up’, i.e. from the submucosa [550]. Moreover, in the intestine, immune protection of the intestinal mucosa has been shown to depend on IgA secretion by plasma cells residing in subepithelial connective tissue which

gets transported into the gut lumen to provide continuous protection of the mucosal barrier [495], [551]. Thus, B cells may reside in subepithelial layers in the oesophageal mucosa, and B cells that have differentiated into plasma cells may be actively secreting IgA to provide protection for the oesophageal mucosal barrier which is highly compromised in patients with ERD.

In summary, the findings presented in this section of the study highlight several important mucosal differences between asymptomatic individuals and GORD patients- namely patients with a macroscopically normal oesophagus- which may underlie oesophageal sensitivity. First, increased expression of NGF on tryptase+ mast cells in the oesophageal mucosa of GORD patients compared to healthy controls is likely to be of pathophysiological relevance to heartburn sensation. Second, our findings of reduced dendritic cells in the GORD patient population, and particularly in FH patients whose symptom generation is not associated with acid reflux, highlights a potential peripheral mechanism for food-induced heartburn symptoms in patients with GORD. Third, heartburn symptoms in FH may be partially explained by the expression of CXCR2 on deep sensory afferent nerves. These findings highlight the enticing possibility of novel therapeutic targets for anti-inflammatory treatment of heartburn.

4.4.1 Limitations of Methodology

There are limitations within our experimental methods which may have affected our results. Differences in antibodies used in IF-IHC can produce different results from existing literature which looked at some of the same markers that we assessed using a different antibody, and tissue fixed in a different way as seen with CD3 T lymphocytes. However, given the nature of our starting materials, IF-IHC was the best way to assess protein expression and localisation for the inflammatory cytokine receptors which have previously never been assessed in the oesophageal mucosa of patients with GORD or in healthy individuals. By ensuring that all antibodies selected for use in the study underwent vigorous optimisation, we ensured specific staining in our samples. With the lack of appropriate animal model to enable the oesophagus to be studied in a way that is comparable to the human conditions, assessing protein expression in patient endoscopic biopsies was best done using IF-IHC. Moreover, the assessment of spatial relationship between afferent nerve endings innervating oesophageal mucosa of GORD patients and immune cells was only qualitative in nature and cannot ascertain whether immune cells and nerve endings are actually in communication. To this end, functional studies that assess the response of *ex vivo* nerve preparations when challenged with inflammatory cytokines may help to elucidate this mechanism. Training in and utilisation

of quantitative software such as QuPath will also enable more conclusive results from the existing dataset, including in assessing the morphology and granularity of mast cells.

Biopsies represent only a small percentage of oesophageal surface area, and thus only give a snapshot for anatomical localisation studies. The method of biopsy taking is also imprecise, and a more defined protocol for future studies would improve the comparability between patient samples. However, as patients with GORD rarely undergo surgical procedures, it was not possible to obtain larger tissue from patients with heartburn symptoms. Moreover, although the *ex vivo* biopsy culture was a useful tool to maximise the information obtained from limited patient samples, due to increased time constraints posed by the global pandemic which started in the second year of this project and is ongoing, the number of fresh biopsies collected from ERD patients was very low. However, these preliminary results give an indication of the feasibility of using this model to test different challenging solutions on biopsies obtained from heartburn patients and suggest a neat functional method of obtaining useful quantitative data from the available starting materials, adding an important angle to the project.

4.4.2 Future Work

It will be useful to expand several aspects of the study to obtain more information on neuro-immune interactions in the oesophageal mucosa of patients with GORD. First, expanding CXCR2/CGRP staining on greater numbers of subjects would help us reach a clearer understanding on the role of CXCR2 in heartburn pathogenesis in FH compared to ERD, NERD, and BO patients. Secondly, assessing GAP43 expression on CGRP-immunoreactive nerves, and NTRK1/TrkA expression on CGRP/PGP-immunoreactive nerves will help to complete the sensory characterisation of the oesophageal mucosa and cement the mechanism of action of mast cell release of NGF in heartburn pathogenesis. Moreover, expanding the immune cell characterisation to assess the localisation of CD4+ and CD8+ T cells will help to answer the question of T cell infiltration in the oesophageal mucosa of patients with different phenotypes of GORD. Assessing the relative level of *TNF-α* gene expression in the oesophageal mucosa of patients with GORD via qPCR studies will be useful to elucidate the role of TNF-signalling in the pathogenesis of heartburn. Observing the effect of dendritic cell infiltration after PPI therapy and assessing tight junction proteins in relation to dendritic cells will constitute an interesting follow-up study.

Given more time in future, it would be very useful to expand the multiplex assays to assess whether the changes seen in inflammatory cytokine release might be more significant. Moreover, it will also help to perform the *ex vivo* experiments on oesophageal mucosal

biopsies from patients with NERD, BO, and FH to understand differences between mucosal cytokine response to different acid buffers. Furthermore, combining bile salt and acid, repeating exposure for a longer time, dose response to intermittent pH concentrations, conducting multiple treatments over 24h to mimic the multiple reflux mechanisms that GORD patients usually experience, and the effect of PPIs, will enable a more comprehensive understanding of the mucosal response to refluxate. It is also important to consider that the blood supply to biopsies is cut off. This induces the death of lymphocytes, so assessing for cell death markers at baseline will be an important follow-up experiment using cell viability assays to ensure that the cytokine release response we see in biopsies is not just a physiological response to cell death. Finally, utilising *in vitro* systems such as organotypic or organ-on-chip models to enable prolonged testing of different challenge conditions may be a fulfilling research avenue to explore in future.

5 General Discussion

5.1 Summary of Data

Sensory mucosal mechanisms in patients with GORD were investigated with anatomical neuronal characterisation studies. To clarify the pathogenic role of oesophageal epithelial cells making up the bulk of the mucosa and the role of residing immune cell populations in the response to noxious luminal stimulus, bulk RNA sequencing experiments were done on oesophageal biopsy samples from healthy controls and GORD patient groups. Data from these experiments led to further studies to validate immune cell profiles of individual disease groups and healthy controls, and co-localisation studies to elucidate the role of neuro-immune interactions in heartburn pathogenesis. These led to preliminary functional experiments to test the effect of acid exposure on inflammatory cytokine release in the oesophageal mucosa.

The contribution of central sensitisation to the development of oesophageal chest pain has been well established in prior studies by Aziz *et al*. which infused acid into the oesophagus, measured cortical responses to electrical stimulation, and found central enhancement of sensory transfer in patients with visceral hypersensitivity [552], [553]. Earlier studies have also addressed the question of whether peripheral sensitisation contributes to visceral hypersensitivity in GORD patients where 0.1M HCl was infused into the distal oesophagus, and GORD patients demonstrated increased sensitivity to infusion [554], [555]. In this study, we document novel mucosal features that can potentially underlie sensory mechanisms involved in increased pain perception in heartburn patients by showing neurochemical, genetic, and cellular changes to the oesophageal mucosa itself. These changes are similar to the peripheral mechanisms that have been extensively reported in the colon, where differential molecular fingerprints of colonic sensory neurons have been shown to be responsible for response to IBS treatment [436]. A more detailed account of these concepts will be given below.

5.2 NERD is a unique phenotype of visceral hypersensitivity

The first and most important findings were the molecular sensory pathways that can potentially underlie increased pain perception in patients with non-erosive reflux disease. The expression of acid-sensing ion channel TRPV1 on superficial $CGRP^{+}$ afferent mucosal nerves, and increased ASIC3 expression on oesophageal epithelial cells in NERD patients raises the potential for topical therapy. These findings confirmed the group's previous descriptions of superficial afferent nerves in NERD, but not in other GORD phenotypes. The novel finding of this investigation was the expression of TRPV1 on these superficially located sensory nerves in patients with NERD, while deep afferent nerves in patients with ERD, FH, and BO did not

express TRPV1 (Figure 81). The uniquely superficial nerves in NERD can explain why in patients without significant breach of the oesophageal mucosal barrier integrity, but with pathological acid exposure, sensory nerves can be activated by acidic luminal stimuli and thus experience similar symptom severity as patients with erosive disease. Moreover, we saw a near significant increase in NGF-expressing mast cell infiltration in the NERD oesophageal mucosa compared to healthy controls. The release of NGF into the oesophageal mucosa from mast cells could increase the excitability of these superficial sensory nerves via TRPV1. However, a greater numbers of NERD patient samples are required to establish this concept. A similar concept has also been demonstrated in IBS, where a dramatic increase in the numbers of CD3+ lymphocytes and ckit+ mast cells in the vicinity of TRPV1+ sensory fibres suggested an increased likelihood for these immune cells to release mediators to activate the TRPV1 channel [186], [556].

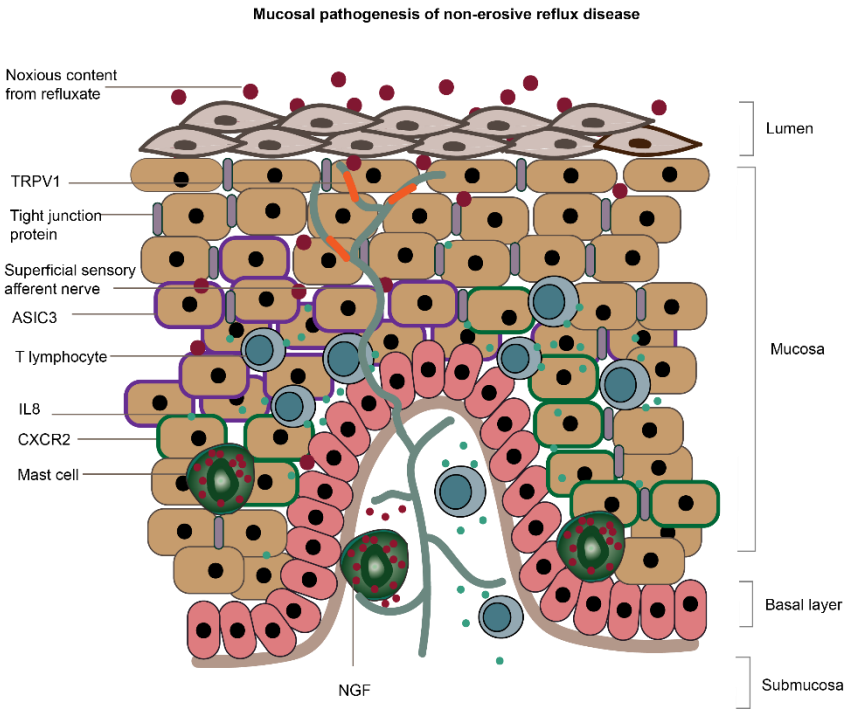

Figure 81 Illustration of NERD oesophageal mucosa

Mucosal factors contributing to the pathogenesis of NERD. The protective mucus barrier is lost, but epithelial lining remains intact. There are superficial sensory nerves expressing TRPV1 which are positioned close enough to the lumen to be activated by H+ from the refluxate. ASIC3 expression on epithelial cells is increased, and NGF+ mast cells are increased.

ASIC3 protein, unlike TRPV1, was not expressed on superficial nor deep afferent nerves, but was detected most frequently on oesophageal epithelial cells in patients with NERD and ERD (Figure 81 and Figure 82). This suggests that ASIC3 is unlikely to be directly involved in the

activation of sensory nerves in heartburn pathogenesis. Rather, the activation of ASIC3 on epithelial cells may involve the inflammatory pathways. The increased expression of ASIC3 on NERD and ERD patients, who have increased acid exposure, compared to FH patients, who do not have increased acid exposure, suggests that ASIC3 expression may be induced by acid exposure of squamous epithelium. Our finding of significantly reduced ASIC3 expression in BO patients who experience chronic acid exposure suggests an inherent difference in the squamous epithelium of these patients compared to NERD and ERD patients. This is supported by our transcriptomic data which revealed a higher number of differentially expressed genes associated with epithelial cell structure between NERD/ERD and BO than between NERD/ERD and healthy controls. Recently, a strong correlation was shown for increased release of proinflammatory cytokines by cultured PBMCs from IBS patients, indicating an activated immune system in these patients in the absence of overt colonic damage [557]. Our data collectively highlight important mucosal mechanisms that may underlie heartburn perception in NERD patients in the absence of pathologic oesophageal damage.

5.3 ERD has a distinct adaptive immune response

From the transcriptomic studies, it was clear that ERD has an adaptive immune response, unlike FH, NERD, and healthy controls. Cellular deconvolution analysis of the sequencing dataset highlighted an increased Th2 and CD8+ T cell population in ERD patients compared to the other GORD phenotypes and healthy controls, suggesting a T-cell mediated inflammatory response in these patients (Figure 82). This data confirms findings from recent studies in an *in vitro* ERD model which demonstrated increased T cell migration induced by acidic bile salts [275], [422]. Moreover, in patients with erosive oesophagitis, CD8 T lymphocytes were recently identified as the predominant immunophenotype in the lymphocytic infiltration associated with this inflammatory group [547]. As such, our results can be considered unsurprising. However, we offer a transcriptomic characterisation of ERD which has not previously been done. Differential expression analysis between healthy controls/FH and ERD patients also significantly highlighted cytokine-mediated signalling pathways, leukocyte migration, and immune response as some of the top biological processes associated with DE genes between these disease groups. In contrast, in BO patients, cellular deconvolution detected an increased memory B cell and plasma cell presence, suggesting a predominant humoral immune response in patients with this premalignant lesion (Figure 83). This could reflect an inherent difference in the squamous epithelium of patients with BO, or could be explained by the fact that BO patients were biopsied while being on PPI treatment (due to the ethical restrictions of stopping PPI in patients with known Barrett's)– the only 'on PPI' group included in the study. This transcriptomic data provided a useful signpost of

immune cell populations which were further validated using IF-IH. The functional studies assessing release of inflammatory cytokines from the oesophageal mucosa detected a significantly higher level of IL8 secretion when exposed to pH2 and pH5 acid buffer compared to the other cytokines assessed, suggesting that the response to acid challenge in ERD patients is through the recruitment of T cells and IL8 release is a relatively rapid response to luminal acidic content. These findings were further supported by the qPCR studies which showed an upregulation of IL8 in GORD, with the highest relative gene expression of IL8 in the ERD subgroup.

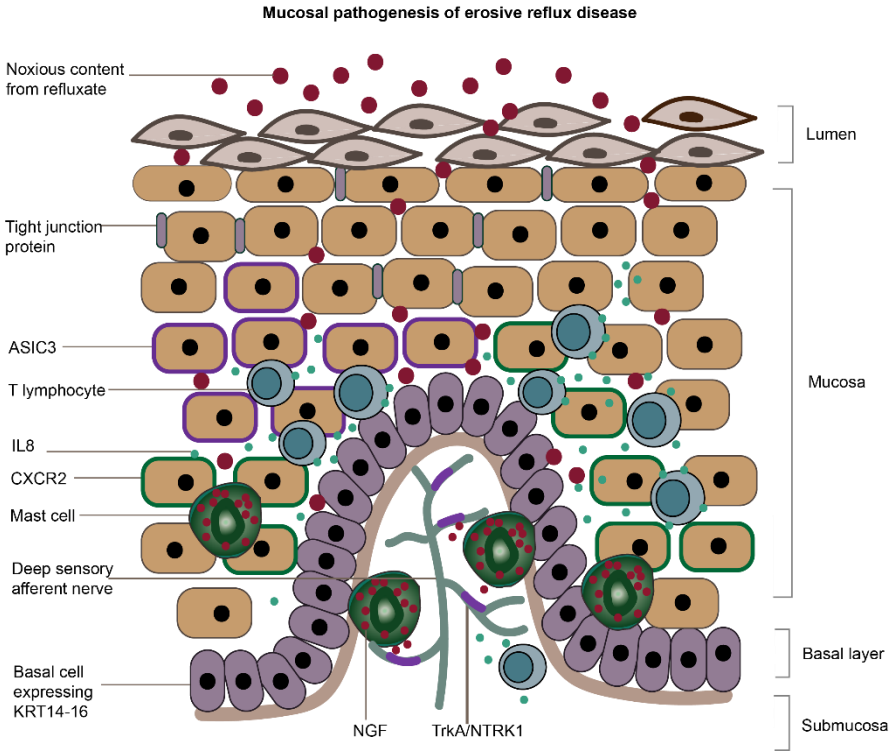

Figure 82 Illustration of the ERD oesophageal mucosa

Figure illustrating mucosal factors contributing to the pathogenesis of ERD. The protective mucus barrier is lost, and there are lesions in the oesophageal mucosa. There is increased ASIC3 expression on epithelial cells, and increased NGF+ mast cells infiltrating the oesophageal mucosa in close apposition to deep intrapapillary nerves (which likely express NGF receptors). The basal cell layer is characterised by KRT14-16 expression, and there is increased IL8 secretion from T lymphocytes infiltrating the oesophageal epithelium.

5.4 NGF-expressing mast cells in heartburn pathogenesis

This study identified increased NGF expression on mast cells infiltrating the oesophageal mucosa of patients with GORD, and detected a very close apposition between these mast cells and deep afferent nerves in patients with ERD. These data suggest that, unlike NERD, in patients where superficial sensory nerves are not detected, (ERD), increased pain perception may be achieved through release of neurotrophins such as NGF or inflammatory mediators such as histamine from mast cells, and their binding and activation of TrkA/NTRK1

or histamine receptor, respectively, thereby inducing activation of deep afferent nerves (Figure 82). Moreover, increased NGF expression on mast cells could also indirectly result in oesophageal hypersensitivity by inducing nerve growth and sprouting. This is similar to what has been found in the colon of IBS patients, where the close proximity of mast cells to mucosal innervation was positively associated with the frequency and severity of abdominal pain [558]. More recently, NGF staining was demonstrated to be significantly increased in the intestinal mucosa of IBS patients compared to controls, and most of this NGF staining was co-expressed on mucosal mast cells, much like our own findings [268]. Moreover, in a post-inflammatory animal model induced by DSS, direct effects of mast cell degranulation on the sensitivity of colonic sensory nerve endings were demonstrated [557]. Taken together, these results highlight an important neuro-immune mechanism that might underlie heartburn sensation in patients with GORD, particularly in patient groups where superficial afferent nerves have not been detected.

Our computational deconvolution analyses revealed a significantly increased mast cell and M2 macrophage abundance in patients with BO, ERD, and NERD compared to FH and normal oesophageal mucosa. An implication of this is the possibility that mast cells and M2 macrophages play a pathogenic role in the elicitation of heartburn symptoms in these patients, and may be recruited upon acid-induced mechanisms in the oesophageal mucosa. The functional experiments performed in this study further support this notion, as NGF release was increased in ERD patients when exposed to pH2 HCl (Figure 82). This strongly supports the hypothesis that NGF expression and release by mast cells in the oesophageal mucosa of patients with ERD is increased upon exposure to acid. This finding was supported by our qPCR experiments which also detected a significant upregulation of NGF in patients with ERD and NERD when compared to the normal oesophageal mucosa. Coupled with the anatomical data demonstrating the close apposition of NGF^{+} mast cells and deep afferent papillary nerve endings in patients with ERD, these data strongly highlight a novel neuro-immune mechanism for heartburn sensation in patients with NERD and ERD.

5.5 Molecular similarities between GORD phenotypes

Transcriptomic experiments identified important differences in the expression profile of keratin proteins between healthy controls and GORD, but also some structural similarities among GORD phenotypes. The loss of *KRT78* from the basal and parabasal layers in GORD patients compared to healthy controls suggests altered structural integrity of the barrier (Figure 84). This may enable luminal content to access deep sensory afferent nerves located in the papillae, a submucosal structure that is otherwise separated from the mucosa by an intact basement membrane, and thereby enable neuronal sensitisation. The downregulation of

MUC17 presents another key structural difference between the normal and GORD oesophageal mucosal lining, whereby the loss of mucous barrier in the epithelial lining may explain the increased permeability of the oesophageal mucosa in patients with GORD. Our findings of *KRT17, KRT14, KRT16*, and *KRT6A-C* upregulation in ERD patients compared to healthy controls suggests active epithelial regeneration in this group of patients. Functional enrichment analysis of these DE basal keratins in ERD and NERD highlighted increased epithelial cell differentiation, ECM assembly, and actin cytoskeleton organisation, suggesting their regulatory role in signalling pathways that control the differentiation of the oesophageal epithelium. Similarly, we detected upregulation of *KRT14* in NERD compared to healthy controls. This offers a molecular explanation for the basal cell hyperplasia and papillary elongation seen in NERD patients, and could explain the superficial localisation of $TRPV1^{+}$ sensory nerves in NERD patients.

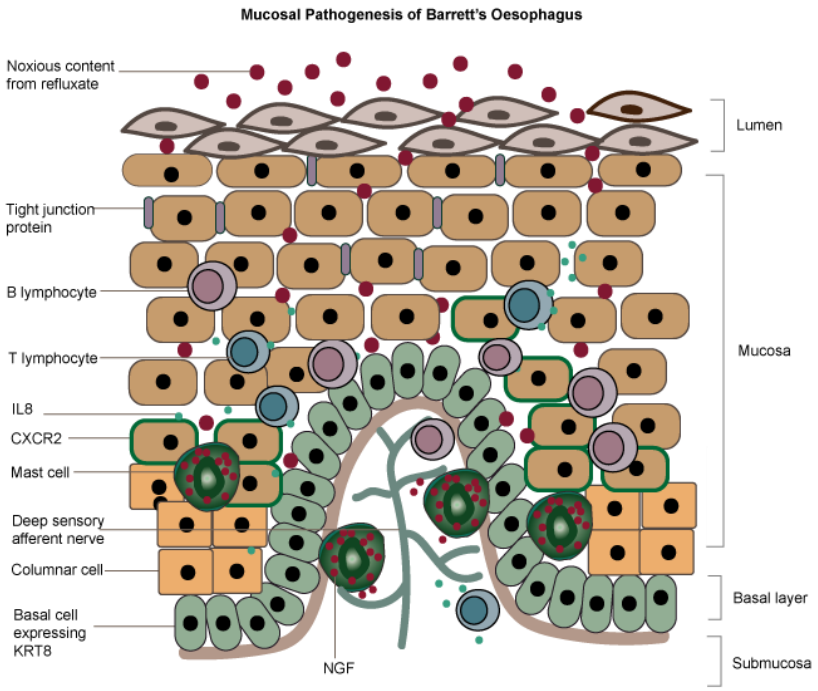

Figure 83 Illustration of the BO oesophageal mucosa

Mucosal factors contributing to the pathogenesis BO. The protective mucus barrier is lost, and there are erosions in the oesophageal epithelium. There is no ASIC3 expression, but some CXCR2 expression on squamous epithelial cells. Inflammation is characterised by infiltration of B and T lymphocytes, and increased NGF+ mast cell infiltration. There is differentiation of some epithelial cells into columnar cells of the stomach. Basal cell layer is characterised by KRT8 expression.

The finding of similar upregulation levels of basal keratin genes between NERD and ERD patients is also a clear demonstration of similar structural integrity of the barrier between these two groups which present very differently at endoscopy. This also suggests that the

differentiation between NERD and ERD is likely due to differences in the composition of luminal contents and exposure. Although there are no overt inflammatory defects in the NERD oesophageal mucosa, *in vivo* studies have previously demonstrated impaired mucosal integrity in these patients who were found to have lower baseline impedance and slower post-acid impedance recovery compared to FH patients [559]. Baseline oesophageal impedance can be seen to represent oesophageal mucosal integrity, and the findings of lower baseline impedance in NERD patients compared to healthy controls and FH patients suggests that increased acid perception could be associated with a more vulnerable mucosal structure. *In vitro* studies in patients with heartburn without oesophagitis also demonstrated a greater reduction of TER in heartburn patients than controls when exposed to acidic and weakly acidic buffer, further highlighting distinct vulnerability of the oesophageal mucosa in these patients [560]. Collectively, our gene expression data on basal keratin overexpression and mucin downregulation could be a possible molecular explanation for this breached structural integrity in patients with NERD (and ERD). Conversely, the finding of increased expression of *KRT8* only in BO compared to normal oesophageal mucosa highlights the distinct structural ability of oesophageal epithelial cells in premalignant BO to have augmented cell motility, as supported by animal studies which show increased migratory properties in cells overexpressing *KRT8* [561], [562] (Figure 83).

5.6 Dendritic cells are important sentinel cells within the normal oesophageal mucosa

IF-IHC experiments revealed a significantly higher CD1a+ dendritic cell infiltration in the oesophageal mucosa of asymptomatic subjects compared to patients with GORD (Figure 84). Dendritic cell abundance in the healthy oesophageal mucosa likely primes naïve T cells to release anti-inflammatory cytokines to suppress an adaptive immune response. The loss of dendritic cells in patients experiencing heartburn symptoms likely highlights a switch to the adaptive immune response, where other immune cell populations are recruited to protect the oesophageal mucosa against luminal antigens, and oral tolerance is no longer maintained. This data highlights an important homeostatic mucosal mechanism that is followed by inflammation in the oesophageal epithelium in GORD. The finding of increased adaptive immune response mechanisms such as complement activation and leukocyte migration in GORD groups compared to healthy controls with the biological interpretation analyses of our transcriptomic data further supports this notion. Moreover, cellular deconvolution of RNA sequencing data also partially confirmed the finding of decreased dendritic cell composition in BO, ERD, and NERD compared to healthy controls and FH. The small discrepancy between IF and sequencing findings for FH patients could be ascribed, at least in part, to the

heterogeneity of the FH population, or the distinctions that exist between subpopulations of dendritic cells according to cell surface receptor expression [563]. This is similar to what has been observed in the intestine, where intestinal dendritic cells are integral for preventing pathological immune responses to harmless antigens [563]. An animal study which assessed dendritic cells from the gut of germ-free mice demonstrated expression of maturation markers in dendritic cells as being similar to those in normal mice, suggesting that the phenotypic maturation of DCs is regulated in the steady state by the release of low levels of inflammatory antigens from normal tissues, even in the absence of commensal flora [564]. These results collectively suggest a sentinel role for these immune cells in the normal, and perhaps also FH oesophageal mucosa, against the activation of an adaptive immune response resulting in inflammation.

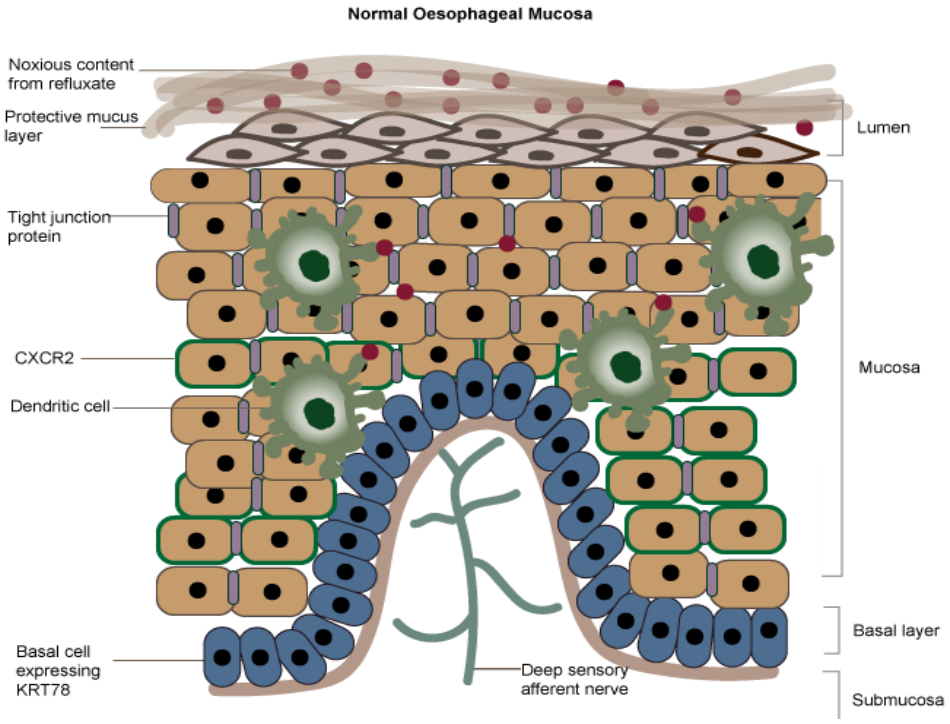

Figure 84 Illustration of the Normal Oesophageal Mucosa

Figure illustrating the normal oesophageal mucosa in asymptomatic individuals based on our findings in this study. A mucus layer protects the epithelial lining from noxious content of the refluxate. There are tight junction proteins that hold epithelial cells tightly together. Dendritic cells act as sentinels of the oesophageal mucosa from antigens ingested through food. There is CXCR2 expression on squamous epithelial cells under physiologic conditions. The basal layer is characterised by high KRT78 expression. Deep afferent nerves do not express inflammatory cytokine receptors.

Interestingly, the majority of literature on the regulatory role of CGRP on dendritic cell function suggests a predominant anti-inflammatory rather than pro-inflammatory role. CGRP expressing nociceptive C fibres were found to be closely associated with dendritic cells

residing in the epidermis of the skin, and CGRP was also reported to be expressed on the surface of some dendritic cells where functional assays reported CGRP to inhibit antigen presentation by dendritic cells [264]. Our finding of reduced CD1a+ dendritic cells in the oesophageal mucosa of GORD could be linked to the presence of CGRP+ sensory nerves in these patients. However, we did not detect a close apposition between dendritic cells and nerve endings, nor found any CGRP expression on dendritic cells, so this is an unlikely mechanism in the context of GORD.

5.7 Functional heartburn patients are microscopically different to healthy controls

FH patients have normal endoscopy, no pathological amount of reflux and no clear association between reflux episodes and symptoms. However, they have typical heartburn, yet the mechanism for heartburn in these patients remains unknown. We identified interesting oesophageal mucosal and molecular differences between patients with FH and healthy controls. The most important finding was co-expression of IL8 receptor CXCR2 on intrapapillary CGRP-immunoreactive nerves in FH, but not healthy controls. This suggests a potential neuroinflammatory signalling mechanism whereby hypersensitivity in these patients may be achieved through IL8 release activating CXCR2 expressed on deep afferent nerves, leading to neuronal activation. We also detected membranous expression of CXCR2 on oesophageal squamous epithelial cells in both healthy controls and FH patients. However, CXCR2 expression was detected on epithelial cells in very close proximity to deep CGRP-immunoreactive nerves in FH, but not controls. The close vicinity of these $CXCR2^{+}CGRP^{+}$ sensory nerves to the $CXCR2^{+}$ epithelial cells may highlight a crosstalk mechanism underlying the onset of increased sensitivity in patients with FH (Figure 85). This also suggests that deep sensory afferent nerves innervating papillary structures in patients with heartburn are likely to become sensitised by increased IL8 secretion. Heartburn sensation in FH patients may be explained by the increased abundance of CD8+ T cells detected by transcriptomic analysis, which may result in increased IL8 secretion in the oesophageal mucosa and thus increased sensitisation of deep sensory nerves via CXCR2 activation.

Moreover, compared with the oesophageal mucosa of healthy asymptomatic subjects, FH patients had 521 significantly DE genes highlighted in 87 molecular pathways including increased circadian regulation of gene expression, establishment of epithelial cell apical/basal polarity, and desmosome assembly, as statistically significative. The downregulation of ‘clock genes’ such as *PER1* and *TEF* in FH patients might be related to the psychological comorbidities frequently associated with this group of patients [565]. Clock gene polymorphisms were associated with bipolar syndrome and alcohol dependence in a case-

control study which assessed single nucleotide polymorphisms in 4 clock genes including *PER*1 [566]. This suggests that changes in the expression pattern of circadian pacemakers in the brain have a knock-on effect in the form of psychological morbidities which likely contribute to the perception of pain in the form of FH.

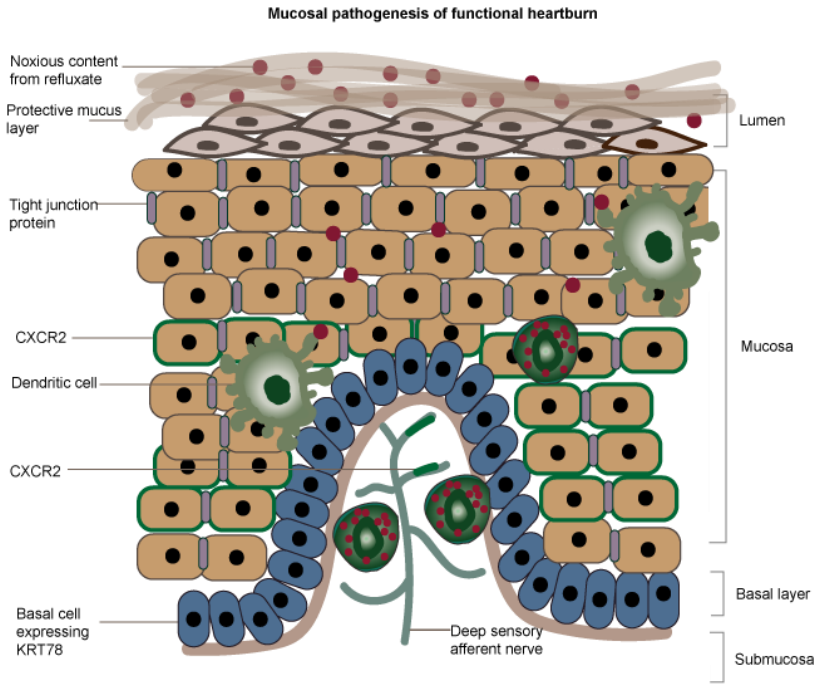

Figure 85 Illustration of the FH oesophageal mucosa

Figure illustrating the mucosal factors contributing to the pathogenesis of FH. A mucus layer protects the epithelial lining from noxious content of the refluxate. There are tight junction proteins that hold epithelial cells tightly together. There is CXCR2 expression on epithelial cells in close apposition to deep sensory nerves, and some CXCR2 expression on these intrapapillary nerve endings. Basal cell layer is characterised by KRT78 expression as in the normal oesophageal mucosa. NGF+ mast cell infiltration is increased in FH compared to healthy controls

5.8 Limitations and future work

Being limited to characterisation, this study lacks significant functional data explaining the mechanistic involvement of the mucosal factors identified. Although the preliminary functional data from the *ex vivo* cytokine release assay provides interesting data to build on, it is far from complete. However, the study has fulfilled its aim of characterising mucosal factors that hold translational relevance and may become potential topical treatment targets with further research. Moreover, due to additional challenges posed by the ongoing SARS-CoV2 pandemic, healthy control biopsies were collected at a later date than the time at which patient samples were collected and experimented. While the latter IF-IHC experiments in the study were done simultaneously on healthy controls and patient samples, RNA sequencing and qPCR experiments for patient biopsy samples and healthy controls were completed at different

time points, in different batches. Due to the limitation of sample collection and preparations, technical variations may exist among reads from different batches of experiments, such as varying sequencing depth and amplification bias. However, batch effects were minimised by sequencing all healthy controls in the same batch, and all GORD samples in a separate batch, thus minimising unwanted technical variations within GORD phenotypes and among healthy control samples. Finally, this study suffered loss of statistical power due to being based on a small sample of biopsies due to the nature of consenting patients, and recruiting asymptomatic participants following ethical approval being granted. In spite of its limitations, this study adds to our understanding of the mucosal factors contributing to the oesophageal hypersensitivity experienced by GORD patients.

The mucosal targets identified in this study are intriguing and could be usefully explored in further research. The *ex vivo* biopsy culture is a useful system for exploring the effect of acid challenge on GORD oesophageal mucosa and topical protective agents on a preclinical, human-like, well-preserved GORD model that is readily translational into responses in patients. Thus, a natural progression of this work is to analyse the effect of acid exposure on a larger cohort of ERD and healthy control samples, and secondly, to apply topical protectant onto the apical aspect of the biopsies to test the efficacy of these protectant therapies at a molecular level by measuring the change in cytokine release with and without topical treatment. Second, topical antagonists for mucosal factors identified, such as TRPV1, ASIC3, NGF receptors, and CXCR2 should be investigated using this *ex vivo* biopsy culture system to measure whether antagonising these targets may reduce the release of inflammatory and/or pain-inducing cytokines.

This study has also highlighted important questions on the structure of the oesophageal mucosa in need of further investigation. Further work into the differences in structural mechanisms for keratin proteins and MUC glycoproteins through IF-IHC experiments, and validation studies using qPCR will provide important information on the oesophageal structural barrier integrity across GORD phenotypes in relation to the patients' acid exposure profile and symptomatology. The question of oesophageal epithelial regeneration is also interesting to consider, and is an avenue signposted by our transcriptomic data worth exploring, particularly to help us further understand why some patients develop ERD, while others develop NERD.

5.9 Conclusions

The main goal of this study was to determine the mucosal factors potentially underlying heartburn perception in patients with GORD. In summary, based on our characterisation and

transcriptomic studies, it is possible to infer a model for heartburn pathogenesis in the different phenotypes of GORD. Sensory mechanisms of pain transmission have a critical role in NERD, where we have demonstrated a likely pathogenic role for superficial sensory nerves expressing TRPV1, and epithelial cells expressing ASIC3. In ERD patients where superficial nerves were not identified, NGF-expressing mast cells in close vicinity to deep afferent nerves are likely to have an indirect role in inducing pain transmission upon NGF release into the oesophageal mucosa, and subsequent activation of the neighbouring nerves. FH patients are different to healthy subjects at the mucosal level, where they express IL8 receptor CXCR2 on deep intrapapillary nerves. These findings have significant translational implications for oesophageal therapies that raise the enticing possibility of topical antagonists in the treatment of NERD, ERD, and FH. Further studies are needed to link these mucosal differences with symptoms in heartburn patients.

6 Appendix

Table 10 Clinical and Demographic Data for GORD Patients

Table includes RDQ score, LA grade for patients with ERD, and total acid exposure time (AET) where clinical data was available for recruited patients.

Sample ID	Phenotype	Gender	Age	Ethnicity	RDQ Score	LA grade	Total AET (%)	Studies	Notes
AE161118	NERD	Male	19	White British	40	n/a	n/a	IF, qPCR, RNA-seq	Sensory testing showed patient to have increased sensitivity to painful stimuli. He has oesophageal atresia which is almost always associated with pathological reflux.
JF110219	ERD	Male	45	White British	30	2	n/a	IF, qPCR	
RQ110219	NERD	Female	70	White British	16	n/a	15.5	IF, qPCR	2cm hiatus hernia with severe pathological acid exposure
JG120219	ERD	Male	60	White British	n/a	3	n/a	IF, qPCR	4cm sliding hiatus hernia
AG140219	NERD	Male	40	Indian	12	n/a	8	IF, qPCR	
MS161118	ERD	Male	58	White other	12	4	n/a	IF, qPCR	4cm sliding hiatus hernia, 18mm balloon distention
AG200219	FH	Male	42	White British	28	n/a	3.4	IF, qPCR, RNA-seq	1cm sliding hiatus hernia
DS200219	NERD	Male	54	Other	60	1	7	IF, qPCR, RNA-seq	2cm hiatus hernia
JM010319	ERD	Male	32	Other	5	3	n/a	IF, qPCR, RNA-seq	4cm sliding hiatus hernia
JH050319	FH	Male	69	White British	45	n/a	n/a	IF, qPCR	Patient had no PPI response, suggesting absence of pathological reflux
BA060319	NERD	Male	54	White British	15	n/a	14.1	IF, qPCR, RNA-seq	2cm hiatus hernia
JU130319	FH	Female	37	White British	54	n/a	Physiological	IF, qPCR, RNA-seq	2cm hiatus hernia
SSG130319	ERD	Male	39	Other	57	2	n/a	IF, qPCR, RNA-seq	
JD220319	ERD	Male	50	Other	0	2	n/a	IF, qPCR	

EM230519	BO	Male	61	White other	12	n/a	n/a	IF, qPCR	Short-segment BO
CB120419	FH	Female	72	White British	58	n/a	1.3	IF, qPCR, RNA-seq	
EB120419	FH	Female	33	Bangladeshi	40	n/a	3	IF, qPCR, RNA-seq	
RM120419	FH	Male	34	Bangladeshi	38	n/a	4	IF, qPCR, RNA-seq	
SC160519	NERD	Female	46	White other	47	n/a	6.6	IF, qPCR, RNA-seq	
BT150519	ERD	Male	48	White British	33	2	n/a	IF, qPCR	
LJ300519	NERD	Female	52	Indian	24	n/a	n/a	IF, qPCR, RNA-seq	Reflux symptoms reduced with PPI, suggesting pathological reflux.
RM250619	ERD	Male	46	White British	8	3	n/a	IF, qPCR, RNA-seq	Large hiatus hernia
AO190719	NERD	Female	52	Black	0	n/a	n/a	IF, qPCR, RNA-seq	2cm hiatus hernia. Reflux changes on histology
JW140819	BO	Male	29	White British	29	1	n/a	IF, qPCR, RNA-seq	BO prague C 0 and M2
MK210819	NERD	Female	32	White British	32	n/a	13.4	IF, qPCR	3cm sliding hernia
SV210819	NERD	Female	39	Indian	16	n/a	6.3	IF, qPCR, RNA-seq	Reflux symptoms were reduced with PPI
ML290819	FH	Female	58	n/a	60	n/a	3.7	IF, qPCR	Shatzki ring and hiatus hernia
DS120919	NERD	Male	29	n/a	8	3	n/a	IF, qPCR, RNA-seq	4cm hiatus hernia. He is technically ERD due to previous grade 3, but did not have inflammation at time of endoscopy.
WB081019	ERD	Male	40	White British	27	2	n/a	IF, qPCR, RNA-seq	3cm hiatus hernia
PB091019	BO	Female	61	White British	0	n/a	n/a	IF, qPCR, RNA-seq	Prague COM1 tongue of BO at 37cm
LK091019	BO	Female	73	White British	0	n/a	n/a	IF, qPCR, RNA-seq	
SM211019	BO	Female	36	Other	38	n/a	n/a	IF, qPCR	
BA221019	BO	Female	67	White British	0	n/a	n/a	IF, qPCR, RNA-seq	Lip of BO with large hiatus hernia
CF231019	BO	Female	55	Other	28	1	n/a	IF, qPCR, RNA-seq	3cm hiatus hernia
SH061119	BO	Female	57	n/a	0	n/a	n/a	IF, qPCR, RNA-seq	

SG131119	FH	Male	53	Ethiopian	n/a	n/a	n/a	IF, qPCR, RNA-seq	
JI050220	NERD	Female	54	Arab	27	n/a	8.4	IF, qPCR, RNA-seq	2cm hiatus hernia
SM050220	ERD	Female	73	White British	11	4	n/a	IF, qPCR, RNA-seq	7cm hiatus hernia
GK190220	BO	Male	37	Greek	33	n/a	n/a	IF, qPCR, RNA-seq	Short BO tongue COM1 at 42cm
CB050320	ERD	Male	19	White British	27	3	n/a	IF, qPCR, RNA-seq	
JB110320	BO	Male	54	White Irish	6	n/a	n/a	IF, qPCR, RNA-seq	COM2 short segment BO with 3cm hiatus hernia
RC110320	BO	Male	73	White British	0	n/a	n/a	IF, qPCR, RNA-seq	
SF030320	ERD	Male	56	White British	0	2	n/a	IF	
CB050320	ERD	Male	19	White British	27	3	n/a	Functional assay	
SJ010921	ERD	Female	33	White British	38	3	n/a	Functional assay	
SF270921	ERD	Female	76	White British	25	3	n/a	Functional assay	

Table 11 Healthy Volunteer Demographics

Sample ID	RDQ Score	Gender	Age
HF040320	0	F	34
MV120521	0	F	35
BB260521	0	M	25
HD090621	0	M	70
AV140721	0	F	25
ZP280721	0	F	20
MG050821	0	F	24
CL180821	0	F	26
TG010921	0	M	26
SZ290921	0	M	20
NU061021	0	F	25
MRM201021	0	F	27
RD271021	2	M	27
MA031121	0	M	45

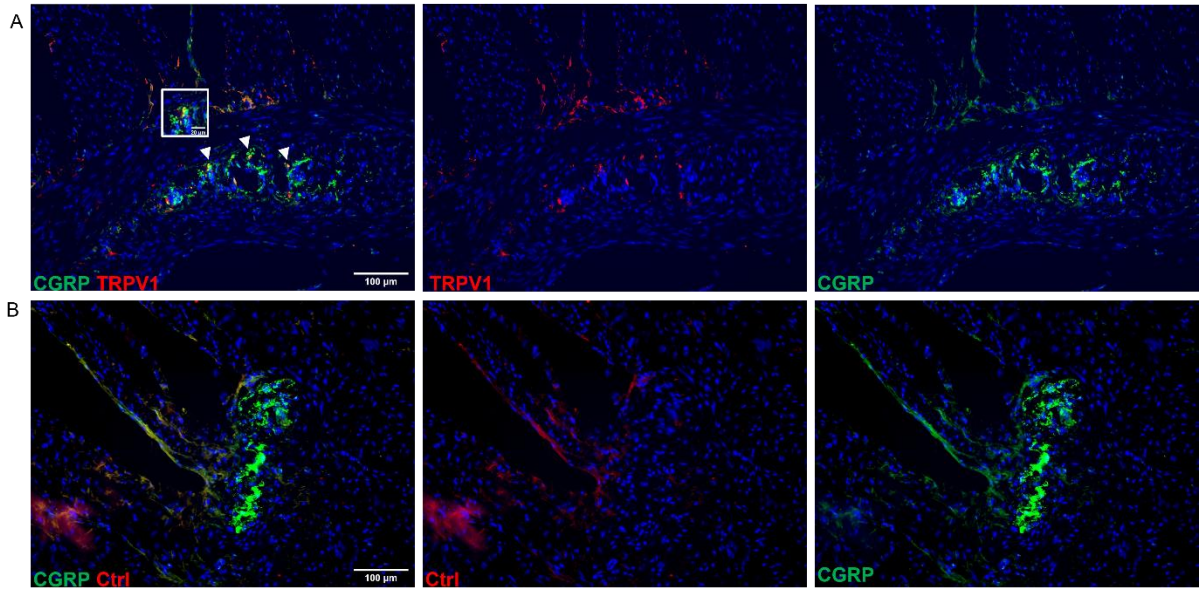

Appendix 1: Control Antigen Staining blocks TRPV1 staining in the myenteric plexus of the inflamed human colon

A) TRPV1 optimisation in the myenteric plexus of IBD colon co-stained with CGRP, showing TRPV1-immunoreactivity on CGRP-expressing neurons in the plexus. Arrowheads highlight TRPV1+CGRP+ colocalisation B) Control antigen staining showing no TRPV1 immunoreactivity in the myenteric plexus of the same IBD colon sample. A total of 2 IBD colon samples and 2 normal colon samples were used for optimisation. Scale bar*:* 100µm, Insert scale bar 20 µm.

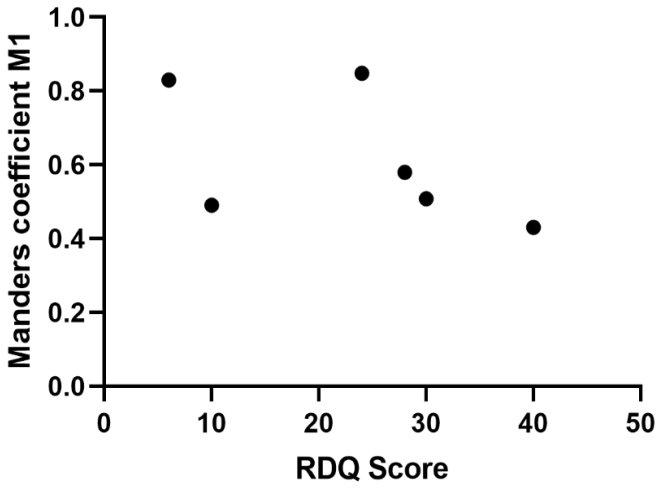

Appendix 3: Correlation between TRPV1:CGRP Co-expression and RDQ Score

There was no correlation between reflux disease questionnaire score and TRPV1 expression by mucosal sensory nerves for the 6 NERD patients whose RDQ scores could be retrieved.

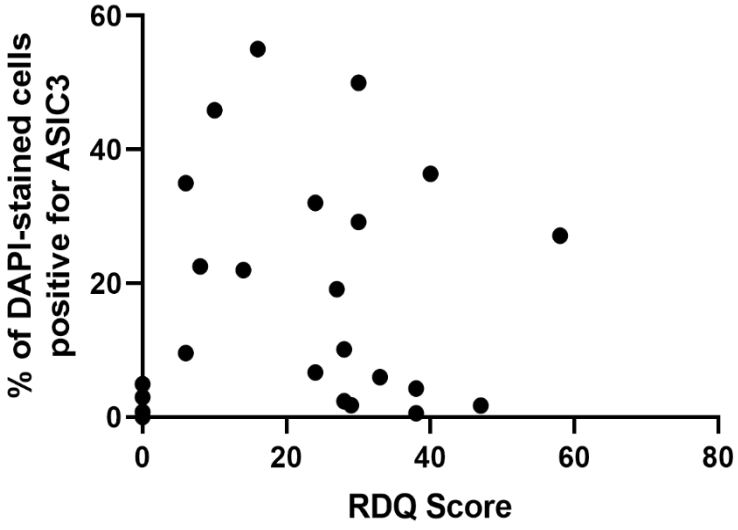

Appendix 2: Correlation between ASIC3 immunoreactivity and RDQ score

There was no correlation between reflux disease questionnaire score and ASIC3 expression by oesophageal epithelial cells for the 24 GORD patients whose RDQ scores could be retrieved.

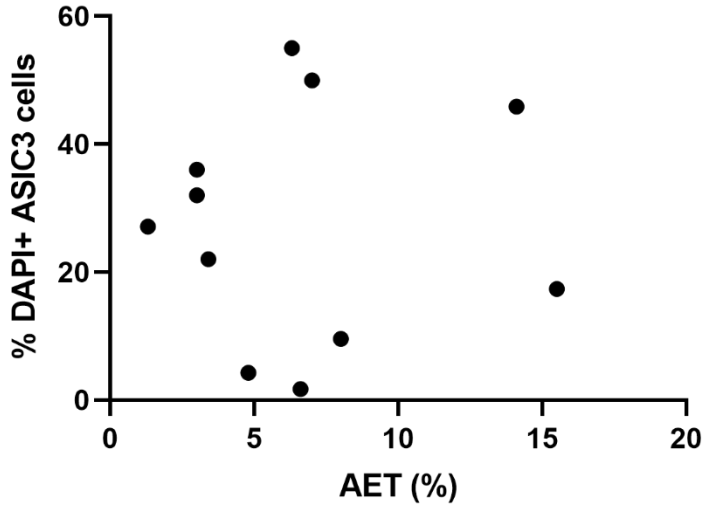

Appendix 4 Correlation between acid exposure time and ASIC3 expression

No correlation was found between acid exposure time in patients with FH and NERD (N=9) and ASIC3 expression (Spearman correlation: $p = 0.41$). AET data was not accessible for all patients.

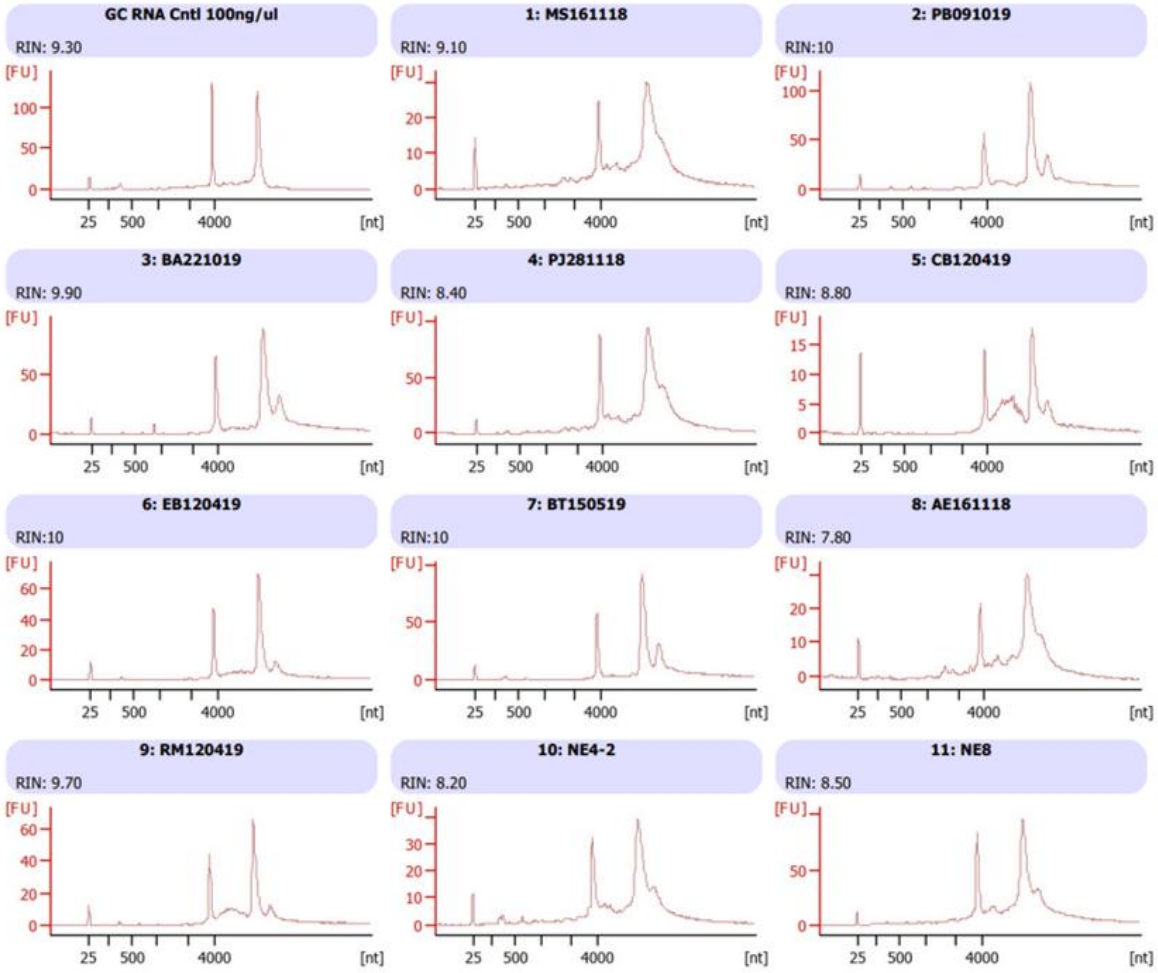

Appendix 5 RNA Sample QC Overview of RNA Integrity

Electrophoresis file run overview from Bioanalyser showing all samples in batch one to have RIN above 7.

Table 12 Pre-alignment QC for RNA-sequenced samples

The quality of raw reads was assessed by performing pre-alignment QC on Partek. This overview table presents input files per row, with corresponding typical metrics on columns. (%GC: fraction of GC content; %N: fraction of no-calls).

Sample ID	Batch	Phenotype	RIN	Disease group	Total reads	Read length	Avg. read quality	% N	% GC
AE161118	2	FH	8	GORD	16915905	76	34.52	0.0854339	52.7687
AG200219	1	FH	9.8	GORD	19397676	76	34.7969	0.0146707	49.8261
AO190719	1	NERD	10	GORD	20668827	76	34.7962	0.0145458	50.4245
AV140721	3	HC	8.1	Control	20152438	76	34.4088	0.0050293	51.2916
BA060319	1	NERD	10	GORD	15403330	76	34.7991	0.0143659	48.5226
BA221019	2	BO	10	GORD	20917085	76	34.6326	0.0853905	49.6187
BB260521	3	HC	9	Control	23869132	76	34.3163	0.0051738	50.4601
BT150519	2	ERD	10	GORD	14711530	76	34.6393	0.0860101	49.8247
CB050220	2	ERD	10	GORD	19988855	76	34.6477	0.0854044	49.9026
CB120419	2	FH	9	GORD	19322257	76	34.6436	0.0855278	49.4475
CF231019	1	BO	9.9	GORD	19819499	76	34.7865	0.0147845	49.8263
CL190821	3	HC	8.7	Control	21079473	76	34.3114	0.0050263	51.939
DS120919	1	NERD	9.9	GORD	18229780	76	34.8012	0.015035	49.6413
DS200219	1	NERD	10	GORD	17959504	76	34.7962	0.0144555	49.5498
E4	2	NERD	8	GORD	18401151	76	34.4501	0.0847827	49.9044
E6	2	NERD	9	GORD	19203679	76	34.6421	0.0859442	47.6206
EB120419	2	FH	10	GORD	20642696	76	34.6106	0.0851622	50.2585
GK190220	2	BO	10	GORD	18985574	76	34.6237	0.0853391	49.8338
HF040320	2	HC	10	Control	19316231	76	34.6533	0.0850024	49.275
JB110320	2	BO	10	GORD	19370522	76	34.6211	0.0857708	47.6722
JG120219	1	ERD	10	GORD	17100589	76	34.7682	0.0146092	50.7695
JI050220	2	NERD	10	GORD	19345177	76	34.6134	0.0865534	50.0331
JM010319	1	ERD	10	GORD	19211167	76	34.7928	0.0146589	49.6816
JU130319	1	FH	9.6	GORD	16543398	76	34.7807	0.0145011	49.832
JW140819	1	BO	9.8	GORD	18639482	76	34.8002	0.0146646	50.5281
LJ300319	2	NERD	10	GORD	15867118	76	34.6663	0.0869433	49.0337

MG050821	3	HC	8.2	Control	21870116	76	34.4313	0.0051368	50.0048
MS161118	2	ERD	9	GORD	19173461	76	34.5769	0.0853171	51.5548
MV120521	3	HC	10	Control	21625289	76	33.9049	0.0050918	50.7925
NE4-2	2	FH	8	GORD	21034800	76	34.6133	0.0857875	49.9242
NE8	2	FH	9	GORD	18700628	76	34.6108	0.0858786	49.855
PB091019	2	BO	10	GORD	19452692	76	34.6192	0.0865353	49.3819
PJ281118	2	ERD	8	GORD	16608207	76	34.642	0.0851409	50.1508
RC110320	2	BO	10	GORD	17142616	76	34.6233	0.0860132	48.702
RM120419	2	FH	10	GORD	18726703	76	34.5485	0.0856064	48.8732
RM250619	1	ERD	9.8	GORD	17097826	76	34.7548	0.0145546	50.1576
SC160519	1	NERD	9.8	GORD	17147128	76	34.7978	0.0146726	50.6094
SG131119	1	FH	10	GORD	21078537	76	34.7791	0.014801	49.6226
SH061119	1	BO	9.8	GORD	15537215	76	34.781	0.014621	49.0773
SM050220	2	ERD	10	GORD	20498418	76	34.6821	0.0858706	49.0268
SM211019	1	BO	10	GORD	34340582	76	34.7828	0.014743	50.001
SSG130319	1	ERD	10	GORD	15391252	76	34.7431	0.0148291	50.7602
SV210819	1	NERD	9	GORD	17283197	76	34.792	0.0144586	49.5295
TG010921	3	HC	N/A	Control	22622540	76	34.4254	0.0050585	49.4918
WB081019	1	ERD	9.9	GORD	19180512	76	34.7413	0.0145099	51.9509
ZP290721	3	HC	9.5	Control	20575176	76	34.4103	0.0052584	50.2603

Table 13 Post-alignment QC of RNA-sequenced samples

The quality of alignment was assessed by performing post-alignment QC. All samples had above 97% alignment, with most samples having at least 17 million total reads. Base quality scores are in the Phred-33 format. These samples were aligned by STAR.

Sample ID	Phenotype	Total reads	Total alignments	Aligned	Total unaligned	Unaligned	Total unique paired	Unique paired	Total non-unique paired	Non-unique paired	Coverage	Avg. length	Avg. quality	%GC
AE161118	FH	16915905	37813010	98.16418	310545	1.835817	15363100	90.82044	1242260	7.343739516	2.63801	76	34.6025	53.0524
AG200219	FH	19397676	41691072	98.74922	242623	1.250784	18142364	93.52854	1012689	5.220671796	4.68832	76	34.8437	50.0521
AO190719	NERD	20668827	43818810	98.61452	286362	1.385478	19426225	93.98804	956240	4.626484125	4.33815	76	34.8399	50.5103
AV140721	HC	20152438	42291006	98.58865	284422	1.411353	19049084	94.52496	818932	4.063686984	3.95874	76	34.4626	51.3336
BA060319	NERD	15403330	33015148	98.44915	238882	1.550846	14381868	93.36856	782580	5.080589717	5.01349	76	34.8486	48.7822
BA221019	BO	20917085	44537320	98.52442	308648	1.475578	19589581	93.65349	1018856	4.870927283	6.32034	76	34.7066	49.7637
BB260521	HC	23869132	49905112	98.45058	369833	1.54942	22517000	94.33523	982299	4.115352833	4.74135	76	34.3937	50.4782
BT150519	ERD	14711530	31556164	98.70953	189848	1.290471	13772553	93.61741	749129	5.092121622	4.11107	76	34.7137	50.0621
CB050220	ERD	19988855	42249122	98.59781	280282	1.402191	18812184	94.11336	896389	4.484443956	4.84404	76	34.7267	49.993
CB120419	FH	19322257	40913354	98.58739	272949	1.412614	18150895	93.93776	898413	4.649627629	4.34088	76	34.7216	49.5469
CF231019	BO	19819499	43850036	98.75192	247364	1.248084	18326285	92.46593	1245850	6.285981295	5.24221	76	34.8284	50.3276
CL190821	HC	21079473	44170948	98.50027	316136	1.499734	19908785	94.44631	854552	4.053953341	3.8037	76	34.3764	51.9807
DS120919	NERD	18229780	40208244	98.66264	243798	1.337361	16827530	92.30792	1158452	6.354722877	4.80896	76	34.8484	50.0988
DS200219	NERD	17959504	39133154	98.76839	221191	1.23161	16708127	93.03223	1030186	5.736160642	4.31675	76	34.846	49.9206
E4	NERD	18401151	39939250	97.86741	392421	2.132589	16893447	91.80647	1115283	6.060941514	3.58782	76	34.5283	50.1202
E6	NERD	19203679	42343014	98.46636	294516	1.533644	17581867	91.55468	1327296	6.911675622	3.58785	76	34.7234	48.0077
EB120419	FH	20642696	43569480	98.56253	296732	1.437467	19455073	94.24676	890891	4.315768638	4.46431	76	34.6879	50.3392
GK190220	BO	18985574	40182492	98.59304	267120	1.406963	17845797	93.99662	872657	4.596421472	4.63533	76	34.7033	49.9389
HF040320	HC	19316231	40604634	98.18519	350552	1.814805	18141953	93.92077	823726	4.264424048	5.41702	76	34.7304	49.3019
JB110320	BO	19370522	41242502	98.28875	331478	1.71125	18056479	93.21627	982565	5.072475589	6.30901	76	34.7032	47.8267
JG120219	ERD	17100589	39598632	98.50188	256187	1.498118	15402928	90.0725	1441474	8.429382169	3.56892	76	34.8025	51.6035
JI050220	NERD	19345177	41482444	98.53687	283045	1.46313	18116482	93.64857	945650	4.888298515	5.48864	76	34.6834	50.2336
JM010319	ERD	19211167	42671168	98.87005	217077	1.129952	17712122	92.19701	1281968	6.673035532	5.19865	76	34.8417	50.2066
JU130319	FH	16543398	37897300	98.62879	226845	1.371212	14993243	90.62977	1323310	7.999021725	4.32168	76	34.8228	50.5612
JW140819	BO	18639482	41405722	98.46581	285966	1.534195	17107130	91.779	1246386	6.686805996	5.14862	76	34.8425	50.9893
LJ300319	NERD	15867118	33720372	98.64556	214910	1.354436	14904850	93.93546	747358	4.710105515	4.14675	76	34.7434	49.2183
MG050821	HC	21870116	45694148	98.46935	334756	1.530655	20669699	94.51115	865661	3.958191168	4.04242	76	34.4988	50.067

MS161118	ERD	19173461	42793870	97.78227	425215	2.217727	17279024	90.11948	1469222	7.662789728	2.53498	76	34.6731	51.9179
MV120521	HC	21625289	45170388	98.01469	429328	1.985305	20291370	93.83167	904591	4.183023866	5.17267	76	34.008	50.8263
NE4-2	FH	21034800	46613042	98.38736	339215	1.612637	19207495	91.31294	1488090	7.074419533	4.04027	76	34.6829	50.32
NE8	FH	18700628	41525806	97.17349	528575	2.826509	16739117	89.51099	1432936	7.662502029	3.80548	76	34.7004	50.3828
PB091019	BO	19452692	41366370	98.5032	291167	1.496795	18248178	93.80798	913347	4.695221618	6.30868	76	34.6933	49.5348
PJ281118	ERD	16608207	36564892	98.55218	240457	1.44782	15270229	91.94387	1097521	6.608305159	2.91674	76	34.7122	50.4329
RC110320	BO	17142616	38360114	97.68612	396659	2.313877	15620613	91.12152	1125344	6.564599009	5.42984	76	34.7205	49.3975
RM120419	FH	18726703	39260274	98.37722	303893	1.622779	17649353	94.24699	773457	4.130235846	4.63594	76	34.65	48.9161
RM250619	ERD	17097826	37156954	98.76717	210787	1.232829	15912977	93.07018	974062	5.69699329	4.15813	76	34.8018	50.4755
SC160519	NERD	17147128	37521302	98.83985	198933	1.160153	15941621	92.96963	1006574	5.870219199	4.16398	76	34.8392	50.9467
SG131119	FH	21078537	45313888	98.87917	236254	1.120827	19747606	93.68585	1094677	5.193325324	5.33043	76	34.8272	49.841
SH061119	BO	15537215	33858280	98.48874	234808	1.511262	14374332	92.5155	928075	5.973239091	5.65325	76	34.8298	49.4671
SM050220	ERD	20498418	43915174	98.66614	273420	1.333859	19170476	93.52173	1054522	5.144406754	4.09588	76	34.7532	49.2746
SM211019	BO	34340582	75775400	98.83614	399675	1.163856	31790241	92.57339	2150666	6.262753497	6.03973	76	34.8261	50.4685
SSG130319	ERD	15391252	33988658	98.83781	178876	1.162193	14241732	92.53134	970644	6.306465517	4.54431	76	34.7886	51.1818
SV210819	NERD	17283197	37398446	98.43446	270575	1.565538	16061943	92.93387	950679	5.500596909	3.73108	76	34.8384	49.8137
TG010921	HC	22622540	47310480	98.53816	330705	1.461839	21356280	94.40266	935555	4.135499374	4.91051	76	34.4942	49.5112
WB081019	ERD	19180512	41513426	98.24893	335864	1.751069	17765601	92.62318	1079047	5.625746591	4.35283	76	34.8154	52.2216
ZP290721	HC	20575176	42997176	98.36052	337325	1.639476	19403457	94.30518	834394	4.055343196	4.50775	76	34.4809	50.2911

Table 14 DEseq2 Comparison Between Healthy Controls and GORD Oesophageal Mucosa

DEseq2 output with FDR-filtered *p* value less than 0.01 for significantly differentially expressed genes between healthy controls and GORD patients. A negative fold change indicates genes downregulated in healthy controls compared to GORD samples, while positive fold change indicates genes downregulated in GORD compared to HC oesophageal mucosa.

Gene ID	P-value (HC vs. GORD)	FDR step up (HC vs. GORD)	Ratio (HC vs. GORD)	Fold change (HC vs. GORD)	LSMean(HC) (HC vs. GORD)	LSMean(GORD) (HC vs.GORD)
REG4	0.00E+00	0.00E+00	1.00E-06	-1.00E+06	3.88E-23	2.91E+02
GKN2	1.43E-72	1.44E-68	1.00E-06	-1.00E+06	4.13E-07	9.80E+01
CLDN18	7.68E-64	5.13E-60	1.00E-06	-1.00E+06	1.58E-06	2.94E+02
DMBT1	5.58E-57	2.80E-53	1.00E-06	-1.00E+06	5.78E-07	5.07E+01
IGLV3-25	1.70E-53	6.82E-50	1.00E-06	-1.00E+06	1.10E-06	4.27E+01
IGKV1-5	2.34E-51	7.82E-48	1.00E-06	-1.00E+06	4.25E-06	1.44E+02
IGHV1-2	1.36E-40	3.90E-37	1.00E-06	-1.00E+06	1.69E-05	1.13E+02
CCL18	3.24E-39	8.12E-36	1.00E-06	-1.00E+06	6.41E-06	1.51E+01
DAZ1	3.75E-35	8.36E-32	1.00E-06	-1.00E+06	6.36E-08	1.57E+01
ADGRG7	1.68E-34	3.38E-31	1.00E-06	-1.00E+06	3.39E-07	3.52E+01
IGHV3-43	2.29E-32	4.18E-29	1.00E-06	-1.00E+06	9.52E-06	1.63E+01
IGKV1-12	2.21E-30	3.69E-27	1.00E-06	-1.00E+06	1.38E-05	5.62E+01
DCDC2	1.33E-29	2.05E-26	1.61E-06	-6.21E+05	1.47E-05	9.15E+00
SLC5A5	2.55E-29	3.66E-26	1.00E-06	-1.00E+06	1.20E-05	2.08E+01
IGHV1-24	1.46E-27	1.95E-24	1.00E-06	-1.00E+06	2.07E-06	1.36E+01
UGT2B15	1.18E-26	1.49E-23	1.00E-06	-1.00E+06	5.52E-06	1.63E+01
SPINK1	8.89E-26	1.05E-22	1.00E-06	-1.00E+06	1.32E-05	2.96E+01
MUC17	5.44E-25	6.06E-22	1.00E-06	-1.00E+06	6.46E-06	3.13E+01
PRSS2	6.92E-23	7.30E-20	1.00E-06	-1.00E+06	2.83E-06	1.51E+01
IGHV3-72	4.31E-20	4.32E-17	2.02E-06	-4.94E+05	2.30E-05	1.14E+01
CLDN2	3.19E-16	3.05E-13	1.34E-06	-7.46E+05	1.54E-05	1.15E+01
PIGR	2.16E-15	1.97E-12	1.63E-03	-6.15E+02	1.91E+00	1.17E+03
ACTC1	3.39E-15	2.96E-12	3.91E-06	-2.56E+05	1.39E-05	3.56E+00
MYH11	5.33E-15	4.45E-12	5.81E-03	-1.72E+02	2.71E+00	4.66E+02
ARNTL	6.30E-15	5.06E-12	2.40E-01	-4.17E+00	3.19E+01	1.33E+02
TFF1	7.62E-15	5.88E-12	2.85E-04	-3.51E+03	2.44E-01	8.56E+02
CTSE	6.46E-14	4.80E-11	3.63E-04	-2.75E+03	1.18E-01	3.25E+02
TM4SF20	1.37E-13	9.78E-11	1.05E-06	-9.50E+05	4.56E-06	4.33E+00
IGHV3-66	1.66E-13	1.15E-10	6.34E-06	-1.58E+05	2.91E-05	4.60E+00
IGHV4-55	2.73E-13	1.83E-10	1.70E-06	-5.88E+05	9.13E-06	5.37E+00
AC130304.1	3.85E-13	2.49E-10	5.71E+00	5.71E+00	6.06E+01	1.06E+01

IGKC	5.03E-13	3.15E-10	2.87E-03	-3.48E+02	1.93E+01	6.71E+03
TFF2	1.01E-12	6.13E-10	4.41E-04	-2.27E+03	1.18E-01	2.68E+02
DES	2.78E-12	1.64E-09	8.56E-04	-1.17E+03	1.81E-01	2.11E+02
IGKV2D-29	4.14E-12	2.34E-09	8.25E-06	-1.21E+05	2.95E-05	3.57E+00
IGHA1	4.20E-12	2.34E-09	5.12E-03	-1.95E+02	2.21E+01	4.32E+03
JCHAIN	1.33E-11	7.24E-09	7.70E-03	-1.30E+02	1.49E+01	1.94E+03
CLMP	1.45E-11	7.67E-09	2.26E-02	-4.42E+01	1.20E+00	5.29E+01
MUC5AC	1.87E-11	9.64E-09	4.30E-04	-2.33E+03	4.57E-01	1.06E+03
TSPAN8	5.51E-11	2.77E-08	1.14E-02	-8.81E+01	3.45E+00	3.04E+02
ACTG2	1.14E-10	5.57E-08	2.92E-03	-3.43E+02	2.98E-01	1.02E+02
THBS2	1.21E-10	5.76E-08	1.59E-01	-6.30E+00	2.76E+01	1.74E+02
LGALS4	1.38E-10	6.42E-08	3.69E-03	-2.71E+02	8.26E-01	2.24E+02
FN1	1.48E-10	6.75E-08	4.10E-02	-2.44E+01	1.12E+01	2.73E+02
ALDOB	1.55E-10	6.91E-08	1.73E-05	-5.79E+04	1.07E-05	6.21E-01
REG1A	1.69E-10	7.38E-08	6.99E-06	-1.43E+05	7.75E-06	1.11E+00
PER1	1.82E-10	7.77E-08	4.83E+00	4.83E+00	1.68E+03	3.48E+02
TEF	2.79E-10	1.17E-07	2.98E+00	2.98E+00	9.87E+02	3.31E+02
BEST1	3.23E-10	1.32E-07	8.56E+00	8.56E+00	6.36E+02	7.43E+01
LIPG	3.38E-10	1.36E-07	4.32E-02	-2.31E+01	1.90E+00	4.39E+01
DPT	4.54E-10	1.76E-07	3.33E-02	-3.01E+01	1.60E+00	4.82E+01
IGLC3	4.56E-10	1.76E-07	6.07E-03	-1.65E+02	2.87E+00	4.74E+02
IGHA2	5.31E-10	2.01E-07	1.08E-02	-9.27E+01	9.26E+00	8.58E+02
PHLDB2	6.45E-10	2.40E-07	1.98E-01	-5.06E+00	3.36E+01	1.70E+02
IGHV4-59	9.68E-10	3.53E-07	8.78E-04	-1.14E+03	1.15E-01	1.31E+02
SPRR2G	1.10E-09	3.94E-07	9.42E-03	-1.06E+02	7.17E-01	7.61E+01
MAP1B	1.29E-09	4.54E-07	1.11E-01	-9.02E+00	7.98E+00	7.20E+01
SLC6A14	1.39E-09	4.82E-07	5.90E-02	-1.70E+01	1.21E+01	2.04E+02
AC087190.3	2.05E-09	6.96E-07	6.56E-02	-1.53E+01	3.33E+00	5.07E+01
AGR2	2.08E-09	6.96E-07	2.82E-02	-3.55E+01	3.40E+01	1.21E+03
CLCA1	2.76E-09	9.09E-07	5.24E-06	-1.91E+05	1.60E-06	3.05E-01
CCL21	2.89E-09	9.36E-07	1.49E-02	-6.70E+01	4.87E-01	3.26E+01
IGLV3-1	3.15E-09	9.88E-07	2.51E-03	-3.99E+02	2.39E-01	9.53E+01
GREM1	3.15E-09	9.88E-07	9.11E-03	-1.10E+02	1.00E+00	1.10E+02
CIART	3.41E-09	1.05E-06	5.68E+00	5.68E+00	2.25E+02	3.96E+01
CSPG4	3.68E-09	1.12E-06	1.02E-01	-9.84E+00	3.41E+00	3.35E+01
IGKV3-20	4.63E-09	1.39E-06	4.47E-03	-2.24E+02	1.74E+00	3.90E+02
FABP1	4.72E-09	1.39E-06	5.82E-06	-1.72E+05	2.00E-06	3.44E-01
CAPN6	5.51E-09	1.57E-06	1.33E-01	-7.51E+00	1.22E+01	9.16E+01
7SK	5.53E-09	1.57E-06	1.39E-01	-7.18E+00	5.34E+00	3.83E+01

STK40	5.57E-09	1.57E-06	2.04E+00	2.04E+00	1.71E+03	8.39E+02
CXCL1	8.29E-09	2.31E-06	1.23E-02	-8.16E+01	1.15E+00	9.38E+01
NEXN	1.08E-08	2.94E-06	2.85E-02	-3.51E+01	1.10E+00	3.87E+01
AL161665.1	1.10E-08	2.94E-06	4.96E+00	4.96E+00	3.77E+01	7.59E+00
IGHV3-23	1.10E-08	2.94E-06	2.99E-03	-3.34E+02	7.47E-01	2.50E+02
RN7SK	1.26E-08	3.32E-06	1.42E-01	-7.07E+00	8.05E+00	5.69E+01
IGKV2D-28	1.60E-08	4.16E-06	3.33E-03	-3.00E+02	3.05E-01	9.15E+01
GKN1	1.66E-08	4.21E-06	8.72E-03	-1.15E+02	5.42E+00	6.22E+02
AC022400.7	1.66E-08	4.21E-06	2.59E+00	2.59E+00	6.85E+01	2.64E+01
APLNR	1.76E-08	4.43E-06	2.54E-01	-3.93E+00	2.22E+01	8.73E+01
PCDH17	1.82E-08	4.50E-06	2.41E-01	-4.15E+00	1.43E+01	5.92E+01
HOXA7	2.53E-08	6.18E-06	1.62E-01	-6.18E+00	1.19E+01	7.39E+01
GABPB1-AS1	2.56E-08	6.18E-06	4.17E-01	-2.40E+00	1.51E+02	3.61E+02
DBP	2.69E-08	6.43E-06	3.26E+00	3.26E+00	6.26E+02	1.92E+02
FLII	2.91E-08	6.88E-06	1.54E+00	1.54E+00	3.41E+03	2.21E+03
SERPINA3	3.16E-08	7.38E-06	7.53E-03	-1.33E+02	6.26E-01	8.32E+01
NR1D2	3.22E-08	7.43E-06	3.27E+00	3.27E+00	2.07E+03	6.32E+02
MUC6	3.70E-08	8.44E-06	5.61E-04	-1.78E+03	1.17E-01	2.08E+02
TSPAN1	3.99E-08	8.98E-06	3.13E-02	-3.20E+01	8.48E+00	2.71E+02
SPON1	4.71E-08	1.05E-05	1.78E-01	-5.61E+00	1.43E+01	8.01E+01
AZGP1	4.86E-08	1.07E-05	7.62E-03	-1.31E+02	4.92E-01	6.46E+01
TTR	4.93E-08	1.08E-05	6.21E-05	-1.61E+04	1.31E-05	2.11E-01
LTF	5.49E-08	1.18E-05	3.61E-02	-2.77E+01	2.74E+00	7.59E+01
SLCO4A1	5.72E-08	1.22E-05	2.73E+00	2.73E+00	6.74E+02	2.47E+02
OLFM4	5.80E-08	1.22E-05	8.62E-03	-1.16E+02	1.54E+00	1.78E+02
S100A7	6.82E-08	1.43E-05	4.28E-02	-2.34E+01	1.64E+02	3.83E+03
ZC3H6	7.05E-08	1.46E-05	6.55E-01	-1.53E+00	1.22E+02	1.86E+02
SLC44A4	7.48E-08	1.53E-05	3.22E-02	-3.10E+01	4.43E+00	1.38E+02
ACTN4	7.88E-08	1.60E-05	1.66E+00	1.66E+00	1.14E+04	6.86E+03
FADS1	8.58E-08	1.72E-05	2.90E-01	-3.44E+00	1.97E+01	6.80E+01
ANXA10	9.35E-08	1.86E-05	2.20E-03	-4.54E+02	2.54E-01	1.15E+02
LMOD1	9.80E-08	1.93E-05	5.66E-02	-1.77E+01	3.18E+00	5.62E+01
IGKV4-1	9.89E-08	1.93E-05	3.80E-03	-2.63E+02	1.08E+00	2.85E+02
TCIM	1.02E-07	1.97E-05	1.35E-01	-7.43E+00	9.44E+00	7.01E+01
TMEM80	1.09E-07	2.07E-05	2.76E+00	2.76E+00	9.71E+02	3.52E+02
IGKV1D-39	1.16E-07	2.19E-05	3.65E-03	-2.74E+02	5.58E-01	1.53E+02
ADAM23	1.19E-07	2.23E-05	3.34E-01	-2.99E+00	4.19E+01	1.25E+02
LYZ	1.25E-07	2.33E-05	6.31E-02	-1.58E+01	2.81E+02	4.45E+03
RHOA	1.35E-07	2.46E-05	1.24E+00	1.24E+00	7.82E+03	6.29E+03

AP2A1	1.35E-07	2.46E-05	1.46E+00	1.46E+00	1.19E+03	8.15E+02
KRTDAP	1.41E-07	2.56E-05	9.11E-02	-1.10E+01	4.20E+01	4.61E+02
TAGLN	1.45E-07	2.60E-05	8.55E-02	-1.17E+01	2.86E+01	3.34E+02
SYTL2	1.54E-07	2.73E-05	8.21E-02	-1.22E+01	1.60E+01	1.95E+02
HOXA10	1.62E-07	2.85E-05	3.76E-02	-2.66E+01	9.82E-01	2.61E+01
POU2AF1	1.66E-07	2.90E-05	6.70E-02	-1.49E+01	5.72E+00	8.54E+01
IL33	1.89E-07	3.26E-05	1.90E-01	-5.25E+00	2.55E+01	1.34E+02
SEMA3C	1.94E-07	3.32E-05	1.57E-01	-6.36E+00	2.36E+01	1.50E+02
PFKP	2.05E-07	3.49E-05	1.46E+00	1.46E+00	1.60E+03	1.09E+03
ACTA2	2.07E-07	3.49E-05	1.21E-01	-8.26E+00	2.54E+01	2.10E+02
COL5A2	2.14E-07	3.57E-05	1.98E-01	-5.06E+00	3.35E+01	1.69E+02
SERPINA1	2.15E-07	3.57E-05	5.54E-02	-1.81E+01	1.52E+01	2.75E+02
MACO1	2.40E-07	3.94E-05	1.83E+00	1.83E+00	1.81E+03	9.89E+02
AL357033.1	2.51E-07	4.09E-05	4.10E+00	4.10E+00	1.19E+02	2.90E+01
RTP4	2.72E-07	4.37E-05	1.77E-01	-5.64E+00	7.67E+00	4.32E+01
IGHV1-18	2.72E-07	4.37E-05	3.25E-03	-3.08E+02	2.57E-01	7.93E+01
MCAM	2.76E-07	4.40E-05	2.04E-01	-4.91E+00	3.59E+01	1.76E+02
GOLM1	3.02E-07	4.78E-05	7.58E-02	-1.32E+01	3.95E+01	5.21E+02
NR2F1	3.17E-07	4.96E-05	2.08E-01	-4.80E+00	8.77E+00	4.21E+01
IGHV5-51	3.43E-07	5.34E-05	3.05E-03	-3.27E+02	2.77E-01	9.08E+01
VSIG1	3.57E-07	5.50E-05	2.34E-02	-4.28E+01	3.36E+00	1.44E+02
HMGA1P1	3.59E-07	5.50E-05	1.97E+00	1.97E+00	5.96E+01	3.03E+01
PAMR1	3.80E-07	5.78E-05	1.63E-01	-6.13E+00	3.89E+00	2.38E+01
CPT1B	3.98E-07	6.00E-05	4.49E-01	-2.23E+00	5.92E+01	1.32E+02
TMC5	4.06E-07	6.08E-05	6.34E-02	-1.58E+01	1.05E+01	1.65E+02
PI15	4.13E-07	6.14E-05	2.97E-02	-3.37E+01	5.92E-01	1.99E+01
TFF3	4.53E-07	6.68E-05	1.36E-02	-7.34E+01	1.04E+00	7.62E+01
COL1A2	4.64E-07	6.80E-05	1.21E-01	-8.26E+00	8.34E+01	6.89E+02
MMP2	4.67E-07	6.80E-05	1.44E-01	-6.97E+00	3.39E+01	2.36E+02
MEG3	4.89E-07	7.06E-05	1.70E-01	-5.87E+00	1.48E+01	8.71E+01
UBA6-AS1	5.13E-07	7.27E-05	6.36E-01	-1.57E+00	6.34E+01	9.97E+01
SI	5.13E-07	7.27E-05	1.46E-05	-6.83E+04	5.44E-06	3.72E-01
SELENOP	5.14E-07	7.27E-05	5.90E-01	-1.70E+00	1.36E+03	2.31E+03
DEPDC7	5.55E-07	7.78E-05	4.95E-01	-2.02E+00	3.85E+01	7.77E+01
CCDC127	5.65E-07	7.82E-05	1.66E+00	1.66E+00	3.83E+02	2.30E+02
GNAS	5.65E-07	7.82E-05	1.44E+00	1.44E+00	9.27E+03	6.42E+03
POSTN	5.83E-07	8.02E-05	7.20E-02	-1.39E+01	1.29E+01	1.80E+02
PCBP1	6.55E-07	8.94E-05	1.56E+00	1.56E+00	7.10E+03	4.56E+03
AC008875.3	6.63E-07	8.99E-05	1.92E-01	-5.21E+00	1.12E+01	5.83E+01

MEDAG	6.92E-07	9.32E-05	1.62E-01	-6.18E+00	2.96E+00	1.83E+01
FYB1	7.19E-07	9.61E-05	2.54E-01	-3.94E+00	7.24E+01	2.85E+02
HOOK2	7.92E-07	1.05E-04	1.61E+00	1.61E+00	1.13E+03	6.99E+02
CTSL	8.07E-07	1.07E-04	1.81E-01	-5.53E+00	4.46E+01	2.47E+02
MUC5B	8.18E-07	1.07E-04	5.46E-02	-1.83E+01	1.75E+01	3.20E+02
MSMB	8.26E-07	1.08E-04	6.64E-03	-1.51E+02	1.19E-01	1.79E+01
AC078816.1	8.64E-07	1.12E-04	1.01E+01	1.01E+01	8.60E+00	8.54E-01
PGM5	8.69E-07	1.12E-04	1.16E-01	-8.64E+00	4.67E+00	4.03E+01
EPHB2	8.95E-07	1.14E-04	1.20E-01	-8.35E+00	6.33E+00	5.28E+01
BCR	9.32E-07	1.18E-04	1.49E+00	1.49E+00	1.94E+03	1.30E+03
RNASE1	9.92E-07	1.25E-04	1.23E-01	-8.14E+00	2.31E+01	1.88E+02
MUC13	9.98E-07	1.25E-04	2.27E-03	-4.40E+02	2.48E-01	1.09E+02
LUM	1.04E-06	1.28E-04	1.39E-01	-7.21E+00	5.46E+01	3.94E+02
PLEKHB1	1.04E-06	1.28E-04	5.95E-02	-1.68E+01	1.19E+00	2.00E+01
FCRL5	1.05E-06	1.28E-04	6.30E-03	-1.59E+02	1.18E-01	1.88E+01
IGHV3-21	1.05E-06	1.28E-04	2.00E-03	-5.00E+02	1.27E-01	6.34E+01
KCNN4	1.06E-06	1.28E-04	1.32E-01	-7.56E+00	8.48E+00	6.41E+01
MMP9	1.08E-06	1.31E-04	7.52E-02	-1.33E+01	3.77E+00	5.01E+01
SPRY4	1.11E-06	1.34E-04	2.49E-01	-4.01E+00	1.66E+01	6.66E+01
GALNT6	1.16E-06	1.39E-04	1.56E-01	-6.42E+00	3.26E+01	2.09E+02
LURAP1L	1.19E-06	1.41E-04	1.22E-01	-8.18E+00	4.32E+00	3.53E+01
SULT1A4	1.20E-06	1.41E-04	1.47E-01	-6.79E+00	4.03E+00	2.74E+01
CHCHD3	1.29E-06	1.51E-04	7.23E-01	-1.38E+00	3.59E+02	4.97E+02
PMP22	1.30E-06	1.51E-04	2.19E-01	-4.56E+00	1.83E+01	8.36E+01
FAM155A	1.30E-06	1.51E-04	4.86E-02	-2.06E+01	2.98E-01	6.14E+00
IQGAP2	1.31E-06	1.51E-04	1.53E-01	-6.52E+00	2.53E+01	1.65E+02
CLEC2B	1.36E-06	1.56E-04	3.10E-01	-3.22E+00	5.52E+01	1.78E+02
SEMA3G	1.54E-06	1.76E-04	2.50E-01	-4.01E+00	7.77E+00	3.11E+01
KCNMA1	1.58E-06	1.79E-04	2.26E-01	-4.43E+00	1.00E+01	4.45E+01
ABCA12	1.62E-06	1.83E-04	2.23E-01	-4.48E+00	3.93E+01	1.76E+02
S100A7A	1.63E-06	1.83E-04	1.79E-02	-5.59E+01	1.03E+00	5.76E+01
RETREG1	1.67E-06	1.86E-04	2.34E-01	-4.28E+00	1.37E+01	5.87E+01
PLCB4	1.69E-06	1.88E-04	1.10E-01	-9.07E+00	3.37E+00	3.05E+01
HOXB7	1.75E-06	1.93E-04	4.38E-02	-2.28E+01	1.07E+00	2.44E+01
COL12A1	1.76E-06	1.93E-04	1.93E-01	-5.19E+00	4.57E+01	2.37E+02
UBE2MP1	1.82E-06	1.98E-04	1.40E+00	1.40E+00	1.54E+02	1.10E+02
LNX1	1.82E-06	1.98E-04	2.46E+00	2.46E+00	2.01E+03	8.16E+02
VNN3	1.87E-06	2.02E-04	2.03E-02	-4.92E+01	1.81E-01	8.89E+00
NID1	1.89E-06	2.03E-04	1.79E-01	-5.60E+00	1.76E+01	9.86E+01

HAS2	1.92E-06	2.05E-04	2.81E-02	-3.56E+01	4.67E-01	1.66E+01
DIAPH1	1.97E-06	2.10E-04	1.51E+00	1.51E+00	4.67E+03	3.10E+03
AL357033.4	2.00E-06	2.11E-04	3.01E+00	3.01E+00	5.55E+02	1.84E+02
BAG6	2.04E-06	2.14E-04	1.36E+00	1.36E+00	2.27E+03	1.67E+03
MACROH2A1	2.06E-06	2.15E-04	1.41E+00	1.41E+00	4.75E+03	3.36E+03
HTRA3	2.19E-06	2.28E-04	7.57E-02	-1.32E+01	1.54E+00	2.04E+01
EZR	2.21E-06	2.28E-04	1.42E+00	1.42E+00	1.14E+04	8.02E+03
MIR31HG	2.23E-06	2.30E-04	2.76E-01	-3.62E+00	2.04E+01	7.41E+01
CHST2	2.24E-06	2.30E-04	1.56E-01	-6.40E+00	6.99E+00	4.47E+01
AKAP12	2.35E-06	2.40E-04	1.57E-01	-6.35E+00	6.65E+00	4.23E+01
CPNE8	2.48E-06	2.51E-04	4.68E-01	-2.13E+00	3.94E+01	8.42E+01
GATA6	2.60E-06	2.63E-04	2.20E-02	-4.55E+01	7.12E-01	3.24E+01
ANPEP	2.62E-06	2.63E-04	5.96E-02	-1.68E+01	1.21E+01	2.03E+02
ADAMTS5	2.67E-06	2.67E-04	1.11E-01	-9.01E+00	1.66E+00	1.49E+01
MALAT1	2.70E-06	2.68E-04	4.65E-01	-2.15E+00	2.02E+04	4.35E+04
ZBTB25	2.71E-06	2.68E-04	6.73E-01	-1.48E+00	7.42E+01	1.10E+02
HAPLN1	2.74E-06	2.69E-04	1.99E-02	-5.03E+01	2.98E-01	1.50E+01
INPP5A	2.83E-06	2.77E-04	1.51E+00	1.51E+00	5.63E+02	3.73E+02
PROM1	2.90E-06	2.83E-04	7.91E-03	-1.26E+02	6.12E-01	7.74E+01
IGHV3-49	2.92E-06	2.83E-04	2.95E-03	-3.39E+02	1.27E-01	4.30E+01
TMC7	2.96E-06	2.85E-04	1.53E-01	-6.54E+00	3.03E+00	1.98E+01
AC005062.1	2.97E-06	2.85E-04	4.84E+00	4.84E+00	1.34E+01	2.77E+00
SNX9	3.03E-06	2.89E-04	2.19E+00	2.19E+00	5.36E+03	2.45E+03
TSPAN18	3.04E-06	2.89E-04	2.50E-01	-4.01E+00	7.51E+00	3.01E+01
CXCL12	3.21E-06	3.03E-04	2.25E-01	-4.44E+00	2.16E+01	9.61E+01
IL20RA	3.24E-06	3.04E-04	6.75E-01	-1.48E+00	1.51E+02	2.24E+02
KCNA2	3.24E-06	3.04E-04	2.91E-01	-3.43E+00	8.69E+00	2.98E+01
IGHV3-7	3.50E-06	3.26E-04	6.16E-03	-1.62E+02	4.84E-01	7.87E+01
SUSD6	3.53E-06	3.27E-04	1.95E+00	1.95E+00	2.92E+03	1.50E+03
PGK1P2	3.53E-06	3.27E-04	1.53E+00	1.53E+00	1.26E+02	8.21E+01
CA2	3.57E-06	3.29E-04	1.73E-01	-5.78E+00	2.17E+02	1.26E+03
OASL	3.63E-06	3.32E-04	1.25E-01	-8.02E+00	1.15E+01	9.22E+01
IGFBP6	3.73E-06	3.40E-04	1.85E-01	-5.40E+00	3.02E+01	1.63E+02
CMBL	3.78E-06	3.42E-04	1.88E-01	-5.33E+00	2.55E+01	1.36E+02
POMK	3.78E-06	3.42E-04	6.66E-01	-1.50E+00	1.71E+02	2.56E+02
PRSS1	3.82E-06	3.43E-04	1.03E-04	-9.71E+03	1.95E-05	1.89E-01
AL662797.1	3.84E-06	3.44E-04	4.50E+00	4.50E+00	1.07E+01	2.37E+00
CCDC80	3.94E-06	3.51E-04	2.57E-01	-3.88E+00	5.34E+01	2.08E+02
CTHRC1	3.99E-06	3.54E-04	4.06E-02	-2.46E+01	7.15E-01	1.76E+01

MMRN1	4.05E-06	3.57E-04	9.15E-02	-1.09E+01	2.81E+00	3.07E+01
LHFPL2	4.05E-06	3.57E-04	2.31E-01	-4.32E+00	2.55E+01	1.10E+02
PTPRH	4.20E-06	3.68E-04	4.28E-02	-2.33E+01	2.78E+00	6.50E+01
TNIP1	4.22E-06	3.69E-04	1.58E+00	1.58E+00	4.20E+03	2.65E+03
FREM2	4.42E-06	3.84E-04	3.16E-02	-3.17E+01	2.32E-01	7.35E+00
TRIM31	4.61E-06	3.99E-04	2.18E-02	-4.59E+01	7.11E-01	3.27E+01
PLCD4	4.68E-06	4.03E-04	4.62E-01	-2.17E+00	2.07E+01	4.49E+01
CNN1	4.78E-06	4.10E-04	9.15E-03	-1.09E+02	3.83E-01	4.18E+01
GIMAP7	4.80E-06	4.10E-04	3.44E-01	-2.91E+00	2.54E+01	7.39E+01
FBN1	4.85E-06	4.12E-04	1.93E-01	-5.18E+00	1.60E+01	8.27E+01
GNE	4.89E-06	4.14E-04	2.70E+00	2.70E+00	1.68E+03	6.22E+02
CXCL6	4.94E-06	4.15E-04	2.85E-02	-3.51E+01	1.08E+00	3.78E+01
ADAMTS15	4.94E-06	4.15E-04	1.11E-01	-8.99E+00	3.79E+00	3.41E+01
RFTN2	5.07E-06	4.24E-04	1.83E-01	-5.46E+00	1.97E+00	1.08E+01
SLC16A4	5.15E-06	4.29E-04	6.23E-02	-1.61E+01	7.23E-01	1.16E+01
CHN1	5.40E-06	4.48E-04	2.32E-01	-4.31E+00	6.38E+00	2.75E+01
COL1A1	5.51E-06	4.55E-04	1.66E-01	-6.02E+00	9.96E+01	5.99E+02
NR1D1	5.55E-06	4.56E-04	5.00E+00	5.00E+00	1.64E+03	3.28E+02
IGF2	5.69E-06	4.66E-04	1.47E-01	-6.82E+00	4.61E+00	3.14E+01
CA9	5.83E-06	4.76E-04	1.43E-02	-7.00E+01	5.63E-01	3.94E+01
AL049555.1	5.96E-06	4.83E-04	1.19E-02	-8.42E+01	5.19E-01	4.37E+01
CARMN	5.97E-06	4.83E-04	1.85E-01	-5.42E+00	6.13E+00	3.32E+01
ADAMTS4	6.00E-06	4.83E-04	7.27E-02	-1.38E+01	7.08E-01	9.74E+00
TMPRSS3	6.21E-06	4.98E-04	2.65E-02	-3.77E+01	6.44E-01	2.43E+01
DCTN1	6.26E-06	5.00E-04	1.34E+00	1.34E+00	2.15E+03	1.60E+03
LBX2-AS1	6.30E-06	5.02E-04	1.21E-01	-8.30E+00	1.30E+00	1.08E+01
TGFB3	6.43E-06	5.08E-04	4.19E-01	-2.39E+00	3.28E+01	7.81E+01
CDH11	6.43E-06	5.08E-04	1.59E-01	-6.30E+00	7.70E+00	4.85E+01
ERN2	6.64E-06	5.21E-04	1.28E-02	-7.82E+01	5.99E-01	4.68E+01
IGHV3-48	6.66E-06	5.21E-04	3.45E-03	-2.90E+02	1.12E-01	3.24E+01
ROR2	6.68E-06	5.21E-04	1.42E-01	-7.02E+00	3.30E+00	2.31E+01
MYL9	6.75E-06	5.25E-04	1.76E-01	-5.68E+00	3.70E+01	2.10E+02
QRFPR	6.81E-06	5.25E-04	3.99E-02	-2.51E+01	2.98E-01	7.48E+00
CADPS2	6.82E-06	5.25E-04	2.86E-01	-3.50E+00	2.22E+01	7.77E+01
MYLK	6.83E-06	5.25E-04	2.06E-01	-4.85E+00	3.58E+01	1.74E+02
GCNT2	6.94E-06	5.31E-04	5.55E-01	-1.80E+00	9.19E+01	1.66E+02
SAP30-DT	7.06E-06	5.39E-04	3.91E-01	-2.56E+00	4.59E+00	1.18E+01
COL3A1	7.21E-06	5.48E-04	1.69E-01	-5.90E+00	2.51E+02	1.48E+03
VPS52	7.31E-06	5.53E-04	1.42E+00	1.42E+00	9.84E+02	6.93E+02

ELF3	7.37E-06	5.56E-04	1.92E+00	1.92E+00	1.14E+04	5.95E+03
HMGA2	7.45E-06	5.58E-04	1.27E-01	-7.89E+00	3.61E+00	2.85E+01
PER3	7.45E-06	5.58E-04	3.08E+00	3.08E+00	1.47E+03	4.77E+02
RNF122	7.50E-06	5.59E-04	4.55E-01	-2.20E+00	1.30E+01	2.86E+01
WFDC2	7.52E-06	5.59E-04	2.05E-02	-4.88E+01	8.58E-01	4.19E+01
OSMR	7.55E-06	5.59E-04	6.17E-01	-1.62E+00	1.98E+02	3.21E+02
SLIT3	7.58E-06	5.59E-04	2.14E-01	-4.68E+00	1.04E+01	4.88E+01
FOXD1	7.69E-06	5.65E-04	1.18E-01	-8.45E+00	1.36E+00	1.15E+01
FOXF2	7.73E-06	5.66E-04	1.34E-01	-7.47E+00	2.83E+00	2.12E+01
FCF1	7.81E-06	5.70E-04	8.01E-01	-1.25E+00	4.41E+02	5.51E+02
ATP6AP1	7.84E-06	5.70E-04	1.40E+00	1.40E+00	1.66E+03	1.18E+03
DNAJC22	8.25E-06	5.96E-04	1.86E-02	-5.38E+01	3.83E-01	2.06E+01
PAX5	8.28E-06	5.96E-04	2.87E-02	-3.49E+01	2.32E-01	8.09E+00
NFIL3	8.31E-06	5.96E-04	4.27E-01	-2.34E+00	1.09E+02	2.55E+02
KRT14	8.32E-06	5.96E-04	1.41E-01	-7.09E+00	3.04E+03	2.15E+04
MUC3A	8.38E-06	5.98E-04	4.44E-03	-2.25E+02	1.27E-01	2.85E+01
C1S	8.40E-06	5.98E-04	2.53E-01	-3.96E+00	1.17E+02	4.63E+02
FCGR3A	8.53E-06	6.03E-04	1.42E-01	-7.05E+00	7.85E+00	5.54E+01
SLC7A7	8.53E-06	6.03E-04	1.69E-01	-5.90E+00	6.39E+00	3.77E+01
RCAN2	8.61E-06	6.06E-04	2.29E-01	-4.36E+00	1.10E+01	4.79E+01
SNX33	8.67E-06	6.08E-04	1.55E+00	1.55E+00	2.32E+03	1.50E+03
EBF1	8.73E-06	6.10E-04	2.31E-01	-4.33E+00	4.86E+00	2.10E+01
ELAPOR1	8.85E-06	6.16E-04	7.42E-02	-1.35E+01	6.67E+00	8.98E+01
AL139099.1	8.91E-06	6.18E-04	4.15E+00	4.15E+00	7.83E+00	1.89E+00
LINC01232	8.96E-06	6.20E-04	2.81E-01	-3.56E+00	6.98E+00	2.49E+01
BAIAP2	9.21E-06	6.35E-04	1.81E+00	1.81E+00	2.56E+03	1.42E+03
THY1	9.32E-06	6.40E-04	1.53E-01	-6.53E+00	1.34E+01	8.71E+01
PAK4	9.43E-06	6.45E-04	1.45E+00	1.45E+00	7.51E+02	5.19E+02
ADAMTSL4-AS1	9.44E-06	6.45E-04	2.48E+00	2.48E+00	2.16E+01	8.70E+00
MED24	9.52E-06	6.46E-04	1.29E+00	1.29E+00	6.40E+02	4.97E+02
CTTN	9.53E-06	6.46E-04	1.26E+00	1.26E+00	4.59E+03	3.65E+03
YY1AP1	9.67E-06	6.54E-04	1.37E+00	1.37E+00	1.41E+03	1.03E+03
HSD17B2	9.78E-06	6.58E-04	6.85E-02	-1.46E+01	3.18E+00	4.63E+01
MDM2	9.89E-06	6.64E-04	8.04E-01	-1.24E+00	7.98E+02	9.94E+02
CYSTM1	9.93E-06	6.64E-04	1.20E-01	-8.30E+00	3.45E+01	2.86E+02
PPP2R1A	1.00E-05	6.65E-04	1.48E+00	1.48E+00	3.41E+03	2.30E+03
CCDC68	1.00E-05	6.65E-04	1.89E-01	-5.29E+00	1.27E+01	6.71E+01
SLC25A21	1.00E-05	6.65E-04	2.14E+00	2.14E+00	2.92E+01	1.37E+01
MAP2K6	1.01E-05	6.66E-04	5.65E-01	-1.77E+00	1.16E+02	2.05E+02

FLNC	1.01E-05	6.67E-04	1.78E-01	-5.62E+00	5.87E+00	3.30E+01
ZFYVE1	1.04E-05	6.80E-04	1.67E+00	1.67E+00	9.59E+02	5.76E+02
UBA1	1.04E-05	6.80E-04	1.41E+00	1.41E+00	4.00E+03	2.83E+03
KRT20	1.04E-05	6.80E-04	1.56E-02	-6.42E+01	1.39E+00	8.92E+01
SULT1C2	1.06E-05	6.87E-04	7.27E-03	-1.38E+02	3.67E-01	5.05E+01
CDK6	1.06E-05	6.89E-04	5.76E-01	-1.74E+00	2.88E+02	5.01E+02
NFIB	1.07E-05	6.91E-04	6.32E-01	-1.58E+00	3.45E+02	5.45E+02
NRCAM	1.08E-05	6.95E-04	1.73E-01	-5.77E+00	3.25E+00	1.88E+01
TBX3	1.11E-05	7.09E-04	3.80E-01	-2.63E+00	3.28E+01	8.64E+01
UNC13D	1.12E-05	7.17E-04	1.65E+00	1.65E+00	9.79E+02	5.95E+02
NRP2	1.15E-05	7.32E-04	3.21E-01	-3.12E+00	3.98E+01	1.24E+02
BCAR3	1.18E-05	7.51E-04	1.95E+00	1.95E+00	4.35E+02	2.23E+02
BMERB1	1.20E-05	7.60E-04	1.85E-01	-5.40E+00	5.79E+00	3.13E+01
CSNK1D	1.21E-05	7.61E-04	1.37E+00	1.37E+00	2.07E+03	1.51E+03
TPM1	1.23E-05	7.75E-04	2.45E-01	-4.08E+00	1.08E+02	4.42E+02
TFEC	1.24E-05	7.80E-04	2.32E-01	-4.31E+00	4.42E+00	1.91E+01
PRUNE2	1.25E-05	7.82E-04	4.64E-02	-2.16E+01	1.22E+00	2.62E+01
AEBP1	1.27E-05	7.90E-04	1.80E-01	-5.54E+00	1.88E+01	1.04E+02
GSN	1.28E-05	7.93E-04	1.50E+00	1.50E+00	8.32E+03	5.54E+03
AKR1B10	1.29E-05	7.99E-04	4.19E-01	-2.39E+00	1.33E+03	3.17E+03
MFAP4	1.31E-05	8.12E-04	1.92E-01	-5.20E+00	2.04E+01	1.06E+02
AC024592.2	1.32E-05	8.12E-04	2.85E+00	2.85E+00	1.52E+02	5.34E+01
ADCY9	1.35E-05	8.24E-04	1.77E+00	1.77E+00	4.46E+02	2.52E+02
TGM2	1.35E-05	8.24E-04	1.02E-01	-9.81E+00	9.90E+00	9.71E+01
AC010422.3	1.36E-05	8.32E-04	4.81E-01	-2.08E+00	1.80E+01	3.73E+01
IGLV1-40	1.40E-05	8.49E-04	8.76E-03	-1.14E+02	1.27E+00	1.45E+02
NCAM1	1.44E-05	8.73E-04	6.80E-02	-1.47E+01	7.50E-01	1.10E+01
TENT5C	1.45E-05	8.73E-04	1.11E-01	-9.03E+00	1.71E+01	1.54E+02
PRDM1	1.45E-05	8.73E-04	1.90E+00	1.90E+00	3.58E+03	1.88E+03
STK24	1.48E-05	8.87E-04	1.61E+00	1.61E+00	7.73E+03	4.80E+03
CFH	1.49E-05	8.91E-04	2.93E-01	-3.42E+00	1.34E+02	4.58E+02
C2orf16	1.50E-05	8.97E-04	4.25E+00	4.25E+00	7.72E+01	1.82E+01
USP11	1.56E-05	9.27E-04	1.40E+00	1.40E+00	3.02E+02	2.15E+02
RARRES1	1.58E-05	9.37E-04	3.13E-02	-3.20E+01	6.13E-01	1.96E+01
TMEM127	1.59E-05	9.40E-04	1.58E+00	1.58E+00	2.81E+03	1.78E+03
KAZALD1	1.59E-05	9.40E-04	2.11E-01	-4.74E+00	6.97E+00	3.31E+01
RAB7A	1.61E-05	9.46E-04	1.31E+00	1.31E+00	4.27E+03	3.27E+03
IGFBP7	1.62E-05	9.49E-04	3.28E-01	-3.05E+00	8.73E+01	2.66E+02
SNAP29	1.64E-05	9.57E-04	1.36E+00	1.36E+00	7.49E+02	5.49E+02

MIR100HG	1.65E-05	9.60E-04	3.72E-01	-2.69E+00	2.23E+01	5.99E+01
AC024560.5	1.66E-05	9.63E-04	5.40E+00	5.40E+00	8.47E+00	1.57E+00
SERTAD2	1.66E-05	9.65E-04	1.90E+00	1.90E+00	2.54E+03	1.34E+03
CXCL14	1.68E-05	9.69E-04	3.65E-01	-2.74E+00	6.96E+02	1.91E+03
TCF4	1.68E-05	9.70E-04	6.22E-01	-1.61E+00	2.58E+02	4.15E+02
ERH	1.70E-05	9.72E-04	7.01E-01	-1.43E+00	5.82E+02	8.30E+02
SLC4A7	1.70E-05	9.72E-04	5.44E-01	-1.84E+00	1.16E+02	2.14E+02
ADRA2A	1.71E-05	9.74E-04	1.45E-01	-6.87E+00	4.47E+00	3.07E+01
VCAM1	1.71E-05	9.74E-04	1.60E-01	-6.25E+00	6.54E+00	4.09E+01
SMARCA4	1.72E-05	9.77E-04	1.51E+00	1.51E+00	3.03E+03	2.00E+03
CACNA1C	1.72E-05	9.77E-04	2.43E-01	-4.11E+00	5.33E+00	2.19E+01
COL4A6	1.73E-05	9.79E-04	2.47E-01	-4.05E+00	8.00E+00	3.24E+01
JAM2	1.76E-05	9.90E-04	4.00E-01	-2.50E+00	2.53E+01	6.33E+01
RELA	1.80E-05	1.01E-03	1.27E+00	1.27E+00	9.39E+02	7.38E+02
MIA	1.81E-05	1.02E-03	1.94E-02	-5.15E+01	1.81E-01	9.32E+00
MAB21L1	1.84E-05	1.03E-03	3.44E-02	-2.90E+01	1.81E-01	5.25E+00
RAB20	1.84E-05	1.03E-03	1.32E-01	-7.58E+00	6.14E+00	4.66E+01
NNMT	1.85E-05	1.03E-03	9.38E-02	-1.07E+01	2.39E+00	2.55E+01
LPCAT1	1.87E-05	1.04E-03	2.89E-01	-3.46E+00	6.30E+01	2.18E+02
MSRB3	1.88E-05	1.04E-03	2.34E-01	-4.28E+00	1.50E+01	6.44E+01
ADAMTS1	1.88E-05	1.04E-03	2.49E-01	-4.01E+00	2.15E+01	8.61E+01
MLPH	1.91E-05	1.05E-03	1.55E-01	-6.43E+00	2.58E+01	1.66E+02
TEK	1.96E-05	1.07E-03	3.36E-01	-2.98E+00	1.20E+01	3.57E+01
F5	1.96E-05	1.07E-03	4.90E-02	-2.04E+01	1.11E+00	2.27E+01
IFNE	1.97E-05	1.07E-03	2.25E-01	-4.44E+00	3.87E+00	1.72E+01
HOXD8	1.97E-05	1.07E-03	4.18E-01	-2.39E+00	5.86E+00	1.40E+01
AL136084.1	1.99E-05	1.08E-03	7.90E+00	7.90E+00	1.54E+01	1.95E+00
SEL1L3	2.02E-05	1.09E-03	2.18E-01	-4.60E+00	6.59E+01	3.03E+02
CD200	2.05E-05	1.10E-03	2.86E-01	-3.49E+00	5.95E+00	2.08E+01
PRSS12	2.07E-05	1.12E-03	4.97E-01	-2.01E+00	6.12E+01	1.23E+02
CTNNA1	2.09E-05	1.12E-03	1.45E+00	1.45E+00	1.06E+04	7.25E+03
FKBP5	2.09E-05	1.12E-03	1.81E+00	1.81E+00	7.96E+02	4.40E+02
MROH6	2.16E-05	1.15E-03	2.40E+00	2.40E+00	1.59E+03	6.62E+02
EMILIN1	2.22E-05	1.18E-03	1.69E-01	-5.93E+00	1.15E+01	6.85E+01
ANTXR2	2.24E-05	1.19E-03	2.10E-01	-4.75E+00	2.08E+01	9.89E+01
PROCR	2.28E-05	1.20E-03	2.97E-01	-3.36E+00	1.31E+01	4.40E+01
CRY2	2.29E-05	1.21E-03	1.59E+00	1.59E+00	3.58E+02	2.24E+02
PITX2	2.33E-05	1.23E-03	1.70E-01	-5.90E+00	4.82E+00	2.84E+01
ARHGEF18	2.35E-05	1.23E-03	1.53E+00	1.53E+00	1.36E+03	8.87E+02

CFAP251	2.37E-05	1.24E-03	2.09E-01	-4.79E+00	5.26E+00	2.52E+01
ZEB2	2.43E-05	1.27E-03	2.38E-01	-4.20E+00	3.01E+01	1.26E+02
MMP7	2.49E-05	1.30E-03	2.20E-02	-4.55E+01	1.09E+00	4.95E+01
ZFP36	2.54E-05	1.32E-03	2.12E+00	2.12E+00	5.43E+03	2.57E+03
TTC7A	2.66E-05	1.38E-03	1.38E+00	1.38E+00	1.02E+03	7.43E+02
B3GAT2	2.68E-05	1.39E-03	2.95E+00	2.95E+00	1.89E+01	6.40E+00
AC007191.1	2.73E-05	1.41E-03	3.53E-01	-2.83E+00	5.26E+00	1.49E+01
TESC	2.76E-05	1.42E-03	9.14E-02	-1.09E+01	2.84E+00	3.11E+01
CCDC85C	2.77E-05	1.42E-03	1.55E+00	1.55E+00	1.75E+03	1.12E+03
SHH	2.78E-05	1.42E-03	1.81E-02	-5.53E+01	2.32E-01	1.28E+01
GRN	2.80E-05	1.43E-03	1.65E+00	1.65E+00	9.14E+03	5.55E+03
GJC1	2.84E-05	1.45E-03	2.56E-01	-3.91E+00	7.28E+00	2.85E+01
FEZ1	2.85E-05	1.45E-03	1.41E-01	-7.07E+00	2.83E+00	2.00E+01
PNPLA6	2.87E-05	1.45E-03	1.54E+00	1.54E+00	8.53E+02	5.55E+02
KCNK3	2.89E-05	1.46E-03	7.70E-02	-1.30E+01	7.59E-01	9.86E+00
LINC00294	2.97E-05	1.50E-03	6.34E-01	-1.58E+00	5.95E+01	9.40E+01
ASRGL1	2.99E-05	1.51E-03	9.83E-02	-1.02E+01	2.35E+00	2.39E+01
TICAM1	3.01E-05	1.51E-03	2.20E+00	2.20E+00	1.79E+03	8.14E+02
AL357033.3	3.01E-05	1.51E-03	3.07E+00	3.07E+00	6.96E+01	2.26E+01
TMEM140	3.03E-05	1.51E-03	1.60E-01	-6.27E+00	5.08E+00	3.19E+01
CELSR1	3.05E-05	1.52E-03	1.88E+00	1.88E+00	2.81E+03	1.50E+03
PCDH18	3.06E-05	1.52E-03	2.89E-01	-3.46E+00	1.63E+01	5.64E+01
WFDC1	3.08E-05	1.53E-03	1.33E-01	-7.50E+00	2.67E+00	2.01E+01
F2R	3.13E-05	1.54E-03	3.06E-01	-3.26E+00	2.54E+01	8.29E+01
RWDD3	3.14E-05	1.54E-03	6.69E-01	-1.49E+00	4.31E+01	6.43E+01
PER2	3.14E-05	1.54E-03	1.94E+00	1.94E+00	5.48E+02	2.83E+02
SERPINB4	3.15E-05	1.54E-03	2.85E-01	-3.51E+00	1.75E+03	6.13E+03
SRSF2	3.15E-05	1.54E-03	1.20E+00	1.20E+00	2.25E+03	1.86E+03
SPINT1	3.16E-05	1.54E-03	1.79E+00	1.79E+00	9.06E+03	5.07E+03
COL6A3	3.21E-05	1.56E-03	1.93E-01	-5.18E+00	7.91E+01	4.09E+02
LGALS1	3.22E-05	1.56E-03	2.75E-01	-3.64E+00	6.32E+01	2.30E+02
GNG11	3.24E-05	1.57E-03	3.62E-01	-2.76E+00	2.57E+01	7.10E+01
IFI44L	3.24E-05	1.57E-03	1.97E-01	-5.07E+00	1.34E+01	6.77E+01
CSGALNACT1	3.26E-05	1.57E-03	2.66E-01	-3.75E+00	1.86E+01	6.99E+01
CASK	3.27E-05	1.57E-03	6.72E-01	-1.49E+00	3.49E+02	5.19E+02
FGF10	3.29E-05	1.58E-03	3.86E-02	-2.59E+01	2.98E-01	7.72E+00
KIZ	3.29E-05	1.58E-03	5.10E-01	-1.96E+00	7.83E+01	1.53E+02
PGPEP1	3.33E-05	1.59E-03	3.13E-01	-3.19E+00	3.52E+01	1.12E+02
TMEM176A	3.35E-05	1.60E-03	1.57E-01	-6.37E+00	8.53E+00	5.43E+01

MYO1D	3.36E-05	1.60E-03	1.37E+00	1.37E+00	2.25E+03	1.65E+03
FER1L4	3.41E-05	1.62E-03	1.53E-01	-6.54E+00	1.25E+01	8.16E+01
DOCK11	3.43E-05	1.62E-03	3.41E-01	-2.93E+00	2.71E+01	7.94E+01
EDN2	3.49E-05	1.65E-03	4.84E+00	4.84E+00	3.57E+02	7.37E+01
ABHD12	3.54E-05	1.67E-03	1.63E+00	1.63E+00	1.28E+03	7.85E+02
PNPLA1	3.55E-05	1.67E-03	3.53E-02	-2.83E+01	1.81E-01	5.13E+00
AC025171.1	3.57E-05	1.67E-03	2.82E-01	-3.54E+00	7.81E+00	2.77E+01
HOXA9	3.58E-05	1.67E-03	1.33E-01	-7.49E+00	5.28E+00	3.96E+01
CCNA1	3.63E-05	1.69E-03	3.47E-02	-2.88E+01	2.98E-01	8.60E+00
SPECC1	3.66E-05	1.70E-03	1.88E+00	1.88E+00	9.65E+02	5.13E+02
SAA1	3.70E-05	1.72E-03	6.30E-02	-1.59E+01	1.92E+00	3.04E+01
TMEM45A	3.72E-05	1.72E-03	3.23E-01	-3.09E+00	5.85E+01	1.81E+02
ZSCAN31	3.75E-05	1.74E-03	5.21E-01	-1.92E+00	1.25E+02	2.39E+02
SERPINA4	3.78E-05	1.74E-03	3.65E-04	-2.74E+03	2.92E-06	8.00E-03
RECQL4	3.81E-05	1.75E-03	2.80E+00	2.80E+00	5.66E+02	2.02E+02
AC027290.1	3.82E-05	1.75E-03	8.71E+00	8.71E+00	8.53E+00	9.79E-01
ANXA11	3.83E-05	1.76E-03	1.75E+00	1.75E+00	7.10E+03	4.07E+03
HTRA1	3.85E-05	1.76E-03	3.96E-01	-2.53E+00	5.50E+01	1.39E+02
PRAP1	3.85E-05	1.76E-03	1.05E-04	-9.53E+03	1.46E-05	1.39E-01
ANXA2R	3.88E-05	1.76E-03	2.44E-01	-4.09E+00	3.18E+00	1.30E+01
IGF1	3.95E-05	1.80E-03	1.87E-01	-5.33E+00	5.45E+00	2.91E+01
NAGA	3.99E-05	1.81E-03	1.29E+00	1.29E+00	3.86E+02	3.00E+02
LRRC32	4.00E-05	1.81E-03	2.31E-01	-4.34E+00	8.59E+00	3.73E+01
FCN1	4.01E-05	1.81E-03	6.48E-02	-1.54E+01	1.18E+00	1.82E+01
RENBP	4.04E-05	1.82E-03	1.01E-01	-9.90E+00	1.19E+00	1.17E+01
VCAN	4.12E-05	1.85E-03	1.22E-01	-8.19E+00	1.23E+01	1.01E+02
AC018557.1	4.13E-05	1.85E-03	3.72E+00	3.72E+00	1.19E+01	3.19E+00
TMEM263	4.13E-05	1.85E-03	3.74E-01	-2.68E+00	6.22E+01	1.67E+02
GDPD5	4.16E-05	1.86E-03	2.10E-01	-4.76E+00	2.52E+00	1.20E+01
VASN	4.18E-05	1.86E-03	2.25E+00	2.25E+00	1.01E+03	4.48E+02
CCND1	4.19E-05	1.86E-03	1.57E+00	1.57E+00	5.00E+03	3.19E+03
FAM13C	4.20E-05	1.86E-03	5.05E-01	-1.98E+00	2.64E+01	5.22E+01
CLEC7A	4.22E-05	1.87E-03	3.51E-01	-2.85E+00	5.77E+01	1.65E+02
RMRP	4.24E-05	1.87E-03	2.32E-01	-4.31E+00	6.70E+00	2.89E+01
AC025171.4	4.28E-05	1.88E-03	8.14E-02	-1.23E+01	2.32E-01	2.85E+00
TIMP1	4.60E-05	2.02E-03	2.28E-01	-4.39E+00	6.34E+01	2.78E+02
PIP5K1B	4.64E-05	2.03E-03	1.05E-01	-9.57E+00	3.25E+00	3.11E+01
ACOT11	4.70E-05	2.05E-03	1.51E+00	1.51E+00	7.28E+02	4.82E+02
CES1	4.72E-05	2.06E-03	5.24E+00	5.24E+00	3.38E+03	6.45E+02

TMEM176B	4.73E-05	2.06E-03	1.86E-01	-5.38E+00	1.90E+01	1.02E+02
CDS2	4.74E-05	2.06E-03	7.49E-01	-1.33E+00	2.72E+02	3.63E+02
KCTD21	4.77E-05	2.07E-03	1.32E+00	1.32E+00	3.94E+02	2.99E+02
HMOX1	4.82E-05	2.08E-03	2.20E+00	2.20E+00	1.69E+03	7.66E+02
DTX2	4.88E-05	2.11E-03	1.87E+00	1.87E+00	1.87E+03	1.00E+03
BCAT1	4.91E-05	2.11E-03	1.66E-01	-6.01E+00	1.50E+01	9.03E+01
ZBTB20	4.93E-05	2.12E-03	4.59E-01	-2.18E+00	6.17E+01	1.34E+02
TIPARP	4.99E-05	2.14E-03	1.74E+00	1.74E+00	1.68E+03	9.66E+02
FBLIM1	5.05E-05	2.15E-03	4.60E-01	-2.17E+00	1.85E+02	4.02E+02
SPDEF	5.05E-05	2.15E-03	1.78E-02	-5.61E+01	2.32E-01	1.30E+01
UBE2R2	5.06E-05	2.15E-03	1.36E+00	1.36E+00	1.65E+03	1.22E+03
TTC7B	5.07E-05	2.15E-03	3.70E-01	-2.70E+00	1.30E+01	3.51E+01
TRIP10	5.08E-05	2.15E-03	2.03E+00	2.03E+00	7.38E+03	3.63E+03
TFPI	5.08E-05	2.15E-03	3.35E-01	-2.98E+00	3.31E+01	9.86E+01
AC005261.1	5.17E-05	2.18E-03	6.29E-01	-1.59E+00	1.77E+02	2.81E+02
MISP	5.23E-05	2.21E-03	6.24E-02	-1.60E+01	5.06E+00	8.10E+01
CTSC	5.28E-05	2.22E-03	5.00E-01	-2.00E+00	5.80E+02	1.16E+03
AIFM2	5.29E-05	2.22E-03	2.15E+00	2.15E+00	7.01E+02	3.26E+02
DEAF1	5.29E-05	2.22E-03	1.60E+00	1.60E+00	4.72E+02	2.95E+02
HNF4G	5.31E-05	2.22E-03	1.49E-01	-6.72E+00	5.84E+00	3.93E+01
LMO7	5.35E-05	2.23E-03	2.08E+00	2.08E+00	1.73E+04	8.30E+03
GJA4	5.36E-05	2.23E-03	2.41E-01	-4.15E+00	3.77E+00	1.56E+01
RAMP3	5.40E-05	2.24E-03	2.78E-01	-3.60E+00	1.50E+01	5.38E+01
GDA	5.41E-05	2.24E-03	8.66E-02	-1.15E+01	1.86E+00	2.14E+01
PXDN	5.43E-05	2.25E-03	2.46E-01	-4.06E+00	2.24E+01	9.11E+01
TNFRSF10B	5.50E-05	2.27E-03	5.43E-01	-1.84E+00	1.52E+02	2.80E+02
SH3TC1	5.52E-05	2.27E-03	1.90E+00	1.90E+00	6.19E+02	3.26E+02
FBLN5	5.56E-05	2.28E-03	2.00E-01	-5.00E+00	5.43E+00	2.71E+01
C8orf82	5.56E-05	2.28E-03	2.05E+00	2.05E+00	5.41E+02	2.64E+02
FSTL1	5.58E-05	2.28E-03	3.29E-01	-3.04E+00	1.28E+02	3.88E+02
LRP10	5.64E-05	2.30E-03	1.49E+00	1.49E+00	8.32E+03	5.58E+03
HNF4A	5.73E-05	2.34E-03	2.98E-02	-3.36E+01	1.02E+00	3.43E+01
SGCE	5.79E-05	2.35E-03	1.11E-01	-9.00E+00	1.54E+00	1.38E+01
INSYN1-AS1	5.80E-05	2.35E-03	3.25E+00	3.25E+00	1.30E+01	3.98E+00
NFKBIA	5.80E-05	2.35E-03	1.92E+00	1.92E+00	2.87E+03	1.50E+03
TRIM58	5.80E-05	2.35E-03	1.26E-01	-7.95E+00	1.56E+00	1.24E+01
PLCE1	5.81E-05	2.35E-03	2.62E-01	-3.82E+00	1.56E+01	5.97E+01
MED25	5.87E-05	2.37E-03	1.35E+00	1.35E+00	6.28E+02	4.67E+02
FRZB	5.89E-05	2.37E-03	1.73E-01	-5.78E+00	2.43E+00	1.40E+01

SCNN1A	5.90E-05	2.37E-03	1.51E+00	1.51E+00	3.99E+03	2.65E+03
PFKL	5.91E-05	2.37E-03	1.50E+00	1.50E+00	3.25E+03	2.17E+03
ETF1	5.98E-05	2.39E-03	1.34E+00	1.34E+00	3.81E+03	2.85E+03
MAP1S	6.04E-05	2.41E-03	2.31E+00	2.31E+00	2.09E+02	9.06E+01
CTNNAL1	6.08E-05	2.42E-03	2.38E+00	2.38E+00	1.08E+03	4.53E+02
DNM2	6.10E-05	2.42E-03	1.38E+00	1.38E+00	2.63E+03	1.91E+03
ABALON	6.13E-05	2.43E-03	4.07E+00	4.07E+00	6.97E+00	1.71E+00
AL158206.1	6.19E-05	2.45E-03	3.38E-01	-2.96E+00	3.51E+01	1.04E+02
ACTN4P1	6.26E-05	2.47E-03	1.72E+00	1.72E+00	6.60E+01	3.84E+01
PLAUR	6.29E-05	2.48E-03	1.52E-01	-6.57E+00	1.71E+01	1.12E+02
DDR2	6.35E-05	2.50E-03	2.69E-01	-3.71E+00	2.32E+01	8.60E+01
WWP2	6.36E-05	2.50E-03	1.34E+00	1.34E+00	9.18E+02	6.84E+02
KIF3C	6.40E-05	2.51E-03	5.11E-01	-1.96E+00	2.14E+01	4.18E+01
SYT13	6.48E-05	2.54E-03	2.55E-02	-3.92E+01	2.32E-01	9.11E+00
DTX2P1	6.52E-05	2.54E-03	2.54E+00	2.54E+00	7.19E+01	2.83E+01
FHL1	6.53E-05	2.55E-03	2.69E-01	-3.72E+00	3.23E+01	1.20E+02
HABP2	6.57E-05	2.55E-03	1.26E-02	-7.92E+01	1.81E-01	1.43E+01
MYO1A	6.60E-05	2.56E-03	4.66E-02	-2.15E+01	1.45E+00	3.11E+01
QRICH1	6.63E-05	2.57E-03	1.27E+00	1.27E+00	8.32E+02	6.56E+02
SH3GL1	6.65E-05	2.57E-03	1.81E+00	1.81E+00	5.36E+03	2.96E+03
PGDP1	6.82E-05	2.63E-03	1.77E+00	1.77E+00	9.77E+01	5.53E+01
CXCL9	6.85E-05	2.64E-03	1.51E-01	-6.64E+00	1.02E+01	6.76E+01
CREB3L1	6.88E-05	2.65E-03	4.63E-02	-2.16E+01	3.44E+00	7.43E+01
AL359922.3	6.90E-05	2.65E-03	3.16E-01	-3.16E+00	3.49E+00	1.10E+01
NEDD4L	6.99E-05	2.68E-03	1.80E+00	1.80E+00	7.86E+02	4.36E+02
P2RX4	7.00E-05	2.68E-03	3.10E-01	-3.23E+00	2.23E+01	7.19E+01
NCK2	7.04E-05	2.69E-03	1.63E+00	1.63E+00	2.55E+03	1.57E+03
SEC14L1	7.09E-05	2.70E-03	1.71E+00	1.71E+00	1.79E+03	1.05E+03
TNFSF18	7.15E-05	2.72E-03	5.80E-02	-1.72E+01	2.04E+00	3.52E+01
ATP6V0A4	7.24E-05	2.74E-03	2.77E+00	2.77E+00	4.21E+02	1.52E+02
SLC7A11	7.25E-05	2.74E-03	3.13E-01	-3.20E+00	5.11E+01	1.63E+02
KIAA1191	7.31E-05	2.76E-03	1.34E+00	1.34E+00	1.54E+03	1.15E+03
CGAS	7.47E-05	2.81E-03	4.30E-01	-2.33E+00	2.93E+01	6.83E+01
DACH1	7.47E-05	2.81E-03	1.23E-01	-8.14E+00	1.45E+00	1.18E+01
ECM2	7.50E-05	2.82E-03	2.30E-01	-4.34E+00	3.87E+00	1.68E+01
AC025171.2	7.62E-05	2.86E-03	4.39E-01	-2.28E+00	1.28E+01	2.92E+01
OTUD5	7.69E-05	2.87E-03	1.28E+00	1.28E+00	6.38E+02	4.97E+02
FAM30A	7.70E-05	2.87E-03	3.16E-02	-3.17E+01	7.72E-01	2.44E+01
AC003681.1	7.71E-05	2.87E-03	3.96E+00	3.96E+00	1.81E+01	4.56E+00

CLDN10	7.72E-05	2.87E-03	4.30E+00	4.30E+00	2.46E+02	5.72E+01
LILRB2	7.72E-05	2.87E-03	1.33E-01	-7.51E+00	2.95E+00	2.22E+01
EGLN3	7.77E-05	2.88E-03	1.75E+00	1.75E+00	9.95E+02	5.70E+02
AC093484.3	7.79E-05	2.88E-03	3.33E+00	3.33E+00	8.35E+00	2.51E+00
ITGA8	7.80E-05	2.88E-03	2.40E-01	-4.16E+00	1.33E+01	5.55E+01
ATP6V1H	7.82E-05	2.89E-03	1.28E+00	1.28E+00	7.91E+02	6.17E+02
CAPN5	7.93E-05	2.92E-03	1.90E+00	1.90E+00	2.73E+03	1.44E+03
CAPN1	7.94E-05	2.92E-03	1.56E+00	1.56E+00	9.96E+03	6.40E+03
CAPN2	8.01E-05	2.94E-03	1.40E+00	1.40E+00	7.26E+03	5.18E+03
TPM2	8.10E-05	2.96E-03	2.77E-01	-3.61E+00	6.87E+01	2.48E+02
NUP42	8.11E-05	2.96E-03	7.58E-01	-1.32E+00	1.31E+02	1.73E+02
TPSB2	8.12E-05	2.96E-03	3.37E-01	-2.97E+00	4.38E+01	1.30E+02
HKDC1	8.29E-05	3.02E-03	7.63E-02	-1.31E+01	1.31E+00	1.71E+01
COL4A2	8.30E-05	3.02E-03	3.04E-01	-3.29E+00	9.80E+01	3.22E+02
CAPNS1	8.37E-05	3.03E-03	1.44E+00	1.44E+00	5.88E+03	4.07E+03
PHLDB3	8.39E-05	3.03E-03	1.94E+00	1.94E+00	9.03E+02	4.65E+02
AMBRA1	8.39E-05	3.03E-03	1.47E+00	1.47E+00	5.50E+02	3.75E+02
DZIP1	8.41E-05	3.03E-03	4.03E-01	-2.48E+00	2.17E+01	5.40E+01
KCNG1	8.45E-05	3.04E-03	2.09E+00	2.09E+00	1.48E+02	7.09E+01
AC006141.1	8.52E-05	3.06E-03	2.34E-01	-4.27E+00	3.48E+00	1.49E+01
BHLHE40	8.65E-05	3.10E-03	1.59E+00	1.59E+00	5.99E+03	3.77E+03
CD163	8.75E-05	3.13E-03	2.31E-01	-4.34E+00	1.15E+01	4.98E+01
HMOX2	8.76E-05	3.13E-03	1.55E+00	1.55E+00	1.66E+03	1.07E+03
OLFML1	8.81E-05	3.15E-03	1.14E-01	-8.74E+00	1.29E+00	1.13E+01
HOXA10-AS	8.83E-05	3.15E-03	3.50E-02	-2.86E+01	2.32E-01	6.63E+00
SFXN3	8.88E-05	3.16E-03	4.81E-01	-2.08E+00	5.43E+01	1.13E+02
ALG6	8.91E-05	3.17E-03	7.75E-01	-1.29E+00	1.26E+02	1.62E+02
CEP290	8.96E-05	3.18E-03	5.06E-01	-1.98E+00	7.28E+01	1.44E+02
ZG16B	8.99E-05	3.18E-03	8.93E-02	-1.12E+01	5.95E+00	6.67E+01
ADGRF5	9.05E-05	3.19E-03	4.57E-01	-2.19E+00	4.33E+01	9.47E+01
AC011497.2	9.06E-05	3.19E-03	1.87E+00	1.87E+00	3.38E+02	1.81E+02
CDC42SE2	9.12E-05	3.21E-03	5.35E-01	-1.87E+00	1.95E+02	3.65E+02
REP15	9.13E-05	3.21E-03	2.17E-01	-4.62E+00	6.61E+00	3.05E+01
ANK1	9.20E-05	3.23E-03	1.85E-01	-5.40E+00	4.03E+00	2.18E+01
SCARA5	9.41E-05	3.29E-03	2.07E-02	-4.84E+01	1.81E-01	8.75E+00
AC016747.1	9.51E-05	3.32E-03	5.19E-01	-1.93E+00	1.77E+01	3.40E+01
ZCCHC9	9.55E-05	3.33E-03	8.01E-01	-1.25E+00	2.48E+02	3.10E+02
RFTN1	9.63E-05	3.35E-03	3.10E-01	-3.22E+00	2.72E+01	8.78E+01
CD38	9.64E-05	3.35E-03	5.00E-01	-2.00E+00	3.82E+01	7.64E+01

ADAMDEC1	9.68E-05	3.36E-03	1.19E-01	-8.39E+00	1.74E+00	1.46E+01
MT-ND6	9.70E-05	3.36E-03	2.25E+00	2.25E+00	5.66E+02	2.51E+02
MAFF	9.70E-05	3.36E-03	2.20E+00	2.20E+00	2.55E+03	1.16E+03
PLA2G2F	9.72E-05	3.36E-03	3.28E-02	-3.04E+01	2.32E-01	7.07E+00
ZER1	1.00E-04	3.46E-03	1.30E+00	1.30E+00	6.80E+02	5.22E+02
C4B	1.01E-04	3.48E-03	2.34E-01	-4.27E+00	1.01E+01	4.33E+01
ZFAND3	1.01E-04	3.48E-03	1.26E+00	1.26E+00	1.06E+03	8.41E+02
AP2A2	1.01E-04	3.48E-03	1.24E+00	1.24E+00	5.41E+02	4.38E+02
ITGA5	1.02E-04	3.49E-03	2.84E-01	-3.52E+00	3.52E+01	1.24E+02
NT5E	1.04E-04	3.54E-03	1.84E-01	-5.42E+00	1.48E+01	8.04E+01
NMNAT3	1.04E-04	3.54E-03	5.53E-01	-1.81E+00	2.74E+01	4.96E+01
STRN4	1.04E-04	3.54E-03	1.32E+00	1.32E+00	1.01E+03	7.69E+02
DEFB103A	1.05E-04	3.58E-03	9.29E-02	-1.08E+01	5.08E+00	5.46E+01
COA1	1.06E-04	3.60E-03	8.42E-01	-1.19E+00	2.52E+02	2.99E+02
FAM214B	1.06E-04	3.60E-03	1.60E+00	1.60E+00	7.41E+02	4.62E+02
LIMD1-AS1	1.07E-04	3.60E-03	2.38E+00	2.38E+00	8.38E+00	3.52E+00
RAB6B	1.07E-04	3.60E-03	2.35E+00	2.35E+00	1.39E+02	5.94E+01
RFLNA	1.08E-04	3.63E-03	3.82E-02	-2.62E+01	1.28E+00	3.34E+01
MTDH	1.08E-04	3.63E-03	8.37E-01	-1.19E+00	1.89E+03	2.26E+03
CCRL2	1.08E-04	3.63E-03	6.88E-02	-1.45E+01	1.40E+00	2.03E+01
CERS6-AS1	1.09E-04	3.65E-03	2.87E+00	2.87E+00	1.82E+01	6.33E+00
PECAM1	1.09E-04	3.65E-03	3.15E-01	-3.17E+00	1.31E+02	4.16E+02
FRMD8P1	1.09E-04	3.65E-03	2.34E+00	2.34E+00	1.05E+01	4.46E+00
HGF	1.10E-04	3.67E-03	9.61E-02	-1.04E+01	1.28E+00	1.33E+01
PAXIP1-AS2	1.10E-04	3.68E-03	5.34E-01	-1.87E+00	3.20E+01	5.99E+01
FER1L6	1.11E-04	3.71E-03	1.28E-01	-7.81E+00	1.20E+01	9.38E+01
ZNF214	1.12E-04	3.72E-03	4.93E-01	-2.03E+00	1.23E+01	2.50E+01
ATP12A	1.12E-04	3.72E-03	3.86E+00	3.86E+00	8.88E+02	2.30E+02
PTBP2	1.12E-04	3.72E-03	6.79E-01	-1.47E+00	7.01E+01	1.03E+02
ADIPOR2	1.13E-04	3.74E-03	1.67E+00	1.67E+00	3.72E+03	2.23E+03
DDX60	1.14E-04	3.75E-03	2.56E-01	-3.90E+00	6.85E+01	2.67E+02
RSPO3	1.14E-04	3.75E-03	2.64E-02	-3.79E+01	1.81E-01	6.85E+00
LINC00888	1.14E-04	3.75E-03	1.12E-01	-8.90E+00	8.29E-01	7.37E+00
EHD4	1.14E-04	3.75E-03	1.44E+00	1.44E+00	1.02E+03	7.08E+02
NR2F2	1.15E-04	3.76E-03	3.89E-01	-2.57E+00	5.27E+01	1.35E+02
PLN	1.15E-04	3.78E-03	3.36E-02	-2.98E+01	2.98E-01	8.87E+00
IFIT3	1.16E-04	3.78E-03	2.64E-01	-3.78E+00	5.64E+01	2.13E+02
NEGR1	1.16E-04	3.79E-03	1.88E-01	-5.31E+00	3.19E+00	1.69E+01
RAB3C	1.17E-04	3.80E-03	4.22E-02	-2.37E+01	2.32E-01	5.50E+00

PMEPA1	1.17E-04	3.82E-03	3.02E-01	-3.31E+00	3.41E+01	1.13E+02
TPBG	1.18E-04	3.82E-03	6.43E-01	-1.56E+00	1.67E+02	2.60E+02
CDH6	1.20E-04	3.90E-03	2.35E-01	-4.25E+00	6.61E+00	2.81E+01
CLDN5	1.21E-04	3.93E-03	3.74E-01	-2.67E+00	1.24E+01	3.32E+01
TECR	1.23E-04	3.96E-03	1.62E+00	1.62E+00	3.13E+03	1.93E+03
AC114546.3	1.25E-04	4.04E-03	3.16E+00	3.16E+00	2.21E+01	6.98E+00
SERPING1	1.26E-04	4.04E-03	2.20E-01	-4.55E+00	4.61E+01	2.10E+02
HSPA2	1.27E-04	4.08E-03	2.10E+00	2.10E+00	1.43E+03	6.83E+02
THSD7A	1.27E-04	4.08E-03	3.62E-01	-2.77E+00	6.00E+00	1.66E+01
FERMT2	1.27E-04	4.09E-03	2.72E-01	-3.68E+00	1.35E+01	4.98E+01
PIP5K1C	1.29E-04	4.12E-03	1.52E+00	1.52E+00	7.15E+02	4.70E+02
FILIP1	1.30E-04	4.15E-03	1.96E-01	-5.11E+00	2.99E+00	1.53E+01
ACTG1	1.31E-04	4.18E-03	1.61E+00	1.61E+00	5.59E+04	3.48E+04
GORASP1	1.32E-04	4.22E-03	1.23E+00	1.23E+00	6.89E+02	5.60E+02
SMPD1	1.33E-04	4.22E-03	1.54E+00	1.54E+00	5.18E+02	3.37E+02
CAPN8	1.34E-04	4.26E-03	4.95E-02	-2.02E+01	3.15E+00	6.37E+01
ARHGAP27	1.35E-04	4.26E-03	1.81E+00	1.81E+00	4.68E+03	2.59E+03
MAP1A	1.35E-04	4.26E-03	1.72E-01	-5.83E+00	2.34E+00	1.36E+01
UCKL1-AS1	1.36E-04	4.28E-03	2.05E+00	2.05E+00	7.64E+01	3.72E+01
SLCO4A1-AS1	1.36E-04	4.28E-03	3.44E+00	3.44E+00	4.19E+01	1.22E+01
MAN1A1	1.37E-04	4.32E-03	3.14E-01	-3.18E+00	5.64E+01	1.79E+02
PHTF2	1.38E-04	4.32E-03	1.65E+00	1.65E+00	4.37E+02	2.64E+02
MFHAS1	1.38E-04	4.32E-03	5.22E-01	-1.91E+00	1.18E+02	2.26E+02
VNN1	1.39E-04	4.34E-03	5.24E-02	-1.91E+01	1.44E+00	2.74E+01
TBC1D9B	1.39E-04	4.34E-03	1.31E+00	1.31E+00	1.93E+03	1.48E+03
ATRX	1.40E-04	4.36E-03	7.05E-01	-1.42E+00	1.05E+03	1.50E+03
TMSB4XP6	1.40E-04	4.37E-03	3.74E-01	-2.67E+00	5.81E+00	1.55E+01
ERG	1.41E-04	4.39E-03	4.94E-01	-2.02E+00	3.02E+01	6.11E+01
FKBP7	1.42E-04	4.42E-03	3.27E-01	-3.05E+00	6.99E+00	2.13E+01
TAS1R3	1.42E-04	4.42E-03	2.42E+00	2.42E+00	8.41E+01	3.47E+01
FENDRR	1.44E-04	4.46E-03	1.50E-01	-6.68E+00	4.81E+00	3.21E+01
FUT8	1.46E-04	4.53E-03	3.32E-01	-3.01E+00	3.74E+01	1.13E+02
SLC44A1	1.48E-04	4.57E-03	6.84E-01	-1.46E+00	9.93E+02	1.45E+03
FAT4	1.48E-04	4.58E-03	2.60E-01	-3.85E+00	7.56E+00	2.91E+01
CHRDL1	1.50E-04	4.63E-03	3.24E-02	-3.09E+01	2.98E-01	9.21E+00
CTSK	1.53E-04	4.69E-03	3.36E-01	-2.97E+00	4.53E+01	1.35E+02
VAT1	1.53E-04	4.69E-03	1.84E+00	1.84E+00	6.72E+03	3.66E+03
ASPHD2	1.53E-04	4.70E-03	3.30E-01	-3.03E+00	2.14E+01	6.48E+01
PRDM16	1.54E-04	4.71E-03	5.78E-02	-1.73E+01	6.88E-01	1.19E+01

SYT11	1.54E-04	4.71E-03	3.35E-01	-2.99E+00	1.31E+01	3.91E+01
C1orf116	1.55E-04	4.75E-03	1.73E+00	1.73E+00	1.08E+04	6.24E+03
KRT78	1.56E-04	4.77E-03	2.58E+00	2.58E+00	6.10E+04	2.36E+04
FAM133B	1.58E-04	4.82E-03	7.71E-01	-1.30E+00	1.45E+02	1.88E+02
CACNA1H	1.59E-04	4.84E-03	1.82E-01	-5.50E+00	2.77E+00	1.52E+01
IL2RA	1.60E-04	4.85E-03	1.98E-01	-5.04E+00	2.91E+00	1.47E+01
LRCH4	1.61E-04	4.87E-03	1.47E+00	1.47E+00	6.27E+02	4.26E+02
GLIPR2	1.61E-04	4.87E-03	2.95E-01	-3.39E+00	2.12E+01	7.20E+01
DEPP1	1.61E-04	4.87E-03	2.47E-01	-4.05E+00	1.20E+01	4.88E+01
TOX3	1.62E-04	4.87E-03	2.49E-02	-4.02E+01	3.83E-01	1.54E+01
FGF7	1.62E-04	4.87E-03	3.92E-02	-2.55E+01	8.84E-01	2.26E+01
ADGRA2	1.64E-04	4.92E-03	2.94E-01	-3.40E+00	2.18E+01	7.42E+01
CADM3-AS1	1.64E-04	4.93E-03	2.05E-01	-4.87E+00	1.93E+00	9.41E+00
N4BP1	1.64E-04	4.93E-03	1.43E+00	1.43E+00	2.27E+03	1.59E+03
ST6GAL1	1.66E-04	4.98E-03	3.10E-01	-3.23E+00	5.01E+01	1.62E+02
PCDHB14	1.67E-04	4.98E-03	4.79E-01	-2.09E+00	1.77E+01	3.70E+01
HYAL1	1.67E-04	4.98E-03	3.61E-01	-2.77E+00	2.33E+01	6.46E+01
BMP4	1.68E-04	5.00E-03	3.90E-01	-2.57E+00	2.03E+01	5.21E+01
WBP2	1.69E-04	5.03E-03	1.35E+00	1.35E+00	1.30E+03	9.64E+02
RPS6KA5	1.71E-04	5.10E-03	6.76E-01	-1.48E+00	9.57E+01	1.41E+02
FAM204A	1.73E-04	5.14E-03	7.93E-01	-1.26E+00	2.63E+02	3.32E+02
ZNF800	1.75E-04	5.18E-03	1.56E+00	1.56E+00	6.39E+02	4.09E+02
AVPI1	1.75E-04	5.18E-03	2.06E+00	2.06E+00	4.78E+02	2.32E+02
LOX	1.77E-04	5.22E-03	3.77E-01	-2.65E+00	6.97E+01	1.85E+02
PDGFRB	1.78E-04	5.26E-03	3.36E-01	-2.98E+00	3.55E+01	1.06E+02
ZFAND5	1.79E-04	5.26E-03	1.68E+00	1.68E+00	5.10E+03	3.04E+03
HSPA12B	1.79E-04	5.26E-03	3.39E-01	-2.95E+00	5.83E+00	1.72E+01
KLF7	1.79E-04	5.26E-03	6.17E-01	-1.62E+00	1.50E+02	2.43E+02
A2M	1.81E-04	5.30E-03	3.71E-01	-2.70E+00	3.97E+02	1.07E+03
CALD1	1.81E-04	5.30E-03	4.08E-01	-2.45E+00	3.53E+02	8.67E+02
SPRED1	1.81E-04	5.30E-03	6.10E-01	-1.64E+00	1.48E+02	2.42E+02
AGMAT	1.82E-04	5.32E-03	2.67E-01	-3.74E+00	7.61E+00	2.84E+01
ACKR4	1.83E-04	5.34E-03	5.93E-02	-1.69E+01	1.50E+00	2.52E+01
ENPEP	1.84E-04	5.36E-03	6.95E-02	-1.44E+01	4.87E-01	7.00E+00
TCN1	1.84E-04	5.36E-03	3.23E-01	-3.09E+00	9.73E+01	3.01E+02
COQ10B	1.85E-04	5.36E-03	1.33E+00	1.33E+00	3.73E+02	2.80E+02
MASP1	1.85E-04	5.36E-03	1.16E-01	-8.65E+00	1.82E+00	1.57E+01
IFI6	1.86E-04	5.37E-03	1.51E-01	-6.64E+00	2.50E+01	1.66E+02
AGR3	1.86E-04	5.37E-03	1.03E-02	-9.75E+01	1.81E-01	1.76E+01

IGHV4-34	1.87E-04	5.40E-03	8.39E-03	-1.19E+02	2.44E-01	2.90E+01
PRKG2	1.87E-04	5.40E-03	4.68E-01	-2.14E+00	1.10E+01	2.35E+01
TNFSF13B	1.88E-04	5.40E-03	2.47E-01	-4.05E+00	1.04E+01	4.22E+01
C11orf95	1.89E-04	5.42E-03	6.60E-01	-1.52E+00	6.02E+01	9.13E+01
MRAS	1.89E-04	5.42E-03	2.25E-01	-4.45E+00	5.53E+00	2.46E+01
TADA2A	1.89E-04	5.42E-03	7.84E-01	-1.27E+00	1.28E+02	1.63E+02
ACOX1	1.89E-04	5.42E-03	1.52E+00	1.52E+00	3.66E+03	2.40E+03
PDK4	1.91E-04	5.46E-03	2.11E-01	-4.75E+00	8.01E+00	3.80E+01
SLC38A11	1.94E-04	5.54E-03	1.41E-01	-7.10E+00	1.86E+00	1.32E+01
UBD	1.94E-04	5.54E-03	1.96E-01	-5.11E+00	1.67E+01	8.52E+01
YBX3	1.96E-04	5.57E-03	1.53E+00	1.53E+00	6.82E+03	4.45E+03
TP53INP2	1.96E-04	5.58E-03	2.15E+00	2.15E+00	6.27E+03	2.91E+03
SYNPO2	1.97E-04	5.58E-03	3.39E-01	-2.95E+00	8.29E+01	2.44E+02
LGMN	1.98E-04	5.60E-03	1.31E+00	1.31E+00	1.11E+03	8.49E+02
VTCN1	2.00E-04	5.67E-03	3.18E-02	-3.14E+01	2.32E-01	7.30E+00
PITPNC1	2.01E-04	5.67E-03	4.64E-01	-2.16E+00	9.46E+01	2.04E+02
HSD17B11	2.01E-04	5.68E-03	3.46E-01	-2.89E+00	4.72E+01	1.36E+02
PHACTR4	2.03E-04	5.72E-03	1.74E+00	1.74E+00	4.48E+03	2.57E+03
LAMA4	2.03E-04	5.72E-03	3.39E-01	-2.95E+00	3.98E+01	1.18E+02
RPL21P93	2.04E-04	5.73E-03	4.66E-01	-2.14E+00	1.78E+01	3.82E+01
SCN1B	2.05E-04	5.74E-03	1.85E-01	-5.41E+00	1.57E+00	8.48E+00
CNST	2.05E-04	5.74E-03	1.94E+00	1.94E+00	1.15E+03	5.93E+02
SOX4	2.05E-04	5.74E-03	5.47E-01	-1.83E+00	2.25E+02	4.12E+02
MYO5B	2.06E-04	5.75E-03	1.57E+00	1.57E+00	3.27E+03	2.08E+03
ISLR	2.08E-04	5.80E-03	1.98E-01	-5.05E+00	5.78E+00	2.92E+01
STK24P1	2.08E-04	5.80E-03	2.27E+00	2.27E+00	1.24E+01	5.46E+00
RUSC1	2.10E-04	5.86E-03	1.28E+00	1.28E+00	6.89E+02	5.39E+02
CYB5R3	2.13E-04	5.92E-03	1.29E+00	1.29E+00	1.26E+03	9.77E+02
FAM241A	2.13E-04	5.93E-03	6.73E-01	-1.49E+00	1.33E+02	1.98E+02
DUSP19	2.17E-04	6.00E-03	5.41E-01	-1.85E+00	1.40E+01	2.59E+01
ITPKC	2.18E-04	6.03E-03	1.87E+00	1.87E+00	4.31E+03	2.31E+03
NCCRP1	2.19E-04	6.05E-03	2.01E+00	2.01E+00	1.50E+04	7.46E+03
MXD1	2.19E-04	6.05E-03	2.02E+00	2.02E+00	1.75E+04	8.66E+03
BRD4	2.20E-04	6.05E-03	1.29E+00	1.29E+00	1.00E+03	7.81E+02
PPL	2.21E-04	6.09E-03	2.15E+00	2.15E+00	1.23E+05	5.73E+04
NRIP2	2.22E-04	6.10E-03	7.50E-02	-1.33E+01	2.32E-01	3.09E+00
SLC44A2	2.22E-04	6.10E-03	1.23E+00	1.23E+00	2.97E+03	2.42E+03
NES	2.24E-04	6.14E-03	4.01E-01	-2.50E+00	6.77E+01	1.69E+02
MGP	2.24E-04	6.14E-03	3.12E-01	-3.20E+00	1.74E+01	5.58E+01

AL109628.2	2.25E-04	6.14E-03	3.05E+00	3.05E+00	5.88E+00	1.93E+00
ATP6V1C2	2.26E-04	6.17E-03	2.05E+00	2.05E+00	1.17E+03	5.68E+02
COL6A2	2.26E-04	6.17E-03	3.19E-01	-3.13E+00	1.21E+02	3.79E+02
PLIN3	2.27E-04	6.18E-03	1.77E+00	1.77E+00	5.18E+03	2.93E+03
TWIST1	2.27E-04	6.18E-03	8.18E-02	-1.22E+01	4.83E-01	5.91E+00
CELF1	2.28E-04	6.18E-03	8.45E-01	-1.18E+00	7.98E+02	9.44E+02
PCIF1	2.28E-04	6.19E-03	1.33E+00	1.33E+00	2.94E+02	2.22E+02
G6PD	2.29E-04	6.19E-03	1.45E+00	1.45E+00	1.08E+03	7.40E+02
BAG2	2.29E-04	6.19E-03	2.91E-01	-3.43E+00	5.81E+00	1.99E+01
SELP	2.29E-04	6.19E-03	1.86E-01	-5.39E+00	5.19E+00	2.80E+01
IFITM1	2.30E-04	6.21E-03	3.89E-01	-2.57E+00	1.32E+02	3.39E+02
CCDC88A	2.31E-04	6.22E-03	5.07E-01	-1.97E+00	1.86E+02	3.66E+02
SVEP1	2.32E-04	6.25E-03	1.74E-01	-5.76E+00	2.77E+00	1.60E+01
THSD1	2.33E-04	6.25E-03	4.56E-01	-2.19E+00	2.32E+01	5.09E+01
APOL2	2.34E-04	6.26E-03	3.72E-01	-2.69E+00	1.25E+02	3.36E+02
CHI3L2	2.34E-04	6.26E-03	1.94E-01	-5.15E+00	3.40E+00	1.75E+01
ADGRL4	2.36E-04	6.30E-03	4.42E-01	-2.26E+00	2.97E+01	6.73E+01
FRG1CP	2.36E-04	6.30E-03	5.29E-01	-1.89E+00	3.32E+01	6.28E+01
RASGEF1B	2.40E-04	6.40E-03	2.09E+00	2.09E+00	1.38E+03	6.59E+02
CDC42EP3	2.41E-04	6.42E-03	3.37E-01	-2.97E+00	2.72E+01	8.08E+01
ARID4B	2.43E-04	6.47E-03	7.60E-01	-1.32E+00	6.68E+02	8.80E+02
TMBIM6	2.44E-04	6.47E-03	1.13E+00	1.13E+00	9.72E+03	8.58E+03
GPA33	2.44E-04	6.47E-03	3.67E-02	-2.73E+01	6.38E-01	1.74E+01
DTNA	2.44E-04	6.47E-03	1.85E-01	-5.40E+00	2.04E+00	1.10E+01
PPP3CA	2.45E-04	6.47E-03	7.19E-01	-1.39E+00	3.51E+02	4.89E+02
STK39	2.45E-04	6.48E-03	1.57E+00	1.57E+00	2.16E+03	1.38E+03
NID2	2.46E-04	6.49E-03	2.37E-01	-4.22E+00	6.31E+00	2.66E+01
EDN1	2.46E-04	6.49E-03	3.65E-01	-2.74E+00	1.04E+01	2.83E+01
STN1	2.49E-04	6.56E-03	1.52E+00	1.52E+00	1.37E+03	9.01E+02
RHOJ	2.49E-04	6.56E-03	3.56E-01	-2.81E+00	9.99E+00	2.80E+01
ZSCAN2	2.51E-04	6.59E-03	4.48E-01	-2.23E+00	1.02E+01	2.27E+01
PRR3	2.52E-04	6.61E-03	7.06E-01	-1.42E+00	3.35E+01	4.75E+01
KLK9	2.52E-04	6.61E-03	1.47E-01	-6.78E+00	1.51E+01	1.02E+02
TMEM273	2.53E-04	6.61E-03	4.06E-01	-2.46E+00	1.71E+01	4.20E+01
HOXC10	2.53E-04	6.61E-03	2.59E-02	-3.87E+01	3.83E-01	1.48E+01
PLK3	2.54E-04	6.62E-03	2.00E+00	2.00E+00	5.91E+02	2.96E+02
PIM2	2.55E-04	6.64E-03	2.48E-01	-4.04E+00	2.71E+01	1.09E+02
HSD17B7P2	2.55E-04	6.64E-03	5.29E-01	-1.89E+00	1.12E+01	2.11E+01
HOXC4	2.56E-04	6.66E-03	1.62E+00	1.62E+00	1.64E+02	1.01E+02

FOS	2.57E-04	6.68E-03	2.35E-01	-4.25E+00	1.20E+02	5.13E+02
MAPK3	2.58E-04	6.69E-03	1.54E+00	1.54E+00	2.83E+03	1.84E+03
CDHR2	2.58E-04	6.69E-03	1.84E-02	-5.44E+01	3.83E-01	2.08E+01
SAMD4B	2.59E-04	6.70E-03	1.55E+00	1.55E+00	1.42E+03	9.16E+02
TMEM14A	2.60E-04	6.71E-03	6.99E-01	-1.43E+00	2.21E+02	3.16E+02
DACT1	2.61E-04	6.72E-03	6.39E-02	-1.56E+01	4.92E-01	7.69E+00
COL4A1	2.61E-04	6.73E-03	2.97E-01	-3.37E+00	9.65E+01	3.25E+02
RIPOR3	2.64E-04	6.80E-03	1.94E-01	-5.16E+00	2.89E+00	1.49E+01
SLC40A1	2.65E-04	6.82E-03	4.49E-01	-2.23E+00	2.29E+02	5.11E+02
PRDM8	2.68E-04	6.88E-03	5.79E-02	-1.73E+01	3.83E-01	6.61E+00
SF3B3	2.70E-04	6.91E-03	1.41E+00	1.41E+00	3.00E+03	2.13E+03
TNRC6B	2.70E-04	6.91E-03	7.40E-01	-1.35E+00	3.96E+02	5.35E+02
ADAMTSL3	2.70E-04	6.91E-03	1.67E-01	-6.00E+00	2.05E+00	1.23E+01
CYP2T1P	2.72E-04	6.93E-03	2.22E+00	2.22E+00	7.29E+01	3.28E+01
IGIP	2.73E-04	6.95E-03	7.10E-01	-1.41E+00	9.43E+01	1.33E+02
HEPH	2.74E-04	6.97E-03	1.93E-01	-5.19E+00	1.64E+01	8.53E+01
ZNF385D	2.74E-04	6.97E-03	2.97E-01	-3.37E+00	3.17E+00	1.07E+01
RNF10	2.75E-04	6.97E-03	1.33E+00	1.33E+00	3.96E+03	2.97E+03
SLC12A2	2.75E-04	6.99E-03	3.77E-01	-2.65E+00	1.38E+02	3.65E+02
TREM2	2.77E-04	7.01E-03	1.17E-01	-8.53E+00	7.59E-01	6.47E+00
MAGOH	2.78E-04	7.03E-03	7.34E-01	-1.36E+00	2.00E+02	2.72E+02
SAA2	2.79E-04	7.04E-03	4.29E-02	-2.33E+01	6.03E-01	1.41E+01
VDAC1	2.79E-04	7.05E-03	1.21E+00	1.21E+00	2.95E+03	2.45E+03
EIF2AK2	2.80E-04	7.06E-03	7.05E-01	-1.42E+00	3.79E+02	5.38E+02
SLC19A3	2.80E-04	7.06E-03	8.74E-02	-1.14E+01	3.83E-01	4.38E+00
DIPK1A	2.81E-04	7.06E-03	4.35E-01	-2.30E+00	3.44E+01	7.91E+01
XAF1	2.81E-04	7.06E-03	4.34E-01	-2.30E+00	1.93E+02	4.43E+02
FADS6	2.81E-04	7.06E-03	2.08E+00	2.08E+00	8.29E+01	3.99E+01
ZC3H3	2.82E-04	7.06E-03	1.40E+00	1.40E+00	2.59E+02	1.85E+02
LPIN2	2.83E-04	7.07E-03	1.76E+00	1.76E+00	1.16E+03	6.60E+02
TIMP2	2.83E-04	7.08E-03	1.86E+00	1.86E+00	2.63E+03	1.41E+03
VDAC2P5	2.84E-04	7.08E-03	1.38E+00	1.38E+00	3.05E+03	2.21E+03
ANKRD26	2.87E-04	7.15E-03	6.57E-01	-1.52E+00	1.74E+02	2.64E+02
PCSK5	2.88E-04	7.16E-03	1.72E+00	1.72E+00	9.02E+02	5.23E+02
ESAM	2.88E-04	7.16E-03	1.86E+00	1.86E+00	6.08E+02	3.26E+02
RAB11FIP1	2.89E-04	7.16E-03	1.64E+00	1.64E+00	7.42E+03	4.53E+03
PLEKHS1	2.89E-04	7.16E-03	1.64E-02	-6.11E+01	2.98E-01	1.82E+01
PTPRB	2.91E-04	7.22E-03	4.31E-01	-2.32E+00	3.95E+01	9.18E+01
CASP6	2.94E-04	7.28E-03	6.10E-01	-1.64E+00	8.45E+01	1.39E+02

CHAC1	2.97E-04	7.33E-03	2.44E+00	2.44E+00	7.41E+02	3.03E+02
FKBP10	2.97E-04	7.33E-03	2.73E-01	-3.67E+00	1.33E+01	4.86E+01
OMA1	2.99E-04	7.37E-03	7.66E-01	-1.31E+00	1.53E+02	2.00E+02
NAIP	3.01E-04	7.40E-03	5.21E-01	-1.92E+00	6.69E+01	1.28E+02
PGF	3.01E-04	7.40E-03	4.17E-01	-2.40E+00	9.30E+00	2.23E+01
FAXDC2	3.01E-04	7.40E-03	4.51E-01	-2.22E+00	2.72E+01	6.02E+01
SEC11A	3.02E-04	7.40E-03	8.30E-01	-1.20E+00	6.73E+02	8.11E+02
TPPP3	3.02E-04	7.41E-03	3.37E-01	-2.97E+00	5.46E+01	1.62E+02
CYP27C1	3.03E-04	7.41E-03	3.83E-01	-2.61E+00	2.64E+01	6.89E+01
MED16	3.03E-04	7.41E-03	1.51E+00	1.51E+00	5.96E+02	3.94E+02
MYH14	3.05E-04	7.45E-03	1.50E+00	1.50E+00	4.44E+03	2.96E+03
PGM1	3.06E-04	7.46E-03	1.26E+00	1.26E+00	8.16E+02	6.49E+02
ENAH	3.07E-04	7.47E-03	4.70E-01	-2.13E+00	2.59E+02	5.51E+02
CUX1	3.11E-04	7.57E-03	1.28E+00	1.28E+00	1.24E+03	9.66E+02
XCR1	3.12E-04	7.57E-03	2.14E+00	2.14E+00	5.62E+01	2.63E+01
TMEM64	3.12E-04	7.57E-03	6.81E-01	-1.47E+00	1.22E+02	1.79E+02
BCKDHA	3.13E-04	7.59E-03	1.53E+00	1.53E+00	1.01E+03	6.57E+02
ARHGAP1	3.14E-04	7.59E-03	1.26E+00	1.26E+00	1.47E+03	1.17E+03
MTRES1	3.14E-04	7.59E-03	7.01E-01	-1.43E+00	9.84E+01	1.40E+02
PRSS23	3.15E-04	7.62E-03	3.42E-01	-2.93E+00	6.57E+01	1.92E+02
SPOCD1	3.18E-04	7.66E-03	4.27E-02	-2.34E+01	2.32E-01	5.44E+00
DYRK3	3.18E-04	7.67E-03	5.50E-01	-1.82E+00	3.72E+01	6.77E+01
ACAD8	3.19E-04	7.67E-03	1.27E+00	1.27E+00	4.16E+02	3.29E+02
RIC8B	3.20E-04	7.67E-03	6.42E-01	-1.56E+00	4.28E+01	6.67E+01
LRRC24	3.20E-04	7.67E-03	3.98E+00	3.98E+00	1.28E+02	3.21E+01
LOXL2	3.20E-04	7.68E-03	2.61E-01	-3.83E+00	1.19E+01	4.54E+01
VPS37B	3.21E-04	7.69E-03	1.65E+00	1.65E+00	3.25E+03	1.98E+03
MPI	3.24E-04	7.75E-03	1.31E+00	1.31E+00	4.57E+02	3.49E+02
ZNRF1	3.25E-04	7.76E-03	1.71E+00	1.71E+00	1.75E+03	1.03E+03
CLIC5	3.26E-04	7.77E-03	2.60E-01	-3.85E+00	3.91E+00	1.51E+01
DPH5	3.26E-04	7.77E-03	7.37E-01	-1.36E+00	1.14E+02	1.55E+02
SEC24C	3.26E-04	7.77E-03	1.54E+00	1.54E+00	5.08E+03	3.29E+03
RGS5	3.30E-04	7.84E-03	3.97E-01	-2.52E+00	3.08E+02	7.77E+02
SLC6A20	3.30E-04	7.84E-03	1.27E-02	-7.87E+01	1.81E-01	1.42E+01
DDX60L	3.30E-04	7.84E-03	3.07E-01	-3.26E+00	5.43E+01	1.77E+02
CA1	3.31E-04	7.85E-03	1.11E-04	-9.00E+03	9.04E-05	8.13E-01
OGN	3.32E-04	7.85E-03	4.64E-02	-2.16E+01	4.82E-01	1.04E+01
ATP2A3	3.32E-04	7.85E-03	2.49E-01	-4.02E+00	7.65E+01	3.07E+02
FAM214A	3.33E-04	7.85E-03	1.93E+00	1.93E+00	3.48E+03	1.80E+03

MGLL	3.33E-04	7.85E-03	1.74E+00	1.74E+00	9.24E+03	5.31E+03
KCTD12	3.33E-04	7.85E-03	5.64E-01	-1.77E+00	2.52E+02	4.47E+02
CCL19	3.35E-04	7.88E-03	1.62E-01	-6.18E+00	2.42E+00	1.49E+01
TBX2	3.37E-04	7.91E-03	2.79E-01	-3.58E+00	8.45E+00	3.02E+01
FAM25G	3.37E-04	7.91E-03	8.00E+00	8.00E+00	2.73E+01	3.41E+00
EPS8L2	3.38E-04	7.92E-03	1.73E+00	1.73E+00	9.24E+03	5.34E+03
TBC1D15	3.39E-04	7.94E-03	1.40E+00	1.40E+00	6.99E+02	5.00E+02
SMIM3	3.40E-04	7.95E-03	5.18E-01	-1.93E+00	4.11E+01	7.94E+01
KCNN3	3.42E-04	8.00E-03	2.61E-01	-3.83E+00	6.91E+00	2.64E+01
LAMP1	3.43E-04	8.00E-03	1.24E+00	1.24E+00	3.32E+03	2.68E+03
BCO1	3.44E-04	8.03E-03	2.62E-01	-3.82E+00	4.22E+00	1.61E+01
PDE3B	3.46E-04	8.05E-03	1.97E-01	-5.08E+00	4.57E+00	2.32E+01
TNFRSF10D	3.46E-04	8.05E-03	3.99E-01	-2.50E+00	2.66E+01	6.66E+01
CCDC134	3.47E-04	8.06E-03	7.45E-01	-1.34E+00	1.36E+02	1.83E+02
JPH2	3.48E-04	8.07E-03	6.56E-02	-1.52E+01	7.11E-01	1.08E+01
KBTBD11	3.48E-04	8.07E-03	1.99E-01	-5.01E+00	6.18E+00	3.10E+01
IGFBP3	3.50E-04	8.10E-03	3.76E-01	-2.66E+00	1.01E+02	2.69E+02
LY96	3.50E-04	8.10E-03	1.74E-01	-5.74E+00	2.86E+00	1.64E+01
ANKRD10	3.52E-04	8.12E-03	6.36E-01	-1.57E+00	1.55E+02	2.44E+02
GDI1	3.52E-04	8.12E-03	1.22E+00	1.22E+00	8.97E+02	7.37E+02
PLEKHG6	3.55E-04	8.18E-03	1.77E+00	1.77E+00	1.15E+03	6.53E+02
TUBB4B	3.57E-04	8.23E-03	1.44E+00	1.44E+00	6.53E+03	4.53E+03
POLDIP3	3.61E-04	8.29E-03	1.18E+00	1.18E+00	1.25E+03	1.06E+03
CCNI	3.63E-04	8.33E-03	1.29E+00	1.29E+00	4.79E+03	3.70E+03
CAPZB	3.64E-04	8.34E-03	1.23E+00	1.23E+00	3.97E+03	3.23E+03
TLR4	3.67E-04	8.41E-03	2.62E-01	-3.81E+00	1.79E+01	6.82E+01
CLN8	3.69E-04	8.44E-03	1.53E+00	1.53E+00	8.01E+02	5.24E+02
ABTB2	3.71E-04	8.48E-03	2.27E+00	2.27E+00	6.20E+02	2.73E+02
CPE	3.72E-04	8.48E-03	5.32E-01	-1.88E+00	7.68E+01	1.44E+02
DCN	3.74E-04	8.52E-03	3.44E-01	-2.91E+00	2.16E+02	6.28E+02
AC090994.1	3.75E-04	8.52E-03	4.51E+00	4.51E+00	1.08E+01	2.41E+00
SLC41A2	3.75E-04	8.52E-03	2.07E-01	-4.82E+00	9.04E+00	4.36E+01
LINC00492	3.75E-04	8.52E-03	7.37E+00	7.37E+00	6.22E+00	8.44E-01
IGLV3-19	3.76E-04	8.53E-03	1.75E-02	-5.71E+01	6.30E-01	3.60E+01
ITGA11	3.77E-04	8.53E-03	2.07E-01	-4.82E+00	3.29E+00	1.58E+01
RECQL5	3.77E-04	8.53E-03	1.55E+00	1.55E+00	1.02E+03	6.55E+02
MAP2K1	3.77E-04	8.53E-03	1.56E+00	1.56E+00	1.61E+03	1.04E+03
MYOCD	3.78E-04	8.54E-03	2.16E-02	-4.63E+01	1.81E-01	8.38E+00
BHLHE22	3.79E-04	8.56E-03	8.43E-02	-1.19E+01	2.98E-01	3.54E+00

B3GNT3	3.82E-04	8.62E-03	1.94E+00	1.94E+00	1.76E+03	9.05E+02
LINC02762	3.84E-04	8.64E-03	3.92E-01	-2.55E+00	6.17E+00	1.57E+01
CCDC102B	3.84E-04	8.64E-03	2.69E-01	-3.71E+00	3.11E+00	1.15E+01
EPHA2	3.85E-04	8.64E-03	1.77E+00	1.77E+00	5.21E+03	2.94E+03
POU2F2	3.86E-04	8.66E-03	2.38E-01	-4.20E+00	1.01E+01	4.26E+01
ESYT3	3.87E-04	8.66E-03	1.62E+00	1.62E+00	5.20E+01	3.22E+01
AF117829.1	3.87E-04	8.66E-03	5.23E-01	-1.91E+00	1.56E+01	2.98E+01
BRD1	3.87E-04	8.66E-03	1.47E+00	1.47E+00	7.98E+02	5.44E+02
MYBBP1A	3.89E-04	8.69E-03	1.30E+00	1.30E+00	5.07E+02	3.89E+02
MORF4L1	3.89E-04	8.69E-03	8.07E-01	-1.24E+00	7.44E+02	9.22E+02
BMP6	3.91E-04	8.71E-03	1.95E-01	-5.12E+00	3.22E+00	1.65E+01
CHMP1B-AS1	3.91E-04	8.71E-03	4.30E+00	4.30E+00	1.05E+01	2.44E+00
XPNPEP3	3.92E-04	8.71E-03	7.79E-01	-1.28E+00	1.38E+02	1.77E+02
BTN3A2	3.92E-04	8.71E-03	4.49E-01	-2.23E+00	1.99E+02	4.44E+02
MYCT1	3.93E-04	8.72E-03	3.53E-01	-2.83E+00	8.27E+00	2.34E+01
ALAS1	3.93E-04	8.72E-03	1.29E+00	1.29E+00	8.15E+02	6.31E+02
MRGPRF	3.95E-04	8.74E-03	1.83E-01	-5.45E+00	2.83E+00	1.54E+01
SUN2	3.97E-04	8.78E-03	1.41E+00	1.41E+00	2.33E+03	1.66E+03
PDE5A	4.00E-04	8.84E-03	3.79E-01	-2.64E+00	3.27E+01	8.62E+01
AC044860.1	4.02E-04	8.88E-03	2.25E+00	2.25E+00	3.02E+01	1.34E+01
NRG1	4.07E-04	8.97E-03	3.53E-01	-2.84E+00	2.93E+01	8.30E+01
GAK	4.07E-04	8.97E-03	1.38E+00	1.38E+00	1.57E+03	1.14E+03
AC016026.1	4.08E-04	8.97E-03	4.14E-01	-2.41E+00	2.28E+01	5.51E+01
TJP2	4.08E-04	8.97E-03	1.46E+00	1.46E+00	3.90E+03	2.68E+03
SOCS3	4.10E-04	9.00E-03	2.01E-01	-4.98E+00	3.10E+01	1.55E+02
PDIA2	4.14E-04	9.07E-03	5.54E-02	-1.81E+01	8.21E-01	1.48E+01
ADAMTS2	4.15E-04	9.08E-03	2.66E-01	-3.75E+00	7.95E+00	2.98E+01
RRAS2	4.15E-04	9.08E-03	6.96E-01	-1.44E+00	1.30E+02	1.87E+02
CFB	4.15E-04	9.08E-03	3.11E-01	-3.21E+00	1.21E+02	3.90E+02
ST8SIA4	4.18E-04	9.11E-03	4.16E-01	-2.40E+00	2.11E+01	5.07E+01
ADAM28	4.18E-04	9.11E-03	2.76E-01	-3.63E+00	3.44E+01	1.25E+02
SEMA3B	4.19E-04	9.12E-03	2.83E-01	-3.53E+00	1.95E+01	6.90E+01
AF131215.6	4.20E-04	9.15E-03	5.59E-01	-1.79E+00	1.54E+01	2.75E+01
TINAGL1	4.22E-04	9.18E-03	4.50E-01	-2.22E+00	1.34E+02	2.97E+02
EXTL2	4.23E-04	9.18E-03	5.41E-01	-1.85E+00	3.29E+01	6.07E+01
RNF223	4.24E-04	9.19E-03	2.29E+00	2.29E+00	1.09E+03	4.74E+02
GJB1	4.24E-04	9.19E-03	4.28E-02	-2.34E+01	6.38E-01	1.49E+01
GTF2IRD1P1	4.25E-04	9.20E-03	3.08E+00	3.08E+00	1.14E+01	3.70E+00
C6orf223	4.29E-04	9.27E-03	5.97E-02	-1.68E+01	2.98E-01	5.00E+00

ABHD10	4.32E-04	9.31E-03	7.19E-01	-1.39E+00	1.33E+02	1.85E+02
HLA-DQB2	4.32E-04	9.31E-03	2.41E+00	2.41E+00	2.22E+02	9.20E+01
CYGB	4.32E-04	9.31E-03	2.76E-01	-3.62E+00	9.85E+00	3.57E+01
OPTN	4.34E-04	9.35E-03	1.43E+00	1.43E+00	2.62E+03	1.83E+03
MEP1A	4.37E-04	9.39E-03	2.15E-02	-4.65E+01	2.32E-01	1.08E+01
SLC17A9	4.37E-04	9.39E-03	1.20E-01	-8.30E+00	3.71E+00	3.08E+01
ARHGAP10	4.38E-04	9.39E-03	1.76E+00	1.76E+00	2.08E+03	1.18E+03
SCNN1B	4.38E-04	9.39E-03	1.86E+00	1.86E+00	2.22E+03	1.20E+03
CD300LF	4.41E-04	9.45E-03	2.03E-01	-4.94E+00	1.91E+00	9.42E+00
NEDD9	4.44E-04	9.49E-03	3.08E-01	-3.25E+00	2.75E+01	8.92E+01
ZNF521	4.46E-04	9.52E-03	3.75E-01	-2.67E+00	1.14E+01	3.03E+01
ALDH3B1	4.46E-04	9.53E-03	1.76E+00	1.76E+00	6.56E+02	3.72E+02
WFDC12	4.48E-04	9.55E-03	2.80E-01	-3.57E+00	8.32E+00	2.97E+01
NECTIN3	4.49E-04	9.56E-03	2.39E-01	-4.19E+00	8.49E+00	3.55E+01
CP	4.51E-04	9.60E-03	4.80E-02	-2.08E+01	1.32E+00	2.75E+01
MS4A1	4.52E-04	9.60E-03	7.67E-02	-1.30E+01	1.29E+00	1.68E+01
ASNS	4.55E-04	9.64E-03	5.75E-01	-1.74E+00	9.46E+01	1.65E+02
MUC2	4.55E-04	9.64E-03	1.75E-02	-5.71E+01	3.79E-01	2.17E+01
PHF14	4.55E-04	9.64E-03	6.63E-01	-1.51E+00	3.25E+02	4.90E+02
ADGRL3	4.58E-04	9.68E-03	1.99E-01	-5.03E+00	3.16E+00	1.59E+01
GIMAP2	4.62E-04	9.76E-03	3.79E-01	-2.64E+00	1.31E+01	3.47E+01
MRAP2	4.64E-04	9.76E-03	3.48E-01	-2.87E+00	1.53E+01	4.38E+01
AL732437.1	4.64E-04	9.76E-03	2.24E+00	2.24E+00	5.15E+01	2.31E+01
ZBTB7C	4.65E-04	9.76E-03	1.53E+00	1.53E+00	1.95E+03	1.28E+03
RSF1	4.65E-04	9.76E-03	7.43E-01	-1.35E+00	6.08E+02	8.19E+02
SLC25A23	4.65E-04	9.76E-03	1.61E+00	1.61E+00	2.00E+03	1.24E+03
PTPN23	4.66E-04	9.76E-03	1.36E+00	1.36E+00	5.83E+02	4.28E+02
ST3GAL5	4.66E-04	9.76E-03	3.53E-01	-2.83E+00	1.24E+01	3.51E+01
TSHZ3	4.66E-04	9.76E-03	4.13E-01	-2.42E+00	1.28E+01	3.09E+01
AL137003.1	4.66E-04	9.77E-03	6.15E-01	-1.63E+00	1.77E+01	2.88E+01
STBD1	4.73E-04	9.89E-03	5.64E-01	-1.77E+00	5.98E+01	1.06E+02
TYRO3	4.73E-04	9.89E-03	1.69E+00	1.69E+00	1.37E+03	8.12E+02
APOL1	4.75E-04	9.89E-03	2.44E-01	-4.10E+00	1.92E+02	7.87E+02
LRFN2	4.75E-04	9.89E-03	2.89E+00	2.89E+00	2.48E+01	8.59E+00
PCBP1-AS1	4.75E-04	9.89E-03	1.76E+00	1.76E+00	6.79E+02	3.86E+02
ADH1B	4.75E-04	9.89E-03	1.63E-01	-6.13E+00	1.18E+01	7.24E+01
PTCHD4	4.76E-04	9.90E-03	8.25E-02	-1.21E+01	2.32E-01	2.81E+00
AC026785.2	4.80E-04	9.96E-03	5.45E+00	5.45E+00	6.02E+00	1.10E+00
GDPD2	4.80E-04	9.96E-03	1.38E-01	-7.27E+00	1.56E+00	1.13E+01

CRYBG2	4.83E-04	9.98E-03	1.84E+00	1.84E+00	4.21E+03	2.29E+03
ATP1B1	4.83E-04	9.98E-03	1.43E+00	1.43E+00	6.73E+03	4.71E+03
C1orf198	4.83E-04	9.98E-03	1.22E+00	1.22E+00	4.35E+02	3.58E+02
ZNF101	4.83E-04	9.98E-03	1.61E+00	1.61E+00	5.89E+02	3.66E+02
CTIF	4.83E-04	9.98E-03	1.52E+00	1.52E+00	6.40E+02	4.21E+02
ADGRE2	4.84E-04	9.99E-03	2.77E-01	-3.61E+00	1.02E+01	3.69E+01
AL353622.1	4.85E-04	9.99E-03	4.63E-01	-2.16E+00	7.10E+00	1.53E+01
CD34	4.86E-04	9.99E-03	5.61E-01	-1.78E+00	7.71E+01	1.37E+02
CCL28	4.87E-04	9.99E-03	3.80E-01	-2.63E+00	4.24E+01	1.12E+02
SULF1	4.87E-04	9.99E-03	4.58E-01	-2.18E+00	4.30E+01	9.39E+01
PCDH12	4.87E-04	9.99E-03	3.73E-01	-2.68E+00	7.29E+00	1.95E+01
MARCKSL1	4.87E-04	9.99E-03	2.52E-01	-3.97E+00	7.26E+01	2.88E+02

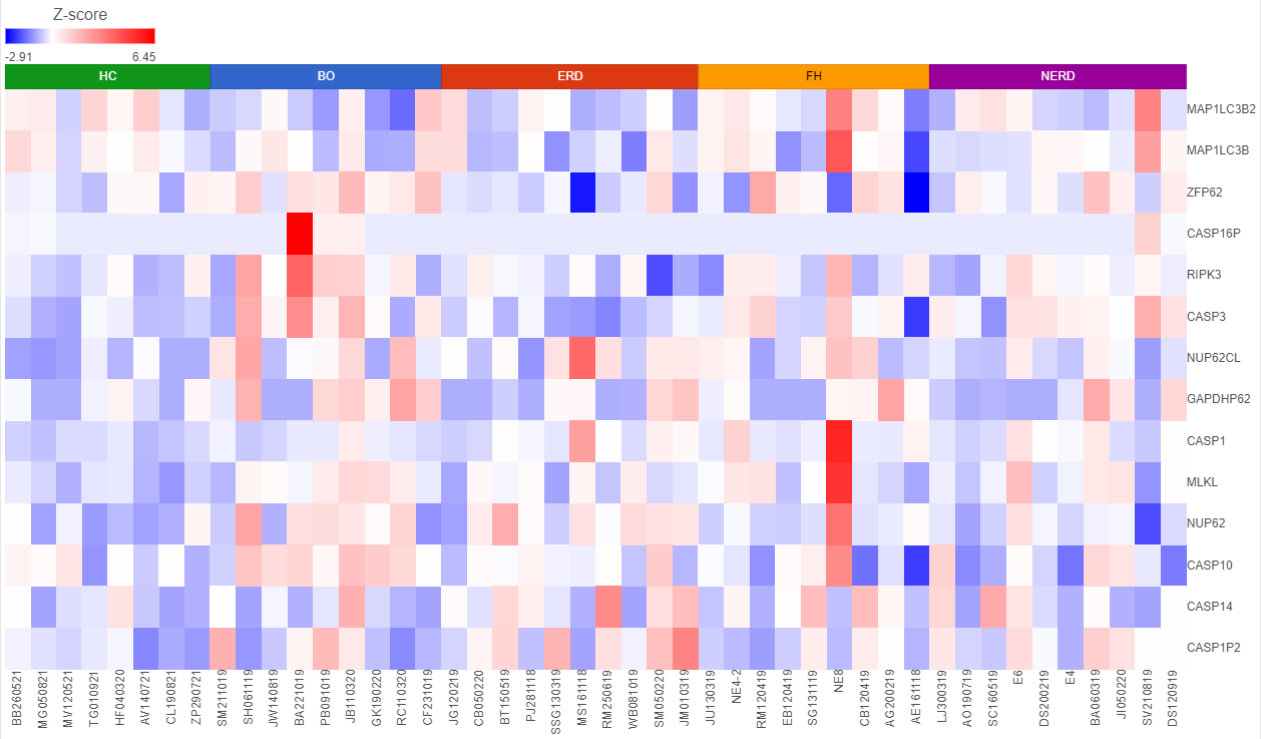

Appendix 6 Expression of Cell Death Markers Among Samples used for RNA Sequencing

Normalised gene expression matrix was filtered for genes involved in cell death using Partek. A significant difference in expression of cell death markers was not detected among groups. Of note, sample BA221019 and NE8 may be flagged for having high level of expression of more than 3 cell death genes, suggesting necrosis in the tissue upon collection and transportation.

Appendix 7 Heatmap of Most Differentially Expressed Genes Between Normal and GORD Oesophageal Mucosa

Heatmap displaying filtered DE genes with TPM over 100, and with adjusted p<0.01. Graph coded manually using R. HC: N=8, BO: N=9, ERD: N=10, FH: N=9, NERD: N=9

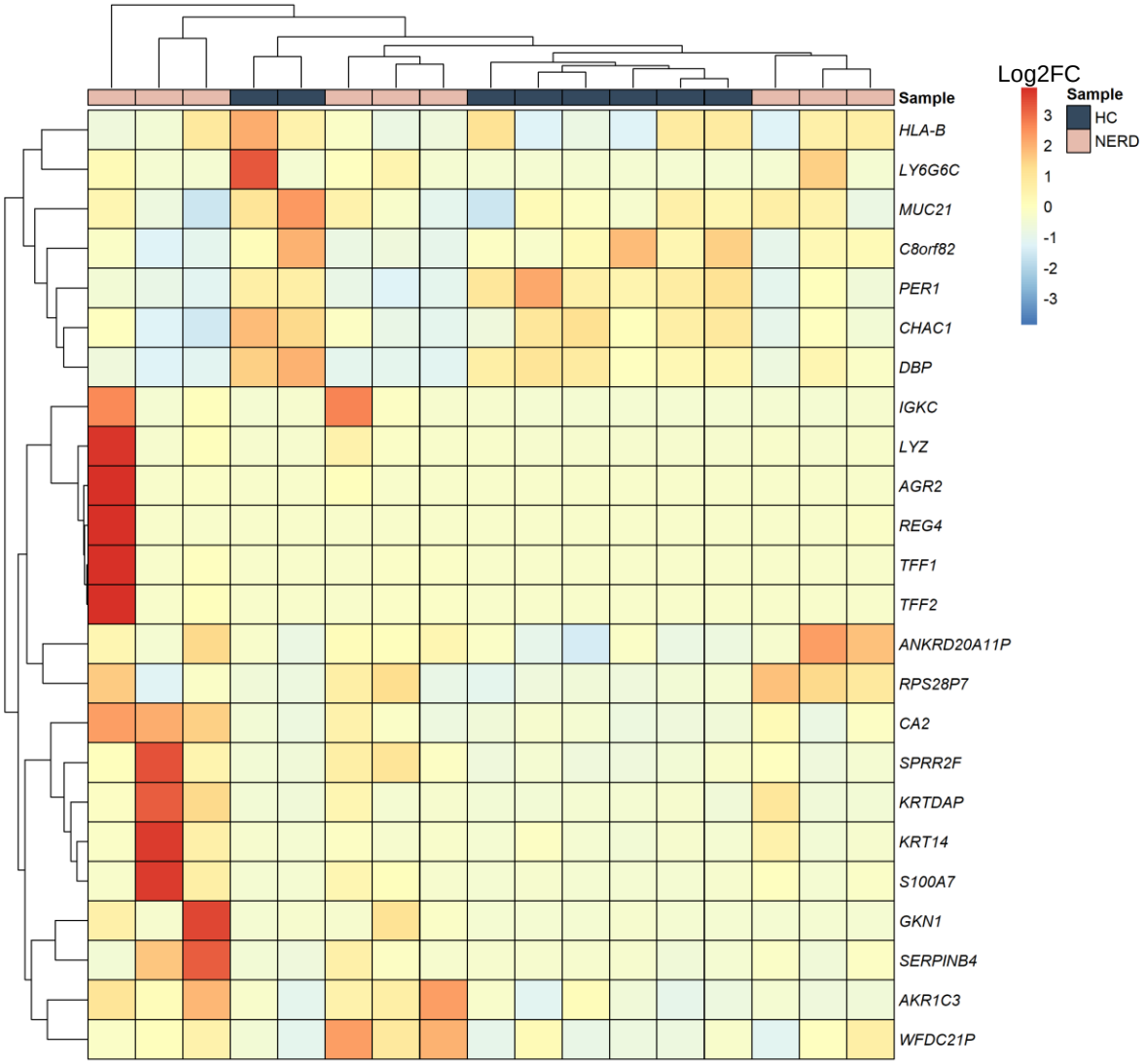

Appendix 8 Heatmap of Most Significantly Differentially Expressed Genes Between Normal and NERD Oesophageal Mucosa

Heatmap displaying filtered DE genes with TPM over 25, and with adjusted p<0.01. Graph coded manually using R. HC: N=8, NERD: N=9. Log2FC= Log2 fold change in gene expression

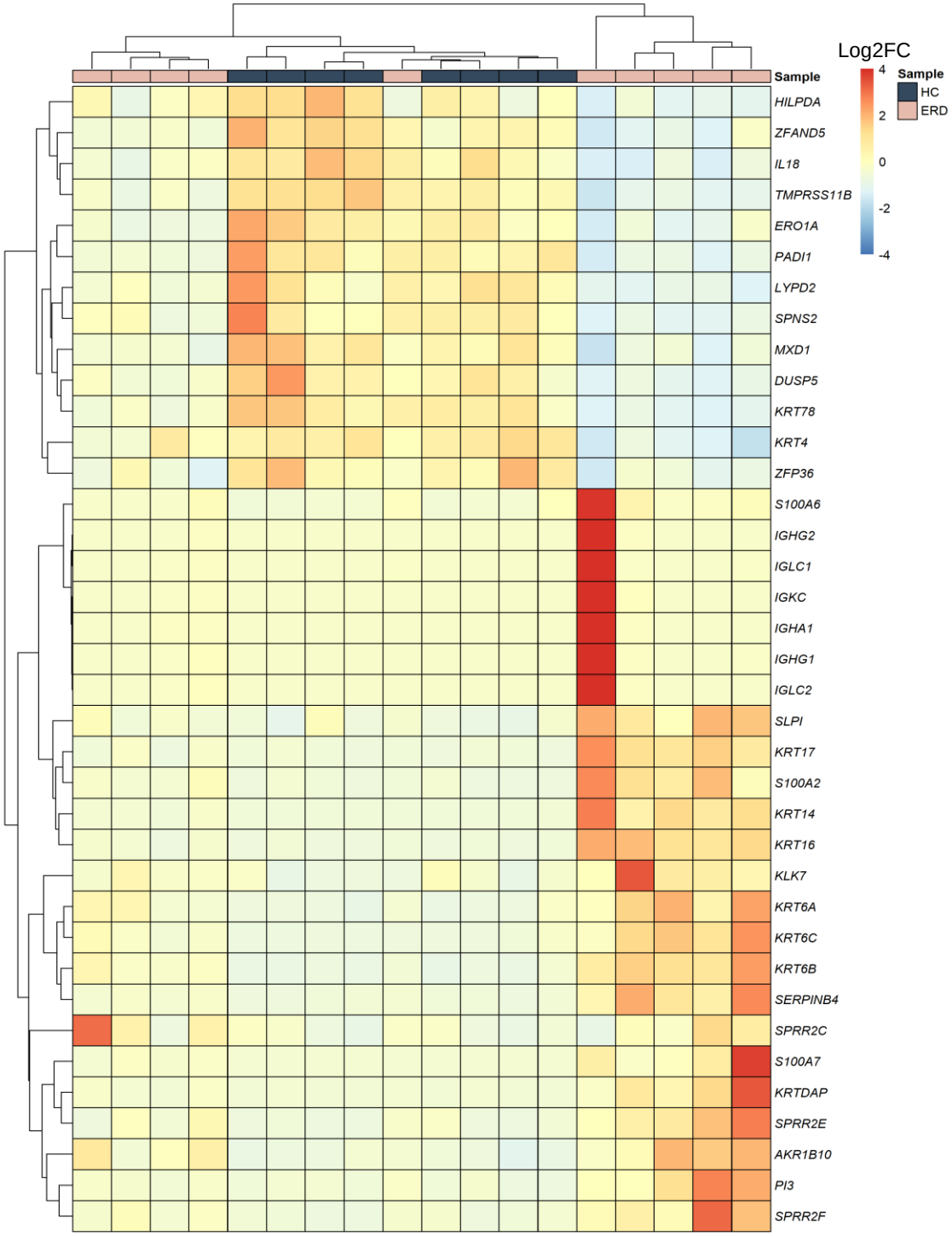

Appendix 9 Most Significantly Differentially Expressed Genes Between ERD and Normal Oesophageal Mucosa

Heatmap displaying filtered DE genes with TPM over 150, and with adjusted p<0.01. Graph coded manually using R. HC: N=8, ERD: N=10. Log2FC= Log2 fold change in gene expression

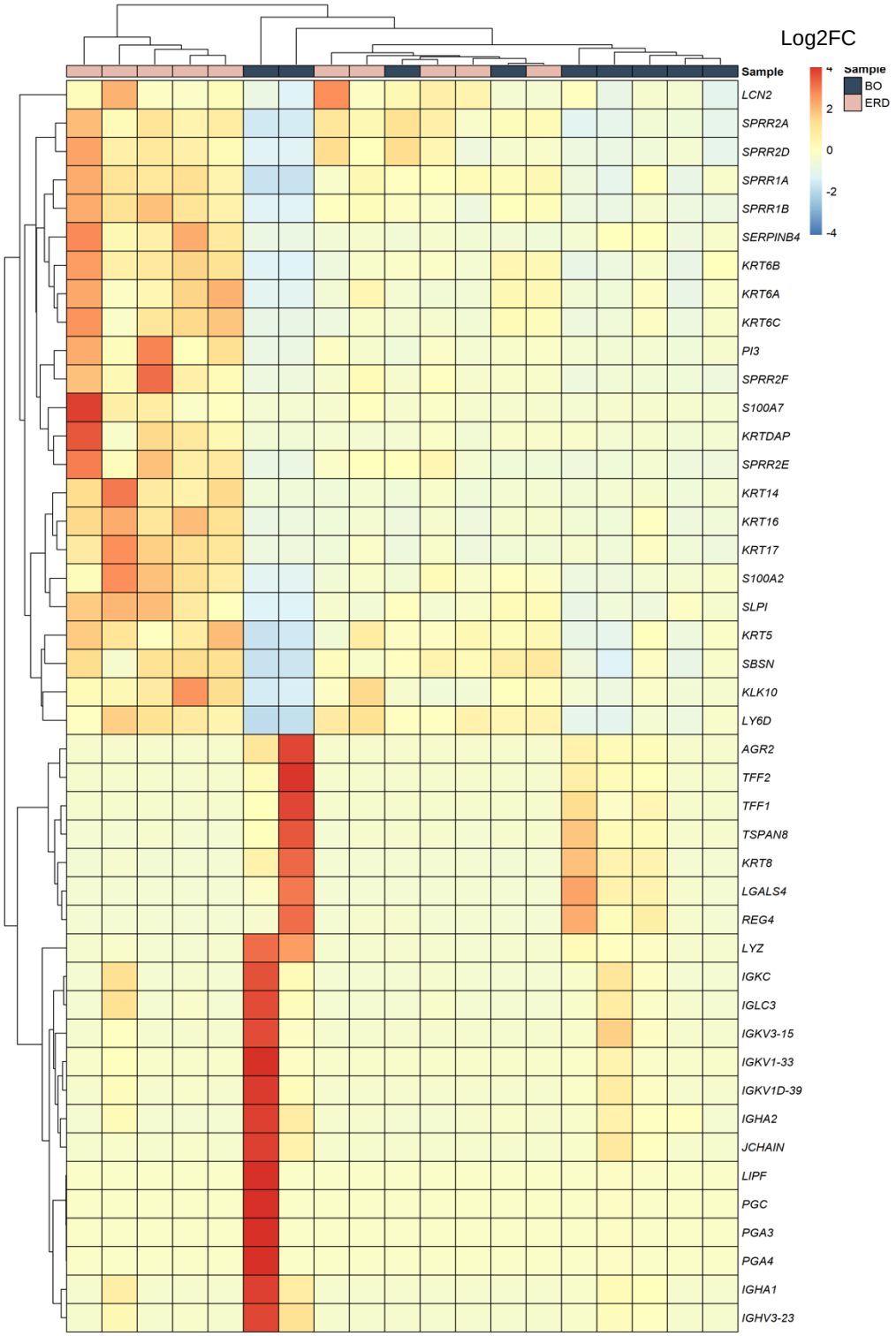

Appendix 10 Most Significantly Differentially Expressed Genes Between BO and ERD Oesophageal Mucosa

Heatmap displaying filtered DE genes with TPM>100, and adjusted p<0.01. Graph coded manually using R. ERD: N=10, BO: N=9. Log2FC= Log2 fold change in gene expression

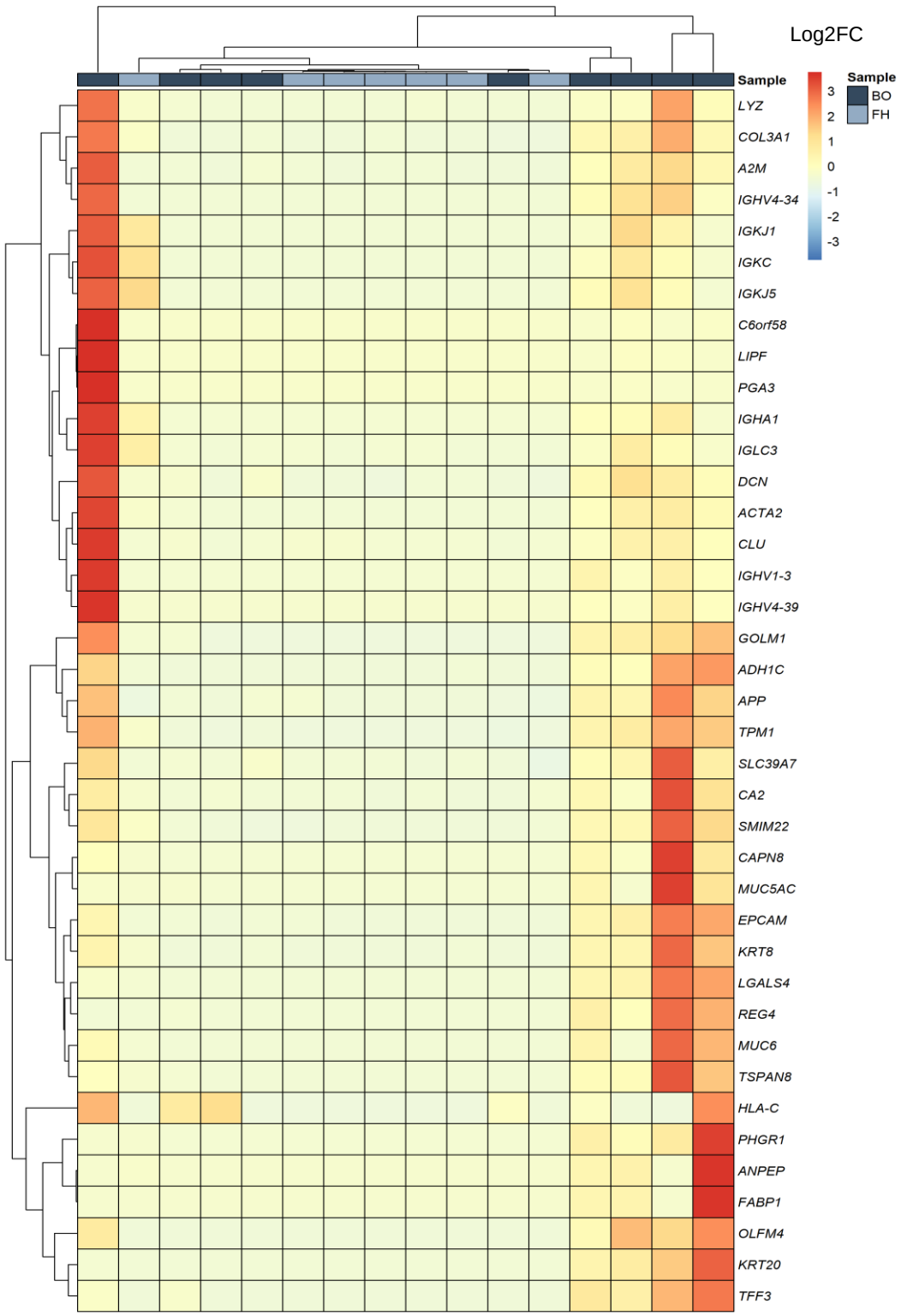

Appendix 11 Most Significantly Differentially Expressed Genes Between BO and FH Oesophageal Mucosa

Heatmap showing filtered DE genes with TPM>50, and adjusted p<0.01. Graph coded manually using R. BO: N=9, FH: N=7. Log2FC= Log2 fold change in gene expression

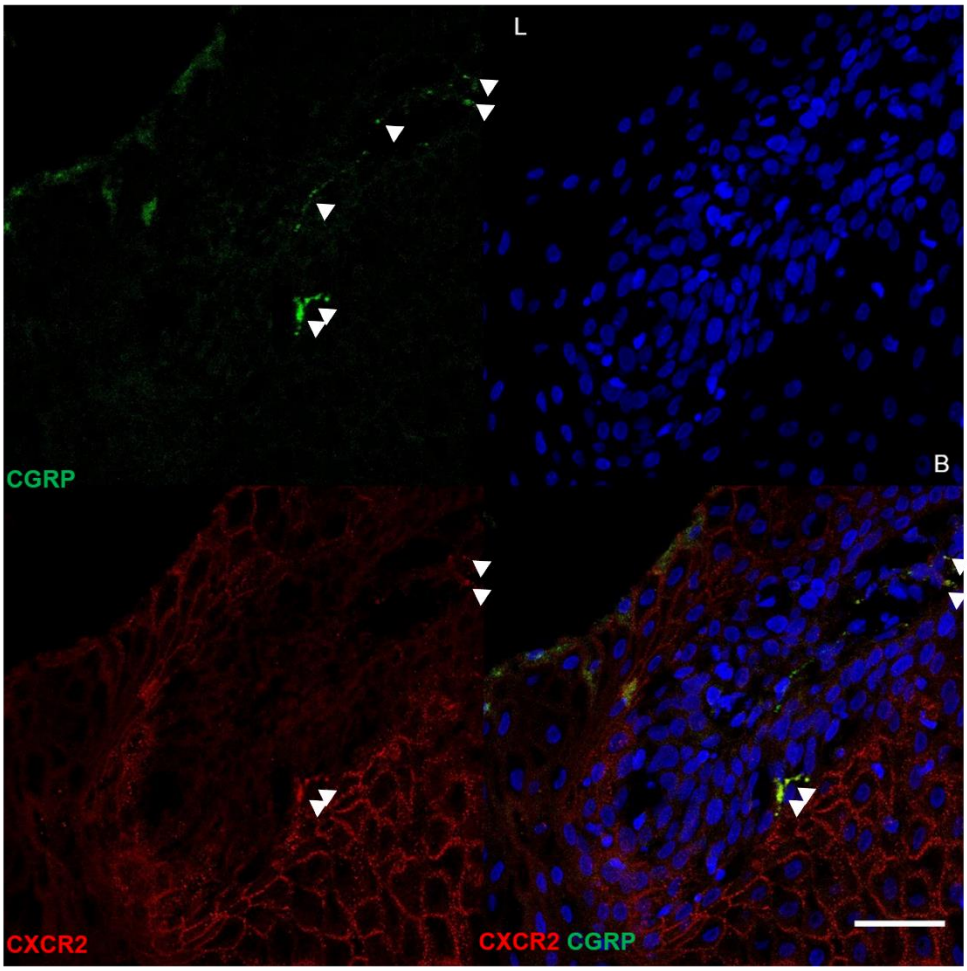

Appendix 12 CXCR2 Expression on a deep sensory nerve in a patient with functional heartburn

Confocal Z-stack maximum intensity projection of a representative functional heartburn patient co-expressing CXCR2 on a deep sensory afferent nerve in the papillae in close association with CXCR2-immunoreactive epithelial cells surrounding the papillae. L=lumen, B= basal layer. Scale bar represents 10µm

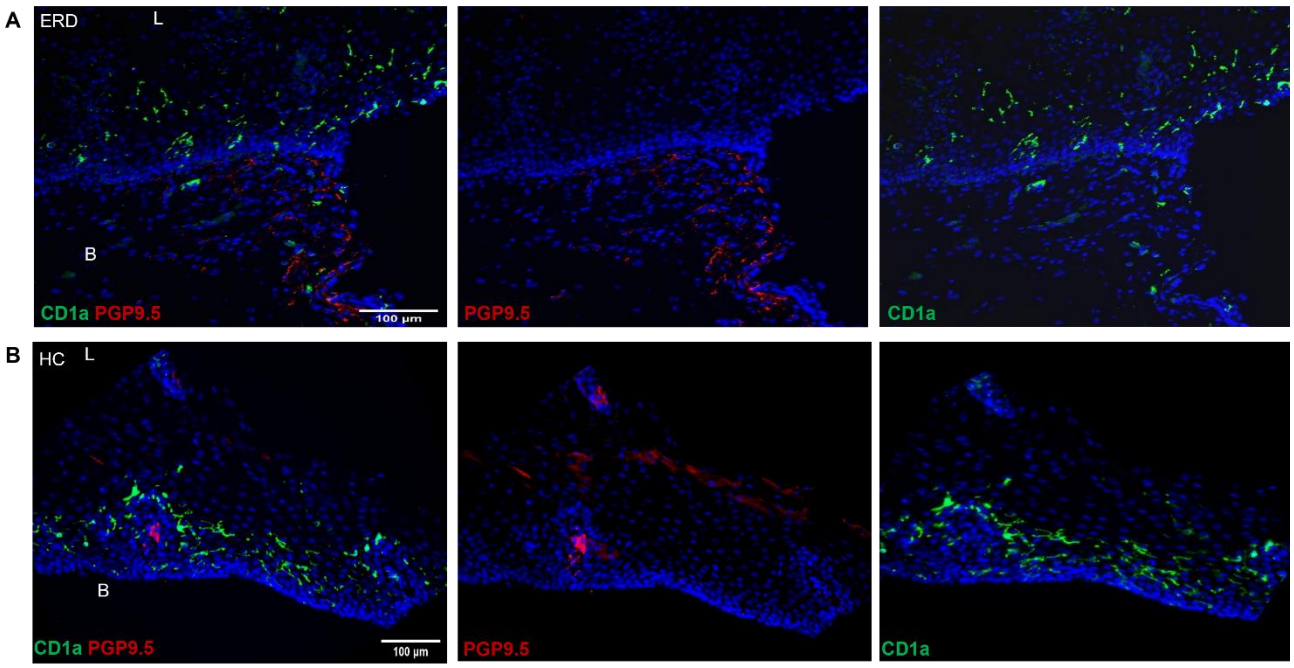

Appendix 13 CD1a+ dendritic cells and PGP9.5+ deep nerve endings are not closely apposed

A) Interpapillary CD1a^{+} dendritic cells in a representative ERD sample and submucosal PGP9.5^{+} afferent nerves. B) Interpapillary CD1a^{+} dendritic cells and submucosal PGP9.5^{+} afferent nerves in a representative healthy control sample. Scale bar: 100µm.

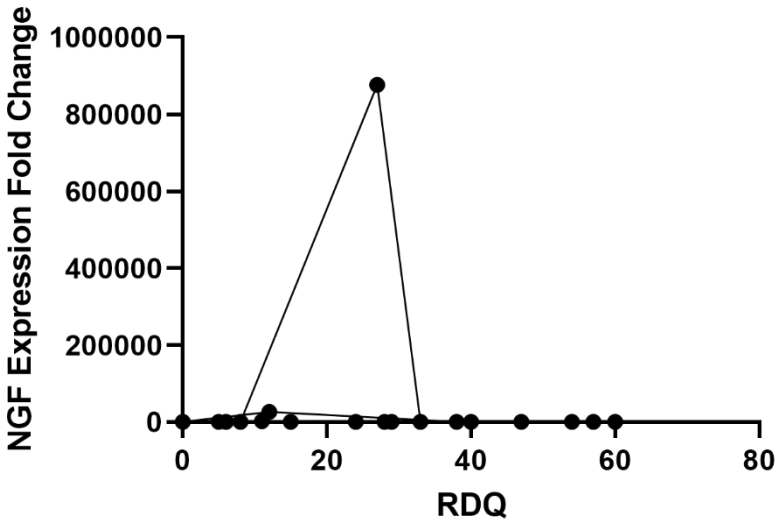

Appendix 15 Correlation Between NGF RNA Expression and Symptom Burden Data

No correlation was found between reflux disease questionnaire score in GORD patients and *NGF* expression ($2^{-\Delta\Delta CT}$).

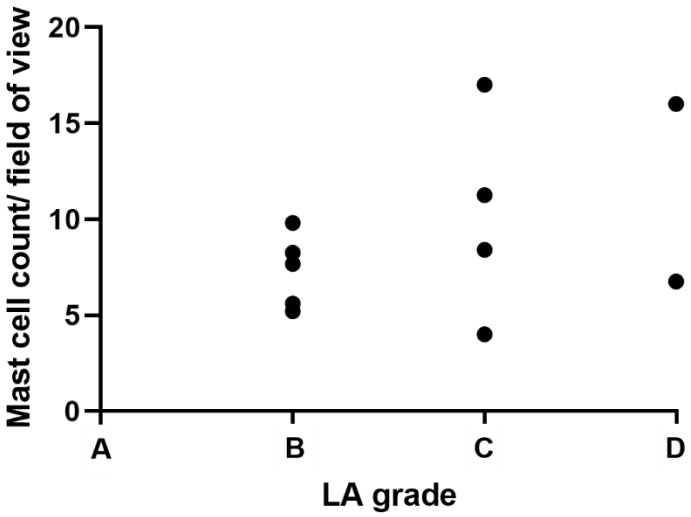

Appendix 14 Correlation of Mast Cell Quantification and Degree of Inflammation in ERD

No correlation was found between LA grade of ERD and mast cells quantified per field of view (Logistic regression: p= 0.34). ERD: N=11.

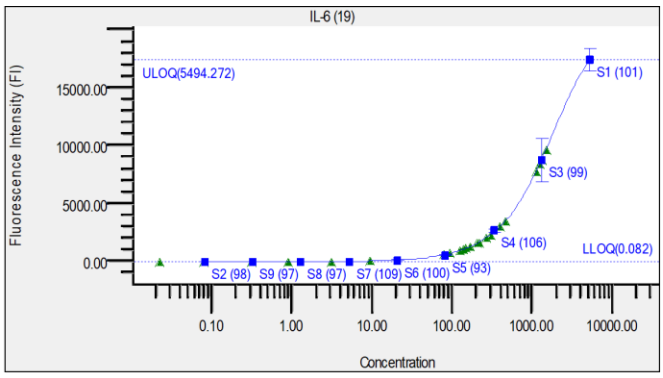

Regression Type: Logistic - 5PL
Std. Curve: FI = 2.30483 + (20143.4 - 2.30483) / ((1 + (Conc / 2663.64)^-1.75706))^0.562692
FitProb = 0.4535, ResVar = 0.9158
Standard Partial Outlier Outlier
Unknown Control

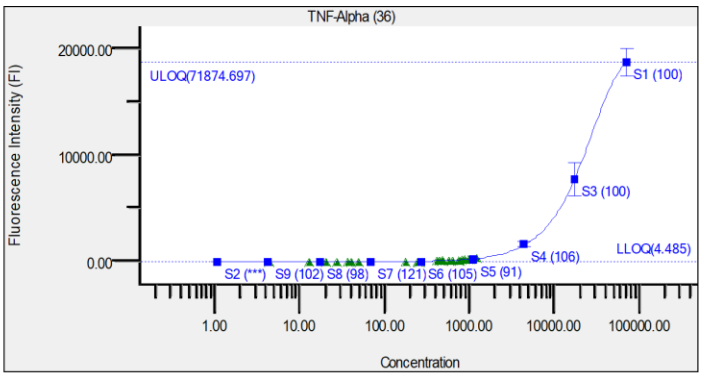

Regression Type: Logistic - 5PL
Std. Curve: FI = 4.13361 + (20722.5 - 4.13361) / ((1 + (Conc / 37403.1)^-2.41729))^0.501388
FitProb = 0.1124, ResVar = 1.8714
Standard Partial Outlier Outlier
Unknown Control

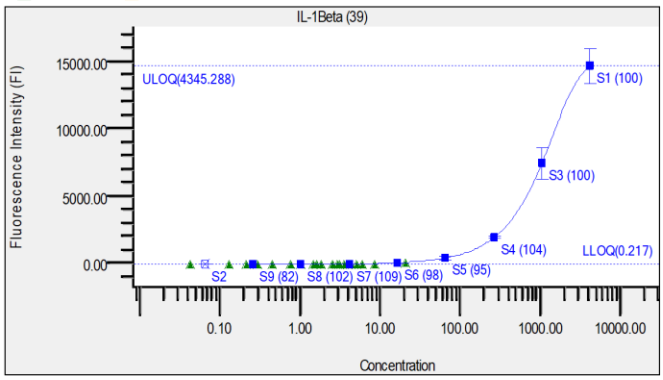

Regression Type: Logistic - 5PL
Std. Curve: FI = 0.761329 + (15772.9 - 0.761329) / ((1 + (Conc / 2026.16)^-2.35973))^0.438123
FitProb = 0.5403, ResVar = 0.7193
Standard Partial Outlier Outlier
Unknown Control

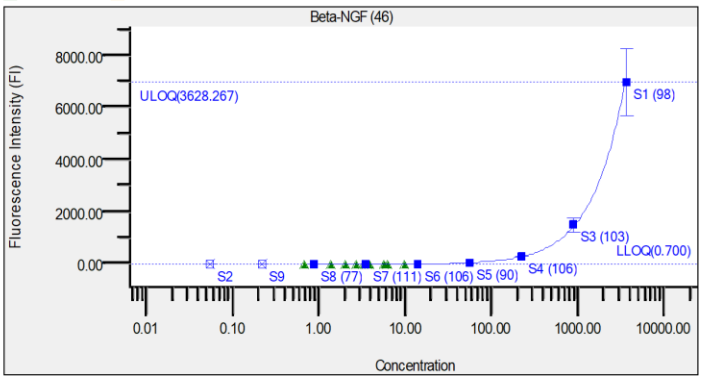

Regression Type: Logistic - 5PL
Std. Curve: FI = 0.606781 + (53562.1 - 0.606781) / ((1 + (Conc / 21464)^-11.0519))^0.103549
FitProb = 0.1101, ResVar = 2.2066
Standard Partial Outlier Outlier
Unknown Control

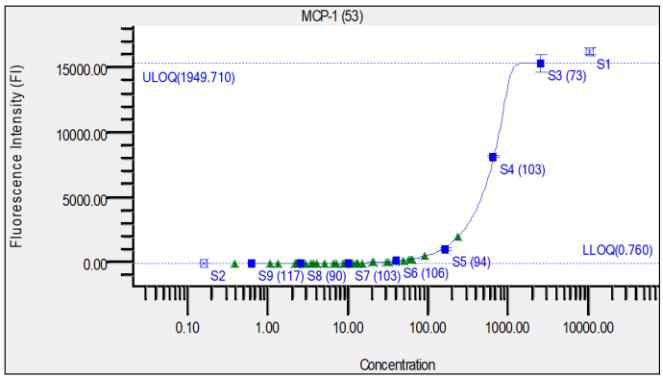

Regression Type: Logistic - 5PL
Std. Curve: FI = 5.15853 + (15441.6 - 5.15853) / ((1 + (Conc / 1089.23)^-13.5077))^0.0999982
FitProb = 0.0918, ResVar = 2.3886
Standard Partial Outlier Outlier
Unknown Control

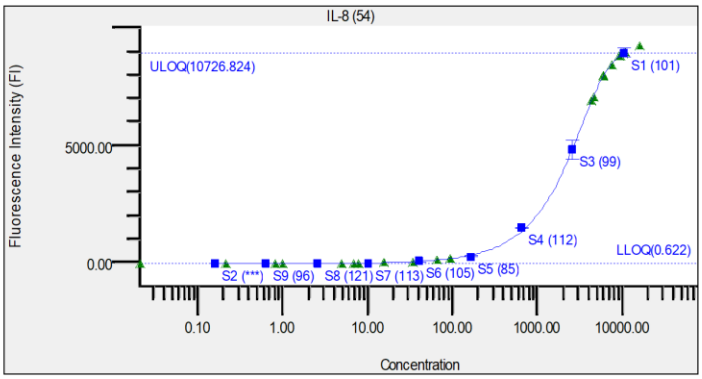

Regression Type: Logistic - 5PL
Std. Curve: FI = 2.94246 + (9446.48 - 2.94246) / ((1 + (Conc / 4874.29)^-2.55238))^0.380599
FitProb = 0.0067, ResVar = 3.5473
Standard Partial Outlier Outlier
Unknown Control

Appendix 16 Standard curves for Bioplex 6-plex cytokine release assay

Standard curves for all inflammatory cytokines investigated in the Bioplex assay fell within the range of the standards, showing accuracy of readouts.

References

[1] N. Vakil, “The Montreal definition and classification of gastroesophageal reflux disease: a global evidence-based consensus,” *Am J Gastroenterol*, vol. 101, 2006.

[2] R. K. Mittal, R. H. Holloway, R. Penagini, L. A. Blackshaw, and J. Dent, “Transient lower esophageal sphincter relaxation.,” *Gastroenterology*, vol. 109, no. 2, pp. 601–610, Aug. 1995.

[3] C. Reimer and P. Bytzer, “Gastroesophageal reflux disease: current state-of-the-art management.,” *Best practice & research. Clinical gastroenterology*, vol. 27, no. 3. Netherlands, p. 323, Jun. 2013. doi: 10.1016/j.bpg.2013.07.001.

[4] J. M. Shin and G. Sachs, “Pharmacology of proton pump inhibitors,” *Curr Gastroenterol Rep*, vol. 10, no. 6, pp. 528–534, Dec. 2008, doi: 10.1007/s11894-008-0098-4.

[5] P. J. Kahrilas, G. Boeckxstaens, and A. J. P. M. Smout, “Management of the patient with incomplete response to PPI therapy,” *Best Practice and Research: Clinical Gastroenterology*, vol. 27, no. 3. Bailliere Tindall Ltd, pp. 401–414, 2013. doi: 10.1016/j.bpg.2013.06.005.

[6] S. Toghanian, P. Wahlqvist, D. A. Johnson, S. C. Bolge, and B. Liljas, “The burden of disrupting gastro-oesophageal reflux disease: a database study in US and European cohorts.,” *Clin Drug Investig*, vol. 30, no. 3, pp. 167–178, 2010, doi: 10.2165/11531670-000000000-00000.

[7] A. F. Peery *et al.*, “Burden and Cost of Gastrointestinal, Liver, and Pancreatic Diseases in the United States: Update 2018,” *Gastroenterology*, vol. 156, no. 1. 2019. doi: 10.1053/j.gastro.2018.08.063.

[8] P. Woodland and D. Sifrim, “The refluxate: The impact of its magnitude, composition and distribution.,” *Best Pract Res Clin Gastroenterol*, vol. 24, no. 6, pp. 861–871, Dec. 2010, doi: 10.1016/j.bpg.2010.09.002.

[9] A. Goldman *et al.*, “Characterization of squamous esophageal cells resistant to bile acids at acidic pH: implication for Barrett’s esophagus pathogenesis.,” *Am J Physiol Gastrointest Liver Physiol*, vol. 300, no. 2, pp. G292-302, Feb. 2011, doi: 10.1152/ajpgi.00461.2010.

[10] R. K. Mittal and D. H. Balaban, “The esophagogastric junction,” *N Engl J Med*, vol. 336(13), pp. 924–932, 1997.

[11] Y. Y. Lee and K. E. L. McColl, “Pathophysiology of gastroesophageal reflux disease,” *Best Practice and Research: Clinical Gastroenterology*, vol. 27, no. 3. Bailliere Tindall Ltd, pp. 339–351, Jun. 01, 2013. doi: 10.1016/j.bpg.2013.06.002.

[12] R. K. Goyal and S. Rattan, “Nature of the vagal inhibitory innervation to the lower esophageal sphincter,” *Journal of Clinical Investigation*, vol. 55, no. 5, pp. 1119–1126, May 1975, doi: 10.1172/JCI108013.

[13] S. Roman *et al.*, “Validation of criteria for the definition of transient lower esophageal sphincter relaxations using high-resolution manometry,” *Neurogastroenterology and Motility*, vol. 29, no. 2, Feb. 2017, doi: 10.1111/nmo.12920.

[14] Y. Y. Lee *et al.*, “Kinetics of transient hiatus hernia during transient lower esophageal sphincter relaxations and swallows in healthy subjects,” *Neurogastroenterology & Motility*, vol. 24, no. 11, pp. 990-e539, Nov. 2012, doi: 10.1111/j.1365-2982.2012.01948.x.

[15] V. P. Zagorodnyuk, B. N. Chen, and S. J. H. Brookes, “Intraganglionic laminar endings are mechano-transduction sites of vagal tension receptors in the guinea-pig stomach,” *Journal of Physiology*, vol. 534, no. 1, pp. 255–268, Jul. 2001, doi: 10.1111/j.1469-7793.2001.00255.x.

[16] S. Lin, M. Ke, J. Xu, and P. J. Kahrilas, “Impaired Esophageal Emptying in Reflux Disease,” *Am J Gastroenterol*, vol. 89, no. 7, pp. 1003–1006, Jan. 1994, doi: 10.1111/j.1572-0241.1994.tb03213.x.

[17] P. J. Kahrilas, H. C. Kim, and J. E. Pandolfino, “Approaches to the diagnosis and grading of hiatal hernia,” *Best Pract Res Clin Gastroenterol*, vol. 22, no. 4, pp. 601–616, Aug. 2008, doi: 10.1016/j.bpg.2007.12.007.

[18] J. Tack and J. E. Pandolfino, “Pathophysiology of Gastroesophageal Reflux Disease,” *Gastroenterology*, vol. 154, no. 2, pp. 277–288, Jan. 2018, doi: 10.1053/j.gastro.2017.09.047.

[19] J. Fletcher, A. Wirz, J. Young, R. Vallance, and K. E. L. McColl, “Unbuffered highly acidic gastric juice exists at the gastroesophageal junction after a meal,” *Gastroenterology*, vol. 121, no. 4, pp. 775–783, Oct. 2001, doi: 10.1053/gast.2001.27997.

[20] A. T. Clarke, A. A. Wirz, J. P. Seenan, J. J. Manning, D. Gillen, and K. E. L. McColl, “Paradox of gastric cardia: It becomes more acidic following meals while the rest of stomach becomes less acidic,” *Gut*, vol. 58, no. 7, pp. 904–909, Jul. 2009, doi: 10.1136/gut.2008.161927.

[21] K. E. L. McColl, A. Clarke, and J. Seenan, “Acid pocket, hiatus hernia and acid reflux,” *Gut*, vol. 59, no. 4. BMJ Publishing Group, pp. 430–431, Apr. 01, 2010. doi: 10.1136/gut.2009.192922.

[22] S. Sloan and P. J. Kahrilas, “Impairment of esophageal emptying with hiatal hernia,” *Gastroenterology*, vol. 100, no. 3, pp. 596–605, Jan. 1991, doi: 10.1016/0016-5085(91)80003-R.

[23] J. E. Pandolfino, G. Shi, B. Trueworthy, and P. J. Kahrilas, “Esophagogastric junction opening during relaxation distinguishes nonhernia reflux patients, hernia patients, and normal subjects,” *Gastroenterology*, vol. 125, no. 4, pp. 1018–1024, Oct. 2003, doi: 10.1016/S0016-5085(03)01210-1.

[24] D. Pohl *et al.*, “Do We Need Gastric Acid?,” *Digestion*, vol. 77, no. 3–4, pp. 184–197, Aug. 2008, doi: 10.1159/000142726.

[25] P. T. Ramsay and A. Carr, “Gastric acid and digestive physiology,” *Surgical Clinics of North America*, vol. 91, no. 5. Elsevier, pp. 977–982, Oct. 01, 2011. doi: 10.1016/j.suc.2011.06.010.

[26] P. Holzer, “Acid sensing by visceral afferent neurones,” *Acta Physiologica*, vol. 201, no. 1. John Wiley & Sons, Ltd, pp. 63–75, Jan. 01, 2011. doi: 10.1111/j.1748-1716.2010.02143.x.

[27] M. Hsu and F. Lui, *Physiology, Stomach*. StatPearls Publishing, 2018. Accessed: Apr. 02, 2020. [Online]. Available: http://www.ncbi.nlm.nih.gov/pubmed/30571046

[28] J. M. Manson, M. Rauch, and M. S. Gilmore, “The commensal microbiology of the gastrointestinal tract,” *Adv Exp Med Biol*, vol. 635, pp. 15–28, 2008, doi: 10.1007/978-0-387-09550-9_2.

[29] A. Sheh and J. G. Fox, “The role of the gastrointestinal microbiome in Helicobacter pylori pathogenesis,” *Gut Microbes*, vol. 4, no. 6. Taylor & Francis, p. 505, Aug. 19, 2013. doi: 10.4161/gmic.26205.

[30] K. R. Bhaskar *et al.*, “Viscous fingering of HCI through gastric mucin,” *Nature*, vol. 360, no. 6403, pp. 458–461, Dec. 1992, doi: 10.1038/360458a0.

[31] A. Allen, A. Bell, M. Mantle, and J. P. Pearson, “The structure and physiology of gastrointestinal mucus.,” *Advances in Experimental Medicine and Biology*, vol. 144. pp. 115–133, 1982. doi: 10.1007/978-1-4615-9254-9_15.

[32] P. Guillem *et al.*, “Mucin gene expression and cell differentiation in human normal, premalignant and malignant esophagus,” *Int J Cancer*, vol. 88, no. 6, pp. 856–861, Dec. 2000, doi: 10.1002/1097-0215(20001215)88:6<856::AID-IJC3>3.0.CO;2-D.

[33] R. C. Orlando, “Esophageal Epithelial Resistance,” in *The Esophagus: Fifth Edition*, Wiley-Blackwell, 2012, pp. 419–433. doi: 10.1002/9781444346220.ch22.

[34] S. E. Williams and L. A. Turnberg, “Studies of the protective properties of gastric mucus.,” *Adv Exp Med Biol*, vol. 144, pp. 187–188, 1982, doi: 10.1007/978-1-4615-9254-9_28.

[35] S. E. Williams and L. A. Turnberg, “Demonstration of a pH gradient across mucus adherent to rabbit gastric mucosa: Evidence for a ‘mucus-bicarbonate’ barrier,” *Gut*, vol. 22, no. 2, pp. 94–96, Feb. 1981, doi: 10.1136/gut.22.2.94.

[36] E. M. M. Quigley and L. A. Turnberg, “pH of the Microclimate Lining Human Gastric and Duodenal Mucosa In Vivo Studies in Control Subjects and in Duodenal Ulcer Patients,” 1987.

[37] B. H. Hamilton and R. C. Orlando, “In vivo alkaline secretion by mammalian esophagus,” *Gastroenterology*, vol. 97, no. 3, pp. 640–648, Sep. 1989, doi: 10.1016/0016-5085(89)90635-5.

[38] N. A. Tobey, C. M. Argote, M. S. Awayda, X. C. Vanegas, and R. C. Orlando, “Effect of luminal acidity on the apical cation channel in rabbit esophageal epithelium,” *American Journal of Physiology-Gastrointestinal and Liver Physiology*, vol. 292, no. 3, pp. G796–G805, Mar. 2007, doi: 10.1152/ajpgi.00385.2005.

[39] P. Holzer, “Acid-sensing ion channels in gastrointestinal function,” *Neuropharmacology*, vol. 94. Elsevier Ltd, pp. 72–79, Jul. 01, 2015. doi: 10.1016/j.neuropharm.2014.12.009.

[40] “Esophagus | Gastrointestinal Tract.” https://histologyguide.com/slideview/MHS-234-esophagus/14-slide-1.html?x=13205&y=6078&z=7.2 (accessed Mar. 02, 2022).

[41] K. R. McQuaid, L. Laine, M. B. Fennerty, R. Souza, and S. J. Spechler, “Systematic review: the role of bile acids in the pathogenesis of gastro-oesophageal reflux disease and related neoplasia,” *Aliment Pharmacol Ther*, vol. 34, no. 2, pp. 146–165, Jul. 2011, doi: 10.1111/j.1365-2036.2011.04709.x.

[42] N. B. ROBERTS, “Review article: human pepsins - their multiplicity, function and role in reflux disease,” *Aliment Pharmacol Ther*, vol. 24, pp. 2–9, Aug. 2006, doi: 10.1111/j.1365-2036.2006.03038.x.

[43] W. J. Barlow and R. C. Orlando, “The pathogenesis of heartburn in nonerosive reflux disease: A unifying hypothesis,” *Gastroenterology*, vol. 128, no. 3, pp. 771–778, Mar. 2005, doi: 10.1053/j.gastro.2004.08.014.

[44] N. A. Tobey, T. M. Gambling, X. C. Vanegas, J. L. Carson, and R. C. Orlando, “Physicochemical basis for dilated intercellular spaces in non-erosive acid-damaged rabbit esophageal epithelium,” *Diseases of the Esophagus*, vol. 21, no. 8, pp. 757–764, Nov. 2008, doi: 10.1111/j.1442-2050.2008.00841.x.

[45] P. Woodland, C. Lee, Y. Duraisamy, R. Farre, P. Dettmar, and D. Sifrim, “Assessment and protection of esophageal mucosal integrity in patients with heartburn without esophagitis.,” *Am J Gastroenterol*, vol. 108, no. 4, pp. 535–543, Apr. 2013, doi: 10.1038/ajg.2012.469.

[46] H. Van Malenstein, R. Farré, and D. Sifrim, “Esophageal dilated intercellular spaces (DIS) and nonerosive reflux disease,” *American Journal of Gastroenterology*, vol. 103, no. 4. pp. 1021–1028, Apr. 2008. doi: 10.1111/j.1572-0241.2007.01688.x.

[47] A. Ravelli, V. Villanacci, M. Cadei, M. Fuoti, G. Gennati, and M. Salemme, “Dilated intercellular spaces in eosinophilic esophagitis,” *J Pediatr Gastroenterol Nutr*, vol. 59, no. 5, pp. 589–593, Nov. 2014, doi: 10.1097/MPG.0000000000000491.

[48] D. Asaoka *et al.*, “Altered localization and expression of tight-junction proteins in a rat model with chronic acid reflux esophagitis,” *J Gastroenterol*, vol. 40, no. 8, pp. 781–790, Aug. 2005, doi: 10.1007/s00535-005-1628-6.

[49] F. Y. Li and Y. Li, “Interleukin-6, desmosome and tight junction protein expression levels in reflux esophagitis-affected mucosa,” *World J Gastroenterol*, vol. 15, no. 29, pp. 3621–3630, Aug. 2009, doi: 10.3748/wjg.15.3621.

[50] B. Jovov, J. Que, N. A. Tobey, Z. Djukic, B. L. M. Hogan, and R. C. Orlando, “Role of e-cadherin in the pathogenesis of gastroesophageal reflux disease,” *American Journal of Gastroenterology*, vol. 106, no. 6, pp. 1039–1047, Jun. 2011, doi: 10.1038/ajg.2011.102.

[51] P. W. Weijenborg and A. J. Bredenoord, “How reflux causes symptoms: Reflux perception in gastroesophageal reflux disease,” *Best Practice and Research: Clinical Gastroenterology*, vol. 27, no. 3. Bailliere Tindall Ltd, pp. 353–364, Jun. 01, 2013. doi: 10.1016/j.bpg.2013.06.003.

[52] a. j. bredenoord, g. j. m. hemmink, and a. j. p. m. smout, “Relationship between gastro-oesophageal reflux pattern and severity of mucosal damage,” *Neurogastroenterology & Motility*, vol. 21, no. 8, pp. 807–812, Aug. 2009, doi: 10.1111/j.1365-2982.2009.01306.x.

[53] L. R. Lundell *et al.*, “Endoscopic assessment of oesophagitis: clinical and functional correlates and further validation of the Los Angeles classification,” *Gut*, vol. 45, no. 2, pp. 172–180, 1999, doi: 10.1136/gut.45.2.172.

[54] Q. Aziz, R. Fass, C. P. Gyawali, H. Miwa, J. E. Pandolfino, and F. Zerbib, “Esophageal disorders,” *Gastroenterology*, vol. 150, no. 6, pp. 1368–1379, May 2016, doi: 10.1053/j.gastro.2016.02.012.

[55] D. Ang, D. Sifrim, and J. Tack, “Mechanisms of heartburn,” *Nat Clin Pract Gastroenterol Hepatol*, vol. 5, no. 7, pp. 383–392, Jul. 2008, doi: 10.1038/ncpgasthep1160.

[56] P. W. Weijenborg *et al.*, “Hypersensitivity to acid is associated with impaired esophageal mucosal integrity in patients with gastroesophageal reflux disease with and without esophagitis,” *Am J Physiol Gastrointest Liver Physiol*, vol. 307, no. 3, pp. G323-9, Aug. 2014, doi: 10.1152/ajpgi.00345.2013.

[57] M. Yang *et al.*, “Quantitative assessment and characterization of visceral hyperalgesia evoked by esophageal balloon distention and acid perfusion in patients with functional heartburn, nonerosive reflux disease, and erosive esophagitis,” *Clinical Journal of Pain*, vol. 26, no. 4, pp. 326–331, May 2010, doi: 10.1097/AJP.0b013e3181c8fc83.

[58] H. Miwa *et al.*, “Oesophageal hypersensitivity in Japanese patients with non-erosive gastro-oesophageal reflux diseases,” *Aliment Pharmacol Ther*, vol. 20, no. s1, pp. 112–117, Jul. 2004, doi: 10.1111/j.1365-2036.2004.01990.x.

[59] A. Nagahara *et al.*, “Increased esophageal sensitivity to acid and saline in patients with nonerosive gastro-esophageal reflux disease,” *J Clin Gastroenterol*, vol. 40, no. 10, pp. 891–895, Nov. 2006, doi: 10.1097/01.mcg.0000225673.76475.9d.

[60] J. Fletcher, “Barrett’s esophagus evokes a quantitatively and qualitatively altered response to both acid and hypertonic solutions,” *Am J Gastroenterol*, vol. 98, no. 7, pp. 1480–1486, Jul. 2003, doi: 10.1016/s0002-9270(03)00376-9.

[61] A. L. Krarup, Sø. S. Olesen, P. Funch-Jensen, H. Gregersen, and A. M. Drewes, “Proximal and distal esophageal sensitivity is decreased in patients with barrett’s esophagus,” *World J Gastroenterol*, vol. 17, no. 4, pp. 514–521, Jan. 2011, doi: 10.3748/wjg.v17.i4.514.

[62] C. Lottrup, A. L. Krarup, H. Gregersen, P. Ejstrud, and A. M. Drewes, “Patients with Barrett’s esophagus are hypersensitive to acid but hyposensitive to other stimuli compared with healthy controls,” *Neurogastroenterology & Motility*, vol. 29, no. 4, p. e12992, Apr. 2017, doi: 10.1111/nmo.12992.

[63] G. H. Koek, D. Sifrim, T. Lerut, J. Janssens, and J. Tack, “Multivariate analysis of the association of acid and duodeno-gastro- oesophageal reflux exposure with the presence of oesophagitis, the severity of oesophagitis and Barrett’s oesophagus,” *Gut*, vol. 57, no. 8, pp. 1056–1064, Aug. 2008, doi: 10.1136/gut.2006.119206.

[64] R. F. Souza, “The role of acid and bile reflux in oesophagitis and Barrett’s metaplasia,” *Biochem Soc Trans*, vol. 38, no. 2, pp. 348–352, Apr. 2010, doi: 10.1042/BST0380348.

[65] M. Jiang *et al.*, “Transitional basal cells at the squamous-columnar junction generate Barrett’s oesophagus,” *Nature*, vol. 550, no. 7677, pp. 529–533, Oct. 2017, doi: 10.1038/nature24269.

[66] C. H. Knowles and Q. Aziz, “Visceral hypersensitivity in non-erosive reflux disease.,” *Gut*, vol. 57, no. 5, pp. 674–683, May 2008, doi: 10.1136/gut.2007.127886.

[67] B. D. Naliboff *et al.*, “The effect of life stress on symptoms of heartburn,” *Psychosom Med*, vol. 66, no. 3, pp. 426–434, 2004, doi: 10.1097/01.psy.0000124756.37520.84.

[68] R. Fass *et al.*, “The Effect of Auditory Stress on Perception of Intraesophageal Acid in Patients With Gastroesophageal Reflux Disease,” *Gastroenterology*, vol. 134, no. 3, pp. 696–705, 2008, doi: 10.1053/j.gastro.2007.12.010.

[69] L. Guadagnoli, R. Yadlapati, T. Taft, J. E. Pandolfino, M. Tye, and L. Keefer, “Esophageal hypervigilance is prevalent across gastroesophageal reflux disease presentations,” *Neurogastroenterol Motil*, vol. 33, no. 8, Aug. 2021, doi: 10.1111/NMO.14081.

[70] D. A. Carlson *et al.*, “Esophageal Hypervigilance and Visceral Anxiety Are Contributors to Symptom Severity Among Patients Evaluated With High-Resolution Esophageal Manometry,” *Am J Gastroenterol*, vol. 115, no. 3, pp. 367–375, Mar. 2020, doi: 10.14309/AJG.0000000000000536.

[71] P. J. Kahrilas, L. Keefer, and J. E. Pandolfino, “Patients with refractory reflux symptoms: What do they have and how should they be managed?,” *Neurogastroenterol Motil*, vol. 27, no. 9, pp. 1195–1201, Sep. 2015, doi: 10.1111/NMO.12644.

[72] R. Schey *et al.*, “Sleep Deprivation Is Hyperalgesic in Patients With Gastroesophageal Reflux Disease,” *Gastroenterology*, vol. 133, no. 6, pp. 1787–1795, Dec. 2007, doi: 10.1053/j.gastro.2007.09.039.

[73] B. F. Kessing, A. J. Bredenoord, C. M. G. Saleh, and A. J. P. M. Smout, “Effects of Anxiety and Depression in Patients With Gastroesophageal Reflux Disease,” *Clinical Gastroenterology and Hepatology*, vol. 13, no. 6, pp. 1089-1095.e1, Jun. 2015, doi: 10.1016/j.cgh.2014.11.034.

[74] L. Van Oudenhove, K. Demyttenaere, J. Tack, and Q. Aziz, “Central nervous system involvement in functional gastrointestinal disorders,” *Best Pract Res Clin Gastroenterol*, vol. 18, no. 4, pp. 663–680, Aug. 2004, doi: 10.1016/j.bpg.2004.04.010.

[75] D. A. Carlson *et al.*, “Esophageal Hypervigilance and Visceral Anxiety Are Contributors to Symptom Severity Among Patients Evaluated With High-Resolution Esophageal Manometry,” *Am J Gastroenterol*, vol. 115, no. 3, pp. 367–375, Mar. 2020, doi: 10.14309/ajg.0000000000000536.

[76] K. N. Browning and R. A. Travagli, “Central nervous system control of gastrointestinal motility and secretion and modulation of gastrointestinal functions,” *Compr Physiol*, vol. 4, no. 4, pp. 1339–1368, Oct. 2014, doi: 10.1002/cphy.c130055.

[77] S. Breit, A. Kupferberg, G. Rogler, and G. Hasler, “Vagus Nerve as Modulator of the Brain-Gut Axis in Psychiatric and Inflammatory Disorders,” *Front Psychiatry*, vol. 9, p. 44, Mar. 2018, doi: 10.3389/fpsyt.2018.00044.

[78] W. J. Dodds, J. Dent, W. J. Hogan, and R. C. Arndorfer, “Effect of atropine on esophageal motor function in humans.,” *Am J Physiol*, vol. 240, no. 4, pp. G290-6, Apr. 1981, doi: 10.1152/ajpgi.1981.240.4.G290.

[79] P. I. Collman, L. Tremblay, and N. E. Diamant, “The distribution of spinal and vagal sensory neurons that innervate the esophagus of the cat.,” *Gastroenterology*, vol. 103, no. 3, pp. 817–22, Sep. 1992, doi: 10.1016/0016-5085(92)90012-n.

[80] R. K. Mittal, “Pathophysiology of Gastroesophageal Reflux Disease: Motility Factors,” in *The Esophagus*, Oxford, UK: Wiley-Blackwell, 2012, pp. 405–418. doi: 10.1002/9781444346220.ch21.

[81] S. M. Brierley, P. Hughes, A. Harrington, and L. Ashley Blackshaw, “Innervation of the Gastrointestinal Tract by Spinal and Vagal Afferent Nerves,” in *Physiology of the Gastrointestinal Tract*, vol. 1, Elsevier Inc., 2012, pp. 703–731. doi: 10.1016/B978-0-12-382026-6.00024-5.

[82] X. Yu, M. Yu, Y. Liu, and S. Yu, “TRP channel functions in the gastrointestinal tract.,” *Semin Immunopathol*, vol. 38, no. 3, pp. 385–396, May 2016, doi: 10.1007/s00281-015-0528-y.

[83] M. Dutsch, U. Eichhorn, J. Worl, M. Wank, H. R. Berthoud, and W. L. Neuhuber, “Vagal and spinal afferent innervation of the rat esophagus: a combined retrograde tracing and immunocytochemical

study with special emphasis on calcium-binding proteins.," *J Comp Neurol*, vol. 398, no. 2, pp. 289–307, Aug. 1998.

[84] M. Wank and W. L. Neuhuber, "Local differences in vagal afferent innervation of the rat esophagus are reflected by neurochemical differences at the level of the sensory ganglia and by different brainstem projections.," *J Comp Neurol*, vol. 435, no. 1, pp. 41–59, Jun. 2001.

[85] R. K. Khurana and J. M. Petras, "Sensory innervation of the canine esophagus, stomach, and duodenum.," *Am J Anat*, vol. 192, no. 3, pp. 293–306, Nov. 1991, doi: 10.1002/aja.1001920309.

[86] R. Uddman, T. Grunditz, A. Luts, H. Desai, G. Fernstrom, and F. Sundler, "Distribution and origin of the peripheral innervation of rat cervical esophagus.," *Dysphagia*, vol. 10, no. 3, pp. 203–212, 1995.

[87] T. Hayakawa, S. Kuwahara, S. Maeda, K. Tanaka, and M. Seki, "Distribution of vagal CGRP-immunoreactive fibers in the lower esophagus and the cardia of the stomach of the rat," *J Chem Neuroanat*, vol. 38, no. 2, pp. 124–129, Oct. 2009, doi: 10.1016/j.jchemneu.2009.04.001.

[88] O. A. Krishtal and V. I. Pidoplichko, "A receptor for protons in the membrane of sensory neurons may participate in nociception," *Neuroscience*, vol. 6, no. 12, pp. 2599–2601, Dec. 1981, doi: 10.1016/0306-4522(81)90105-6.

[89] O. Krishtal, "The ASICs: Signaling molecules? Modulators?," *Trends Neurosci*, vol. 26, no. 9, pp. 477–483, Sep. 2003, doi: 10.1016/S0166-2236(03)00210-8.

[90] M. Petersen and R. H. LaMotte, "Effect of protons on the inward current evoked by capsaicin in isolated dorsal root ganglion cells," *Pain*, vol. 54, no. 1, pp. 37–42, Jul. 1993, doi: 10.1016/0304-3959(93)90097-9.

[91] H. U. Zeilhofer, M. Kress, and D. Swandulla, "Fractional Ca 2+ currents through capsaicin- and proton-activated ion channels in rat dorsal root ganglion neurones," *Journal of Physiology*, vol. 503, no. 1, pp. 67–78, Aug. 1997, doi: 10.1111/j.1469-7793.1997.067bi.x.

[92] R. Waldmann, G. Champigny, F. Bassilana, C. Heurteaux, and M. Lazdunski, "A proton-gated cation channel involved in acid-sensing," *Nature*, vol. 386, no. 6621, pp. 173–177, Mar. 1997, doi: 10.1038/386173a0.

[93] S. Bevan and P. Geppetti, "Protons: small stimulants of capsaicin-sensitive sensory nerves," *Trends Neurosci*, vol. 17, no. 12, pp. 509–512, Jan. 1994, doi: 10.1016/0166-2236(94)90149-X.

[94] P. Holzer, "Local effector functions of capsaicin-sensitive sensory nerve endings: Involvement of tachykinins, calcitonin gene-related peptide and other neuropeptides," *Neuroscience*, vol. 24, no. 3, pp. 739–768, Mar. 1988, doi: 10.1016/0306-4522(88)90064-4.

[95] D. Julius, "TRP channels and pain.," *Annu Rev Cell Dev Biol*, vol. 29, pp. 355–384, 2013, doi: 10.1146/annurev-cellbio-101011-155833.

[96] H. Miwa, T. Kondo, T. Oshima, H. Fukui, T. Tomita, and J. Watari, "Esophageal sensation and esophageal hypersensitivity - overview from bench to bedside.," *J Neurogastroenterol Motil*, vol. 16, no. 4, pp. 353–362, Oct. 2010, doi: 10.5056/jnm.2010.16.4.353.

[97] A. E. Dubin and A. Patapoutian, "Nociceptors: the sensors of the pain pathway.," *J Clin Invest*, vol. 120, no. 11, pp. 3760–3772, Nov. 2010, doi: 10.1172/JCI42843.

[98] A. I. Basbaum, D. M. Bautista, G. Scherrer, and D. Julius, "Cellular and molecular mechanisms of pain.," *Cell*, vol. 139, no. 2, pp. 267–284, Oct. 2009, doi: 10.1016/j.cell.2009.09.028.

[99] P. Anand, Q. Aziz, R. Willert, and L. Van Oudenhove, "Peripheral and central mechanisms of visceral sensitization in man," in *Neurogastroenterology and Motility*, Jan. 2007, vol. 19, no. SUPPL.1, pp. 29–46. doi: 10.1111/j.1365-2982.2006.00873.x.

[100] Y. Kawasaki *et al.*, "Journal of Neuroscience," *J. Neurosci.*, vol. 22, no. 5, pp. 1532–1540, Sep. 2004, doi: 20026611.

[101] C. J. Woolf and M. W. Salter, “Neuronal plasticity: Increasing the gain in pain,” *Science*, vol. 288, no. 5472. American Association for the Advancement of Science, pp. 1765–1768, Jun. 09, 2000. doi: 10.1126/science.288.5472.1765.

[102] D. W. Garrison, M. J. Chandler, and R. D. Foreman, “Viscerosomatic convergence onto feline spinal neurons from esophagus, heart and somatic fields: effects of inflammation,” *Pain*, vol. 49, no. 3, pp. 373–382, Jun. 1992, doi: 10.1016/0304-3959(92)90245-7.

[103] B. K. Medda, J. N. Sengupta, I. M. Lang, and R. Shaker, “Response properties of the brainstem neurons of the cat following intra-esophageal acid–pepsin infusion,” *Neuroscience*, vol. 135, no. 4, pp. 1285–1294, 2005, doi: https://doi.org/10.1016/j.neuroscience.2005.07.016.

[104] B. Banerjee *et al.*, “Alterations in N-methyl-D-aspartate receptor subunits in primary sensory neurons following acid-induced esophagitis in cats,” *Am J Physiol Gastrointest Liver Physiol*, vol. 296, no. 1, Jan. 2009, doi: 10.1152/ajpgi.90419.2008.

[105] S. Sarkar, Q. Aziz, C. J. Woolf, A. R. Hobson, and D. G. Thompson, “Contribution of central sensitisation to the development of non-cardiac chest pain,” *Lancet*, vol. 356, no. 9236, pp. 1154–1159, Sep. 2000, doi: 10.1016/S0140-6736(00)02758-6.

[106] S. Sarkar *et al.*, “The prostaglandin E2 receptor-1 (EP-1) mediates acid-induced visceral pain hypersensitivity in humans,” *Gastroenterology*, vol. 124, no. 1, pp. 18–25, Jan. 2003, doi: 10.1053/gast.2003.50022.

[107] A. B. Maimberg and T. L. Yaksh, “Cyclooxygenase inhibition and the spinal release of prostaglandin E2 and amino acids evoked by paw formalin injection: A microdialysis study in unanesthetized rats,” *Journal of Neuroscience*, vol. 15, no. 4, pp. 2768–2776, 1995, doi: 10.1523/jneurosci.15-04-02768.1995.

[108] H. Baba, T. Kohno, K. A. Moore, and C. J. Woolf, “Direct activation of rat spinal dorsal horn neurons by prostaglandin E2,” *Journal of Neuroscience*, vol. 21, no. 5, pp. 1750–1756, Mar. 2001, doi: 10.1523/jneurosci.21-05-01750.2001.

[109] R. P. Willert, C. J. Woolf, A. R. Hobson, C. Delaney, D. G. Thompson, and Q. Aziz, “The Development and Maintenance of Human Visceral Pain Hypersensitivity Is Dependent on the N-Methyl-D-Aspartate Receptor,” *Gastroenterology*, vol. 126, no. 3, pp. 683–692, Mar. 2004, doi: 10.1053/j.gastro.2003.11.047.

[110] J. B. Furness, “The enteric nervous system and neurogastroenterology,” *Nature Reviews Gastroenterology and Hepatology*, vol. 9, no. 5. Nature Publishing Group, pp. 286–294, May 06, 2012. doi: 10.1038/nrgastro.2012.32.

[111] H. R. Mertz, “Overview of functional gastrointestinal disorders: Dysfunction of the brain-gut axis,” *Gastroenterology Clinics of North America*, vol. 32, no. 2. W.B. Saunders, pp. 463–476, 2003. doi: 10.1016/S0889-8553(03)00019-0.

[112] T. Uesaka, H. M. Young, V. Pachnis, and H. Enomoto, “Development of the intrinsic and extrinsic innervation of the gut,” *Dev Biol*, vol. 417, no. 2, pp. 158–167, 2016, doi: https://doi.org/10.1016/j.ydbio.2016.04.016.

[113] Y. Jiang, H. Dong, L. Eckmann, E. M. Hanson, K. C. Ihn, and R. K. Mittal, “Visualizing the enteric nervous system using genetically engineered double reporter mice: Comparison with immunofluorescence,” *PLoS One*, vol. 12, no. 2, p. e0171239, Feb. 2017, doi: 10.1371/journal.pone.0171239.

[114] W. B. Cannon, “ŒSOPHAGEAL PERISTALSIS AFTER BILATERAL VAGOTOMY,” *American Journal of Physiology-Legacy Content*, vol. 19, no. 3, pp. 436–444, Aug. 1907, doi: 10.1152/ajplegacy.1907.19.3.436.

[115] V. P. Zagorodnyuk, B. N. Chen, M. Costa, and S. J. H. Brookes, “Mechanotransduction by intraganglionic laminar endings of vagal tension receptors in the guinea-pig oesophagus,” *Journal of*

Physiology, vol. 553, no. 2. Wiley-Blackwell, pp. 575–587, Dec. 01, 2003. doi: 10.1113/jphysiol.2003.051862.

[116] V. P. Zagorodnyuk, B. N. Chen, and S. J. Brookes, “Intraganglionic laminar endings are mechano-transduction sites of vagal tension receptors in the guinea-pig stomach.,” *J Physiol*, vol. 534, no. Pt 1, pp. 255–268, Jul. 2001, doi: 10.1111/j.1469-7793.2001.00255.x.

[117] H. -R Berthoud and T. L. Powley, “Vagal afferent innervation of the rat fundic stomach: Morphological characterization of the gastric tension receptor,” *Journal of Comparative Neurology*, vol. 319, no. 2, pp. 261–276, May 1992, doi: 10.1002/cne.903190206.

[118] H. R. Berthoud and T. L. Powley, “Vagal afferent innervation of the rat fundic stomach: morphological characterization of the gastric tension receptor.,” *J Comp Neurol*, vol. 319, no. 2, pp. 261–276, May 1992, doi: 10.1002/cne.903190206.

[119] G. A. Hicks *et al.*, “Excitation of rat colonic afferent fibres by 5-HT3 receptors,” *Journal of Physiology*, vol. 544, no. 3, pp. 861–869, Nov. 2002, doi: 10.1113/jphysiol.2002.025452.

[120] S. M. Brierley, R. C. W. 3rd Jones, G. F. Gebhart, and L. A. Blackshaw, “Splanchnic and pelvic mechanosensory afferents signal different qualities of colonic stimuli in mice.,” *Gastroenterology*, vol. 127, no. 1, pp. 166–178, Jul. 2004.

[121] M. Koltzenburg, C. L. Stucky, and G. R. Lewin, “Receptive Properties of Mouse Sensory Neurons Innervating Hairy Skin,” *J Neurophysiol*, vol. 78, no. 4, pp. 1841–1850, Oct. 1997, doi: 10.1152/jn.1997.78.4.1841.

[122] S. K. Joshi and G. F. Gebhart, “Visceral pain.,” *Curr Rev Pain*, vol. 4, no. 6, pp. 499–506, 2000.

[123] R. D. Brtva, G. A. Iwamoto, and J. C. Longhurst, “Distribution of cell bodies for primary afferent fibers from the stomach of the cat,” *Neurosci Lett*, vol. 105, no. 3, pp. 287–293, Nov. 1989, doi: 10.1016/0304-3940(89)90635-6.

[124] N. Clerc and C. Mazzia, “Morphological relationships of choleragenoid horseradish peroxidase-labeled spinal primary afferents with myenteric ganglia and mucosal associated lymphoid tissue in the cat esophagogastric junction.,” *J Comp Neurol*, vol. 347, no. 2, pp. 171–186, Sep. 1994, doi: 10.1002/cne.903470203.

[125] A. J. Page and L. A. Blackshaw, “An in vitro study of the properties of vagal afferent fibres innervating the ferret oesophagus and stomach.,” *J Physiol*, vol. 512 (Pt 3, pp. 907–916, Nov. 1998, doi: 10.1111/j.1469-7793.1998.907bd.x.

[126] S. Sekizawa, T. Ishikawa, F. B. Sant’Ambrogio, and G. Sant’Ambrogio, “Vagal esophageal receptors in anesthetized dogs: mechanical and chemical responsiveness.,” *J Appl Physiol (1985)*, vol. 86, no. 4, pp. 1231–1235, Apr. 1999, doi: 10.1152/jappl.1999.86.4.1231.

[127] B. K. Medda, J. N. Sengupta, I. M. Lang, and R. Shaker, “Response properties of the brainstem neurons of the cat following intra-esophageal acid-pepsin infusion,” *Neuroscience*, vol. 135, no. 4, pp. 1285–1294, 2005, doi: 10.1016/j.neuroscience.2005.07.016.

[128] C. McGuire *et al.*, “Ex vivo study of human visceral nociceptors,” *Gut*, vol. 67, no. 1, pp. 86–96, Jan. 2018, doi: 10.1136/gutjnl-2016-311629.

[129] M. Falempin, N. Mei, and J. P. Rousseau, “Vagal mechanoreceptors of the inferior thoracic oesophagus, the lower oesophageal sphincter and the stomach in the sheep.,” *Pflugers Arch*, vol. 373, no. 1, pp. 25–30, Jan. 1978.

[130] R. W. Hamill, R. E. Shapiro, and M. A. Vizzard, “Peripheral Autonomic Nervous System,” in *Primer on the Autonomic Nervous System*, Elsevier Inc., 2012, pp. 17–26. doi: 10.1016/B978-0-12-386525-0.00004-4.

[131] P. Bessou and E. R. Perl, “Response of cutaneous sensory units with unmyelinated fibers to noxious stimuli.,” *J Neurophysiol*, vol. 32, no. 6, pp. 1025–1043, 1969, doi: 10.1152/jn.1969.32.6.1025.

[132] K. Zimmermann *et al.*, “Phenotyping sensory nerve endings in vitro in the mouse,” *Nat Protoc*, vol. 4, no. 2, pp. 174–196, 2009, doi: 10.1038/nprot.2008.223.

[133] M. S. Gold and G. F. Gebhart, “Nociceptor sensitization in pain pathogenesis,” *Nature Medicine*, vol. 16, no. 11. NIH Public Access, pp. 1248–1257, Nov. 2010. doi: 10.1038/nm.2235.

[134] W. D. Snider and S. B. McMahon, “Tackling pain at the source: New ideas about nociceptors,” *Neuron*, vol. 20, no. 4. Cell Press, pp. 629–632, Apr. 01, 1998. doi: 10.1016/S0896-6273(00)81003-X.

[135] J. N. Wood, J. P. Boorman, K. Okuse, and M. D. Baker, “Voltage-gated sodium channels and pain pathways,” *Journal of Neurobiology*, vol. 61, no. 1. pp. 55–71, Oct. 2004. doi: 10.1002/neu.20094.

[136] J. M. A. Laird, V. Souslova, J. N. Wood, and F. Cervero, “Deficits in visceral pain and referred hyperalgesia in Nav1.8 (SNS/PN3)-null mice,” *Journal of Neuroscience*, vol. 22, no. 19, pp. 8352–8356, Oct. 2002, doi: 10.1523/jneurosci.22-19-08352.2002.

[137] A. M. Harriott and M. S. Gold, “Contribution of primary afferent channels to neuropathic pain,” *Current Pain and Headache Reports*, vol. 13, no. 3. NIH Public Access, pp. 197–207, 2009. doi: 10.1007/s11916-009-0034-9.

[138] T. R. Cummins, P. L. Sheets, and S. G. Waxman, “The roles of sodium channels in nociception: Implications for mechanisms of pain,” *Pain*, vol. 131, no. 3. NIH Public Access, pp. 243–257, Oct. 2007. doi: 10.1016/j.pain.2007.07.026.

[139] M. D. Baker and J. N. Wood, “Involvement of Na+ channels in pain pathways,” *Trends in Pharmacological Sciences*, vol. 22, no. 1. Elsevier, pp. 27–31, Jan. 01, 2001. doi: 10.1016/S0165-6147(00)01585-6.

[140] L. A. Blackshaw, S. M. Brierley, and P. A. Hughes, “TRP channels: new targets for visceral pain,” *Gut*, vol. 59, no. 01, pp. 126–135, 2010, doi: 10.1136/gut.2009.179523.

[141] C. J. Moreau, J. P. Dupuis, J. Revilloud, K. Arumugam, and M. Vivaudou, “Coupling ion channels to receptors for biomolecule sensing,” *Nat Nanotechnol*, vol. 3, no. 10, pp. 620–625, Sep. 2008, doi: 10.1038/nnano.2008.242.

[142] I. M. Fuentes and J. A. Christianson, “Ion channels, ion channel receptors, and visceral hypersensitivity in irritable bowel syndrome,” *Neurogastroenterology and Motility*, vol. 28, no. 11. Blackwell Publishing Ltd, pp. 1613–1618, Nov. 01, 2016. doi: 10.1111/nmo.12979.

[143] R. M. Greene and M. M. Pisano, “Serotonin signaling as a target for craniofacial embryotoxicity,” in *Handbook of Developmental Neurotoxicology*, Elsevier, 2018, pp. 65–74. doi: 10.1016/B978-0-12-809405-1.00006-7.

[144] M. Delvaux, D. Louvel, J. P. Mamet, R. Campos-Oriola, and J. Frexinos, “Effect of alosetron on responses to colonic distension in patients with irritable bowel syndrome,” *Aliment Pharmacol Ther*, vol. 12, no. 9, pp. 849–855, Sep. 1998, doi: 10.1046/j.1365-2036.1998.00375.x.

[145] G. Burnstock and J. N. Wood, “Purinergic receptors: Their role in nociception and primary afferent neurotransmission,” *Curr Opin Neurobiol*, vol. 6, no. 4, pp. 526–532, Aug. 1996, doi: 10.1016/S0959-4388(96)80060-2.

[146] B. Banerjee *et al.*, “Altered expression of P2X3 in vagal and spinal afferents following esophagitis in rats,” *Histochem Cell Biol*, vol. 132, no. 6, pp. 585–597, Dec. 2009, doi: 10.1007/s00418-009-0639-4.

[147] Y. Yiangou *et al.*, “ATP-gated ion channel P2X3 is increased in human inflammatory bowel disease,” *Neurogastroenterology and Motility*, vol. 13, no. 4, pp. 365–369, Aug. 2001, doi: 10.1046/j.1365-2982.2001.00276.x.

[148] Y. Yiangou *et al.*, “Vanilloid receptor 1 immunoreactivity in inflamed human bowel,” *Lancet*, vol. 357, no. 9265, pp. 1338–1339, Apr. 2001, doi: 10.1016/S0140-6736(00)04503-7.

[149] B. Banerjee, B. K. Medda, Z. Lazarova, N. Bansal, R. Shaker, and J. N. Sengupta, “Effect of reflux-induced inflammation on transient receptor potential vanilloid one (TRPV1) expression in primary sensory neurons innervating the oesophagus of rats.,” *Neurogastroenterol Motil*, vol. 19, no. 8, pp. 681–691, Aug. 2007, doi: 10.1111/j.1365-2982.2007.00947.x.

[150] C. C. Chen, A. Zimmer, W. H. Sun, J. Hall, M. J. Brownstein, and A. Zimmer, “A role for ASIC3 in the modulation of high-intensity pain stimuli,” *Proc Natl Acad Sci U S A*, vol. 99, no. 13, pp. 8992–8997, Jun. 2002, doi: 10.1073/pnas.122245999.

[151] Y. Yiangou *et al.*, “Increased acid-sensing ion channel ASIC-3 in inflamed human intestine,” *Eur J Gastroenterol Hepatol*, vol. 13, no. 8, pp. 891–896, 2001, doi: 10.1097/00042737-200108000-00003.

[152] G. Owsianik, K. Talavera, T. Voets, and B. Nilius, “Permeation and selectivity of TRP channels.,” *Annu Rev Physiol*, vol. 68, pp. 685–717, 2006, doi: 10.1146/annurev.physiol.68.040204.101406.

[153] L. J. Wu, T. B. Sweet, and D. E. Clapham, “International Union of Basic and Clinical Pharmacology. LXXVI. Current progress in the Mammalian TRP ion channel family,” *Pharmacological Reviews*, vol. 62, no. 3. American Society for Pharmacology and Experimental Therapeutics, pp. 381–404, Sep. 2010. doi: 10.1124/pr.110.002725.

[154] V. Lehen’Kyi and N. Prevarskaya, “Oncogenic TRP channels,” in *Advances in Experimental Medicine and Biology*, 2011, vol. 704, pp. 929–945. doi: 10.1007/978-94-007-0265-3_48.

[155] M. J. Caterina, M. A. Schumacher, M. Tominaga, T. A. Rosen, J. D. Levine, and D. Julius, “The capsaicin receptor: A heat-activated ion channel in the pain pathway,” *Nature*, vol. 389, no. 6653, pp. 816–824, 1997, doi: 10.1038/39807.

[156] M. M. Moran, M. A. McAlexander, T. Bíró, and A. Szallasi, “Transient receptor potential channels as therapeutic targets,” *Nature Reviews Drug Discovery*, vol. 10, no. 8. Nature Publishing Group, pp. 601–620, Aug. 01, 2011. doi: 10.1038/nrd3456.

[157] D. E. Clapham, “TRP channels as cellular sensors,” *Nature*, vol. 426, no. 6966. Nature Publishing Group, pp. 517–524, Dec. 04, 2003. doi: 10.1038/nature02196.

[158] E. V. Kuzhikandathil, H. Wang, T. Szabo, N. Morozova, P. M. Blumberg, and G. S. Oxford, “Functional analysis of capsaicin receptor (vanilloid receptor subtype 1) multimerization and agonist responsiveness using a dominant negative mutation,” *Journal of Neuroscience*, vol. 21, no. 22, pp. 8697–8706, Nov. 2001, doi: 10.1523/jneurosci.21-22-08697.2001.

[159] K. Singh, N. Luo, and P. Rosenberg, “TRP Channels in Cardiovascular Disease,” in *TRP Channels as Therapeutic Targets: From Basic Science to Clinical Use*, Elsevier Inc., 2015, pp. 365–383. doi: 10.1016/B978-0-12-420024-1.00020-5.

[160] S. E. Jordt and D. Julius, “Molecular basis for species-specific sensitivity to ‘hot’ chili peppers,” *Cell*, vol. 108, no. 3, pp. 421–430, 2002, doi: 10.1016/S0092-8674(02)00637-2.

[161] H. H. Chuang *et al.*, “Bradykinin and nerve growth factor release the capsaicin receptor from PtdIns(4,5)P2-mediated inhibition,” *Nature*, vol. 411, no. 6840, pp. 957–962, Jun. 2001, doi: 10.1038/35082088.

[162] P. V. Lishko, E. Procko, X. Jin, C. B. Phelps, and R. Gaudet, “The Ankyrin Repeats of TRPV1 Bind Multiple Ligands and Modulate Channel Sensitivity,” *Neuron*, vol. 54, no. 6, pp. 905–918, Jun. 2007, doi: 10.1016/j.neuron.2007.05.027.

[163] Y. Kwon, T. Hofmann, and C. Montell, “Integration of Phosphoinositide- and Calmodulin-Mediated Regulation of TRPC6,” *Mol Cell*, vol. 25, no. 4, pp. 491–503, Feb. 2007, doi: 10.1016/j.molcel.2007.01.021.

[164] R. J. Docherty, J. C. Yeats, S. Bevan, and H. W. G. M. Boddeke, “Inhibition of calcineurin inhibits the desensitization of capsaicin-evoked currents in cultured dorsal root ganglion neurones from adult rats,” *Pflugers Arch*, vol. 431, no. 6, pp. 828–837, 1996, doi: 10.1007/s004240050074.

[165] B. Minke and B. Cook, “TRP channel proteins and signal transduction,” *Physiological Reviews*, vol. 82, no. 2. American Physiological Society, pp. 429–472, 2002. doi: 10.1152/physrev.00001.2002.

[166] M. J. Berridge, P. Lipp, and M. D. Bootman, “The calcium entry pas de deux,” *Science*, vol. 287, no. 5458. pp. 1604–1605, Mar. 03, 2000. doi: 10.1126/science.287.5458.1604.

[167] P. A. Rutecki, “Neuronal excitability: Voltage-dependent currents and synaptic transmission,” *Journal of Clinical Neurophysiology*, vol. 9, no. 2, pp. 195–211, 1992, doi: 10.1097/00004691-199204010-00003.

[168] L. S. Premkumar and G. P. Ahern, “Induction of vanilloid receptor channel activity by protein kinase C,” *Nature*, vol. 408, no. 6815, pp. 985–990, Dec. 2000, doi: 10.1038/35050121.

[169] L. De Petrocellis *et al.*, “The vanilloid receptor (VR1)-mediated effects of anandamide are potently enhanced by the cAMP-dependent protein kinase,” *J Neurochem*, vol. 77, no. 6, pp. 1660–1663, 2001, doi: 10.1046/j.1471-4159.2001.00406.x.

[170] A. Dray, C. A. Forbes, and G. M. Burgess, “Ruthenium red blocks the capsaicin-induced increase in intracellular calcium and activation of membrane currents in sensory neurones as well as the activation of peripheral nociceptors in vitro,” *Neurosci Lett*, vol. 110, no. 1–2, pp. 52–59, Mar. 1990, doi: 10.1016/0304-3940(90)90786-9.

[171] M. J. Caterina *et al.*, “Impaired nociception and pain sensation in mice lacking the capsaicin receptor,” *Science (1979)*, vol. 288, no. 5464, pp. 306–313, Apr. 2000, doi: 10.1126/science.288.5464.306.

[172] B. Nilius and G. Owsianik, “The transient receptor potential family of ion channels,” *Genome Biol*, vol. 12, no. 3, p. 218, Mar. 2011, doi: 10.1186/gb-2011-12-3-218.

[173] P. Hayes *et al.*, “Cloning and functional expression of a human orthologue of rat vanilloid receptor-1,” *Pain*, vol. 88, no. 2, pp. 205–215, Nov. 2000, doi: 10.1016/S0304-3959(00)00353-5.

[174] J. D. Nathan *et al.*, “Capsaicin vanilloid receptor-1 mediates substance P release in experimental pancreatitis,” *Am J Physiol Gastrointest Liver Physiol*, vol. 281, no. 5 44-5, 2001, doi: 10.1152/ajpgi.2001.281.5.g1322.

[175] A. Charrua, C. D. Cruz, F. Cruz, and A. Avelino, “Transient Receptor Potential Vanilloid Subfamily 1 is Essential for the Generation of Noxious Bladder Input and Bladder Overactivity in Cystitis,” *Journal of Urology*, vol. 177, no. 4, pp. 1537–1541, Apr. 2007, doi: 10.1016/j.juro.2006.11.046.

[176] Z. Y. Wang, P. Wang, F. V. Merriam, and D. E. Bjorling, “Lack of TRPV1 inhibits cystitis-induced increased mechanical sensitivity in mice,” *Pain*, vol. 139, no. 1, pp. 158–167, Sep. 2008, doi: 10.1016/j.pain.2008.03.020.

[177] S. M. Ward, J. Bayguinov, K.-J. Won, D. Grundy, and H. R. Berthoud, “Distribution of the vanilloid receptor (VR1) in the gastrointestinal tract.,” *J Comp Neurol*, vol. 465, no. 1, pp. 121–135, Oct. 2003, doi: 10.1002/cne.10801.

[178] J. Sakurai *et al.*, “Activation of Extracellular Signal-Regulated Protein Kinase in Sensory Neurons After Noxious Gastric Distention and Its Involvement in Acute Visceral Pain in Rats,” *Gastroenterology*, vol. 134, no. 4, pp. 1094–1103, Apr. 2008, doi: 10.1053/j.gastro.2008.01.031.

[179] Y. Dai *et al.*, “Phosphorylation of extracellular signal-regulated kinase in primary afferent neurons by noxious stimuli and its involvement in peripheral sensitization,” *Journal of Neuroscience*, vol. 22, no. 17, pp. 7737–7745, Sep. 2002, doi: 10.1523/jneurosci.22-17-07737.2002.

[180] W. Rong, K. Hillsley, J. B. Davis, G. Hicks, W. J. Winchester, and D. Grundy, “Jejunal afferent nerve sensitivity in wild-type and TRPV1 knockout mice,” *Journal of Physiology*, vol. 560, no. 3, pp. 867–881, Nov. 2004, doi: 10.1113/jphysiol.2004.071746.

[181] B. Y. De Winter *et al.*, “Involvement of afferent neurons in the pathogenesis of endotoxin-induced ileus in mice: Role of CGRP and TRPV1 receptors,” *Eur J Pharmacol*, vol. 615, no. 1–3, pp. 177–184, Aug. 2009, doi: 10.1016/j.ejphar.2009.04.055.

[182] A. Türler *et al.*, “Endogenous endotoxin participates in causing a panenteric inflammatory ileus after colonic surgery,” *Ann Surg*, vol. 245, no. 5, pp. 734–744, May 2007, doi: 10.1097/01.sla.0000255595.98041.6b.

[183] B. Wang, J. Glatzle, M. H. Mueller, M. Kreis, P. Enck, and D. Grundy, “Lipopolysaccharide-induced changes in mesenteric afferent sensitivity of rat jejunum in vitro: role of prostaglandins,” *American Journal of Physiology-Gastrointestinal and Liver Physiology*, vol. 289, no. 2, pp. G254–G260, Aug. 2005, doi: 10.1152/ajpgi.00329.2004.

[184] S. A. Malin, J. A. Christianson, K. Bielefeldt, and B. M. Davis, “TPRV1 expression defines functionally distinct pelvic colon afferents,” *Journal of Neuroscience*, vol. 29, no. 3, pp. 743–752, Jan. 2009, doi: 10.1523/JNEUROSCI.3791-08.2009.

[185] A. Miranda, E. Nordstrom, A. Mannem, C. Smith, B. Banerjee, and J. N. Sengupta, “The role of transient receptor potential vanilloid 1 in mechanical and chemical visceral hyperalgesia following experimental colitis,” *Neuroscience*, vol. 148, no. 4, pp. 1021–1032, Sep. 2007, doi: 10.1016/j.neuroscience.2007.05.034.

[186] A. Akbar *et al.*, “Expression of the TRPV1 receptor differs in quiescent inflammatory bowel disease with or without abdominal pain,” *Gut*, vol. 59, no. 6, pp. 767–774, Jun. 2010, doi: 10.1136/gut.2009.194449.

[187] K. Fujino, S. G. de la Fuente, Y. Takami, T. Takahashi, and C. R. Mantyh, “Attenuation of acid induced oesophagitis in VR-1 deficient mice.,” *Gut*, vol. 55, no. 1, pp. 34–40, Jan. 2006, doi: 10.1136/gut.2005.066795.

[188] S. Peles *et al.*, “Differential effects of transient receptor vanilloid one (TRPV1) antagonists in acid-induced excitation of esophageal vagal afferent fibers of rats.,” *Neuroscience*, vol. 161, no. 2, pp. 515–525, Jun. 2009, doi: 10.1016/j.neuroscience.2009.03.040.

[189] R. O. Silva *et al.*, “Role of TRPV1 receptor in inflammation and impairment of esophageal mucosal integrity in a murine model of nonerosive reflux disease,” *Neurogastroenterology & Motility*, vol. 30, no. 8, p. e13340, Aug. 2018, doi: 10.1111/nmo.13340.

[190] L. Cheng *et al.*, “HCl-activated neural and epithelial vanilloid receptors (TRPV1) in cat esophageal mucosa,” *Am J Physiol Gastrointest Liver Physiol*, vol. 297, no. 1, Jul. 2009, doi: 10.1152/ajpgi.90386.2008.

[191] J. Ma, K. M. Harnett, J. Behar, P. Biancani, and W. Cao, “Signaling in TRPV1-induced platelet activating factor (PAF) in human esophageal epithelial cells.,” *Am J Physiol Gastrointest Liver Physiol*, vol. 298, no. 2, pp. G233-40, Feb. 2010, doi: 10.1152/ajpgi.00409.2009.

[192] A. J. Wardlaw, R. Moqbel, O. Cromwell, and A. B. Kay, “Platelet-activating factor. A potent chemotactic and chemokinetic factor for human eosinophils.,” *J Clin Invest*, vol. 78, no. 6, pp. 1701–1706, Dec. 1986, doi: 10.1172/JCI112765.

[193] W. G. Paterson, C. A. Kieffer, M. J. Feldman, D. v Miller, and G. P. Morris, “Role of platelet-activating factor in acid-induced esophageal mucosal injury.,” *Dig Dis Sci*, vol. 52, no. 8, pp. 1861–1866, Aug. 2007, doi: 10.1007/s10620-006-9385-9.

[194] L. Wu *et al.*, “PAR-2 activation enhances weak acid-induced ATP release through TRPV1 and ASIC sensitization in human esophageal epithelial cells,” *American Journal of Physiology-Gastrointestinal and Liver Physiology*, vol. 309, no. 8, pp. G695–G702, Oct. 2015, doi: 10.1152/ajpgi.00162.2015.

[195] J. J. Kim, N. Kim, Y. J. Choi, J. S. Kim, and H. C. Jung, “Increased TRPV1 and PAR2 mRNA expression levels are associated only with the esophageal reflux symptoms, but not with the extraesophageal reflux symptoms.,” *Medicine*, vol. 95, no. 32, p. e4387, Aug. 2016, doi: 10.1097/MD.0000000000004387.

[196] P. J. Matthews, Q. Aziz, P. Facer, J. B. Davis, D. G. Thompson, and P. Anand, “Increased capsaicin receptor TRPV1 nerve fibres in the inflamed human oesophagus.,” *Eur J Gastroenterol Hepatol*, vol. 16, no. 9, pp. 897–902, Sep. 2004.

[197] P. Boadas-Vaello, S. Castany, J. Homs, B. Alvarez-Perez, M. Deulofeu, and E. Verdu, “Neuroplasticity of ascending and descending pathways after somatosensory system injury: reviewing knowledge to identify neuropathic pain therapeutic targets.,” *Spinal Cord*, vol. 54, no. 5, pp. 330–340, May 2016, doi: 10.1038/sc.2015.225.

[198] A. L. Krarup *et al.*, “Randomised clinical trial: The efficacy of a transient receptor potential vanilloid 1 antagonist AZD1386 in human oesophageal pain,” *Aliment Pharmacol Ther*, vol. 33, no. 10, pp. 1113–1122, May 2011, doi: 10.1111/j.1365-2036.2011.04629.x.

[199] B. Nilius, G. Appendino, and G. Owsianik, “The transient receptor potential channel TRPA1: from gene to pathophysiology.,” *Pflugers Arch*, vol. 464, no. 5, pp. 425–458, Nov. 2012, doi: 10.1007/s00424-012-1158-z.

[200] D. M. Bautista *et al.*, “TRPA1 mediates the inflammatory actions of environmental irritants and proalgesic agents.,” *Cell*, vol. 124, no. 6, pp. 1269–1282, Mar. 2006, doi: 10.1016/j.cell.2006.02.023.

[201] M. Z. P. Guimaraes and S.-E. Jordt, *TRPA1 : A Sensory Channel of Many Talents*. CRC Press/Taylor & Francis, 2007.

[202] S.-E. Jordt *et al.*, “Mustard oils and cannabinoids excite sensory nerve fibres through the TRP channel ANKTM1.,” *Nature*, vol. 427, no. 6971, pp. 260–265, Jan. 2004, doi: 10.1038/nature02282.

[203] G. M. Story *et al.*, “ANKTM1, a TRP-like channel expressed in nociceptive neurons, is activated by cold temperatures,” *Cell*, vol. 112, no. 6, pp. 819–829, Mar. 2003, doi: 10.1016/S0092-8674(03)00158-2.

[204] A. M. Peier *et al.*, “A TRP channel that senses cold stimuli and menthol.,” *Cell*, vol. 108, no. 5, pp. 705–715, Mar. 2002.

[205] S. M. Louis, D. Johnstone, N. J. W. Russell, A. Jamieson, and G. J. Dockray, “Antibodies to calcitonin-gene related peptide reduce inflammation induced by topical mustard oil but not that due to carrageenin in the rat,” *Neurosci Lett*, vol. 102, no. 2–3, pp. 257–260, Jul. 1989, doi: 10.1016/0304-3940(89)90088-8.

[206] M. Bandell *et al.*, “Noxious cold ion channel TRPA1 is activated by pungent compounds and bradykinin,” *Neuron*, vol. 41, no. 6, pp. 849–857, Mar. 2004, doi: 10.1016/S0896-6273(04)00150-3.

[207] R. Couture, M. Harrisson, R. M. Vianna, and F. Cloutier, “Kinin receptors in pain and inflammation,” *European Journal of Pharmacology*, vol. 429, no. 1–3. pp. 161–176, Oct. 10, 2001. doi: 10.1016/S0014-2999(01)01318-8.

[208] B. Minke, “The TRP channel and phospholipase C-mediated signaling.,” *Cell Mol Neurobiol*, vol. 21, no. 6, pp. 629–43, Dec. 2001, doi: 10.1023/a:1015191702536.

[209] T. K. Lapointe and C. Altier, “The role of TRPA1 in visceral inflammation and pain,” *Channels*, vol. 5, no. 6, pp. 525–529, Nov. 2011, doi: 10.4161/chan.5.6.18016.

[210] S. M. Brierley *et al.*, “The Ion Channel TRPA1 Is Required for Normal Mechanosensation and Is Modulated by Algesic Stimuli,” *Gastroenterology*, vol. 137, no. 6, p. 2084, 2009, doi: 10.1053/j.gastro.2009.07.048.

[211] S. Wang *et al.*, “Phospholipase C and protein kinase A mediate bradykinin sensitization of TRPA1: a molecular mechanism of inflammatory pain.,” *Brain*, vol. 131, no. Pt 5, pp. 1241–51, May 2008, doi: 10.1093/brain/awn060.

[212] F. Cattaruzza, I. Spreadbury, M. Miranda-Morales, E. F. Grady, S. Vanner, and N. W. Bunnett, “Transient receptor potential ankyrin-1 has a major role in mediating visceral pain in mice,” *Am J Physiol Gastrointest Liver Physiol*, vol. 298, no. 1, p. G81, Jan. 2010, doi: 10.1152/ajpgi.00221.2009.

[213] S. Bertin *et al.*, “The TRPA1 ion channel is expressed in CD4+ T cells and restrains T-cell-mediated colitis through inhibition of TRPV1,” *Gut*, vol. 66, no. 9, pp. 1584–1596, 2017, doi: 10.1136/gutjnl-2015-310710.

[214] S. Yu, G. Gao, B. Z. Peterson, and A. Ouyang, “TRPA1 in mast cell activation-induced long-lasting mechanical hypersensitivity of vagal afferent C-fibers in guinea pig esophagus,” *Am J Physiol Gastrointest Liver Physiol*, vol. 297, pp. 34–42, 2009, doi: 10.1152/ajpgi.00068.2009.-Sensitization.

[215] S. Yu and A. Ouyang, “TRPA1 in bradykinin-induced mechanical hypersensitivity of vagal C fibers in guinea pig esophagus.,” *Am J Physiol Gastrointest Liver Physiol*, vol. 296, no. 2, pp. G255-65, Feb. 2009, doi: 10.1152/ajpgi.90530.2008.

[216] A. M. Peier *et al.*, “A TRP channel that senses cold stimuli and menthol,” *Cell*, vol. 108, no. 5, pp. 705–715, Mar. 2002, doi: 10.1016/S0092-8674(02)00652-9.

[217] L. Tsavaler, M. H. Shapero, S. Morkowski, and R. Laus, “Trp-p8, a novel prostate-specific gene, is up-regulated in prostate cancer and other malignancies and shares high homology with transient receptor potential calcium channel proteins,” *Cancer Res*, vol. 61, no. 9, pp. 3760–3769, May 2001.

[218] D. D. McKemy, W. M. Neuhausser, and D. Julius, “Identification of a cold receptor reveals a general role for TRP channels in thermosensation.,” *Nature*, vol. 416, no. 6876, pp. 52–58, Mar. 2002, doi: 10.1038/nature719.

[219] M. Bandell *et al.*, “High-throughput random mutagenesis screen reveals TRPM8 residues specifically required for activation by menthol,” *Nat Neurosci*, vol. 9, no. 4, pp. 493–500, Apr. 2006, doi: 10.1038/nn1665.

[220] H. H. Chuang, W. M. Neuhausser, and D. Julius, “The super-cooling agent icilin reveals a mechanism of coincidence detection by a temperature-sensitive TRP channel,” *Neuron*, vol. 43, no. 6, pp. 859–869, Sep. 2004, doi: 10.1016/j.neuron.2004.08.038.

[221] R. W. Colburn *et al.*, “Attenuated Cold Sensitivity in TRPM8 Null Mice,” *Neuron*, vol. 54, no. 3, pp. 379–386, May 2007, doi: 10.1016/j.neuron.2007.04.017.

[222] D. M. Bautista *et al.*, “The menthol receptor TRPM8 is the principal detector of environmental cold,” *Nature*, vol. 448, no. 7150, pp. 204–208, Jul. 2007, doi: 10.1038/nature05910.

[223] X. Zhang *et al.*, “Direct inhibition of the cold-Activated TRPM8 ion channel by Gα q,” *Nat Cell Biol*, vol. 14, no. 8, pp. 850–858, Aug. 2012, doi: 10.1038/ncb2529.

[224] T. Rohács, C. M. B. Lopes, I. Michailidis, and D. E. Logothetis, “PI(4,5)P2 regulates the activation and desensitization of TRPM8 channels through the TRP domain,” *Nat Neurosci*, vol. 8, no. 5, pp. 626–634, May 2005, doi: 10.1038/nn1451.

[225] B. Nilius *et al.*, “The Ca2+-activated cation channel TRPM4 is regulated by phosphatidylinositol 4,5-biphosphate,” *EMBO Journal*, vol. 25, no. 3, pp. 467–478, Feb. 2006, doi: 10.1038/sj.emboj.7600963.

[226] L. S. Premkumar, M. Raisinghani, S. C. Pingle, C. Long, and F. Pimentel, “Downregulation of transient receptor potential melastatin 8 by protein kinase C-mediated dephosphorylation,” *Journal of Neuroscience*, vol. 25, no. 49, pp. 11322–11329, Dec. 2005, doi: 10.1523/JNEUROSCI.3006-05.2005.

[227] G. Bhave *et al.*, “Protein kinase C phosphorylation sensitizes but does not activate the capsaicin receptor transient receptor potential vanilloid 1 (TRPV1),” *Proc Natl Acad Sci U S A*, vol. 100, no. 21, pp. 12480–12485, Oct. 2003, doi: 10.1073/pnas.2032100100.

[228] A. M. Harrington *et al.*, “A novel role for TRPM8 in visceral afferent function.,” *Pain*, vol. 152, no. 7, pp. 1459–1468, Jul. 2011, doi: 10.1016/j.pain.2011.01.027.

[229] T. Hosoya *et al.*, “TRPM8 has a key role in experimental colitis-induced visceral hyperalgesia in mice.,” *Neurogastroenterol Motil*, vol. 26, no. 8, pp. 1112–1121, Aug. 2014, doi: 10.1111/nmo.12368.

[230] S. M. Mueller-Tribbensee, M. Karna, M. Khalil, M. F. Neurath, P. W. Reeh, and M. A. Engel, “Differential Contribution of TRPA1, TRPV4 and TRPM8 to Colonic Nociception in Mice.,” *PLoS One*, vol. 10, no. 7, p. e0128242, 2015, doi: 10.1371/journal.pone.0128242.

[231] R. Ramachandran *et al.*, “TRPM8 activation attenuates inflammatory responses in mouse models of colitis.,” *Proc Natl Acad Sci U S A*, vol. 110, no. 18, pp. 7476–7481, Apr. 2013, doi: 10.1073/pnas.1217431110.

[232] P. R. de Jong *et al.*, “TRPM8 on mucosal sensory nerves regulates colitogenic responses by innate immune cells via CGRP,” *Mucosal Immunol*, vol. 8, p. 491, Oct. 2014.

[233] R. Khanna, J. K. MacDonald, and B. G. Levesque, “Peppermint oil for the treatment of irritable bowel syndrome: a systematic review and meta-analysis.,” *J Clin Gastroenterol*, vol. 48, no. 6, pp. 505–512, Jul. 2014, doi: 10.1097/MCG.0b013e3182a88357.

[234] X. Yu, Y. Hu, F. Ru, M. Kollarik, B. J. Undem, and S. Yu, “TRPM8 function and expression in vagal sensory neurons and afferent nerves innervating guinea pig esophagus.,” *Am J Physiol Gastrointest Liver Physiol*, vol. 308, no. 6, pp. G489-96, Mar. 2015, doi: 10.1152/ajpgi.00336.2014.

[235] X. Yu, Y. Hu, and S. Yu, “Effects of acid on vagal nociceptive afferent subtypes in guinea pig esophagus,” *Am J Physiol Gastrointest Liver Physiol*, vol. 307, no. 4, pp. G471-8, Aug. 2014, doi: 10.1152/ajpgi.00156.2014.

[236] P. Banovcin, M. Duricek, T. Zatko, P. Liptak, R. Hyrdel, and M. Kollarik, “The infusion of menthol into the esophagus evokes cold sensations in healthy subjects but induces heartburn in patients with gastroesophageal reflux disease (GERD).,” *Dis Esophagus*, Apr. 2019, doi: 10.1093/dote/doz038.

[237] N. Yoder, C. Yoshioka, and E. Gouaux, “Gating mechanisms of acid-sensing ion channels,” *Nature*, vol. 555, no. 7696, pp. 397–401, Mar. 2018, doi: 10.1038/nature25782.

[238] M. Kress and R. Waldmann, “Chapter 8 Acid Sensing Ionic Channels,” *Current Topics in Membranes*, vol. 57. Academic Press, pp. 241–276, Jan. 01, 2006. doi: 10.1016/S1063-5823(06)57007-3.

[239] P. Holzer, “Acid-sensitive ion channels and receptors,” *Handbook of Experimental Pharmacology*, vol. 194, no. 194. Routledge, pp. 283–332, 2009. doi: 10.1007/978-3-540-79090-7_9.

[240] J. Jasti, H. Furukawa, E. B. Gonzales, and E. Gouaux, “Structure of acid-sensing ion channel 1 at 1.9 Å resolution and low pH,” *Nature*, vol. 449, no. 7160, pp. 316–323, Sep. 2007, doi: 10.1038/nature06163.

[241] J. A. Wemmie, M. P. Price, and M. J. Welsh, “Acid-sensing ion channels: advances, questions and therapeutic opportunities,” *Trends in Neurosciences*, vol. 29, no. 10. Elsevier Current Trends, pp. 578–586, Oct. 01, 2006. doi: 10.1016/j.tins.2006.06.014.

[242] J. Mamet, A. Baron, M. Lazdunski, and N. Voilley, “Proinflammatory mediators, stimulators of sensory neuron excitability via the expression of acid-sensing ion channels,” *Journal of Neuroscience*, vol. 22, no. 24, pp. 10662–10670, Dec. 2002, doi: 10.1523/jneurosci.22-24-10662.2002.

[243] Q. Gu and L. Y. Lee, “Acid-Sensing ion channels and pain,” *Pharmaceuticals*, vol. 3, no. 5. Multidisciplinary Digital Publishing Institute (MDPI), pp. 1411–1425, 2010. doi: 10.3390/ph3051411.

[244] M. P. Price *et al.*, “The DRASIC cation channel contributes to the detection of cutaneous touch and acid stimuli in mice,” *Neuron*, vol. 32, no. 6, pp. 1071–1083, Dec. 2001, doi: 10.1016/S0896-6273(01)00547-5.

[245] F. Ru, P. Banovcin, and M. Kollarik, “Acid sensitivity of the spinal dorsal root ganglia C-fiber nociceptors innervating the guinea pig esophagus,” *Neurogastroenterology and Motility*, vol. 27, no. 6, pp. 865–874, Jun. 2015, doi: 10.1111/nmo.12561.

[246] Y. Akiba *et al.*, “CO2 chemosensing in rat oesophagus,” *Gut*, vol. 57, no. 12, pp. 1654–1664, Dec. 2008, doi: 10.1136/gut.2007.144378.

[247] T. Wultsch *et al.*, “Deletion of the acid-sensing ion channel ASIC3 prevents gastritis-induced acid hyperresponsiveness of the stomach-brainstem axis,” *Pain*, vol. 134, no. 3, pp. 245–253, Feb. 2008, doi: 10.1016/j.pain.2007.04.025.

[248] “Gastroduodenal Mucosal Defense,” pp. 1259–1291, Jan. 2006, doi: 10.1016/B978-012088394-3/50053-2.

[249] Y. Akiba and J. D. Kaunitz, “Luminal chemosensing and upper gastrointestinal mucosal defenses,” *Am J Clin Nutr*, vol. 90, no. 3, pp. 826S-831S, Sep. 2009, doi: 10.3945/ajcn.2009.27462U.

[250] R. Schuligoi, M. Jocic, A. Heinemann, E. Schoninkle, M. A. Pabst, and P. Holzer, “Gastric acid-evoked c-los messenger RNA expression in rat brainstem is signaled by capsaicin-resistant vagal afferents,” *Gastroenterology*, vol. 115, no. 3, pp. 649–660, Sep. 1998, doi: 10.1016/S0016-5085(98)70144-1.

[251] K. Bielefeldt and B. M. Davis, “Differential effects of ASIC3 and TRPV1 deletion on gastroesophageal sensation in mice,” *American Journal of Physiology-Gastrointestinal and Liver Physiology*, vol. 294, no. 1, pp. G130–G138, Jan. 2008, doi: 10.1152/ajpgi.00388.2007.

[252] A. S. Rothmeier and W. Ruf, “Protease-activated receptor 2 signaling in inflammation,” *Seminars in Immunopathology*, vol. 34, no. 1. pp. 133–149, Jan. 2012. doi: 10.1007/s00281-011-0289-1.

[253] G. Flaubert and G. Flaubert, “Titel,” in *Bouvard und Pécuchet*, vol. 5, no. 50, Wallstein Verlag, 2017, pp. IV-1-IV–4. doi: 10.5771/9783835341579-iv-1.

[254] P. Woodland *et al.*, “Distinct afferent innervation patterns within the human proximal and distal esophageal mucosa,” *Am J Physiol Gastrointest Liver Physiol*, vol. 308, no. 6, pp. G525–G531, 2015, doi: 10.1152/ajpgi.00175.2014.

[255] M. Kollarik, F. Ru, and M. Brozmanova, “Vagal afferent nerves with the properties of nociceptors,” *Auton Neurosci*, vol. 153, no. 1–2, pp. 12–20, Feb. 2010, doi: 10.1016/j.autneu.2009.08.001.

[256] P. Woodland *et al.*, “Superficial Esophageal Mucosal Afferent Nerves May Contribute to Reflux Hypersensitivity in Nonerosive Reflux Disease,” *Gastroenterology*, vol. 153, no. 5, pp. 1230–1239, Nov. 2017, doi: 10.1053/j.gastro.2017.07.017.

[257] M. Vieth *et al.*, “Epithelial Thickness is a Marker of Gastroesophageal Reflux Disease,” *Clinical Gastroenterology and Hepatology*, vol. 14, no. 11, pp. 1544-1551.e1, Nov. 2016, doi: 10.1016/j.cgh.2016.06.018.

[258] Y. M. Bhat and K. Bielefeldt, “Capsaicin receptor (TRPV1) and non-erosive reflux disease.,” *Eur J Gastroenterol Hepatol*, vol. 18, no. 3, pp. 263–270, Mar. 2006.

[259] A. M. Harrington, S. M. Brierley, N. J. Isaacs, R. L. Young, and L. Ashley Blackshaw, “Identifying spinal sensory pathways activated by noxious esophageal acid,” *Neurogastroenterology and Motility*, vol. 25, no. 10, pp. e660-8, Oct. 2013, doi: 10.1111/nmo.12180.

[260] R.-R. Ji, A. Chamessian, and Y.-Q. Zhang, “Pain regulation by non-neuronal cells and inflammation.,” *Science*, vol. 354, no. 6312, pp. 572–577, Nov. 2016, doi: 10.1126/science.aaf8924.

[261] J. A. M. Coull *et al.*, “BDNF from microglia causes the shift in neuronal anion gradient underlying neuropathic pain,” *Nature*, vol. 438, no. 7070, pp. 1017–1021, Dec. 2005, doi: 10.1038/nature04223.

[262] M. Zelenka, M. Schäfers, and C. Sommer, “Intraneural injection of interleukin-1β and tumor necrosis factor-alpha into rat sciatic nerve at physiological doses induces signs of neuropathic pain,” *Pain*, vol. 116, no. 3, pp. 257–263, Aug. 2005, doi: 10.1016/j.pain.2005.04.018.

[263] J. C. Ansel, J. R. Brown, D. G. Payan, and M. A. Brown, “Substance P selectively activates TNF-alpha gene expression in murine mast cells.,” *J Immunol*, vol. 150, no. 10, pp. 4478–85, May 1993, Accessed: Apr. 28, 2020. [Online]. Available: http://www.ncbi.nlm.nih.gov/pubmed/7683320

[264] J. Hosoi *et al.*, “Regulation of Langerhans cell function by nerves containing calcitonin gene-related peptide,” *Nature*, vol. 363, no. 6425, pp. 159–163, 1993, doi: 10.1038/363159A0.

[265] W. Ding, L. L. Stohl, J. A. Wagner, and R. D. Granstein, “Calcitonin Gene-Related Peptide Biases Langerhans Cells toward Th2-Type Immunity,” *The Journal of Immunology*, vol. 181, no. 9, pp. 6020–6026, Nov. 2008, doi: 10.4049/jimmunol.181.9.6020.

[266] A. Diogenes, C. C. R. Ferraz, A. N. Akopian, M. A. Henry, and K. M. Hargreaves, “LPS sensitizes TRPV1 via activation of TLR4 in trigeminal sensory neurons.,” *J Dent Res*, vol. 90, no. 6, pp. 759–64, Jun. 2011, doi: 10.1177/0022034511400225.

[267] Y. Li *et al.*, “The cancer chemotherapeutic paclitaxel increases human and rodent sensory neuron responses to TRPV1 by activation of TLR4,” *Journal of Neuroscience*, vol. 35, no. 39, pp. 13487–13500, Sep. 2015, doi: 10.1523/JNEUROSCI.1956-15.2015.

[268] G. Dothel *et al.*, “Nerve fiber outgrowth is increased in the intestinal mucosa of patients with irritable bowel syndrome.,” *Gastroenterology*, vol. 148, no. 5, pp. 1002-1011.e4, May 2015, doi: 10.1053/j.gastro.2015.01.042.

[269] N. de Bortoli *et al.*, “Gastroesophageal reflux disease, functional dyspepsia and irritable bowel syndrome: Common overlapping gastrointestinal disorders,” *Annals of Gastroenterology*, vol. 31, no. 6. Hellenic Society of Gastroenterology, pp. 639–648, Oct. 20, 2018. doi: 10.20524/aog.2018.0314.

[270] L. I. Benowitz and A. Routtenberg, “GAP-43: an intrinsic determinant of neuronal development and plasticity.,” *Trends Neurosci*, vol. 20, no. 2, pp. 84–91, Feb. 1997.

[271] D. Diolaiti *et al.*, “Functional cooperation between TrkA and p75NTR accelerates neuronal differentiation by increased transcription of GAP-43 and p21(CIP/WAF) genes via ERK1/2 and AP-1 activities,” *Exp Cell Res*, vol. 313, no. 14, pp. 2980–2992, Aug. 2007, doi: 10.1016/j.yexcr.2007.06.002.

[272] I. E. Demir, K.-H. Schäfer, E. Tieftrunk, H. Friess, and G. O. Ceyhan, “Neural plasticity in the gastrointestinal tract: chronic inflammation, neurotrophic signals, and hypersensitivity,” *Acta Neuropathol*, vol. 125, no. 4, pp. 491–509, 2013, doi: 10.1007/s00401-013-1099-4.

[273] A. Altomare, M. P. L. Guarino, S. Cocca, S. Emerenziani, and M. Cicala, “Gastroesophageal reflux disease: Update on inflammation and symptom perception,” *World J Gastroenterol*, vol. 19, no. 39, pp. 6523–6528, Oct. 2013, doi: 10.3748/wjg.v19.i39.6523.

[274] N. Yoshida, “Inflammation and oxidative stress in gastroesophageal reflux disease,” *Journal of Clinical Biochemistry and Nutrition*, vol. 40, no. 1. The Society for Free Radical Research Japan, pp. 13–23, Jan. 2007. doi: 10.3164/jcbn.40.13.

[275] K. B. Dunbar *et al.*, “Association of Acute Gastroesophageal Reflux Disease With Esophageal Histologic Changes,” *JAMA*, vol. 315, no. 19, pp. 2104–2112, 2016, doi: 10.1001/jama.2016.5657.

[276] H. Isomoto *et al.*, “Enhanced expression of interleukin-8 and activation of nuclear factor kappa-B in endoscopy-negative gastroesophageal reflux disease,” *Am J Gastroenterol*, vol. 99, no. 4, pp. 589–597, 2004, doi: 10.1111/j.1572-0241.2004.04110.x.

[277] R. C. Fitzgerald *et al.*, “Inflammatory gradient in Barrett’s oesophagus: implications for disease complications,” *Gut*, vol. 51, no. 3, p. 316, Sep. 2002, doi: 10.1136/GUT.51.3.316.

[278] J. Ma *et al.*, “HCl-induced and ATP-dependent upregulation of TRPV1 receptor expression and cytokine production by human esophageal epithelial cells,” *Am J Physiol Gastrointest Liver Physiol*, vol. 303, no. 5, pp. G635-45, Sep. 2012, doi: 10.1152/ajpgi.00097.2012.

[279] C. Singaram, A. Sengupta, C. Stevens, S. J. Spechler, and R. K. Goyal, “Localization of calcitonin gene-related peptide in human esophageal langerhans cells,” *Gastroenterology*, vol. 100, no. 2, pp. 560–563, 1991, doi: 10.1016/0016-5085(91)90231-9.

[280] A. D. Cook, A. D. Christensen, D. Tewari, S. B. McMahon, and J. A. Hamilton, “Immune Cytokines and Their Receptors in Inflammatory Pain,” *Trends in Immunology*, vol. 39, no. 3. Elsevier Ltd, pp. 240–255, Mar. 01, 2018. doi: 10.1016/j.it.2017.12.003.

[281] H. G. Schaible, “Nociceptive neurons detect cytokines in arthritis,” *Arthritis Research and Therapy*, vol. 16, no. 1. BioMed Central Ltd., Oct. 30, 2014. doi: 10.1186/s13075-014-0470-8.

[282] J. Scholz and C. J. Woolf, “The neuropathic pain triad: neurons, immune cells and glia,” *Nat Neurosci*, vol. 10, no. 11, pp. 1361–1368, Nov. 2007, doi: 10.1038/NN1992.

[283] W. A. Verri, T. M. Cunha, C. A. Parada, S. Poole, F. Q. Cunha, and S. H. Ferreira, “Hypernociceptive role of cytokines and chemokines: Targets for analgesic drug development?,” *Pharmacology and Therapeutics*, vol. 112, no. 1. Pharmacol Ther, pp. 116–138, Oct. 2006. doi: 10.1016/j.pharmthera.2006.04.001.

[284] R. Dubner, T. Berta, Y. J. Qadri, G. Chen, and R. R. Ji, “Microglial Signaling in Chronic Pain with a Special Focus on Caspase 6, p38 MAP Kinase, and Sex Dependence,” *J Dent Res*, vol. 95, no. 10, pp. 1124–1131, Sep. 2016, doi: 10.1177/0022034516653604.

[285] G. Chen and D. v. Goeddel, “TNF-R1 signaling: A beautiful pathway,” *Science*, vol. 296, no. 5573. American Association for the Advancement of Science, pp. 1634–1635, May 31, 2002. doi: 10.1126/science.1071924.

[286] H. Wajant and D. Siegmund, “TNFR1 and TNFR2 in the control of the life and death balance of macrophages,” *Frontiers in Cell and Developmental Biology*, vol. 7, no. May. Frontiers Media S.A., p. 91, May 29, 2019. doi: 10.3389/fcell.2019.00091.

[287] R. M. Locksley, N. Killeen, and M. J. Lenardo, “The TNF and TNF receptor superfamilies: Integrating mammalian biology,” *Cell*, vol. 104, no. 4. Cell Press, pp. 487–501, Feb. 23, 2001. doi: 10.1016/S0092-8674(01)00237-9.

[288] A. P. Gregory *et al.*, “TNF receptor 1 genetic risk mirrors outcome of anti-TNF therapy in multiple sclerosis,” *Nature*, vol. 488, no. 7412, pp. 508–511, Aug. 2012, doi: 10.1038/nature11307.

[289] F. K. M. Chan, H. J. Chun, L. Zheng, R. M. Siegel, K. L. Bui, and M. J. Lenardo, “A domain in TNF receptors that mediates ligand-independent receptor assembty and signaling,” *Science (1979)*, vol. 288, no. 5475, pp. 2351–2354, Jun. 2000, doi: 10.1126/science.288.5475.2351.

[290] B. Lainez *et al.*, “Identification and characterization of a novel spliced variant that encodes human soluble tumor necrosis factor receptor 2,” *Int Immunol*, vol. 16, no. 1, pp. 169–177, Jan. 2004, doi: 10.1093/intimm/dxh014.

[291] B. Galve-de Rochemonteix, L. P. Nicod, and J. M. Dayer, “Tumor Necrosis Factor Soluble Receptor 75: The Principal Receptor Form Released by Human Alveolar Macrophages and Monocytes in the Presence of Interferon γ,” *Am J Respir Cell Mol Biol*, vol. 14, no. 3, pp. 279–287, Dec. 1996, doi: 10.1165/ajrcmb.14.3.8845179.

[292] H. P. Hyun, Y. C. Lo, S. C. Lin, L. Wang, K. Y. Jin, and H. Wu, “The death domain superfamily in intracellular signaling of apoptosis and inflammation,” *Annual Review of Immunology*, vol. 25. Annu Rev Immunol, pp. 561–586, 2007. doi: 10.1146/annurev.immunol.25.022106.141656.

[293] H. Wajant and P. Scheurich, “TNFR1-induced activation of the classical NF-κB pathway,” *FEBS Journal*, vol. 278, no. 6, pp. 862–876, Apr. 2011, doi: 10.1111/j.1742-4658.2011.08015.x.

[294] D. W. Banner *et al.*, “Crystal structure of the soluble human 55 kd TNF receptor-human TNFβ complex: Implications for TNF receptor activation,” *Cell*, vol. 73, no. 3, pp. 431–445, May 1993, doi: 10.1016/0092-8674(93)90132-A.

[295] H. Hsu, J. Xiong, and D. v. Goeddel, “The TNF receptor 1-associated protein TRADD signals cell death and NF-κB activation,” *Cell*, vol. 81, no. 4, pp. 495–504, May 1995, doi: 10.1016/0092-8674(95)90070-5.

[296] H. Hsu, H. B. Shu, M. G. Pan, and D. v. Goeddel, “TRADD-TRAF2 and TRADD-FADD interactions define two distinct TNF receptor 1 signal transduction pathways,” *Cell*, vol. 84, no. 2, pp. 299–308, Jan. 1996, doi: 10.1016/S0092-8674(00)80984-8.

[297] H. Hsu, J. Huang, H. B. Shu, V. Baichwal, and D. v. Goeddel, “TNF-dependent recruitment of the protein kinase RIP to the TNF receptor-1 signaling complex,” *Immunity*, vol. 4, no. 4, pp. 387–396, 1996, doi: 10.1016/S1074-7613(00)80252-6.

[298] C. Dostert, M. Grusdat, E. Letellier, and D. Brenner, “The TNF family of ligands and receptors: Communication modules in the immune system and beyond,” *Physiol Rev*, vol. 99, no. 1, pp. 115–160, Jan. 2019, doi: 10.1152/physrev.00045.2017.

[299] M. J. M. Bertrand *et al.*, “cIAP1 and cIAP2 Facilitate Cancer Cell Survival by Functioning as E3 Ligases that Promote RIP1 Ubiquitination,” *Mol Cell*, vol. 30, no. 6, pp. 689–700, Jun. 2008, doi: 10.1016/j.molcel.2008.05.014.

[300] J. E. Vince *et al.*, “TRAF2 must bind to cellular inhibitors of apoptosis for tumor necrosis factor (TNF) to efficiently activate NF-κB and to prevent TNF-induced apoptosis,” *Journal of Biological Chemistry*, vol. 284, no. 51, pp. 35906–35915, Dec. 2009, doi: 10.1074/jbc.M109.072256.

[301] J. R. Bradley, “TNF-mediated inflammatory disease,” *Journal of Pathology*, vol. 214, no. 2. John Wiley & Sons, Ltd, pp. 149–160, Jan. 01, 2008. doi: 10.1002/path.2287.

[302] P. J. W. Naudé, J. A. den Boer, P. G. M. Luiten, and U. L. M. Eisel, “Tumor necrosis factor receptor cross-talk,” *FEBS Journal*, vol. 278, no. 6. FEBS J, pp. 888–898, Apr. 2011. doi: 10.1111/j.1742-4658.2011.08017.x.

[303] J. Medler and H. Wajant, “Tumor necrosis factor receptor-2 (TNFR2): An overview of an emerging drug target,” *Expert Opinion on Therapeutic Targets*, vol. 23, no. 4. Taylor and Francis Ltd, pp. 295–307, 2019. doi: 10.1080/14728222.2019.1586886.

[304] M. Bennett, K. Macdonald, S. W. Chan, J. P. Luzio, R. Simari, and P. Weissberg, “Cell surface trafficking of Fas: A rapid mechanism of p53-mediated apoptosis,” *Science (1979)*, vol. 282, no. 5387, pp. 290–293, Oct. 1998, doi: 10.1126/science.282.5387.290.

[305] T. Hino *et al.*, “Hydrogen peroxide enhances shedding of type I soluble tumor necrosis factor receptor from pulmonary epithelial cells,” *Am J Respir Cell Mol Biol*, vol. 20, no. 1, pp. 122–128, Jan. 1999, doi: 10.1165/ajrcmb.20.1.3217.

[306] J. R. Bradley, D. R. Johnson, and J. S. Pober, “Endothelial activation by hydrogen peroxide: Selective increases of intercellular adhesion molecule-1 and major histocompatibility complex class I,” *American Journal of Pathology*, vol. 142, no. 5, pp. 1598–1609, 1993, Accessed: Jan. 28, 2021. [Online]. Available: /pmc/articles/PMC1886909/?report=abstract

[307] L. A. Madge, M. R. Sierra-Honigmann, and J. S. Pober, “Apoptosis-inducing agents cause rapid shedding of tumor necrosis factor receptor 1 (TNFR1). A nonpharmacological explanation foil inhibition of TNF- mediated activation,” *Journal of Biological Chemistry*, vol. 274, no. 19, pp. 13643–13649, May 1999, doi: 10.1074/jbc.274.19.13643.

[308] M. K. Boettger *et al.*, “Antinociceptive effects of tumor necrosis factor α neutralization in a rat model of antigen-induced arthritis: Evidence of a neuronal target,” *Arthritis Rheum*, vol. 58, no. 8, pp. 2368–2378, Aug. 2008, doi: 10.1002/art.23608.

[309] M. Schäfers, C. I. Svensson, C. Sommer, and L. S. Sorkin, “Tumor necrosis factor-α induces mechanical allodynia after spinal nerve ligation by activation of p38 MAPK in primary sensory neurons,” *Journal of Neuroscience*, vol. 23, no. 7, pp. 2517–2521, Apr. 2003, doi: 10.1523/jneurosci.23-07-02517.2003.

[310] V. I. Shubayev and R. R. Myers, “Axonal transport of TNF-α in painful neuropathy: Distribution of ligand tracer and TNF receptors,” *J Neuroimmunol*, vol. 114, no. 1–2, pp. 48–56, Mar. 2001, doi: 10.1016/S0165-5728(00)00453-7.

[311] S. Hensellek, P. Brell, H. G. Schaible, R. Bräuer, and G. Segond von Banchet, “The cytokine TNFα increases the proportion of DRG neurones expressing the TRPV1 receptor via the TNFR1 receptor and ERK activation,” *Molecular and Cellular Neuroscience*, vol. 36, no. 3, pp. 381–391, Nov. 2007, doi: 10.1016/j.mcn.2007.07.010.

[312] S. Ohtori, K. Takahashi, H. Moriya, and R. R. Myers, “TNF-α and TNF-α receptor type 1 upregulation in glia and neurons after peripheral nerve injury: Studies in murine DRG and spinal cord,” *Spine*

(Phila Pa 1976), vol. 29, no. 10, pp. 1082–1088, May 2004, doi: 10.1097/00007632-200405150-00006.

[313] A. Oprée and M. Kress, “Involvement of the proinflammatory cytokines tumor necrosis factor-alpha, IL-1 beta, and IL-6 but not IL-8 in the development of heat hyperalgesia: effects on heat-evoked calcitonin gene-related peptide release from rat skin,” *J Neurosci*, vol. 20, no. 16, pp. 6289–6293, Aug. 2000, doi: 10.1523/JNEUROSCI.20-16-06289.2000.

[314] Y. T. Lin, L. S. Ro, H. L. Wang, and J. C. Chen, “Up-regulation of dorsal root ganglia BDNF and trkB receptor in inflammatory pain: An in vivo and in vitro study,” *J Neuroinflammation*, vol. 8, Sep. 2011, doi: 10.1186/1742-2094-8-126.

[315] K. Liu *et al.*, “Structural basis of CXC chemokine receptor 2 activation and signalling,” *Nature 2020 585:7823*, vol. 585, no. 7823, pp. 135–140, Jul. 2020, doi: 10.1038/s41586-020-2492-5.

[316] J. Korzenik, M. D. Larsen, J. Nielsen, J. Kjeldsen, and B. M. Nørgård, “Increased risk of developing Crohn’s disease or ulcerative colitis in 17 018 patients while under treatment with anti-TNFα agents, particularly etanercept, for autoimmune diseases other than inflammatory bowel disease,” *Aliment Pharmacol Ther*, vol. 50, no. 3, pp. 289–294, Aug. 2019, doi: 10.1111/apt.15370.

[317] T. Scheinin, D. M. Butler, F. Salway, B. Scallon, and M. Feldmann, “Validation of the interleukin-10 knockout mouse model of colitis: Antitumour necrosis factor-antibodies suppress the progression of colitis,” *Clin Exp Immunol*, vol. 133, no. 1, pp. 38–43, Jul. 2003, doi: 10.1046/j.1365-2249.2003.02193.x.

[318] T. Goretsky *et al.*, “P53 mediates TNF-induced epithelial cell apoptosis in IBD,” *American Journal of Pathology*, vol. 181, no. 4, pp. 1306–1315, Oct. 2012, doi: 10.1016/j.ajpath.2012.06.016.

[319] R. Stillie and A. W. Stadnyk, “Role of TNF receptors, TNFR1 and TNFR2, in dextran sodium sulfate-induced colitis,” *Inflamm Bowel Dis*, vol. 15, no. 10, pp. 1515–1525, Oct. 2009, doi: 10.1002/ibd.20951.

[320] H. Oshima *et al.*, “TNF-/TNFR1 signaling promotes gastric tumorigenesis through induction of Noxo1 and Gna14 in tumor cells,” *Oncogene*, vol. 33, no. 29, pp. 3820–3829, Jul. 2014, doi: 10.1038/onc.2013.356.

[321] I. Perry *et al.*, “Reduced cadherin/catenin complex expression in celiac disease can be reproduced in vitro by cytokine stimulation,” *Laboratory Investigation*, vol. 79, no. 12, pp. 1489–1499, Dec. 1999, Accessed: Jan. 29, 2021. [Online]. Available: https://europepmc.org/article/med/10616200

[322] C. Tselepis *et al.*, “Tumour necrosis factor-α in Barrett’s oesophagus: A potential novel mechanism of action,” *Oncogene*, vol. 21, no. 39, pp. 6071–6081, 2002, doi: 10.1038/sj.onc.1205731.

[323] K. Ren and R. Torres, “Role of interleukin-1β during pain and inflammation,” *Brain Res Rev*, vol. 60, no. 1, p. 57, Apr. 2009, doi: 10.1016/J.BRAINRESREV.2008.12.020.

[324] O. Ludwiczek *et al.*, “Imbalance between interleukin-1 agonists and antagonists: relationship to severity of inflammatory bowel disease,” *Clin Exp Immunol*, vol. 138, no. 2, pp. 323–329, Nov. 2004, doi: 10.1111/J.1365-2249.2004.02599.X.

[325] I. C. Chikanza, P. Roux-Lombard, J. -M Dayer, and G. S. Panayi, “Dysregulation of the in vivo production of interleukin-1 receptor antagonist in patients with rheumatoid arthritis. Pathogenetic implications,” *Arthritis Rheum*, vol. 38, no. 5, pp. 642–648, 1995, doi: 10.1002/ART.1780380511.

[326] F. Martinon, A. Mayor, and J. Tschopp, “The inflammasomes: guardians of the body,” *Annu Rev Immunol*, vol. 27, pp. 229–265, 2009, doi: 10.1146/ANNUREV.IMMUNOL.021908.132715.

[327] S. Tassi, S. Carta, R. Vené, L. Delfino, M. R. Ciriolo, and A. Rubartelli, “Pathogen-Induced Interleukin-1β Processing and Secretion Is Regulated by a Biphasic Redox Response,” *The Journal of Immunology*, vol. 183, no. 2, pp. 1456–1462, Jul. 2009, doi: 10.4049/JIMMUNOL.0900578.

[328] “Inflammasome Activation Pathways: R&D Systems.” https://www.rndsystems.com/pathways/inflammasome-activation-pathways (accessed Nov. 15, 2021).

[329] L. Agostini, F. Martinon, K. Burns, M. F. McDermott, P. N. Hawkins, and J. Tschopp, “NALP3 forms an IL-1beta-processing inflammasome with increased activity in Muckle-Wells autoinflammatory disorder,” *Immunity*, vol. 20, no. 3, pp. 319–325, Mar. 2004, doi: 10.1016/S1074-7613(04)00046-9.

[330] M. Braddock and A. Quinn, “Targeting IL-1 in inflammatory disease: new opportunities for therapeutic intervention,” *Nat Rev Drug Discov*, vol. 3, no. 4, pp. 330–339, 2004, doi: 10.1038/NRD1342.

[331] D. Boraschi, P. Italiani, S. Weil, and M. U. Martin, “The family of the interleukin-1 receptors,” *Immunol Rev*, vol. 281, no. 1, pp. 197–232, Jan. 2018, doi: 10.1111/IMR.12606.

[332] R. Medzhitov *et al.*, “MyD88 is an adaptor protein in the hToll/IL-1 receptor family signaling pathways,” *Mol Cell*, vol. 2, no. 2, pp. 253–258, 1998, doi: 10.1016/S1097-2765(00)80136-7.

[333] A. Weber, P. Wasiliew, and M. Kracht, “Interleukin-1 (IL-1) pathway,” *Sci Signal*, vol. 3, no. 105, Jan. 2010, doi: 10.1126/SCISIGNAL.3105CM1.

[334] S. J. Martin and S. J. Martin, “Cell death and inflammation: the case for IL-1 family cytokines as the canonical DAMPs of the immune system,” *FEBS J*, vol. 283, no. 14, pp. 2599–2615, Jul. 2016, doi: 10.1111/FEBS.13775.

[335] N. T. Martin and M. U. Martin, “Interleukin 33 is a guardian of barriers and a local alarmin,” *Nat Immunol*, vol. 17, no. 2, pp. 122–131, Feb. 2016, doi: 10.1038/NI.3370.

[336] C. Garlanda, C. A. Dinarello, and A. Mantovani, “The interleukin-1 family: back to the future,” *Immunity*, vol. 39, no. 6, pp. 1003–1018, Dec. 2013, doi: 10.1016/J.IMMUNI.2013.11.010.

[337] O. Obreja, P. K. Rathee, K. S. Lips, C. Distler, and M. Kress, “IL-1 beta potentiates heat-activated currents in rat sensory neurons: involvement of IL-1RI, tyrosine kinase, and protein kinase C,” *FASEB J*, vol. 16, no. 12, pp. 1497–1503, Oct. 2002, doi: 10.1096/FJ.02-0101COM.

[338] J. C. V. M. Copray *et al.*, “Expression of interleukin-1 beta in rat dorsal root ganglia,” *J Neuroimmunol*, vol. 118, no. 2, pp. 203–211, Aug. 2001, doi: 10.1016/S0165-5728(01)00324-1.

[339] W. Guo *et al.*, “Glial–Cytokine–Neuronal Interactions Underlying the Mechanisms of Persistent Pain,” *Journal of Neuroscience*, vol. 27, no. 22, pp. 6006–6018, May 2007, doi: 10.1523/JNEUROSCI.0176-07.2007.

[340] A. Churg, S. Zhou, X. Wang, R. Wang, and J. L. Wright, “The role of interleukin-1beta in murine cigarette smoke-induced emphysema and small airway remodeling,” *Am J Respir Cell Mol Biol*, vol. 40, no. 4, pp. 482–490, Apr. 2009, doi: 10.1165/RCMB.2008-0038OC.

[341] S. Provoost *et al.*, “NLRP3/caspase-1-independent IL-1beta production mediates diesel exhaust particle-induced pulmonary inflammation,” *J Immunol*, vol. 187, no. 6, pp. 3331–3337, Sep. 2011, doi: 10.4049/JIMMUNOL.1004062.

[342] Y. Kawasaki *et al.*, “Distinct roles of matrix metalloproteases in the early- and late-phase development of neuropathic pain,” *Nat Med*, vol. 14, no. 3, pp. 331–336, Mar. 2008, doi: 10.1038/NM1723.

[343] N. Üçeyler, A. Tscharke, and C. Sommer, “Early cytokine expression in mouse sciatic nerve after chronic constriction nerve injury depends on calpain,” *Brain Behav Immun*, vol. 21, no. 5, pp. 553–560, Jul. 2007, doi: 10.1016/J.BBI.2006.10.003.

[344] C. Sommer and M. Schäfers, “Painful mononeuropathy in C57BL/Wld mice with delayed Wallerian degeneration: differential effects of cytokine production and nerve regeneration on thermal and mechanical hypersensitivity,” *Brain Res*, vol. 784, no. 1–2, pp. 154–162, Feb. 1998, doi: 10.1016/S0006-8993(97)01327-9.

[345] M. Schäfers and L. Sorkin, “Effect of cytokines on neuronal excitability,” *Neurosci Lett*, vol. 437, no. 3, pp. 188–193, Jun. 2008, doi: 10.1016/J.NEULET.2008.03.052.

[346] H. Fukuoka, M. Kawatani, T. Hisamitsu, and C. Takeshige, “Cutaneous hyperalgesia induced by peripheral injection of interleukin-1 beta in the rat,” *Brain Res*, vol. 657, no. 1–2, pp. 133–140, Sep. 1994, doi: 10.1016/0006-8993(94)90960-1.

[347] G. Wolf, E. Gabay, M. Tal, R. Yirmiya, and Y. Shavit, “Genetic impairment of interleukin-1 signaling attenuates neuropathic pain, autotomy, and spontaneous ectopic neuronal activity, following nerve injury in mice,” *Pain*, vol. 120, no. 3, pp. 315–324, Feb. 2006, doi: 10.1016/J.PAIN.2005.11.011.

[348] L. Franchi *et al.*, “NLRC4-driven production of IL-1β discriminates between pathogenic and commensal bacteria and promotes host intestinal defense,” *Nat Immunol*, vol. 13, no. 5, pp. 449–456, May 2012, doi: 10.1038/NI.2263.

[349] M. E. Sellin *et al.*, “Epithelium-intrinsic NAIP/NLRC4 inflammasome drives infected enterocyte expulsion to restrict Salmonella replication in the intestinal mucosa,” *Cell Host Microbe*, vol. 16, no. 2, pp. 237–248, Aug. 2014, doi: 10.1016/J.CHOM.2014.07.001.

[350] I. Rauch *et al.*, “NAIP-NLRC4 Inflammasomes Coordinate Intestinal Epithelial Cell Expulsion with Eicosanoid and IL-18 Release via Activation of Caspase-1 and -8,” *Immunity*, vol. 46, no. 4, pp. 649–659, Apr. 2017, doi: 10.1016/J.IMMUNI.2017.03.016.

[351] M. Rawat *et al.*, “IL1B Increases Intestinal Tight Junction Permeability by Up-regulation of MIR200C-3p, Which Degrades Occludin mRNA,” *Gastroenterology*, vol. 159, no. 4, pp. 1375–1389, Oct. 2020, doi: 10.1053/J.GASTRO.2020.06.038.

[352] L. W. Kaminsky, R. Al-Sadi, and T. Y. Ma, “IL-1β and the Intestinal Epithelial Tight Junction Barrier,” *Front Immunol*, vol. 12, p. 767456, 2021, doi: 10.3389/FIMMU.2021.767456.

[353] J. S. Silver and C. A. Hunter, “gp130 at the nexus of inflammation, autoimmunity, and cancer,” *J Leukoc Biol*, vol. 88, no. 6, pp. 1145–1156, Dec. 2010, doi: 10.1189/JLB.0410217.

[354] M. Hibi, M. Murakami, M. Saito, T. Hirano, T. Taga, and T. Kishimoto, “Molecular cloning and expression of an IL-6 signal transducer, gp130,” *Cell*, vol. 63, no. 6, pp. 1149–1157, Dec. 1990, doi: 10.1016/0092-8674(90)90411-7.

[355] T. Taga *et al.*, “Interleukin-6 triggers the association of its receptor with a possible signal transducer, gp130,” *Cell*, vol. 58, no. 3, pp. 573–581, Aug. 1989, doi: 10.1016/0092-8674(89)90438-8.

[356] C. Martínez-Pérez *et al.*, “The Signal Transducer IL6ST (gp130) as a Predictive and Prognostic Biomarker in Breast Cancer,” *J Pers Med*, vol. 11, no. 7, p. 618, Jul. 2021, doi: 10.3390/JPM11070618.

[357] M. J. Boulanger, D. chone Chow, E. E. Brevnova, and K. C. Garcia, “Hexameric structure and assembly of the interleukin-6/IL-6 alpha-receptor/gp130 complex,” *Science*, vol. 300, no. 5628, pp. 2101–2104, Jun. 2003, doi: 10.1126/SCIENCE.1083901.

[358] N. Stahl *et al.*, “Association and activation of Jak-Tyk kinases by CNTF-LIF-OSM-IL-6 beta receptor components,” *Science*, vol. 263, no. 5143, pp. 92–95, 1994, doi: 10.1126/SCIENCE.8272873.

[359] U. A. K. Betz and W. Müller, “Regulated expression of gp130 and IL-6 receptor alpha chain in T cell maturation and activation,” *Int Immunol*, vol. 10, no. 8, pp. 1175–1184, 1998, doi: 10.1093/INTIMM/10.8.1175.

[360] F. Al-Sammak, T. Kalinski, S. Weinert, A. Link, T. Wex, and P. Malfertheiner, “Gastric Epithelial Expression of IL-12 Cytokine Family in Helicobacter pylori Infection in Human: Is it Head or Tail of the Coin?,” *PLoS One*, vol. 8, no. 9, p. e75192, Sep. 2013, doi: 10.1371/JOURNAL.PONE.0075192.

[361] L. Hong, H. Huang, and B. Wu, “Metabolites of intestinal microflora upregulate microRNA-200c-3p expression level to suppress airway epithelial inflammation via the IL6ST/JNK/STAT3 signaling pathway,” *Exp Ther Med*, vol. 22, no. 3, Jul. 2021, doi: 10.3892/ETM.2021.10431.

[362] K. Yoshida *et al.*, “Targeted disruption of gp130, a common signal transducer for the interleukin 6 family of cytokines, leads to myocardial and hematological disorders,” *Proc Natl Acad Sci U S A*, vol. 93, no. 1, pp. 407–411, Jan. 1996, doi: 10.1073/PNAS.93.1.407.

[363] Y. Tian *et al.*, “MicroRNA-31 Reduces Inflammatory Signaling and Promotes Regeneration in Colon Epithelium, and Delivery of Mimics in Microspheres Reduces Colitis in Mice,” *Gastroenterology*, vol. 156, no. 8, pp. 2281-2296.e6, Jun. 2019, doi: 10.1053/J.GASTRO.2019.02.023.

[364] D. G. Hill *et al.*, “Hyperactive gp130/STAT3-driven gastric tumourigenesis promotes submucosal tertiary lymphoid structure development,” *Int J Cancer*, vol. 143, no. 1, pp. 167–178, Jul. 2018, doi: 10.1002/IJC.31298.

[365] M. Andratsch *et al.*, “A key role for gp130 expressed on peripheral sensory nerves in pathological pain,” *J Neurosci*, vol. 29, no. 43, pp. 13473–13483, Oct. 2009, doi: 10.1523/JNEUROSCI.1822-09.2009.

[366] Kalpachidou T *et al.*, “Genetic and functional evidence for gp130/IL6ST-induced TRPA1 upregulation in uninjured but not injured neurons in a mouse model of neuropathic pain,” *Pain* , 2021.

[367] K. Dvorakova *et al.*, “Increased expression and secretion of interleukin-6 in patients with Barrett’s esophagus,” *Clin Cancer Res*, vol. 10, no. 6, pp. 2020–2028, Mar. 2004, doi: 10.1158/1078-0432.CCR-0437-03.

[368] Y. Qiao *et al.*, “IL6 derived from cancer-associated fibroblasts promotes chemoresistance via CXCR7 in esophageal squamous cell carcinoma,” *Oncogene 2018 37:7*, vol. 37, no. 7, pp. 873–883, Oct. 2017, doi: 10.1038/onc.2017.387.

[369] G. Romero, M. von Zastrow, and P. A. Friedman, “Role of PDZ Proteins in Regulating Trafficking, Signaling, and Function of GPCRs. Means, Motif, and Opportunity,” *Adv Pharmacol*, vol. 62, pp. 279–314, 2011, doi: 10.1016/B978-0-12-385952-5.00003-8.

[370] Q. Liu *et al.*, “The CXCL8-CXCR1/2 pathways in cancer,” *Cytokine Growth Factor Rev*, vol. 31, pp. 61–71, Oct. 2016, doi: 10.1016/J.CYTOGFR.2016.08.002.

[371] W. E. Holmes, J. Lee, W. J. Kuang, G. C. Rice, and W. I. Wood, “Structure and functional expression of a human interleukin-8 receptor,” *Science*, vol. 253, no. 5025, pp. 1278–1280, 1991, doi: 10.1126/SCIENCE.1840701.

[372] D. BB, M. SR, M. W, C. MF, and N. PH, “Physical association of Gi2alpha with interleukin-8 receptors,” *J Biol Chem*, vol. 271, no. 22, 1996, doi: 10.1074/JBC.271.22.12783.

[373] D. Wu, G. J. LaRosa, and M. I. Simon, “G protein-coupled signal transduction pathways for interleukin-8,” *Science*, vol. 261, no. 5117, pp. 101–103, 1993, doi: 10.1126/SCIENCE.8316840.

[374] Y. Wu *et al.*, “A chemokine receptor CXCR2 macromolecular complex regulates neutrophil functions in inflammatory diseases,” *J Biol Chem*, vol. 287, no. 8, pp. 5744–5755, Feb. 2012, doi: 10.1074/JBC.M111.315762.

[375] D. Xythalis, M. B. Frewin, and P. W. Gudewicz, “Inhibition of IL-8-mediated MAPK activation in human neutrophils by beta1 integrin ligands,” *Inflammation*, vol. 26, no. 2, pp. 83–88, 2002, doi: 10.1023/A:1014836211643.

[376] A. Chuntharapai, J. Lee, C. A. Hébert, and K. J. Kim, “Monoclonal antibodies detect different distribution patterns of IL-8 receptor A and IL-8 receptor B on human peripheral blood leukocytes,” vol. 153, no. 12, pp. 5682–8, 1994.

[377] X. Han *et al.*, “CXCR2 expression on granulocyte and macrophage progenitors under tumor conditions contributes to mo-MDSC generation via SAP18/ERK/STAT3,” *Cell Death & Disease 2019 10:8*, vol. 10, no. 8, pp. 1–15, Aug. 2019, doi: 10.1038/s41419-019-1837-1.

[378] T. Tecimer, J. Dlott, A. Chuntharapai, A. W. Martin, and S. C. Peiper, “Expression of the Chemokine Receptor CXCR2 in Normal and Neoplastic Neuroendocrine Cells,” *Arch Pathol Lab Med*, vol. 124, no. 4, pp. 520–525, Apr. 2000, doi: 10.5858/2000-124-0520-EOTCRC.

[379] Z. J. Zhang, D. L. Cao, X. Zhang, R. R. Ji, and Y. J. Gao, “Chemokine contribution to neuropathic pain: respective induction of CXCL1 and CXCR2 in spinal cord astrocytes and neurons,” *Pain*, vol. 154, no. 10, p. 2185, 2013, doi: 10.1016/J.PAIN.2013.07.002.

[380] D. L. Cao, Z. J. Zhang, R. G. Xie, B. C. Jiang, R. R. Ji, and Y. J. Gao, “Chemokine CXCL1 enhances inflammatory pain and increases NMDA receptor activity and COX-2 expression in spinal cord neurons via activation of CXCR2,” *Exp Neurol*, vol. 261, pp. 328–336, 2014, doi: 10.1016/J.EXPNEUROL.2014.05.014.

[381] C. DL, Q. B, Z. ZJ, G. YJ, and W. XB, “Chemokine receptor CXCR2 in dorsal root ganglion contributes to the maintenance of inflammatory pain,” *Brain Res Bull*, vol. 127, pp. 219–225, Oct. 2016, doi: 10.1016/J.BRAINRESBULL.2016.09.016.

[382] Y. Zhou *et al.*, “Overexpression of GRK6 attenuates neuropathic pain via suppression of CXCR2 in rat dorsal root ganglion,” *Mol Pain*, vol. 12, May 2016, doi: 10.1177/1744806916646381.

[383] X. Zhang, R. Guo, H. Kambara, F. Ma, and H. R. Luo, “The role of CXCR2 in acute inflammatory responses and its antagonists as anti-inflammatory therapeutics,” *Curr Opin Hematol*, vol. 26, no. 1, pp. 28–33, Jan. 2019, doi: 10.1097/MOH.0000000000000476.

[384] R. C. Chou *et al.*, “Lipid-cytokine-chemokine cascade drives neutrophil recruitment in a murine model of inflammatory arthritis,” *Immunity*, vol. 33, no. 2, pp. 266–278, Aug. 2010, doi: 10.1016/J.IMMUNI.2010.07.018.

[385] Y. Naito, T. Takagi, and T. Yoshikawa, “Molecular fingerprints of neutrophil-dependent oxidative stress in inflammatory bowel disease,” *J Gastroenterol*, vol. 42, no. 10, pp. 787–798, Oct. 2007, doi: 10.1007/S00535-007-2096-Y.

[386] M. Inoue *et al.*, “IL-8/CXCR2 Signalling Promotes Cell Proliferation in Oesophageal Squamous Cell Carcinoma and Correlates With Poor Prognosis,” *Anticancer Res*, vol. 41, no. 2, pp. 783–794, Feb. 2021, doi: 10.21873/ANTICANRES.14830.

[387] T. Nishi *et al.*, “CXCR2 expression and postoperative complications affect long-term survival in patients with esophageal cancer,” *World J Surg Oncol*, vol. 13, no. 1, pp. 1–9, Aug. 2015, doi: 10.1186/S12957-015-0658-7/TABLES/5.

[388] K. Wu *et al.*, “Silencing of CXCR2 and CXCR7 protects against esophageal cancer.,” *Am J Transl Res*, vol. 8, no. 8, pp. 3398–3408, Aug. 2016, Accessed: Mar. 12, 2022. [Online]. Available: https://europepmc.org/articles/PMC5009392

[389] N. YOSHIDA *et al.*, “Molecular mechanisms involved in interleukin-8 production by normal human oesophageal epithelial cells,” *Aliment Pharmacol Ther*, vol. 24, no. SUPPL.4, pp. 219–226, Jan. 2007, doi: 10.1111/j.1365-2036.2006.00049.x.

[390] N. Yoshida *et al.*, “Interleukin-8 expression in the esophageal mucosa of patients with gastroesophageal reflux disease,” *Scand J Gastroenterol*, vol. 39, no. 9, pp. 816–822, Sep. 2004, doi: 10.1080/00365520410006729.

[391] M. Majima, Y. Ito, K. Hosono, and H. Amano, “CGRP/CGRP Receptor Antibodies: Potential Adverse Effects Due to Blockade of Neovascularization?,” *Trends Pharmacol Sci*, vol. 40, no. 1, pp. 11–21, Jan. 2019, doi: 10.1016/J.TIPS.2018.11.003.

[392] D. L. Hay, G. Christopoulos, A. Christopoulos, D. R. Poyner, and P. M. Sexton, “Pharmacological discrimination of calcitonin receptor: receptor activity-modifying protein complexes,” *Mol Pharmacol*, vol. 67, no. 5, pp. 1655–1665, 2005, doi: 10.1124/MOL.104.008615.

[393] L. M. McLatchie *et al.*, “RAMPs regulate the transport and ligand specificity of the calcitonin-receptor-like receptor,” *Nature 1998 393:6683*, vol. 393, no. 6683, pp. 333–339, May 1998, doi: 10.1038/30666.

[394] B. N. Evans, M. I. Rosenblatt, L. O. Mnayer, K. R. Oliver, and I. M. Dickerson, “CGRP-RCP, a Novel Protein Required for Signal Transduction at Calcitonin Gene-related Peptide and Adrenomedullin

Receptors *," *Journal of Biological Chemistry*, vol. 275, no. 40, pp. 31438–31443, Oct. 2000, doi: 10.1074/JBC.M005604200.

[395] Z. Zhang, C. S. Winborn, B. M. de Prado, and A. F. Russo, "Sensitization of calcitonin gene-related peptide receptors by receptor activity-modifying protein-1 in the trigeminal ganglion," *J Neurosci*, vol. 27, no. 10, pp. 2693–2703, Mar. 2007, doi: 10.1523/JNEUROSCI.4542-06.2007.

[396] A. F. Russo, "Calcitonin Gene-Related Peptide (CGRP): A New Target for Migraine," *Annu Rev Pharmacol Toxicol*, vol. 55, p. 533, Jan. 2015, doi: 10.1146/ANNUREV-PHARMTOX-010814-124701.

[397] G. S. Cottrell, "CGRP Receptor Signalling Pathways," *Handb Exp Pharmacol*, vol. 255, pp. 37–64, 2018, doi: 10.1007/164_2018_130.

[398] S. Hilairet, C. Bélanger, J. Bertrand, A. Laperrière, S. M. Foord, and M. Bouvier, "Agonist-promoted Internalization of a Ternary Complex between Calcitonin Receptor-like Receptor, Receptor Activity-modifying Protein 1 (RAMP1), and β-Arrestin *," *Journal of Biological Chemistry*, vol. 276, no. 45, pp. 42182–42190, Nov. 2001, doi: 10.1074/JBC.M107323200.

[399] L. Edvinsson, K. A. Haanes, K. Warfvinge, and Di. N. Krause, "CGRP as the target of new migraine therapies - successful translation from bench to clinic," *Nat Rev Neurol*, vol. 14, no. 6, pp. 338–350, Jun. 2018, doi: 10.1038/S41582-018-0003-1.

[400] L. Edvinsson, A. S. Grell, and K. Warfvinge, "Expression of the CGRP Family of Neuropeptides and their Receptors in the Trigeminal Ganglion," *J Mol Neurosci*, vol. 70, no. 6, pp. 930–944, Jun. 2020, doi: 10.1007/S12031-020-01493-Z.

[401] J. K. Lennerz *et al.*, "Calcitonin receptor-like receptor (CLR), receptor activity-modifying protein 1 (RAMP1), and calcitonin gene-related peptide (CGRP) immunoreactivity in the rat trigeminovascular system: differences between peripheral and central CGRP receptor distribution," *J Comp Neurol*, vol. 507, no. 3, pp. 1277–1299, Mar. 2008, doi: 10.1002/CNE.21607.

[402] M. Honda *et al.*, "Inhibition of receptor activity–modifying protein 1 suppresses the development of endometriosis and the formation of blood and lymphatic vessels," *J Cell Mol Med*, vol. 24, no. 20, pp. 11984–11997, Oct. 2020, doi: 10.1111/JCMM.15823.

[403] N. Kawashima-Takeda *et al.*, "RAMP1 suppresses mucosal injury from dextran sodium sulfate-induced colitis in mice," *J Gastroenterol Hepatol*, vol. 32, no. 4, pp. 809–818, Apr. 2017, doi: 10.1111/JGH.13505.

[404] T. Inoue *et al.*, "RAMP1 in Kupffer cells is a critical regulator in immune-mediated hepatitis," *PLoS One*, vol. 13, no. 11, p. e0200432, Nov. 2018, doi: 10.1371/JOURNAL.PONE.0200432.

[405] N. Kawashima-Takeda *et al.*, "RAMP1 suppresses mucosal injury from dextran sodium sulfate-induced colitis in mice," *J Gastroenterol Hepatol*, vol. 32, no. 4, pp. 809–818, Apr. 2017, doi: 10.1111/JGH.13505.

[406] S. Tsuru *et al.*, "RAMP1 signaling in immune cells regulates inflammation-associated lymphangiogenesis," *Lab Invest*, vol. 100, no. 5, pp. 738–750, May 2020, doi: 10.1038/S41374-019-0364-0.

[407] C. Kurashige, K. Hosono, H. Matsuda, K. Tsujikawa, H. Okamoto, and M. Majima, "Roles of receptor activity-modifying protein 1 in angiogenesis and lymphangiogenesis during skin wound healing in mice," *FASEB J*, vol. 28, no. 3, pp. 1237–1247, 2014, doi: 10.1096/FJ.13-238998.

[408] K. Tsujikawa *et al.*, "Hypertension and dysregulated proinflammatory cytokine production in receptor activity-modifying protein 1-deficient mice," *Proc Natl Acad Sci U S A*, vol. 104, no. 42, pp. 16702–16707, Oct. 2007, doi: 10.1073/PNAS.0705974104.

[409] K. Seiler, J. I. Nusser, J. K. Lennerz, W. L. Neuhuber, and K. Messlinger, "Changes in calcitonin gene-related peptide (CGRP) receptor component and nitric oxide receptor (sGC) immunoreactivity

in rat trigeminal ganglion following glyceroltrinitrate pretreatment," *J Headache Pain*, vol. 14, no. 1, p. 74, 2013, doi: 10.1186/1129-2377-14-74.

[410] S. Eftekhari, C. A. Salvatore, A. Calamari, S. A. Kane, J. Tajti, and L. Edvinsson, "Differential distribution of calcitonin gene-related peptide and its receptor components in the human trigeminal ganglion," *Neuroscience*, vol. 169, no. 2, pp. 683–696, Aug. 2010, doi: 10.1016/J.NEUROSCIENCE.2010.05.016.

[411] L. Ohlsson, K. A. Haanes, E. Kronvall, C. Xu, J. Snellman, and L. Edvinsson, "Erenumab (AMG 334), a monoclonal antagonist antibody against the canonical CGRP receptor, does not impair vasodilatory or contractile responses to other vasoactive agents in human isolated cranial arteries," *Cephalalgia*, vol. 39, no. 14, pp. 1745–1752, Dec. 2019, doi: 10.1177/0333102419867282.

[412] L. Horling, N. W. Bunnett, K. Messlinger, W. L. Neuhuber, and M. Raab, "Localization of receptors for calcitonin-gene-related peptide to intraganglionic laminar endings of the mouse esophagus: peripheral interaction between vagal and spinal afferents?," *Histochem Cell Biol*, vol. 141, no. 3, pp. 321–335, Mar. 2014, doi: 10.1007/S00418-013-1162-1.

[413] W. H. MALONEY, "Peptic esophagitis," *J Lancet*, vol. 79, no. 1, pp. 14–16, Jan. 1959, doi: 10.1001/jama.1935.02760110034008.

[414] R. F. Souza *et al.*, "Gastroesophageal Reflux Might Cause Esophagitis Through a Cytokine-Mediated Mechanism Rather Than Caustic Acid Injury," *Gastroenterology*, vol. 137, no. 5, pp. 1776–1784, 2009, doi: 10.1053/j.gastro.2009.07.055.

[415] H. K. Eltzschig and P. Carmeliet, "Hypoxia and inflammation," *New England Journal of Medicine*, vol. 364, no. 7. Massachussetts Medical Society, pp. 656–665, Feb. 17, 2011. doi: 10.1056/NEJMra0910283.

[416] X. Huo *et al.*, "Hypoxia-inducible factor-2α plays a role in mediating oesophagitis in GORD," *Gut*, vol. 66, no. 9, pp. 1542–1554, Sep. 2017, doi: 10.1136/gutjnl-2016-312595.

[417] C. C. Scholz and C. T. Taylor, "Hydroxylase-dependent regulation of the NF-κb pathway," *Biological Chemistry*, vol. 394, no. 4. pp. 479–493, Apr. 2013. doi: 10.1515/hsz-2012-0338.

[418] A. Loboda, A. Jozkowicz, and J. Dulak, "HIF-1 and HIF-2 transcription factors--similar but not identical.," *Molecules and cells*, vol. 29, no. 5. pp. 435–442, May 2010. doi: 10.1007/s10059-010-0067-2.

[419] C. T. Taylor, "Interdependent roles for hypoxia inducible factor and nuclear factor-κB in hypoxic inflammation," *Journal of Physiology*, vol. 586, no. 17. Wiley-Blackwell, pp. 4055–4059, 2008. doi: 10.1113/jphysiol.2008.157669.

[420] X. Huo *et al.*, "Hypoxia-inducible factor-2alpha plays a role in mediating oesophagitis in GORD," *Gut*, vol. 66, no. 9, pp. 1542–1554, 2017, doi: 10.1136/gutjnl-2016-312595.

[421] H. Isomoto, "Elevated levels of chemokines in esophageal mucosa of patients with reflux esophagitis," *Am J Gastroenterol*, vol. 98, no. 3, pp. 551–556, Mar. 2003, doi: 10.1016/s0002-9270(02)06025-2.

[422] X. Huo *et al.*, "In oesophageal squamous cells exposed to acidic bile salt medium, omeprazole inhibits IL-8 expression through effects on nuclear factor-κB and activator protein-1," *Gut*, vol. 63, no. 7, pp. 1042–1052, 2014, doi: 10.1136/gutjnl-2013-305533.

[423] K. Mönkemüller *et al.*, "Interleukin-1beta and interleukin-8 expression correlate with the histomorphological changes in esophageal mucosa of patients with erosive and non-erosive reflux disease," *Digestion*, vol. 79, no. 3, pp. 186–195, Apr. 2009, doi: 10.1159/000211714.

[424] J. E. Pandolfino, H. B. El-Serag, Q. Zhang, N. Shah, S. K. Ghosh, and P. J. Kahrilas, "Obesity: a challenge to esophagogastric junction integrity," *Gastroenterology*, vol. 130, no. 3, pp. 639–649, 2006, doi: 10.1053/J.GASTRO.2005.12.016.

[425] S. Paris, R. Ekeanyanwu, Y. Jiang, D. Davis, S. J. Spechler, and R. F. Souza, “Obesity and its effects on the esophageal mucosal barrier,” *Am J Physiol Gastrointest Liver Physiol*, vol. 321, no. 3, pp. G335–G343, 2021, doi: 10.1152/AJPGI.00199.2021/ASSET/IMAGES/LARGE/AJPGI.00199.2021_F002.JPEG.

[426] C. H. Blevins, P. G. Iyer, M. F. Vela, and D. A. Katzka, “The Esophageal Epithelial Barrier in Health and Disease,” *Clinical Gastroenterology and Hepatology*, vol. 16, no. 5, pp. 608–617, May 2018, doi: 10.1016/J.CGH.2017.06.035.

[427] J. Dent, “Microscopic Esophageal Mucosal Injury in Nonerosive Reflux Disease,” *Clinical Gastroenterology and Hepatology*, vol. 5, no. 1. W.B. Saunders, pp. 4–16, Jan. 2007. doi: 10.1016/j.cgh.2006.08.006.

[428] H. Isomoto *et al.*, “Enhanced Expression of Interleukin-8 and Activation of Nuclear Factor Kappa-B in Endoscopy-negative Gastroesophageal Reflux Disease,” *American Journal of Gastroenterology*, vol. 99, no. 4, pp. 589–597, Apr. 2004, doi: 10.1111/j.1572-0241.2004.04110.x.

[429] N. A. Tobey, J. L. Carson, R. A. Alkiek, and R. C. Orlando, “Dilated intercellular spaces: A morphological feature of acid reflux- damaged human esophageal epithelium,” *Gastroenterology*, vol. 111, no. 5, pp. 1200–1205, 1996, doi: 10.1053/gast.1996.v111.pm8898633.

[430] R. Fiocca *et al.*, “Development of consensus guidelines for the histologic recognition of microscopic esophagitis in patients with gastroesophageal reflux disease: the Esohisto project,” *Hum Pathol*, vol. 41, no. 2, pp. 223–231, 2010, doi: 10.1016/j.humpath.2009.07.016.

[431] E. Savarino *et al.*, “Microscopic esophagitis distinguishes patients with non-erosive reflux disease from those with functional heartburn,” *J Gastroenterol*, vol. 48, no. 4, pp. 473–482, Apr. 2013, doi: 10.1007/s00535-012-0672-2.

[432] C. Triantos, N. Koukias, G. Karamanolis, and K. Thomopoulos, “Changes in the esophageal mucosa of patients with non erosive reflux disease: How far have we gone?,” *World J Gastroenterol*, vol. 21, no. 19, pp. 5762–5767, May 2015, doi: 10.3748/wjg.v21.i19.5762.

[433] N. Manabe, T. Yamamoto, M. Matsusaki, M. Akashi, and K. Haruma, “Measurement of low-grade inflammation of the esophageal mucosa with electrical conductivity shows promise in assessing PPI responsiveness in patients with GERD,” *Am J Physiol Gastrointest Liver Physiol*, vol. 321, no. 1, pp. G29–G40, Jul. 2021, doi: 10.1152/AJPGI.00365.2020/ASSET/IMAGES/MEDIUM/GI-00365-2020R01.PNG.

[434] S. Iyengar, M. H. Ossipov, and K. W. Johnson, “The role of calcitonin gene-related peptide in peripheral and central pain mechanisms including migraine,” *Pain*, vol. 158, no. 4. Lippincott Williams and Wilkins, pp. 543–559, Apr. 01, 2017. doi: 10.1097/j.pain.0000000000000831.

[435] S. J. H. Brookes, N. J. Spencer, M. Costa, and V. P. Zagorodnyuk, “Extrinsic primary afferent signalling in the gut,” *Nature Reviews Gastroenterology and Hepatology*, vol. 10, no. 5. Nature Publishing Group, pp. 286–296, May 26, 2013. doi: 10.1038/nrgastro.2013.29.

[436] J. R. F. Hockley *et al.*, “Single-cell RNAseq reveals seven classes of colonic sensory neuron,” *Gut*, vol. 68, no. 4, pp. 633–644, Apr. 2019, doi: 10.1136/gutjnl-2017-315631.

[437] P. Holzer, “The pharmacological challenge to tame the transient receptor potential vanilloid-1 (TRPV1) nocisensor,” *British Journal of Pharmacology*, vol. 155, no. 8. John Wiley & Sons, Ltd, pp. 1145–1162, Dec. 25, 2008. doi: 10.1038/bjp.2008.351.

[438] R. H. Lee, H. Korsapati, V. Bhalla, N. Varki, and R. K. Mittal, “Esophageal Submucosal Injection of Capsaicin but Not Acid Induces Symptoms in Normal Subjects,” *Mucosa Acid Injection and Heartburn Sensation*, vol. 22, no. 3, pp. 436–443, 2016, doi: 10.5056/jnm15166.

[439] S. Kindt, R. Vos, K. Blondeau, and J. Tack, “Influence of intra-oesophageal capsaicin instillation on heartburn induction and oesophageal sensitivity in man,” *Neurogastroenterology and Motility*, vol. 21, no. 10, Oct. 2009, doi: 10.1111/j.1365-2982.2009.01332.x.

[440] E. S. Kimball, S. P. Prouty, K. P. Pavlick, N. H. Wallace, C. R. Schneider, and P. J. Hornby, “Stimulation of neuronal receptors, neuropeptides and cytokines during experimental oil of mustard colitis,” *Neurogastroenterology and Motility*, vol. 19, no. 5, pp. 390–400, May 2007, doi: 10.1111/j.1365-2982.2007.00939.x.

[441] Y. C. Chua *et al.*, “Oesophageal epithelial ASIC3 is associated with increase in severity of symptoms in patients with gastro-oesophageal reflux disease (GORD),” *Gut*, vol. 60, no. Suppl 1, pp. A171–A171, Apr. 2011, doi: 10.1136/gut.2011.239301.363.

[442] I. Mainie *et al.*, “Acid and non-acid reflux in patients with persistent symptoms despite acid suppressive therapy: A multicentre study using combined ambulatory impedance-pH monitoring,” *Gut*, vol. 55, no. 10, pp. 1398–1402, Oct. 2006, doi: 10.1136/gut.2005.087668.

[443] J. Kun *et al.*, “Upregulation of the transient receptor potential ankyrin 1 ion channel in the inflamed human and mouse colon and its protective roles.,” *PLoS One*, vol. 9, no. 9, p. e108164, 2014, doi: 10.1371/journal.pone.0108164.

[444] B. I. Tõth, A. Oláh, A. G. Szöllósi, and T. Bírõ, “TRP channels in the skin,” *British Journal of Pharmacology*, vol. 171, no. 10. John Wiley and Sons Inc., pp. 2568–2581, 2014. doi: 10.1111/bph.12569.

[445] A. Ustaoglu *et al.*, “Heartburn Sensation in Non-Erosive Reflux Disease: Pattern of Superficial Sensory Nerves Expressing TRPV1 and Epithelial Cells Expressing ASIC3 Receptors,” *American Journal of Physiology-Gastrointestinal and Liver Physiology*, p. ajpgi.00013.2021, Mar. 2021, doi: 10.1152/ajpgi.00013.2021.

[446] M. Morgan, S. Nencini, J. Thai, and J. J. Ivanusic, “TRPV1 activation alters the function of Aδ and C fiber sensory neurons that innervate bone,” *Bone*, vol. 123, pp. 168–175, 2019, doi: https://doi.org/10.1016/j.bone.2019.03.040.

[447] K. R. Shieh *et al.*, “Evidence for neurotrophic factors associating with TRPV1 gene expression in the inflamed human esophagus,” *Neurogastroenterology and Motility*, vol. 22, no. 9, pp. 971–7, e252, Sep. 2010, doi: 10.1111/j.1365-2982.2010.01530.x.

[448] M. P. L. Guarino *et al.*, “Increased TRPV1 gene expression in esophageal mucosa of patients with non-erosive and erosive reflux disease,” *Neurogastroenterology and Motility*, vol. 22, no. 7, pp. 746-e219, Jul. 2010, doi: 10.1111/j.1365-2982.2010.01514.x.

[449] X. Han *et al.*, “Upregulation of acid sensing ion channels is associated with esophageal hypersensitivity in GERD,” *The FASEB Journal*, vol. 36, no. 1, p. e22083, Jan. 2022, doi: 10.1096/FJ.202100606R.

[450] W. G. Li and T. Le Xu, “ASIC3 channels in multimodal sensory perception,” *ACS Chemical Neuroscience*, vol. 2, no. 1. American Chemical Society, pp. 26–37, Jan. 19, 2011. doi: 10.1021/cn100094b.

[451] M. Khalil *et al.*, “Transient receptor potential melastatin 8 ion channel in macrophages modulates colitis through a balance-shift in TNF-alpha and interleukin-10 production,” *Mucosal Immunol*, vol. 9, no. 6, 2016, doi: 10.1038/mi.2016.16.

[452] S. Singh, S. K. Garg, P. P. Singh, P. G. Iyer, and H. B. El-Serag, “Acid-suppressive medications and risk of oesophageal adenocarcinoma in patients with barrett’s oesophagus: A systematic review and meta- Analysis,” *Gut*, vol. 63, no. 8. BMJ Publishing Group, pp. 1229–1237, 2014. doi: 10.1136/gutjnl-2013-305997.

[453] C. Calabrese *et al.*, “Reversibility of GERD ultrastructural alterations and relief of symptoms after omeprazole treatment,” *American Journal of Gastroenterology*, vol. 100, no. 3, pp. 537–542, Mar. 2005, doi: 10.1111/j.1572-0241.2005.40476.x.

[454] J. Wang *et al.*, “Differential gene expression in normal esophagus and Barrett’s esophagus,” *J Gastroenterol*, vol. 44, no. 9, pp. 897–911, May 2009, doi: 10.1007/s00535-009-0082-2.

[455] E. Bonora *et al.*, “INPP4B overexpression and c-KIT downregulation in human achalasia,” *Neurogastroenterology and Motility*, vol. 30, no. 9, Sep. 2018, doi: 10.1111/nmo.13346.

[456] L. I. Gomes *et al.*, “Expression profile of malignant and nonmalignant lesions of esophagus and stomach: Differential activity of functional modules related to inflammation and lipid metabolism,” *Cancer Res*, vol. 65, no. 16, pp. 7127–7136, Aug. 2005, doi: 10.1158/0008-5472.CAN-05-1035.

[457] D. M. Greenawalt *et al.*, “Gene expression profiling of esophageal cancer: Comparative analysis of Barrett’s esophagus, adenocarcinoma, and squamous cell carcinoma,” *Int J Cancer*, vol. 120, no. 9, pp. 1914–1921, May 2007, doi: 10.1002/ijc.22501.

[458] Y. Hao, G. Triadafilopoulos, P. Sahbaie, H. S. Young, M. B. Omary, and A. W. Lowe, “Gene Expression Profiling Reveals Stromal Genes Expressed in Common Between Barrett’s Esophagus and Adenocarcinoma,” *Gastroenterology*, vol. 131, no. 3, pp. 925–933, Sep. 2006, doi: 10.1053/j.gastro.2006.04.026.

[459] E. T. Kimchi *et al.*, “Progression of Barrett’s metaplasia to adenocarcinoma is associated with the suppression of the transcriptional programs of epidermal differentiation,” *Cancer Res*, vol. 65, no. 8, pp. 3146–3154, Apr. 2005, doi: 10.1158/0008-5472.CAN-04-2490.

[460] J. Ostrowski *et al.*, “Molecular defense mechanisms of Barrett’s metaplasia estimated by an integrative genomics,” *J Mol Med*, vol. 85, no. 7, pp. 733–743, Jul. 2007, doi: 10.1007/s00109-007-0176-3.

[461] J. W. P. M. Van Baal *et al.*, “A comparative analysis by SAGE of gene expression profiles of Barrett’s esophagus, normal squamous esophagus, and gastric cardia,” *Gastroenterology*, vol. 129, no. 4, pp. 1274–1281, 2005, doi: 10.1053/j.gastro.2005.07.026.

[462] G. A. Busslinger, B. L. A. Weusten, A. Bogte, H. Begthel, L. A. A. Brosens, and H. Clevers, “Human gastrointestinal epithelia of the esophagus, stomach, and duodenum resolved at single-cell resolution,” *Cell Rep*, vol. 34, no. 10, p. 108819, Mar. 2021, doi: 10.1016/j.celrep.2021.108819.

[463] A. Dobin *et al.*, “STAR: Ultrafast universal RNA-seq aligner,” *Bioinformatics*, vol. 29, no. 1, pp. 15–21, Jan. 2013, doi: 10.1093/bioinformatics/bts635.

[464] M. I. Love, W. Huber, and S. Anders, “Moderated estimation of fold change and dispersion for RNA-seq data with DESeq2,” *Genome Biol*, vol. 15, no. 12, pp. 1–21, Dec. 2014, doi: 10.1186/S13059-014-0550-8/FIGURES/9.

[465] Y. Zhou *et al.*, “Metascape provides a biologist-oriented resource for the analysis of systems-level datasets,” *Nat Commun*, vol. 10, no. 1, Dec. 2019, doi: 10.1038/S41467-019-09234-6.

[466] D. Aran, Z. Hu, and A. J. Butte, “xCell: Digitally portraying the tissue cellular heterogeneity landscape,” *Genome Biol*, vol. 18, no. 1, Nov. 2017, doi: 10.1186/s13059-017-1349-1.

[467] H. H. Bragulla and D. G. Homberger, “Structure and functions of keratin proteins in simple, stratified, keratinized and cornified epithelia,” *J Anat*, vol. 214, no. 4, p. 516, 2009, doi: 10.1111/J.1469-7580.2009.01066.X.

[468] “PER1 period circadian regulator 1 [Homo sapiens (human)] - Gene - NCBI.” https://www.ncbi.nlm.nih.gov/gene/5187 (accessed Feb. 22, 2022).

[469] “CIART circadian associated repressor of transcription [Homo sapiens (human)] - Gene - NCBI.” https://www.ncbi.nlm.nih.gov/gene/148523 (accessed Feb. 22, 2022).

[470] V. Aksenova *et al.*, “Actin-binding protein alpha-actinin 4 (ACTN4) is a transcriptional co-activator of RelA/p65 sub-unit of NF-kB,” *Oncotarget*, vol. 4, no. 2, pp. 362–372, 2013, doi: 10.18632/ONCOTARGET.901.

[471] “IL33 interleukin 33 [Homo sapiens (human)] - Gene - NCBI.” https://www.ncbi.nlm.nih.gov/gene/90865#gene-expression (accessed Dec. 08, 2021).

[472] K. J. Hewitt, R. Agarwal, and P. J. Morin, “The claudin gene family: Expression in normal and neoplastic tissues,” *BMC Cancer*, vol. 6, no. 1, pp. 1–8, Jul. 2006, doi: 10.1186/1471-2407-6-186/FIGURES/3.

[473] Y. Itoh *et al.*, “Identification and Expression of Human Epiglycanin/MUC21: a Novel Transmembrane Mucin,” *Glycobiology*, vol. 18, no. 1, pp. 74–83, Jan. 2008, doi: 10.1093/GLYCOB/CWM118.

[474] “TGM1 transglutaminase 1 - Gene - GTR - NCBI.” https://www.ncbi.nlm.nih.gov/gtr/genes/7051/ (accessed Feb. 22, 2022).

[475] A. D. Gruber, R. C. Elble, H. L. Ji, K. D. Schreur, C. M. Fuller, and B. U. Pauli, “Genomic cloning, molecular characterization, and functional analysis of human CLCA1, the first human member of the family of Ca2+-activated Cl- channel proteins,” *Genomics*, vol. 54, no. 2, pp. 200–214, Dec. 1998, doi: 10.1006/geno.1998.5562.

[476] “MUCL3 mucin like 3 [Homo sapiens (human)] - Gene - NCBI.” https://www.ncbi.nlm.nih.gov/gene/135656 (accessed Aug. 20, 2022).

[477] “CLDN18 claudin 18 [Homo sapiens (human)] - Gene - NCBI.” https://www.ncbi.nlm.nih.gov/gene?Cmd=DetailsSearch&Term=51208 (accessed Aug. 18, 2022).

[478] “TFF3 trefoil factor 3 [Homo sapiens (human)] - Gene - NCBI.” https://www.ncbi.nlm.nih.gov/gene?Cmd=DetailsSearch&Term=7033 (accessed Aug. 18, 2022).

[479] A. M. Newman *et al.*, “Robust enumeration of cell subsets from tissue expression profiles,” *Nature Methods 2015 12:5*, vol. 12, no. 5, pp. 453–457, Mar. 2015, doi: 10.1038/nmeth.3337.

[480] M. C. Takenaka, M. G. Guereschi, and A. S. Basso, “Neuroimmune interactions: dendritic cell modulation by the sympathetic nervous system,” *Seminars in Immunopathology 2016 39:2*, vol. 39, no. 2, pp. 165–176, Oct. 2016, doi: 10.1007/S00281-016-0590-0.

[481] M. C. Takenaka *et al.*, “Norepinephrine Controls Effector T Cell Differentiation through β2-Adrenergic Receptor-Mediated Inhibition of NF-κB and AP-1 in Dendritic Cells,” *J Immunol*, vol. 196, no. 2, pp. 637–644, Jan. 2016, doi: 10.4049/JIMMUNOL.1501206.

[482] Y. Yanagawa, M. Matsumoto, and H. Togashi, “Enhanced dendritic cell antigen uptake via alpha2 adrenoceptor-mediated PI3K activation following brief exposure to noradrenaline,” *J Immunol*, vol. 185, no. 10, pp. 5762–5768, Nov. 2010, doi: 10.4049/JIMMUNOL.1001899.

[483] M. Cernadas, J. Lu, G. Watts, and M. B. Brenner, “CD1a expression defines an interleukin-12 producing population of human dendritic cells,” *Clin Exp Immunol*, vol. 155, no. 3, p. 523, Mar. 2009, doi: 10.1111/J.1365-2249.2008.03853.X.

[484] M. Mohajeri, P. T. Kovanen, V. Bianconi, M. Pirro, A. F. G. Cicero, and A. Sahebkar, “Mast cell tryptase - Marker and maker of cardiovascular diseases,” *Pharmacol Ther*, vol. 199, pp. 91–110, Jul. 2019, doi: 10.1016/J.PHARMTHERA.2019.03.008.

[485] “ACTN4 actinin alpha 4 [Homo sapiens (human)] - Gene - NCBI.” https://www.ncbi.nlm.nih.gov/gene/81 (accessed Aug. 24, 2022).

[486] “CLDN10 claudin 10 [Homo sapiens (human)] - Gene - NCBI.” https://www.ncbi.nlm.nih.gov/gene/9071 (accessed Aug. 24, 2022).

[487] “MUC17 mucin 17, cell surface associated [Homo sapiens (human)] - Gene - NCBI.” https://www.ncbi.nlm.nih.gov/gene/140453 (accessed Aug. 24, 2022).

[488] Y. Niv *et al.*, “Membrane-bound mucins and mucin terminal glycans expression in idiopathic or Helicobacter pylori, NSAID associated peptic ulcers,” *World J Gastroenterol*, vol. 20, no. 40, pp. 14913–14920, Oct. 2014, doi: 10.3748/WJG.V20.I40.14913.

[489] “ADAM23 ADAM metallopeptidase domain 23 [Homo sapiens (human)] - Gene - NCBI.” https://www.ncbi.nlm.nih.gov/gene/8745 (accessed Aug. 24, 2022).

[490] L. Langbein *et al.*, “Localisation of keratin K78 in the basal layer and first suprabasal layers of stratified epithelia completes expression catalogue of type II keratins and provides new insights into sequential keratin expression,” *Cell Tissue Res*, vol. 363, no. 3, pp. 735–750, Mar. 2016, doi: 10.1007/S00441-015-2278-5.

[491] R. D. Paladini and P. A. Coulombe, “Directed Expression of Keratin 16 to the Progenitor Basal Cells of Transgenic Mouse Skin Delays Skin Maturation,” *Journal of Cell Biology*, vol. 142, no. 4, pp. 1035–1051, Aug. 1998, doi: 10.1083/JCB.142.4.1035.

[492] H. Alam, L. Sehgal, S. T. Kundu, S. N. Dalal, and M. M. Vaidya, “Novel function of keratins 5 and 14 in proliferation and differentiation of stratified epithelial cells,” *Mol Biol Cell*, vol. 22, no. 21, pp. 4068–4078, Nov. 2011, doi: 10.1091/MBC.E10-08-0703/ASSET/IMAGES/LARGE/4068FIG7.JPEG.

[493] S. Mazzalupo, P. Wong, P. Martin, and P. A. Coulombe, “Role for keratins 6 and 17 during wound closure in embryonic mouse skin,” *Developmental Dynamics*, vol. 226, no. 2, pp. 356–365, Feb. 2003, doi: 10.1002/DVDY.10245.

[494] “JCHAIN joining chain of multimeric IgA and IgM [Homo sapiens (human)] - Gene - NCBI.” https://www.ncbi.nlm.nih.gov/gene/3512 (accessed Dec. 15, 2021).

[495] N. W. Palm *et al.*, “Immunoglobulin A coating identifies colitogenic bacteria in inflammatory bowel disease,” *Cell*, vol. 158, no. 5, p. 1000, Aug. 2014, doi: 10.1016/J.CELL.2014.08.006.

[496] N. Mohy-ud-din *et al.*, “Barrett’s esophagus: What do we need to know?,” *Dis Mon*, vol. 66, no. 1, Jan. 2020, doi: 10.1016/J.DISAMONTH.2019.02.003.

[497] R. Fass, “Nicht-erosive refluxerkrankung (Non-erosive Reflux Disease, NERD) und erosive ösophagitis - Ein krankheitsspektrum oder verschiedene erscheinungsbilder derselben krankheit?,” *Z Gastroenterol*, vol. 45, no. 11, pp. 1156–1163, Nov. 2007, doi: 10.1055/S-2007-963628/ID/52.

[498] A. Shah, F. Shibli, Y. Kitayama, and R. Fass, “The Natural Course of Gastroesophageal Reflux Disease: A Critical Appraisal of the Literature,” *J Clin Gastroenterol*, vol. 55, no. 1, pp. 12–20, Jan. 2021, doi: 10.1097/MCG.0000000000001419.

[499] S. B. des Varannes, F. Zerbib, and J. P. Galmiche, “Functional heartburn.,” *Gastroenterol Hepatol (N Y)*, vol. 10, no. 6, pp. 381–383, Jun. 2014, doi: 10.1002/9781118444788.ch8.

[500] B. Terris *et al.*, “Mucin gene expression in intraductal papillary-mucinous pancreatic tumours and related lesions,” *Journal of Pathology*, vol. 197, no. 5, pp. 632–637, 2002, doi: 10.1002/path.1146.

[501] S. Y. Kim and M. G. Nair, “Macrophages in wound healing: activation and plasticity,” *Immunol Cell Biol*, vol. 97, no. 3, pp. 258–267, Mar. 2019, doi: 10.1111/IMCB.12236.

[502] A. M. I. Mowat, “Anatomical basis of tolerance and immunity to intestinal antigens,” *Nat Rev Immunol*, vol. 3, no. 4, pp. 331–341, 2003, doi: 10.1038/NRI1057.

[503] T. B. Bertolini, M. Biswas, C. Terhorst, H. Daniell, R. W. Herzog, and A. R. Piñeros, “Role of orally induced regulatory T cells in immunotherapy and tolerance,” *Cell Immunol*, vol. 359, p. 104251, Jan. 2021, doi: 10.1016/J.CELLIMM.2020.104251.

[504] B. E. Clausen and P. Stoitzner, “Functional specialization of skin dendritic cell subsets in regulating T cell responses,” *Front Immunol*, vol. 6, no. OCT, p. 534, 2015, doi: 10.3389/FIMMU.2015.00534/BIBTEX.

[505] A. Nishibu, B. R. Ward, J. v. Jester, H. L. Ploegh, M. Boes, and A. Takashima, “Behavioral responses of epidermal Langerhans cells in situ to local pathological stimuli,” *J Invest Dermatol*, vol. 126, no. 4, pp. 787–796, Apr. 2006, doi: 10.1038/SJ.JID.5700107.

[506] J. Aguilera-Lizarraga *et al.*, “Local immune response to food antigens drives meal-induced abdominal pain,” *Nature 2021 590:7844*, vol. 590, no. 7844, pp. 151–156, Jan. 2021, doi: 10.1038/s41586-020-03118-2.

[507] K. Gupta and I. T. Harvima, “Mast cell-neural interactions contribute to pain and itch,” *Immunol Rev*, vol. 282, no. 1, pp. 168–187, Mar. 2018, doi: 10.1111/IMR.12622.

[508] G. Barbara *et al.*, “Mast cell-dependent excitation of visceral-nociceptive sensory neurons in irritable bowel syndrome,” *Gastroenterology*, vol. 132, no. 1, pp. 26–37, 2007, doi: 10.1053/J.GASTRO.2006.11.039.

[509] A. Leon *et al.*, “Mast cells synthesize, store, and release nerve growth factor.,” *Proc Natl Acad Sci U S A*, vol. 91, no. 9, p. 3739, Apr. 1994, doi: 10.1073/PNAS.91.9.3739.

[510] M. Kubo, “Innate and adaptive type 2 immunity in lung allergic inflammation,” *Immunol Rev*, vol. 278, no. 1, pp. 162–172, Jul. 2017, doi: 10.1111/IMR.12557.

[511] P. Krzyszczyk, R. Schloss, A. Palmer, and F. Berthiaume, “The role of macrophages in acute and chronic wound healing and interventions to promote pro-wound healing phenotypes,” *Front Physiol*, vol. 9, no. MAY, p. 419, May 2018, doi: 10.3389/FPHYS.2018.00419/BIBTEX.

[512] R. Simeoli *et al.*, “Exosomal cargo including microRNA regulates sensory neuron to macrophage communication after nerve trauma,” *Nat Commun*, vol. 8, no. 1, Dec. 2017, doi: 10.1038/S41467-017-01841-5.

[513] M. Akkaya, K. Kwak, and S. K. Pierce, “B cell memory: building two walls of protection against pathogens,” *Nature Reviews Immunology 2019 20:4*, vol. 20, no. 4, pp. 229–238, Dec. 2019, doi: 10.1038/s41577-019-0244-2.

[514] P. A. Revell, V. Mayston, P. Lalor, and P. Mapp, “The synovial membrane in osteoarthritis: a histological study including the characterisation of the cellular infiltrate present in inflammatory osteoarthritis using monoclonal antibodies,” *Ann Rheum Dis*, vol. 47, no. 4, pp. 300–307, 1988, doi: 10.1136/ARD.47.4.300.

[515] A. G. Vanderwall and E. D. Milligan, “Cytokines in Pain: Harnessing Endogenous Anti-Inflammatory Signaling for Improved Pain Management,” *Front Immunol*, vol. 10, p. 3009, Dec. 2019, doi: 10.3389/FIMMU.2019.03009.

[516] M. Peiris *et al.*, “Human visceral afferent recordings: Preliminary report,” *Gut*, vol. 60, no. 2, pp. 204–208, Feb. 2011, doi: 10.1136/gut.2010.221820.

[517] U. D *et al.*, “Unbiased classification of sensory neuron types by large-scale single-cell RNA sequencing,” *Nat Neurosci*, vol. 18, no. 1, pp. 145–153, Jan. 2015, doi: 10.1038/NN.3881.

[518] L. CL *et al.*, “Somatosensory neuron types identified by high-coverage single-cell RNA-sequencing and functional heterogeneity,” *Cell Res*, vol. 26, no. 1, pp. 83–102, Jan. 2016, doi: 10.1038/CR.2015.149.

[519] L. M *et al.*, “Effects of complete Freund’s adjuvant on immunohistochemical distribution of IL-1beta and IL-1R I in neurons and glia cells of dorsal root ganglion,” *Acta Pharmacol Sin*, vol. 26, no. 2, pp. 192–198, Feb. 2005, doi: 10.1111/J.1745-7254.2005.00522.X.

[520] W. JG *et al.*, “The chemokine CXCL1/growth related oncogene increases sodium currents and neuronal excitability in small diameter sensory neurons,” *Mol Pain*, vol. 4, Sep. 2008, doi: 10.1186/1744-8069-4-38.

[521] T. Crosson *et al.*, “Profiling of how nociceptor neurons detect danger – new and old foes,” *J Intern Med*, vol. 286, no. 3, pp. 268–289, 2019, doi: 10.1111/JOIM.12957.

[522] T. SK and S. RE, “Immune System Involvement in Specific Pain Conditions,” *Mol Pain*, vol. 13, Aug. 2017, doi: 10.1177/1744806917724559.

[523] M. R. Zavala-Solares *et al.*, “Gene expression profiling of inflammatory cytokines in esophageal biopsies of different phenotypes of gastroesophageal reflux disease: a cross-sectional study,” *BMC Gastroenterol*, vol. 21, p. 201, 2020, doi: 10.1186/s12876-021-01707-7.

[524] K. J. Livak and T. D. Schmittgen, “Analysis of relative gene expression data using real-time quantitative PCR and the 2(-Delta Delta C(T)) Method,” *Methods*, vol. 25, no. 4, pp. 402–408, 2001, doi: 10.1006/METH.2001.1262.

[525] K. L. Edelblum, J. A. Goettel, T. Koyama, S. J. McElroy, F. Yan, and D. B. Polk, “TNFR1 promotes tumor necrosis factor-mediated mouse colon epithelial cell survival through RAF activation of NF-κB,” *Journal of Biological Chemistry*, vol. 283, no. 43, pp. 29485–29494, Oct. 2008, doi: 10.1074/jbc.M801269200.

[526] Y. Nishitani *et al.*, “Intestinal Anti-Inflammatory Activity of Lentinan: Influence on IL-8 and TNFR1 Expression in Intestinal Epithelial Cells,” *PLoS One*, vol. 8, no. 4, p. 62441, Apr. 2013, doi: 10.1371/journal.pone.0062441.

[527] E. Mizoguchi *et al.*, “TNF Receptor Type I-Dependent Activation of Innate Responses to Reduce Intestinal Damage-Associated Mortality,” *Gastroenterology*, vol. 134, no. 2, pp. 470–480, Feb. 2008, doi: 10.1053/j.gastro.2007.11.055.

[528] M. CT *et al.*, “Use of bioluminescence imaging to track neutrophil migration and its inhibition in experimental colitis,” *Clin Exp Immunol*, vol. 162, no. 1, pp. 188–196, Oct. 2010, doi: 10.1111/J.1365-2249.2010.04234.X.

[529] F. Zhu *et al.*, “Original Article Blockade of CXCR2 suppresses proinflammatory activities of neutrophils in ulcerative colitis,” 2020. [Online]. Available: www.ajtr.org

[530] B. Villeret *et al.*, “Blockade of IL-1R signaling diminishes Paneth cell depletion and Toxoplasma gondii induced ileitis in mice,” *Am J Clin Exp Immunol*, vol. 2, no. 1, p. 107, 2013, Accessed: Nov. 16, 2021. [Online]. Available: /pmc/articles/PMC3714202/

[531] G. Laumet, J. Ma, A. J. Robison, S. Kumari, C. J. Heijnen, and A. Kavelaars, “T Cells as an Emerging Target for Chronic Pain Therapy,” *Front Mol Neurosci*, vol. 12, Sep. 2019, doi: 10.3389/FNMOL.2019.00216.

[532] Y. Kobayashi, N. Kiguchi, Y. Fukazawa, F. Saika, T. Maeda, and S. Kishioka, “Macrophage-T cell interactions mediate neuropathic pain through the glucocorticoid-induced tumor necrosis factor ligand system,” *J Biol Chem*, vol. 290, no. 20, pp. 12603–12613, May 2015, doi: 10.1074/JBC.M115.636506.

[533] R. J. Jaken *et al.*, “Neuropathy-Induced Spinal GAP-43 Expression Is Not a Main Player in the Onset of Mechanical Pain Hypersensitivity,” *J Neurotrauma*, vol. 28, no. 12, p. 2463, Dec. 2011, doi: 10.1089/NEU.2011.1833.

[534] A. Akbar, Y. Yiangou, P. Facer, J. R. F. Walters, P. Anand, and S. Ghosh, “Increased capsaicin receptor TRPV1-expressing sensory fibres in irritable bowel syndrome and their correlation with abdominal pain,” *Gut*, vol. 57, no. 7, p. 923, Jul. 2008, doi: 10.1136/GUT.2007.138982.

[535] G. Minnone, F. de Benedetti, and L. Bracci-Laudiero, “NGF and Its Receptors in the Regulation of Inflammatory Response,” *Int J Mol Sci*, vol. 18, no. 5, May 2017, doi: 10.3390/IJMS18051028.

[536] K. Vadstrup *et al.*, “Validation and Optimization of an Ex Vivo Assay of Intestinal Mucosal Biopsies in Crohn’s Disease: Reflects Inflammation and Drug Effects OPEN ACCESS,” 2016, doi: 10.1371/journal.pone.0155335.

[537] J. D. Levine, T. J. Coderre, K. Covinsky, and A. I. Basbaum, “Neural influences on synovial mast cell density in rat,” *J Neurosci Res*, vol. 26, no. 3, pp. 301–307, 1990, doi: 10.1002/jnr.490260306.

[538] S. Yukawa *et al.*, “Dermal mast cell density in fingers reflects severity of skin sclerosis in systemic sclerosis,” *Mod Rheumatol*, vol. 23, no. 6, pp. 1151–1157, Nov. 2013, doi: 10.1007/s10165-012-0813-8.

[539] F. F. di Mola *et al.*, “Nerve growth factor and Trk high affinity receptor (TrkA) gene expression in inflammatory bowel disease,” *Gut*, vol. 46, no. 5, pp. 670–678, 2000, doi: 10.1136/GUT.46.5.670.

[540] I. Kinkelin, S. Mötzing, M. Koltzenburg, and E. B. Bröcker, “Increase in NGF content and nerve fiber sprouting in human allergic contact eczema,” *Cell Tissue Res*, vol. 302, no. 1, pp. 31–37, 2000, doi: 10.1007/S004410000202.

[541] R. H. Stead, U. Kosecka-Janiszewska, A. B. Oestreicher, M. F. Dixon, and J. Bienenstock, “Remodeling of B-50 (GAP-43)- and NSE-immunoreactive mucosal nerves in the intestines of rats infected with Nippostrongylus brasiliensis,” *J Neurosci*, vol. 11, no. 12, pp. 3809–3821, 1991, doi: 10.1523/JNEUROSCI.11-12-03809.1991.

[542] B. M. Davis, G. R. Lewin, L. M. Mendell, M. E. Jones, and K. M. Albers, “Altered expression of nerve growth factor in the skin of transgenic mice leads to changes in response to mechanical stimuli,” *Neuroscience*, vol. 56, no. 4, pp. 789–792, 1993, doi: 10.1016/0306-4522(93)90127-2.

[543] P. G. Nagappan, H. Chen, and D.-Y. Wang, “Neuroregeneration and plasticity: a review of the physiological mechanisms for achieving functional recovery postinjury”, doi: 10.1186/s40779-020-00259-3.

[544] D. L. Cao, B. Qian, Z. J. Zhang, Y. J. Gao, and X. B. Wu, “Chemokine receptor CXCR2 in dorsal root ganglion contributes to the maintenance of inflammatory pain,” *Brain Res Bull*, vol. 127, pp. 219–225, Oct. 2016, doi: 10.1016/J.BRAINRESBULL.2016.09.016.

[545] J. Shan, T. Oshima, H. Fukui, J. Watari, and H. Miwa, “Acidic deoxycholic acid and chenodeoxycholic acid induce interleukin-8 production through p38 mitogen-activated protein kinase and protein kinase A in a squamous epithelial model,” *Journal of Gastroenterology and Hepatology (Australia)*, vol. 28, no. 5, pp. 823–828, 2013, doi: 10.1111/jgh.12139.

[546] J. Shan, T. Oshima, X. Chen, H. Fukui, J. Watari, and H. Miwa, “Trypsin impaired epithelial barrier function and induced IL-8 secretion through basolateral PAR-2: a lesson from a stratified squamous epithelial model,” *American Journal of Physiology-Gastrointestinal and Liver Physiology*, vol. 303, no. 10, pp. G1105–G1112, Nov. 2012, doi: 10.1152/ajpgi.00220.2012.

[547] R. Moiseff, N. Olson, A. A. Suriawinata, R. I. Rothstein, and M. Lisovsky, “CD8 T-Cell–Predominant Lymphocytic Esophagitis is One of the Major Patterns of Lymphocytic Inflammation in Gastroesophageal Reflux Disease,” *Arch Pathol Lab Med*, vol. 145, no. 9, pp. 1138–1143, Sep. 2021, doi: 10.5858/ARPA.2020-0430-OA.

[548] K. B. Dunbar *et al.*, “Association of acute gastroesophageal reflux disease with esophageal histologic changes,” *JAMA - Journal of the American Medical Association*, vol. 315, no. 19, pp. 2104–2112, May 2016, doi: 10.1001/jama.2016.5657.

[549] V. V. V. Hira, A. L. de Jong, K. Ferro, M. Khurshed, R. J. Molenaar, and C. J. F. van Noorden, “Comparison of different methodologies and cryostat versus paraffin sections for chromogenic immunohistochemistry,” *Acta Histochem*, vol. 121, no. 2, pp. 125–134, Feb. 2019, doi: 10.1016/J.ACTHIS.2018.10.011.

[550] A. Ustaoglu, A. Nguyen, S. Spechler, D. Sifrim, R. Souza, and P. Woodland, “Mucosal pathogenesis in gastro-esophageal reflux disease,” *Neurogastroenterology & Motility*, Oct. 2020, doi: 10.1111/nmo.14022.

[551] J. Spencer and L. M. Sollid, “The human intestinal B-cell response,” *Mucosal Immunology 2016 9:5*, vol. 9, no. 5, pp. 1113–1124, Jul. 2016, doi: 10.1038/mi.2016.59.

[552] S. Sarkar, Q. Aziz, C. J. Woolf, A. R. Hobson, and D. G. Thompson, “Contribution of central sensitisation to the development of non-cardiac chest pain,” *Lancet*, vol. 356, no. 9236, pp. 1154–1159, Sep. 2000, doi: 10.1016/S0140-6736(00)02758-6.

[553] A. R. Hobson and Q. Aziz, “Brain processing of esophageal sensation in health and disease,” *Gastroenterology Clinics*, vol. 33, no. 1, pp. 69–91, Mar. 2004, doi: 10.1016/S0889-8553(03)00132-8.

[554] R. Fass, “Differential effect of long-term esophageal acid exposure on mechanosensitivity and chemosensitivity in humans,” *Gastroenterology*, vol. 115(6), pp. 1363–1373, 1998.

[555] J. L. Smith, A. R. Opekun, E. Larkai, and D. Y. Graham, “Sensitivity of the Esophageal Mucosa to pH in Gastroesophageal Reflux Disease,” *Gastroenterology*, vol. 96, pp. 683–692, 1989.

[556] T. Liebregts *et al.*, “Immune activation in patients with irritable bowel syndrome,” *Gastroenterology*, vol. 132, no. 3, pp. 913–920, 2007, doi: 10.1053/J.GASTRO.2007.01.046.

[557] J. R. Coldwell, B. D. Phillis, K. Sutherland, G. S. Howarth, and L. A. Blackshaw, “Increased responsiveness of rat colonic splanchnic afferents to 5-HT after inflammation and recovery,” *J Physiol*, vol. 579, no. Pt 1, pp. 203–213, Feb. 2007, doi: 10.1113/JPHYSIOL.2006.123158.

[558] G. Barbara *et al.*, “Activated Mast Cells in Proximity to Colonic Nerves Correlate with Abdominal Pain in Irritable Bowel Syndrome,” *Gastroenterology*, vol. 126, no. 3, pp. 693–702, Mar. 2004, doi: 10.1053/j.gastro.2003.11.055.

[559] P. Woodland, M. Al-Zinaty, E. Yazaki, and D. Sifrim, “In vivo evaluation of acid-induced changes in oesophageal mucosa integrity and sensitivity in non-erosive reflux disease,” *Gut*, vol. 62, no. 9, pp. 1256–1261, Sep. 2013, doi: 10.1136/gutjnl-2012-302645.

[560] P. Woodland, C. Lee, Y. Duraysami, R. Farré, P. Dettmar, and D. Sifrim, “Assessment and protection of esophageal mucosal integrity in patients with heartburn without esophagitis,” *American Journal of Gastroenterology*, vol. 108, no. 4, pp. 535–543, 2013, doi: 10.1038/ajg.2012.469.

[561] Y. W. Chu, R. B. Runyan, R. G. Oshima, and M. J. C. Hendrix, “Expression of complete keratin filaments in mouse L cells augments cell migration and invasion,” *Proc Natl Acad Sci U S A*, vol. 90, no. 9, pp. 4261–4265, May 1993, doi: 10.1073/PNAS.90.9.4261.

[562] C. Matthias, B. Mack, A. Berghaus, and O. Gires, “Keratin 8 expression in head and neck epithelia,” *BMC Cancer*, vol. 8, no. 1, pp. 1–10, Sep. 2008, doi: 10.1186/1471-2407-8-267/FIGURES/4.

[563] J. L. Coombes and F. Powrie, “Dendritic cells in intestinal immune regulation,” *Nat Rev Immunol*, vol. 8, no. 6, p. 435, Jun. 2008, doi: 10.1038/NRI2335.

[564] N. S. Wilson *et al.*, “Normal proportion and expression of maturation markers in migratory dendritic cells in the absence of germs or Toll-like receptor signaling,” *Immunol Cell Biol*, vol. 86, no. 2, pp. 200–205, Feb. 2008, doi: 10.1038/SJ.ICB.7100125.

[565] T. Yamasaki, J. O’Neil, and R. Fass, “Update on Functional Heartburn,” *Gastroenterol Hepatol (N Y)*, vol. 13, no. 12, p. 725, Dec. 2017, Accessed: Feb. 25, 2022. [Online]. Available: /pmc/articles/PMC5763558/

[566] G. Yang, Y. Yang, H. Tang, and K. Yang, “Loss of the clock gene Per1 promotes oral squamous cell carcinoma progression via the AKT/mTOR pathway,” *Cancer Sci*, vol. 111, no. 5, pp. 1542–1554, May 2020, doi: 10.1111/CAS.14362.